Optimizing the Processes for Isolation, Preservation, and Transportation of Human Limbus-derived Stromal/ Mesenchymal Stem Cells for Corneal Regeneration

Thesis submitted for the degree of

DOCTOR OF PHILOSOPHY

To

THE DEPARTMENT OF ANIMAL BIOLOGY
SCHOOL OF LIFE SCIENCES
UNIVERSITY OF HYDERABAD
HYDERABAD – 500 046
INDIA

By

Damala Mukesh

Under the supervision of

Supervisor (External):
Dr. Vivek Singh
Centre for Ocular Regeneration
L V Prasad Eye Institute

Supervisor (UoH):
Dr. A. Bindu Madhava Reddy
Dept. of Animal Biology
School of Life Sciences

Centre for Ocular Regeneration
Prof. Brien Holden Eye Research Centre
LV Prasad Eye Institute
Hyderabad - 500 034

July 2023

Enrolment No: 17LAPH16

University of Hyderabad

School of Life Sciences

Department of Animal Biology

Hyderabad-500 046, India

CERTIFICATE

This is to certify that this thesis entitled "Optimizing the Processes for Isolation, Preservation, and Transportation of Human Limbus-derived Stromal/ Mesenchymal Stem Cells for Corneal Regeneration" submitted by Mr. Damala Mukesh bearing registration number 17LAPH16 for the degree of Doctor of Philosophy to the University of Hyderabad is a bonafide record of research work carried out by him at the LV Prasad Eye Institute, Hyderabad under my supervision. The contents of this thesis, in full or in parts have not been submitted to any other University or Institution for the award of any degree or diploma. I hereby, recommend his thesis for submission, for the award of the degree of Doctor of Philosophy from the University.

Dr. Vivek Singh
Supervisor, Centre for Ocular Regeneration
Brien Holden Eye Research Centre, LV Prasad Eye Institute

Dr. VIVEK SINGH, PhD
Scientist
Prof. Brien Holden Eye Research Center,
Champalimaud Translational Centre for Eye Research,
L V Prasad Eye Institute (LVPEI), Kallam Anji Reddy Campus,
L V Prasad Marg, Hyderabad – 500 034.

Dr. A. Bindu Madhava Reddy
Supervisor (UoH)

Dr. A. Bindu Madhava Reddy
Assistant Professor
Dept. of Animal Biology
School of Life Sciences
University of Hyderabad
Hyderabad-500 046.

Director of Research,
Brien Holden Eye Research Centre,
LV Prasad Eye Institute

Dr. SAYAN BASU
Director of Research
Hyderabad Eye Research Foundation
L V Prasad Eye Institute
Road No.2, Banjara Hills,
Hyderabad-500 034, Telangana, India

Head,
Department of Animal Biology,
School of Life Sciences, UoH

अध्यक्ष / HEAD
जंतु जैविकी विभाग
Department of Animal Biology

Dean,
School of Life Sciences, UoH

07/07/21

डीन / Dean
जीव विज्ञान संकाय / School of Life Sciences
हैदराबाद विश्वविद्यालय / University of Hyderabad
हैदराबाद / Hyderabad-500 046.

University of Hyderabad

School of Life Sciences

Department of Animal Biology

Hyderabad-500 046, India

DECLARATION

I, Damala Mukesh, hereby declare that this thesis entitled "Optimizing the Processes for Isolation, Preservation, and Transportation of Human Limbus-derived Stromal/Mesenchymal Stem Cells for Corneal Regeneration" submitted by me under the guidance and supervision of Dr. Vivek Singh and Dr. A Bindu Madhava Reddy, is original and independent research work. I also declare that it has not been submitted to any other University or Institution for the award of any degree or diploma.

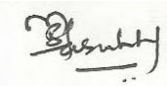

Date

20 July 2023

Damala Mukesh

17LAPH16

University of Hyderabad
Hyderabad-500 046, India

CERTIFICATE

This is to certify that this thesis entitled "Optimizing the Processes for Isolation, Preservation, and Transportation of Human Limbus-derived Stromal/Mesenchymal Stem Cells for Corneal Regeneration" submitted by Mr. Damala Mukesh bearing registration number 17LAPH16 in partial fulfilment of the requirements for the award of Doctor of Philosophy in the Department of Animal Biology, School of Life Sciences, is a bonafide work carried out by him under our supervision and guidance. This thesis is free from plagiarism and has not been submitted previously in full or in parts, have not been submitted to any other University or Institution for the award of any degree or diploma.

Parts of this thesis have been:

A. Published

1. **Mukesh Damala** Stephen Swioklo, Madhuri A. Koduri, Noopur S. Mitragotri, Sayan Basu, Che J. Connon, and Vivek Singh. "Encapsulation of human limbus-derived stromal/mesenchymal stem cells for biological preservation and transportation in extreme Indian conditions for clinical use." ***Scientific Reports*** 9, no. 1 (2019): 16950. DOI: 10.1038/s41598-019-53315-x , **IF: 4.122**
2. Arun Chandru, Parinita Agrawal, Sanjay Kumar Ojha, Kamalnath Selvakumar, Vaishnavi K. Shiva, Tanmay Gharat, Shivaram Selvam, Midhun Ben Thomas, **Mukesh Damala,** Deeksha Prasad, Sayan Basu, Tuhin Bhowmick, Virender Singh Sangwan and Vivek Singh. "Human cadaveric donor cornea derived extra cellular matrix microparticles for minimally invasive healing/regeneration of corneal wounds." ***Biomolecules*** 11, no. 4 (2021): 532. DOI:10.3390/biom11040532, **IF:6.064**
3. Fatemeh Tavakkoli, **Mukesh Damala,** Madhuri Amulya Koduri, Abhilash Gangadharan, Amit K. Rai, Debasis Dash, Sayan Basu, and Vivek Singh. "Transcriptomic profiling of human limbus-derived stromal/mesenchymal stem cells—novel mechanistic insights into the pathways involved in corneal wound healing." *International Journal of Molecular Sciences* 23, no. 15 (2022): 8226. DOI:10.3390/ijms23158226, **IF:6.028**
4. **Mukesh Damala**, Abhishek Sahoo, Naveen Pakalapati, Vivek Singh, and Sayan Basu. "Pre Clinical Evaluation of Efficacy and Safety of Human Limbus-Derived Stromal/Mesenchymal Stem Cells with and without Alginate Encapsulation for Future Clinical Applications." *Cells* 12, no. 6 (2023): 876. DOI:10.3390/cells12060876, **IF:7.666**
5. Abhishek Sahoo, **Mukesh Damala,** Jilu Jaffet, Deeksha Prasad, Sayan Basu, and Vivek Singh. "Expansion and characterization of human limbus-derived stromal/mesenchymal stem cells in xeno-free medium for therapeutic applications." ***Stem Cell Research & Therapy*** 14, no. 1 (2023): 1-16. DOI:10.1186/s13287-023-03299-3, **IF:8.088**
6. **Mukesh Damala**, Naveen Pakalapati, Vivek Singh, and Sayan Basu. "Safety and toxicity of human limbus-derived stromal/mesenchymal stem cells with and without alginate encapsulation for clinical application." (2021). DOI: 10.21203/rs.3.rs-789579/v1. ***An open-access pre-print submission.*** Available at: https://assets.researchsquare.com/files/rs-789579/v1/38c54e5c-a528-4171-b1e1-5e7be43a4da7.pdf?c=1636053801 ; https://www.researchsquare.com/article/rs-789579/v1
7. Sayan Basu, **Mukesh Damala,** and Vivek Singh. "Limbal stromal stem cell therapy for acute and chronic superficial corneal pathologies: early clinical outcomes of the Funderburgh technique." ***Investigative ophthalmology & visual science*** 58, no. 8 (2017): 3371-3371. **IF: 3.303** (Proceeding Publication)

8. Funderburgh, James, Sayan Basu, **Mukesh Damala,** Fateme Tavakkoli, Virender Sangwan, and Vivek Singh. "Limbal stromal stem cell therapy for acute and chronic superficial corneal pathologies: one-year outcomes." *Investigative ophthalmology & visual science* 59, no. 9 (2018): 3455-3455. (Proceeding Publication)
9. Basu, Sayan, **Mukesh Damala,** Fateme Tavakkoli, Noopur Mitragotri, and Vivek Singh. "Human limbus-derived mesenchymal/stromal stem cell therapy for superficial corneal pathologies: Two-year outcomes." *Investigative Ophthalmology & Visual Science* 60, no. 9 (2019): 4146-4146. (Proceeding Publication)
10. **Damala, Mukesh,** Stephen Swioklo, Madhuri Amulya Kondapaka, Noopur Mitragotri, Sayan Basu, Che John Connon, and Vivek Singh. "Encapsulation of human limbus-derived stromal/mesenchymal stem cells for storage and transportation at room temperature." *Investigative Ophthalmology & Visual Science* 60, no. 9 (2019): 4654-4654. (Proceeding Publication)
11. Singh, Vivek, **Mukesh Damala**, Tanmay Gharat, Shivaram Selvam, Sanjay Kumar Ojha, Tuhin Bhowmick, Arun Chandru, Virender Singh Sangwan, and Sayan Basu. "A Novel Extracellular Matrix-Mimetic Hydrogel for Corneal Regeneration." *Investigative Ophthalmology & Visual Science* 60, no. 9 (2019): 4687-4687. (Proceeding Publication)

B. Presented in the following International and National Conferences

1. Poster presentation: "In vivo assessment of the toxicity of human limbus-derived stromal/mesenchymal stem cells with or without alginate encapsulation for clinical use" at the 27th IERG Annual Meeting, 2021– Hyderabad (International).
2. Poster presentation: "Encapsulation of human limbus-derived stromal/mesenchymal stem cells for storage and transportation at room temperature" at the ARVO Annual Conference, 2019 – Vancouver, Canada (International).
3. Poster presentation: "Characterization and optimization of human limbus-derived mesenchymal/ stromal stem cells for clinical application" at 86th SBC Annual Conference, 2017 – New Delhi (National).

Further, the student has passed the following courses towards the fulfilment of coursework requirements for a Ph.D.

Name	Credits	Credits Obtained	Pass/Fail
Research Methodology / Laboratory Rotation	6	6	Passed
Analytical Techniques / Biostatistics	6	6	Passed
Scientific Writing	3	3	Passed
Clinical Orientation	2	2	Passed

08/07/23

Dr. Vivek Singh
Supervisor (External)

Dr. VIVEK SINGH, PhD
Scientist
Prof. Brien Holden Eye Research Center,
Champalimaud Translational Centre for Eye Research,
L V Prasad Eye Institute (LVPEI), Kallam Anji Reddy Campus,
L V Prasad Marg, Hyderabad – 500 034

Dr. A. Bindu Madhava Reddy
Supervisor (UoH)

Dr. A. Bindu Madhava Reddy
Assistant Professor
Dept. of Animal Biology
School of Life Sciences
University of Hyderabad
Hyderabad-500 046.

Director of Research,
Brien Holden Eye Research Centre,
I.V Prasad Eye Institute

Head,
Department of Animal Biology,
School of Life Sciences, UoH

Dean,
School of Life
Sciences, UoH

अध्यक्ष / HEAD
जंतु जैविकी विभाग
Department of Animal Biology

जीव विज्ञान संकाय / School of Life Sciences
हैदराबाद विश्वविद्यालय / University of Hyderabad
हैदराबाद / Hyderabad-500 046

Dr. SAYAN BASU
Director of Research
Hyderabad **Eye Research Foundation**
L V Prasad **Eye Institute**
Road No.2, **Banjara Hills,**
Hyderabad-500 034, **Telangana, India**

Optimizing the Processes for Isolation, Preservation, and Transportation of Human Limbus-derived Stromal/Mesenchymal Stem Cells for Corneal Regeneration

Dedicated to

This doctoral thesis work is dedicated to

My *Guru*s

(Drs. Vivek Singh, Sayan Basu, and Abhinav R Kethiri)

My Parents

(Shri Vijaya Bhaskar and Shri Swarupa Rani)

&

Every little *Squirrel* * that is fighting

Blindness – the *forestallment*, the *Cure* and the *Aftermath*

---

* Referring to a character from the Indian mythological epic *Ramayana,* which conveys the moral:

"No task or contribution towards the ultimate pinnacle, however small, is unimportant !".

Acknowledgements

I would like to dedicate this section to expressing my great gratitude and heartfelt acknowledgements to all of these exceptional individuals and organisations that have shaped my PhD research. Their continuous assistance, counsel, and contributions have been monumental, and I owe them a great debt.

First and foremost, I extend my deepest appreciation to the visionary **Dr. Vivek Singh**, LV Prasad Eye Institute (LVPEI), my supervisor and PhD guide. His unwavering patience, or let's say tolerance and unparalleled expertise have been the cornerstone of my research journey. I am really appreciative of his mentorship and all the opportunities he has afforded me during my scientific career. *Many thanks, Dr Vivek!*

I would like to extend my heartfelt appreciation to **Dr. Bindu Madhava Reddy**, University of Hyderabad, my supervisor and PhD guide, whose administrative support and unwavering patience have been nothing short of extraordinary.

I owe **Dr. Sayan Basu**, the Director of Research at the Prof Brien Holden Eye Research Centre (BHERC), and a renowned mentor, an inexpressible debt of gratitude. Dr. Basu's continuous support, observations, and direction have shaped my study in ways that have exceeded my greatest hopes. He has been a beacon of insight, guiding me back on course when necessary.

Dr. Gullapalli Nageswara Rao, the founder and Chairman Emeritus, LVPEI, **Dr. Prashant Garg,** Chairman, LVPEI, **Dr. Bala Subramaniam**, Director Emeritus - BHERC, and **Dr. Virender Sangwan**, the Ex-Director - Centre for Ocular Regeneration, and **Dr. Sayan Basu**, Director - Centre for Ocular Regeneration, deserve my heartfelt gratitude. Their foresight has built great infrastructure and cutting-edge laboratory facilities, allowing me to do my research study. I am really grateful to LVPEI for providing me with the essential chance to pursue my research interests. In addition, **Drs. Sangwan and Balu** have been incredibly supportive during the difficult PhD admissions process. I am grateful to them.

I cannot forget the distinguished **LVPEI faculty,** whose insight, skill, and guidance have greatly improved my research. Their passion to quality and knowledge advancement has always encouraged me to achieve.

The **Indian Council of Medical Research** (ICMR) and the **Science and Engineering Research Board** (SERB), Government of India, are the esteemed funders of my research. I am humbled and honoured to have their support and trust.

The **Ramayamma International Eye Bank** in Hyderabad has generously supplied therapeutic donor corneas that have served as the basis for my study. My research would have remained aspirational in the absence of their contributions. I will always be grateful for their great assistance.

I'd like to thank **Atelerix Co Ltd.** in Britain for their assistance and collaboration in alginate work. My research has advanced into greater territories, thanks to their support and raw material supplies. I'd also want to thank **Dr. Mick McLean** of Atelerix for financing my first international travel to the ARVO Conference.

I would like to extend my heartfelt thanks to the staff at the **Centre for Cellular and Molecular Biology** (CCMB), particularly **Dr. Mahesh** and **Mr. Sai**, for their support and assistance with the animal experiments that were an integral part of my research.

My heartfelt gratitude goes out to my remarkable lab colleagues, whose friendship, intellectual exchanges, and shared experiences have helped mould me into the person and the researcher I am today. **Dr Abhinav R Kethiri,** my Guru from the very beginning of this journey, should be singled out for his countless helpful suggestions and constant encouragement and training. I'm also grateful to **Madhuri K Amulya** and **Abhishek Sahoo**, who assisted me with molecular studies and animal experimentation. I will be eternally grateful to my former labmates, **Enoch Raju, Harsha Agarwal, Dr Fatemeh Tavakkoli, Noopur Mitragotri, Veena**, and **Ajay Jhakar,** for their helpful hands and unflinching support. My sincere gratitude is extended to **Jilu Jaffet, Mohd Salman, Deeksha Prasad,** and **Aniruth Reddy** for their support in the laboratory and animal facilities when it was required.

I'm grateful to **Drs Vijay Singh, Anshuman Verma, Om Prakash and Sanjay Kumar**, esteemed postdoctoral fellows, who have guided, advised, and helped me with my academic writing and research. Their skills and wisdom have helped my study be clear and rigorous.

The GMP (Good Manufacturing Practice) gurus, Mr **Ashwin,** and Mr **Chetan AJ**, deserve my deepest appreciation for their unwavering support, expert guidance, and meticulous oversight in ensuring adherence to rigorous certifications, training protocols, and batch manufacturing records. Their invaluable contribution has set the highest standards for my research.

I thank LVPEI's Pathology and Microbiology labs for processing my samples. I'd want to thank **Mr. Sridhar, Dr. Soumya Jakati,** and **Dr. Dilip Mishra** of Pathology Services for always helping with samples.

I must thank the administrative staff who made my research run smoothly. **Ms Elena D Roopchandra**, BHERC -Assistant Director, **Mr Poorna Chandar Rao, Mr Ramulu, and Mr Srinivas Ayyagari** helped me with their administrative support.

I thank **Mr. Malkaiah** from the Stores Department and **Mr. Jagadish** from the Purchase Department for their constant support in providing research supplies. Their efficiency and attention have made my work run smoothly. I'd also want to thank **Mr. Sunil** from the Internet Services Desk for his help providing softwares to ensure uninterrupted access to vital resources. I

love the library and am grateful to **Mr. Sudhakar, Banu ji,** and **Mr. Kuddoos** for their consistent support in facilitating access to prints and documents, enriching my research journey.

Dr. Vinay Pulimamidi, Dr. Praveen Jospeh, Dr. Meha, Dr. Shahna, Dr. Ranjith, Mrs. Pooja Kethiri, Sudipta Mahato, Dr Jayshree Gandhi and all the other LVPEI colleagues have my deepest respect and gratitude. Their friendship, encouragement, and shared experiences have added immeasurably to the value of my experiences at LVPEI. I reserve a special mention for **Dr. Poonam,** who's been a *'reset'* button on any challenging day and for being that, *Keeper*.

I thank my longtime *Mama,* **Mr. Naveen Kola (Pakalapati).** His continuous support, encouragement, and conviction in my abilities have sustained me through personal and professional challenges. It's so rare of him to say No to me.

I'd want to single out **Ms**. **Swatilekha Hazra,** also known as Motu. She has been an exceptional part of my life, a dependable chum who has always been there for me no matter what. Her unending encouragement, unbounded optimism, and undying faith in my abilities have been invaluable. Can't thank her enough!

Last but certainly not least, I owe an immeasurable debt of gratitude to my beloved parents **Shri Vijaya Bhaskar and Swarupa Rani Damala**, and my sister **Sucharitha**. Without their unwavering support, sacrifice, and belief in me, this journey would not have been possible. Their unconditional love and encouragement have been the driving force behind my achievements. I'm forever grateful to my sister, fondly known as *Ammu,* for selflessly prioritizing my needs and dreams above her own.

Lastly, I extend my heartfelt appreciation to **all the donors and their families**, without whom this research would not have been possible. Their selfless act of donating corneas has provided the foundation for my work, offering hope and potential breakthroughs in the field of ocular research. Their contributions have touched countless lives and will continue to do so.

I'm grateful to everyone listed above. My PhD thesis was shaped by their encouragement, mentoring, and contributions. I carry their tremendous insights, knowledge, and inspiration with me as I begin my next academic and career adventure.

- *Mukesh Damala*

Contents

Annexures

List of Tables

List of Figures

List of Abbreviations

Short Form	Abbreviation
µL	Microliter
ABCB5	ATP-Binding Cassette Sub-Family B Member 5
ABCG2	ATP-binding cassette sub-family G member 2
ARVO	Association for Research in Vision and Ophthalmology
ASC	Adult Stem Cell Suite
BET	Bacterial Endotoxin
BSA	Bovine Serum Albumin
CCMB	Center for Cellular and Molecular Biology
CD	Cluster of Differentiation
CD105	Endoglin
CD105	Cluster of Differentiation 105
CD34	Cluster of Differentiation 34
CD45	Cluster of Differentiation 45
CD73	Ecto-5'-nucleotidase
CD73	Cluster of Differentiation 73
CD90	Thy-1 cell surface antigen
cDNA	Complementary DNA
CDSCO	Central Drugs Standard Control Organization
cGMP	Current Good Manufacturing Practices
CO_2	Carbon Dioxide
CoA	Certificate of Analysis
Collagen I	Collagen type I
Collagen II	Collagen type II
Collagen III	Collagen type III
Collagen IV	Collagen type IV
Collagen V	Collagen type V
CPCSEA	Committee for the Purpose of Control and Supervision of Experiments on Animals
DAPI	4',6-diamidino-2-phenylindole
DMEM	Dulbecco's Modified Eagle Medium

DMEM/F12	Dulbecco's Modified Eagle Medium/Nutrient Mixture F-12
DMSO	Dimethyl Sulfoxide
DNA	Deoxyribonucleic Acid
DNAse	Deoxyribonuclease
DPBS	Dulbecco's Phosphate-Buffered Saline
E-Cadherin	Epithelial Cadherin
EGF	Epidermal Growth Factor
FBS	Fetal Bovine Serum
FDA	Food and Drug Administration (U.S)
G	Gauge
GAPDH	Glyceraldehyde 3-Phosphate Dehydrogenase
GLP	Good Laboratory Practice
GMP	Good Manufacturing Practices
HLA-DR	Human Leukocyte Antigen-DR
hLMSCs	Human Limbus-derived Stromal/Mesenchymal Stem Cells
IAEC	Institutional Animal Ethics Committee
IC-SCR	Institutional Committee for Stem Cell Research
IHC	Immunohistochemistry
IOP	Intraocular Pressure
IU	International Units
KERA	Keratocan
Keratin	Keratin
Kg	Kilograms
MK	Mc Carey-Kaufman
mL	Milliliter
MPR	Media Preparation Room
MTT	3-(4,5-dimethylthiazol-2-yl)-2,5-diphenyltetrazolium bromide
NA	Not Applicable
N-Cadherin	Neural Cadherin
NDCT	New Drugs and Clinical Trials
OECD	Organization for Economic Co-operation and Development
P63-α	Tumor protein p63 isoform α
PAX-6	Paired Box Protein Pax-6

PBS	Phosphate Buffered Saline
PCR	Polymerase Chain Reaction
PFA	Paraformaldehyde
QC	Quality Control
RNA	Ribonucleic Acid
RNAse	Ribonuclease
RT	Room Temperature
SOP	Standard Operating Procedure
SYBR	Sybr Green
TC	Tissue Culture
TrypLE	Trypsin-like Enzyme
VIM	Vimentin
α-SMA	Alpha-Smooth Muscle Actin
µ	Micro

Chapter 1

Introduction

1. Introduction

The visual system is one of the most prominent sensory functions of the human body. It is the basis for perceiving one's surroundings. The sensory organ of the visual system is the eye. The brain and eye communicate and work together in sensing and interpreting our surroundings to us. This occurs through the transmission of light into the eye, which is then processed and transferred to the thalamus of the brain through the optic nerve for interpreting the information for visual perception. More than 70% of people are afraid of losing vision compared to the rest of the senses (Hutmacher, 2019), which explains the prominence of this system.

On the anterior side of the eye, lies the transparent cornea, which transcribes the light entering the eye. Along with the sclera and conjunctiva, it also acts as a protective barrier from the external surroundings offering protection to the internal parts of the eye. Two-thirds of the eye's total refractive power is located in the cornea, sometimes known as the "window of the eye," a transparent structure responsible for focusing light on the retina. The cornea's stroma is transparent because of its smooth surface and the uniform arrangement of collagen fibrils. Maintenance of the shape and the transparency of the cornea is essential for the refraction of light, a prerequisite for optimal vision (Mannis & Holland, 2021).

Any disturbance to the physiology and structural damage to the cornea due to factors including, but not limited to, infection, inflammations, trauma, chemical or thermal burns, etc. can cause opacification to the transparent cornea, causing moderate to severe visual impairment or blindness. The etiology of corneal blindness includes a variety of physical, inflammatory, and congenital factors, and to which the most commonly generated form of the response is corneal scarring. This opacification or the haze of the corneal surface, which follows a mechanical trauma or a burn or necrosis, is part of the natural healing mechanism and tissue repair.

After an injury to the corneal stroma, which forms a majority of its structural components and accounts for >90% of the corneal thickness, the surrounding area is recruited with fibroblast cells. These cells generate the fibrotic matrix in an uncontrolled or irregular fashion and replace the damaged or lost tissue. However, this irregular formation of the collagen fibrils affects the transparency of the cornea, obscuring the entry of light into the eye. Based on the size and depth of the damage, the scarring can remain for as low as a few weeks to several years, affecting the vision of the individuals. This unfavorable way of healing the cornea affects the day-to-day life of the people as long as the scar remains in the cornea (Basu et al., 2014a).

Such pathologies involving the cornea are the third leading cause of reversible blindness, affecting millions of people worldwide. More than 83% of the eye injuries that required tertiary care involved cornea and conjunctiva (Blaszkowska et al., 2022) and nearly 98% of the corneally blind individuals are from underdeveloped nations (Mathews et al., 2018a).

The most commonly performed surgical intervention aimed at restoring corneal clarity and vision is corneal transplantation (keratoplasty), where the whole of the affected cornea or in part is replaced by a fresh cornea obtained from cadaver donors. Despite being the most widely performed type of organ transplantation worldwide, only 1 in 70 corneally blind people, receive this intervention, due to a combination of various regional and socio-economic factors (Flaxman et al., 2017; Gain et al., 2016).

In addition to the logistical constraint, corneal transplantation is majorly limited by post-operative complications such as graft failures over a period of time, graft rejections, graft dislocation or detachment, the incidence of glaucoma, infections, long follow-up, etc. (Singh et al., 2019). This necessitates the need for exploring other alternatives to overcome these limitations.

The recent advances in regenerative therapy have opened up the possibilities of using cell-based therapeutics as an alternative therapy to restore vision. The cell-based therapy which offers a minimally invasive and multiplied availability to a greater number of individuals can reduce the risk of postoperative complications and the need for donor corneas. With their unique immunomodulatory properties and significant regenerative potential, mesenchymal stem cells (MSCs) are an excellent alternative for the regeneration of the ocular surface. With no expression of the HLA-DR, these cells also would not elicit any type of immune response (Bray et al., 2014a).

Limbus, a brown-pigmented layer surrounding the cornea, harbors such MSCs capable of regenerating the damaged corneal tissue (Branch et al., 2012a; J. L. Funderburgh et al., 2016a). These limbal stem cells repopulate the cells of the epithelium and stroma, which may be lost owing to the regular wear and tear of the ocular surface as a result of exposure to the external environment or even just blinking, as well as after an injury. The stem cells derived from limbal stroma are similar to the keratocytes, native cells of the corneal stroma, which differentiate to and replace the lost keratocytes (Mann et al., 2011; Kumar et al., 2018).

Various pre-clinical studies in animal models, where the human limbus-derived stromal/mesenchymal stem cells (hLMSCs) have been applied as a xenograft and explored for their regenerative potential, have proven their safety (Basu et al., 2014a) and the efficacy in regenerating the cornea (Coppola et al., 2017; Hertsenberg et al., 2017a). The early intervention of

the corneal scar with hLMSCs can repair the corneal surface and regenerate the tissue without causing any fibrosis (Basu et al., 2014a), offering an early recovery.

Despite their therapeutic potential, currently, there are no studies that have explored the regenerative potential of hLMSCs in humans. In the translation of this cell-based therapy to a definitive treatment for blinding corneal pathologies, certain bottlenecks have to be addressed. This includes: (1) optimized and reliable cell culture methods of isolating and expanding hLMSCs, (2) the development of methods to store and transport the hLMSCs over prolonged distances and time without hindering their phenotypic properties, (3) the establishment of their safety and stability profiles in a regulated manner. Overcoming these challenges improves the quality of the cells and enhances the availability of these cells to millions of people in need.

To safeguard patient safety and ensure the efficacy of cell-based therapeutics, the *Drugs and Cosmetics act, 1940, India,* and the *National Guidelines for Stem Cell Research, 2017* (*National Guidelines for Stem Cell Research, 2017*, n.d.; *Schedule Y(Ammended Version) - CDSCO*, n.d.-a) mandate the practice of Current Good Manufacturing Practice (cGMP) in the generation and the testing the cells and cell-derivatives. The guidelines issued by the Central Drugs Standard Control Organization (CDSCO), the Indian regulatory body (the equivalent of the Food and Drug Administration (FDA), USA), necessitate the conduct of research involving human subjects in an ethically and socially responsible manner, in compliance with the regulations. This requires the optimization of the protocols of generating and testing any new investigational medicinal product (IMP, also referred to as an *Investigational New Drug* or *Investigational New Entity*) in a standardized, regulated and controlled manner.

The protocols to design, validate and streamline the processes of generating the IMPs in the clean-room facility, should be drafted, optimized, and tested to ensure consistent quality and quantity of the product, with minimal or no impurities. The stability of the IMP over long durations without any mutations or changes in the characteristic properties has to be tested and established, to ensure no harmful or undesirable aftereffects to the recipient, other than the anticipated outcomes. The product should be free of any microbial contaminants such as bacteria, fungi, and viruses to ensure safety.

The product should be well-characterized and consistent testing has to be done to ensure the identity, functionality, and effectiveness of the product intended for definite use. The testing of all raw materials including human tissues, plastics, chemicals, and reagents ensures that the product meets all requirements and specifications set for a desired activity or purpose. Many such practices

are required to be performed to guarantee the highest possible standards of the safety, efficacy, and quality of medicinal products.

The GMPs are a compilation of such guidelines and directives suggested and mandated by the regulatory authorities of a given nation. These guidelines govern the activities of production, distribution, and end-use of the products designed. This requires the design of Standard Operating Protocols (SOPs) to streamline, document, track and validate every activity of production, distribution, and testing with the criterion set for required specifications (Abdellah et al., 2015; Gouveia et al., 2015a).

Biologics and cell-based products must be transported between labs and institutions to expand research and therapy options. The current modes of shipping cells or cell-based therapeutics are dominated by cryopreservation methods that transport the cells with suspended metabolism. The cryopreservation methods do not offer optimal viability and hamper the functionality of the cells, changing their cell survival and potentiality. These methods require longer durations for the cell populations to stabilize in a culture post-thaw and can affect the timeframe of consumption by the end-user (Chinnadurai et al., 2016; Karlsson & Toner, 1996).

Cryopreservation methods demand equipment of high cost and maintenance, and also skilled personnel at both the sites of production and end-use. On the other hand, the logistical issues of using restricted items as cryo-coolants (For example dry ice) for maintaining ultra-low temperatures always persist (*Dangerous Goods & Prohibited Items | FedEx India*, n.d.). Hence, the expedited shipping of the biologics requires a separate channel for the handling of the shipments which can be 10-25x expensive compared to a regular shipment. This calls for exploring new and reliable alternatives that offer the preservation and transport of cells and biologics that offer the maintenance of stable and unaffected characteristic properties of the cells, optimal viability, easy handling, and low-cost logistics.

One of the alternative methods widely explored in recent years to store and preserve biologics is the encapsulation of biological samples or plant seeds. Encapsulation offers the preservation of cell viability and the properties of their proliferation and differentiation. Alginates are the most widely used encapsulating agents for cell encapsulation and drug delivery. They are natural polysaccharides derived from seaweeds (Brown Algae), with excellent biocompatibility and biodegradability (J. Sun & Tan, 2013a). Alginate encapsulation enhances the differentiation ability (Richardson et al., 2014) of the stem cells and maintains cell viability (H. J. Kong et al., 2003). Sodium alginate was shown to be a safe hydrogel matrix to store and preserve ovarian follicles

(Camboni et al. 2013) and improved the preservation of adipose-derived stem cells at hypothermic temperatures (less than room temperature)(Swioklo et al., 2016).

Additionally, the alginates are inert in nature and offer excellent customizations to alter the viscosity and the gelation properties of the hydrogels, with controllable stiffness and polymerization periods. This would enable the testing of these hydrogels in cells of various sizes and tissues with various dimensions. Above all, the reagents required for the encapsulation procedures are all "regarded as safe" for human consumption. The reagents used for the encapsulation procedure i.e. sodium alginate (*CFR - Code of Federal Regulations Title 21*, n.d.-a) and calcium chloride (Tran, n.d.) are safe for human consumption and are widely used in the food industry. Sodium citrate, used for releasing the cells from encapsulation by breaking the calcium alginate ionic cross-linking, besides being considered safe (Office of the Federal Register, 1994) is widely used to treat alkali burns to reduce ulcers (Pfister et al., 1981, 1982) and also in artificial tears to treat dry eye disease(Drew et al., 2018). Thus, these agents can be an excellent choice for encapsulating hLMSCs, being used as non-invasive therapy, and treating corneal pathologies.

The assessment of the safety and toxicity of Alginate-encapsulated hLMSCs (*En*+ hLMSCs) in an animal model of corneal wound or scar is mandatory before they could be tested for their potential of regenerating the ocular surface in humans. The guidelines of CDSCO suggest the safety of any IMP be established in two animals (one rodent, and one non-rodent) before they could be used for human applications. Maintaining sterility in all the activities involved in the cultivation, encapsulation, transport, release, and final delivery of the hLMSCs onto the ocular surface is obligatory and crucial to ensure the safety of the recipient. Assessing the toxicity of the and the immune response on the site of application i.e. ocular surface and internal (systemic) body would help to understand the effect of *En*+ hLMSCs on the recipient. Any immune response elicited can be quantified and tested to understand and amend the procedures accordingly to make a safer and more efficacious formulation. Assessing the same with non-encapsulated hLMSCs (*En*- hLMSCs) would help to differentiate the effect of encapsulation versus non-encapsulation on the functionality of the hLMSCs.

To test the efficacy of the *En*+ hLMSCs, the generation of an animal model of the corneal scar would provide a real-time understanding of the efficacy of these cells, and differentiate the same between *En*+ or *En*- hLMSCs. Assessing the same in two separate groups of animal models providing prophylaxis care before the onset of the scar in one group and treatment post-development of the scar in the other group would enable us to understand the ability of *En*+

hLMSCs in preventing corneal scars. Altogether, this would enable the establishment of the safety and efficacy profiles of the hLMSCs for corneal regeneration.

In this thesis work, we aimed to design, standardize and optimize the protocols of cultivation, storage, and transport of the hLMSCs and assess their characteristic features and stabilities in compliance with the cGMP directives and regulatory guidelines. Additionally, to design a framework for taking this potential therapy, from bench to bedside.

Chapter 2

Objectives

2. Objectives

1. Optimizing the methods for isolation, characterization of hLMSCs, and assessment of their quality and stability complying with the current GMP norms.
2. Optimizing the cold-chain-free methods of preservation and transport of hLMSCs over prolonged durations and distances at varying temperatures.
3. Evaluation of the safety and toxicity of the hLMSCs with and without encapsulation.
4. Assessment of the efficacy of hLMSCs with and without encapsulation in healing the corneal scar in an animal model.

Chapter 3

Review of Literature

3.1.1. Beyond the Horizon of Sight: The Potential of Human Visual Perception

Human vision holds great prominence among the various senses due to its complexity, versatility, and the amount of information it provides (Knauer & Pfeiffer, 2008). Considered the primary sense for many individuals, vision allows us to perceive and interpret the world around us in remarkable detail.

Visual perception plays a crucial role in gathering information about our environment. It provides us with a comprehensive understanding of the shape, color, size, and movement of objects, enabling us to navigate and interact with our surroundings effectively. The ability to see allows us to recognize faces, read written language, and appreciate the beauty of the visual world.

Vision also contributes significantly to our safety and well-being. It alerts us to potential dangers and helps us avoid obstacles, both in our immediate surroundings and when navigating complex environments. Depth perception, peripheral vision, and visual acuity enable us to perform various tasks that require precise hand-eye coordination (Brown, 1999).

3.1.2. The Human Eye: A Gateway to Visual Perception and Beyond

- The eye is a complex organ that is responsible for capturing and processing visual information. It consists of several structures, including the cornea, iris, lens, retina, and optic nerve (**Figure 3.1 A-B**).
- The cornea, the eye's most transparent layer, aids in focusing light onto the retina. The iris, which is the colorful component of the eye, controls how much light enters through the pupil. The lens, a transparent structure situated behind the iris that aids in enhancing light's focus on the retina (Remington, 2012).
- The retina, the eye's innermost layer, includes photoreceptor cells that sense light and provide visual information to the brain. The retina has numerous layers, including the photoreceptor layer, which includes rod and cone cells that sense light, and the ganglion cell layer, which contains optic nerve cells (Purves, 2001).
- The optic nerve transmits visual information from the retina to the brain. It exits via the optic disc on the back of the eye (Kanski & Bowling, 2016).
- The optic cup, a depression in the embryo, becomes the optic nerve and retina. The neural tube-derived optic vesicle invaginates to create the optic cup during embryogenesis. The optic cup has two layers—inner and exterior. The inner layer becomes the retina, while the outer layer becomes the retinal pigment epithelium and other supporting cells (Sadler & Langman, 2012)

3.1.3. The Visual Symphony: Exploring the Intricate Process of Seeing.

The brain and eye process visual input to form our worldview. The cornea, pupil, and lens concentrate light onto the retina (Remington, 2012). Rods and cones are retinal photoreceptors. Cones offer color vision in strong light, whereas rods provide low-light vision. When light hits photoreceptor cells, a chemical reaction creates electrical impulses. The optic nerve sends these electrical impulses to the brain, which interprets them as visual images (M. Gupta et al., 2023).

3.1.4. Development of eye:

The neural plate folds into the neural tube to produce the eye early in embryonic development. In the third week of gestation, neurulation creates the central nervous system, including the brain and spinal cord. The anterior portion of the neural tube begins to bulge outward, forming a structure known as the optic vesicle. The optic vesicle grows and invaginates inward, forming a double-walled structure known as the optic cup (Remington, 2012)

The optic cup is composed of two layers, the outer layer and the inner layer, which give rise to different structures in the eye. The outer layer gives rise to the pigmented layer of the retina, the ciliary body, and the iris, while the inner layer gives rise to the neural layer of the retina. The optic stalk, which connects the optic cup to the developing brain, eventually forms the optic nerve. As the optic cup forms, the ectoderm adjacent to it thickens to form the lens placode. The lens placode invaginates inward to form the lens vesicle, which eventually separates from the surface ectoderm to become a free-floating structure in the developing eye. The lens vesicle differentiates into the lens, which is responsible for focusing light onto the retina (Sadler & Langman, 2012).

The differentiation of the retina and lens involves the expression of specific genes and the production of signaling molecules that regulate cell fate and development. For example, the differentiation of the neural retina involves the expression of transcription factors such as Pax6, which regulates the development of the optic cup and neural retina. Similarly, the differentiation of the lens involves the expression of specific transcription factors, such as Sox2 and Pax6, which are essential for lens development (Kondoh et al., 2004; Matsushima et al., 2011).

The lens and epithelium of the cornea are the first structures to emerge during development. Next, cells derived from the neural crest migrate in waves between the epithelium and lens to create the stroma and endothelium. The former eventually thickens as it secretes Descemet's membrane (Eghrari et al., 2015).

The corneal limbus develops from surface ectoderm cells surrounding the developing lens placode, which give rise to the corneal epithelium and limbal stem cells. The corneal limbus first becomes

macroscopically visible around 17 weeks of gestation as a distinct region at the junction of the cornea and sclera. Up to 16 weeks, the cornea and eyeball diameters increase in parallel, but after 16 weeks the cornea's growth rate declines relative to the rest of the eyeball. By 20 weeks, the corneal limbus is distinctly visible, and between 21 and 23 weeks it takes on a more convex shape and curvature. The corneal limbus ultimately develops into a reservoir of stem cells that maintain the corneal epithelium throughout life (Harayama et al., 1980).

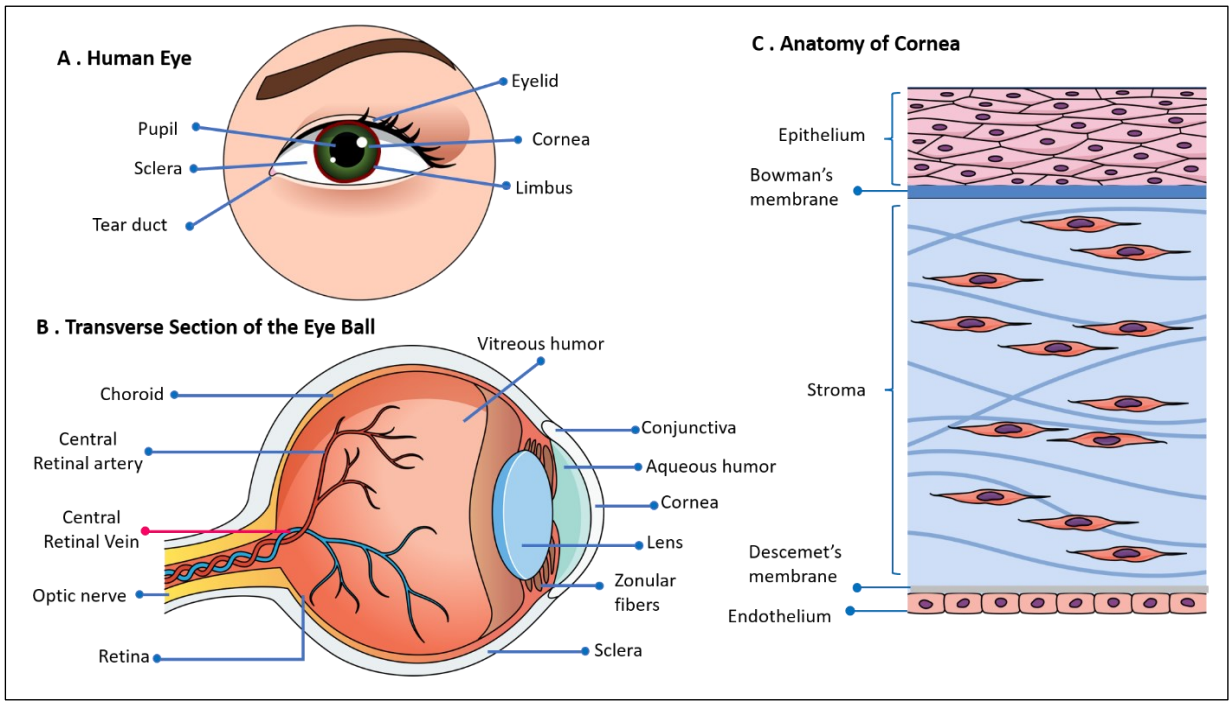

Figure 3.1: Illustration demonstrating the anatomy of human eye (**A**), transverse rection of the whole eye ball (B) and the layers of cornea (**C**).

3.2. Anatomy of cornea

The cornea is composed of five main layers, including the epithelium, Bowman's layer, stroma, Descemet's membrane, and endothelium (DelMonte & Kim, 2011) (**Figure 3.1 C**).

3.2.1. **Epithelium:** The Outermost Protective Layer

The epithelium is the outermost layer of the cornea and serves as a protective barrier against injury and infection. Composed of several layers of cells, it plays a vital role in safeguarding the cornea. The primary functions of the epithelium include preventing the entry of harmful substances, such as bacteria and foreign particles, into the cornea. Additionally, it helps maintain the smooth surface of the cornea, which is essential for clear and sharp vision (Maurice, 1957; Sadler & Langman, 2012).

2.2.1. **Bowman's Layer:** Structural Support

Beneath the epithelium lies Bowman's layer, a thin layer of collagen fibers. Although acellular, it provides structural support to the cornea. Bowman's layer contributes to the cornea's overall strength and stability, helping it maintain its shape and resist deformation. While injuries to Bowman's layer can impair its regenerative capacity, its presence is crucial for the cornea's integrity (Maurice, 1957).

3.2.2. **Stroma:** Transparency and Refractive Properties

The stroma, which is the thickest layer of the cornea, constitutes approximately 90% of its total thickness. It is primarily composed of collagen fibers arranged in a precise lattice pattern, with the quiescent cells called keratocytes, embedded in the spatial arrangement. This unique arrangement contributes to the cornea's transparency, allowing light to pass through it without scattering. The stroma's regular organization also plays a pivotal role in the cornea's refractive properties, bending and focusing incoming light onto the retina (Espana & Birk, 2020; Maurice, 1957)

3.2.3. **Descemet's Membrane:** Separating Stroma and Endothelium

Descemet's membrane is a thin layer situated between the stroma and the endothelium. Composed of specialized collagen fibers, it acts as a barrier between these two layers. Descemet's membrane provides structural support to the cornea, preventing bulging or protrusion of the stroma. Furthermore, it serves as a substrate for endothelial cell attachment and plays a role in cell migration during wound healing processes (DelMonte & Kim, 2011; Maurice, 1957).

3.2.4. **Endothelium:** Fluid Regulation and Transparency Maintenance

The endothelium is a single layer of cells that lines the inner surface of the cornea. It is responsible for regulating the flow of fluid into and out of the cornea. The endothelial cells have an essential function in maintaining the cornea's transparency by actively pumping excess fluid out of the stroma. This pump action prevents fluid accumulation and edema, which would otherwise result in impaired vision. The endothelium's efficient fluid management ensures the cornea remains clear and optically functional (DelMonte & Kim, 2011; Espana & Birk, 2020; Maurice, 1957)

These distinct layers of the cornea work together harmoniously to maintain the cornea's integrity, transparency, and visual function. Any disruption or damage to these layers can lead to vision problems and ocular disorders, emphasizing the importance of their proper functioning and care. The anatomy of the cornea with its delicate arrangement of the layers, is essential for its proper function in the visual system. The transparency of the cornea is maintained by the regular arrangement of collagen fibers in the stroma and the absence of blood vessels, which would otherwise scatter light and impair vision. These refractive properties are quite important for focusing light onto the retina for visual processing (Eghrari et al., 2015; Maurice, 1957).

3.3. Corneal stroma – Essential contribution to optical clarity/transparency

The corneal stroma, which constitutes approximately 90% of the cornea's thickness, is primarily composed of collagen fibrils and extracellular matrix. It consists of multiple lamellae, each containing parallel collagen fibrils, while adjacent lamellae have collagen fibrils arranged in orthogonal orientations. This crisscross arrangement of collagen fibrils scatters light in all directions, minimizing forward scatter and enhancing transparency. The spacing between collagen fibrils and lamellae is uniform, further contributing to light scattering in all directions and reducing reflection and absorption. With a small diameter of around 25-35 nm, the collagen fibrils allow light to pass through the spaces between them with minimal scattering, absorption, or reflection. The organized and highly regulated structure of the corneal stroma ensures transparency by maintaining the orthogonal arrangement, uniform spacing, and small diameter of collagen fibrils. Disruptions to this organization, such as corneal edema, scarring, or dystrophy, can impair transparency by affecting the uniform spacing and orthogonal arrangement of collagen. Overall, the orthogonal arrangement and uniform spacing of collagen fibrils in the corneal stroma play a crucial role in promoting transparency by reducing forward light scatter, maintaining a uniform refractive index, allowing minimal interaction with small-diameter fibrils, and providing a consistent optical pathway through the organized stromal structure (Espana & Birk, 2020; Jester et al., 1999; Maurice, 1957).

3.3.1. Functions of cornea

The cornea is the transparent, dome-shaped tissue located at the front of the eye, covering the iris, pupil, and anterior chamber. Cornea plays a vital role in the overall function of the eye. Its functions range from protecting the eye from environmental threats to refraction and focusing light onto the retina, ultimately contributing to the clarity and quality of vision. Any abnormalities or changes to the cornea can lead to significant visual impairment, underscoring the critical role it plays in vision.

3.3.1.1. Protection: The cornea acts as a protective layer for the eye, preventing foreign particles and dust from entering the eye. It also provides a barrier against infection and injury, as it is rich in nerve endings and immune cells. The cornea contains several types of cells, including epithelial cells, which form a protective barrier against the external environment, and endothelial cells, which regulate fluid movement and prevent excess fluid accumulation within the cornea. Any damage to the cornea can cause a significant impact on vision, underscoring its critical protective function (Sridhar, 2018).

3.3.1.2. Refraction: The cornea is responsible for about 75% of the eye's refractive power, which is the ability of the eye to bend and focus light. It acts as a convex lens, refracting light that enters the eye and focusing it on the retina, located at the back of the eye. The cornea is responsible for the majority of the eye's focusing power and contributes to the clarity and sharpness of vision. The refractive power of the cornea is determined by its curvature, thickness, and refractive index, which refers to the speed of light as it passes through the cornea (Espana & Birk, 2020; Meek & Boote, 2004).

3.3.1.3. Vision: The cornea plays an essential role in the visual process. It not only refracts and focuses light onto the retina, but it also contributes to the quality and clarity of vision. The cornea has a unique structure that allows for high levels of light transmission, which is critical for optimal visual function. The cornea's transparency is due to its unique extracellular matrix, which is composed of collagen fibrils that are precisely arranged to allow for light transmission. Any abnormalities or changes to the cornea can significantly impact vision, leading to visual impairment and other vision problems (Espana & Birk, 2020; Meek & Boote, 2004; Torricelli et al., 2016; S. E. Wilson, 2020).

3.3.2. Immune privilege of cornea

The immune system is an essential part of the body's defense mechanism against foreign invaders, including pathogens and cancer cells. However, in certain organs and tissues, such as the brain and the eye, the immune system is tightly regulated to prevent excessive inflammation and tissue damage. Immune privilege is a term used to describe the state in which an organ or tissue can evade or suppress an immune response The cornea, is one such tissue that exhibits immune privilege, a phenomenon that enables it to maintain transparency and function despite its exposure to the external environment.

The cornea is one of the most immune-privileged tissues in the body, as it is avascular, lacks lymphatics, and is separated from the surrounding tissues by a basement membrane. These features

limit the access of immune cells to the cornea, reducing the risk of inflammation and tissue damage. However, the absence of immune surveillance also makes the cornea vulnerable to infections and injuries, sometimes (Ambati et al., 2006; Subbannayya et al., 2020; Taylor, 2016).

The immune privilege of the cornea is maintained by several mechanisms, including antigen sequestration, immune deviation, and immune privilege-associated molecules.

1. Antigen sequestration refers to the process by which the cornea sequesters foreign antigens, preventing their recognition by the immune system. This is achieved through the expression of tight junction proteins, such as occludin and claudin-5, which prevent the movement of antigens across the corneal epithelium. In addition, the cornea expresses several immunosuppressive factors, such as alpha-melanocyte-stimulating hormone (α-MSH) and transforming growth factor-beta (TGF-β), which inhibit the activation and proliferation of immune cells (Taylor, 2016).
2. Immune deviation is another mechanism that contributes to the immune privilege of the cornea. This refers to the process by which the immune response to a particular antigen is redirected to a non-inflammatory pathway. In the case of the cornea, immune deviation is achieved through the induction of regulatory T cells (Tregs), which suppress the activation of effector T cells and prevent excessive inflammation. The cornea also expresses Fas ligand (FasL), which induces apoptosis of infiltrating T cells, further contributing to immune tolerance (Keino et al., 2018).
3. Several molecules have been identified that are involved in the maintenance of immune privilege in the cornea. Few of them include
    - programmed death-ligand 1 (PD-L1), which binds to the PD-1 receptor on T cells and induces their apoptosis or suppression (Jeon et al., 2018; L.-L. Wang et al., 2017);
    - complement inhibitor CD46, which prevents the activation of the complement system (Hori, 2008)
    - galectin-9, which induces apoptosis of Th1 and Th17 cells (Shimmura-Tomita et al., 2013).

These molecules are expressed by the corneal epithelium and endothelium and contribute to the suppression of immune responses.

3.4. Limbus

The limbus, meaning "border" in Latin, refers to the junction between the transparent cornea and opaque sclera in the eye This specialized structure is responsible for maintaining the homeostasis of the ocular surface and is involved in the regeneration of corneal epithelial cells. The limbus also contains stem cells that play a critical role in the maintenance and repair of the corneal epithelium (Thoft, 1989; Thoft et al., 1989; Van Buskirk & Michael, 1989).

3.4.1. Discovery of limbus

The discovery of the corneal limbus is not attributed to a specific individual, as its existence and characteristics have been observed and described by various researchers and anatomists over the course of history. Early descriptions of the limbus can be found in anatomical studies and observations by renowned scientists and anatomists throughout history, even in the 1600s. However, the limbus as a distinct anatomical structure was not specifically attributed to an individual discoverer. The limbus itself did not become a prominent focus of research and discovery until the 1980s, when its regenerative capacity and role in corneal stem cells were understood. This led to a surge of research interest in the limbus and its functions (Pellegrini et al., 1999; Schermer et al., 1986).

3.4.2. Limbus: Anatomy, Cell Composition, and their functions

The limbus, situated at the junction of the cornea and conjunctiva, plays a crucial role in maintaining corneal homeostasis and supporting regenerative processes. Comprised of specialized cell populations and unique anatomical structures, the limbus serves as a microenvironment for limbal stem cells (LSCs) and orchestrates the continuous renewal of the corneal epithelium and stroma (J. L. Funderburgh et al., 2016b; Li et al., 2007; Neil, 2020).

3.4.2.1. Limbal Stem Cells (LSCs):

- Located within structures such as limbal crypts or Palisades of Vogt, LSCs are responsible for the continuous regeneration of the corneal epithelium.
- LSCs possess self-renewal and differentiation capabilities, enabling them to replenish and repair the corneal epithelium throughout an individual's lifetime.
- These cells contribute to corneal homeostasis by maintaining a balance between cell proliferation and differentiation (O'Sullivan & Clynes, 2007).

3.4.2.2. Palisades of Vogt:

- The Palisades of Vogt are finger-like projections at the peripheral edge of the corneal epithelium.

- They were first reported in 1921 by a German ophthalmologist named Alfred Vogt.
- Serving as a reservoir for LSCs, these structures provide a specialized niche that supports the self-renewal and regeneration of corneal epithelial cells.
- The Palisades of Vogt are composed of basal, wing, and intermediate cells, each playing a distinct role in the maintenance and differentiation of LSCs (Goldberg & Bron, 1982).

3.4.2.3. Melanocytes:

- Melanocytes are present in the limbus and produce melanin, which provides photoprotection to LSCs and the corneal epithelium.
- By shielding LSCs from UV radiation and oxidative stress, melanocytes help maintain the viability and functionality of these critical stem cells (Dziasko et al., 2015a; Gonzalez et al., 2018a).

3.4.2.4. Immune Cells:

- The limbus harbors various immune cells, including Langerhans cells and dendritic cells.
- These immune cells play a vital role in immune surveillance, detecting and responding to pathogens or foreign antigens that may threaten ocular surface health.
- By modulating immune responses, these cells contribute to the maintenance of corneal homeostasis and protection against infections (Gonzalez et al., 2018b).

3.4.2.5. Stromal Cells:

- Supporting the structure of the limbus, stromal cells contribute to the organization and integrity of this microenvironment.
- Additionally, stromal cells may play a role in regulating the behavior of LSCs and the overall balance of corneal epithelial cell proliferation and differentiation (Espana et al., 2003).

3.4.2.6. Vascular Cells:

- Unlike the avascular cornea, the limbus is a vascularized region. Vascular cells within the limbus, such as blood vessels, provide essential nutrients and oxygen to the limbal cells, including LSCs, promoting their viability and function (Van Buskirk, 1989; Papas, 2003).

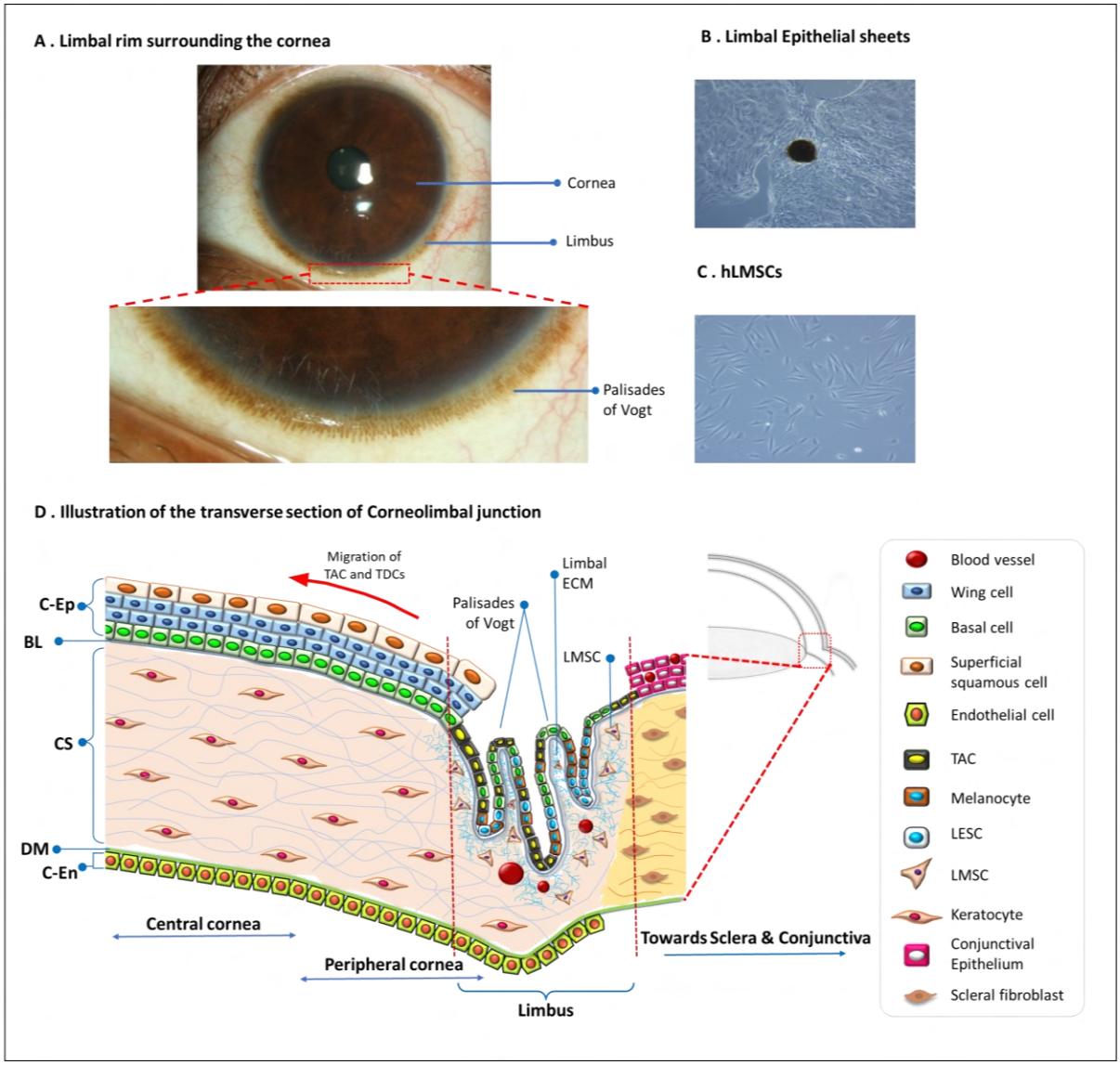

Figure 3.2: (A) Clinical image of the human eye showing the limbal rim surrounding the cornea, inset: magnified section of the limbal rim showing finger-like invaginations called palisades of Vogt. **(B-C)** Micro-photograph of the limbal epithelial stem cells and hLMSCs in a culture flask. **(D)** Illustration showing the anatomical and cellular arrangement in the corneolimbal junction. The hLMSCs are located in the stromal extracellular matrix beneath limbal basal membrane in the finger-like projections called Palisades of Vogt. The TACs (Transiently Amplifying Cells) and TDCs (Terminally Differentiated Cells) of corneal epithelia and stroma, derived and differentiated from the limbal progenitor cells move in centripetal direction towards the central cornea, replacing the dead or lost cells, for the maintenance of corneal layers. The illustration is shown for the representational purposes only, and does not proportionally specify or correlate to the actual dimensions of the corneal cells or layers. *C-Ep*: Corneal Epithelium; *BL*: Bowman's Layer; *CS*: Corneal Stroma; *DM*: Descemet's Membrane; C-En: Corneal Endothelium, *LESC*: Limbal Epithelial Stem Cell; *LMSC*: Limbus-derived Mesenchymal/Stromal stem cell.

3.4.3. Role of Limbus in homeostasis and maintenance of corneal (ocular) surface

1. The corneal limbus is a transitional zone between the cornea and the sclera, which is responsible for the homeostasis and maintenance of the corneal (ocular) surface. The limbus contains a population of stem cells known as limbal stem cells (LSCs), which are responsible for the continuous renewal of the corneal epithelium and maintenance of the corneal surface (Schlötzer-Schrehardt et al., 2007; Secker & Daniels, 2008; Dziasko et al., 2015b).
2. LSCs play a crucial role in maintaining the corneal surface by providing a constant supply of new corneal epithelial cells. These cells migrate centripetally from the limbus to the corneal surface, where they differentiate and replace older cells that have been shed from the surface (Thoft & Friend, 1983; Thoft, 1989; Thoft et al., 1989). The proper function of LSCs is essential for the maintenance of a healthy corneal epithelium and the prevention of ocular surface diseases such as corneal ulcers and limbal stem cell deficiency (Sangwan et al., 2006; Kolli et al., 2019)
3. The limbus also plays an important role in the immune privilege of the cornea, which is the unique ability of the cornea to avoid rejection by the body's immune system (Bray et al., 2014b). LSCs produce immunosuppressive factors that help to regulate the immune response in the cornea and maintain the immune privilege (Garfias et al., 2012a). For example, LSCs produce high levels of transforming growth factor-beta (TGF-β), which has been shown to have immunosuppressive effects and play a role in corneal wound healing (Joyce & Zieske, 1997).
4. Dysfunction of the limbus can result in limbal stem cell deficiency (LSCD), a condition characterized by the loss or dysfunction of LSCs and subsequent corneal surface defects. LSCD can lead to corneal scarring, neovascularization, and vision loss. Treatments for LSCD include limbal stem cell transplantation, which involves transplanting healthy LSCs from the patient's own eye or a donor eye to the affected eye (Sangwan et al., 2006; Gonzalez et al., 2018c; Kate & Basu, 2022).

3.4.4. Stem cells in Limbus: Types and their functions

3.4.4.1. Limbal Epithelial Stem Cells

Limbal epithelial stem cells (LESCs) were first discovered and identified in the early 1980s. These cells are responsible for renewing the corneal epithelium. They self-renew by asymmetric cell division, producing one stem cell and one transient amplifying cell. The transient amplifying cells

then migrate onto the corneal surface and differentiate into the various cell types that make up the corneal epithelium. Limbal stem cells play an important role in maintaining a healthy corneal surface and enabling corneal wound healing. Damage or loss of limbal stem cells can lead to limbal stem cell deficiency (LSCD), which impairs the cornea's ability to renew its epithelial cells. This can result in corneal opacity, neovascularization, and vision loss. Transplantation of limbal stem cells from a donor, has been shown to restore the stem cell population and regenerate the corneal epithelium in patients with limbal stem cell deficiency (Sharma & Coles, 1989; Secker & Daniels, 2008; Gonzalez et al., 2018c).

3.4.4.2. LESC – Side population cells and non-side population cells

Limbal epithelial stem cells (LESCs) can be categorized into two main types based on their ability to efflux the dye Hoechst 33342. The first type is called side population (SP) cells, which are capable of dye efflux and appear on the "side" of the fluorescence histogram. SP cells constitute approximately 1-5% of limbal epithelial cells. These cells possess distinct stem cell properties such as slow cycling, high clonogenicity, and notable differentiation potential, making them considered as more primitive stem cells (Umemoto et al., 2006). The second type is known as non-side population (NSP) cells, which are unable to efflux the Hoechst dye and appear in the main population on the fluorescence histogram. NSP cells make up the majority (95-99%) of limbal epithelial cells. In contrast to SP cells, NSP cells exhibit lower stem cell characteristics. They demonstrate lower expression of stem cell markers, faster cell cycling, reduced clonogenic and sphere-forming ability, and diminished differentiation potential, indicating a more differentiated progenitor cell population (Chang et al., 2011).

Both SP cells and NSP cells are capable of regenerating the corneal epithelium, although SP cells may be more effective due to their higher stemness. These cell populations represent distinct subsets within the LESC niche, with SP cells representing more primitive stem cells and NSP cells representing a progenitor cell population (Akinci et al., 2009).

3.4.4.3. Limbal Progenitor Cells

Limbal progenitor cells are a crucial population of epithelial stem cells and transient amplifying cells that reside in the basal layer of the limbus. Their primary role is to continuously renew and replenish the corneal epithelial cells. Limbal progenitor cells encompass both slow-cycling limbal epithelial stem cells and their fast-dividing progenitor daughters, collectively known as limbal

progenitor cells. The responsibility of limbal progenitor cells lies in the process of self-renewal and differentiation to sustain the corneal epithelium. Through asymmetric cell division, limbal epithelial stem cells give rise to two distinct cell types: one stem cell and one transient amplifying cell. Subsequently, the transient amplifying cells migrate onto the surface of the cornea and undergo differentiation, ultimately becoming corneal epithelial cells. While limbal progenitor cells express certain stem cell markers such as p63, ABCG2, and integrins, their expression levels are lower compared to LESCs. Damage or impairment to the limbal progenitor cells also leads to LSCD (S.-Y. Chen et al., 2011; Nieto-Miguel et al., 2011).

3.4.4.4. LSSCs – Discovery, location, function

Limbal stromal stem cells, residing within the stromal layer of the limbus, play a pivotal role in maintaining the integrity and replenishing the corneal stroma. Reported in early 2000s (Choong et al., 2007; Dominici et al., 2006; Du et al., 2005; M. L. Funderburgh et al., 2005), the functional properties and potential of these cells is since then being explored by various teams across the globe. The limbal stroma encompasses a specialized microenvironment, known as the niche, that supports the presence and function of these stem cells. Functionally, limbal stromal stem cells exhibit the remarkable ability to self-renew and differentiate into keratocytes, the primary cellular constituents of the corneal stroma. Keratocytes actively maintain the extracellular matrix of the corneal stroma, which is fundamentally crucial for maintaining corneal transparency (Choong et al., 2007; Mann et al., 2011; West-Mays & Dwivedi, 2006).

In response to corneal injury or wound healing, limbal stromal stem cells become activated, undergoing proliferation and differentiation into keratocytes. This regenerative process facilitates the restoration of the corneal stroma by replenishing the depleted population of keratocytes, ensuring its structural and functional integrity. Extensive research has revealed the distinctive stem cell properties of limbal stromal stem cells (Du et al., 2005; J. L. Funderburgh et al., 2016a; M. L. Funderburgh et al., 2005; Hertsenberg & Funderburgh, 2015), including their high clonogenic potential (Branch et al., 2012a; Du et al., 2005), and capacity for differentiation(Chang et al., 2011; Gonzalez et al., 2018d; Mann et al., 2011; Ghoubay et al., 2020). These cells express multiple specific markers/genes associated with stemness and proteins that contribute to the wound healing cascade (Kamil & Mohan, 2021a; Morgan et al., 2016; Weng et al., 2020; S. E. Wilson, 2020).

3.4.4.5. Interactions and Combined function/action of LESC-LSSC in regeneration and homeostasis of the cornea

Several studies have demonstrated that limbal epithelial stem cells and limbal stromal stem cells interact and support each other to enable corneal regeneration and wound healing. In the study by Kothwarapu et al. (2018), as well as independent studies by Dziasko et al., McKay et al., and other researchers, it was found that limbal stromal fibroblasts play a critical role in promoting the survival, proliferation, and differentiation of limbal epithelial stem cells during corneal wound healing through multiple factors and interactions with the extracellular matrix secreted (Dziasko et al., 2014; Kowtharapu et al., 2018; McKay et al., 2019). Similarly, in a study by Jabbehdari et al, it was reported that limbal stromal stem cells can differentiate into keratocytes that support the growth and differentiation of limbal epithelial stem cells. They showed that conditioned medium from limbal stromal stem cell-derived keratocytes promoted limbal epithelial stem cell proliferation and corneal epithelial differentiation(Jabbehdari et al., 2020). Higa *et al* also showed that limbal epithelial stem cells and limbal stromal fibroblasts communicate bidirectionally, with each cell type secreting factors (cadherins and aquaporins) that maintain the other (Higa et al., 2013). In their review, Di Girolamo et al (2015) discussed evidence that limbal epithelial stem cells and limbal stromal cells form an integrated functional unit that enables corneal regeneration, with factors secreted by both cell types regulating the behavior of the other to maintain corneal homeostasis (Di Girolamo, 2015).

Taken together, these studies demonstrate that limbal epithelial stem cells and limbal stromal stem cells interact through secreted factors to support each other's function, enabling them to renew the cornea and promote wound healing. The coordinated response of these limbal cell types, along with immune cells, allows for effective corneal wound healing.

3.5. The Big Ambiguity: CSSCs/Keratocytes/Keratinocytes/Limbal Peripheral cells/Limbal stromal stem cells

There seems to be some confusion and ambiguity around the terminology for various corneal stem cells, in the literature published over the last decade and a half. There seems to be some overlap and lack of standardization in the terminology used to describe various corneal stem cell populations. Corneal stromal stem cells (CSSCs) may refer either specifically to quiescent keratocytes or more broadly to any stromal stem cells.

Table 3.1 and **Figure 3.3** elucidate this ambiguity in detail.

Term	Description	Reference
Corneal stromal stem cells (CSSCs)	Refers broadly to any stem cells residing in the corneal stroma. It may specifically denote quiescent keratocytes with stem cell properties or other stromal stem cell populations.	(Pinnamaneni & Funderburgh, 2012)
Keratocytes	The main cell type residing in the corneal stroma. Traditionally considered static cells, but now recognized that a subset can act as stem cells (CSSCs) and give rise to new keratocytes.	(M. L. Funderburgh et al., 2005)
Keratinocytes	Epithelial cells producing keratin. Found in the skin, corneo-limbal epithelium, and eyelids, but not in the corneal stroma. Different from Keratocytes of cornea	(T. T. Sun & Green, 1977; Popova et al., 2006)
Peripheral Limbal (Stem) cells	Broadly refers to cells in the limbal region, the junction between the cornea and sclera. This includes limbal epithelial stem cells and other supporting cells.	(Branch et al., 2012b)
Limbal stromal stem cells	Some studies propose the existence of a distinct population of stem cells in the limbal stroma, separate from CSSCs. And some argue that CSSCs and limbal stromal stem cells may refer to the same population.	(Branch et al., 2012b; Rodríguez & Vecino, 2016)

Table 3.1: List of the types of cells, often mistaken to be limbal stem cells (stromal), and their description

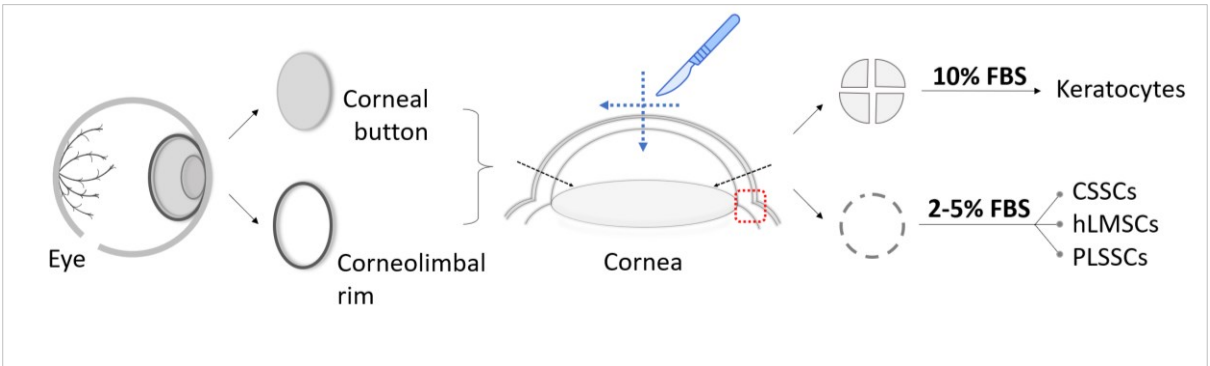

Figure 3.3: Illustration showing the cells types derived from the sources – corneal button and limbal tissues.

It is crucial to establish a precise understanding of the aforementioned cell types. In this chapter, the term "Keratocytes" specifically denotes the native cells present in the corneal button or those cultured from it, excluding any cells originating from the limbus. "Limbus-derived stromal stem cells" or CSSCs, on the other hand, are derived from the corneolimbal rims (**Figure 3.3**), as observed in the majority of studies. Therefore, for the purpose of clarity and consistency, it is advisable to consider these cells under a unified terminology. Thus, to address this population of stem cells, the term hLMSCs (human limbus-derived stromal/mesenchymal stem cells) is used throughout the study.

3.6. Corneal blindness and vision impairment: Etiology, incidence, and demographics

Corneal blindness and vision impairment are significant global health concerns that have a profound impact on individuals and communities. The cornea, being the transparent front part of the eye, plays a crucial role in focusing light onto the retina, enabling clear vision. However, various factors can lead to corneal diseases and conditions, resulting in vision loss or impairment. Understanding the etiology, incidence, and demographics of corneal blindness and vision impairment is essential for developing effective prevention strategies, improving access to treatment, and addressing the specific needs of affected populations.

3.6.1.1. Etiology:

- Trauma: Corneal trauma, such as abrasions, lacerations, or foreign body injuries, is a common cause of corneal pathologies and vision impairment (Kanski & Bowling, 2016).
- Infections: Bacterial, viral, fungal, or parasitic infections of the cornea can lead to a range of conditions, including corneal ulcers and scarring (Cabrera-Aguas et al., 2022).
- Inflammation: Inflammatory conditions such as uveitis or scleritis can affect the cornea and lead to vision loss (Duplechain et al., 2023).
- Dystrophies: Corneal dystrophies are a group of inherited disorders that affect the cornea and can lead to vision impairment, such as Fuchs' endothelial dystrophy or lattice dystrophy (Matthaei et al., 2019).
- Degeneration: Corneal degeneration can be caused by a range of factors, including aging, exposure to UV light, and systemic diseases such as diabetes (Golubović, 1994; Kamil & Mohan, 2021b).

3.6.1.2. Incidence and demographics:

The incidence and demographics of corneal pathologies and vision impairment can vary depending on the underlying cause. According to a study published by Mathews et al. (2018), globally, 4.9 million people suffer from corneal blindness, with the majority residing in low and middle-income countries (Mathews et al., 2018b). Cataracts were identified as the leading cause of blindness worldwide, followed by glaucoma, age-related macular degeneration, and diabetic retinopathy (Bourne et al., 2017). Additionally, a report by the World Health Organization (WHO) in 2019 stated that approximately 2.2 billion individuals worldwide have a vision impairment or blindness, with nearly 1 billion cases being preventable or treatable. Age was found to be a contributing factor, with older age groups having a higher incidence of vision impairment and blindness compared to younger age groups (Mathews et al., 2018b; *Vision Impairment and Blindness*, n.d.).

In India, corneal blindness is a significant concern. Vashist et al. (2022) reported that corneal causes accounted for ~10% of blindness in India, with the highest incidence observed in individuals aged 21-50 years (Vashist et al., 2022).

The incidence of corneal abrasion is higher among individuals of working age, with automotive workers between the ages of 20 and 29 years having the highest incidence of eye injuries. Furthermore, ocular chemical burns are considered emergencies and account for 11.5%–22.1% of all ocular injuries (Wong et al., 1998; Willmann et al., 2023).

When it comes to corneal damage, minor abrasions are typically healed by the resilient cornea itself. However, major corneal damage can lead to the formation of corneal scars. These scars can be caused by various factors, including the improper use of contact lenses, deep scratches, lacerations, burns, and certain diseases such as shingles and syphilis.

3.6.2. Corneal scarring: the underlying causes and mechanisms and factors

Corneal scarring is a common cause of visual impairment and is often a result of injury, infection, or inflammation. The scarring process involves the accumulation of extracellular matrix proteins, such as collagen, fibronectin, and laminin, in the corneal stroma, leading to the formation of fibrous tissue (Maurice, 1957). Several pathways and mechanisms have been implicated in corneal scarring, including oxidative stress, paracrine signaling, and inflammation (Fuest et al., 2023; S. Wilson, 2012). Reactive oxygen species and oxidative stress can lead to corneal endothelial cell death, reduce corneal thickness, and increase matrix metalloproteinase activity, which degrades tissue inhibitor of metalloproteinase-1 and promotes extracellular matrix remodeling (Nita & Grzybowski, 2016)

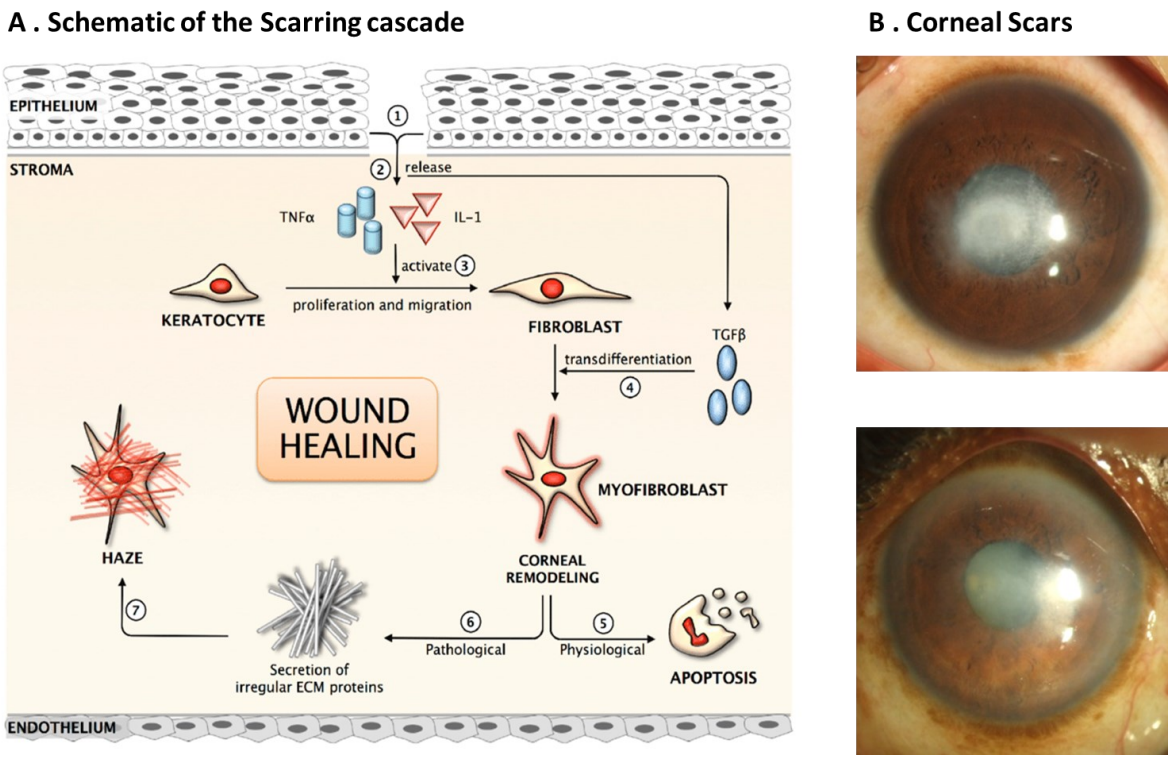

Figure 3.4: (A) Illustration (adapted) depicting the cascade of events after an injury to the ocular surface, that lead to formation of scarring (Chaurasia et al., 2015), **(B)** Collage of the clinical photographs showing the cloudy haze/scar in cornea.

Paracrine signaling pathways play a role in corneal scarring, whereby cytokines and growth factors produced by cells in the cornea and the immune system can trigger the activation of fibroblasts and myofibroblasts, leading to fibrogenesis and matrix deposition. Inflammation is also a critical component of corneal scarring, with pro-inflammatory cytokines such as IL-1β, TNF-α, and TGF-β playing a major role in the process by promoting cell activation, migration, and differentiation (S. Wilson, 2012; S. E. Wilson, 2020). When the cornea experiences significant abrasion, it can disrupt the basement and Bowman's membranes, leading to interactions between the epithelial and stromal layers of the cornea. This interaction triggers a complex wound-healing process (Chaurasia et al., 2015). Transforming growth factor-beta (TGF-β), in its active form, binds to the TGF-β type I/II receptor (TBRI/II) on the keratocyte plasma membrane, initiating a downstream SMAD-dependent signaling cascade. This cascade increases the expression of fibrotic genes, including matrix metalloproteinases (MMPs) and connective tissue growth factor (CTGF) (Joyce & Zieske, 1997).

3.6.3. Corneal scars, burns and trauma – management and treatment options

Corneal scars, burns, and trauma can have a profound impact on visual function, leading to significant visual impairment and decreased quality of life for affected individuals.

3.6.3.1. Diagnosis of corneal scarring:

The diagnosis of corneal scarring requires a meticulous evaluation, combining various ophthalmic examinations and corneal imaging techniques. Visual acuity assessment helps quantify the extent of visual impairment, while slit-lamp biomicroscopy allows for detailed examination of the cornea, revealing the presence, location, and characteristics of scars. Corneal imaging techniques, such as anterior segment optical coherence tomography (AS-OCT), provide high-resolution cross-sectional images of the cornea, aiding in the precise visualization and characterization of scars (McCally et al., 2007; K. C. Lee et al., 2019; Han et al., 2022).

3.6.3.2. Management and Treatment modalities

The management of corneal scarring involves a multidimensional approach that considers the severity and location of the scar, as well as the individual patient's specific circumstances. Surgical interventions play a pivotal role in addressing corneal scars that significantly affect vision. Deep anterior lamellar keratoplasty (DALK) and posterior lamellar keratoplasty (PLK) are two prominent surgical techniques used to treat deep stromal corneal abscesses and anterior stromal disorders causing scarring. These procedures involve the selective replacement of the affected corneal layers while preserving the healthy ones, thereby promoting better visual outcomes. On the other hand, penetrating keratoplasty (PK) involves the replacement of the entire cornea and may be considered for more extensive or centrally located scars. However, PK carries a higher risk of complications and graft rejection compared to DALK and PLK, leading to inferior long-term survival rates (Ljubimov & Saghizadeh, 2015a; Barrientez et al., 2019; Dang et al., 2022)

Topical management strategies also play a significant role in the treatment of corneal scarring. Medications such as anti-inflammatory agents, lubricants, and autologous serum eye drops have been employed to alleviate symptoms, reduce inflammation, and promote corneal healing. These approaches aim to improve visual acuity, reduce discomfort, and enhance the overall health of the cornea. Additionally, amniotic membrane transplantation combined with laser ablation has shown promise in corneal scar revision (Buzzonetti et al., 2012). This procedure involves the application of an amniotic membrane graft over the scarred cornea, facilitating tissue regeneration and reducing inflammation and scarring. Anterior segment optical coherence tomography (AS-OCT) is a valuable tool for evaluating the effectiveness of scar-based amniotic membrane transplantation in the treatment of corneal epithelial defects and scars. It allows for precise monitoring of the

healing process, graft integration, and the restoration of corneal architecture (Barrientez et al., 2019; Dang et al., 2022).

Advancements in surgical techniques and topical therapies continue to shape the management of corneal scarring. Ongoing research aims to refine existing procedures and explore novel treatment modalities to improve outcomes further. It is crucial to consider the individual characteristics of each patient's corneal scar, tailoring the treatment approach accordingly to achieve optimal visual rehabilitation and maximize the restoration of corneal integrity.

In summary, treatment options for corneal scars depend on factors such as the type, location, and severity of the scar. Current methods that are either in practice or being explored are listed down in **Table 3.2.**

Surgical Treatments		
Corneal Collagen Cross-Linking	Uses riboflavin eye drops and UV light to strengthen collagen fibers in the cornea and stabilize corneal scars, commonly used for keratoconus	(El-Raggal, 2009)
Surface Ablation	Procedures like phototherapeutic keratectomy (PTK) and laser epithelial keratomileusis (LASEK) remove outer corneal layers to smooth out superficial scars	(Deshmukh et al., 2020)
Intracorneal Ring Segments	Thin synthetic rings implanted into the cornea to reshape it and reduce the effects of scarring, particularly for keratoconus scars	(Zadnik et al., 2019)
Corneal Transplant	In severe cases where scarring significantly affects vision, a corneal transplant replaces the damaged cornea with donor tissue	(Ljubimov & Saghizadeh, 2015b; Kumar et al., 2021)
Amniotic Membrane Grafts	Grafts made from the amniotic membrane surrounding the fetus placed over the cornea to reduce inflammation, promote healing, and stabilize scars	(Mohammadi et al., 2017)
Molecular Methods		
Exosomes	Derived from stem cells, exosomes deliver antifibrotic proteins and microRNAs to modulate the signalling cascade involved in corneal scarring	(Ong et al., 2023)
Targeted Gene Silencing and MicroRNA Therapies	Manipulation of gene expression and microRNA activity to prevent corneal fibrosis and promote scarless regeneration	(Ghosh et al., 2022)

Bioactive Molecules, Biomolecules, and Nanomedicine	Development of therapies using bioactive molecules, biomolecules, and nanomedicine to prevent scarring and promote corneal regeneration	(Mahdavi et al., 2020)
Tissue Engineering	Utilizing scaffolds made from biocompatible materials to create an environment supporting the growth and differentiation of corneal cells	(B. Kong & Mi, 2016; C. Zhang et al., 2020; X. Zhang et al., 2012)
Stem Cell Therapy	Use of stem cells from various sources to replenish damaged corneal epithelial cells, promote regeneration, and improve visual acuity and ocular health	(Basu et al., 2019a)

Table 3.2. Surgical methods available to treat corneal pathologies – scars, trauma, burns etc.,

All these innovative approaches hold promise for the prevention and treatment of corneal scarring by promoting scarless healing, regenerating corneal tissue, and improving visual outcome.

Cell therapy offers promising prospects for the treatment of corneal scars and burns, with limbal stem cell therapy showing particular potential owing to the unique characteristics of limbal stromal stem cells. Numerous studies have demonstrated the efficacy of limbal stem cell transplantation, in restoring and regenerating the corneal epithelium and stroma. This therapeutic approach has shown the potential to enhance vision and alleviate symptoms associated with corneal scars, opacities. This effectiveness of limbal stem cell therapy can be attributed to the unique properties of limbal stromal stem cells, including their capacity for self-renewal, ability to differentiate into corneal cells, and capability to modulate the immune response. Exploring this avenue holds also promise for overcoming the challenges associated with donor scarcity and thus expanding the reach of limbal stem cell therapy.

3.7. The Promising Potential of hLMSCs in Corneal Regeneration

The hLMSCs hold significant promise for corneal wound healing and regeneration. Their differentiation potential enables them to differentiate into keratocytes, which are responsible for producing the corneal stromal matrix, thereby facilitating the replenishment of damaged corneal stroma after injury (S.-Y. Chen et al., 2011). Through their paracrine effects, hLMSCs secrete factors that promote corneal epithelial cell proliferation, wound healing, and anti-fibrosis, supporting corneal regeneration and restoration of transparency (J. L. Funderburgh et al., 2016b;

S. E. Wilson, 2020). Moreover, hLMSCs exhibit immunomodulatory properties by secreting cytokines and growth factors that suppress immune cell activation and inflammation, thereby regulating the microenvironment for optimal wound healing (Matthyssen, Van Den Bogerd, et al., 2018). As stem cells, hLMSCs can self-renew, ensuring a sustainable source of keratocytes to support long-term corneal regeneration. Additionally, their location in the limbal niche plays a crucial role in maintaining their stemness properties and allows them to modulate the limbal microenvironment (X.-N. Liu et al., 2021; Zhu et al., 2022a). To enhance their engraftment and functionality in the cornea, hLMSCs can be delivered using biomaterials such as scaffolds, hydrogels, and carriers (Di Girolamo, 2015). In conclusion, the combination of hLMSCs' differentiation potential, paracrine effects, immunomodulation, self-renewal, and strategic delivery techniques positions them as a promising cell source for corneal wound healing and regeneration therapies

3.7.1. Exploring the Promise of hLMSCs for Corneal Regeneration: From discovery to Therapeutic Applications

In the last 10-15 years, research on human limbal mesenchymal stem cells (hLMSCs) has yielded significant insights into their properties and therapeutic potential for corneal regeneration. Here is a summary of the key findings and developments during this period:

3.7.1.1. Discovery and Characterization:

- hLMSCs were first identified in the early 2000s based on their location in the limbal niche and expression of stem cell markers.
- They possess multilineage differentiation potential, resembling mesenchymal stem cells, and can differentiate into keratocytes, osteocytes, adipocytes, and chondrocytes (J. L. Funderburgh et al., 2016b).

3.7.1.2. Differentiation Potential:

- In vitro and in vivo studies have demonstrated that hLMSCs can differentiate into functional keratocytes, which contribute to the production of the stromal matrix and corneal transparency (Basu et al., 2014a; Branch et al., 2012b; Gonzalez et al., 2018d).
- They may also transdifferentiate into corneal epithelial cells, supporting corneal epithelial homeostasis and regeneration (Basu et al., 2014a).

3.7.1.3. Therapeutic Potential:

- hLMSCs have shown promise in corneal regeneration and repair applications.
- They can replenish corneal stromal cells by differentiating into keratocytes, aiding in the reconstruction of the corneal stromal matrix (Katikireddy et al., 2014; Kowtharapu et al., 2018; Mann et al., 2011; Zhu et al., 2022b).
- hLMSCs secrete factors that support corneal epithelial stem cells, inhibit fibrosis, and promote wound healing (Espana et al., 2003; Kowtharapu et al., 2018; Nili et al., 2019).
- These cells have immunomodulatory effects, suppressing immune cell activation and proliferation, which can be beneficial for corneal transplantation and immune-related ocular diseases (Bray et al., 2014b; Garfias et al., 2012b).
- Studies have demonstrated the wound healing potential of hLMSCs in animal models, where they have regenerated the corneal stroma and restored corneal transparency.

3.7.1.4. Advancements:

- Immortalized hLMSC lines have been generated, maintaining their differentiation potential and anti-inflammatory properties. This offers advantages for research purposes and potential therapeutic applications (Dos Santos et al., 2022).
- Culture conditions for expanding hLMSCs have been optimized, with xeno-free culture media supporting their expansion while preserving their stem cell properties. Encapsulating hLMSCs in hyaluronic acid hydrogel helps protect the cells and provide a suitable environment for their survival and function. This delivery system has shown promising results in promoting corneal wound healing and may be a potential vehicle for delivering hLMSCs in future therapeutic applications (Mörö et al., 2022).
- Specific microRNAs, such as miR-29a, have been identified in hLMSCs, which have anti-fibrotic effects and can be used for cell selection in corneal scarring therapy (Yam et al., 2023a).

Taken together, the above-mentioned studies have shown that hLMSCs can help corneal wounds heal by regenerating the corneal stroma and making the cornea clear again. Their ability to differentiate into keratocytes, modulate the limbal microenvironment, and secrete factors with anti-fibrotic and immunomodulatory effects make them promising candidates for future therapeutic interventions aimed at restoring corneal homeostasis and transparency. Further research and clinical trials are needed to fully understand the potential of hLMSCs and their delivery methods in treating corneal injuries and diseases.

Table 3.3 lists the additional evidences of major studies and reports for each characteristic property of the hLMSCs:

Clinical trials and efficacy studies	Successful use of a tissue-engineered allogeneic implant in severe keratitis patients	(Basu et al., 2019b; González-Gallardo et al., 2023; Jhanji et al., 2022)
Evidence of multipotency	hLMSCs possess self-renewal and multilineage differentiation potential.	(Branch et al., 2012a; Du et al., 2005; Pinnamaneni & Funderburgh, 2012)
Evidence of differentiation in keratocytes	hLMSCs can differentiate into keratocytes that produce stromal matrix.	(Hertsenberg & Funderburgh, 2015; Mann et al., 2011)
Evidence of epithelial support	Conditioned medium from hLMSCs promotes limbal epithelial stem cell proliferation and differentiation.	(Espana et al., 2003; Hashmani et al., 2013; Kowtharapu et al., 2018)
Evidence of corneal transparency restoration	Transplantation of hLMSCs helps restore corneal transparency in animal models.	(Basu et al., 2014b; Popova et al., 2006)
Evidence of scarless corneal wound healing	hLMSCs aid in corneal wound healing with minimal scarring.	(Di Girolamo, 2015; Weng et al., 2020)
Proof that they are anti-fibrotic	hLMSCs and their derivatives secrete factors that inhibit fibrosis and promote corneal transparency.	(Hertsenberg et al., 2017b; Matthyssen, Van den Bogerd, et al., 2018; Yam et al., 2023b)
Evidence of immunomodulatory properties	hLMSCs have an immunoregulatory nature that can control inflammation.	(Jhanji et al., 2021)

Table 3.3: Studies demonstrating the characteristic properties of hLMSCs and their therapeutic potential

3.8. hLMSCs for Clinical Use

To grasp the rationale behind rigorous quality studies conducted on hLMSCs, it is essential to explore the regulatory framework and its significance. This section examines the rules, guidelines, and the need to adhere to them in research of humans with focus on the field of stem cell research, highlighting their crucial role in ensuring safety, efficacy, and ethical conduct.

3.8.1. From National to Global: Navigating Regulatory Frameworks, Bodies and Agencies

Internationally, there are several regulatory bodies that oversee and enforce regulations related to clinical research and drug development. Here are some prominent regulatory bodies at the international and country-specific levels:

3.8.1.1. International Conference on Harmonisation of Technical Requirements for Registration of Pharmaceuticals for Human Use (ICH): ICH is a global organization that brings together regulatory authorities and the pharmaceutical industry to develop and promote harmonized guidelines for drug development, including guidelines for clinical trials.

3.8.1.2. European Medicines Agency (EMA): EMA is responsible for the evaluation and supervision of medicinal products in the European Union (EU). It provides regulatory guidance and oversees the authorization and post-authorization of drugs, including clinical trial oversight.

3.8.1.3. Food and Drug Administration (FDA): FDA is the regulatory body responsible for ensuring the safety and efficacy of drugs and medical devices in the United States. It sets guidelines and regulations for clinical trials conducted in the U.S and majorly affects the guidelines framed by various countries across the world.

Some notable country-specific regulatory bodies include the *Pharmaceuticals and Medical Devices Agency* (PMDA) in Japan, the *Therapeutic Goods Administration* (TGA) in Australia, the *Health Products Regulatory Authority* (HPRA) in Ireland, and *Health Canada* in Canada. These regulatory bodies play a crucial role in setting guidelines, evaluating drug safety and efficacy, and ensuring compliance with regulatory standards in their respective countries.

In India, the rules and guidelines governing research on human subjects are primarily governed by the following regulatory bodies:

3.8.1.4. Indian Council of Medical Research (ICMR): ICMR is the apex body in India for the formulation, coordination, and promotion of biomedical research. It plays a crucial role in formulating guidelines, policies, and ethical standards for clinical research.

ICMR provides support for research activities, promotes ethical conduct, and oversees the functioning of research institutions and ethics committees (*Guidelines | Indian Council of Medical Research | Government of India*, n.d.).

3.8.1.5. Central Drugs Standard Control Organization (CDSCO): CDSCO is the national regulatory authority for pharmaceuticals and medical devices in India. It operates under the Directorate General of Health Services, Ministry of Health and Family Welfare. CDSCO is responsible for the approval, regulation, and quality control of drugs and medical devices in India. It ensures compliance with regulatory requirements, monitors clinical trials, and grants permissions for conducting research (*Acts & Rules*, n.d.).

3.8.1.6. Drugs Controller General of India (DCGI): DCGI is the head of CDSCO and holds the highest regulatory authority for drug approvals and clinical research in India. DCGI is responsible for the overall control and regulation of pharmaceuticals and clinical trials. It grants permissions for clinical trials, assesses study protocols, monitors trial conduct, and ensures compliance with ethical and regulatory guidelines (*Who's Who*, n.d.).

ICMR, CDSCO, and DCGI are interconnected entities and work in collaboration to regulate and control clinical research in India. While ICMR focuses on the formulation of research policies and ethical guidelines, CDSCO and DCGI are responsible for the regulatory oversight, approval, and monitoring of clinical trials to ensure participant safety and compliance with applicable regulations and standards.

In addition to national regulatory governing bodies, states also establish their own regulatory bodies to oversee and enforce drug-related laws and standards. Telangana, for instance, has the *Drug Control Administration* (DCA), which plays a pivotal role in ensuring the safety, quality, and efficacy of drugs within the state. It is responsible for the enforcement of drug-related laws, regulations, and standards. The DCA conducts inspections, grants licenses, and monitors the manufacturing, distribution, and sale of pharmaceutical products. Additionally, it takes measures to prevent the circulation of counterfeit drugs, promotes public awareness on drug safety, and addresses complaints related to drug quality and availability (*DRUGS CONTROL ADMINISTRATION*, n.d.).

At the institutional level, clinical research, with stem cells in focus, is typically regulated and overseen by various entities, including:

3.8.1.7. Institutional Review Boards (IRBs) or Research Ethics Committees (RECs): These are local committees responsible for reviewing and approving research

protocols to ensure the protection of human subjects. IRBs/RECs assess the scientific validity, ethical soundness, and participant safety of research studies conducted within an institution.

3.8.1.8. Institutional Policies and Procedures: Institutions develop their own internal policies and procedures to govern research activities. These policies ensure that researchers and staff are aware of their responsibilities, guidelines, and procedures related to conducting ethical and compliant research.

3.8.1.9. The Institutional Committee for Stem Cell Research (IC-SCR): The IC-SCR serves a crucial role in overseeing and regulating stem cell research within institutions. Its primary purpose is to ensure ethical and scientific integrity in all aspects of stem cell research conducted within the institution. The IC-SCR reviews research proposals, monitors ongoing studies, and ensures compliance with national and international guidelines and regulations. IC-SCR promotes responsible and transparent stem cell research while safeguarding the rights and welfare of participants.

3.8.2. Major Regulatory rules and Guidelines in India.

In India, regulatory compliance and guidelines for various sectors, including clinical research, are enforced under several major rules and acts.

3.8.2.1. Drugs and Cosmetics Act, 1940: This act regulates the import, manufacture, distribution, and sale of drugs and cosmetics in India. It establishes guidelines for the quality, safety, and efficacy of drugs and cosmetics, including regulations for clinical trials (*2016DrugsandCosmeticsAct1940Rules1945.Pdf*, n.d.-a).

3.8.2.2. Schedule Y: Schedule Y is a part of the Drugs and Cosmetics Rules, 1945. It provides detailed guidelines and requirements for conducting clinical trials in India. It covers aspects such as study design, informed consent, ethical considerations, reporting requirements, and safety monitoring (*Schedule Y(Ammended Version) - CDSCO*, n.d.-b).

3.8.2.3. New Drugs and Clinical Trials Rules, 2019: These rules replaced the earlier rules of 1945 and brought significant changes to the regulation of clinical trials in India. They outline the regulatory requirements for conducting clinical trials, including the approval process, responsibilities of stakeholders, compensation, and post-trial obligations (*NewDrugs_CTRules_2019.Pdf*, n.d.-a).

3.8.2.4. Indian Council of Medical Research (ICMR) Ethical Guidelines: ICMR has formulated ethical guidelines for biomedical research involving human participants. These guidelines provide comprehensive ethical considerations and standards for

conducting research, including clinical trials (*ICMR_National_Ethical_Guidelines.Pdf*, n.d.)

3.8.2.5. Good Clinical Practice (GCP) Guidelines: GCP guidelines provide internationally accepted ethical and scientific standards for designing, conducting, recording, and reporting clinical trials. In India, adherence to GCP guidelines is mandatory for conducting clinical trials (*Good-Clinical-Practice-Guideline.Pdf*, n.d.)

Additionally, irrespective of the country-specific regulations for carrying out research related to human subjects/samples, this one set of rules, are followed by every researcher working in this area.

3.8.2.6. Declaration of Helsinki: The Declaration of Helsinki, developed by the World Medical Association, is a set of ethical principles for medical research involving human subjects. It provides guidance on issues such as informed consent, risk-benefit assessment, and participant rights (*WMA Declaration of Helsinki – Ethical Principles for Medical Research Involving Human Subjects – WMA – The World Medical Association*, n.d.).

All these regulations and guidelines play a crucial role in ensuring regulatory compliance, ethical conduct, participant safety, and the overall quality of clinical research in India. It is important for investigators, sponsors, and other stakeholders to familiarize themselves with these regulations and adhere to them during the planning and conduct of clinical trials and research.

3.8.3. Ethical Considerations in Research with Human Subjects

Regulatory frameworks play a critical role in ensuring the appropriate oversight and governance of clinical trials and research involving human subjects and are imperative due to a multitude of reasons, which include:

3.8.3.1. Protection of Human Rights: The Nuremberg Code, established after World War II, laid the foundation for ethical considerations in human research, emphasizing the importance of voluntary consent and the prohibition of experiments where death or disabling injury is expected. The Declaration of Helsinki further expanded these principles, emphasizing the need for protocols to be reviewed by an independent committee. These principles are designed to protect the rights, dignity, autonomy, and welfare of research participants. This includes ensuring informed consent, maintaining

confidentiality (Commissioner, 2020), respecting the autonomy of the subjects, etc., (Group, 1996; W & Al-Sayed, 2018).

3.8.3.2. Scientific Validity: The validity of a study is the degree to which it accurately answers the question it was intended to answer. Without scientific validity, the results of a study could be misleading or incorrect. Regulations ensure that the study design, data collection, and analysis are appropriate and rigorous, and that the results are reliable and can be generalized to a larger population (Hulley, 2013; W & Al-Sayed, 2018).

3.8.3.3. Risk-Benefit Assessment: Before a clinical trial can begin, the potential benefits must be weighed against the potential risks. This includes considering the severity and likelihood of potential harms, the potential for benefit, and the availability of alternative treatments. The goal is to ensure that the potential benefits justify the risks, and that unnecessary harm is not inflicted on participants (W & Al-Sayed, 2018).

3.8.3.4. Avoidance of Exploitation: Vulnerable populations, such as children, pregnant women, prisoners, and economically disadvantaged individuals (Dal-Ré et al., 2016), may be at greater risk of exploitation in research. Regulations help to ensure that these populations are not unduly burdened by research, that their participation is truly voluntary, and that they are not exposed to unnecessary risks (Institute of Medicine (US) Committee on Ethical Considerations for Revisions to DHHS Regulations for Protection of Prisoners Involved in Research, 2007).

3.8.3.5. Transparency and Accountability: Transparency in research involves openly sharing information about the study design, methods, results, and funding. Accountability involves taking responsibility for the conduct and outcomes of the research. Regulations promote both transparency and accountability, helping to prevent misconduct and bias, and ensuring that the results of research can be trusted (Nosek et al., 2015).

3.8.3.6. Ensuring Informed Consent: Informed consent is a process in which a participant is informed about all aspects of the trial, including its purpose, duration, required procedures, and key contacts. Risks and potential benefits, and the right to refuse to participate or to withdraw from the research at any time, without reprisal, are also explained. Regulations ensure that this process is carried out thoroughly and ethically and that subjects are fully informed about the research and that their participation is voluntary (Nishimura et al., 2013).

3.8.3.7. Quality Control and Assurance: Quality control and assurance involve systematic activities implemented in a quality system to ensure that the requirements for a product

or service are fulfilled. In the context of clinical trials, this includes ensuring that the study is conducted and data are generated, documented, and reported in compliance with Good Clinical Practice (GCP) and the applicable regulatory requirements (Al Balooshi et al., 2003; Badrick, 2021).

3.8.4. The Significance of Regulatory Compliance: Advantages for Investigators and Participants in Clinical Research

Regulatory compliance plays a vital role in clinical research, ensuring the ethical conduct of studies and the protection of participants' rights and welfare. By establishing rules and guidelines, regulatory bodies aim to maintain the integrity, reliability, and safety of clinical trials. While the primary focus is on patient safety, regulatory compliance also offers significant advantages to both investigators and participants involved in clinical research.

3.8.4.1. Benefits to Investigators:

- **Guidance and Standardization:** Regulations provide a clear framework and guidelines for investigators to follow, ensuring that all research is conducted to the same high standards. This helps to maintain the integrity and quality of the research (*GUIDELINE FOR GOOD CLINICAL PRACTICE*, n.d.; Saxena & Saxena, 2014).
- **Risk Management:** Investigators can mitigate potential legal and ethical risks associated with conducting clinical trials by ensuring informed consent, protecting participant confidentiality, and conducting a thorough risk-benefit analysis (Sanmukhani & Tripathi, 2011)
- **Credibility and Trust:** Compliance with regulations can enhance the credibility of the research and the trustworthiness of the investigators, which can facilitate recruitment of participants and collaboration with other researchers. (Hocevar et al., 2017; Kerasidou, 2017).
- **Facilitating International Collaboration and Global Harmonization:** Regulations help establish common standards and guidelines for clinical research across countries, facilitating international collaboration and harmonization of research practices. This allows for the exchange of knowledge, resources, and expertise, leading to more efficient and effective research outcomes.

3.8.4.2. Benefits to Patients or Participants:

- **Protection of Rights and Welfare:** Regulations protect the rights, safety, and well-being of research participants by ensuring informed consent, maintaining confidentiality, and respecting the autonomy of the subjects (Group, 1996; Koonrungsesomboon & Karbwang, 2016)

- **Informed Decision-Making:** The requirement for informed consent ensures that participants have all the information they need to make an informed decision about whether to participate in the research. This includes information about the purpose of the research, the procedures involved, the potential risks and benefits, and the participant's rights (U. C. Gupta, 2013).
- **Risk Mitigation:** Regulations require that the potential benefits of the research outweigh the risks to the participants. This is achieved through a thorough evaluation of the potential harms and benefits of the research, and a determination that the research is justified (Pignatti et al., 2015).
- **Transparency:** Regulations promote transparency in research, which allows participants to understand the research process and the results of the research. This includes requirements for registration of clinical trials, reporting of results, and disclosure of conflicts of interest (Joshi & Bhardwaj, 2018; Nosek et al., 2015).

3.8.5. Balancing the *Potential* and the *Ethics*: The Need for Regulation in Stem Cell Research

The field of stem cell research is characterized by its immense medical potential and the ethical considerations it raises. Stem cells possess the remarkable ability to differentiate into various cell types, offering promising prospects for groundbreaking advancements in medicine. However, given the ethical implications and potential risks associated with stem cell research and therapy, there is a strong emphasis on regulatory compliance. Stringent regulations have been established to ensure responsible and safe practices within the field. These regulations aim to create an environment that fosters accountability and upholds ethical standards in stem cell research.

In the Indian context, the ICMR and the Department of Biotechnology (DBT) play crucial roles in providing guidelines and overseeing regulatory compliance in stem cell research and therapy. Through their efforts, regulatory bodies aim to balance the potential benefits of stem cell research with the need for ethical and safe practices, ensuring the field progresses in a responsible manner. Few factors which necessaire the regulations in this field are outlined hereunder:

3.8.5.1. Ethical Considerations: Stem cell research, particularly when it involves human embryonic stem cells, raises significant ethical issues, right from their derivation or collection, to their end use and the fate of these cells after successful transplantation to the patients or subjects. Regulations are needed to ensure that the research is

conducted ethically, respecting the dignity and rights of donors, and that the benefits of the research outweigh the ethical concerns (Hyun, 2010; Lo & Parham, 2009)

3.8.5.2. **Safety and Efficacy:** Stem cell therapies have the potential to treat a wide range of diseases, but they also carry risks, such as the potential for uncontrolled growth or differentiation, depending on the type and origin of cells. Regulations ensure that stem cell therapies are thoroughly tested for safety and efficacy before they are approved for use in patients (Menasché et al., 2015; Research, 2020).

3.8.5.3. **Quality Control:** Regulations ensure that stem cells are collected, processed, stored, and used in a manner that maintains their quality and safety. This includes requirements for sterility, identity, purity, and potency. The purity of the stem cell populations without any contamination of other sorts, is necessary to avoid the risks of cell differentiation (Andrews et al., 2015; Menasché et al., 2015; *StemBook*, 2008)

Regulating stem cell research contributes to achieving the above factors and also ensures the responsible and ethical practices in the field, with respect to the informed consent (King & Perrin, 2014), the accountability for wrongful doings and supervision (Scott & Magnus, 2014) and the transparency of the entire study procedures and outcomes .

3.8.6. Pre-requisites for *in-vivo* and *in-vitro* analyses before translating stem cell research

The New Drugs and Clinical Trials Rules (NDCT), 2019, have specific provisions for stem cell research and therapy. These rules classify stem cell-based products under the category of "new drugs", thus mandating regulatory oversight.

According to the NDCT Rules, 2019, any stem cell-based product intended for clinical use must undergo rigorous pre-clinical and clinical testing to ensure its safety and efficacy. The pre-clinical tests include in vitro and in vivo studies, while the clinical trials are conducted in four phases:

1. **Phase I** *(Safety/Pharmacokinetic Study):* Small-scale study to assess safety, dosage range, and side effects in healthy individuals.
2. **Phase II** *(Exploratory Study):* Larger-scale study to evaluate effectiveness and safety of the drug.
3. **Phase III** *(Confirmatory Study)*: Extensive study to confirm effectiveness, compare to existing treatments, and gather safety information.

4. **Phase IV** *(Post Marketing Surveillance Study)*: To gather additional data on risks, benefits, and optimal use of the drug.

For stem cell-based therapies, the NDCT Rules, 2019, also mandate that the stem cells must be processed as minimally as possible, without altering their original biological characteristics. If the cells are extensively manipulated or combined with a biomaterial, the product is considered a "drug-biological-device combination" and is subject to additional regulations.

It's important to note that these rules are in line with the guidelines issued by the Indian Council of Medical Research (ICMR) and the Department of Biotechnology (DBT) in 2017, which also emphasize the need for rigorous testing and ethical considerations in stem cell research and therapy. And *no investigative drug/ cell-based product can be used in clinical trials without prior approval* (Lahiry et al., 2019; *India's New Drugs and Clinical Trials Rules*, n.d.)

In the context of cell-based therapeutics, pre-clinical tests are crucial to assess the safety, efficacy, and biological activity of the therapeutic cells. In the Indian context, these tests would be guided by the New Drugs and Clinical Trials Rules, 2019, and the ICMR-DBT National Guidelines for Stem Cell Research, 2017. However, depending on the case-to-case criteria, some tests may be exempted and/or additional tests may be insisted, at the discretion of the governing authority, here DCGI. The tests generally performed include:

3.8.6.1. In vitro tests:

- **Cell characterization**: This involves confirming the identity of the cells (e.g., through genetic markers), their purity (absence of unwanted cell types), and their potency (ability to perform their intended function). This is typically done using techniques like flow cytometry, immunocytochemistry, or gene expression analysis.
- **Sterility testing**: This is done to ensure that the cell product is free from contamination by bacteria, fungi, or viruses. This is typically done using culture-based methods or molecular techniques like PCR.
- **Karyotyping or other genetic stability tests**: These tests are done to ensure that the cells have not undergone any harmful genetic changes during culture. This can be done using traditional karyotyping, or more advanced techniques like comparative genomic hybridization or next-generation sequencing.

- **Tumorigenicity tests**: These are performed to ensure that the cells do not form tumors when cultured *in vitro*. This can be done using soft agar colony formation assays or other similar methods.

3.8.6.2. In vivo tests:

- **Biodistribution studies**: These studies are done to determine where the cells go in the body after administration. This is typically done in animal models, and involves labeling the cells with a tracer that can be detected using imaging techniques like Positron Emission Tomography (PET) or Magnetic Resonance Imaging (MRI) (Ding & Wu, 2012)
- **Tumorigenicity studies**: These studies are done to ensure that the cells do not form tumors when administered to animals. This involves injecting the cells into animals and monitoring them for the formation of tumors over a certain period of time.
- **Toxicity studies**: These studies are done to assess the safety of the cells when administered at different doses and monitoring for any adverse effects.
- **Efficacy studies:** These studies are done to assess whether the cells have the desired therapeutic effect in an appropriate animal model of the disease. The specifics of this test would depend on the disease that the therapy is intended to treat.

3.8.7. Guidelines for pre-clinical (animal) studies

In India, the pre-requisites for performing *in vivo* toxicity and efficacy studies in animal models are regulated by the **Committee for Control and Supervision of Experiments on Animals** (CCSEA), [previously, *Committee for the Purpose of Control and Supervision of Experiments on Animals* (CPCSEA)], under the Ministry of Fisheries, Animal Husbandry and Dairying. They include:

1. **Animals and Species:** The choice of animal species depends on the specific study. Commonly used species include mice, rats, rabbits, and guinea pigs. The number of animals used should be the minimum necessary to achieve valid results and depends on the study design.
2. **GLP or GMP:** Good Laboratory Practice (GLP) is required for these studies. GLP ensures the quality and integrity of the test data. Good Manufacturing Practice (GMP) may or may not be directly related to in vivo testing but is a system for ensuring that products are consistently produced and controlled according to quality standards.
3. **Ethical Approval:** Any institution planning to conduct animal experiments must obtain prior approval from the Institutional Animal Ethics Committee (IAEC), which operates under the guidelines of the CPCSEA.
4. **Facility Accreditation:** The test facility should be registered with the CPCSEA.

Globally, there are several guidelines and regulations for animal testing which include the **OECD** Guidelines for the Testing of Chemicals, the International Council for Harmonisation of Technical Requirements for Pharmaceuticals for Human Use (**ICH**) Guidelines, the International Organization for Standardization (**ISO**) guidelines, and the **Three Rs principle**, which stands for *Replacement, Reduction, and Refinement.* All these guidelines ensure the ethical treatment of animals involved in scientific research, promote the responsible use of animals, and minimize their suffering.

However, in the experimental design of the current study involving hLMSCs, these guidelines were followed, in major.

1. **OECD Guidelines for the Testing of Chemicals:** The Organisation for Economic Co-operation and Development (OECD) has developed international guidelines for testing of chemicals, which include several test methods using animals. These guidelines are used by government, industry and independent laboratories to assess the safety of chemical substances.

2. **The ARVO (Association for Research in Vision and Ophthalmology) Statement for the Use of Animals in Ophthalmic and Vision Research:** The key principles of the ARVO statement include:

a. *Justification of Research*: Research must have significant benefits and scientifically valid design.
b. *Personnel:* Qualified and trained personnel are responsible for animal care and use.
c. *Veterinary Care:* Adequate veterinary care, regular consultation with attending veterinarian.
d. *Animal Well-being:* Prioritizing animal well-being through proper housing, feeding, and pain management.
e. *Minimization of Animal Use:* Minimizing the number of animals used through study design and sharing of tissues.
f. *Committee Review:* Research involving animals must be approved by an animal care and use committee

3.8.8. CDSCO-NDCT Rules and ICMR Mandate for GMP standardization and Testing

NDCT rules outline the requirements for GMP manufacturing protocols and GLP toxicity study protocols to ensure the quality, safety, and efficacy of drugs (*NewDrugs_CTRules_2019.Pdf*, n.d.-a).

The GMP are guidelines that provide a system of processes, procedures, and documentation to assure a product has the identity, strength, composition, quality, and purity that it is represented to possess. In the context of stem cell research and therapy, GMP guidelines ensure that stem cells are produced and handled in a way that meets the standards of quality, stability and safety (Aghayan et al., 2015; Jose et al., 2020; Sullivan et al., 2018).

In India, the Central Drugs Standard Control Organization (CDSCO) is responsible for enforcing GMP guidelines. These guidelines mandate that all aspects of the manufacturing process, from the initial procurement of raw materials to the final packaging of the product, are conducted in a controlled environment that minimizes the risk of contamination or errors. This includes rigorous testing of the product at various stages of production, as well as thorough documentation of all procedures and results (George, 2011; Viswanathan et al., 2013).

Internationally, GMP guidelines are enforced by various regulatory bodies, such as the FDA, in Title 21 of the Code of Federal Regulations (*CFR - Code of Federal Regulations Title 21*, n.d.-b; Sensebé et al., 2013) or the EMA (Gouveia et al., 2015b), for cell-based research. These guidelines are broadly similar to those in India, although there may be some differences in specific requirements.

3.8.9. Role of GMP Guidelines in Research and Clinical Trials

The GMP guidelines play a crucial role in both laboratory research, right from the development of the process to the end use (*Does GMP Apply to Development? - ECA Academy*, n.d.); and in human trials ensuring the quality and reliability of the investigational medicinal products (*Medicines*, n.d.). The guidelines have a significant impact, greatly benefitting various factors (Gouveia et al., 2015b) including:

1. **Quality Assurance:** GMP guidelines ensure that products are consistently produced and controlled according to quality standards. This is crucial in research and development (R&D) as it ensures the reliability and reproducibility of experimental results.
2. **Risk Minimization:** GMP is designed to minimize the risks involved in any pharmaceutical production that cannot be eliminated through testing the final product. This includes risks such as unexpected contamination of products, incorrect labels on containers, and variations in the active ingredient amount. In the context of research, this helps to prevent experimental errors and inaccuracies.
3. **Process Validation:** GMP guidelines cover the development, validation, control and transfer of manufacturing processes and analytical procedures. This is particularly important in R&D, where new processes and procedures are often developed. GMP ensures these are validated, meaning they are checked for accuracy and consistency.
4. **Regulatory Compliance:** Compliance with GMP guidelines is often a prerequisite for regulatory approval of clinical trials in humans. This ensures that the investigational medicinal products (IMPs) used in these trials are of high quality and have been produced in a controlled environment.
5. **Patient Safety:** In human trials, GMP ensures that the medicines used are safe and effective. This is achieved by enforcing strict quality control and manufacturing standards, thereby protecting trial participants from potential harm.
6. **Documentation:** GMP requires detailed written procedures for each process and systems – production, distribution, and quality control, to provide documented proof that correct procedures are consistently followed. This is crucial in research and human trials where accurate record-keeping is essential.
7. **Traceability:** Traceability refers to the ability to track and document the movement of raw materials, intermediates, and finished products throughout the manufacturing process. By implementing GMP standards, pharmaceutical companies can establish robust documentation systems, including batch records and product labelling, which enable accurate traceability of each stage of production

8. **Self-inspection:** GMP guidelines emphasize the importance of self-inspection or internal audits. Self-inspection involves a systematic evaluation of a company's manufacturing operations to identify areas of non-compliance and potential risks. Self-inspection also enables companies to proactively address any issues, implement corrective actions, and continuously improve their manufacturing practices

In additional to above, three other key aspects or specific requirements that can vary depending on the type of product being manufactured (Patel & Chotai, 2011), which are:

9. **Premises and Equipment:** The manufacturing premises must be designed, constructed, disinfected and maintained to prevent contamination and errors. Equipment must be appropriately designed, cleaned, and maintained.
10. **Personnel:** All personnel involved in manufacturing must have the necessary qualifications, skills, and training. They should also follow strict hygiene guidelines, and should be trained periodically.
11. **Product Recall:** There should be a system in place for recalling defective products from the market.

3.8.10. Tests performed in Characterization, Safety and Efficacy Studies of biologics

3.8.10.1. Characterization:

Immunohistochemistry or immunostaining techniques are commonly used to analyze the expression and localization of specific proteins or markers in cells or tissues. Flow cytometry (FACS) allows for the identification and quantification of different cell populations based on surface markers. Gene analysis methods, such as PCR or microarray analysis, provide insights into the genetic profile of cells or tissues. Stability studies involve karyotyping to assess chromosomal stability, while sterility testing examines the absence of mycoplasma, endotoxins, and microbial contamination (bacteria and fungi).

1. **Immunostaining (Immunohistochemistry):** Immunostaining, also known as immunohistochemistry, is a technique used to visualize specific proteins or antigens in cells or tissues. It involves the use of antibodies that bind to the target protein, followed by the addition of a detection system that produces a visible signal, such as a coloured dye or fluorescent marker. This technique allows researchers to examine the localization and distribution of proteins within cells or tissues, providing valuable information about their expression patterns.

2. **Flow Cytometry (FACS):** Flow cytometry, or fluorescence-activated cell sorting (FACS), is a powerful method used to analyze and sort individual cells based on their physical and chemical properties. It utilizes fluorescently-labelled antibodies or dyes to label specific cell surface markers or intracellular molecules. The labelled cells are then passed through a flow cytometer, which measures the emitted fluorescence and provides quantitative data about the different cell populations present in a sample. FACS is widely used for cell characterization, cell sorting, and analyzing various cellular parameters.
3. **Polymerase Chain Reaction (PCR):** Polymerase chain reaction (PCR) is a widely used technique in molecular biology that amplifies specific DNA sequences. It involves a series of temperature cycles to denature the DNA, allow primers to anneal to the target sequence, and then amplify the desired DNA region using a DNA polymerase enzyme. PCR allows researchers to generate multiple copies of a specific DNA fragment, enabling various downstream applications such as gene expression analysis, mutation detection, and DNA sequencing.
4. **Karyotyping:** Karyotyping is a cytogenetic technique used to analyze the number, structure, and arrangement of chromosomes in a cell. It involves staining and visualizing the chromosomes under a microscope, typically from cells arrested in metaphase. By examining the size, banding pattern, and overall morphology of the chromosomes, karyotyping can detect chromosomal abnormalities, such as aneuploidy (abnormal chromosome number) or structural rearrangements. This technique is commonly used in genetic research, clinical diagnostics, and reproductive medicine.
5. **Mycoplasma Testing:** Mycoplasma testing is performed to determine the presence or absence of mycoplasma contamination in cell cultures. Mycoplasmas are bacteria-like microorganisms that can infect cell lines, leading to potential changes in cellular behavior and experimental outcomes. Different methods, such as PCR-based assays or microbial culture, can be employed for mycoplasma detection, ensuring the integrity and reliability of cell-based experiments.
6. **Endotoxin Testing:** Endotoxin testing is conducted to assess the presence of bacterial endotoxins, primarily derived from the outer membrane of gram-negative bacteria. Endotoxins can cause adverse effects in biological systems, triggering inflammatory responses and influencing experimental results. The Limulus Amebocyte Lysate (LAL) assay, derived from horseshoe crab blood, is the most common method used for endotoxin detection and quantification in pharmaceutical, biomedical, and research settings.

7. **Microbial Methods:** Microbial methods involve the identification and quantification of microbial contaminants, including bacteria and fungi, to ensure the sterility and safety of samples or products. Various techniques such as microbial culture, molecular methods (e.g., PCR), or next-generation sequencing (NGS) can be utilized for microbial analysis. These methods help detect and identify specific microorganisms, assess microbial load, and evaluate the effectiveness of sterilization processes in research, pharmaceutical, and clinical settings.

3.8.10.2. Safety studies

Safety studies are conducted using various approaches to assess the potential risks and adverse effects of an intervention. These studies can be performed in both in vivo (within a living organism) and in vitro (in a controlled laboratory environment) settings, depending on the nature of the intervention and the research objectives. The selection of the appropriate safety assessment mode or model depends on the research objectives, feasibility, ethical considerations, and regulatory requirements. Often, a combination of in vivo, in vitro, and computational approaches is utilized to comprehensively evaluate the safety profile of an intervention before further development or clinical trials. Here are some common modes or models used in safety studies:

1. **In vivo studies**: These studies involve testing the intervention in living organisms, such as animals (e.g., rodents, non-human primates) or human subjects. The chosen animal models should have similarities to humans in terms of physiological, anatomical, and genetic characteristics to provide relevant safety data.
2. **In vitro studies**: These studies are conducted using isolated cells, tissues, or organ systems outside of a living organism. In vitro models allow researchers to investigate the direct effects of the intervention on specific cellular or molecular targets without the complexities associated with whole organisms.
3. **Animal models:** Animals are often used in safety studies to evaluate the effects of the intervention on various physiological systems. The choice of animal models depends on factors such as genetic similarities, availability, and ethical considerations.
4. **Cell-based models:** These models involve using specific cell lines or cultures to assess the intervention's effects on cellular behaviour, viability, or toxicity. Cell-based assays can provide valuable information about the intervention's impact at the cellular level.
5. **Organotypic models:** These models involve culturing organ-like structures that mimic the complexity and function of specific organs. Organotypic models allow researchers to study the intervention's effects on organ systems, providing insights into potential organ-specific toxicity or adverse effects.

6. **Computational models:** Computational approaches, such as computer simulations or predictive modelling, can be used to assess the safety of an intervention. These models rely on algorithms and mathematical calculations to predict the intervention's effects based on available data.

3.8.10.3. Efficacy studies

Efficacy studies are conducted to evaluate the effectiveness or desired outcomes of an intervention. These studies aim to determine whether the intervention produces the intended therapeutic effects. The assessment of efficacy typically involves a combination of in vitro and in vivo experiments, as well as clinical trials in human subjects. The choice of efficacy assessment methods depends on the nature of the intervention, the specific therapeutic target, and the stage of development. Here are some common approaches used to evaluate efficacy:

1. **In vitro studies:** In vitro experiments are performed using isolated cells or tissues to assess the intervention's effects on specific cellular targets or biological processes. These studies provide insights into the intervention's mechanism of action, its ability to modulate cellular functions, and its potential therapeutic benefits at a cellular level.
2. **Animal models:** Animal models are frequently used to assess the efficacy of an intervention in a controlled and preclinical setting. Animal studies allow researchers to investigate the intervention's effects on physiological systems, disease models, or specific outcomes relevant to the intended therapeutic purpose. These studies provide valuable information about the intervention's efficacy, dosing, and potential side effects before progressing to human trials.
3. **Clinical trials:** Clinical trials involve testing the intervention's efficacy in human subjects under controlled conditions. These trials are typically conducted in multiple phases, starting with small-scale studies to assess safety and dose-ranging, and then progressing to larger-scale trials to evaluate the intervention's efficacy compared to standard treatments or placebo. Clinical trials provide crucial evidence regarding the intervention's effectiveness, optimal dosing, safety profile, and potential side effects in the target population.
4. **Biomarker analysis:** Biomarkers are measurable indicators that can reflect the intervention's effects on a biological process, disease progression, or therapeutic response. Biomarker analysis in both preclinical and clinical studies help to assess the intervention's efficacy by measuring changes in relevant biomarkers associated with the desired therapeutic outcome.

3.8.11. Animal models to study corneal scarring or trauma

Researchers use various models to study corneal scars and wound healing. However, each model has its advantages and limitations, and the choice depends on the specific research objectives and resources available.

- **Animal models -** The most common are rabbit and mouse models where corneal injury is induced through alkali burns, excimer laser ablation, or mechanical wounding. This results in corneal fibrosis and scarring that mimic what is seen in human patients. Researchers can then test potential treatments in these models.
- **Ex vivo models** - Corneal buttons or strips from donor human corneas are cultured ex vivo and treated to induce fibrosis. This allows studying corneal scarring in actual human corneal tissue. However, these models lack the in vivo environment.
- **In vitro models** - Corneal cells, especially keratocytes and fibroblasts, are cultured in vitro and treated to induce myofibroblast differentiation and extracellular matrix deposition. This helps study the cellular and molecular mechanisms of corneal fibrosis. But these models lack the complexity of in vivo tissue.
- **Organ culture models -** Whole eye globes from animal donors are cultured ex vivo. Injury can be induced to study corneal wound healing and scarring in a more intact tissue environment. However, the cornea may degenerate over time in culture.
- **3D tissue models -** Corneal cells are combined with biomaterials to create 3D corneal constructs that can be injured in vitro. While simplified, these models allow studying scar development and treatment in a tissue-like environment.

Animal models, particularly mice, are commonly used to study corneal scars and wound healing. These models are valuable for understanding the function of growth factors and extracellular matrix components in corneal wound healing. Here are some of the models and techniques used:

- **Stromal Injury Techniques:** A study tested three stromal injury techniques in mice to evaluate their effectiveness in inducing corneal scars. The techniques involved creating a linear partial thickness keratotomy, removing the corneal epithelium and debriding the stroma, or a combination of both. The severity of scars was assessed using a modified Fantes haze scale. This study helps in understanding the different methods of inducing corneal scars in mice and provides a standardized approach for evaluating scar severity
- **Rabbit alkali burn model**: This is a well-established model where corneal alkali injury is induced in rabbits, typically using sodium hydroxide. This results in corneal inflammation,

neovascularization, stromal fibrosis and opacity - features that mimic corneal chemical burns in humans. Researchers can then test potential anti-scarring therapies in this model.

- **Mouse excimer laser ablation model:** In this model, a precise stromal wound is created in mice using an excimer laser. This induces corneal fibrosis and haze formation that can be quantified objectively. The mouse model allows use of transgenic strains and genetic manipulation to study the molecular mechanisms of corneal scarring.
- **Rat corneal scrape model:** In this simple model, the corneal epithelium of rats is mechanically scraped using a blade. This results in re-epithelialization and stromal healing associated with fibrosis and opacity. The rat model is cost-effective and allows testing of various anti-scarring treatments.
- **Porcine alkali burn model:** Pigs have a corneal anatomy and physiology similar to humans. In this model, alkali injury is induced in pigs using sodium hydroxide to produce corneal burns, scarring and neovascularization. The large cornea size allows sampling for molecular and histological analyses.
- **Canine corneal abrasion model:** Mechanical corneal abrasion is performed in dogs to induce corneal wound healing and scarring. The dog cornea heals more similarly to humans, making this a relevant large animal model. However, it is more expensive than other models.
- **Chemical Burns, Penetrating Incisional Wounds, or Laser Ablation:** These injury models simulate corneal scarring seen after injuries. The mechanisms of trauma as well as severity of injuries vary greatly. Severe corneal injuries commonly present with a combination of traumatic penetrating or nonpenetrating lacerations accompanied by loss of stromal tissue or surface abrasive damage.
- **Genetically Manipulated Mice:** These are used to study biological processes. Their genes can be manipulated including so-called humanized mice that carry inserted human genes. An injury technique that consistently creates significant stromal scars in mice will complement the current techniques used that apply chemical injuries and laser ablation in the study of stromal trauma and wound healing.

The murine model generated by debridement is a preferred choice for studying corneal wound healing and scar formation. This model allows for controlled and standardized wounds, closely mimicking human corneal trauma and facilitating the study of relevant healing processes. With its simplicity and reproducibility, the debridement technique enables better consistency and comparison of results. Additionally, this model serves as a valuable platform for testing potential treatments, providing insights into their effects on wound healing and scar formation.

3.9.1. Biological Preservation and transport of cells

During cell transport, maintaining the appropriate temperature and preventing contamination are critical. The specific method of transport depends on factors such as the distance, cell type, and preservation method employed. It is essential to create a controlled environment that ensures the optimal conditions for cell viability throughout the transportation process (Pegg, 2007; Hunt, 2011; Woods & Thirumala, 2011).

The main challenge during cell transport is to maintain consistent temperature control to prevent detrimental effects on cell viability. This can be achieved through the use of specialized containers, such as insulated coolers or liquid nitrogen dewars, equipped with temperature monitoring and control systems. These containers help maintain the required temperature range for the specific preservation method employed, whether it is cryopreservation or hypothermic preservation. Additionally, it is crucial to implement proper packaging and handling procedures to minimize the risk of contamination during transport (Woods & Thirumala, 2011).

The ability to safely transport and store cells is essential for a wide range of uses, from basic science research to therapeutic treatments. Common techniques include cryopreservation and hypothermic preservation, both of which have advantages and disadvantages. Understanding these considerations is vital for effective cell management.

3.9.1.1. Cryopreservation: Exploring the *Potential* and the *Uncertainties*

Cryopreservation helps preserving cells at ultra-low temperatures for long-term storage while maintaining their viability. This is a widely used method for long-term storage of cells, tissues, and organs. It involves cooling cells to sub-zero temperatures, typically -196°C using liquid Nitrogen. This preservation technique offers several benefits. It allows for the long-term storage of biological materials, enabling research and clinical applications that require extended preservation. When performed correctly, cryopreservation can maintain the optimal viability and functionality of cells after thawing, ensuring their usefulness in subsequent experiments or clinical procedures (Hunt, 2011; Kapoore et al., 2019).

However, cryopreservation is frequently hindered by its inherent constraints. It requires the use of cryoprotectants or cryoprotective agents (CPA), which can be toxic to cells if not carefully managed. The majorly used cryoprotectant is dimethyl sulfoxide (DMSO), others being glycerol (GLY), ethylene glycol (EG), and propylene glycol (PG) etc., (Whaley et al., 2021). DMSO – despite being considered the most toxic reagent to cells (Bhattacharya, 2018), is ironically the most widely used agent for cryopreservation. Studies by Ha *et al* and Hent *et al* have shown only a 30% recovery of embryonic stem cells (ESC) when used at 5% concentration in the cryopreservation

media or at 10%, but with an extra added agent EG (Ha et al., 2005; Heng et al., 2006). In another report by Heng *et al* cryopreserved ESC have shown decreased viabilities, if not for an additional Matrigel-based matrix, in the preservation media (Heng et al., 2005). On the contrary, when used at 10% levels in the study by Liu *et al*, adipose-derived stem cells (AdSCs) were not hampered in terms of their viability(G. Liu et al., 2008). A similar kind of mixed or ambiguous findings were reported by Kapoore *et al*, Ji *et al* and Boer *et al* in terms of the differentiation abilities. While Ji *et al* and Boer *et al* reported poor viability and reduced differentiation potential in ESCs; decreased or poor functionality and differentiation potential of the CD34+ MSCs respectively, study Kapoore *et al* reported the unaffected functional stability and viability of the cryopreserved cells (de Boer, Dräger, Pinedo, Kessler, Monnee-van Muijen, et al., 2002; de Boer, Dräger, Pinedo, Kessler, van der Wall, et al., 2002; Ji et al., 2004; Kapoore et al., 2019).

In addition to these uncertain notions by the researchers, there is also a risk of contamination between samples during storage and thawing processes. Furthermore, cryopreservation is a costly affair due to the required equipment, materials, and the forever-ongoing storage expenses (Woods & Thirumala, 2011).

3.9.1.2. Cold-chain methods (refrigeration)

Cold-chain methods, the primarily used hypothermic storage methods, offer storing cells at reduced temperatures above freezing to slow down metabolic activity and extend storage time. This method involves storing cells, tissues, or organs at temperatures above freezing, typically between 2°C and 8°C. This method is commonly used for short-term storage purposes. It offers advantages such as preserving cell viability with less damage compared to cryopreservation since it avoids the freezing and thawing processes. It is particularly useful when immediate or short-term storage is required, such as during transportation or in certain clinical settings. However, cold-chain/refrigerating methods have their own limitations. Cells cannot be stored for extended periods, as they're not designed for long-term preservation. There is also a risk of cell death or loss of functionality if cells are not properly maintained during the preservation process.

3.9.1.3. Dry Ice and Hypothermic Preservation methods for Cell Property Retention

Dry ice storage is another commonly employed method for preserving biological samples and perishable items at extremely low temperatures, typically around -80°C. It provides the benefit of maintaining a stable and consistent cold environment, ensuring the preservation of sensitive materials. However, it is important to be aware of the potential harmful effects associated with the use of dry ice. For instance, a study conducted by Til et al. (2016) investigated the effects of storing and transporting cryopreserved semen samples on dry ice. Interestingly, the study revealed that

while transportation did not significantly impact the quality of the samples, the use of dry ice had detrimental effects on sperm parameters, particularly motility and vitality (Til et al., 2016). This highlights the need for careful consideration and optimization of storage methods when utilizing dry ice for preserving delicate biological samples.

On the other hand, hypothermic preservation at temperatures ranging from 15°C to 22°C is emerging as a promising approach for the long-term preservation of various biological materials. This temperature range offers a mild cooling environment that can help maintain the viability and functionality of cells and tissues. Researchers are actively exploring the effectiveness of hypothermic preservation and working towards optimizing storage conditions within this temperature range.

3.9.2. The impact of additional CPAs in cryopreservation/hypothermic preservation

In cryopreservation, the development of advanced biomaterials capable of safeguarding cells against osmotic and ice-induced damage, as well as mitigating oxidative stress, is crucial for enhancing cell survival. Additionally, cold chain shipping may lead to hypothermia-induced injuries or extracellular matrix (ECM) loss caused by cell-permeable agents (Ma et al., 2015). Therefore, the design of new biomaterials and careful consideration of shipping conditions are imperative in cryopreservation techniques. The **table 3.4** summarizes a range of studies highlighting the effectiveness of different cryoprotective agents on various cells and tissues during cryopreservation or hypothermic preservation. All these studies have shown that trehalose, alginate, and other impermeable agents can significantly enhance cell viability and preserve the important characteristics of the cells or tissues.

On the other hand, hypothermic storage at temperatures between 15-22 degrees Celsius is an alternative approach that requires further exploration. This temperature range provides a mild cooling environment that can help preserve the viability and functionality of various biological materials, including cells and tissues. Hypothermic storage has shown promise in maintaining cell integrity, metabolic activity, and overall cellular function. However, there is still a need for more research to optimize the storage conditions, identify the limitations, and fully understand the long-term effects of hypothermic storage on different types of samples.

Cryoprotective Agents	Cells or Tissues Studied	Effect or Benefit	References
Trehalose	Mammalian cells	Effective preservation during cryopreservation, preserving cell viability	(Campbell & Brockbank, 2011)
Trehalose	Human mesenchymal stromal cells	Successful cryopreservation with electroporation, minimal impact on gene expression	(Dovgan et al., 2021)
Trehalose	Primary rat hepatocytes	Improved cell viability, suppressed ice crystal formation, maintained liver function	(Yoshida et al., 2020)
Trehalose glycopolymers	Tissue-engineered constructs	Maintained viability and function of cryopreserved constructs	(J. Wang et al., 2022)
Trehalose, other sugars	Lactic acid bacteria	Protective effect on viability after freezing or freeze-drying	(Giulio et al., 2005)
Alginate-encapsulated recombinant cells	Recombinant cells	Maintained viability, structure, and protein secretion of encapsulated cells	(Stensvaag et al., 2004)
Alginate microspheres	Mesenchymal stromal cells	High viability and metabolic activity after cryopreservation	(Pravdyuk et al., 2013)
Alginate hydrogels	Recombinant myoblasts	Preserved metabolic activity, insulin secretion, and cell morphology	(Ahmad & Sambanis, 2013)
Alginate gel entrapment	Hepatocytes	Improved viability, cell yield, preserved mitochondrial function, reduced apoptosis	(Mahler et al., 2003)

Table 3.4: Studies demonstrating the benefits of impermeable cryoprotective agents on cell viability that cause less or no cell injury

According to the study by Waler C. Oslon, the loss of cells during storage is higher at temperatures of 15°C and 40°C, compared to 22°C. These findings suggest that the temperature range of 22-25°C holds promise for further research in hypothermic storage. Understanding the effects of this temperature range on cell viability and preservation can potentially optimize hypothermic storage methods and improve cell storage outcomes (Olson et al., 2011).

3.9.3. Challenges and Considerations in Shipping Stem Cells

Stem cells, for instance, are particularly delicate and require specialized preservation methods to maintain their unique properties. Different cell types may necessitate alternative approaches such as hypothermic preservation with customized procedures. Regardless of the preservation method, shipping cells, including stem cells, presents several challenges that must be carefully addressed. Few of them are highlighted in **Table 3.5.**

These challenges can be addressed through careful planning, the use of specialized shipping containers, and working with couriers experienced in the transport of biological materials. However, based on the type of cell type and the end-use purpose, each type of shipment of stem cells can present unique challenges that need to be managed to ensure the cells arrive at their destination in a optimal viable and functional state.

3.9.4. Upcoming/alternative methods of cell preservation and transport – Pros & Cons

Traditional cell preservation procedures, such as gradual freezing, frequently provide obstacles and restrictions that might impair cell viability and performance. To address these shortcomings, researchers throughout the world have been investigating new and alternative approaches that may give improvements in cell preservation and transport. A number of procedures, including as vitrification and desiccation, have emerged as potential options. Each strategy has its own set of advantages and disadvantages that must be carefully studied before being put into practise. **Table 3.6** summarises these forthcoming approaches, stressing their benefits and potential downsides.

Risks	Plausible challenge(s)
Temperature Control	Stem cells often need to be kept at very specific temperatures to maintain their viability. This can be particularly challenging during transport, especially over long distances or through areas with extreme temperatures.
Time Sensitivity	Stem cells can be sensitive to the length of time they are in transit. Delays in transport can potentially impact the viability and functionality of the cells.
Risk of contamination	During transport, there's a risk of contamination from various sources. Ensuring the cells remain sterile throughout the journey is crucial.
Cryopreservation Challenges and logistics thereof	If stem cells are being transported in a cryopreserved state, there are additional challenges. These include maintaining the ultra-low temperatures required for cryopreservation and managing the thawing process at the destination to ensure cell viability.
Regulatory Compliance	Transporting biological materials often involves navigating complex regulatory landscapes. This can include everything from packaging requirements to documentation for customs.
Costs involved	The specialized packaging and transport conditions required for stem cells can make shipping expensive.
Specialized media	Stem cells require specific nutrient media and growth factors to remain healthy during shipping. Correct composition of media must be used and changed regularly to nourish the cells, as when needed.

Table 3.5: Table describing the key considerations or essential factors required to be addressed or be minded during transport of biological cells (Yu et al., 2018)

Method	Range	Pros	Cons	References
Vitrification	-196°C	By raising the concentration of cryoprotectants and rapidly freezing the cells, vitrification prevents the production of ice crystals, resulting in a glass-like solidification of the cells.	• Uses more cryoprotectants than typical freezing procedures, which might harm cells. • Needs quick freezing and warming rates, which are hard to control, especially for bigger samples and labour-intensive.	(Fahy et al., 2009; He et al., 2008)
Desiccation	RT	• Desiccation is the process of drying cells to preserve them, which mimics a natural survival strategy in some species. • Possibility to use for a broader spectrum of cell types.	• The drying process can harm cell structures. • The rehydration process following desiccation can potentially cause cell harm. • Complex procedures	(S. Chen et al., 2019)
Use of novel cryo-protectants	Varies	Use of new cryoprotectants that are less toxic to cells, such as antifreeze proteins that can prevent ice formation at sub-zero temperatures.	• Novel cryoprotectants may cause unanticipated cell damage. • Novel cryoprotectants' development can be costly.	(Fahy et al., 2009)
Magnetic freezing	Varies	Magnetic freezing is a novel method that uses a magnetic field to control the freezing process, potentially reducing the damage caused by ice crystal formation.	• This method's efficacy and risks are unknown due to limited studies. • Magnetic field generation and control need special equipment.	(Ito et al., 2020; Manuchehrabadi et al., 2017)
Use of nanoparticles	Varies	• Nanoparticles can be used to control the freezing process and protect cells from damage • This is a developing field of research with the potential for advancements in controlled freezing techniques.	• Nanoparticles' effects on cells are not entirely known, and their usage may pose potential hazards. • The use of nanoparticles in medicine requires regulatory permission, which may be a time-consuming procedure.	(Guven & Demirci, 2012)

Table 3.6: Comparison of cell preservation methods, highlighting their unique characteristics and considerations.

3.10. Enhanced Cell Protection and Viability: Cell Encapsulation for Improved Storage and Transport

Cell encapsulation is a method that involves surrounding cells with a protective layer, typically a gel-like substance, to provide them with stability and facilitate their storage and transport. This technique offers several advantages compared to traditional methods of cell preservation, which include

1. **Protection:** The encapsulating material provides a physical barrier that protects the cells from mechanical, chemical, and biological stresses during handling and transportation. This helps maintain cell viability and functionality.
2. **Isolation:** Encapsulation creates a controlled microenvironment by isolating the cells from the external environment. The encapsulating material allows for the diffusion of nutrients and waste products while preventing the ingress of harmful substances.
3. **Stability:** Encapsulated cells can remain stable at different temperatures, including room temperature. This eliminates the need for complex and costly cold chain logistics associated with cryopreservation methods. It provides greater flexibility in storage and transportation options.
4. **Ease of use:** Encapsulated cells, housed in hydrogels or membranes, are easier to handle and transport compared to frozen cell suspensions. There is no requirement for specialized equipment, such as liquid nitrogen tanks, making encapsulated cells more accessible and practical for a broader range of applications.
5. **Cost-effectiveness:** Storing and transporting encapsulated cells at room temperature or refrigerated temperatures is more cost-effective than cryopreservation. The absence of expensive equipment and infrastructure needed for maintaining a cold chain reduces logistical challenges and expenses.
6. **Scalability:** Encapsulation allows for standardized and controlled cell production and storage. This scalability is crucial for large-scale applications in regenerative medicine and cell-based therapies.

3.10.1. Encapsulating agents

The following table (**Table 3.7**) provides an overview of different materials commonly used as encapsulating agents for cells in various biomedical applications. All these materials offer distinct advantages and disadvantages in cell encapsulation.

Material	Advantages	Disadvantages
Alginate	▪ Derived from brown seaweed, a renewable resource ▪ Biocompatible ▪ Low cost ▪ Forms a gel under mild conditions, which is gentle on cells ▪ Can be used to encapsulate a wide variety of cell types	▪ Gel strength can be variable and may not be suitable for all applications ▪ May require additional cross-linking to improve stability ▪ Difficult to control pore size, which can affect cell release
Polyethylene glycol (PEG)	▪ Synthetic polymer with consistent properties ▪ Biocompatible ▪ Flexible, can be modified to control properties like porosity and degradation rate	▪ More expensive than natural polymers ▪ May require chemical modification for cell attachment ▪ Not biodegradable, which can limit its use in certain applications
Chitosan	▪ Derived from chitin, a renewable resource ▪ Biocompatible ▪ Biodegradable ▪ Can form a gel under mild conditions	▪ Requires acidic conditions to gel, which can be harmful to cells ▪ Gel strength and degradation rate can be variable
Gelatin	▪ Derived from collagen, a natural protein ▪ Biocompatible ▪ Forms a soft gel, which can be gentle on cells	▪ Gel strength is weak and may not be suitable for all applications ▪ Derived from animal sources, which can raise ethical or contamination concerns
Agarose	▪ Derived from seaweed, a renewable resource ▪ Forms a stable gel ▪ Can be used to encapsulate a wide variety of cell types	▪ Gel strength can be weak and may not be suitable for all applications ▪ Not biodegradable, which can limit its use in certain applications
Trehalose	▪ Natural disaccharide with high water retention capabilities ▪ Can protect cells from dehydration ▪ Biocompatible ▪ Can stabilize proteins and cell membranes	▪ Difficult to introduce into cells ▪ May require specific techniques to encapsulate cells ▪ Not suitable for all cell types

Table 3.7: The types of materials used in cell encapsulation, listed against their advantages and disadvantages.

3.10.2. Alginate: A Versatile Hydrogel for Cell Encapsulation

Alginate is a natural, anionic, and non-toxic polysaccharide derived from brown seaweeds, composed of mannuronic acid (M) and guluronic acid (G) residues. Upon contact with divalent cations, such as calcium, it forms a gel matrix that has numerous applications in biomedicine, particularly for cell encapsulation and storage. This matrix is semi-permeable, allowing nutrients and waste to pass through while protecting the cells from the external environment. Alginate has been used extensively for the encapsulation of mammalian and bacterial cells due to its biocompatibility, adjustable viscosity, and permeability to oxygen and nutrients. It can also be formulated into different shapes and sizes, including micro- and macro-beads, fibers, and hydrogels, tailored according to specific needs. Alginate hydrogels provide broad protection for the encapsulated cells from harsh environments, immune rejection, and physical stress during transit, making it an ideal biomaterial for cell delivery (K. Y. Lee & Mooney, 2012a; J. L. Wilson et al., 2014)

Alginate is considered versatile for several reasons:

1. **Gelation:** Alginate can form a gel at room temperature without the need for any harsh conditions, which is beneficial for maintaining cell viability (K. Y. Lee & Mooney, 2012b).
2. **Tunability:** The properties of the alginate gel, such as its stiffness and porosity, can be tuned by adjusting the concentration of alginate and the type and concentration of cross-linking ions. This allows the encapsulation conditions to be optimized for different types of cells (Freeman & Kelly, 2017).
3. **Biocompatibility:** Alginate is generally considered to be biocompatible and has been used in various medical applications, from wound dressings to drug delivery systems (Abourehab et al., 2022)
4. **Inertness:** Alginate is chemically inert and does not interact with or affect the encapsulated cells. This allows the cells to function normally within the alginate matrix (J. Sun & Tan, 2013b).
5. **Porosity:** Alginate hydrogels are porous, allowing the diffusion of nutrients, oxygen, and waste products to and from the encapsulated cells.
6. **Degradability:** Alginate hydrogels can be made to degrade over time by controlling the crosslinking density. This allows for release of the encapsulated cells when desired.
7. **Mechanical stability:** Alginate hydrogels can have sufficient mechanical stability to withstand handling and transport of the encapsulated cells (Becker et al., 2001).

8. **Cost:** Alginate is low-cost and easily available, making it suitable for large-scale cell encapsulation applications (Pereira et al., 2020).

As for safety, alginate has been used in food and pharmaceutical applications for many years and is generally considered safe (Bi et al., 2022; Food and Drug Adminsitration, n.d.). However, like any material, it can potentially cause an immune response or other adverse reactions in some individuals or under certain conditions. Therefore, it's important to thoroughly test any encapsulation system for safety and efficacy before it's used in humans.

Other agents used in encapsulation, such as polyethylene glycol (PEG) and chitosan, also have a long history of use in biomedical applications and are generally considered safe. These materials must also undergo extensive testing for safety and effectiveness, and the same considerations still need to be made (Cao et al., 2021).

Chapter 4

Methodology

4. Methodology

4.1. Workflow

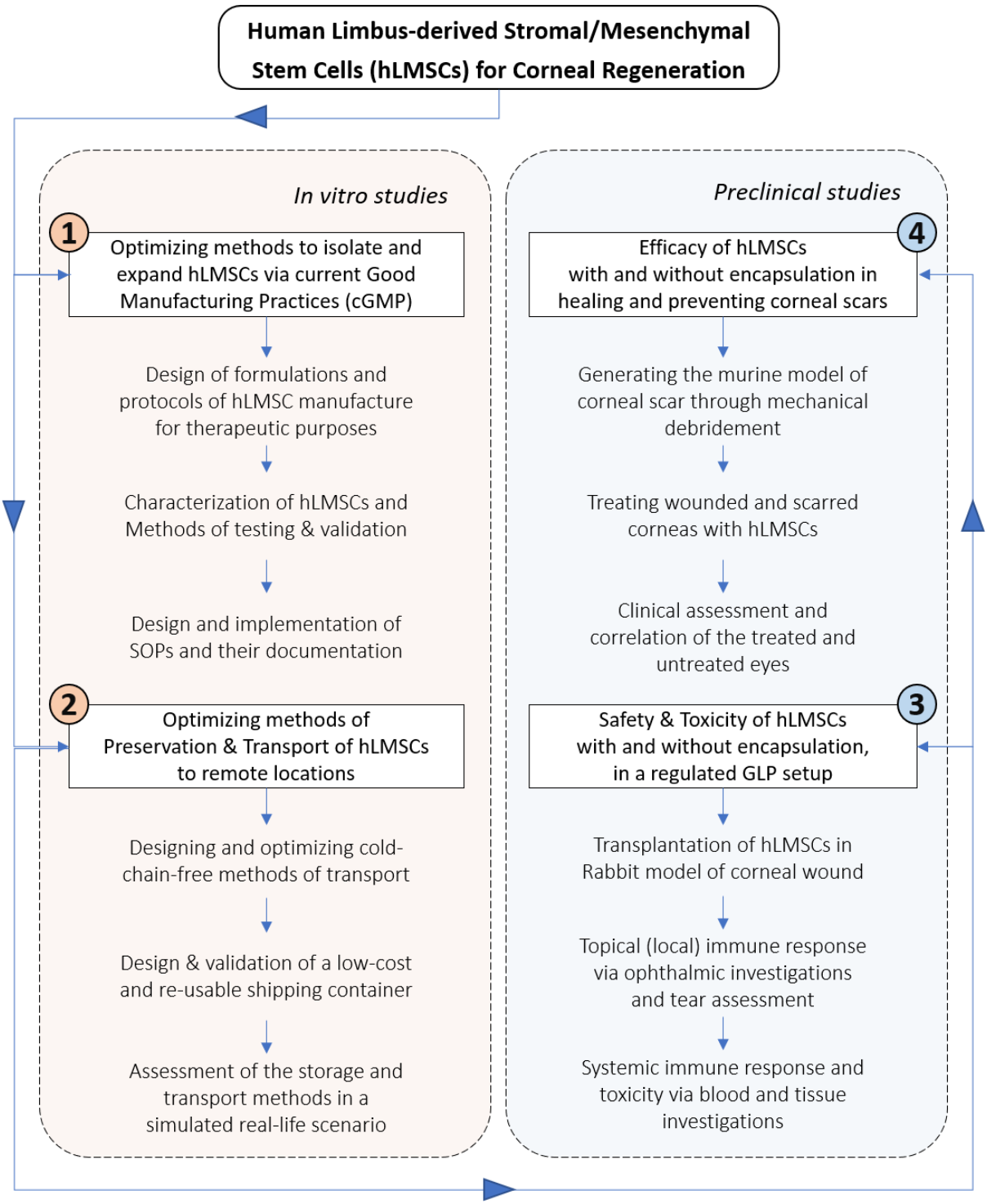

Figure 4.1: Schematic of the study workflow.

4.2. Study approvals and Ethics Statements

All techniques and methods used in this thesis were approved by the Institutional Review Board and Ethics Committee of the LV Prasad Eye Institute in Hyderabad (LEC 05-18-081; Annexure-I) and the Institutional Committee for Stem Cell Research (IC-SCR Ref. No. 08-18-002; Annexure-II). The Declaration of Helsinki was strictly followed in all the research utilizing human tissue. Ramayamma International Eye bank in Hyderabad was the source for the human cadaver donor corneas. Informed consent to use the donor corneas for surgical and research purposes was obtained from the kith and kin of the donors by the eye bank. A masked, reference copy of the informed consent form is enclosed here as *Annexure-III*.

Sipra Labs Limited, Hyderabad (Compliance Certificates of Compliance and Accreditation: GLP/C-107/2017 and TC-5417 respectively), is a GLP-compliant (Good Laboratory Practice) contract research firm with which we conducted the preclinical toxicity and safety investigation in rabbit. Sipra Labs' CPCSEA (Committee for the Purpose of Control and Supervision of Experiments on Animals) gave their clearance to this experimentation with the research number PCT/IAEC/110-19. The Efficacy Study in Murine Models was authorized by the Institutional Animal Ethics Committee (IAEC) of the Center for Cellular and Molecular Biology (CCMB), Hyderabad (study number: IAEC 92/2019) (*Annexure-V*).

Both pre-clinical investigations followed the ARVO Statement for the Use of Animals in Ophthalmic and Vision Research to reduce animal suffering, distress, and discomfort.

4.3. Compliance with the National and International guidelines

All the protocols and experimental designs were performed in compliance with multiple national and international guidelines as listed below.

The development, optimization, validation, and standardization of all protocols were performed by the principles cGMP (Current Good Manufacturing Practices), as stated in the *Schedule M, Part 1A* of the *Drugs and Cosmetics Act 1945,* Government of India (*2016DrugsandCosmeticsAct1940Rules1945.Pdf*, n.d.-b) and *Rule 55, Chapter VIII* of the *NDCT rules*, CDSCO, Government of India (*NewDrugs_CTRules_2019.Pdf*, n.d.-b). The SOPs for all standardized protocols: cultivation, encapsulation of hLMSCs, testing, and analysis from the raw-material stage to the end product, were designed and implemented to maintain consistent uniformity and quality output from all the activities.

The experimental protocols in the toxicity and safety study were carried out in a GLP facility, in congruence with the guidelines of *Schedule Y, Drugs and Cosmetics Rules act, 2019*, Government of India (*2016DrugsandCosmeticsAct1940Rules1945.Pdf*, n.d.-b) and the OECD (Organization for Economic Co-operation and Development) principles of GLP, 1997 (*Publicdisplaydocumentpdf.Pdf*, n.d.). The study was conducted employing calibrated and standardized equipment and following SOPs, as stated by the above-mentioned guidelines.

4.4. Optimization, validation, and standardization of hLMSC cultivation in GMP facility

4.4.1. Overview of GMP cleanroom and batch manufacturing record

The activity of hLMSC isolation, cultivation and expansion was performed in controlled manner in a regulated clean room area. The cell culture activity from processing of the donor corneas to the final harvest was performed in the Grade B facility, where the quality of air doesn't exceed the specifications of 3200 particles (<0.5 μ size) per cubic feet, at rest.

A snapshot of the clean room and the in-process monitoring was illustrated in **Figure 4.2.**

All the activities of the culture procedures, regular maintenance of the clean room, equipment and instrumentation, and the personnel working are continuously monitored, and regulated in a controlled manner with standard operating protocols laid.

Each and every step in all the protocols (**Figure 4.3**), are recorded in a document called the Batch Manufacturing Record (BMR). This record is specific to each batch of cells produced from a single donor cornea. Only upon, the cells of a given batch being found to qualify the given specifications set, in terms of number, viability and the characteristic properties, the BMR shall be approved for therapeutic purposes.

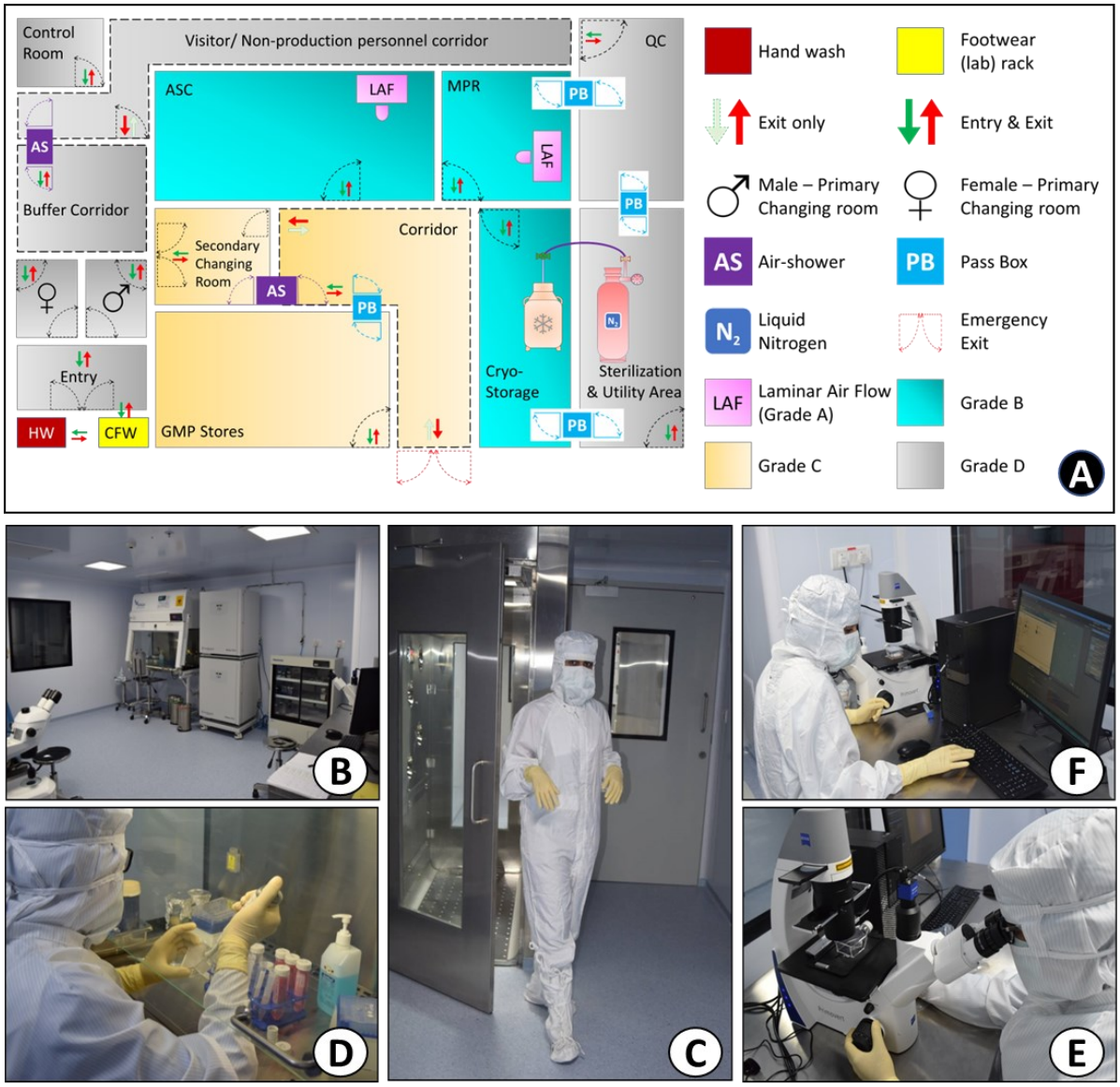

Figure 4.2: Overview of the Clean room facility and GMP procedures: A) Illustration showing the grades of clean room areas and their respective functions, where a particular event or step of the hLMSCs manufacturing process; (Legend in the panel on right). B) Snapshot of the cell culture suite. C) Production personnel in sterile suits. D) Activity in LAF (class A). E) In-process monitoring of hLMSC cultures. F) Spot documentation of the observations and activity for BMR. ASC – Adult stem cell suite; MPR – Media preparation room; QC – Quality control.

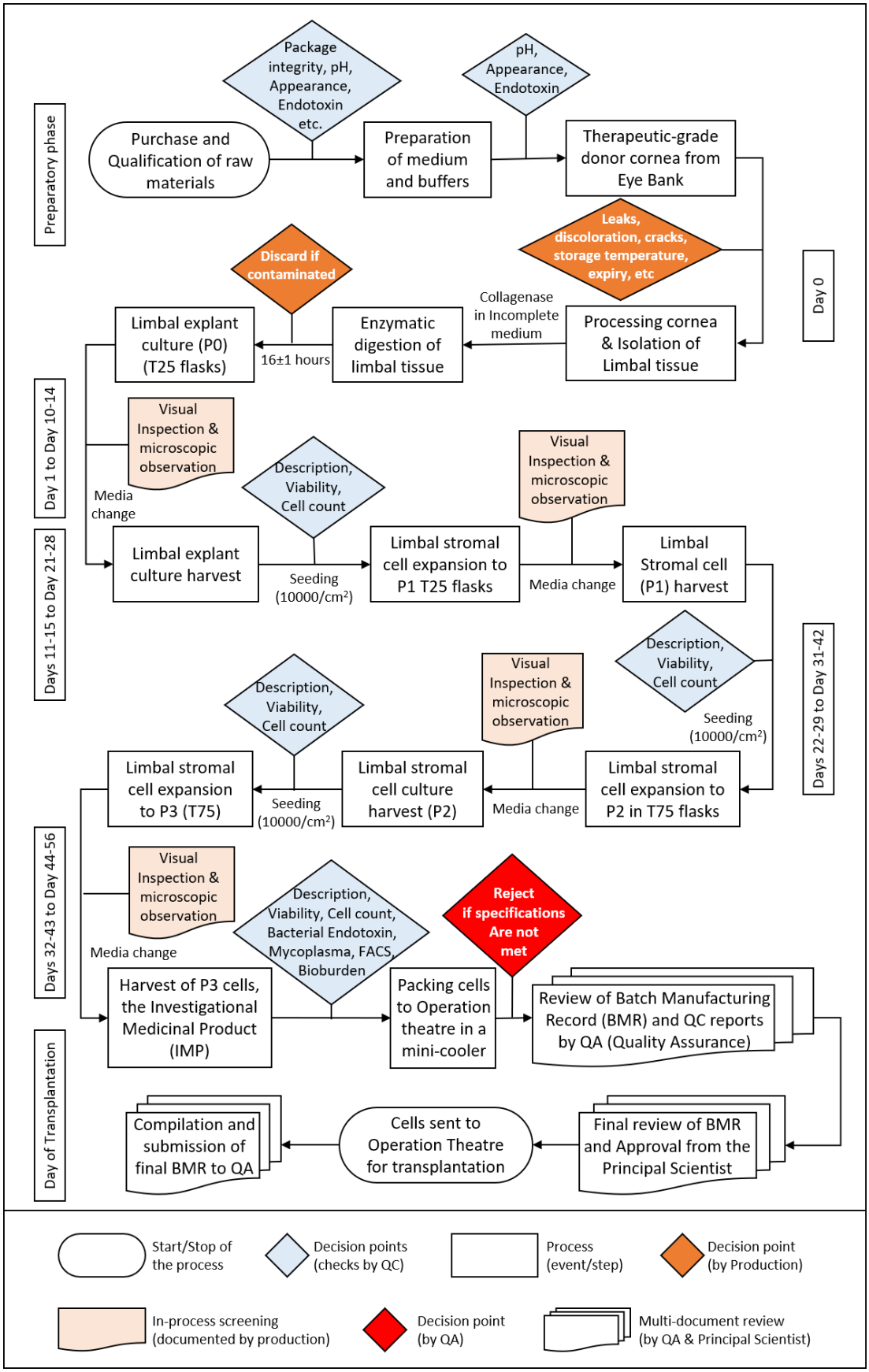
Preparatory phase
Package integrity, pH, Appearance, Endotoxin etc.
pH, Appearance, Endotoxin
Purchase and Qualification of raw materials
Preparation of medium and buffers
Therapeutic-grade donor cornea from Eye Bank
Leaks, discoloration, cracks, storage temperature, expiry, etc
Day 0
Discard if contaminated
Collagenase in Incomplete medium
Limbal explant culture (P0) (T25 flasks)
16±1 hours
Enzymatic digestion of limbal tissue
Processing cornea & Isolation of Limbal tissue
Day 1 to Day 10-14
Visual Inspection & microscopic observation
Media change
Description, Viability, Cell count
Visual Inspection & microscopic observation
Days 11-15 to Day 21-28
Limbal explant culture harvest
Seeding (10000/cm²)
Limbal stromal cell expansion to P1 T25 flasks
Media change
Limbal Stromal cell (P1) harvest
Description, Viability, Cell count
Seeding (10000/cm²)
Days 22-29 to Day 31-42
Description, Viability, Cell count
Visual Inspection & microscopic observation
Limbal stromal cell expansion to P3 (T75)
Seeding (10000/cm²)
Limbal stromal cell culture harvest (P2)
Media change
Limbal stromal cell expansion to P2 in T75 flasks
Days 32-43 to Day 44-56
Visual Inspection & microscopic observation
Media change
Description, Viability, Cell count, Bacterial Endotoxin, Mycoplasma, FACS, Bioburden
Reject if specifications Are not met
Harvest of P3 cells, the Investigational Medicinal Product (IMP)
Packing cells to Operation theatre in a mini-cooler
Review of Batch Manufacturing Record (BMR) and QC reports by QA (Quality Assurance)
Day of Transplantation
Compilation and submission of final BMR to QA
Cells sent to Operation Theatre for transplantation
Final review of BMR and Approval from the Principal Scientist
Start/Stop of the process
Decision points (checks by QC)
Process (event/step)
Decision point (by Production)
In-process screening (documented by production)
Decision point (by QA)
Multi-document review (by QA & Principal Scientist)

Figure 4.3: Schematic of the flow of events in manufacture of hLMSCs and their delivery from bench-to-bedside, as recorded in BMR. (Legend in the lower panel)

4.4.2. Evaluation of the donor corneas and the criteria for inclusion and exclusion

The corneoscleral rims (**Figure** 4.4) harvested from human cadaveric donors were used in this thesis work. The interval of death-to-harvest and preservation was not more than 12 hours. The corneas collected were stored at +2 to +8◦C till use in *Mc Carey-Kaufman* (MK) medium with validity up to 4 days from the time of death. The donor corneas were then evaluated for therapeutic suitability, through gross physical observation and slit lamp biomicroscopy by the eye bank personnel. The results of these evaluations are listed in the *Tissue Evaluation Sheet* for each donor cornea. This forms the basis for accepting or omitting a donor cornea for use in cell culture. A masked copy is enclosed as *Annexure IV*.

4.4.2.1. Inclusion criteria:

The assessment criteria and other parameters (but not limited to) evaluated before the acceptance or disqualification of a donor cornea towards the isolation and cultivation of the hLMSCs are listed in the **Table 4.1**.

Parameters considered/assessed		**Rejected if**
Age	18 – 60 years	Age of <18 or >60 years
Gender	Male and Female	N/App
Anatomical & morphological evaluation (Retro illumination through specular microscopy		
Epithelium	▪ Keratitis (inflammation), ▪ Epithelial defects, ▪ Sloughing of tissue (dead cells/layers), ▪ Presence of debris	▪ Inflammation or ▪ Active ocular infections (uveitis, choroiditis, retinitis) ▪ Sloughing >10%
Stroma	▪ Scars ▪ Edema, ▪ Clarity, ▪ Arcus (fat or lipid deposit), ▪ Infiltrates or foreign bodies,	▪ Scars in the stroma ▪ Foreign bodies ▪ Infiltrates
Descemet's membrane	▪ folds ▪ striae	--- Contd..

Endothelium	▪ cell count/mm^2, ▪ cell dropout, ▪ stress lines, ▪ defects, ▪ polymegathism (variability of cell size) ▪ pleomorphism (variability of cell number)	▪ Cell count of <3000 cells/mm^2
Serological parameters		
Blood-borne diseases	▪ Hepatitis B, ▪ Hepatitis C, ▪ and HIV I/II	▪ Known history or ▪ positive for blood-borne diseases
Sexually transmitted diseases (STDs)	▪ Syphilis	▪ Tested positive for STDs ▪ Known history
Cause of death		
--	--	▪ Consumption of poison ▪ Snake bites ▪ Road traffic accident cases with an open head injury

Table 4.1: List of the acceptance and evaluation criteria for serological and anatomical evaluation of donor corneas.

After screening the donor corneas for all the above parameters by eye bank, the qualified tissues are selected for therapeutic use in penetrating or tectonic (partial) keratoplasty. Such tissues are collected after a secondary visual examination with naked eye and processed for limbal expansion.

4.4.3. Testing the raw material

All the raw material used in the study (plastic ware and reagents) are either manufactured in GMP facilities, or certified for use in therapeutic applications in humans. Every unit of raw material is re-checked internally with individual specifications set, using SOPs to ensure the proper functionality and properties of the products as per the respective certificate of analysis (CoA), and also to prevent any adverse events.

4.4.3.1. Plastic ware

The plasticware are tissue culture-grade, and are certified to be sterile, and free of human DNA, DNAse, RNAse, and pyrogens. They are checked for the validity and shelf life, intactness of the external individual packaging, and physical defects.

4.4.3.2. Corneal tissues

In addition to the tests done by eye bank, the donor corneas are again checked before tissue processing through physical observation via naked eye. The parameters include:

a. Discoloration of MK medium,
b. leaks or cracks in the container,
c. validity, and suitability of the tissue,
d. storage temperature,
e. period between the point of death and cornea harvesting, and
f. presence of scars or infiltrates in the corneal tissue

4.4.3.3. Cell culture media and other reagents

The cell culture media, their individual components and other reagents used in the isolation, expansion and storage of the hLMSCs **(Table 4.2)** are evaluated through one or more tests such as physical appearance, pH, validity, intactness of the vial or outer packaging, level of endotoxin etc. before use. The results of these tests should match with the corresponding results mentioned in the respective certificate of analysis. A list of the tests performed is summarized in **Table 4.2**.

Reagent	Appearance	Container integrity	pH	BET	Microbial screening
Collagenase type IV	+	+	+	+	-
DMEM/ F12	+	+	-	+	-
Insulin	+	+	-	-	-
EGF	+	+	-	-	-
FBS	+	+	+	+	-
Antibiotic - Antimycotic	+	+	+	+	-
TrypLE	+	+	+	+	-
DMSO	+	+	-	+	-
DPBS	+	+	+	+	-

Table 4.2: List of the tests performed on raw materials used in isolation and expansion of hLMSCs. Tests performed are indicated with **(+)** and tests that are not performed are indicated with **(-)**.

4.4.4. Isolation and expansion of hLMSCs

4.4.4.1. Preparation of the media and other reagents

The formulations and units of the reagents, used per one batch of the hLMSCs, which were obtained from a single donor cornea, are listed in **Table 4.3**. All the components stored at freezing temperatures were thawed to 2 to 8˚C before making the reagents. The components of each specific reagent were mixed in their respective quantities, in a fresh 50mL centrifuge tube. These compositions were then filtered into fresh tubes, with 0.22µ syringe (nylon) filters. Samples from randomly chosen aliquots of each formulation were tested for the respective criteria (**Table 4.3**) and then used for the cultivation of hLMSCs. Media and other reagents prepared were specific to each batch of the cells produced, to prevent contaminations of any kind.

Reagents and their components	Concentration	Volume	Storage Temperature
a) Complete medium (50 mL) – 4 to 8 units			+2 to +8˚C
• DMEM/F12	-	48.4125 mL	+2 to +8˚C
• Insulin	4mg/mL	62.5 µL	-20 to -30˚C
• EGF	1mg/mL	25 µL	-20 to -30˚C
• FBS	-	1 mL	-20 to -30˚C
• Antibiotic-Antimycotic	100X	500 µL	-20 to -30˚C
b) Incomplete medium (5mL) – 1 unit			
• DMEM/F12	-	5 mL	+2 to +8˚C
c) Wash buffer with 2X antibiotics (15 mL) – 1 unit			
• DPBS	1X	14.7 mL	+25 to +37˚C -20 to -30˚C
• Antibiotic-Antimycotic	100X	300 µL	

Contd..

d) Cryopreservation medium (15 mL) – 1 unit			
• DMSO	-	1.5 mL	Room temperature (RT)
• DMEM/F12	-	6 mL	+2 to +8˚C
• FBS	-	7.5 mL	-20 to -30˚C
e) Cell dissociation medium (50 mL) – 1 unit			RT
• TrypLE	1X	50 mL	RT

Table 4.3: Details of the reagents, and their respective components used in the cultivation of hLMSCs.

4.4.4.2. Processing donor cornea and enzymatic digestion of limbus

All surgical tools were sterilized and equipment were disinfected prior to use. The donor cornea vial was surface-sterilized prior to opening and reevaluated through physical observation for parameters mentioned in inclusion and exclusion criteria (**Table 4.1; Section 4.4.2.1**). All media and reagents used in the isolation and cultivation (except Collagenase enzyme) were thawed to 37˚C from their respective storage temperatures, using a dry bath filled with Lab Armor™ Beads (Thermo Fisher) before adding them to hLMSC cultures or donor corneas in the processing. The handling of the corneal tissue was done using tying forceps. The processing of corneas was performed in a 55mm Petri dish (Eppendorf), under a dissection microscope (Zeiss Stemi 305).

For isolating the limbus, the cornea was washed with 2X Antibiotic-Antimycotic solution diluted in DPBS (pH 7.4), for 1-2 minutes followed by another wash with DPBS. The posterior side (endothelial side up) of the cornea is placed in 2-3mL of fresh DPBS and the layers of iris and endothelium were scrapped with the help of a surgical blade for better visibility fitted to Bard Parker Handle No.3. The tissue was then laid on its anterior side in fresh 2-3mL DPBS. A clean surgical blade was used to separate the entire 360-degree limbal rim (**Figure 4.4**).

The excised limbal rim is transferred into 1mL of plain DMEM/F12 in a fresh 35mm Petri dish and chopped to 1-2mm wide tissue fragments with the blade. These fragments were minced with Castro Viejo scissors for a couple of minutes and were added with of 20uL of Collagenase-IV enzyme at a concentration 10 IU/μL and gently mixed. This dish was then incubated for 16±1 hours at 37˚C in 5% CO_2 chamber.

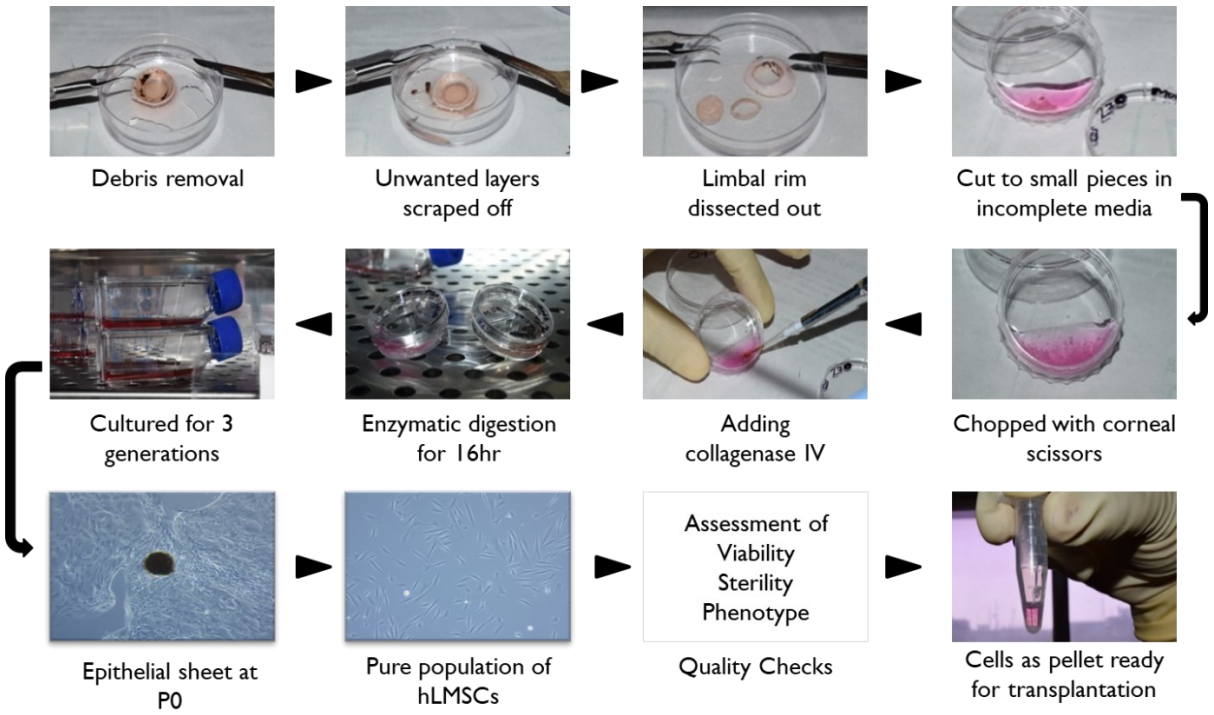

Figure 4.4: Processing of corneoscleral rims: Collage of the photographs elucidating the events of isolation and expansion of hLMSCs

4.4.4.3. Initiation of culture

After collagenase digestion, the enzymatic digestion was halted by adding 2 ml of complete media containing 2% FBS. The digested tissue fragments were then spun down at 1000rpm for 3 minutes at RT, in a 15mL centrifuge tube, with a proper counter-balance. The pelleted fragments were washed twice in DPBS and centrifuged at 1000rpm for 3 minutes, at RT. The tissue fragments were resuspended in 2mL of complete medium. This suspension was aspirated and transferred into a T25 flask with the help of 100-1000uL tips, whose distal ends were cut by ≤5mm long. The cutting of the distal ends of the tips ensures free aspiration of the contents into the passageway of the tip, reducing the shear stress on the tissue fragments. During the transfer, the tissue fragments with the complete medium were dispensed at random locations on the surface of T25, to prevent the attachment of all explants in a single place. The 15mL centrifuge tube is washed with 1mL of complete media and this media is transferred to the same T25 flask to ensure the complete transfer. The flasks were then placed in a chamber with 5% CO_2 and incubated at 37 degrees Celsius.

4.4.4.4. In-process observations, media change, and subculturing

The flasks were left undisturbed till 3 days to facilitate proper attachment of the explants. The flasks were observed for any rapid discoloration in the culture medium, visually without disturbing the flasks. Flaks were then observed under a microscope and imaging was performed every 2-3

days (days 3, 5, 7, 10, and day of confluence). The culture medium (2mL) was replaced following microscopic observation. At each observation, the cultures were assessed for cell morphology, floaters, and color of the medium.

The cultures were passaged on attaining 70-80% confluence. Post microscopic observation and imaging, spent medium at each harvest was collected and stored at 2 to 8°C for in-process testing. The cultures were washed with 2-3 mL of DPBS. Cell dissociation enzyme (2-3 mL), TrypLE was added to the flasks and incubated for 2 minutes at 37°C in a 5% CO_2 chamber. The cells lifted from the surface, are aspirated into a fresh 15mL centrifuge tube containing 1mL of FBS. The flasks were then washed with 1-2mL of DPBS and aspirated into the same centrifuge tube. The suspension was then centrifuged at 1000rpm for 3 minutes at RT. The pellet was washed in 3mL of DPBS and centrifuged at 1000rpm for 3 minutes at RT. The resultant pellet was resuspended in 2mL of complete medium and 10µL of this suspension was collected to quantify viable cells using the Dye-Exclusion assay. The suspension was then seeded at a density of 10^4 cells/cm^2 into new T25 flasks.

This maintenance and subculturing of cultures were performed for four generations (P0 to P3). During passages P2 and P3, the cells were seeded in T75 flasks to facilitate the attachment of more cells and prevent contact inhibition by the hLMSCs. At any stage, 7-8mL of culture medium was maintained in T75 flasks, with 5mL medium replaced on days 3, 5, 7, and 10. The amount of dissociation medium used to harvest cells from P2 and P3 was 2-4 mL. At the end of P3, the cells harvested were subjected to additional tests, listed in **Table 4.4**.

Medium or Suspension	**Description or appearance**	**pH**	**Cell viability**	**BET**	**Microbial screening**	**Mycoplasma**	**FACS**
Complete medium	+	+	-	-	+	-	-
P0 Spent media	+	-	-	+	-	+	-
P1 Spent media	+	-	-	+	-	+	-

Contd..

P2 Spent media	+	-	-	+	-	+	-
P3 Spent media	+	-	-	+	-	+	-
P0 Harvest	+	-	+	-	-	-	-
P1 Harvest	+	-	+	-	-	-	-
P2 Harvest	+	-	+	-	-	-	-
P3 Harvest	+	-	+	+	+	+	+

Table 4.4: List of the in-process tests performed on the culture medium, and the spent medium and cells harvested in each generation of the culture.

4.4.4.5. Cryopreservation

At the end of passage P2, the cells were cryopreserved to assess their stability. Post trypsinization, and quantification of viable cell number, the cell suspension was centrifuged for 3 minutes at 1000rpm/RT. The pellet was resuspended in 500µL - 1mL cryopreservation/freezing medium (**Table 4.3**), based on the cell number. This suspension was aspirated into a cryotube and the centrifuge tube is washed with 500µL - 1mL cryopreservation medium. This medium is transferred into the same cryotube. The cryotubes were then sealed with parafilm and labeled with respective batch numbers.

The density at which the hLMSCs were preserved was 1 million cells/mL of the freezing medium. The cryotubes were then transferred from RT to 2 to 8˚C in a cryocooler filled with Isopropanol, and held for 30 minutes. This was followed by incubation at -20 to -30˚C for 2 hours and then at -80˚C, overnight. The cells were then transferred to the cryo-storage system. The cells were cryopreserved for 3-12 months for further analysis and testing.

4.4.4.6. Cell revival

All reagents required for cell revival: DPBS with 2X antibiotics and complete medium were brought to 37˚C. Cryotubes removed from cryo-storage were immersed in a 37 C dry bath for 15-20 seconds. The contents were then transferred to a fresh 15mL centrifuge tube. The cryotubes were added with 1mL of DPBS with 2X antibiotics and washed or gently agitated if the frozen

blocks still persist. This DPBS is aspirated into the same conical tube and the suspension was centrifuged at 1000rpm for 3 minutes at RT. The pellet was washed with DPBS and centrifuged again at 1000rpm for 3 minutes at RT. The resultant pellet was resuspended in 5mL of complete medium and 10µL of this suspension was collected to quantify viable cells using the Dye-Exclusion assay. The suspension was then seeded to fresh T75 flasks at a density of 10^4 cells/cm^2. The centrifuge tube was washed with 3mL complete medium and was added to the T75 flask.

4.4.4.7. Dye Exclusion Assay

Prior to counting, the cell suspension was titurated to obtain a homogeneously distributed suspension. Ten each microliter of 4% Trypan blue and cell suspension were taken onto a strip of parafilm and gently mixed. The process is repeated on another strip of parafilm. Ten each microliter of these mixtures was taken onto either side of a clean Neubauer chamber and analyzed under a microscope, using a 10x objective. The number of live (unstained) cells and dead cells (stained) in each of the four squares at the vertices of the grid, were counted and noted.

The following factors were taken into consideration during the counting:

a. the number of cells per square was $\lessapprox$15 and $\gtrapprox$50, the suspension was titurated otherwise,
b. the difference between the numbers of cells in any of the squares was $\gtrapprox$20, and
c. cells lying on the edges of these four squares, that were in contact with the five squares in the middle of the grid were excluded.

The formulae used to calculate the cell viability and cell number are as follows:

- *Cell viability (%)* = *[Sum of unstained cells/total number of cells (stained+unstained)] * 100*
- *Viable cells/mL* = *[(Sum of unstained cells/4) * dilution factor] * 10^4*
- *Dilution factor* = *(volume of cell suspension + volume of Trypan Blue)/volume of cell suspension*
- *Total no. of viable cells* = *Viable cells/mL * volume of media in cell suspension in mL*

4.4.4.8. Qualitative assessment of the hLMSC characteristic phenotype

The characteristic phenotype of hLMSCs was qualitatively through immunofluorescence. The cells were plated in a 12-well plate at a density of 10^4 cells per square centimeter and cultured on the surface of sterilized glass coverslips. The culture medium was changed every 2 days till ≥80% confluence.

The confluent cultures were washed twice with 1-2mL of 1X PBS for 5 minutes at RT, after removing the culture medium. After being rinsed twice for 5 minutes with 1X PBS at RT, the cells were fixed with 500 µL of 4% PFA (paraformaldehyde) for 10 minutes at RT. 200µL of 0.3%

Triton-X was used to permeabilize the cells for 20 minutes at room temperature (RT). This was followed by three PBS washes and a 45-minute incubation with 100µL of 2.5 percent BSA in PBS. One hundred microliters of primary antibodies (**Table 4.5**) at appropriate dilutions in 1% BSA were added on to the coverslips and then incubated for overnight at 4˚C. The International Society for Cellular Therapy's minimal standards for multipotent mesenchymal stem cells served as the basis for the establishment of the panel of biomarkers (Dominici et al., 2006).

After three 10-minute PBS washes, 100µL of secondary antibody (**Table 4.6**) diluted in 1 percent BSA was incubated for 45 minutes at RT in dark. Fluoroshield Mounting Medium with DAPI was used to attach the coverslips on a glass slide after three 5-minute PBS washes. DAPI served as a nuclear counterstain. Negative controls were stained without main antibody. An inverted fluorescence microscope captured images (Axio Scope A1, Carl Zeiss).

Primary Antibodies (Unconjugated)	
Ocular biomarkers	**Extracellular / cytoskeletal biomarkers**
PAX-6 (1:100)	α-SMA (1:100)
	Collagen Type I (1:100)
Stem cell biomarkers	Collagen Type II (1:100)
ABCB5 (1:100)	Collagen Type III (1:100)
ABCG2 (1:100)	Collagen Type IV (1:100)
P63-α (1:50)	Collagen Type V (1:100)
	E-Cadherin (1:100)
Mesenchymal/ Surface biomarkers	Keratin (1:100)
CD105 (1:100)	N-Cadherin (1:100)
CD34 (1:100)	Vimentin (1:100)
CD45 (1:100)	
CD73 (1:100)	
CD90 (1:100)	
HLA-DR (1:100)	

Table 4.5: List of the biomarkers assessed for their qualitative expression by hLMSCs.

Secondary Antibody	Dilution ratio
Alexa Fluor 488 anti-rabbit	1:400
Alexa Fluor 488 anti-mouse	1:400
Alexa Fluor 594 anti-rabbit	1:400
Alexa Fluor 594 anti-mouse	1:400

Table 4.6: List of the secondary antibodies used in phenotypic characterization of hLMSCs.

4.4.4.9. Quantitative assessment of the hLMSC characteristic biomarkers

Although the characteristic phenotype of hLMSCs was assessed qualitatively, the logistical constraint of low cell number and limited duration available for quality checks, make it impossible for all the biomarkers be assessed quantitatively as well. Hence, a panel comprising of five major antibodies was chosen to test ever batch of cells produced as part of the quality control. This analysis was done using FACS. The panel of antibodies included P63-α, CD45, CD90, HLA-DR, and ABCG2.

$2x10^4$cells/cm^2 were grown on 18mm coverslips in 12-well culture plates at 37°C with 5% CO_2 in a humidified incubator until confluence. The cells were then incubated for 45-60minutes in dark at 2-8°C. As a comparison, we employed cells that had not been stained, meaning that no primary antibody had been added to the cell solution. After primary antibody incubation, cell suspensions were diluted in 200µL of sheath fluid before being analysed by flow cytometry with a CytoExpert™ analyzer.

4.4.4.10. Evaluation of pelleted hLMSCs viability

Post all quality checks, the hLMSCs were sent for transplantation to the operation theatre. The cells were sent as a pellet in a 1.5mL microcentrifuge tube, with 50uL of complete media supernatant, in a chilled container. The media is left to prevent the cells dying due to unavailability of moisture. However, there could be instances of delayed surgeries due to various reasons. It is necessary for the cells to be alive during this delayed period. Hence, to determine the safe window period between the trypsinization of cells and their delivery onto the recipient eye, the cell viability was assessed when they were stored at +2 to +8◦C.

After determining the viability of hLMSCs using the dye-exclusion technique (identical to that described in **Section 4.4.4.7**), the cell suspension was dispersed evenly among six vials ($5x10^5$ cells/vial/time point) and maintained under ice-cold conditions. At 0.5 hours, 1 hour, 3 hours, 6 hours, 12 hours, and 24 hours, the proportion of viable cells was assessed. This experiment was conducted three times, and the mean viability was determined and graphed.

4.4.4.11. Calculating the growth kinetics

hLMSC cell growth kinetics were also investigated. From hour 0 through Day 6, MTT assay and dye-exclusion were used to count live cells in the culture and determine the doubling times, respectively. For both methods, the cells were plated in triplicates in a 12-well plate, at a density of 20,000cells/cm^2 and cultured for six days. The dye-exclusion test follows the exact same steps as those outlined in **Section 4.4.4.7**.

Each well received 200 mL of 0.25 mg/mL MTT reagent added to culture media free of FBS for the MTT test, which was then incubated for an hour at 37°C in a 5% CO_2 atmosphere. The dimethyl sulfoxide (DMSO, D2650, Sigma Aldrich, USA) was used to solubilize the formazon crystals for 5 minutes at 37°C in a container with 5% CO_2. Using a spectrophotometer and multiple readings of the absorbance at 570 nm against a blank, the concentration was ascertained.

4.4.4.12. Analyzing the hLMSCs' chromosomal stability

An approved third-party laboratory used karyotyping to examine the hLMSCs for chromatin aberrations and mutations. These are the fundamental actions that this procedure entails. Colcemide was used to halt hLMSC cultures that were three to four days old (without encapsulation and post-encapsulation) for spindle development during metaphase. To release the chromosomes from the cell, the cells underwent a hypotonic treatment. The G-banding procedure is then used to make slides, which are subsequently examined using a bright-field microscope. CytoVision® software was used to do the analysis.

4.4.4.13. Microbial screening

The raw materials, medium prepared, and in-process materials like spent media and cell suspension of final harvest were subjected microbial screening. The samples were streaked onto blood-agar plates and were inoculated into thioglycolate media. They were incubated in hot air oven at 37C for 48 hours, to assess the colony formation. Additionally, timely screening (fortnight to quarterly) of the personnel performing the culture activity, LAF and the clean room vents are also screened for possible contaminations using soya-casein-digest agar plates.

4.4.4.14. Mycoplasma testing and analysis

Following the manufacturer's instructions, mycoplasma contamination of the hLMSCs culture was determined (LT07-318, MycoAlert™ Mycoplasma Detection Kit, Lonza, Basel, Switzerland). Mycoplasma contamination was analyzed by measuring the emitted light signal using a

Luminometer (GloMax® 20/20 Illuminometer, E5321, Promega, Madison, USA) in the spent medium of the cells at every passage and the end of passage 3.

4.4.4.15. Determining the endotoxin levels

The levels of bacterial endotoxins in the cell suspension were determined using a gel-clot based kinetic method (N283-125, PYROGENT™ plus Gel Clot LAL Assay, Lonza, Basel, Switzerland) as per the manufacturer's instructions. The procedure involved the preparation of Control Standard Endotoxin (CSE) by rehydrating lyophilized CSE with Limulus Amoebocyte Lysate Reagent Water (LRW). Dilution series of CSE were prepared to obtain desired concentrations. The LAL (Limulus Amoebocyte Lysate) reagent was reconstituted, and the samples were diluted based on the maximum value dilution (MVD) calculated using the known endotoxin limit, potency, and lysate sensitivity provided in the kit.

To calculate the MVD, the formula used was:

$$\textit{Maximum Value Dilution} = \textit{Endotoxin limit X Potency / Sensitivity of Lysate (A)}$$

After calculating the MVD, the samples (cell suspension) were diluted accordingly. For example, if the MVD was determined to be 2, it meant that the sample needed to be diluted two times. The test tubes were then prepared by adding the LAL reagent, the diluted sample, LRW, and positive/negative controls. These test tubes were incubated at 37°C, for 60 minutes in a dry bath. During incubation, gel formation and integrity were observed, and the results were interpreted based on the positive and negative controls. The endotoxin concentration in the unknown samples was determined using serial dilutions and endpoint calculation using the formula:

$$\textit{Endotoxin Concentration} = \textit{Lysate Sensitivity (EU/ml)} \times \textit{Endpoint Dilution}.$$

The lysate sensitivity represents the sensitivity of the LAL reagent used in the assay and is expressed in Endotoxin Units per millilitre (EU/mL). The maximum allowed levels of endotoxins are ≤0.2 EU/mL, as per the FDA guidelines (*Endotoxin Testing Recommendations for Single-Use Intraocular Ophthalmic Devices - Guidance for Industry and Food and Drug Administration Staff*, n.d.; Sharma et al., 2020).

4.5. Storage and transport of hLMSC at ambient temperature

4.5.1. Verification of the insulated container's ability to keep the hypothermic environment

An insulated container with cooling packs (Polybox7, Softbox Systems, India), pre-conditioned to maintain hypothermic temperatures of 30°C, was evaluated in order to have a dependable and reusable system that maintains a normalized range of temperatures regardless of the extreme atmospheric temperatures (**Figure 4.5**). The gel pads surrounding the cell vials were refrigerated 72 hours prior to the hour of encapsulation. 60hours later, the gel pads were arranged in the external Styrofoam container, to obtain the internal temperature to the desired range of 12-15C. 8-12 hours later, when the temperature attains the anticipated range, vials with no cells, were loaded in into the container. The container was then loaded into a standard vehicle with no ventilation or temperature control and transported for 3-5days. This assessment time was constrained to 3-5 days, taking into account how long it would probably take to move cells and across all three seasons in 10 cycles, with at least 3cycles per season. Every four hours throughout this time, the container's inside temperature and the ambient (atmospheric) temperature were both monitored.

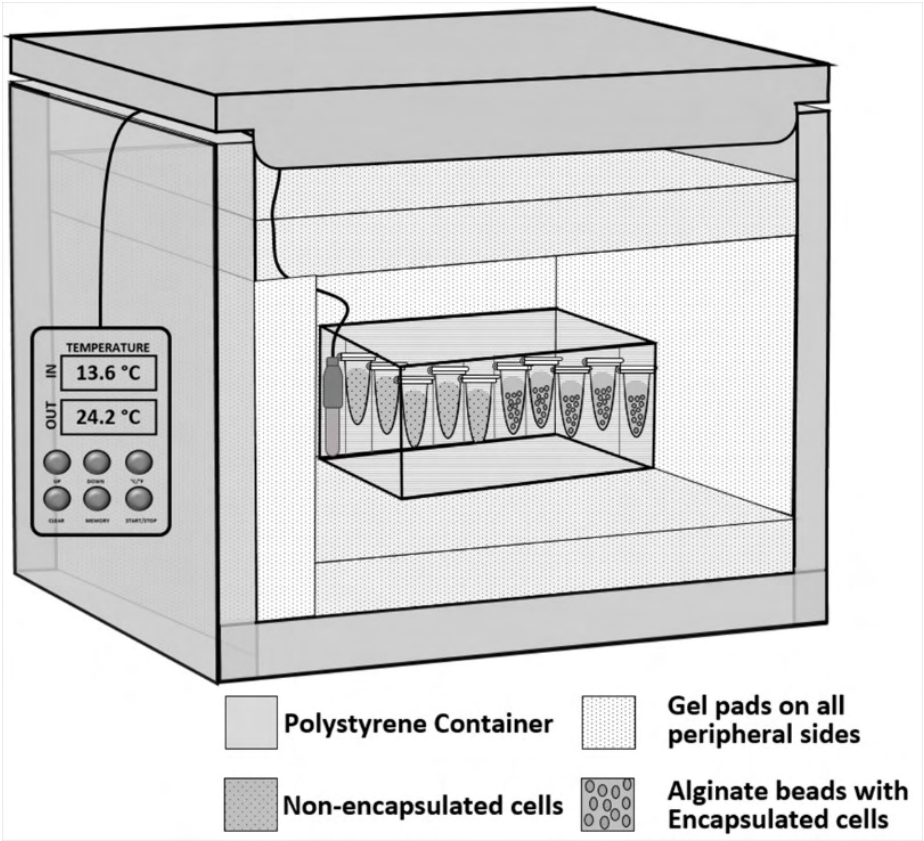

Figure 4.5: Illustration of the insulated container standardized to transport cells at optimal temperatures.

4.5.2. hLMSC encapsulation

A 2.5x10^6 cells/mL cell suspension of hLSMCs was combined with sodium alginate solution from the BeadReady kit, a commercial product offered by Atelerix Ltd. (UK). Through a 21½ G needle, the alginate-cell suspension mixture was gradually dropped into the calcium-chloride based gelation buffer. These alginate-cell suspension droplets were stabilized in the gelation buffer for 8 minutes, causing the beads to polymerize and gel (**Figure 4.6**). After being treated with complete media, the polymerized beads were resuspended in 1mL of fresh complete media.

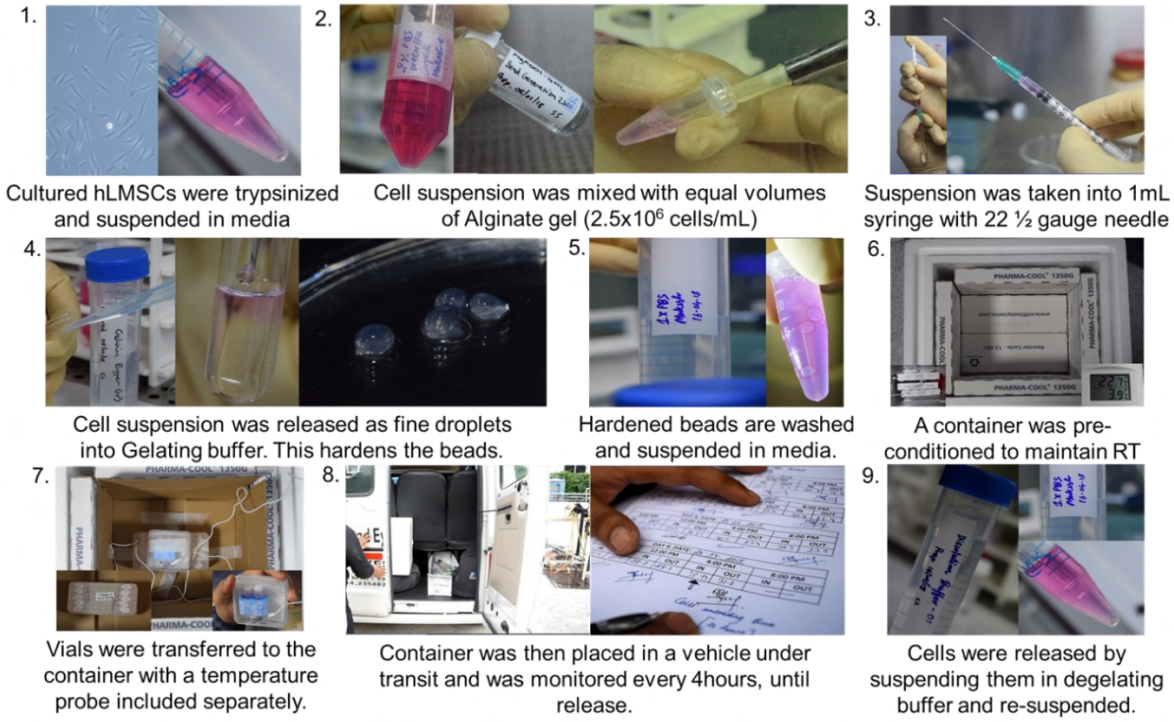

Figure 4.6: Descriptive schematic of the encapsulation procedure and the standardization steps for transporting hLMSCs at optimal temperatures.

4.5.3. Storage and transport of hLMSCs

The alginate-encapsulated cells in the form of polymerized beads were stored in either chilled (4°C) or room temperature (RT) vials (n=5). Up until 3-5 days, the container's interior temperature and the ambient (external) temperature were monitored every 4 hours (**Figure** 4.**6**). The encapsulated cells were transported over a distance of 528.67±64.2 kilometres between three locations in the vicinity of Hyderabad. The transportation was provided by a regular carrier vehicle. The container's outside temperature was used as the control temperature. Similar to above, an equal number of the non-encapsulated cells were either stored or transported. Everything was packaged under carefully controlled conditions. There were three repetitions of this experiment.

4.5.4. **Recovery of hLMSCs from encapsulation**

Alginate beads that contained the cells were rinsed with PBS after transit. They were added with 1.3 mL of the trisodium citrate-based dissolving buffer from the BeadReady kit, and gently stirred while it dissolved for 5 minutes to release the cells from the alginate beads. Centrifugation at 1500 rpm for 5 minutes was used to separate the cells that were suspended in the dissolving buffer. A complete medium was used to resuspend the sedimented cell pellet.

4.5.5. Assessment of viability of recovered cells

A hemocytometer was used to count the number of live (unstained) cells that were extracted from each vial and either transported at room temperature (RT) or kept at 4°C. Following quantification, cells from vials with identical storage conditions (n=5, each at RT and 4°C) were combined. To further analyze their relative survival, gene expression, and expression of phenotypic biomarkers, pooled cells were plated in equal numbers alongwith non-encapsulated cells (cultured under conventional culture conditions) as a control.

4.5.6. Survival of hLMSC in culture (LIVE-DEAD assay)

Recovered cells after transport and storage were assessed for their viability. These cells responded in complete medium were seeded at 20000 cells/cm^2 onto a 18mm coverslip in a 12-well plate and assessed for their survival in cultures, using the LIVE-DEAD assay kit (R37601, Thermofisher, USA) as per manufacturer's instructions. After 48hours of culture, the unattached cells were washed off and wells were added with 1 each mL of LIVE-DEAD reagent. As an experimental control, standard set of cells were pre-treated with 70% EtOH to have dead cells an added with 1mL of LIVE-DEAD reagent. Excess reagent was removed after 15 minutes of incubation at 37°C, and coverslips were mounted on a glass slide using Fluoroshield mounting media with DAPI. Then, fluorescent microscopy (Axio Scope A1, Carl Zeiss AG, Germany) with a 488/570nm filter was used to capture images of the cells.

4.5.7. Relative rate of cell growth of hLMSC in culture (MTT assay)

The cells were plated in triplicates on a 12-well plate, at a density of $2x10^4$cells/cm^2, after being released from 3-day and 5-day storage or transit and having their vitality quantified. The cells were then grown for 48 and 96 hours at 37°C with 5% CO_2 in a humidified incubator. MTT reagent was used to compare the relative survival rates of the cells to the non-encapsulated (cultured in standard culture conditions) control group (M6494, Thermo Fisher, USA).

4.5.8. Qualitative assessment of the characteristic phenotype

Released cells were assessed for viability after RT transit or storage at 4 °C for 3-5 days. For 48 hours, $2x10^4$ cells/cm^2 were grown on coverslips in 12-well culture plates at 37°C with 5% CO_2 in a humidified incubator. These cells were screened for hLMSC biomarkers.

Cultured cells were rinsed twice in PBS before being fixed for 20 minutes in a solution of 4% paraformaldehyde in PBS. Triton-X 0.03 % [vol/vol] in PBS was used to permeabilize the cells, which was followed by two PBS washes that lasted five minutes each. To prevent the non-specific protein-protein interactions, cells were treated for 1 hour with 2.5% BSA in PBS. At RT, moist conditions were used for all of the incubations. Cells were then treated for two hours with primary antibodies in 100 microliters of 1% BSA in PBS after the blocking solution had been removed.

The antibody panel used in this study consisted of several markers to identify specific cell phenotypes. The positive markers for the human limbal stem cell phenotype included ABCG2, Pax6, p63-α, and Col-III. These markers are known to be associated with limbal stem cells. On the other hand, HLA-DR and CD45 were used as negative markers, indicating the absence of mesenchymal origin. In addition to the limbal stem cell markers, the panel also included positive markers for the mesenchymal phenotype, namely CD73, CD105, and VIM. These markers are commonly expressed in mesenchymal cells.

Following the incubation with primary antibodies, cells on coverslips were rinsed twice in PBS for five minutes each. Following a 45-minute incubation with secondary antibodies (1:400) diluted in 100μL of PBS containing one percent BSA, the cells were washed three times for ten minutes each. The panel of secondary antibodies includes anti-mouse and anti-rabbit Alexa Fluor 488 (A11001, Thermo Fisher, USA) (A11008, Thermo Fisher, USA). Fluorescent microscopy imaging was carried out using an Axio Scope A1 Carl Zeiss AG, Germany, fluorescent microscope with a 20x–40x objective after cells were mounted using Fluorosheild mounting media with DAPI (ab104139, Abcam, UK). Three times this experiment was repeated.

The percentage of cells positive for a specific biomarker was determined by analyzing images from the central (1 image) and peripheral areas (2 images) of the coverslip. The results were tabulated, with lack of expression represented as (-), <25% positive cells as (++), 25-50% as (+++), and >90% positive cells as (++++)

4.5.9. Quantitative assessment of the characteristic biomarkers

In order to assess the level of gene expression, one million cells from each storage category were employed after they had been released from their encapsulation. For the control, we utilized freshly

lysed cells derived from the culture. After isolating total RNA with the Trizol (15596018, Thermo Fisher, USA) technique, the RNA was then converted to cDNA with Superscript-III (1808051, Thermo Fisher, USA) at a concentration of 1 μg/μL of RNA per 20 μL of reaction mix. Real-time PCR was performed on the cDNA that had been produced by utilizing a Maxima SYBR Green kit (K0221, Thermo Fisher, USA) with 200ng of template per 25 μL of reaction mix.

Within the confines of the detecting system, the reaction was carried out (Applied Biosystems, USA). The reactions were carried out in parallel. In these investigations, the GAPDH gene served the purpose of a housekeeping gene. The data on gene expression were standardized so that the variation in expression levels could be brought under control and brought closer to the geometric mean of the housekeeping gene. The data were examined via the lens of the $2^{-\Delta\Delta CT}$ approach. The primer sequences are detailed in **Table 4.7**.

Sl #	Primer	Sequence	Size	T_m (°C)
1	GAPDH	Forward: ACCACAGTCCATGCCATCAC	452bp	55°C
		Reverse: TCCACCACCCTGTTGCTGTA		
2	CD90	Forward: CGCTCTCCTGCTAACAGTCTT	142bp	60°C
		Reverse: CAGGCTGAACTCGTACTGGA		
3	PAX-6	Forward: ATAACCTGCCTATGCAACCC	208bp	58°C
		Reverse: GGAACTTGAACTGGAACTGAC		
4	TAp63-α	Forward: GAGGTTGGGCTGTTCATCAT	183bp	57°C
		Reverse: AGGAGATGAGAAGGGGAGGA		

Table 4.7: List of genes (primers) and their nucleotide sequences assessed for the relative expression of the genotype

4.6. Evaluation of the toxicity and safety of hLMSCs

4.6.1. Experimental design

A total of 18 New Zealand White strain rabbits, aged 12 to 16 weeks, were used in the study. The rabbits were evenly distributed into three groups, with 6 rabbits in each group (3 males and 3 females). The groups were as follows: control or sham-treated group (G1), G2 (En- hLMSCs) group treated with hLMSCs that were not encapsulated, and G3 (En+ hLMSCs) group treated with hLMSCs encapsulated in sodium alginate and transported at room temperature. A schematic diagram illustrating the experimental design can be found in **Figure 4.7**.

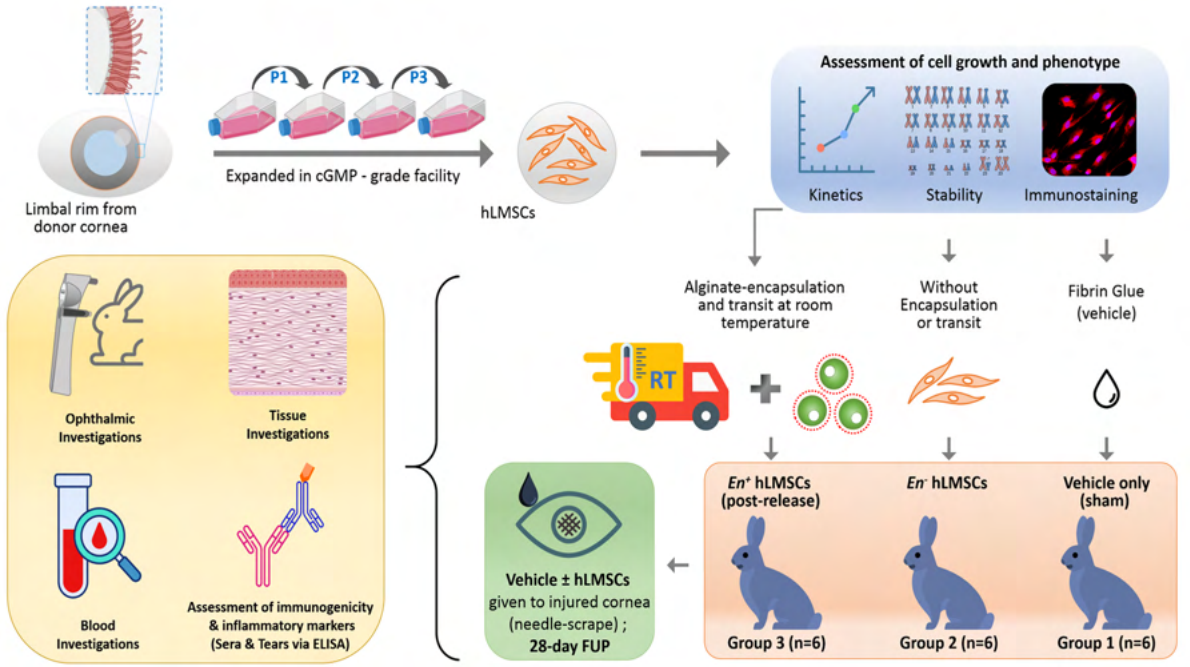

Figure 4.7. Schematic of the safety and toxicity study design.

4.6.2. Animal maintenance and observations

The stratified randomization procedure was used to divide the animals into three groups after at least five days of acclimatization before the experiment. An examination by a veterinarian was done before to the trials to make sure the animals were healthy and appropriate for the research. Throughout the course of the trial, animals were checked twice a day for mortality and morbidity and once a day for clinical symptoms. On the day of therapy and then every week after, individual body weights were noted. Kilograms were used to measure the bodily weights (Kg).

4.6.3. Wounding the ocular surface of rabbits

For the experiment, the rabbits received anesthesia via an intramuscular injection of a Ketamine (35mg/Kg body weight) and Xylazine (10mg/Kg body weight) mixture. Topical anesthesia was applied to the left eye using 1-2 drops of 0.5% proparacaine hydrochloride. To ensure cleanliness, the eyes were gently cleansed using a cotton swab soaked in 0.5% povidone-iodine eye drops. Subsequently, a sterile needle was used to perform a gentle scraping of the eyes.

4.6.4. Dosing of the wounded eyes with hLMSCs

During the experiment, the rabbits in groups G2 and G3 had their test eyes treated with 50×10^4 En- hLMSCs and En+ hLMSCs, respectively. The cells were dissolved in 100µL of a commercially available fibrin glue composition (TISSEEL LYO, Baxter International Inc., Illinois, USA). In contrast, the control or sham-treated group received only the fibrin glue composition without any cells. After administering the substances, the eyelids were gently closed for 3-5 seconds to ensure retention of the test items. Following the procedure, the treated eyes were covered with sterile dressing pads until the rabbits recovered from anesthesia. The animals were closely monitored for irritant and corrosive effects at specified time points, including hours 1, 24, 48, and 72 post-dosing.

4.6.5. Grading of the ocular surface of rabbits after dosing

To find alterations in the cornea, conjunctiva, iris, and aqueous humor, slit-lamp examination (PSLAIA-11, Appasamy Associates, India) was carried out. Ophthalmic exams of the cornea and conjunctiva were performed using fluorescein sodium ophthalmic strips. The ocular observations were graded in accordance with Schedule Y and the numerical scoring system specified in Test No. 405 "Grading of Ocular Lesions" of the OECD Guidelines for the Testing of Chemicals. Prior to dosing, during the third, sixth, twelfth, and twenty-fourth hours of day one, and on days 7, 14, and 28 after dosing, slit lamp and IOP observations were made. **Table 4.8** lists the scoring guidelines.

Observation	Score
Corneal opacity	
• *No ulceration or opacity*	0
• *Scattered or diffuse areas of opacity (other than slight dulling of normal lustre); details of iris clearly visible*	1
• *Easily discernible translucent area; details of iris slightly obscured*	2
• *Nacreous area; no details of iris visible; size of pupil barely discernible*	3
• *Opaque cornea; iris not discernible through the opacity*	4
Iris	
• *Normal*	0
• *Markedly deepened rugae, congestion, swelling, moderate circumcorneal hyperaemia; or injection; iris reactive to light (a sluggish reaction is considered to be an effect)*	1
• *Haemorrhage, gross destruction, or no reaction to light (any or all of these)*	2
Conjunctival Redness (Refers to palpebral and bulbar conjunctivae; excluding cornea and iris)	
• *Normal blood vessels*	0
• *Some blood vessels definitely hyperaemic (injected)*	1
• *Diffuse, crimson colour; individual vessels not easily discernible*	2
• *Diffuse beefy red*	3
Chemosis (swelling of lids and/or nictitating membranes**)**	
• *No swelling (Normal)*	0
• *Some swelling above normal (includes nictitating membranes)*	1
• *Obvious swelling with partial eversion of lids*	2
• *Swelling, with lids about half closed*	3
• *Swelling, with lids more than half closed*	4

Table 4.8. List of the parameters of ophthalmic observations and their respective scores for grading of the severity.

4.6.6. Blood and tear sample collection

At various time intervals, including 1, 6, 12, and 24 hours, as well as on days 7, 14, 21, and 28 after administration, blood samples were collected from the animals. Approximately 3-4 mL of blood was obtained from each animal using plain vacutainers. The collected blood samples were then processed to isolate the serum, which was subsequently stored at -80°C for further analysis.

In addition to blood samples, tear fluid samples were also collected at specific time points throughout the study. Tear strips were used to collect tear fluid from the animals at 1, 3, 6, 12, and 24 hours, as well as on days 7, 14, 21, and 28 after administration. These tear fluid samples were carefully collected and stored at -80°C for the assessment of specific markers including IL-6, TNF-α, and IgE.

4.6.7. Isolation of total protein from tear samples

To extract tear fluid from frozen Schirmer's strips, the protocol described by Posa et al. in 2013 was followed. Firstly, the frozen strips, obtained from Tear Strips by Care Group, Gujarat, India, were carefully positioned close to the base of a sterile 0.5mL microcentrifuge tube using forceps. A sterile 22 ½ gauge needle was used to puncture the 0.5mL microcentrifuge tube, allowing the tear fluid to be collected. To facilitate the collection process, the entire assembly was inserted into a 1.5mL microcentrifuge tube.

Next, approximately 10-50µL of 1x PBS (phosphate-buffered saline) was added to the strip, taking into account the length (mm) of the strip and the absorption capacity of the tear fluid. The setup was then incubated at 2-4°C for a duration of 30 minutes to allow for proper fluid extraction. Following the incubation, the assembly was centrifuged at 13,000rpm for 5 minutes at 4°C. After centrifugation, 1µL of the extracted tear fluid was utilized for protein quantification, while the remaining tear fluid was promptly stored at -80°C for future analysis purposes.

4.6.8. Protein estimation by Bicinchoninic acid (BCA) assay

The protein quantification in the tear fluid was conducted using the BCA assay, which is a colorimetric assay. The BCA assay kit (786-570) from G-Biosciences, Geno Technology Inc., Missouri, USA, was employed following the manufacturer's protocol.

For the assay, standard solutions with concentrations ranging from 2000 µg/mL to 0 µg/mL were prepared. The tear fluid samples, along with the standards, were subjected to the BCA assay. The absorbance of the resulting solutions was measured at 562nm using a SpectraMax M3 microplate reader system from Molecular Devices, California, USA.

Based on the standard graph obtained using the known concentrations of the standards, the protein concentrations of the tear fluid samples were determined. The absorbance values of the unknown samples were compared to the standard curve to calculate their corresponding protein concentrations. This quantitative analysis allowed for the assessment of protein levels in the tear fluid samples.

4.6.9. Determination of inflammatory cytokines by ELISA

The inflammatory markers in the rabbits' samples were quantified using sandwich ELISA methods. Commercially available antibody-coated kits from KinesisDx, Krishgen Biosystems, USA, were used for this purpose. The specific kits used were IgE (K09-0071), IL-6 (Ref: KLX0003), and TNF-α (KLX0065).

In the assay, 40µL of each sample (sera/tear) was added to the respective wells of the ELISA plate. Subsequently, 10µL of the corresponding biotinylated antibodies was added to each well, except for the standards which did not require biotinylated antibodies. The plate was then incubated at 37°C in the dark for 1 hour.

After the incubation, the wells were washed four times with 1x wash buffer using an automated washer system (Erba Lisa Wash II, Erba Mannheim, London, UK). The residual buffer was removed by tapping the plate firmly onto an absorbent paper. Next, 50µL of Streptavidin-HRP conjugate solution was added to each well, followed by another incubation period.

Following this, the wells were washed again, and 50µL each of substrate A and substrate B were added to induce a color reaction. The plate was incubated for 10 minutes, and then the reaction was stopped by adding 50µL of stop solution to each well. The resulting color developed in each well was measured at 450nm using the SpectraMax M3 microplate reader system from Molecular Devices, USA. This allowed for the quantification of the inflammatory markers in the samples based on the absorbance readings.

4.6.10. Necropsy, Organ Weights, and Histological Examination following Euthanasia

Following the completion of the experimental study on day 29, humane euthanasia was performed on all the animals in the sham, En- hLMSCs, and En+ hLMSCs groups. After euthanasia, a series of procedures were conducted to evaluate the animals' tissues and organs in detail. This included necropsy, organ weight measurement, and histopathological examination, which aimed to provide comprehensive insights into the overall health and potential morphological changes associated with the different treatment groups.

Necropsy began with a thorough observation of the external features of each animal to identify any visible abnormalities or signs of pathology. This initial assessment served as an important screening step to detect any gross morphological changes that might have occurred as a result of the experimental interventions.

Following the external observations, an in-situ examination of the organs was carried out. Each organ was carefully examined to identify any gross alterations in shape, color, texture, or consistency. This meticulous evaluation aimed to detect any macroscopic changes or abnormalities that might have developed during the study.

After the completion of the gross pathology examination, specific organs of interest were collected, and their individual weights were recorded. The weights of these organs were expressed as ratios relative to the animals' body weights, allowing for a quantitative assessment of any potential alterations in organ size or mass.

To complement the macroscopic observations, histopathological examination was performed on the collected organs. The organs were preserved in a 10% buffered formalin solution. Histopathological examination involved the preparation of thin sections from the preserved organs. These sections were stained with various histological dyes to enhance the visualization of cellular structures and to identify any histopathological changes – presence of cellular abnormalities, inflammation, necrosis, or any other histological alterations.

4.6.11. Hematology Analysis of Blood samples

In order to gain insights into the hematological profile of the animals, blood samples were collected and subjected to comprehensive hematological analysis using a Hematology cell counter, SYSMEX-XP 100, Japan. To prepare blood smears for microscopic examination, a small amount of the collected blood sample was carefully spread onto glass slides. These slides were then subjected to staining using Leishman stain for better visualization of cellular structures and identification and characterization of different blood cell types.

Once the blood smears were appropriately stained, a differential leukocyte count was performed using conventional microscopy. All the parameters were evaluated based on established reference ranges, enabling a comparative assessment of the animals' hematological status and any potential deviations from normal values.

S. No.	Parameter	Abbreviation	Unit	Purpose/Use
1	Haematocrit	HCT	%	Measures the percentage of red blood cells in the blood.
2	Haemoglobin	Hb	gm/dL	Quantifies the concentration of hemoglobin in the blood.
3	Mean Corpuscular Volume	MCV	fL	Indicates the average volume of red blood cells.
4	Platelets	Plat	10^3/µL	Measures the number of platelets involved in clotting.
5	Red Blood Corpuscles	RBC	10^6/µL	Quantifies the count of red blood cells in the blood.
6	White Blood Corpuscles	WBC	10^3/µL	Measures the count of white blood cells in the blood.
7	Differential Count	DLC	%	Percentage of different types of white blood cells in the blood, including neutrophils, lymphocytes, monocytes, eosinophils, and basophils.
	a) Neutrophils	Neut		
	b) Lymphocytes	Lymph		
	c) Monocytes	Mono		
	d) Eosinophil	Eos		
	e) Basophils	Baso		
8	Reticulocyte Count	RC	%	Measures the percentage of immature red blood cells.
9	Terminal Bone Marrow Examination	BME	-	Involves the examination of bone marrow for diagnostic purposes.
10	Abnormal Immature Cells	AIC	-	Identifies the presence of abnormal immature cells in the blood.
11	Bleeding Time	BT	Minutes	Measures the time taken for bleeding to stop after an injury.
12	Coagulation Time	CT	Minutes	Determines the time required for blood to clot.
13	Prothrombin Time	PT	Seconds	Assesses the time taken for blood to clot through the extrinsic pathway.
14	Activated Partial Thromboplastin Time	APTT	Seconds	Measures the time needed for blood clotting through the intrinsic pathway.
15	Erythrocyte Sedimentation Rate	ESR	mm/1st hr	Indicates the rate at which red blood cells settle in a vertical tube over time.

Table 4.9: The table provides a comprehensive list of hematological parameters measured during the study, along with their respective abbreviations and units of measurement

4.6.12. Clinical biochemistry of blood samples

Sera collected from the blood samples were analyzed for clinical chemistry parameters using an automated Random Access Biochemical Analyzer (EM-360, Erba Mannheim, London UK). The parameters measured and analyzed are listed in **Table 4.10**.

S. No.	Parameter	Abbreviation	Units
1.	Serum Glucose (GLU)	GLU	mg/dL
2.	Blood Urea Nitrogen	BUN	mg/dL
3.	Serum Creatinine	CREAT	mg/dL
4.	Serum Total Bilirubin	TBILL	mg/dL
5.	Alanine Aminotransferase	ALT	IU/L
6.	Aspartate Aminotransferase	AST	IU/L
7.	Serum Alkaline phosphatase	ALP	IU/L
8.	Serum Total Protein	PRO	g/dL
9.	Serum Albumin	ALB	g/dL
10.	Globulin	GLB	g/dL
11.	Serum Total Cholesterol	CHOL	mg/dL
12.	High-density lipoprotein	HDL	mg/dL
13.	Low-density lipoprotein	LDL	mg/dL
14.	Serum Phosphorous	PHOS	mg/dL
15.	Serum Calcium	Ca	mg/dL
16.	Serum Sodium	Na	mmol/L
17.	Serum Potassium	K	mmol/L
18.	Gamma-glutamyl transferase	GGT	IU/L

Table 4.10: List of clinical chemistry parameters observed, along with their corresponding abbreviations and units of measurement.

4.7. Assessment of the efficacy of hLMSCs in healing and preventing corneal scars

4.7.1. Experimental design

A total of fifty-six, 6 to 8-week-old C57BL/6 mice, weighing 22-25grams, were used for this study. Simple or unrestricted randomization was followed in the allocation of the mice to the study groups and subgroups. The study has three treatment arms – (i) scar group, (ii) prophylaxis and (iii) untreated groups. The scar and prophylaxis groups had three each subgroups, with 8 mice per every subgroup, similar to the toxicity study. The subgroup 1 was treated with sham (vehicle only), the subgroup 2 was treated En- hLMSCs and subgroup 3 was treated with En+ hLMSCs. The treatment was given immediately post debridement of the corneal layers in the prophylaxis group. The scar group mice were treated two-weeks post corneal debridement. The mice were allowed to develop corneal scars during this period. The mice of untreated group (n=8), did undergo debridement of the corneal layers, but were not provided with any treatment. The mice were allowed to develop the scar and the extent of the clearing of scarred area was tracked till the end of 8 weeks post debridement.

4.7.2. Animal maintenance – C57BL/6 mice

Mice were acclimatized at least one week before the beginning of the study. Four to five mice per cage were maintained in individually ventilated cages (IVC) with ad libitum feeding.

4.7.3. Generating corneal scar

During the course of the experiment, the mice were anesthetized using a combination of Xylazine and Ketamine diluted in normal saline. Xylazine (ilium Xylazil-100, Troy Laboratories Australia PTY LTD, New South Wales, Australia) was administered at a dosage of 100mg/kg of body weight, while Ketamine (Aneket®, Neon Laboratories Limited, Mumbai, India) was administered at a dosage of 10mg/kg of body weight. The anesthesia was delivered intraperitoneally to induce general anesthesia in the mice.

To prevent the eyes from drying during the experimental procedures, TearsPlus lubricating eye drops (Allergan India Pvt Ltd, Bangalore, India) were applied to both eyes of the mice. In case of any dust particles present in the eyes, they were carefully removed using a surgical spear (EYETEC, Gujarat, India) and the eyes were lubricated again. Topical anesthesia was then administered to both eyes using 0.5% proparacaine (Paracain, Sunways India Pvt Ltd, India).

For the purpose of the experiment, Algerbrush II (Accutome Inc., Pennsylvania, United States) equipped with a 0.5 mm burr was used. The burr was gently rotated in a circular motion on the central cornea of the right eye, extending towards the peripheral cornea, for a duration of 15-20 seconds. This procedure aimed to selectively remove the epithelium and a portion of the anterior stroma in the central cornea, while keeping the limbus, sclera, and other parts of the ocular surface unaffected. Following this, the mice were allowed a two-week period for scar development or were immediately subjected to further treatment as per the experimental design.

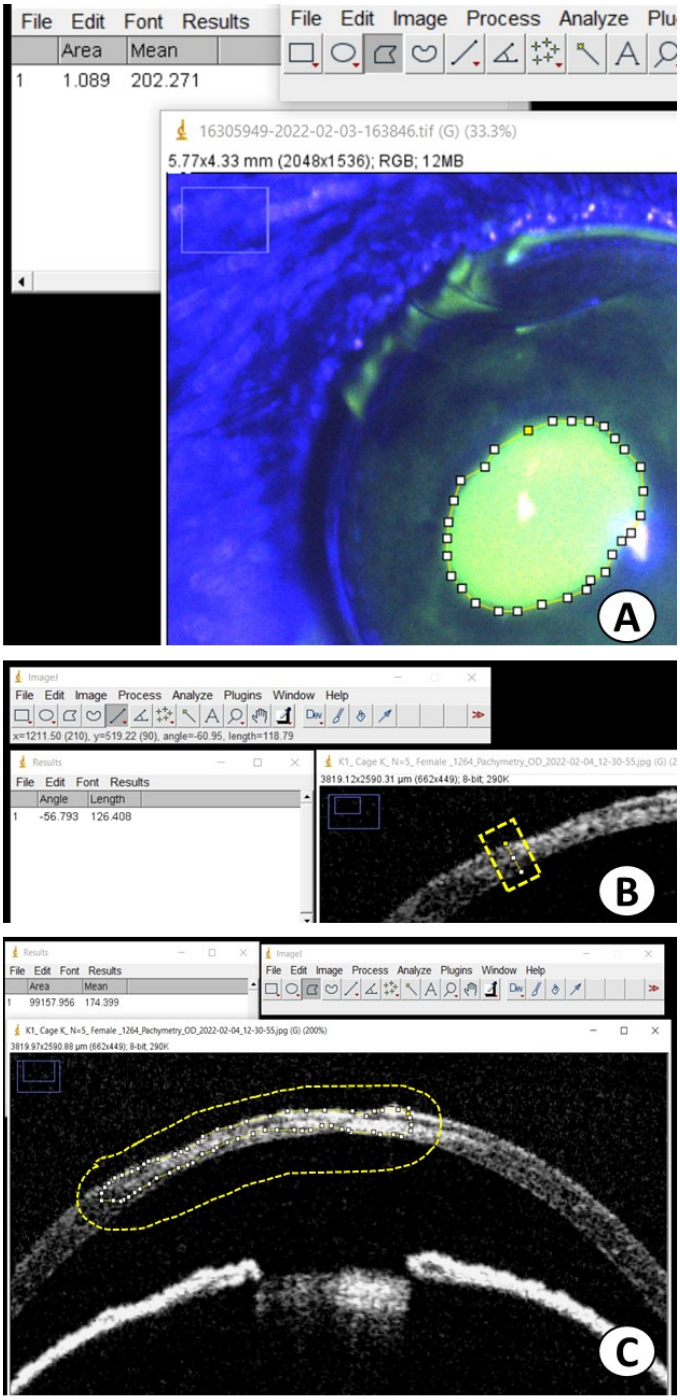

Figure 4.8: Assessment of the corneal thickness and transparency: A) Snapshot illustrating the calculation of wounded corneal surface using ImageJ software to quantify the reepithelization B) Representative image showing the Measuring of corneal thickness and its individual layers C) Representative image illustrating the quantifying the scarred area and mean grayscale value using free-hand.

4.7.4. Transplantation of hLMSCs to scarred corneas

The scarred/debrided corneas were scraped gently with surgical blade #15 to remove the damaged tissue and then treated with 50×10^3 En-/En+ hLMSCs mixed in 2μL of fibrin glue. This fibrin glue cured to form a gel-clot within 1 minute of application. The contralateral eye (right) was used as normal control in all the groups.

4.7.5. Clinical follow-up and imaging

The clinical assessment of the mice included several procedures to evaluate the condition of their eyes. These procedures included clinical photography, optical coherence tomography (OCT) scans using pachymetry to obtain detailed cross-sectional images of the corneal layers, and fluorescein staining of the ocular surface. The purpose of these assessments was to examine the transparency and thickness of the corneal layers, detect the extent of damage in the central cornea, and monitor the closure of the created wound.

The clinical assessments were performed on both eyes of the mice before the surgical wounding and prior to the treatment with human limbal mesenchymal stem cells (hLMSCs). Following the surgery and wounding, the mice's eyes were evaluated at specific time points, including day 1, day 3, day 7, day 10, day 14, and then once a week thereafter until the end of the study, which was 4 weeks post-treatment in both the scar group and the prophylaxis groups to observe and compare the effects of the treatment.

4.7.6. Corneal thickness and transparency measurement

The clinical images were evaluated using ImageJ software (**Figure** 4.**8**) to determine the scarred area (normalized to baseline/post-debridement), and grayscale units (GSU) of the OCT scans to determine the transparency of corneal cross sections.

The rate of reepithelization was assessed by quantifying the wounded area (mm^2) from the fluorescein stain images (**Figure** 4.**8A**) relative to the pre-wound image of the same eye. The E:S (epithelium to stroma) was measured by taking the mean of 10 thickness reads of each layer in the wounded area. The scar area and the mean gray scale value of the scarred cornea was measured by selecting the area of scar using free-hand and quantifying the respective area (**Figure** 4.**8C**) and comparative analysis of these values to the respective baseline readings.

4.7.7. Euthanization and histological analysis of corneas

At the conclusion of the study, the mice were euthanized to allow for further analysis. The whole eyeballs of both eyes from each mouse were carefully collected for histological analysis. This involved preserving the eyeballs in 10% formalin solution.

4.8. Statistical analysis of the experimental data

To ensure the reliability and robustness of the experimental results, all experiments were conducted in at least biological triplicates or more, as necessary. Additionally, wherever applicable, two or more independent readings were taken to account for any variability and increase the accuracy of the data.

For the statistical analysis of the data, appropriate methods were employed to determine the significance of the observed differences or associations – such as the Student's t-test and the Kruskal-Wallis test, were employed based on the nature of the data and the experimental design.

The Student's t-test is a parametric statistical test used for comparing the means of two groups. It assesses whether the observed differences between the groups are statistically significant or simply due to chance. This test calculates a p-value, which represents the probability that the observed differences occurred by random chance. If the p-value is below a predetermined significance level (usually 0.05), it indicates that the differences between the groups are statistically significant.

The Kruskal-Wallis test, on the other hand, is a non-parametric test used when comparing the medians of three or more groups. It is employed when the assumptions required for the t-test are not met, such as when the data is not normally distributed or the sample sizes are small. This test ranks the data and determines whether there are significant differences among the groups based on the ranked values.

The significance level for both tests was set at 0.05, which means that if the calculated p-value is less than 0.05, the differences or associations observed in the data are considered statistically significant.

For the statistical analysis, GraphPad Prism software version 5.0 was utilized.

Chapter 5

Results

5.1. Optimizing the methods for isolation, characterization of hLMSCs, and the assessment of their quality and stability

5.1.1. Continuous Control, Regulation, and Monitoring of activities in the clean room

- All the set parameters of the clean room specifications, for example, maintenance of set temperature and humidity, particle count per cubic feet of air, etc., were all maintained during the entire course of this study, which ensured the cell culture activity was carried in controlled and aseptic conditions.
- No deviations of any kind were found with the quality of air evident from the negligible colonies (i.e., ≤2 colonies, specified alert limit) of microbes grown in soybean casein digest agar plates (settle-plate method) (**Figure 5**.1).
- The personnel involved in the clean room activities and the sterile gowns were also monitored periodically to ensure no transfer of microbes or skin cells shed into the production line. The suit contact plates and finger dab plates have not shown any colonies of the microorganisms, beyond the specified alert limit (i.e., ≤2 colonies).

Conclusively, all the set parameters of the specifications laid down for the control, regulation, and monitoring of the activities, facility, and personnel of the clean room, were within the permissible levels or allowed limits.

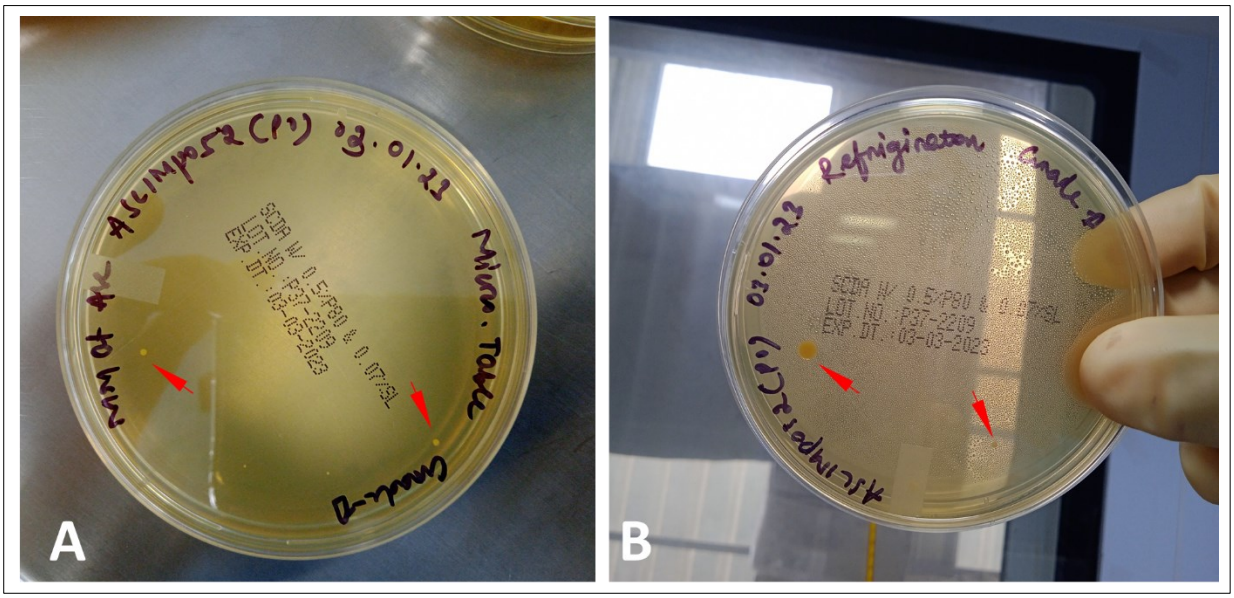

Figure 5.1: Monitoring the aseptic conditions for cell culture activity: **(A-B)** Photographs of the soybean casein digest agar plates showing the negligible number of colonies (red arrow) within specified alert limit, indicating the quality of air and environment in the clean room.

Expansion of hLMSCs in culture

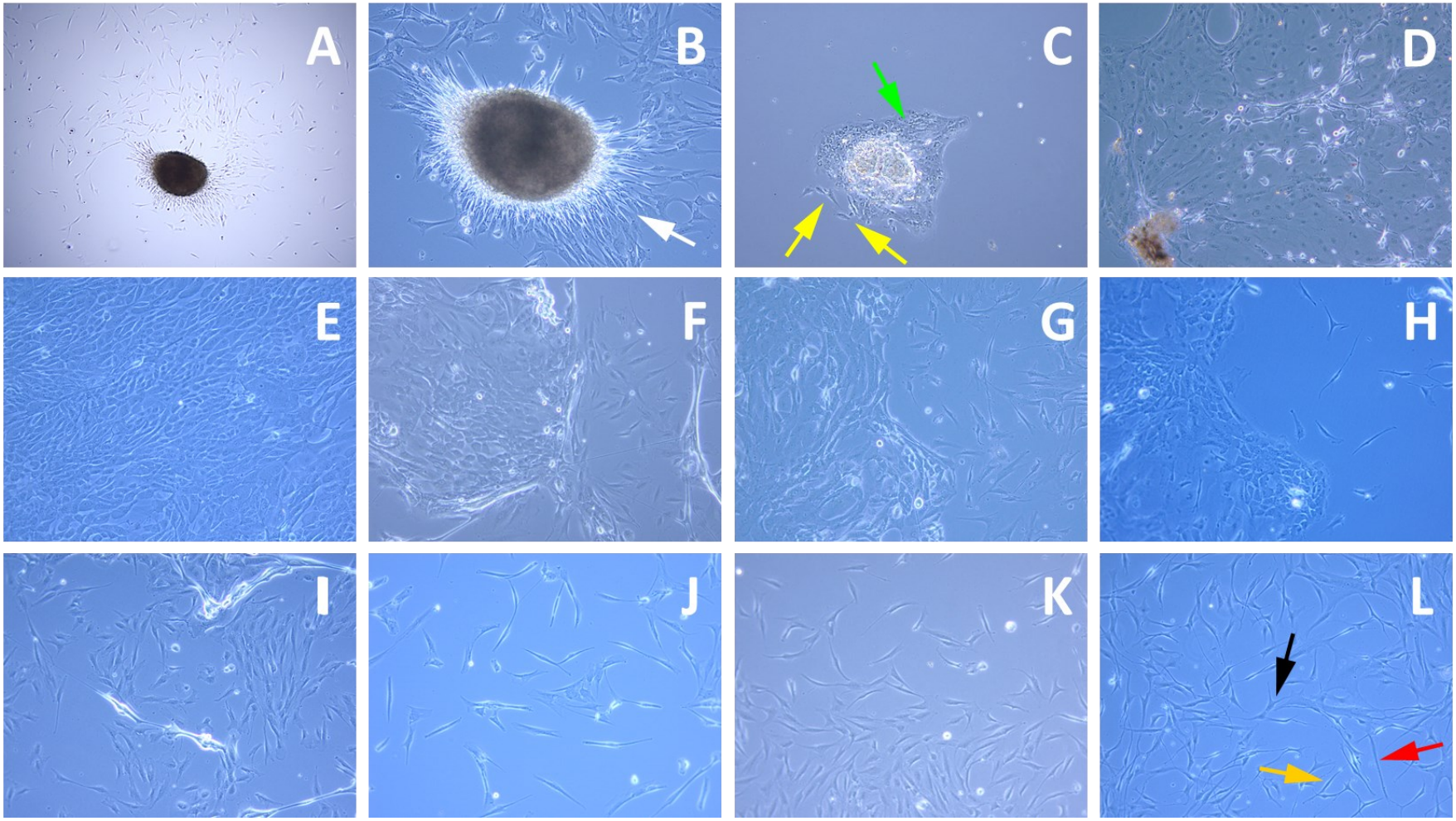

Figure 5.2: Expansion of the hLMSCs in culture: Spindle-shaped stromal cells initiating from the limbal explant, at primary generation (P0) image at 40X magnification (**A**) and 100X magnification (**B**). Both epithelial (cuboidal, indicated with a green arrow) and stromal phenotype cells (indicated with yellow arrows) initiating from the same explant in primary culture (**C**). The primary culture is mostly dominated by epithelial phenotype at the early stages (**D**, on day 3) and at the confluence (**E**, on day 13). The stromal cells gradually increase in number (**F**) after a passage with the epithelial phenotype diminishing in number in the late P1 (**G**) and early P2 generations (**H**). By end of the P2 generation (**I**), ~10% of the epithelial cells were found to be surviving. A pure population of the stromal phenotype in P3 generation (**J-L**). The hLMSCs at early (**J**), mid (**K**), and confluence (**L**) stages, which also include dendritic cells (indicated with a black arrow), undifferentiated fibroblastic cells (indicated with an orange arrow), and quiescent fibroblastic cells (indicated with a red arrow). Magnification (**B-L**): 100X. This data was published in part at DOI: 10.3390/ijms23158226, by (Damala et al., 2022).

5.1.2. Isolation and expansion of hLMSCs

The human limbus-derived mesenchymal/stromal stem cells (hLMSCs) isolated and expanded from the corneal limbal explants were observed to have grown from the explants (**Figure 5.2 A-C**) in the primary generation itself (P0). However, this generation was dominated by the limbal epithelial cells covering 70–90% of the culture flask's surface area.

With the serum maintained at very low levels of ≤2%, the epithelial sheets started to grow in fewer numbers in P1, relative to P0 generation, providing more room for the hLMSCs to expand in the P1 stage (**Figure 5.2 F-G**). By the end of the P2 stage, the number of hLMSCs outnumbered the epithelial population with a smaller number of the epithelial phenotype growing (**Figure 5.2 I**). In P3 generation, a population of the stromal cells were obtained without any epithelial phenotype growing along with the hLMSCs. The cells also included dendritic cells, and cells with fibroblast and myofibroblast morphology in negligible numbers (**Figure 5.2 L**).

5.1.3. Yield, Viability and Adverse events

- In terms of numbers, at confluence the yield per flask, i.e., the number of viable hLMSCs per one T75 flask has ranged at 1×10^6 to 2.5×10^6. Each corneolimbal rim (from one donor cornea) gave rise to 6-8 T75 flasks. This enables the availability of hLMSCs in at least 4–5 doses per one donor cornea, after all the testing procedures. A single dosage to one recipient eye consists of 0.5×10^6 hLMSCs (J. Funderburgh et al., 2018; Basu et al., 2019a).

- The viability of the cells after trypsinization assessed through dye-exclusion assay was always >90%, where the acceptable levels were ≥70%.
- The morphology of cells was found to be cuboidal/spindle/dendritic throughout the cultivation period, as per the set specifications. Cell infiltration of no other kinds (conjunctival/scleral epithelia) were observed.
- Any culture that did not grow to the minimal cell yield at any of the culture, to the set specifications was discarded and the respective batch thereafter, was discontinued.
- No other observations like rapid discoloration of media during the culture, or a change in the turbidity were noticed.

5.1.4. Determination of the characteristic phenotype of hLMSCs

5.1.4.1. Qualitative assessment of the hLMSCs' characteristic phenotype of hLMSCs - Immunofluorescence

The expression of biomarkers for the characteristic phenotype was assessed through immunofluorescence.

The panel of biomarkers included various ocular, stem cell, mesenchymal/surface, and cytoskeletal biomarkers (**Table 4.5 of Methods**).

- The hLMSCs were tested positive for the ocular biomarker Pax6 and stem cell biomarkers ABCG2 and p63-α (panel on top, **Figure 5.3**).
- The surface biomarkers of MSC phenotype CD105. CD73 and CD90 were also found to be constantly expressed by hLMSCs (panel in the middle, **Figure 5.3**).
- The surface biomarkers of MSC phenotype which are ideally expected, not to be expressed by MSCs in general i.e., CD45, CD34 and HLA-DR were found to be negatively expressed by hLSMCs (lower panel, **Figure 5.3**).

All the other cytoskeletal biomarkers were also found to be expressed by the hLMSCs in all the batches of cells tested.

- The collagens of the extracellular matrix, Collagen I, II, III, IV and V were found to be expressed by hLMSCs (**Figure 5.4**).
- Neural cadherins (Cadherin-1 or N-Cad), the transmembrane proteins which mediate cell-to-cell adhesion, were found to be positively expressed by hLMSCs (bottom left, **Figure 5.4**).

- However, the epithelial cadherin (E-Cad or Cadherin-2) did not show any expression in hLMSCs population (bottom right, **Figure 5.4**).
- Vimentin, the intermediary filament biomarker of MSCs, was also observed to be positively expressed by hLMSCs (panel in middle, **Figure 5.4**).
- Additionally, the hLMSCs have also shown positive expression of the Keratocan (KERA, lower panel, **Figure 5.4**), a biomarker for keratocytes of corneal stroma, the cells that responsible for degradation and generation of the stromal collagens, contributing to the corneal transparency.

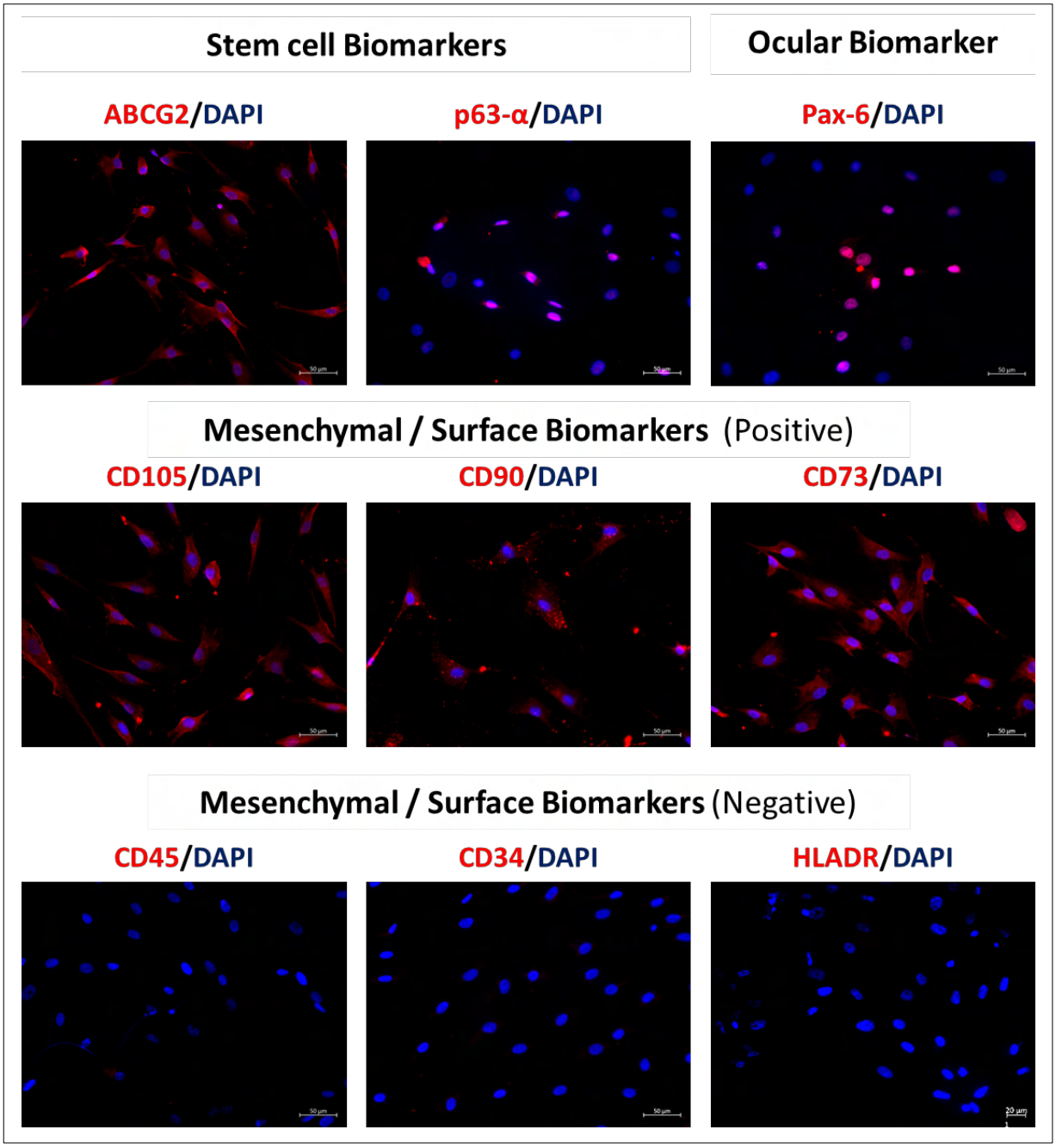

Figure 5.3: Expression of the characteristic biomarkers by hLMSCs. Micrographs (panel on top) showing the positive expression of ocular (Pax6^{+}) and stem cell biomarkers (ABCG2^{+}, p63-α^{+}). hLMSCs showing positive (middle panel) expression of MSC biomarkers CD105^{+}, CD90^{+} and CD73^{+} and negative (lower panel) expression of CD45-, CD34^{-} and HLA-DR^{-}). All hLMSCs culture were counterstained by nuclear stain DAPI (blue). Scale: 50µM. This data was published in part at DOI: 10.3390/ijms23158226, by (Damala et al., 2022).

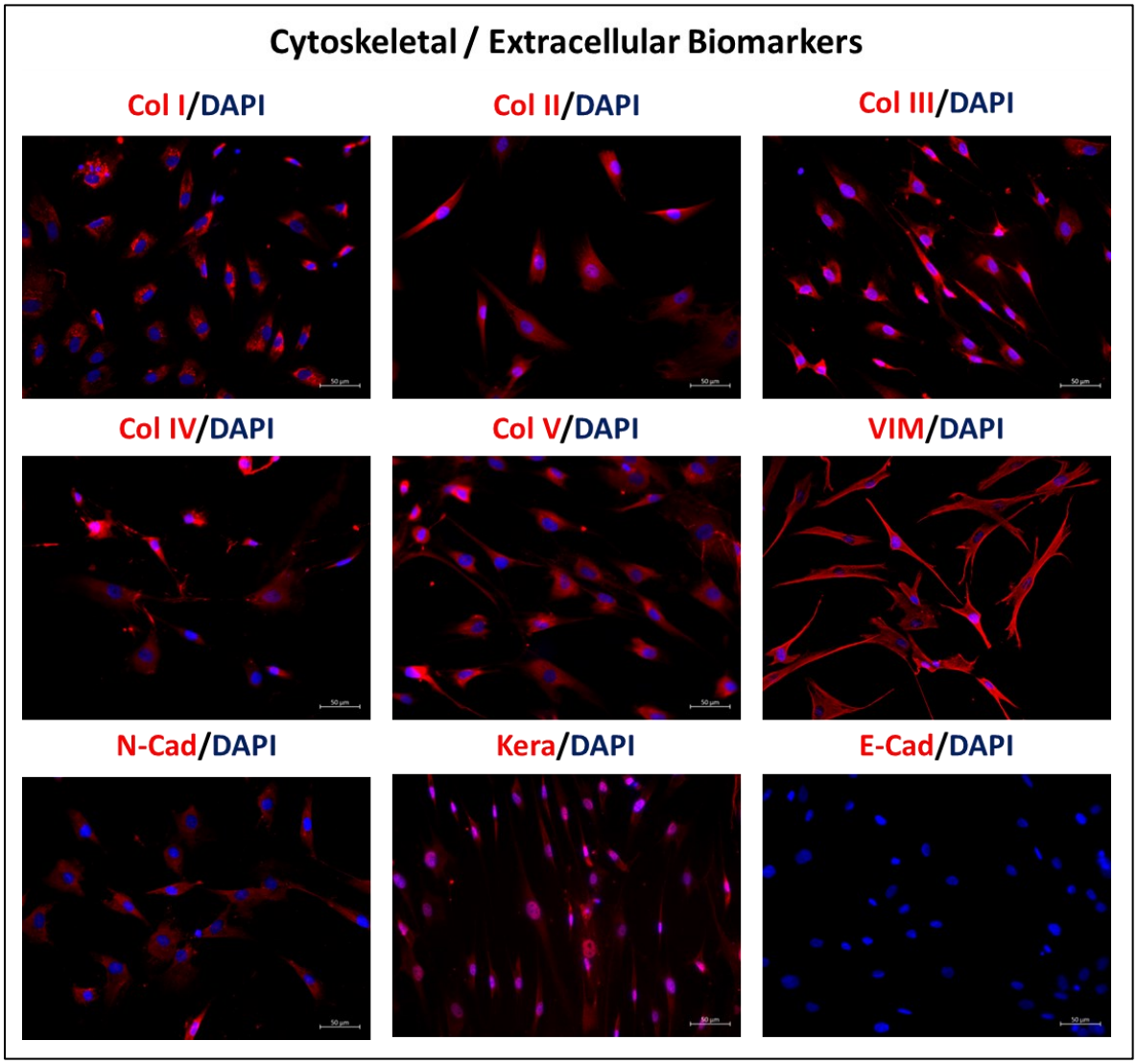

Figure 5.4: Expression of the cytoskeletal biomarkers by hLMSCs. Micrographs showing the positive expression of collagens I, II, III, IV and V (red) and intermediary filaments VIM (red) by hLMSCs. Lower panel showing the positive expression of N-Cad, KERA (red) and no expression of E-Cad. All the hLMSCs culture were counterstained by nuclear stain DAPI (blue). Scale: 50µM. This data was published in part at DOI: 10.3390/ijms23158226, by (Damala et al., 2022).

5.1.4.2. Quantitative assessment of the hLMSCs' characteristic biomarkers: Fluorescence Assisted Cell Sorting (FACS)

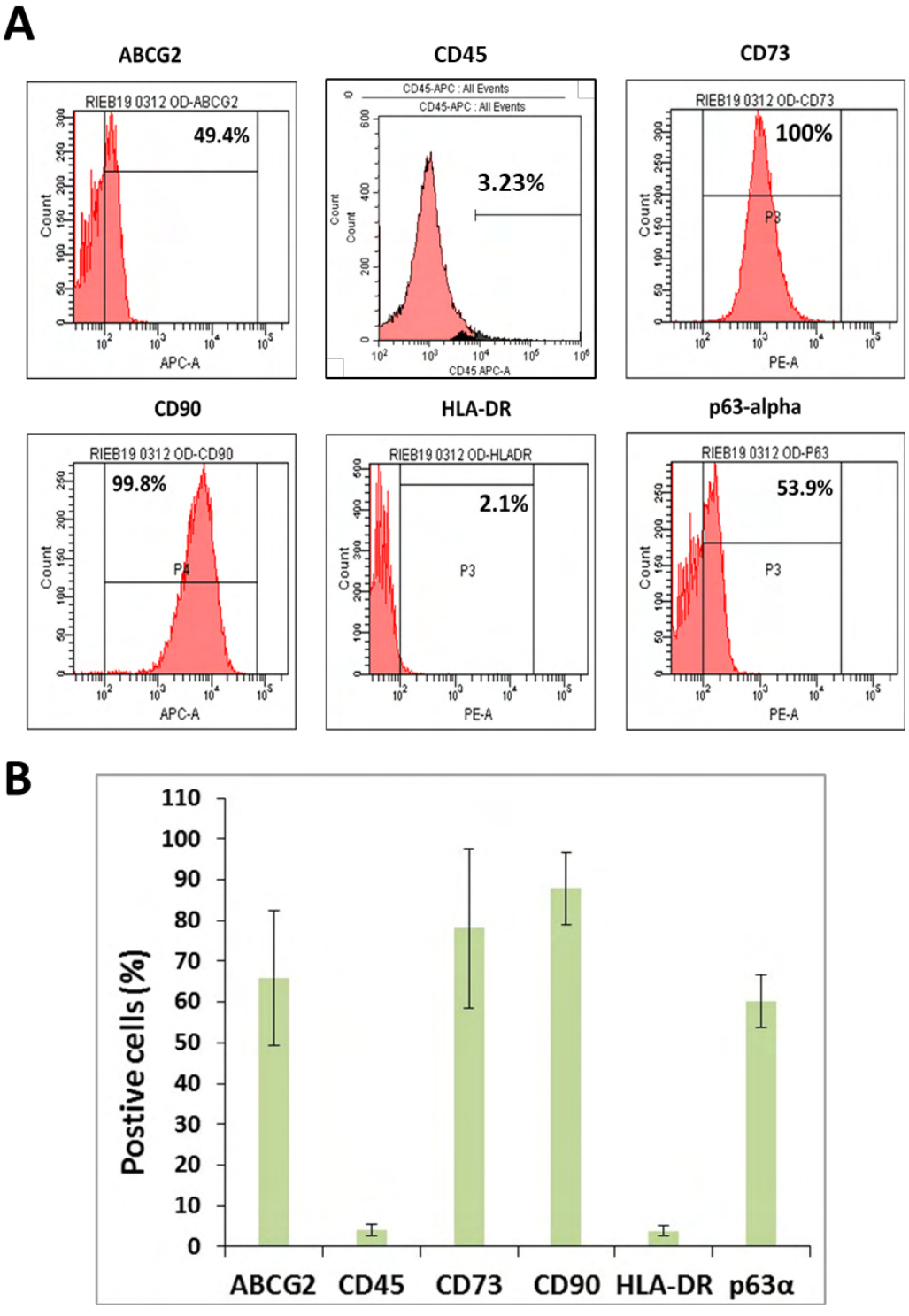

Figure 5.5: Quantifying the biomarker expression by hLMSCs. **(A)** Collage of the representative graph plots showing the percentage of cells expressing the stem cell and mesenchymal biomarkers. **(B)** Bar-graph showing the amount of the biomarker expression (in percentage) by hLMSCs. *n*=12.

The quantification for the phenotypic biomarker expression by the hLMSCs was assessed through Fluorescence-assisted cell sorting (FACS).

- 60.24 ± 6.33 % of cells were positive for the stem cell biomarker p63-α and 65.88 ± 16.48% of the cell population have expressed ABCG2.
- The mesenchymal biomarkers CD90 and CD73 were expressed by 87.89 ± 8.77% and 78.12 ± 19.52% cells respectively.
- The expression of hematopoietic marker CD45 was limited to 3.96 ± 1.39% and HLA-DR was expressed by < 3.91 ± 1.16% cells.

The FACS analysis was performed for every batch cultured, for characteristic analysis and for the pre-clinical studies. The average expression of 12 batches was shown in **Figure 5.5 B**.

5.1.5. Stability and Sterility of hLMSCs

5.1.5.1. Evaluation of the chromosomal stability through karyotyping

hLMSCs were assessed for their genetic or chromosomal instability through karyotyping. The cells of concurrently produced batches and cells after 6-9months of cryo-storage, both were assessed, at an accredited third-party laboratory. All the cells were arrested at the Metaphase stage before analysis.

- No signs of any chromosomal instability in terms of the chromosomal number or structure were found in the cells of concurrently produced batches (**Figure 5.6A**).
- The hLMSCs revived after 6-9months of cryopreservation also did not show any changes (**Figure 5.6B**) in the chromatic aberrations.
- Additionally, the cells cultured from the donors of both sexes also were found with to have no aberrations.
- Overall, hLMSCs were found to have no chromosomal or genetic instabilities in all the cells and their progeny after long-term preservations as well.

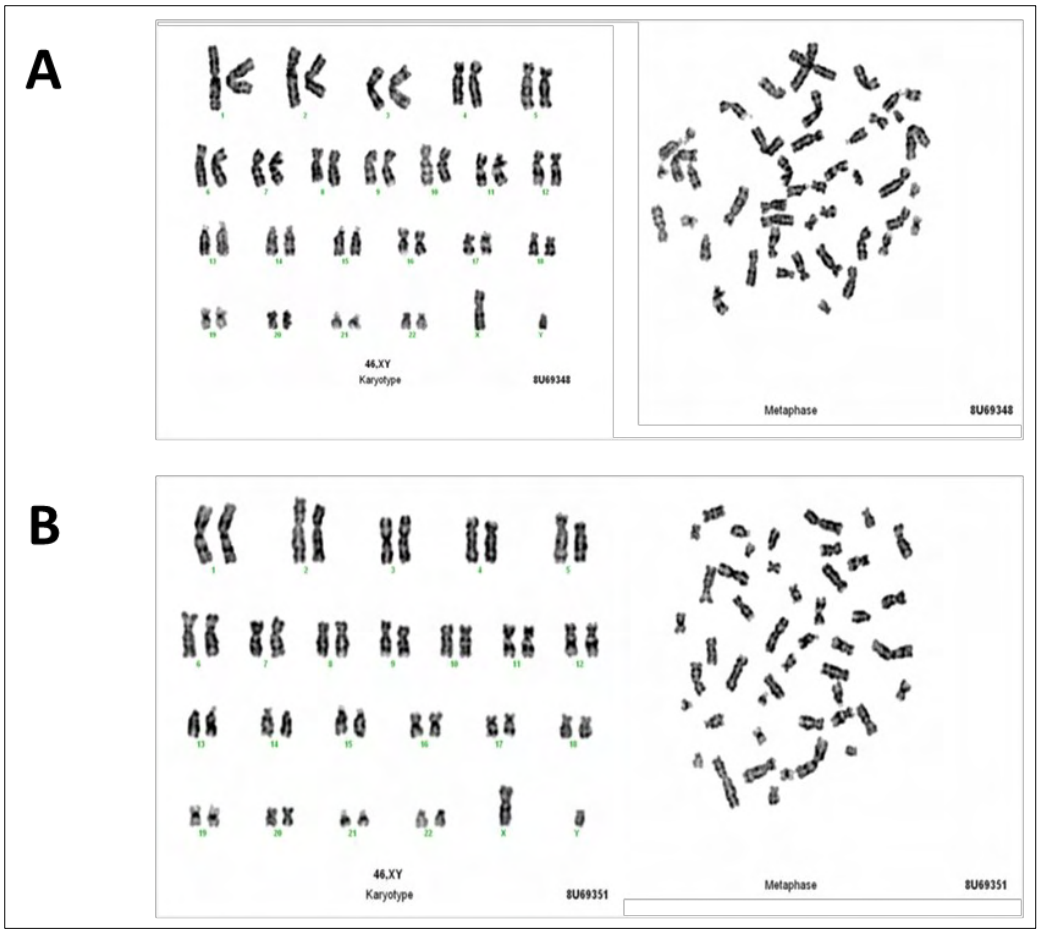

Figure 5.6: Representative karyograms showing stable chromosomes of hLMSCs assessed from the concurrent culture **(A)** and the cells revived from cryopreservation **(B).** This data was published in part, as a pre-print at DOI: 10.21203/rs.3.rs-789579/v1 by (Damala et al., 2021).

5.1.5.2. Evaluation of the viability of pelletized hLMSCs

The hLMSCs were assessed for their stability in terms of cell viability, when stored as a pellet for >3-4 hours in ice-cold conditions, in the event of an unforeseen operational delay at the sites of end use. The assessment was done by storing the hLMSCs as a pellet with <50µL of complete medium, in ice for 24 hours, followed by dye-exclusion assay analysis of the resuspended hLMSCs.

- After 3 hours of incubation on ice, it was found that ≥90% of the hLMSCs remained viable. This indicates that the majority of cells maintained their viability under these conditions.
- At the end of 6 hours, it was observed that 88.33 ± 2.05% of the hLMSCs in the pellet were viable. This suggests that the cells retained a high level of viability even after 6 hours of incubation.

- By the end of 24 hours, the viability of the cells decreased slightly to 78.21 ± 1.28%. This indicates that there was a gradual decline in cell viability over time, but a significant proportion of cells remained viable even after 24 hours.

These viability percentages were depicted in **Figure 5.7 and Table 5.1**, which visually represent the trends in cell viability over the specified time points.

	Time Point	**0th hour**	**0.5 hours**	**1 hour**	**3 hours**	**6 hours**	**12 hours**	**24 hours**
Percentage of viable hLMSCs	***Cycle 1***	93.44	90.48	90.32	90.32	91.67	84.13	76.19
	Cycle 2	91.67	90.32	90.32	90.77	86.44	83.87	79.66
	Cycle 3	94.92	91.53	91.67	89.19	86.89	83.61	78.79
	Mean	93.34	90.77	90.77	90.09	88.33	83.87	78.21
	SD	1.15	0.46	0.55	0.58	2.05	0.18	1.28

Table 5.1. Table showing the percentage of hLMSCs viable after respective hours of storage in ice-cold conditions. SD: Standard deviation.

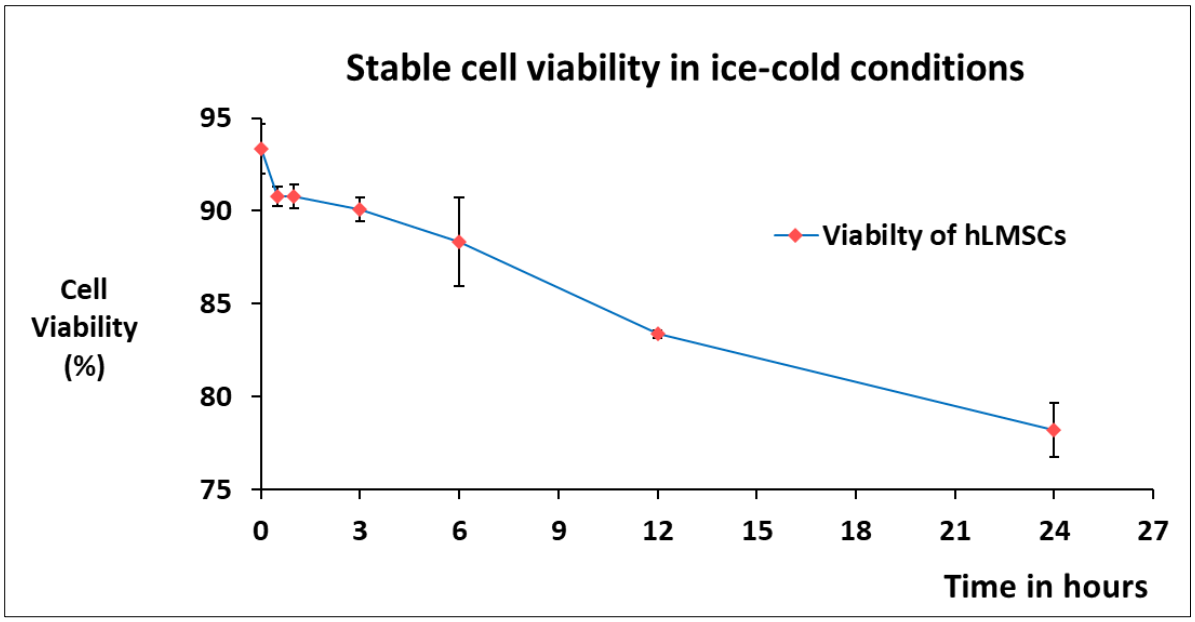

Figure 5.7: A line chart depicting the cell viability trend of hLMSCs during storage in ice. The data, represented as mean ± SD, is based on three sets of experiments (n=3).

5.1.5.3. Growth kinetics of hLMSCs

- The cell doubling time of the pure population of the hLMSCs was found to be ~61 hours.
- The cumulative growth of hLMSCs in terms of cell number assessed through dye-exclusion method and in terms of the optical density values assessed through MTT assay are given in **Figure 5.8A** and **Figure 5.8B** respectively.

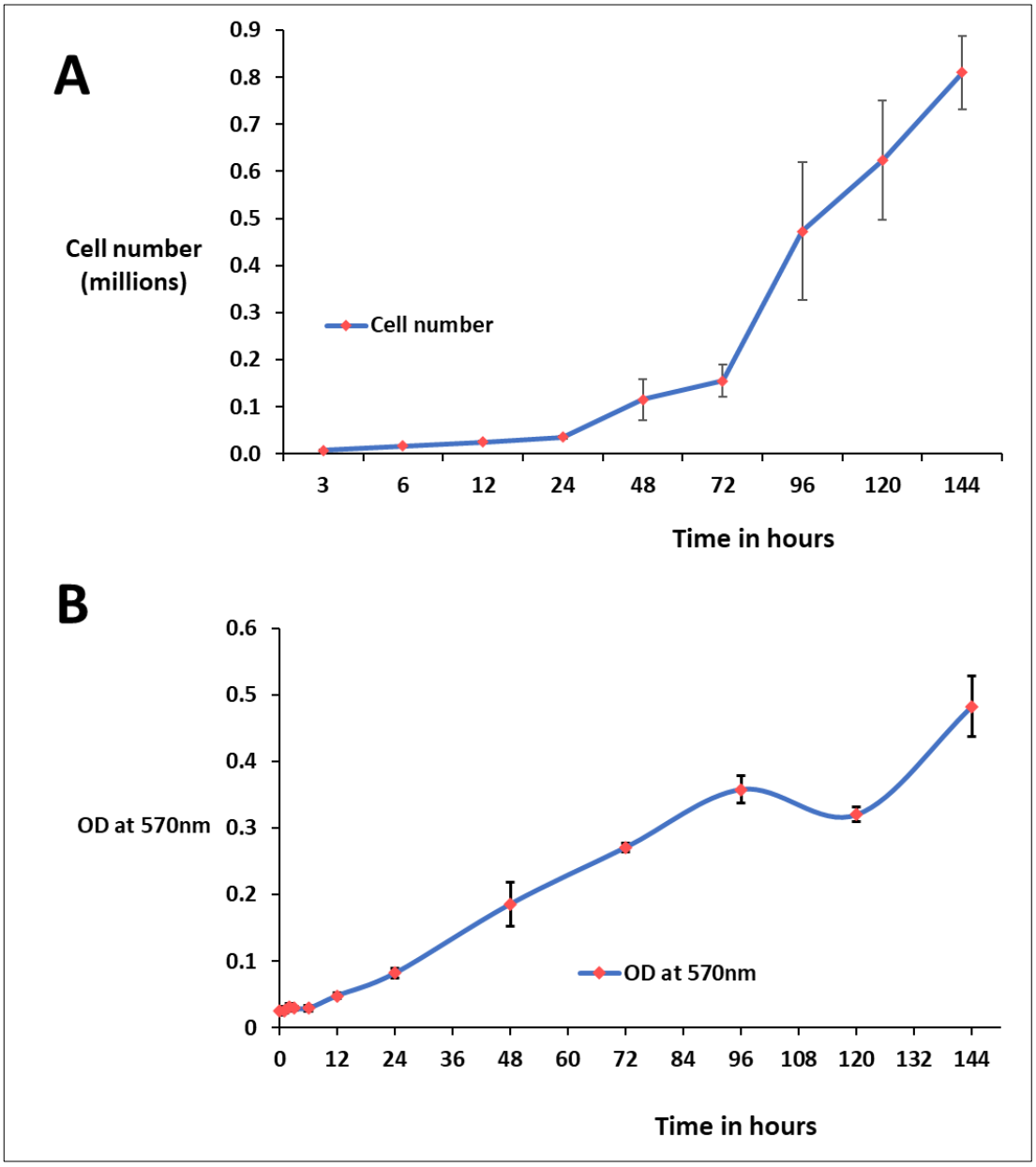

Figure 5.8: Line graph showing the cell growth curve of hLMSCs. The cumulative growth in the number of cells, against the respective duration (hours) in culture is plotted. *n=3*. This data was published in part, as a pre-print at DOI: 10.21203/rs.3.rs-789579/v1 by (Damala et al., 2021).

5.1.5.4. Microbial screening

During the course of the study, all the raw material such as complete medium and the in-process materials such as spent media and the end product (hLMSC cell suspension), were checked for microbial contaminations. All the materials tested were found to have zero colonies of microbial growth and thus no incidence of any bacterial or fungal contamination.

A snapshot of an analytical test report, assessed by an independent quality control team, is given in **Figure 5.9C.**

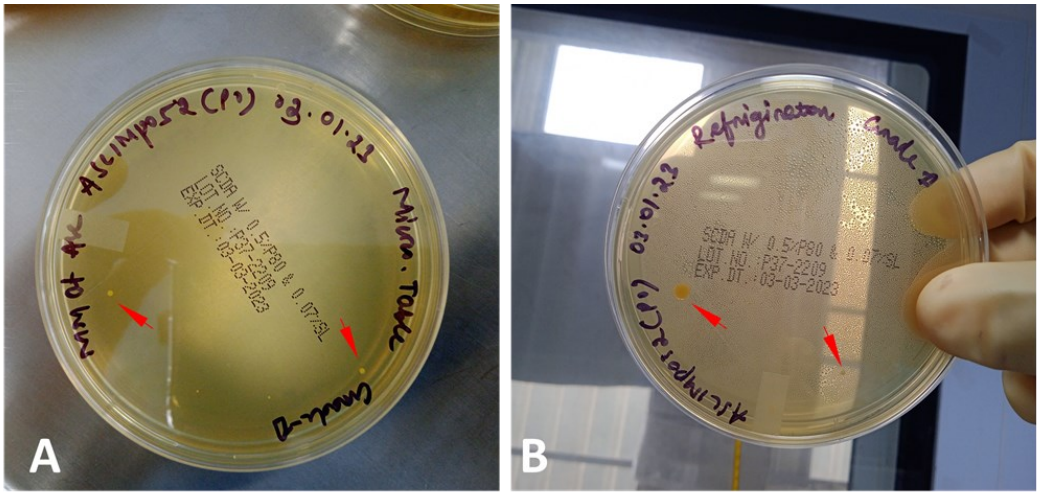

C

Date of Report	23.04.22	AR No.	IPM/22/050
Name of the Material	Spent Media (P3) 48hrs before harvest		
Lot/Batch No.	ASCIMP011		
Specification No.	QCSPCIPM-003		

S. No.	Tests	Acceptance Criteria	Results
01	Description	Clear, Pale brick red to pale yellow color liquid	Complies
02	Bio-burden	No Growth	Complies

Release:

The material complies/~~does not comply~~ as per specification no. QCSPCIPM-003 and is approved ~~/rejected.~~

Figure 5.9: (A-B) Representative images of the media plates showing no growth of bacterial colonies (Permissible Limit: <5). **(C)** A snapshot of the sterility report generated after assessing the sterility of the in-process materials.

5.1.5.5. Assessment of mycoplasma contamination

There was no evidence of Mycoplasma species contamination in any of the in-process materials, or the final cell suspensions of hLMSCs.

Both of these approaches (based on PCR and calorimetry) were utilized in order to ascertain whether or not mycoplasma was present. Both of these approaches have produced quite comparable findings (**Figure 5.10**).

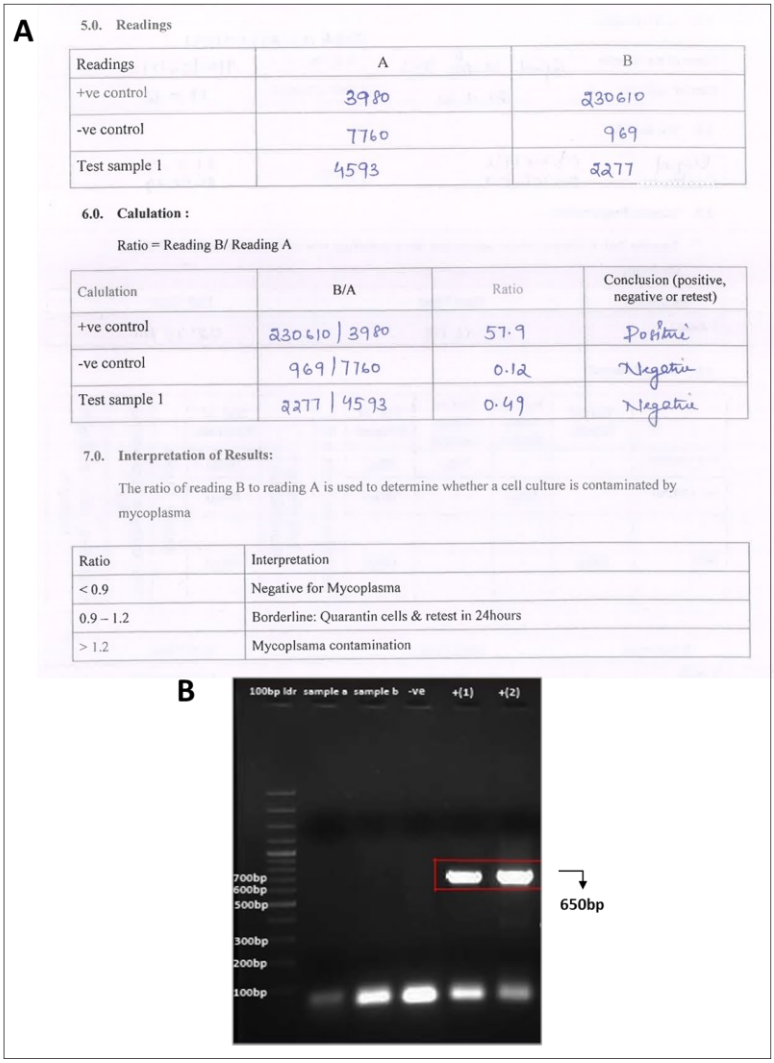

Figure 5.10. (A) A snapshot of the analytical test report generated after assessing the presence of mycoplasma in a given sample, through colorimetry-based method. A ratio of <0.9 indicates that the sample tested is negative. **(B)** Agarose gel electrophoresis image showing the products formed in PCR reaction. *Sample a* and *b* represent the spent media from hLMSC cell suspension. *-ve*: negative sample for mycoplasma, *+(1)* and *+(2)* are positive controls for mycoplasma.

5.1.5.6. Determining the levels of bacterial endotoxin

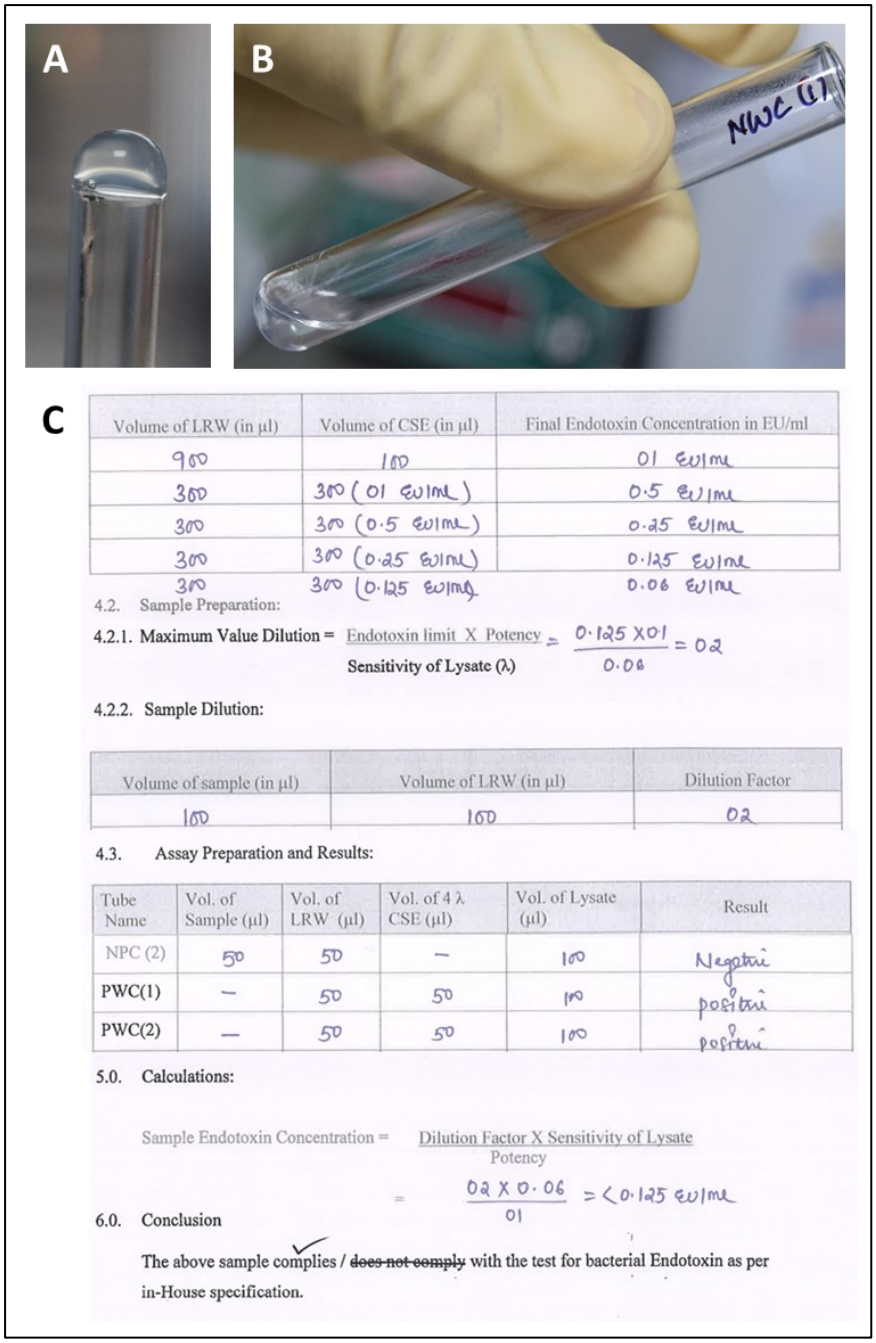

Figure 5.11. (A-B) Representative images showing the clot formation **(A)** depicting the levels of >0.125EU/mL in the positive control, and free flowing suspension without any formation in the negative sample **(B)**. A snapshot of the analytical test report generated after assessing the presence of mycoplasma in a given sample, through colorimetry-based method. A ratio of <0.9 indicates that the sample tested is negative. **(B)** Agarose gel electrophoresis image showing the products formed in PCR reaction. *Sample a* and *b* represent the spent media from hLMSC cell suspension. *(-ve)*: negative sample for mycoplasma, *+(1)* and *+(2)* are positive controls for mycoplasma.

Gel Clot LAL (Limulus amebocyte lysate) assay was performed to determine the levels of bacterial endotoxins in most of the raw materials used in the isolation and cultivation of hLMSCs and the spent media of every generation of the cell culture.

Before releasing a particular batch of hLMSCs for therapeutic purposes, the cell suspension the hLMSCs was also tested for the levels of endotoxins.

At every stage of the cell culture the levels of endotoxins were found less than the permissible levels i.e., ≤0.125 EU/mL (for ophthalmic devices or solutions intended for superficial use).

5.2. Storage and transport of hLMSCs at ambient temperature

5.2.1. Validating an insulated container

The pre-conditioned container was able to successfully maintain an average ambient/ hypothermic (internal) temperature of 18.62 ± 1.82 °C. The average temperature at the time of loading or packing was 13.91°C whereas the average of highest temperatures recorded inside the container was 27.52°C. During this standardization period (80 hours), the mean atmospheric (i.e., external temperature in the cargo carrier) was 31.43 ± 1.2°C. The average of lowest atmospheric temperature recorded was 28.85°C and the average of highest atmospheric temperature was 38.40°C (**Table 5.2**). Over the various seasons of weather, the container was tested, the internal temperature has remained within the desired range of the usual room temperature (**Table 5.2**). This process of container's standardization, however did not employ any cells. After 10 cycles of validation, the container was then used to transport encapsulated hLMSCs.

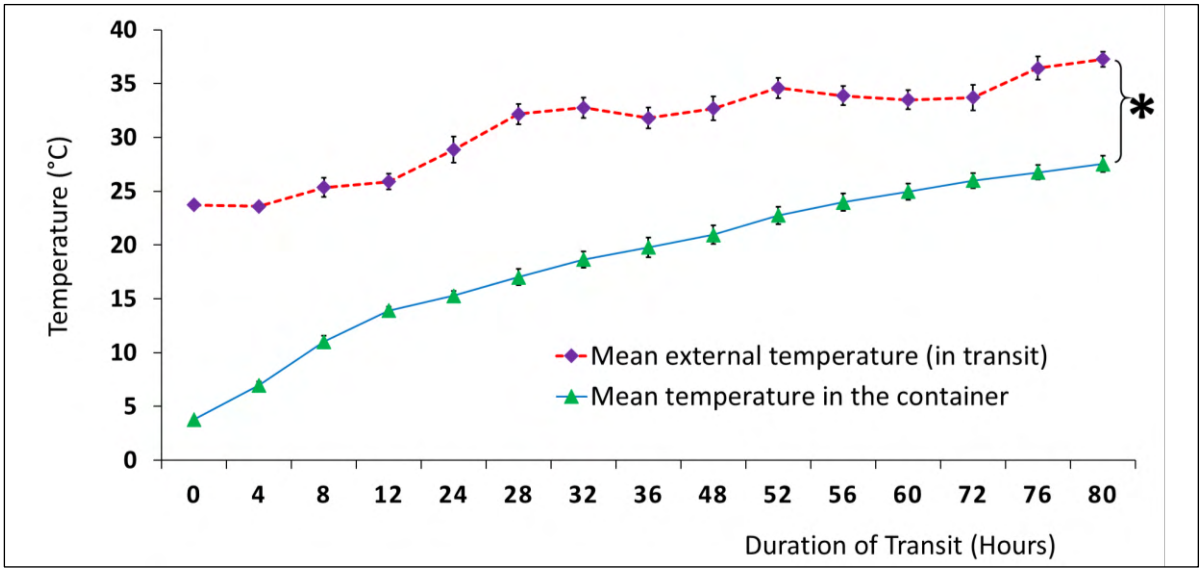

Figure 5.12: Line chart summarizing the relative levels of the external and internal temperatures of the shipping container recorded during the transit for its validation. This pre-conditioned container was validated to check for the maintenance of hypothermic temperatures. This data was published in part at DOI: 10.1038/s41598-019-53315-x, by Damala M *et al*, 2019.

5.2.2. Encapsulation of hLMSCs

The hLMSC cell suspension was encapsulated using Alginate formulation (Section 4.5.2 of Methods) at a density of $2.5x10^6$/mL. The Alg-hLMSCs suspension was dropped into $CaCl_2$-based buffer, as small droplets, that polymerize and harden to form a bead-like structure. The number of resultant beads ranged between 18-24 with at least 18000 to 24000 cells per bead (**Figure 5.13**). These beads with hLMSCs encapsulated in them, were packed for transit.

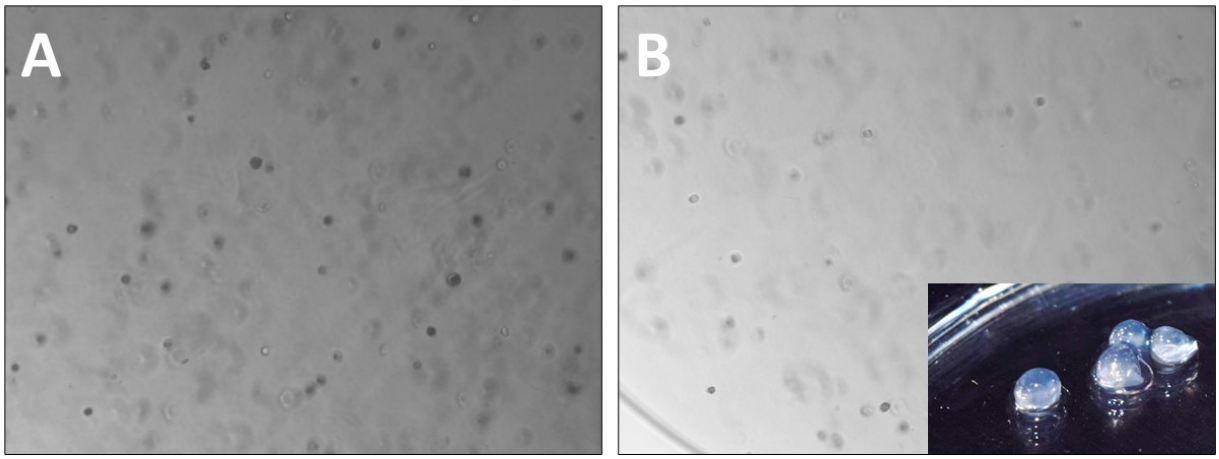

Figure 5.13: Encapsulated hLMSCs in alginate bead: **(A-B)** Phase contrast microphotographs of the alginate beads encapsulating hLMSCs at 40X magnification. Inserted picture showing the alginate beads with cells encapsulated, as seen with the naked eye.

Optimizing the insulated and reusable shipping container																				
Time (hrs)	Cycle 1		Cycle 2		Cycle 3		Cycle 4		Cycle 5		Cycle 6		Cycle 7		Cycle 8		Cycle 9		Cycle 10	
	Atm (Ext)	**Con** (int)	**Atm** (Ext)	**Con** (int)	**Atm** (Ext)	**Con** (int)	**Atm** (Ext)	**Con** (int)	**Atm** (Ext)	**Con** (int)	**Atm** (Ext)	**Con** (int)	**Atm** (Ext)	**Con** (int)	**Atm** (Ext)	**Con** (int)	**Atm** (Ext)	**Con** (int)	**Atm** (Ext)	**Con** (int)
0	22.7	3.9	22.6	3.1	23.4	4.2	22.9	4.9	26.4	3.8	23.6	4.2	23.8	3.6	24.1	4.1	23.3	3.1	24.5	2.9
4	23.2	8.5	21.9	8.3	22.5	7.6	23.8	7.9	23.1	6.1	24.3	6.3	23.2	5.7	24.5	7.6	24.2	5.6	25.3	6.1
8	22.4	13.4	23.4	12.1	31.9	13.7	29.2	13.3	23.6	9.3	23.2	9.5	25.1	9.7	25.2	9.8	25.3	9.1	24.1	10.2
12	29.7	16.4	25.6	14.7	29.8	14.6	27.8	14.2	24.6	13.7	24.1	13.2	24.2	12.8	25.8	13.1	23.4	12.9	23.9	13.5
24	36.4	18.4	31.8	17.4	26.2	16.1	28.6	15.3	23.0	14.6	23.6	14.4	27.6	13.6	29.3	14.2	30.2	14.6	31.8	14.2
28	37.2	21.7	30.6	21.2	37.3	17.2	34.0	16.9	29.6	16.7	28.2	15.1	29.1	15.4	31.5	15.0	31.5	15.3	32.6	15.6
32	40.8	23.6	31.0	23.0	32.1	18.4	30.6	18.1	30.5	17.5	31.1	17.9	30.7	18.3	34.2	16.7	32.6	16.9	33.9	16.1
36	30.4	25.4	35.2	25.1	27.5	19.7	27.8	19.2	29.1	18.0	31.6	19.0	32.5	19.5	36.4	17.5	31.9	17.2	35.6	17.2
48	31.2	25.9	40.3	26.2	29.9	20.4	29.1	20.1	28.4	18.6	32.8	21.1	34.2	21.2	37.5	18.6	33.5	19.0	34.1	18.3
52	39.2	26.8	39.3	27.2	36.4	23.2	37.6	22.9	29.2	21.1	37.6	23.6	33.0	22.8	32.8	20.1	35.8	20.7	36.2	19.0
56	40.5	27.4	36.8	28.5	33.2	25.1	34.3	24.2	31.0	23.2	34.1	25.1	38.6	23.5	33.7	21.3	37.2	21.1	38.3	20.3
60	34.3	27.9	37.2	29.3	30.7	26.4	29.0	25.1	29.6	24.1	36.2	25.9	35.1	24.1	35.6	22.4	33.9	22.5	36.8	21.8
72	33.4	28.4	39.6	29.8	28.6	28.3	29.8	26.6	28.8	24.9	38.2	26.4	34.0	24.8	36.2	24.3	35.1	23.7	37.4	22.6
76	38.7	29.1	45.2	30.2	36.8	29.4	35.6	27.1	32.7	25.1	33.7	27.7	32.6	25.4	37.2	25.1	36.8	24.6	35.1	23.8
80	38.0	31.2	44.3	30.9	37.2	30.1	36.2	27.7	37.2	26.3	36.1	28.1	38.6	26.0	38.6	25.4	39.1	25.2	38.7	24.3

Table 5.2: Table showing the internal and external temperatures (°C) of the insulated shipping container, recorded every 4 hours, during the cycles (n=10) of standardization and validation. Atm – Atmospheric or Container's external temperature, Con – Container's internal temperature.

5.2.3. Recovery from encapsulation after transit

The hLMSCs were recovered at optimal rate irrespective of the external temperature and conditions (**Figure 5.14**).

- The average recovery rate of viable cells after a 3-day transport at room temperature was 82.5% ± 0.9% (n = 3).
- Encapsulated cells stored at 4°C showed a lower recovery rate of 65.2% ± 1.2% (n = 3, p = 0.0008) viability.
- Cells that underwent a 5-day transit were recovered with a viability of 77.0% ± 2.0% (n = 3).
- The viability of cells stored for 5 days at 4°C after encapsulation was 64.5% ± 0.8% (n = 3, p = 0.0104).
- Non-encapsulated cells transported at room temperature had a viability of ≤1% after both 3-day and 5-day transit.
- Cells stored at 4°C without encapsulation showed a mean recovery of approximately 5.3% ± 0.1% after 3 days and ≤4% after 5 days.

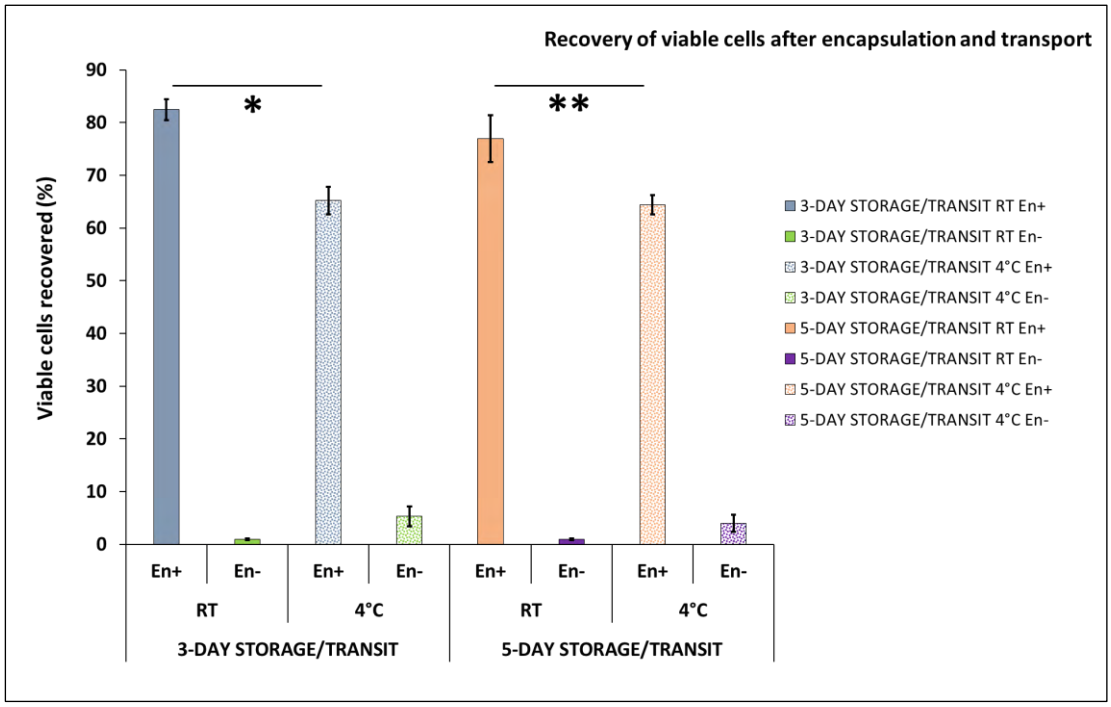

Figure 5.14: Bar graph summarizing the mean recovery of viable cells from 3-5 days of storage or transport, after encapsulation. *En*+ - Encapsulated, *En*- - Non-encapsulated, RT – transported at room temperature, 4◦C – stored at refrigerated conditions. *p = 0.0104, **p = 0.0008. This data was published in part at DOI: 10.1038/s41598-019-53315-x, by Damala M *et al*, 2019.

5.2.4. Relative survival rate

The hLMSCs recovered from storage or transit after encapsulation were assessed for their survival rate in culture (from the adherent cells), relative to a standard ongoing culture of hLMSCs from the same origin. The non-encapsulated cells that were recovered after transit and storage at RT and 4◦C respectively, with 1-4% of viability were excluded from the assessment due to low numbers.

- After 48 hours in culture, cells transported at RT for 3-days, have shown a relative survival rate of 61.93 ± 1.68% compared to a standard culture (normalized to 100%), which after 96 hours in culture, increased to 74.34 ± 2.89%.
- Whereas the cells in transit for 5-days, have exhibited 51.24 ± 1.38% survival after 48 hours that increased to 67.74 ± 9.78% in the subsequent 48 hours (**Figure 5.15**).
- Around 39.67 ± 5.32% of cells stored at 4◦C for 3-days, have shown attachment after 48 hours and this value increased to 54.8 ± 9.04% after 96 hours.
- Cells that were stored for 5 days in refrigerating conditions, had 43.77 ± 3.53% of relative survival after 48 hours that rose to 52.35 ± 8.07% after 96 hours.

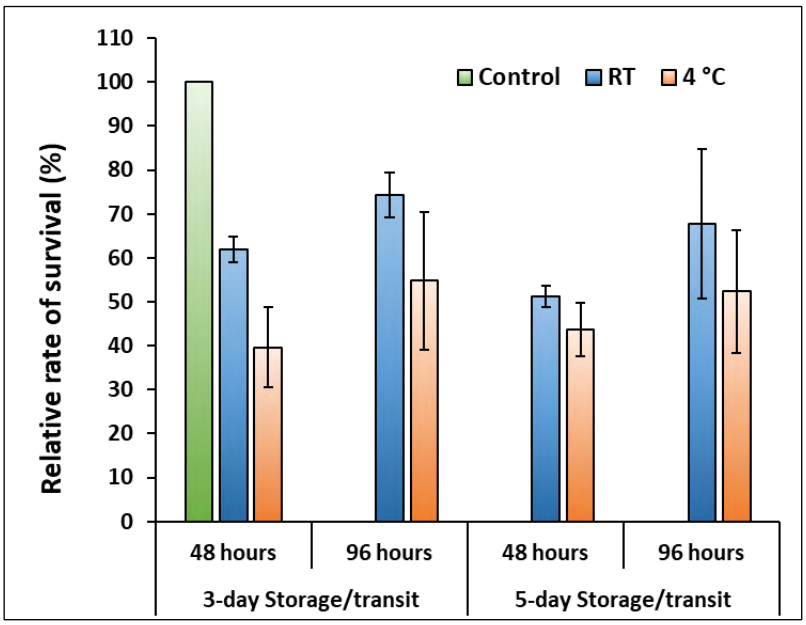

Figure 5.15: Graph plot showing the survival rate of the encapsulated cells in culture, relative to the control cells, capped to 100% (neither stored nor transported). This data was published in part at DOI: 10.1038/s41598-019-53315-x, by Damala M *et al*, 2019.

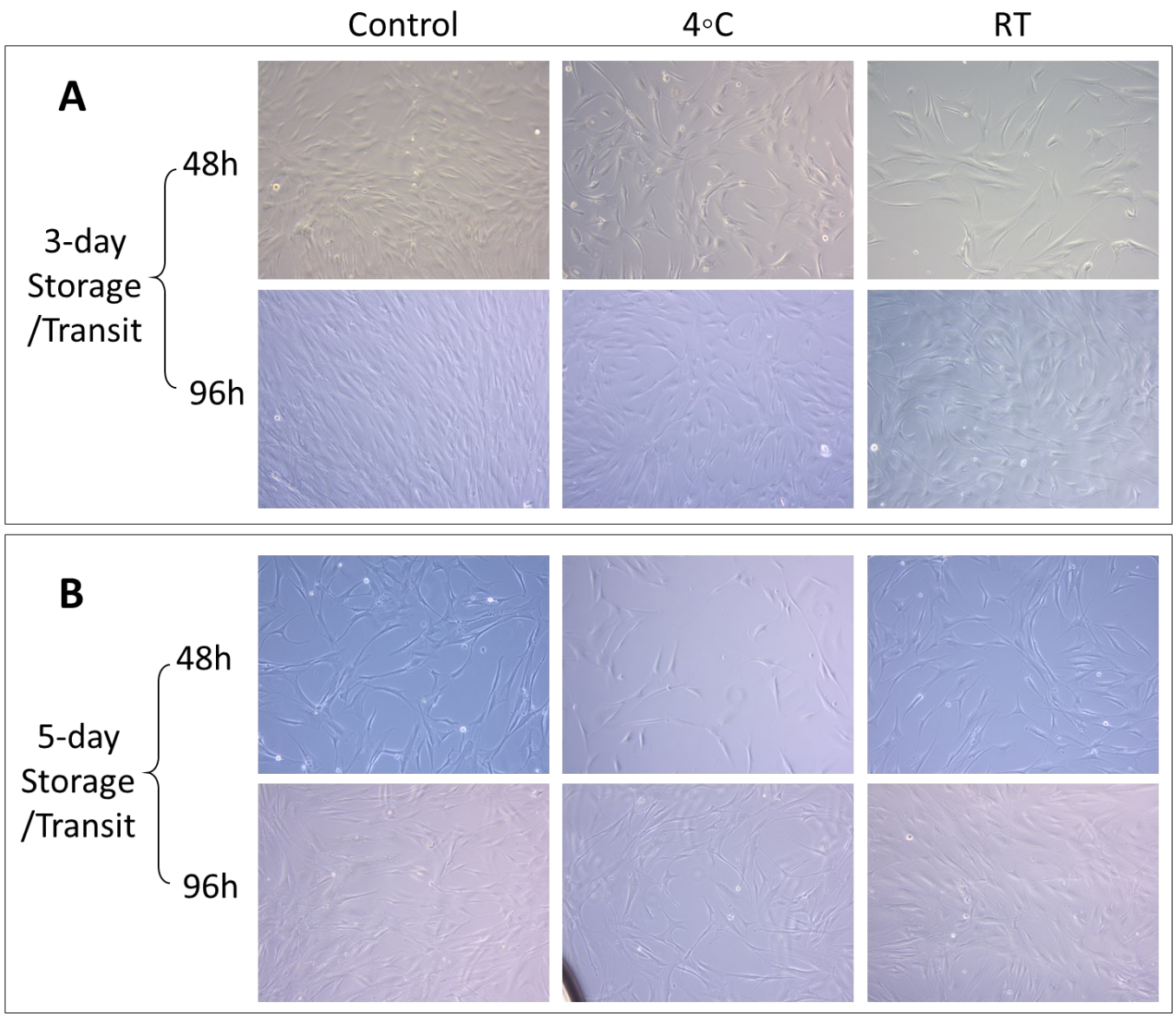

Figure 5.16: hLMSCs in culture after release from encapsulation: **(A)** Panel showing a collage of hLMSCs attached and growing in the cultures, at 48 hours (top) and after 96 hours (lower panel), after 3-days of storage at 4◦C or transit at RT. Both groups have cells grown to 70-80% confluence with respect to the control group cells.

(B) Collage of the micrographs of the hLMSCs in culture after 5-day storage or transit. After 96 hours in culture, these hLMSCs have exhibited 60-70% confluence compared to the control group. Magnification: *100X, n=3*.

5.2.5. Phenotypic Assessment

5.2.5.1. Qualitative assessment of the characteristic phenotype

On both 3-day and 5-day transit, the hLMSCs transported at RT after encapsulation retained their default characteristic phenotype on par with the control cells, which were neither encapsulated nor underwent any kind of transit and storage **(Figure 5.17).**

In the same vein, the cells that were encapsulated and then kept at a temperature of 4 degrees Celsius for three days exhibited no change in their phenotype over this time period. However, the alginate-encapsulated human LSMCs that were kept at a temperature of 4 degrees Celsius did not display expression of the stem cell biomarker ABCG2 after five days of preservation. The remainder of the biomarkers in the panel, including CD73+, Col-III+, Pax6+, p63-+, VIM+, CD105+, CD90+, and Col-III+; all showed that the cells were positive. According to the hypothesis, the cells did not express CD45, which is a hallmark of the hematopoietic system.

Table 5.3 illustrates the individual expression profile (expressed as per percentage) by comparing the number of cells that stained positively for a particular biomarker to the total number of cells that were present in the examined region. This ratio is used to characterize the expression profile.

Type of biomarker	Biomarker	3-day transit			5-day transit		
		Control	4°C	RT	Control	4°C	RT
Ocular biomarker	Pax6	++	++	++	++	++	++
Stem cell biomarkers	p63-α	+	+	+	+	+	+
	ABCG2	+++	+++	+++	+++	–	+++
Mesenchymal/surface biomarkers	VIM	++++	++++	++++	++++	++++	++++
	CD45	–	–	–	–	–	–
	CD90	++++	++++	++++	++++	++++	++++
	CD73	++++	++++	++++	++++	++++	++++
	CD105	++++	++++	++++	++++	++++	++++
Surface biomarkers	Col III	++++	++++	++++	++++	++++	++++

Table 5.3: Expression profile of the characteristic biomarkers by encapsulated hLMSCs under transit/storage at RT/4°C. Key: (-) - No expression, (+) - <25% cells are positive, (++) - 25-50% cells are positive, (+++) - 50-90% cells are positive, (++++) - >90% cells are positive for a given biomarker. This data was published in part at DOI: 10.1038/s41598-019-53315-x, by Damala M *et al*, 2019.

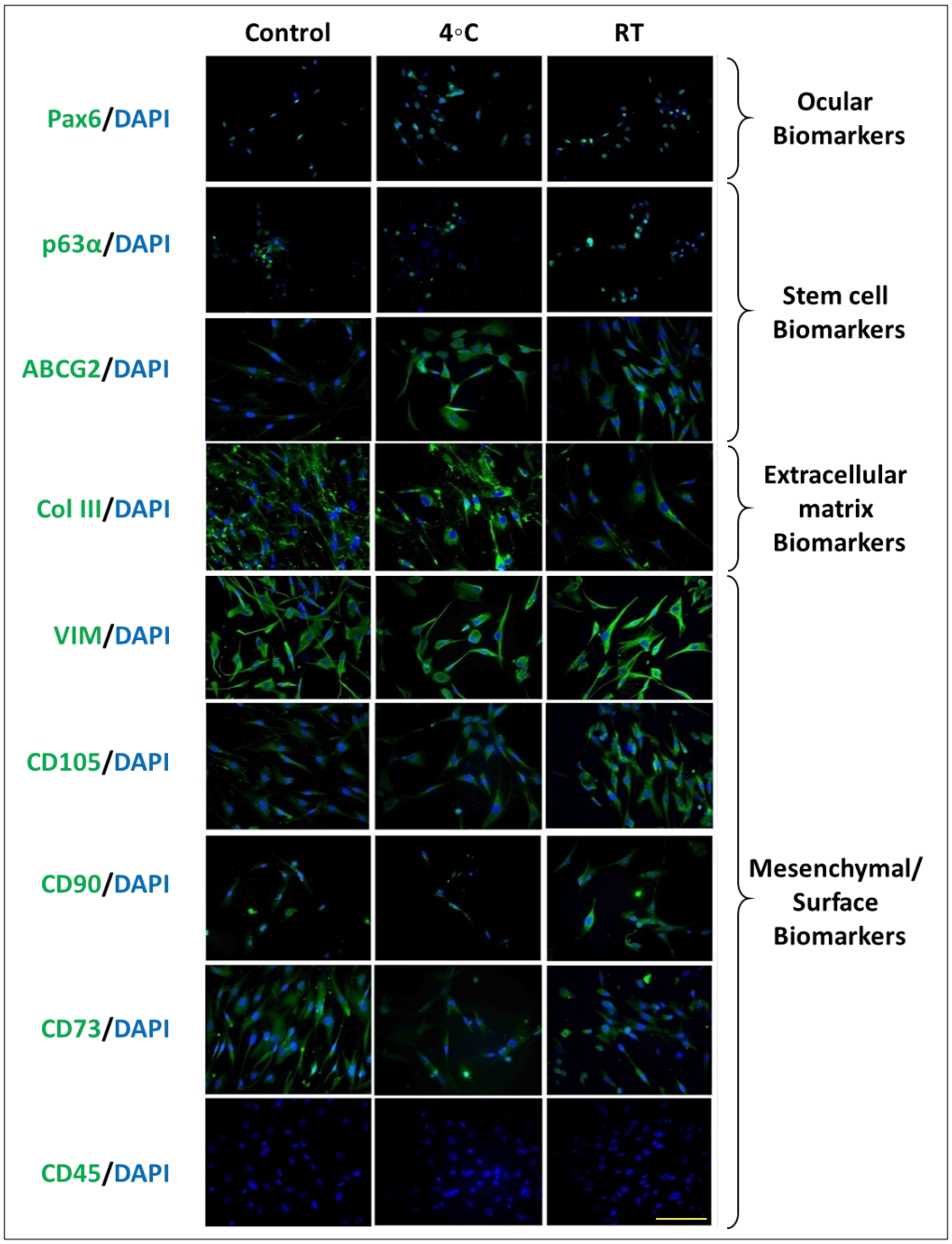

Figure 5.17: Microscopic snapshots of phenotypic assessment after 3-day encapsulation: The figure shows the results of immunostaining performed on alginate encapsulated hLSMCs from both groups that were stored/under transit for 3 days. The encapsulated hLSMCs exhibited positive expression of the following biomarkers: Pax6+ (ocular biomarker), ABCG2+ (stem-cell biomarker), p63-α+ (stem-cell biomarker), VIM+ (mesenchymal biomarker), CD90+ (mesenchymal biomarker), CD105+ (mesenchymal biomarker). The cells were also negative for CD45- (hematopoietic marker). The immunostaining images were visualized using a blue DAPI nuclear stain, and the scale bar represents a distance of 100 μM. This data was published in part at DOI: 10.1038/s41598-019-53315-x, by Damala M *et al*, 2019.

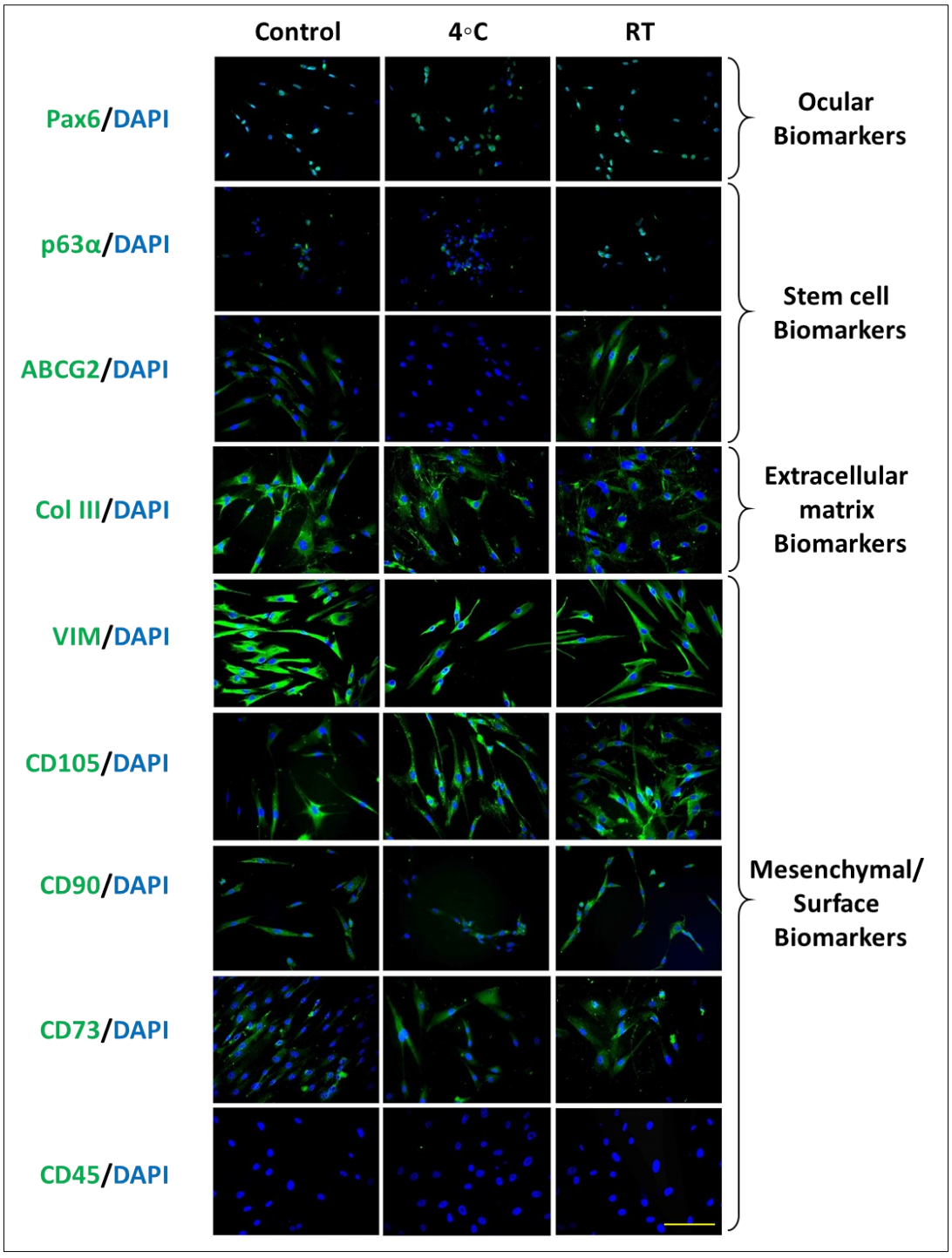

Figure 5.18: Microscopic snapshots of phenotypic assessment after 3-day encapsulation: The figure presents the immunostaining results of alginate encapsulated hLSMCs stored at 4 °C for 5 days. The immunostaining reveals the expression or absence of specific biomarkers in these cells compared to the control group. The alginate encapsulated hLSMCs stored at 4 °C did not exhibit expression of the stem-cell biomarker ABCG2-. However, the cells from the group stored at room temperature (RT) showed a phenotype similar to the control group, expressing the following biomarkers: ABCG2+ (stem-cell biomarker), Pax6+, p63-α+, VIM+, CD90+, CD105+, CD45-

(hematopoietic marker), Col-III+, CD73+. The immunostaining images were visualized using a blue DAPI nuclear stain, and the scale bar represents a distance of 100 μM. This data was published in part at DOI: 10.1038/s41598-019-53315-x, by Damala M *et al*, 2019.

5.2.5.2. Quantitative assessment of the characteristic phenotype

To validate the analysis of characteristic phenotype performed through immunostaining, a panel of limited selective biomarkers was chosen to quantitatively assess hLMSCs under 3-day transit/storage, through RT-PCR. The panel included PAX6, CD90, and p63α biomarkers.

The hLMSCs cultured through standard protocols were used as a reference control. Relative to these non-encapsulated cells, the cells that were under transit o storage after encapsulation has shown a comparable expression of the tested biomarkers, without any statistically significant ($p > 0.11$) differences **(Figure 5.19).** Cells of both the groups (RT and 4◦C) have retained the biomarkers expression, equivalent to the control cells.

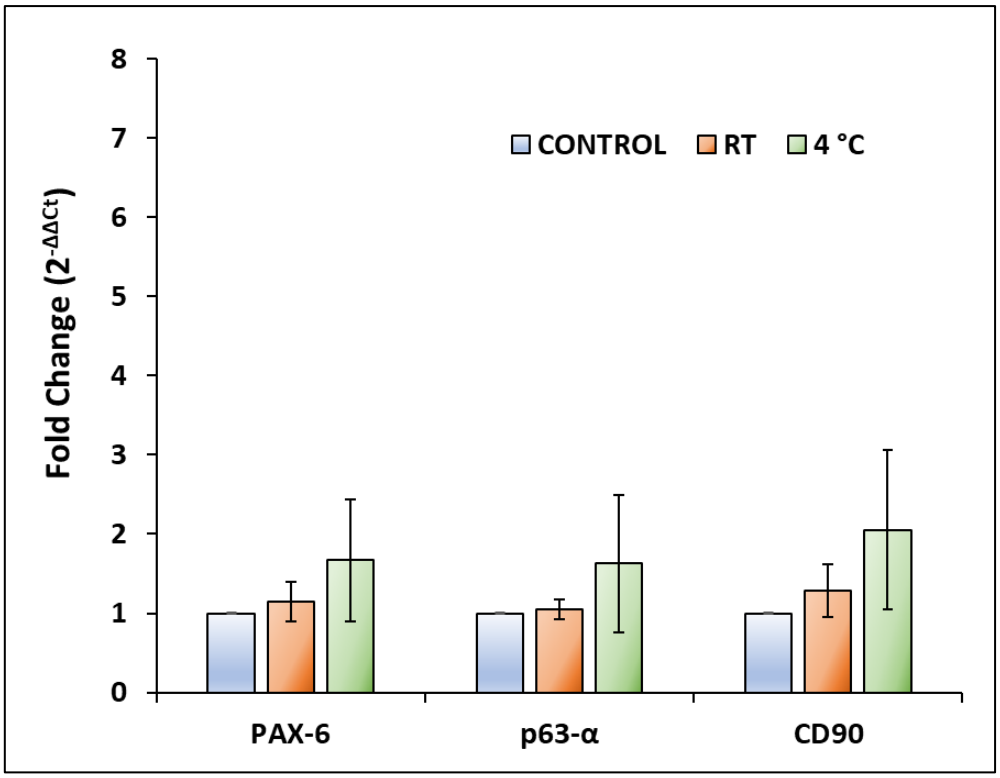

Figure 5.19: Quantitative analysis of the characteristic phenotype of hLMSCs after encapsulation and transit/storage. An insignificant (#p > 0.11) fold change in the expression of all the biomarkers was found among all three groups of cells. This data was published in part at DOI: 10.1038/s41598-019-53315-x, by Damala M *et al*, 2019.

5.3. Safety and Toxicity of the hLMSCs

5.3.1. Mortality and health

All the sham and test (*En+/En-* hLMSCs) group animals were found normal for clinical signs. No signs of morbidity and mortality were observed in both the vehicle control (sham) and the test groups.

5.3.2. Ophthalmic observations

During the ophthalmic observations, no major signs of severe ocular inflammation or redness were detected, and all findings were within the normal range. However, Grade 1 conjunctival inflammation was observed in the treated eyes of all three groups after 3 hours of treatment. By the end of the 6-hour post-treatment period, the animals in Group 2 (G2) showed no inflammation and returned to normal conditions. In contrast, one animal in the sham group and all six animals in Group 3 (G3) still exhibited Grade 1 inflammation. No ocular inflammation was noticed post 12 hours of the dosing, in all the groups (**Figure 5.20 and Table 5.4**). There were no signs of any corrosive and irritant effect in the treated groups, as well.

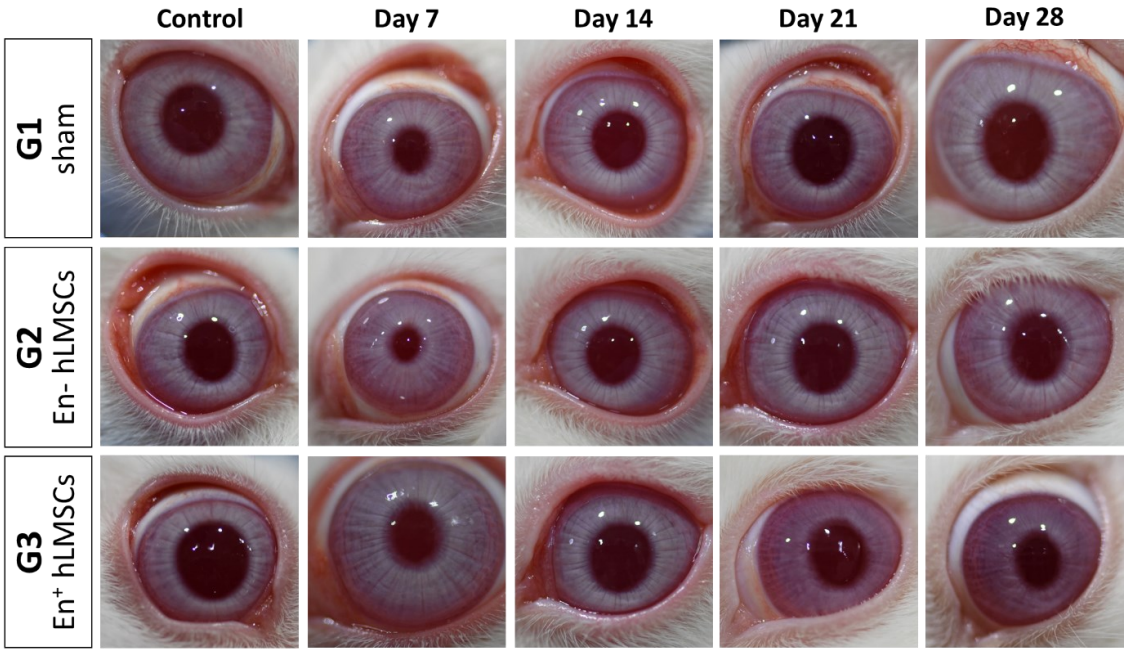

Figure 5.20: Collage of the clinical photographs of both the treated (left eye) and the untreated (*Control*, right eye) eyes of the rabbits, showing no major ophthalmic signs such as redness or inflammation, after treatment with hLMSCs. This data was published in part at DOI: 10.21203/rs.3.rs-789579/v1, by Damala M *et al*, 2021.

Time Point	**G1** (Normal)	**G1** (Treated)	**G2** (Normal)	**G2** (Treated)	**G3** (Normal)	**G3** (Treated)
			Conjunctival redness			
Pre-dose	0 (6 of 6)	0 (6 of 6)	0 (6 of 6)	0 (6 of 6)	0 (6 of 6)	0 (6 of 6)
3 hours	0 (6 of 6)	**1 (6 of 6)**	0 (6 of 6)	**1 (6 of 6)**	0 (6 of 6)	0 (6 of 6)
6 hours	0 (6 of 6)	**1 (1 of 6)**	0 (6 of 6)	**1 (6 of 6)**	0 (6 of 6)	0 (6 of 6)
12 hours	0 (6 of 6)	0 (6 of 6)	0 (6 of 6)	0 (6 of 6)	0 (6 of 6)	0 (6 of 6)
24 hours	0 (6 of 6)	0 (6 of 6)	0 (6 of 6)	0 (6 of 6)	0 (6 of 6)	0 (6 of 6)
day 7	0 (6 of 6)	0 (6 of 6)	0 (6 of 6)	0 (6 of 6)	0 (6 of 6)	0 (6 of 6)
day 14	0 (6 of 6)	0 (6 of 6)	0 (6 of 6)	0 (6 of 6)	0 (6 of 6)	0 (6 of 6)
day 21	0 (6 of 6)	0 (6 of 6)	0 (6 of 6)	0 (6 of 6)	0 (6 of 6)	0 (6 of 6)
day 28	0 (6 of 6)	0 (6 of 6)	0 (6 of 6)	0 (6 of 6)	0 (6 of 6)	0 (6 of 6)
			Corneal opacity			
Pre-dose	0 (6 of 6)	0 (6 of 6)	0 (6 of 6)	0 (6 of 6)	0 (6 of 6)	0 (6 of 6)
3 hours	0 (6 of 6)	0 (6 of 6)	0 (6 of 6)	0 (6 of 6)	0 (6 of 6)	0 (6 of 6)
6 hours	0 (6 of 6)	0 (6 of 6)	0 (6 of 6)	0 (6 of 6)	0 (6 of 6)	0 (6 of 6)
12 hours	0 (6 of 6)	0 (6 of 6)	0 (6 of 6)	0 (6 of 6)	0 (6 of 6)	0 (6 of 6)
24 hours	0 (6 of 6)	0 (6 of 6)	0 (6 of 6)	0 (6 of 6)	0 (6 of 6)	0 (6 of 6)
day 7	0 (6 of 6)	0 (6 of 6)	0 (6 of 6)	0 (6 of 6)	0 (6 of 6)	0 (6 of 6)
day 14	0 (6 of 6)	0 (6 of 6)	0 (6 of 6)	0 (6 of 6)	0 (6 of 6)	0 (6 of 6)
day 21	0 (6 of 6)	0 (6 of 6)	0 (6 of 6)	0 (6 of 6)	0 (6 of 6)	0 (6 of 6)
day 28	0 (6 of 6)	0 (6 of 6)	0 (6 of 6)	0 (6 of 6)	0 (6 of 6)	0 (6 of 6)
			Lesions in Iris			
Pre-dose	0 (6 of 6)	0 (6 of 6)	0 (6 of 6)	0 (6 of 6)	0 (6 of 6)	0 (6 of 6)
3 hours	0 (6 of 6)	0 (6 of 6)	0 (6 of 6)	0 (6 of 6)	0 (6 of 6)	0 (6 of 6)
6 hours	0 (6 of 6)	0 (6 of 6)	0 (6 of 6)	0 (6 of 6)	0 (6 of 6)	0 (6 of 6)
12 hours	0 (6 of 6)	0 (6 of 6)	0 (6 of 6)	0 (6 of 6)	0 (6 of 6)	0 (6 of 6)
24 hours	0 (6 of 6)	0 (6 of 6)	0 (6 of 6)	0 (6 of 6)	0 (6 of 6)	0 (6 of 6)
day 7	0 (6 of 6)	0 (6 of 6)	0 (6 of 6)	0 (6 of 6)	0 (6 of 6)	0 (6 of 6)
day 14	0 (6 of 6)	0 (6 of 6)	0 (6 of 6)	0 (6 of 6)	0 (6 of 6)	0 (6 of 6)
day 21	0 (6 of 6)	0 (6 of 6)	0 (6 of 6)	0 (6 of 6)	0 (6 of 6)	0 (6 of 6)
day 28	0 (6 of 6)	0 (6 of 6)	0 (6 of 6)	0 (6 of 6)	0 (6 of 6)	0 (6 of 6)
			Aqueous humour			
Pre-dose	0 (6 of 6)	0 (6 of 6)	0 (6 of 6)	0 (6 of 6)	0 (6 of 6)	0 (6 of 6)
3 hours	0 (6 of 6)	0 (6 of 6)	0 (6 of 6)	0 (6 of 6)	0 (6 of 6)	0 (6 of 6)
6 hours	0 (6 of 6)	0 (6 of 6)	0 (6 of 6)	0 (6 of 6)	0 (6 of 6)	0 (6 of 6)
12 hours	0 (6 of 6)	0 (6 of 6)	0 (6 of 6)	0 (6 of 6)	0 (6 of 6)	0 (6 of 6)
24 hours	0 (6 of 6)	0 (6 of 6)	0 (6 of 6)	0 (6 of 6)	0 (6 of 6)	0 (6 of 6)
day 7	0 (6 of 6)	0 (6 of 6)	0 (6 of 6)	0 (6 of 6)	0 (6 of 6)	0 (6 of 6)
day 14	0 (6 of 6)	0 (6 of 6)	0 (6 of 6)	0 (6 of 6)	0 (6 of 6)	0 (6 of 6)
day 21	0 (6 of 6)	0 (6 of 6)	0 (6 of 6)	0 (6 of 6)	0 (6 of 6)	0 (6 of 6)
day 28	0 (6 of 6)	0 (6 of 6)	0 (6 of 6)	0 (6 of 6)	0 (6 of 6)	0 (6 of 6)

Table 5.4: Scores of the parameters of ophthalmic observations made, as per the grading of the severity (**Table 4.8** of Methods) of ocular lesions. G1: Sham treated group; G2: Group treated with En- hLMSCs, G3: Group treated with En+ hLMSCs.

5.3.3. Intraocular pressure

The intraocular pressure (IOP) was within normal range and comparable across all study groups. There were no significant differences in the IOP of the treated eyes (right eyes) in both test groups compared to the sham-treated (control) group. The IOP of the contralateral eyes (normal, left eyes) in all groups remained within normal levels with no significant changes, except for one rabbit in the G3 group on day 28, where there was a deviation from the normal range. However, this change did not impact the overall findings (**Figure 5.21 and Table 5.5**).

A table of the individual readings of the IOP of both eyes was provided in **Table 5.6**. The median levels of the IOP of both test (G2 & G3) groups and the vehicle control/test (groups) were provided in **Table 5.5**. The median levels of En+/En- hLMSCs treated groups were comparatively analyzed to that of the sham-treated group. The Kruskal-Wallis test, which is a non-parametric version of the one-way analysis of variance, was used for the statistical study. A pictorial representation of the same is shown in **Figure 5.21**.

Group	Pre-dose	3 hours	6 hours	12 hours	24 hours	Day 7	Day 14	Day 21	Day 28
				IOP of the treated eyes					
G1	10.5	10.0	11.0	11.0	13.0	13.0	12.0	13.0	12.5
G2	12.5	9.0	10.0	11.5	13.0	11.0	12.0	15.0	12.0
G3	12.0	12.0	9.0	11.0	12.5	13.0	13.0	11.0	12.5
p-value	0.185	0.063	0.268	0.855	0.953	0.154	0.718	0.069	0.349
				IOP of the normal eyes					
G1	12	10.5	13	13.5	13.5	14	13	13.5	13
G2	13.5	8	13.5	13	13.5	12.5	12	13	12
G3	12.5	10	12.5	13.5	13.5	12	13.5	12.5	12
p- value	0.715	0.067	0.877	0.792	0.999	0.056	0.586	0.498	*0.017*

Table 5.5: Median levels of intraocular pressure (IOP) measured in the rabbit eyes at various time periods (n=6 for each group). G1: Sham treated group; G2: Group treated with En- hLMSCs, G3:

Group treated with En+ hLMSCs. This data was published in part at DOI: 10.21203/rs.3.rs-789579/v1, by Damala M *et al*, 2021.

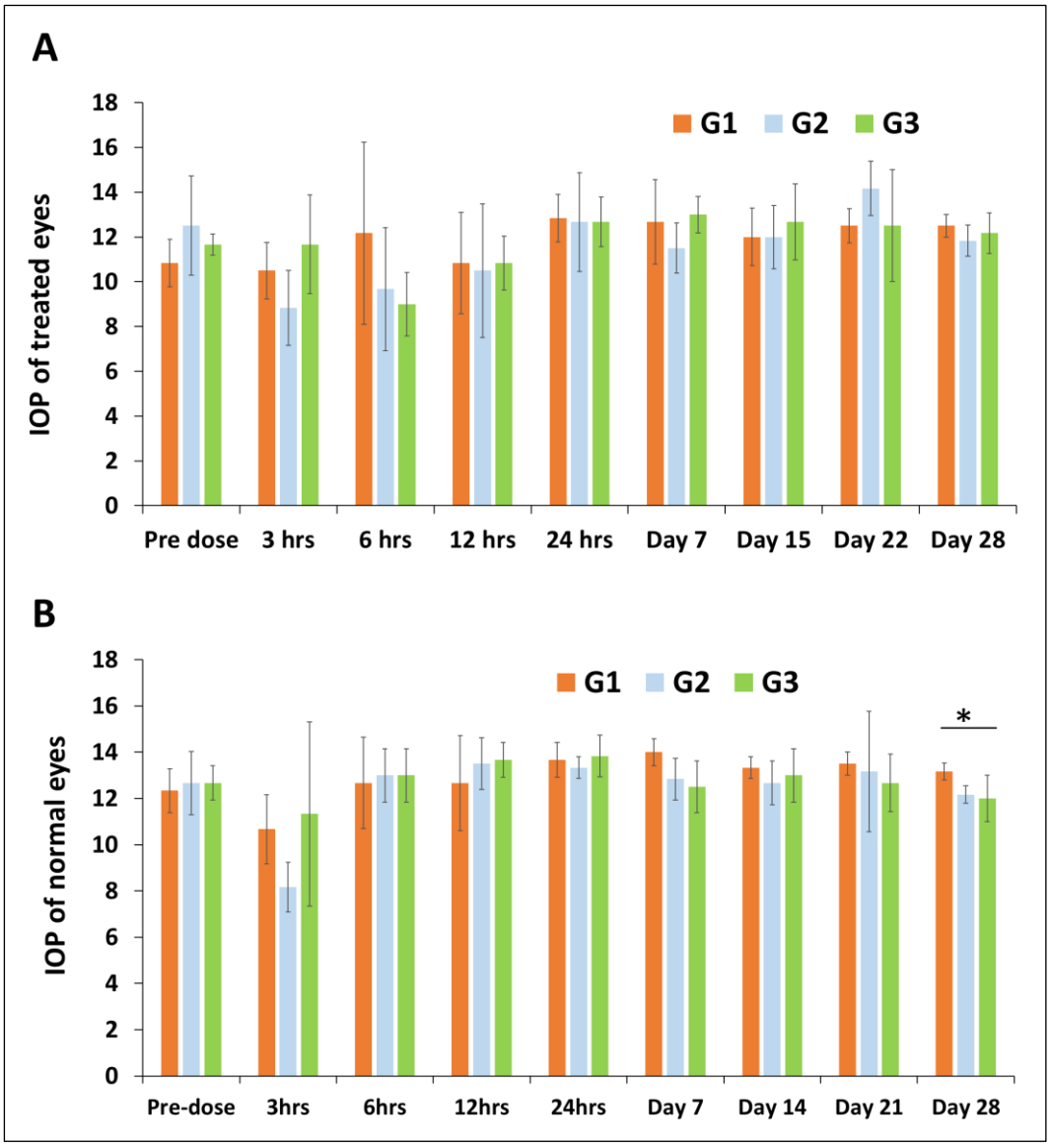

Figure 5.21. **(A)** The graph plot illustrates the changes in intraocular pressure (IOP) of the treated (left) eyes of rabbits following treatment with En+/En- hLMSCs. The data is based on a sample size of n=6. Statistical significance is denoted by *p<0.05, indicating a significant difference compared to the control group. **(B)** The graph plot displays the changes in intraocular pressure (IOP) of the normal (right) eyes of rabbits throughout the study. The data is based on a sample size of n=6. Statistical significance is denoted by *p<0.05, indicating a significant difference compared to the control group. G1: Sham treated group; G2: Group treated with En- hLMSCs, G3: Group treated with En+ hLMSCs. This data was published in part at DOI: 10.21203/rs.3.rs-789579/v1, by Damala M *et al*, 2021.

Individual readings of the Intraocular Pressure																			
GROUP	**ID**	**Pre dose**		**Day 1**								**Day 7**		**Day 15**		**Day 22**		**Day 28**	
				3 hours		**6 hours**		**12 hours**		**24 hours**									
		LE	RE	LE	RE	LE	RE	LE	RE	LE	RE	LE	RE	LE	RE	LE	RE	LE	RE
G1 (*sham*)	***1.***	10	13	10	9	20	13	14	9	13	14	13	14	12	14	12	13	13	13
	2.	10	12	10	12	11	11	11	14	14	13	12	13	10	13	13	14	12	13
	3.	10	12	13	10	10	13	8	11	13	13	13	14	11	13	13	13	13	13
	4.	11	11	10	13	7	13	11	13	14	15	15	15	12	13	13	14	12	13
	5.	13	14	11	11	14	14	13	15	12	14	14	14	14	14	11	13	12	13
	6.	11	12	9	9	11	11	8	14	11	13	9	14	13	13	13	14	13	14
G2 (*En-* hLMSCs)	***7.***	14	14	7	7	5	10	12	13	12	13	11	13	11	13	15	12	11	12
	8.	12	12	9	9	8	10	4	13	9	13	10	12	13	11	12	10	11	12
	9.	9	10	9	8	10	13	12	16	11	14	11	14	10	12	15	11	12	12
	10.	11	13	7	10	10	15	13	13	15	14	11	14	13	13	15	18	12	12
	11.	16	14	9	7	14	14	11	13	15	13	13	12	14	13	15	14	13	13
	12.	13	13	12	8	11	14	11	13	14	15	13	12	11	14	13	14	12	12
G3 (*En+ hLMSCs*)	***13.***	12	12	11	6	8	12	10	13	14	13	13	14	11	14	11	11	12	13
	14.	12	14	14	9	10	15	11	15	14	15	13	14	15	13	11	13	13	12
	15.	11	12	8	10	7	12	11	13	12	13	14	12	13	14	12	12	13	13
	16.	11	13	14	10	8	12	9	13	12	15	12	11	14	12	12	13	13	12
	17.	12	13	10	15	11	13	13	14	11	14	12	12	10	11	11	12	11	12
	18.	12	9	13	18	10	14	11	14	13	13	14	12	13	14	18	15	11	10

Table 5.6: IOP of the treated (left) and normal (right) eyes at different the time-points of the study. Key: *LE* – Left Eye, *RE* – Right Eye. G1: Sham treated group; G2: Group treated with En- hLMSCs, G3: Group treated with En+ hLMSCs.

5.3.4. Clinical chemistry

Most of the clinical chemistry parameters were found to be within normal ranges, indicating no significant abnormalities (**Table 5.7**). However, the following observations were noted:

- Alanine Aminotransferase (ALT) levels were significantly higher in the G3 group (81.7 ± 32.0 IU/L) compared to G1 (61.8 ± 12.6 IU/L) and G2 (59.5 ± 26.9 IU/L).
- Aspartate Aminotransferase (AST) levels were significantly higher in G2 (74.2 ± 67.7 IU/L) compared to G1 (62.2 ± 13.0 IU/L) and G3 (61.0 ± 11.7 IU/L).
- Phosphorous levels were relatively higher in G3 (7.4 ± 1.1 mg/dL) compared to G1 (5.8 ± 0.4 mg/dL), but the difference was not statistically significant.
- Total protein levels were lower in both hLMSCs-treated groups compared to the sham-treated group.
- Total cholesterol and low-density lipoproteins (LDL) levels were higher in G3 compared to the other groups.
- Sodium levels were significantly lower in G3 (152.5 ± 1.9 mmol/L) compared to the sham group (158.4 ± 3.2 mmol/L).

These changes did not have any significant impact on the systemic organs of the tested animals. (**Table 5.7 and Figure 5.25**).

A list of the individual observations of all parameters in the rabbits (arranged group-wise) is provided in **Table 5.8.** The summary of mean observations of all the parameters are given in **Table 5.7**.

S.No.	Parameter	Abbreviation	G1 (sham)	G2 (*En-* hLMSCs)	G3 (*En+* hLMSCs)	Units
1.	Serum Glucose	GLU	112.83 ± 17.49	117.67 ± 12.76	115.33 ± 6.39	mg/dL
2.	Blood Urea Nitrogen	BUN	21.50 ± 2.99	21.67 ± 3.35	22.50 ± 3.64	mg/dL
3.	Serum Creatinine	CREAT	0.95 ± 0.13	0.85 ± 0.08	0.98 ± 0.29	mg/dL
4.	Serum Total Bilirubin	TBILL	0.05 ± 0.00	0.05 ± 0.01	0.05 ± 0.00	mg/dL
5.	Alanine Aminotransferase	ALT	61.83 ± 12.56	59.50 ± 26.91	81.67 ± 32.03*	IU/L
6.	Aspartate Aminotransferase	AST	62.17 ± 13.03	74.17 ± 67.73*	61.00 ± 11.65	IU/L
7.	Serum Alkaline phosphatase	ALP	86.67 ± 39.77	134.83 ± 48.47	107.83 ± 28.37	IU/L
8.	Serum Total Protein	PRO	6.0 ± 0.18	5.63 ± 0.38	5.82 ± 0.25	g/dL
9.	Serum Albumin	ALB	2.40 ± 0.07	2.36 ± 0.20	2.46 ± 0.10	g/dL
10.	Globulin	GLB	3.60 ± 0.21	3.27 ± 0.21*	3.38 ± 0.23	g/dL
11.	Serum Total Cholesterol	CHOL	56.33 ± 29.03	59.00 ± 13.76	74.83 ± 37.75*	mg/dL
12.	High-density Lipoprotein	HDL	23.50 ± 11.91	29.17 ± 9.15	30.83 ± 10.35	mg/dL
13.	Low-density Lipoprotein	LDL	27.00 ± 16.90	25.67 ± 7.36	36.50 ± 23.68*	mg/dL
14.	Serum Phosphorous	PHOS	5.83 ± 0.39	6.22 ± 0.46	7.35 ± 1.11	mg/dL
15.	Serum Calcium	Ca	12.98 ± 0.19	12.80 ± 0.46	12.67 ± 0.40	mg/dL
16.	Serum Sodium	Na	158.40 ± 3.19	153.26 ± 5.01	152.47 ± 1.86*	mmol/L
17.	Serum Potassium	K	4.84 ± 0.21	4.73 ± 0.36	5.50 ± 0.91	mmol/L
18.	Gamma-glutamyl Transferase	GGT	8.42 ± 3.30	10.65 ± 3.46	9.48 ± 4.33	IU/L

Table 5.7: Summary of the group-wise biochemical parameters of the rabbits. Levels observed with significant difference are marked with *. Values are expressed as mean ± SD. *p≤ 0.05. G1: Sham treated group; G2: Group treated with En- hLMSCs, G3: Group treated with En+ hLMSCs.

GROUP	ID	GLU	BUN	CREAT	TBILL	ALT	AST	ALP	PRO	ALB	GLB	CHOL	HDL	LDL	PHOS	Ca	Na	K	GGT
		mg/dL	mg/dL	mg/dL	mg/dL	IU/L	IU/L	IU/L	g/dL	g/dL	g/dL	mg/dL	mg/dL	mg/dL	mg/dL	mg/dL	mmol/L	mmol/L	IU/L
G1 (sham)	***1***	104	16	0.8	0.1	59	61	61	6.2	2.4	3.8	26	11	10	5.9	12.8	159.1	5.1	15.4
	2	110	21	0.9	0.1	59	54	69	6.2	2.4	3.8	32	15	13	5.6	13.2	156.9	4.8	8.1
	3	147	24	1.1	0.1	39	64	32	6.1	2.3	3.8	35	13	15	5.1	13.1	164.8	4.6	5.9
	4	116	20	0.8	0.0	62	63	116	5.9	2.4	3.5	55	29	24	6.2	12.8	154.5	5.0	8.7
	5	111	23	1.1	0.1	74	44	87	5.7	2.4	3.3	88	28	47	6.0	12.8	157.0	4.6	5.9
	6	89	25	1.0	0.1	78	87	155	5.9	2.5	3.4	102	45	53	6.2	13.2	158.1	5.0	6.5
G2 (*En+* hLMSCs)	***7***	113	27	0.9	0.1	37	37	100	5.3	2.1	3.2	52	16	25	5.8	13.1	155.2	5.2	7.9
	8	116	23	0.9	0.0	53	43	155	5.1	2.2	2.9	45	25	17	6.1	13.1	147.7	5.0	6.7
	9	102	17	0.9	0.1	43	41	235	5.8	2.4	3.4	52	21	23	7.0	11.8	151.2	4.2	9.8
	10	124	23	0.7	0.0	56	65	108	5.7	2.5	3.2	59	36	25	6.4	13.0	147.7	4.7	12.9
	11	142	18	0.9	0.1	118	224	104	6.3	2.7	3.6	88	42	41	6.4	12.8	161.9	4.4	17.1
	12	109	22	0.8	0.0	50	35	107	5.6	2.3	3.3	58	35	23	5.6	13.0	149.7	5.0	9.5
G3 (*En- hLMSCs*)	***13***	106	19	1.0	0.1	74	59	142	6.0	2.6	3.4	56	27	24	8.3	11.8	151.5	6.5	5.6
	14	117	21	0.9	0.1	58	49	134	5.8	2.5	3.3	31	16	11	7.1	12.8	153.2	5.3	3.6
	15	113	27	0.9	0.1	28	58	57	6.1	2.3	3.8	44	22	19	7.1	13.0	151.9	7.0	7.3
	16	112	21	0.8	0.0	120	57	91	5.9	2.5	3.4	98	47	46	6.6	12.9	154.5	5.0	16.0
	17	117	28	1.6	0.1	98	86	118	5.3	2.3	3.0	144	35	83	9.2	12.8	154.5	5.0	11.5
	18	127	19	0.7	0.0	112	57	105	5.8	2.4	3.4	76	38	36	5.8	12.7	149.2	4.3	12.9

Table 5.8: Table of the individual observations of the clinical chemistry parameters. Key: G1: Sham treated group; G2: Group treated with En- hLMSCs, G3: Group treated with En+ hLMSCs. *GLU* – Serum Glucose, *BUN* – Blood Urea Nitrogen, *CREAT* – Serum Creatinine, *TBILL* – Serum Total Bilirubin, *ALT* – Alanine Aminotransferase, *AST* – Aspartate Aminotransferase, *ALP*-Serum Alkaline phosphatase, *PRO*-Serum Total Protein, *ALB*-Serum Albumin, *GLB*-Globulin, *CHOL*-Serum Total Cholesterol, *HDL*-High-density lipoprotein, *LDL*-Low-density lipoprotein, *PHOS*-Serum Phosphorous, *Ca*-Serum Calcium, *Na*-Serum Sodium, *K*-Serum Potassium, *GGT*-Gamma-glutamyl transferase.

5.3.5. Hematology

All the hematological parameters were found to be normal in both hLMSC-treated groups, with respect to the sham-treated groups. There were no significant differences in the mean values or levels of the analytes in all three groups. The findings are summarized hereunder:

- Bone marrow observation also had revealed no major or significant changes, in the hematopoietic system in both groups that were treated with hLMSCs.
- No signs of any changes in cellularity such as erythropoiesis, granulopoiesis or lymphopoiesis were observed i.e., the hypocellularity or hypercellularity (presence of lower or higher number of cells than normal levels, respectively) of the red blood cells, neutrophils, eosinophils, basophils and lymphocytes such as B-cells or NK cells; or their precursor cells.
- The number of neutrophils in 2 out of 6 rabbits in the G3 (En+ hLMSCs) group showed a mild variation compared to the sham-treated (G1) group. However, this difference was not statistically significant. This observation was further supported by the absence of dose-dependent variations or toxicity in the myeloid, lymphoid, and erythroid precursor cells observed in the bone marrow smears of the hLMSC-treated animals.
- None of the animals in both sham-treated group and hLMSC-treated groups have shown any signs hyperchromasia or hypochromia in their blood cells.

5.3.6. Isolation of total protein from Tears

The total protein isolated from tears collected from the rabbits of all groups, at all the time points (Section 4.6.7 of Methodology). The isolated proteins were then quantified using BCA method, against the known standards. The amount of protein isolated has ranged between 3.4 μg to 16.2 μg. The volume of a given sample was then diluted accordingly to ensure the concentration of proteins is equal across all samples for ELISA.

S.No.	Parameter	G1 (sham)	G2 (*En-* hLMSCs)	G3 (*En+* hLMSCs)	Units
1)	Haematocrit	44.8 ± 3.31	42.5 ± 4.87	40.73 ± 2.35	%
2)	Hemoglobin	13.83 ± 1.06	13.10 ± 1.61	12.93 ± 0.72	gm/dL
3)	Mean Corpuscular Volume	72.35 ± 2.59	70.33 ± 3.23	70.90 ± 1.97	fL
4)	Platelets	384 ± 152.69	330.5 ± 69.85	461.17 ± 215.31	$10^3/\mu L$
5)	Red Blood Corpuscles	6.19 ± 0.4	6.06 ± 0.77	5.75 ± 0.24	$10^6/\mu L$
6)	White blood Corpuscles	9.97 ± 3.04	7.93 ± 1.54	8.63 ± 3.01	$10^3/\mu L$
7)	Differential Count				
	a) Neutrophils	40.67 ± 8.90	32.0 ± 5.29	43.83 ±15.68	%
	b) Lymphocytes	52.50 ± 10.08	62.67 ± 5.76	50.17 ± 15.42	%
	c) Monocytes	4.5 ± 1.38	3.67 ± 0.75	4.00 ± 0.58	%
	d) Eosinophil	2.33 ± 0.75	1.67 ± 0.47	2.0 ± 0.58	%
	e) Basophils	0.00 ± 0.00	0.00 ± 0.00	0.00 ± 0.00	%
8)	Reticulocyte Count	1.83 ± 0.08	1.86 ± 0.06	1.87 ± 0.05	%
9)	Bleeding Time	3.06 ± 0.29	3.25 ± 0.14	3.08 ± 0.30	minutes
10)	Coagulation Time	6.98 ± 0.33	7.22 ± 0.37	6.98 ± 0.33	minutes
11)	Prothrombin Time	16.17 ± 1.07	16.33 ± 0.94	16.67 ± 1.11	seconds
12)	Activated Partial Thromboplastin Time	39.67 ± 4.03	41.00 ± 2.08	40.33 ± 1.70	seconds
13)	Erythrocyte Sedimentation Rate	4.0 ± 3.21	5.67 ± 3.35	5.33 ± 1.89	mm/1st hour

Table 5.9: Summary of the levels of blood parameters of the rabbits of groups G1, G2 and G3. Key: G1: Sham treated group; G2: Group treated with En- hLMSCs, G3: Group treated with En+ hLMSCs. This data was published in part at DOI: 10.21203/rs.3.rs-789579/v1, by Damala M *et al*, 2021.

GROUP	ID	WBC	RBC	HGB	HCT	MCV	PLT	Neut	Lymph	Mono	Eos	Baso	RC	BT	CT	PT	APTT	ESR
		10^3/ µL	10^6/ µL	g/ dL	%	fL	10^3/ µL	%	%	%	%	%	%	Min.	Min.	secs	secs	mm/ 1st hr
G1 (sham)	***1***	13.1	6.4	13.5	44.4	69.7	662	40	52	5	3	0	1.74	3.00	7.0	16	36	4
	2	7.9	6.6	14.4	46.1	70.2	432	33	61	3	3	0	1.89	3.30	7.0	18	47	2
	3	13.3	6.2	14.6	46.1	74.1	308	60	31	7	2	0	1.69	3.15	6.3	15	35	2
	4	8.8	5.4	11.7	37.9	69.9	404	36	60	3	1	0	1.89	3.30	7.0	16	40	11
	5	11.8	6.6	14.9	48.5	73.6	343	37	55	5	3	0	1.92	3.15	7.3	15	42	2
	6	4.9	6.0	13.9	45.8	76.6	155	38	56	4	2	0	1.84	2.45	7.3	17	38	3
G2 (*En+* hLMSCs)	***7***	9.5	6.9	14.3	47.6	69.1	463	39	54	5	2	0	1.93	3.30	7.0	17	40	2
	8	9.0	6.2	12.8	41.4	66.8	252	25	70	4	1	0	1.82	3.30	7.0	16	42	6
	9	7.1	6.2	13.4	42.3	68.6	308	25	70	3	2	0	1.86	3.00	7.3	18	45	4
	10	7.9	4.9	11.3	37.4	76.8	370	36	59	3	2	0	1.89	3.45	8.0	16	39	10
	11	5.0	7.0	15.7	49.8	71.7	273	33	61	4	2	0	1.90	3.30	7.0	15	41	2
	12	9.1	5.3	11.1	36.5	69.0	317	34	62	3	1	0	1.74	3.15	7.0	16	39	10
G3 (*En- hLMSCs*)	***13***	6.0	5.8	13.0	39.5	68.1	398	33	61	4	2	0	1.88	3.30	7.0	16	40	5
	14	7.3	6.1	13.7	43.6	71.2	348	43	50	5	2	0	1.78	3.00	7.3	18	38	3
	15	14.9	5.5	12.0	38.4	69.9	923	63	33	3	1	0	1.90	3.30	7.3	15	42	8
	16	7.6	6.0	14.0	44.4	74.4	458	52	42	4	2	0	1.83	2.45	7.0	17	39	3
	17	9.5	5.6	12.4	38.9	69.9	256	16	78	4	2	0	1.95	3.30	7.0	16	43	6
	18	6.5	5.5	12.5	39.6	71.9	384	56	37	4	3	0	1.85	3.15	6.3	18	40	7

Table 5.10: List of the individual observations of the blood parameters of all the rabbits in the study groups. Key: G1: Sham treated group; G2: Group treated with En- hLMSCs, G3: Group treated with En+ hLMSCs. *HCT* – Haematocrit, *Hb* – Haemoglobin, *MCV* – Mean Corpuscular Volume, *Plat* – Platelets, RBC – Red Blood Corpuscles, WBC – White Blood Corpuscles, DLC – Differential Count, RC – Reticulocyte Count, *Neut* – Neutrophils, *Lymph* – Lymphocytes, *Mono* – Monocytes, *Eos* – Eosinophil, *Baso* – Basophils, *BME* – Terminal Bone Marrow Examination, *AIC* – Abnormal Immature Cells, *BT* – Bleeding Time, *CT* – Coagulation Time, *PT* – Prothrombin Time, *APTT* – Activated Partial Thromboplastin Time, *ESR* – Erythrocyte Sedimentation Rate.

5.3.7. Quantification of inflammatory markers

5.3.7.1. Level of TNF-α

A decreasing trend of TNF-α was observed from the point of dosing to the end of the study, in the rabbit sera. This trend remained similar across all the groups **(Figure 5.22A and Table 5.11).**

Whereas in the tear samples, the levels of TNF-α in the hLMSC-treated (G2 & G3 groups) were significantly low relative to the sham-treated group (G1) and followed a decreasing trend by the end of the study, except for few initial time points of hour 3 to end of hour 12, on Day 0. **(Figure 5.22B and Table 5.11).**

In tears, the median levels of TNF-α were found to be higher than (**Table 5.11**) the respective levels during the 1st hour of treatment, in the hLMSCs-treated groups (G2 and G3). However, these levels were significantly lesser than that of the sham-treated group (G1), similar to these differences in the levels across all time points, indicating that hLMSCs may not have caused the increase.

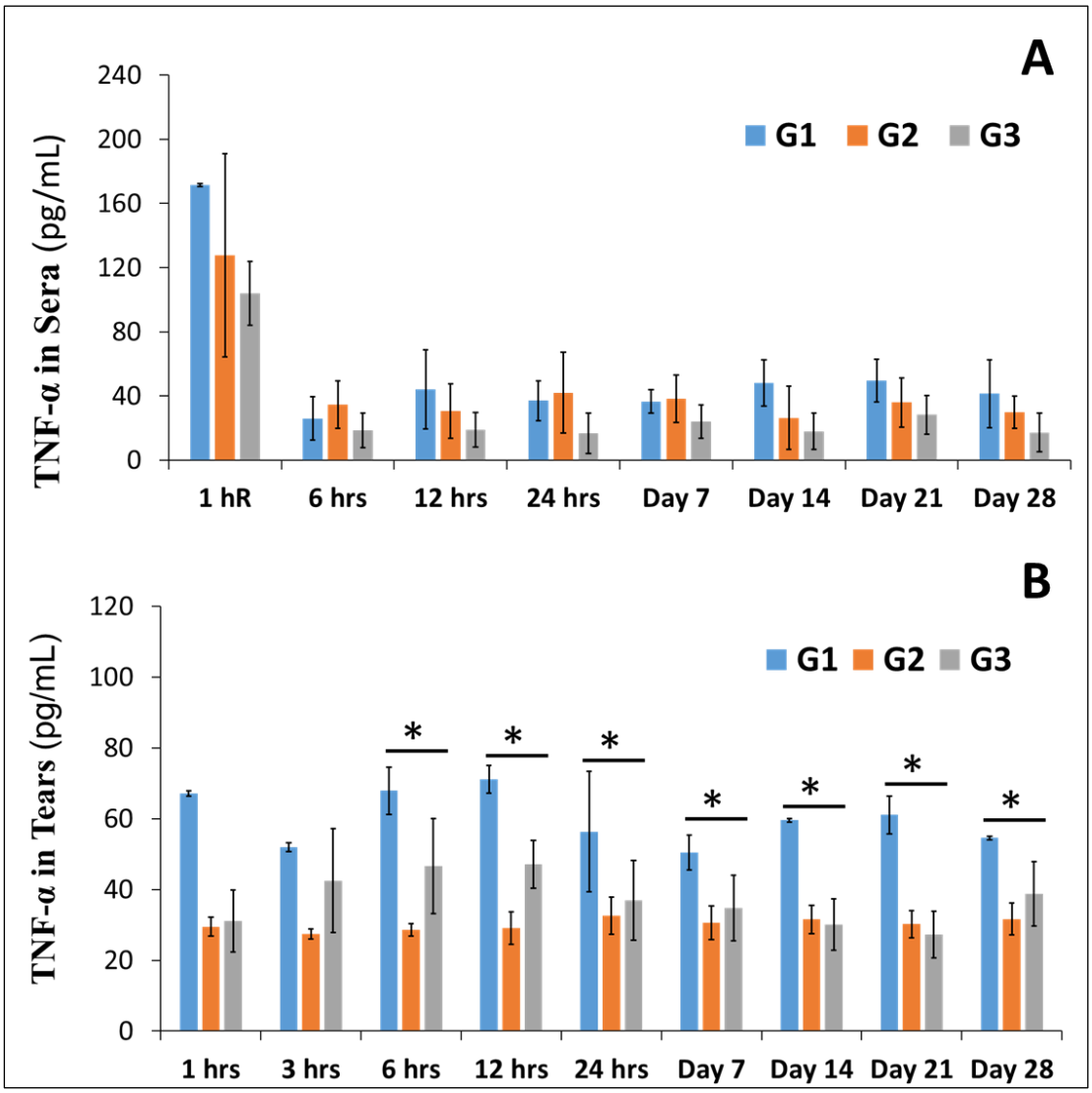

Figure 5.22: Bar-graphs showing the changes in the levels of TNF-α at various time-points in blood (A) and tears (B) of the rabbits treated with hLMSCs. Key: G1: Sham treated group; G2: Group treated with En- hLMSCs, G3: Group treated with En+ hLMSCs. This data was published in part at DOI: 10.21203/rs.3.rs-789579/v1, by Damala M *et al*, 2021.

Group	1hour	3hours	6hours	12hours	24 hours	Day 7	Day 14	Day 21	Day 28
Median levels of TNF-α (pg/mL) in serum									
G1	171.4	NA*	26	44.2	37.1	36.6	31.2	49.5	41.4
G2	165.7	NA*	28.9	23.7	37.3	33.9	25	34.3	27.1
G3	110.9	NA*	18.2	20.1	15.9	26.9	24.1	31.7	23.9
p-value	0.386	NA*	0.199	0.544	0.089	0.354	0.471	0.271	0.187
Median levels of TNF-α (pg/mL) in tears									
G1	67.2	51.9	67.9	71.1	56.4	50.5	59.6	61.1	54.5
G2	28.7	27.6	27.9	30.2	31.9	30.7	31.4	30.8	32.9
G3	31.1	43.1	42.6	47.9	34.7	33.1	27.3	25.6	42.6
p-value	0.091	0.108	*0.005*	*0.004*	*0.253*	*0.109*	*0.071*	*0.071*	*0.028*

Table 5.11: Median levels of the expression of TNF-α in serum and tears at various timepoints during the study. *Blood samples at the 3-hour time-point were not included in methodology. Key: G1: Sham treated group; G2: Group treated with En- hLMSCs, G3: Group treated with En+ hLMSCs. This data was published in part at DOI: 10.21203/rs.3.rs-789579/v1, by Damala M *et al*, 2021.

4.3.7.2. Levels of IL-6

The levels of IL-6 were also observed a similar trend like TNF-α. In the sera of the hLMSC-treated rabbits, IL-6 was observed to decrease toward the end of day 28 from the 1st hour of treatment **(Figure 5.23A).**

In tears, the levels of IL-6 were found to be relatively higher in G3 (En+ hLMSCs) group, immediately post treatment, till the 3rd hour. However, this subsided and followed a relatively

decreasing trend towards the end of day 28, when compared to the sham-treated (G1) group **(Figure 5.23B).**

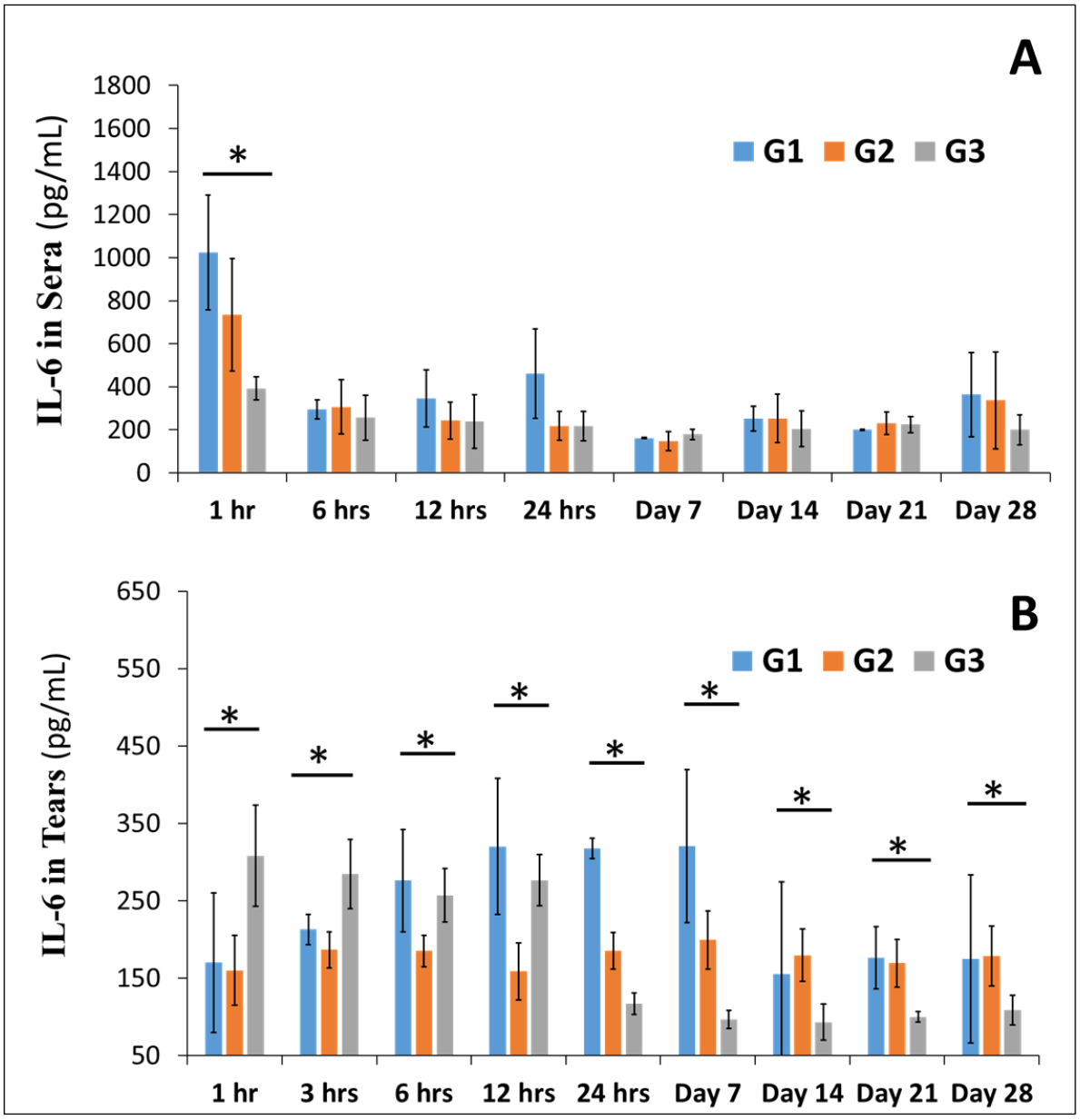

Figure 5.23: Bar-graph showing the levels of IL-6 in blood (A) and tear samples (B)of the rabbits treated with hLMSCs. This data was published in part at DOI: 10.21203/rs.3.rs-789579/v1, by Damala M *et al*, 2021. Key: G1: Sham treated group; G2: Group treated with En- hLMSCs, G3: Group treated with En+ hLMSCs.

Group	1 hours	3 hours	6 hours	12 hours	24 hours	Day 7	Day 14	Day 21	Day 28
Median levels of IL-6 (pg/mL) in serum									
G1	1025	NA*	294.1	345.2	462.2	162.1	251.8	199.9	363.6
G2	735.5	NA*	291.6	209.6	189.8	148.3	212.5	207.9	211.2
G3	373.6	NA*	209.2	176.3	195.6	180.4	171.2	215.6	174.6
p-value	*0.019*	NA*	0.737	0.504	0.258	0.222	0.331	0.549	0.296
Median levels of IL-6 (pg/mL) in tears									
G1	284.3	274.5	345.2	325.5	275.7	316.2	345.2	454.9	357.7
G2	177.9	188.7	192.7	154.5	191.8	198.6	166.2	176.3	195.1
G3	282.2	269	257.8	279.7	114.9	98.3	91.4	100.8	110.6
p-value	*0.021*	*0.008*	*0.012*	*0.012*	*0.006*	*0.005*	*0.004*	*0.004*	*0.014*

Table 5.12: Median levels of the expression of IL-6 in the blood and tears of rabbits treated with hLMSCs. *Blood samples at the 3-hour time-point were not included in methodology. Key: G1: Sham treated group; G2: Group treated with En- hLMSCs, G3: Group treated with En+ hLMSCs. This data was published in part at DOI: 10.21203/rs.3.rs-789579/v1, by Damala M *et al*, 2021.

5.3.7.3. Level of IgE

The levels of IgE were significantly high in the blood samples of the group treated with En+ hLMSCs (G3), in 5 of the 8 timepoints, when compared to the rest of the study groups (G1 & G2). However, a similar trend of the IgE expression was not observed in tear samples.

Except for the immediate hours of treatment with En- hLMSCs, i.e., at hours 1 and 3 post-treatment in group G2, the levels of IgE in the tears were noted to follow a decreasing pattern in all three groups and were comparable **(Figure 5.24).**

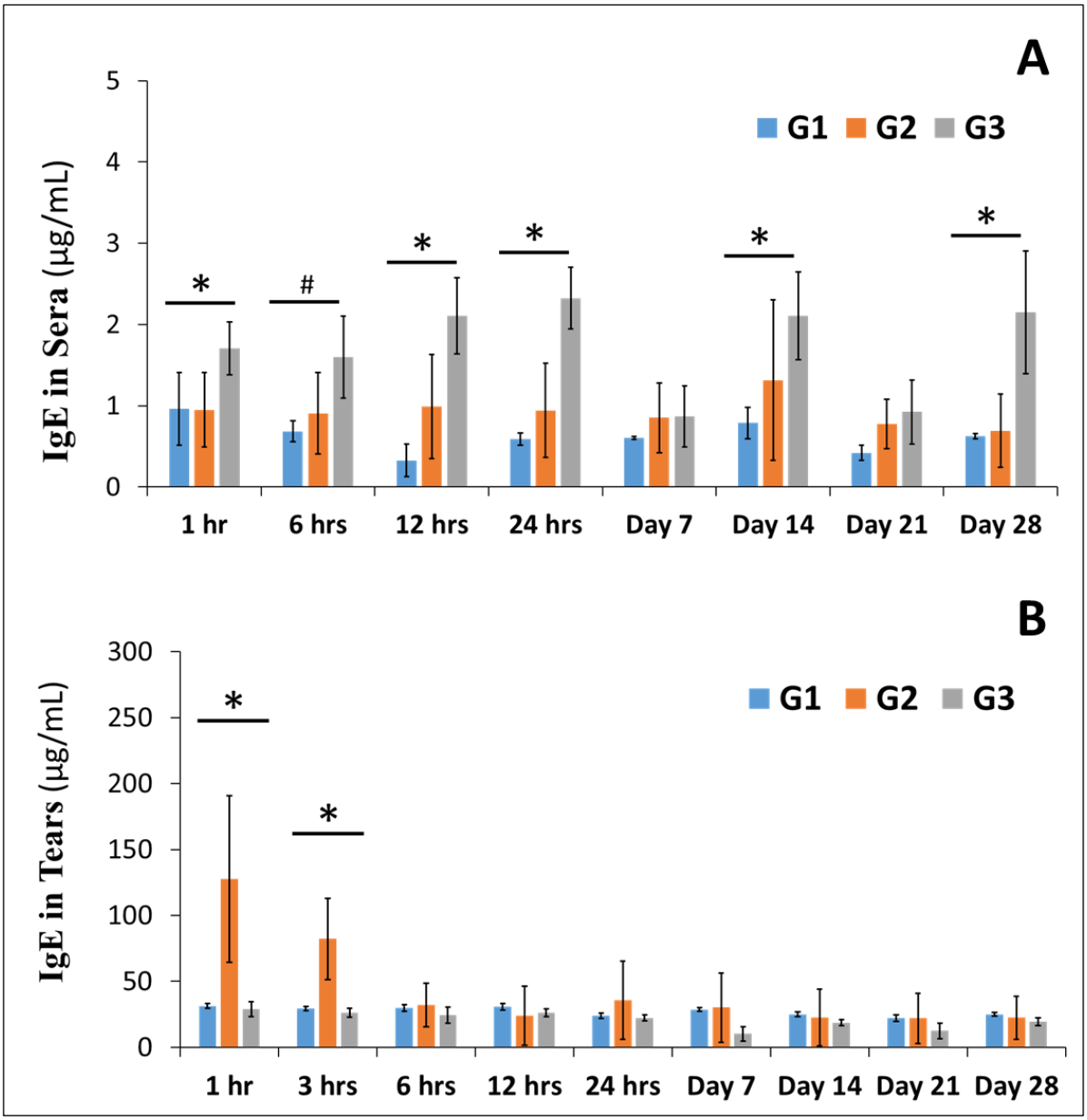

Figure 5.24: Level of IgE in the serum (A) and tears (B) of the rabbits treated with hLMSCs. This data was published in part at DOI: 10.21203/rs.3.rs-789579/v1, by Damala M *et al*, 2021. Key: G1: Sham treated group; G2: Group treated with En- hLMSCs, G3: Group treated with En+ hLMSCs.

Group	1 hours	3 hours	6 hours	12 hours	24 hours	Day 7	Day 14	Day 21	Day 28
Median levels of IgE (µg/mL) in serum									
G1	0.961	NA*	0.684	0.327	0.592	1.205	0.789	0.84	0.626
G2	0.787	NA*	0.659	0.736	0.685	1.555	1.085	1.655	0.537
G3	1.845	NA*	1.588	2.28	2.145	1.875	2.165	1.865	1.95
p-value	*0.048*	NA*	0.067	*0.016*	*0.022*	0.549	*0.024*	0.206	*0.017*
Median levels of IgE (µg/mL) in tears									
G1	32.5	29.5	30.2	31.8	25.5	17.77	25.2	9.7	23.2
G2	165.7	98.5	26.4	17.5	27.1	22.73	17.9	18.5	22.1
G3	30.7	26.4	26.1	26.9	21.1	5.87	18.9	7.4	18
p-value	*0.023*	*0.026*	0.471	0.341	0.737	0.116	0.528	0.344	0.603

Table 5.13: Median levels of the IgE expression in blood and tears are provided. *Blood samples at the 3-hour time-point were not included in methodology. Key: G1: Sham treated group; G2: Group treated with En- hLMSCs, G3: Group treated with En+ hLMSCs. This data was published in part at DOI: 10.21203/rs.3.rs-789579/v1, by Damala M *et al*, 2021.

5.3.8. Necropsy

No abnormalities were detected in any rabbit during the *in situ* and the external examinations of the internal organs (**Table 5.14**).

Test and the Gross Observation	G1 (Sham)	G2 (En- hLMSCs)	G3 (En+ hLMSCs)
External Examination			
No abnormality detected	6 of 6	6 of 6	6 of 6
Abnormality detected	0 of 6	0 of 6	0 of 6
***in situ* Examination**			
No abnormality detected	6 of 6	6 of 6	6 of 6
Abnormality detected	0 of 6	0 of 6	0 of 6

Table 5.14: Summary of the necropsy findings. Key: *No. of animals positive for an observation/Total of animals in the group.* G1: Sham treated group; G2: Group treated with En- hLMSCs, G3: Group treated with En+ hLMSCs.

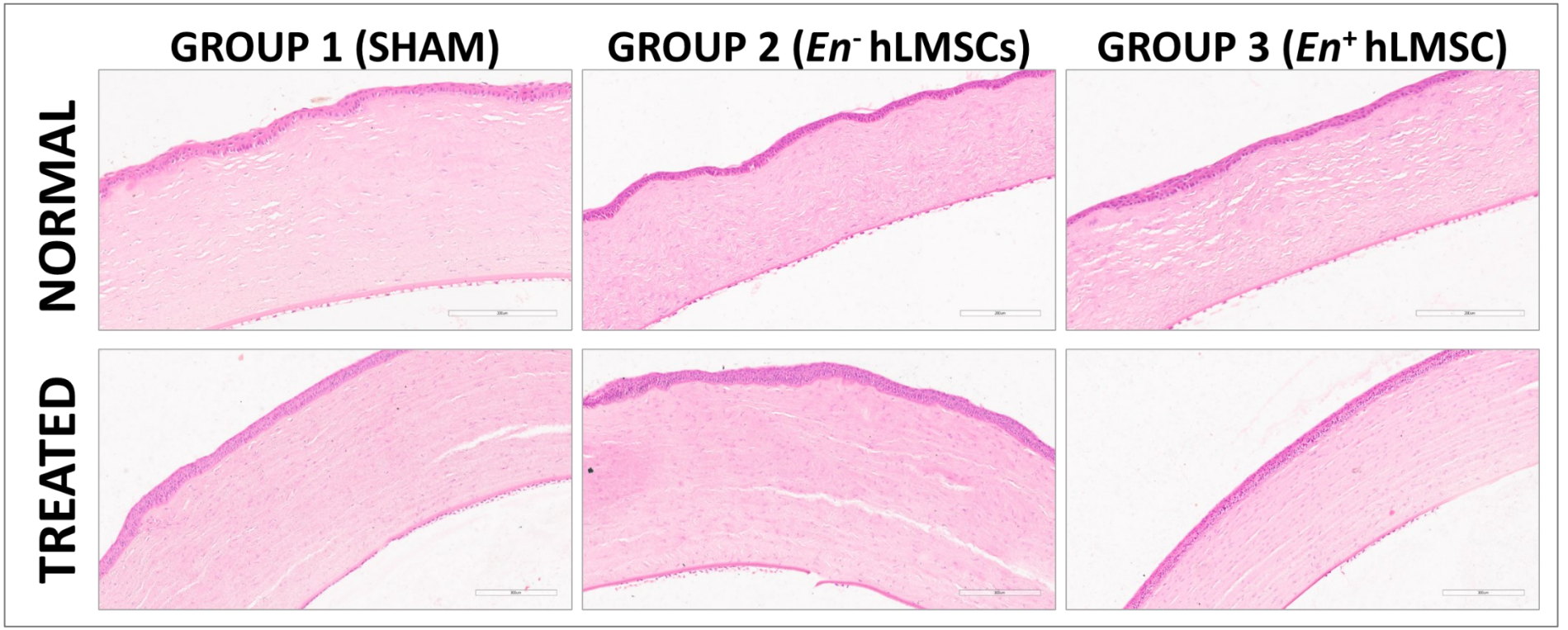

Figure 5.25: Collage of the microphotographs of the rabbit corneas, stained with hematoxylin and eosin, showing normal anatomy of the corneal layers in the treated corneas, with respect to normal corneas. Scale: 200µM. G1: Sham treated group; G2: Group treated with En- hLMSCs, G3: Group treated with En+ hLMSCs. This data was published in part at DOI: 10.21203/rs.3.rs-789579/v1, by Damala M *et al*, 2021.

5.3.9. Histopathology

5.3.9.1. Histopathology of cornea

The corneas were collected on day 29 of the study and subjected to histopathological examinations. The findings show there were no abnormalities in the treated corneas and their layers, when compared to their counterpart (normal/contralateral eyes) (**Figure 5.25**).

5.3.9.2. Histopathology of internal organs

Histopathological examination was carried out for all the groups. The following organs did not show any abnormal changes when compared to the control group: adrenal, aorta, colon, duodenum, epididymis, esophagus, heart, jejunum, lymph node, mammary gland, middle ear, muscle, ovary, pancreas, parathyroid, rectum, skin, spinal cord, spleen, testes, thymus, thyroid, trachea, urinary bladder, and uterus (**Table 5.15**).

- Alveolar wall thickening or inflammation was observed in the lungs of 4 rabbits from G3, 5 rabbits from G2, and 5 rabbits from G1.
- Tubular degeneration was seen in 1 rabbit each from G2, G3, and G1. Additionally, foci of tubular or interstitial inflammation were found in 3 rabbits from G3, 1 rabbit from G2, and 3 rabbits from G1.
- Foci of necrosis and perivascular cuffing were noticed in one male animal from G2 and two animals from G1.
- One animal in each group exhibited submucosal lymphoid tissue hyperplasia in the ileum.
- Sinusoidal hemorrhages were observed in the liver of at least 2 rabbits in all groups. However, foci of necrosis and inflammatory cell infiltration were present only in G1, with no such changes in G2 and G3.

Specific organ changes were observed, but no consistent patterns or significant differences were found between hLMSC-treated and control groups. Similar lesions in sham-treated and hLMSC-treated groups suggest spontaneous occurrences. No major toxic effects were observed in systemic organs, indicating minimal or no impact of hLMSC administration (**Table 5.15**).

Histopathology of internal organs

Organ (s)	Observations	G1	G2	G3
Liver	- Sinusoidal haemorrhage	2 of 6	2 of 6	2 of 6
	- Inflammation or Necrosis or inflammatory cells	1 of 6	0 of 6	0 of 6
	- No Abnormality Detected	3 of 6	4 of 6	4 of 6
Lungs	- Thickening of alveolar wall or inflammation	5 of 6	5 of 6	4 of 6
	- No Abnormality Detected	1 of 6	1 of 6	2 of 6
Kidney	- Tubular degeneration	0 of 6	1 of 6	1 of 6
	- Tubular or interstitial inflammation	3 of 6	1 of 6	1 of 6
	- No Abnormality Detected	3 of 6	4 of 6	4 of 6
Brain	- Foci of cerebral necrosis or peri vascular cuffing	2 of 6	1 of 6	0 of 6
	- No Abnormality Detected	4 of 6	5 of 6	6 of 6
Ileum	- Submucosal lymphoid tissue hyperplasia	1 of 6	1 of 6	1 of 6
	- No Abnormality Detected	5 of 6	5 of 6	5 of 6
Spleen, Heart, Aorta, Adrenals, Colon, Rectum, Lymph nodes, Pancreas, Thymus, Urinary bladder, Stomach, Skeletal muscle, Skin, Spinal cord, Middle ear, Eye, Thyroid, Parathyroid, Trachea, Oesophagus, Duodenum, Jejunum	- No Abnormality Detected	6 of 6	6 of 6	6 of 6

Table 5.15: Summary of histopathological observations and their incidence per group of the rabbits after treatment with hLMSCs. Key: *No. of animals positive for a given indication* of *Total no. of animals per group*. G1: Sham treated group; G2: Group treated with En- hLMSCs, G3: Group treated with En+ hLMSCs.

5.3.10. Organ weights

The weights of the organs in hLMSC-treated groups (G2 and G3) were found have no significant differences with respect to the sham-treated group. A table summarizing these observations is given in **Table 5.16**.

S. No.	Organ	G1 (sham)	G2 (*En-* hLMSCs)	G3 (*En+*hLMSCs)
1.	Brain	8.42 ± 0.85	8.11 ± 0.63	8.10 ± 0.85
2.	Heart	6.28 ± 0.53	7.57 ± 1.17	7.01 ± 1.62
3.	Liver	73.15 ± 10.09	80.70 ± 16.78	71.72 ± 15.87
4.	Spleen	1.05 ± 0.33	1.14 ± 0.39	0.76 ± 0.20
5.	Kidney	14.80 ± 1.17	15.60 ± 1.67	16.53 ± 4.20
6.	Adrenals	0.39 ± 0.25	0.33 ± 0.05	0.31 ± 0.08
7.	Testes (male)	5.39 ± 2.27	6.11 ± 1.23	3.97 ± 1.45
8.	Uterus (female)	6.489 ± 3.31	7.003 ± 1.42	4.309 ± 2.25
9.	Lungs	9.32 ± 0.99	10.13 ± 0.51	9.46 ± 1.84

Table 5.16: Mean organ weights (Mean ± SD, in grams) of the rabbits treated with hLMSCs. No significant differences were observed in the hLMSC-treated groups compared to the control group ($p > 0.05$). G1: Sham treated group; G2: Group treated with En- hLMSCs, G3: Group treated with En+ hLMSCs.

5.3.11. Body weights

In all the test groups, the body weight gain was found normal, when compared to the control group (**Figure 5.26**). The individual body weights and the percentage of weight gain values are given in the **Table 5.17**.

Individual weights (in Kg) of the rabbits

Individual Body Weight (Kg)							Weight Gain (%)			
Group	*ID*	*Day 01*	*Day 08*	*Day 15*	*Day 22*	*Day 28*	*Week 1*	*Week 2*	*Week 3*	*Week 4*
Group 1 *(sham)*	1	1.96	2.40	2.80	2.83	2.75	18.33	30.00	30.74	28.73
	2	2.19	2.30	2.27	2.40	2.35	4.78	3.52	8.75	6.81
	3	2.50	3.00	3.24	3.27	2.97	16.67	22.84	23.55	15.82
	4	1.90	2.21	2.31	2.53	2.55	14.03	17.75	24.90	25.49
	5	2.30	2.35	2.58	2.60	2.66	2.13	10.85	11.54	13.53
	6	2.46	2.67	2.69	2.95	2.94	7.87	8.55	16.61	16.33
Group 2 *(En+ hLMSCs)*	7	1.96	2.21	2.70	2.86	2.63	11.31	27.41	31.47	25.48
	8	2.10	2.33	2.12	2.26	2.39	9.87	0.94	7.08	12.13
	9	2.38	2.54	2.81	2.81	3.11	6.30	15.30	15.30	23.47
	10	1.93	1.95	2.00	2.04	2.38	1.03	3.50	5.39	18.91
	11	2.16	2.34	2.67	2.75	2.39	7.69	19.10	21.45	9.62
	12	2.40	2.45	2.81	2.84	2.94	2.04	14.59	15.49	18.37
Group 3 *(En- hLMSCs)*	13	2.05	2.12	2.17	1.93	2.15	3.30	5.53	-6.22	4.65
	14	2.14	2.30	2.67	2.25	2.59	6.96	19.85	4.89	17.37
	15	2.28	2.35	2.31	2.14	2.36	2.98	1.30	-6.54	3.39
	16	2.10	2.40	2.71	2.86	2.97	12.50	22.51	26.57	29.29
	17	2.30	2.46	2.49	2.44	2.52	6.50	7.63	5.74	8.73
	18	2.38	2.53	2.49	2.49	2.91	5.93	4.42	4.42	18.21

Table 5.17: Table of the individual weights (in Kg) of the rabbits treated with hLMSCs with and without encapsulation and their weight gain ratios recorded during the study. G1: Sham treated group; G2: Group treated with En- hLMSCs, G3: Group treated with En+ hLMSCs.

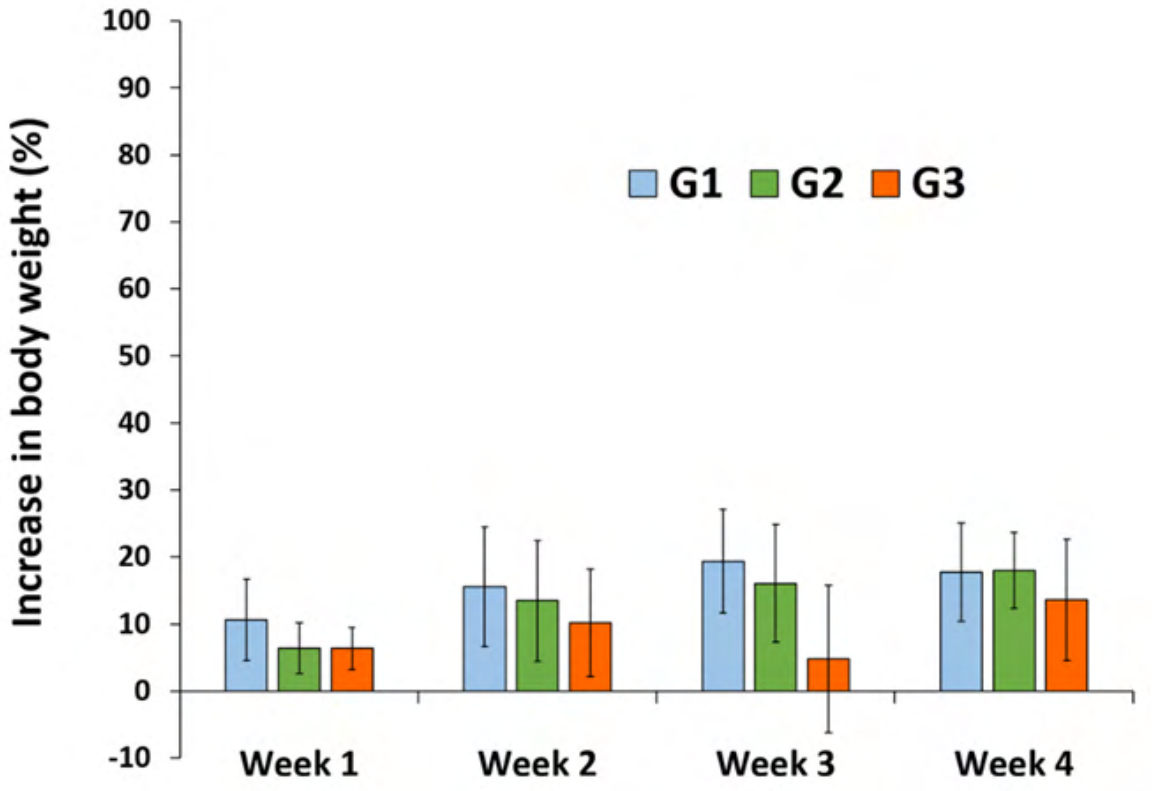

Figure 5.26. Graph plot illustrating the relative increase (%) in body weights of the rabbits following treatment. Three groups of rabbits (n=6) received hLMSCs, and their body weights were measured at the time of treatment and weekly for four weeks. The change in body weight, compared to the day of treatment, is depicted. The data are presented as mean ± SD, and statistical analysis revealed no significant differences ($p > 0.05$). G1: Sham treated group; G2: Group treated with En- hLMSCs, G3: Group treated with En+ hLMSCs. This data was published in part at DOI: 10.21203/rs.3.rs-789579/v1, by Damala M *et al*, 2021.

5.4. Assessment of efficacy of hLMSCs in healing and preventing corneal scars

5.4.1. Corneal scar formation

All the murine corneas that underwent mechanical debridement have developed corneal scaring by the end of week 2 (**Figure 5.27D and Figure 5.28**). The intensity of scarring was evident from the optical coherence tomography (OCT) scan sections of the corneal ultrastructure.

A clear and visually significant haze was evident in the OCT sections. This scarring has found to be gradually decreasing in the corneas treated with hLMSCs (both *Scar* and *Prophylaxis* groups) by the end of day 28, post treatment (**Figure 5.28**).

5.4.2. Mortality

Three mice were found to be dead during the course of the study, due to natural causes. These mice were excluded from the study for further analysis.

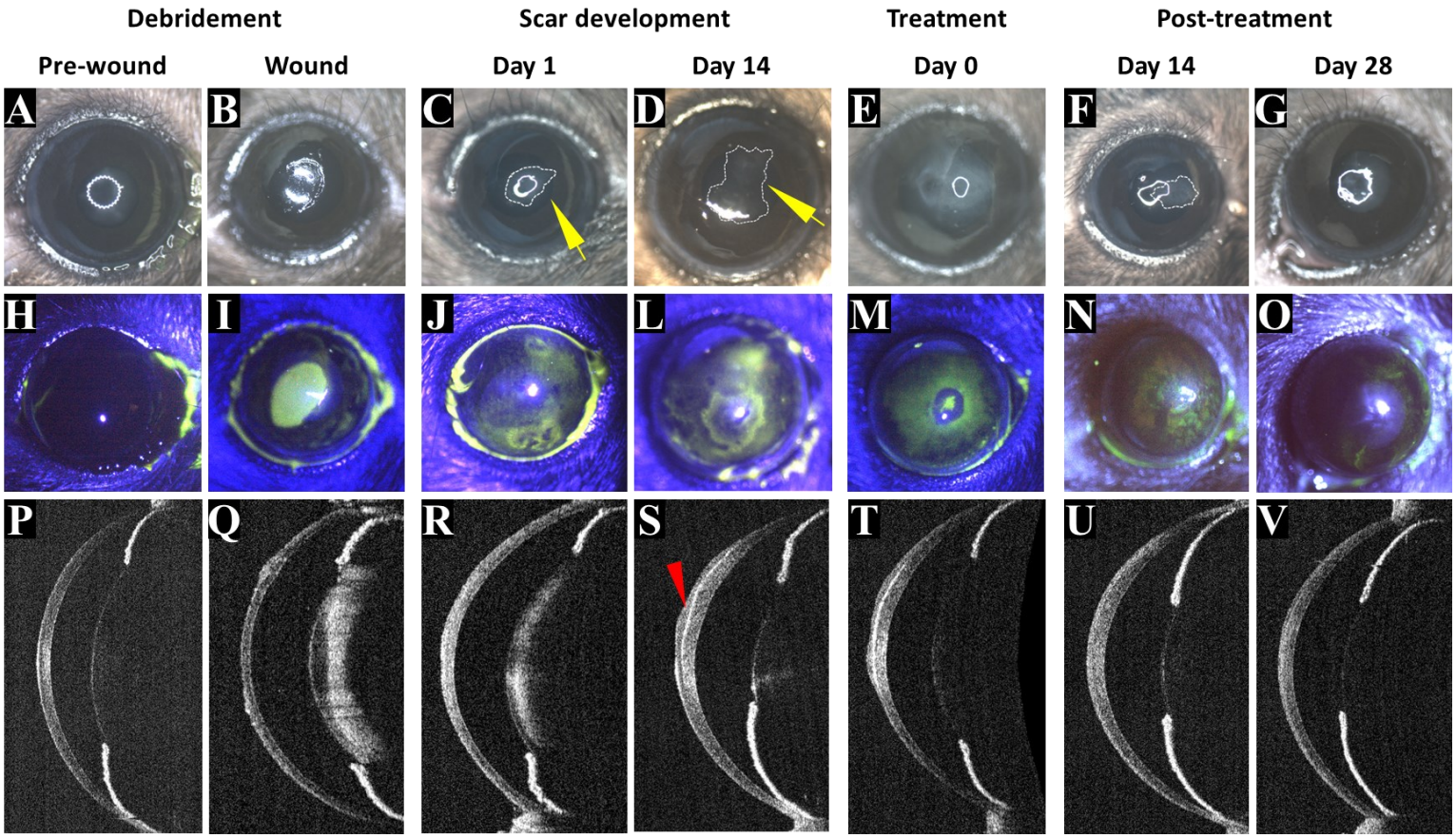

Figure 5.27: A collage of clinical photographs (A-G) showcasing the normal pre-wound corneal surface before central cornea debridement, along with corresponding fluorescein staining images (H-O) confirming compromised epithelial integrity. Following debridement, the corneas exhibited clouding or haze (indicated by a yellow arrow and marked with a dotted line) on day 1, progressing to scar formation within two weeks. The lower panel displays OCT scans (P-V) revealing scarring in the anterior stroma (indicated by a white arrow) and altered corneal thickness. The scarred tissue is subsequently treated with hLMSCs embedded in fibrin glue. On day 28 post-treatment, OCT scans demonstrate stabilized corneal transparency in the treated sections compared to the scarred areas.

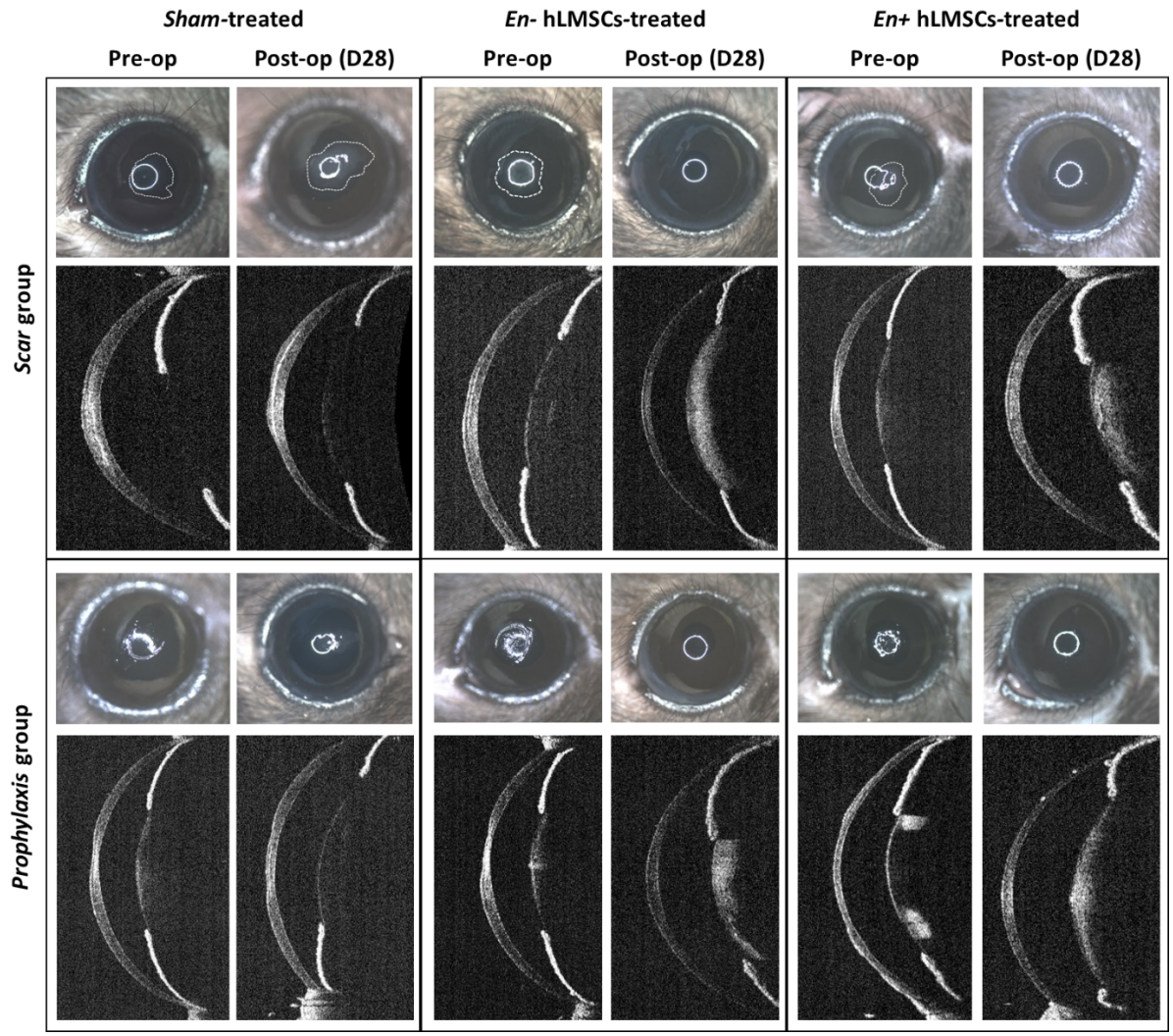

Figure 5.28: Representative microphotographs and scans are presented in a collage to illustrate the scarring of debrided corneas before and after treatment with hLMSCs. The images depict the untreated and sham-treated eyes, which exhibit unhealed corneas following the debridement or treatment. In contrast, the eyes treated with En-/En+ hLMSCs show relatively clear corneas with reduced haze and scarring by the end of day 28. In contrast, the eyes treated with En-/En+ hLMSCs demonstrate improved healing, as evidenced by relatively clear corneas with decreased haze and scarring observed at the end of day 28.

5.4.3. Change in corneal reflectivity (E:S ratio)

The mean E:S reflectivity ratio ranged between 0.87±0.03 and 0.96±0.01 GSU (gray scale units) across the three groups, prior to making any wound.

In the eyes treated with En-/En+ hLMSCs, the E:S ratio returned to baseline levels in all treated arms (**Figure 5.29 A-B**). Conversely, the untreated (**Figure 5.29 C**) and sham-treated arms showed the following changes in the E:S ratio:

- Untreated: decreased from 0.96 GSU to 0.65 GSU
- Sham-treated (scar): decreased from 0.93 GSU to 0.68 GSU
- Sham-treated (Prophylaxis): decreased from 0.96 GSU to 0.76 GSU

These changes indicate increased stromal reflectivity (**Figure 5.29 B**). The reflectivity of the corneas in the untreated groups increased by approximately 32.3%, while the scar and prophylaxis groups showed reflectivity increases of 26.9% and 20.8%, respectively, in the sham-treated arms.

5.4.4. Change in corneal haze

The intensity of corneal scar or haze exhibited a consistent decreasing trend in eyes treated with En-/En+ hLMSCs compared to the pre-treatment levels in both the scar and prophylaxis groups ($p < 0.0001$, n=6). In the scar group, the intensity of corneal haze decreased from 164±12 GSU to 121±6 GSU (26.2% reduction) for mice receiving En- hLMSCs and from 164±11 GSU to 124±11 GSU (24.4% reduction) for mice receiving En+ hLMSCs on day 14 of scar formation to day 28 (**Figure 5.30A**).

Similarly, in the prophylaxis group, the haze decreased from 151±14 GSU to 138±19 GSU (8.6% reduction) for En- hLMSCs and from 173±13 GSU to 136±11 GSU (21.4% reduction) for En+ hLMSCs on day 1 of wounding and transplantation to day 28 (**Figure 5.30B**). In contrast, eyes that received sham-treatment or no treatment showed no significant change in corneal scar intensity compared to the baseline before transplantation (**Figure 5.30A-C**).

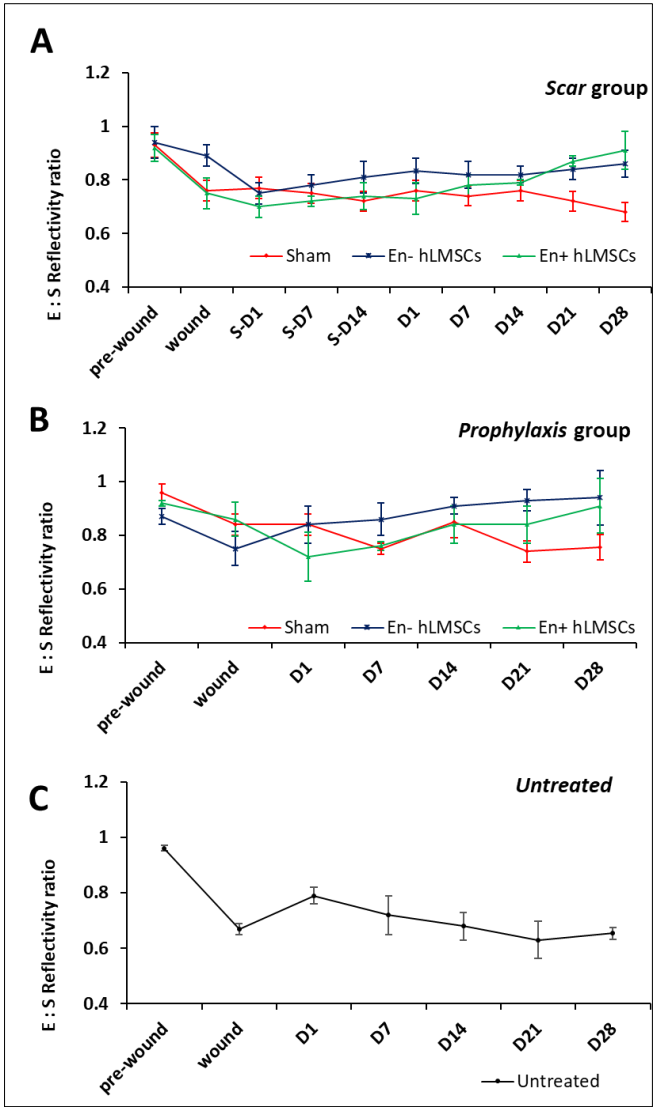

Figure 5.29 (E:S Reflectivity Ratio)

Figure 5.29: The reflectivity of corneal surface has normalized to the baseline readings in the eyes that received hLMSCs in both the scar (A) and prophylaxis (B) groups. The reflectivity of the stroma increased in eyes that received sham (A-B) or no treatment (C). *En-* hLMSCs: hLMSCs without any storage or transport; *En+* hLMSCs – hLMSCs released from encapsulation after storage and transport.

Figure 5.30: (A-C) Graphical representation of scar intensity reduction in corneas. Mice treated with hLMSCs after scar development (A) have shown significant decrease ($p < 0.0001$, n=8) in the scar area, relative to pre-treatment (S-D1 to S-D14), whereas the mice that received hLMSCs prophylactically (B) did not show any significant ($p = 0.08$, n=8) increase the scar area.

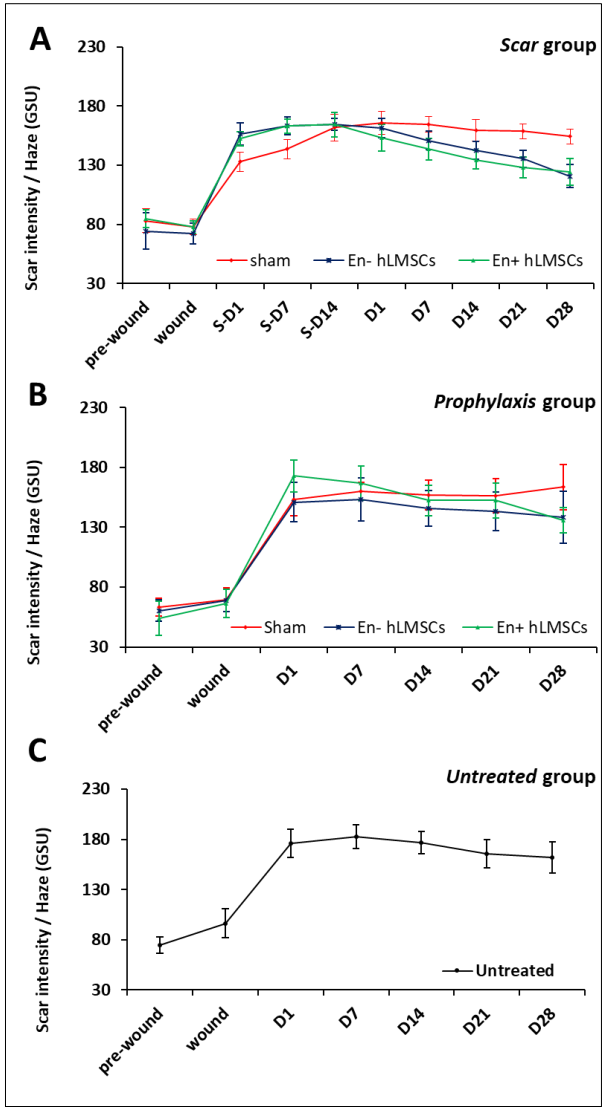

Figure 5.30 (Intensity of Scar or Haze)

5.4.5. Change in the scar area

During the two-week period of scar development, it was observed that the area of the scarred corneal surface increased in all treatment groups. However, after treatment with En- and En+ hLMSCs, there was a gradual decrease in the size of the scarred area (**Figure 5.31A**). This suggests that the hLMSC treatment may have contributed to the reduction of corneal scarring.

On the other hand, mice that received sham treatment did not show a significant change in the size of the corneal scar throughout the follow-up period, indicating that the sham treatment did not have a substantial effect on scar reduction (**Figure 5.31A-B**).

Furthermore, when En-/En+ hLMSCs were administered immediately after debridement, the scarred corneal surface remained relatively stable with a slight decrease in size. Although this decrease was not statistically significant, it suggests that the early application of hLMSCs may have contributed to limiting scar formation ($p = 0.0875$).

In contrast, mice that received prophylactic sham treatment exhibited an increase in the size of the scarred area, which remained consistent over time. This finding further supports the notion that the sham treatment did not have a significant impact on scar reduction. The results from the scar and untreated groups also confirmed the lack of substantial scar reduction ($p < 0.001$, **Figure** 5.31A; $p < 0.0001$, **Figure 5.31C**).

Overall, these observations indicate that treatment with En- and En+ hLMSCs may have the potential to contribute to scar reduction in the cornea, while the sham treatment showed limited effectiveness.

5.4.6. Rate of epithelization

The rate of epithelial recovery within the first week of debridement was comparable in mice treated with either vehicle alone or hLMSCs, irrespective of whether they were encapsulated in alginate or not (**Figure 5.29**). This suggests that the presence of hLMSCs, regardless of the encapsulation, may not have affected the initial healing process of the corneal epithelium during the early phase of debridement.

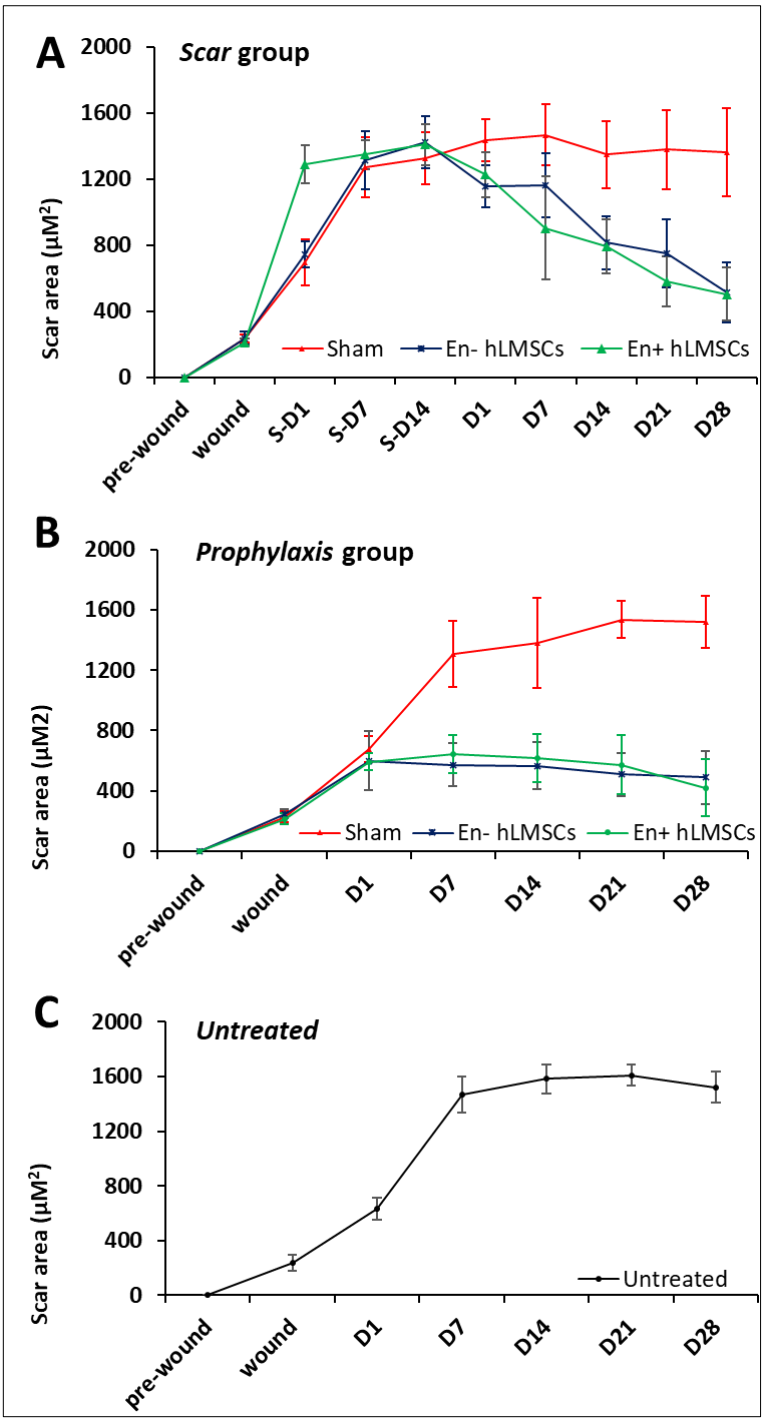

Figure 5.31: Graph plots (A-C) depict the reduction in the size of corneal scars. Mice treated with hLMSCs after scar development (A) exhibited a significant decrease ($p < 0.0001$, n=8) in scar area compared to the pre-treatment period (S-D1 to S-D14). On the other hand, mice that received hLMSCs prophylactically did not show a significant increase ($p = 0.08$, n=8) in scar area. These results indicate that the administration of hLMSCs after scar development effectively reduced the size of corneal scars, while prophylactic treatment with hLMSCs prevented significant scar area increase.

Chapter 6

Discussion

Cell-based therapies are one of the prominent treatment modalities that modern-day regenerative medicine could offer for corneal disorders. These minimally-invasive treatments offer scalability, minimize the risk of postoperative complications, and reduce dependence on donor corneas. With their trilineage differentiation capacity, anti-inflammatory and immunomodulatory properties (Ullah et al., 2015), and regenerative potential (Du et al., 2005), mesenchymal stem cells pose a prominent tool for regenerating the ocular surface. The limbus of the cornea harbors mesenchymal stem cells, capable of regenerating the cornea (Du et al., 2005; Branch et al., 2012; Funderburgh et al., 2016; Pinnamaneni & Funderburgh, 2012).

Earlier studies in mice, where human limbus-derived mesenchymal/stromal stem cells (hLMSCs) were used as a xenograft in mice to prevent fibrosis/scar after a corneal injury, have proven the safety of the mesenchymal originated stem cells, making them immunologically safe (Basu et al., 2014). In addition, many preclinical (Coppola et al., 2017; Ghoubay et al., 2020; Hertsenberg et al., 2017; Wu et al., 2012) and pilot clinical studies (Basu et al., 2017, 2019; Funderburgh et al., 2018) have shown mesenchymal/stromal stem cells derived from corneal limbus to prevent and cure blinding corneal stromal pathologies effectively. However, despite the therapeutic potential of hLMSCs in corneal wound healing, no studies have used the hLMSCs-based cell therapy in humans, conforming to the guidelines stated by the regulatory agencies.

There are several bottlenecks that hinder the translation of this hLMSCs-based cell therapy from bench to bedside, which include the lack of reliable methods of cultivating hLMSCs that conform to the mandatory requirements of current good manufacturing practice (cGMP); viable and cost-effective methods to preserve and transport these cells over extended durations and distances, and establishing the safety profiles of these cells prior to human applications.

The Drugs and Cosmetics Act, 1940, India, included the stem cells and their derivatives under the definition of 'Drugs,' categorizing them as Investigational New Drug or Investigational New Entity when used for clinical applications. To safeguard the vulnerable patients from being exploited and to ensure the efficacy of the stem cell products, the Central Drugs Standard Control Organization (CDSCO), along with the Indian Council of Medical Research (ICMR) and the Department of Biotechnology (DBT), Government of India, has recommended a set of guidelines (National Guidelines for Stem Cell Research, 2017). These guidelines ensure that all studies are conducted ethically and socially responsibly, complying with the regulatory framework (Central Drugs Standard Control Organization, n.d.; Lahiry et al., 2019).

The preservation and shipping of the cells and cell-based products are critical for clinical applications and future studies (Hanna & Hubel, 2009). Methods that offer optimal conservation

of the cell properties increase the outreach of the therapeutic products and offer an established and quality-controlled supply of the cell therapeutics between the sites of production and end-use. Cold-chain methods, mostly cryopreservation, predominate the current methods of storing or transporting cells. However, this inveterate technique fails to provide optimal viability and can induce a genetic drift leading to biological variations (Karlsson & Toner, 1996). Furthermore, the cryoprotectant agents like dimethyl sulfoxide, although meant to protect from cryoinjuries, can be dangerous to the cells, with possibilities of chromosome instability (Jenkins et al., 2012). Developing alternative methods to transport these cells without employing cold-chain methods may significantly improve the availability and affordability of such cell-based therapies.

Encapsulation of cells and cell aggregates is widely being explored and studied in various tissue engineering aspects (Galvez-Martín et al., 2017; Gurruchaga et al., 2015; Santos-Vizcaino et al., 2020). Encapsulation preserves stem cells' viability, proliferation, and differentiation abilities (Hidalgo San Jose et al., 2018). Alginates are the most frequently employed materials for encapsulating cells due to their excellent biocompatibility and biodegradability properties. Furthermore, the inert nature and the customizable viscosity and gelling capacities of the alginate make it the best agent for encapsulation (Li et al., 2015; Mahler et al., 2003; Orive et al., 2006). In addition, the alginate is deemed safe for human consumption by FDA, making it an ideal candidate for cell encapsulation in terms of the regulatory constraint (Cattelan et al., 2020). Encapsulation provides promising alternative methods to preserve the cells without the need for ultra-temperatures and harsh chemicals.

This study validated the cultivation procedures and assess the biological properties of hLMSCs conforming to the regulatory guidelines. In addition, this work focuses on the barriers in translating a potential surgical alternative into therapy and the framework to overcome them.This study focuses on validating cultivation procedures and assessing the biological properties of hLMSCs in accordance with regulatory guidelines. It also highlights the barriers in translating potential surgical alternatives into therapies and proposes strategies to overcome them.

In this study, we successfully isolated and expanded human limbus-derived mesenchymal/stromal stem cells (hLMSCs) from corneal limbal explants. The isolated hLMSCs exhibited distinct characteristics and phenotypes, which were assessed through qualitative and quantitative analyses. Additionally, we evaluated the stability, viability, and sterility of the hLMSCs to ensure their suitability for potential therapeutic applications. In this discussion, we will compare our findings with previous studies and highlight the significance of our results in the context of regenerative medicine.

Our study demonstrated the expression of various biomarkers associated with the characteristic phenotype of hLMSCs. The hLMSCs expressed ocular biomarkers such as Pax6, as well as stem cell markers including ABCG2 and p63-α. These findings are consistent with previous studies that have characterized the phenotype of hLMSCs (Funderburgh et al., 2018; Basu et al., 2019). The expression of surface markers CD105, CD73, and CD90 further confirmed the mesenchymal phenotype of the hLMSCs, while the absence of CD45, CD34, and HLA-DR indicated the absence of hematopoietic markers.

Several studies have reported similar findings regarding the expression of biomarkers in hLMSCs. For example, Xie et al. (2017) isolated and characterized hLMSCs and observed positive expression of Pax6, ABCG2, and p63-α, consistent with our results. Moreover, both studies reported the expression of surface markers CD105, CD73, and CD90, and the absence of CD45, CD34, and HLA-DR.

The expression of cytoskeletal biomarkers, including various collagens, neural cadherins (N-Cad), and vimentin, in hLMSCs was also consistent with previous reports (Xie et al., 2017; Damala et al., 2022). The positive expression of keratocan (KERA), a biomarker specific to corneal stromal keratocytes, further supports the corneal origin and phenotype of the isolated hLMSCs.

Karyotyping analysis revealed no chromosomal abnormalities in the hLMSCs from concurrently produced batches and cells revived from cryopreservation. These results are in line with previous studies that have reported the genetic stability of hLMSCs during long-term cultivation and cryopreservation (Damala et al., 2021).

The viability of hLMSCs stored as a pellet for extended periods was also assessed. Our results showed that the majority of hLMSCs remained viable after 24 hours of storage in ice, with a decline in viability over time. Similar findings have been reported by other studies investigating the viability of MSCs under similar storage conditions (Fekete et al., 2012; Hupfeld et al., 2017). These results indicate that hLMSCs can tolerate short-term storage in a pellet form, which may be useful in scenarios where unexpected delays occur during transportation or processing.

The growth kinetics analysis revealed a doubling time of approximately 61 hours for hLMSCs. This finding aligns with previous studies that have reported similar growth rates for MSCs derived from various sources (Dominici et al., 2006; Basu et al., 2019). The cumulative growth curves demonstrated a steady increase in cell number over time, confirming the proliferative capacity of hLMSCs.

Our study employed rigorous measures to ensure the sterility of the hLMSC cultures and absence of microbial contamination. These measures are essential to minimize the risk of infections and maintain the safety of potential therapeutic applications. All materials used in the isolation and expansion process were thoroughly screened for microbial contamination, following established protocols (European Pharmacopoeia, 2018). These stringent practices align with regulatory guidelines and ensure the suitability of hLMSCs for clinical use.

In conclusion, our study successfully isolated and characterized hLMSCs from corneal limbal explants. The hLMSCs exhibited a phenotype consistent with previous studies, expressing specific biomarkers associated with ocular mesenchymal/stromal stem cells. The stability, viability, and sterility assessments confirmed the suitability of hLMSCs for potential clinical applications.

Our findings align with existing literature, supporting the robustness and reproducibility of the isolation and characterization protocols for hLMSCs. These results contribute to the growing body of knowledge surrounding hLMSCs and their potential use in regenerative medicine and corneal tissue engineering.

Corneal stromal stem cells, including human limbus-derived mesenchymal stem cells (hLMSCs), have shown potential for corneal regeneration and have been explored in clinical trials. However, the lack of proper preservation and transport methods hinders their widespread application. This study aimed to evaluate the efficacy of alginate encapsulation in preserving hLMSC viability and properties during storage and transportation in real-life conditions.

Previous studies have demonstrated the positive expression of HLA-DR in normal cornea and similar findings of viability and maintenance of properties of encapsulated cells stored at room temperature. However, these studies did not test the preservation methods for hLMSCs derived from human tissues in actual transit conditions, nor did they examine the effects of real-life ambient temperature fluctuations.

hLMSCs were encapsulated in alginate and compared with non-encapsulated cells. Viability, survival in culture, and phenotype expression were evaluated. The study also assessed the efficacy of alginate encapsulation in retaining cell properties during storage and transportation in a ground-transportation scenario. The temperature inside the insulated container was maintained at lower levels compared to the external ambient temperature. The number of cells expressing specific biomarkers was analyzed.

Encapsulated hLMSCs maintained high viability and showed good survival in culture and adequate phenotype expression at room temperature and 4°C. The percentage of cells expressing

biomarkers was similar to the control groups. The findings suggest that alginate encapsulation effectively preserves hLMSCs during transit for up to 3 to 5 days at room temperature. This method eliminates the need for dry ice or expensive equipment for maintaining chilled temperature during shipping, potentially reducing storage and transportation costs.

The use of alginate encapsulation for preserving hLMSCs offers several advantages for cell-based therapy in corneal blindness. The simplicity of the encapsulation process combined with cost-effective ground transportation makes it an attractive option, particularly in developing countries where corneal opacification and scarring prevalence is high. The ability to transport cells at room temperature expands the accessibility of cell-based treatments to remote areas without the need for specialized cell culture facilities.

Similar studies have explored alternative treatments for corneal opacification and scarring, such as biomimetic hydrogels, molecular methods, and cell-based therapies. Hydrogels, both with and without cells, have shown effectiveness in stromal replacement using donor tissue. Molecular factors like exosomes and anti-inflammatory agents have also demonstrated potential in preventing or reversing corneal scars. However, hLMSCs have shown promising results in non-scarring wound healing and have the advantage of extended shelf life when encapsulated in alginate.

Preclinical testing and safety evaluations are essential before advancing to human clinical trials. This study conducted a comprehensive evaluation of toxicity and safety in both animal models and in vitro assays. Histopathological examinations of major organs, ophthalmic examinations, and hematological and tissue examinations were performed. The results indicated no abnormalities, inflammatory response, or ocular lesions. The safety profile of hLMSCs supports their potential for clinical applications.

The study has some limitations, such as the lack of serum-free culture methods and the evaluation of therapeutic properties of encapsulated cells, which are ongoing in further phases of the study. Additionally, evaluating the safety of hLMSCs in other delivery routes and testing in untreated or healthy eyes could provide further insights.

Alginate encapsulation is an effective method for preserving human limbus-derived mesenchymal stem cells (hLMSCs) during storage and transportation in real-life conditions. The encapsulated cells maintained high viability, survival in culture, and adequate phenotype expression at room temperature and 4°C. The percentage of cells expressing specific biomarkers was comparable to the non-encapsulated control groups. This study demonstrates the potential of alginate

encapsulation as a practical and cost-effective approach for maintaining the viability and properties of hLMSCs during transit for up to 3 to 5 days at room temperature.

The use of alginate encapsulation offers several advantages for cell-based therapy in corneal blindness. It eliminates the need for expensive equipment or specialized facilities for maintaining chilled temperatures during shipping, making it a viable option, especially in resource-limited settings. The ability to transport cells at room temperature expands access to cell-based treatments in remote areas. Moreover, the simplicity of the encapsulation process reduces the complexity and cost of cell storage and transportation.

Future studies should focus on evaluating the therapeutic properties of encapsulated hLMSCs and their effectiveness in corneal regeneration and wound healing. Additionally, further research is needed to assess the safety and efficacy of hLMSCs in other delivery routes and to explore their potential in untreated or healthy eyes.

The findings of this study contribute to the field of regenerative medicine and provide a promising approach for improving cell-based therapies in corneal blindness. By addressing the challenges of storage and transportation, alginate encapsulation of hLMSCs brings us closer to making these therapies more accessible and affordable for patients worldwide.

Chapter 7

Conclusions

The findings of this study on hLMSCs have significant implications and offer promising prospects for corneal regeneration.

1. **Successful isolation and characterization:** The successful isolation and characterization of hLMSCs through streamlined SOPs in accordance with cGMP guidelines and regulatory framework establish a robust foundation for further research and clinical applications

2. **Enhanced availability of therapy**: The ability to obtain hLMSCs from cadaveric corneas is advantageous as it eliminates the need for invasive procedures and reduces reliance on a limited source. This expanded availability allows for a multiplied supply of this therapy, enabling higher number of patients to benefit from it.

3. **Multipotent nature and differentiation potential**: Extensive characterization of hLMSCs revealed their multipotent nature and their capability to differentiate into various corneal-specific cell types. This suggests their potential for regenerating and restoring damaged corneal tissue, offering new avenues for corneal regeneration therapies.

4. **Purity and identity confirmation**: Immunophenotypic and karyotyping analysis confirmed the purity and identity of hLMSCs, ensuring their suitability for clinical use. These analyses provide reassurance regarding the quality and consistency of the cells used in potential therapies, in addition to the standardized and streamlined methods of all GMP protocols, giving almost no room for errors.

5. **Improved outcomes and reduced complications**: Compared to current treatments like corneal transplantation, hLMSC-based therapies hold the potential for improved outcomes and reduced complications. The non-immunogenic nature of hLMSCs makes them less likely to elicit an immune response, enhancing their safety and effectiveness for use in human patients.

6. **Preservation through encapsulation:** The study explored the encapsulation of hLMSCs in alginate beads, which showed enhanced cell viability during transportation at room temperature compared to storage at 4°C. This finding suggests that encapsulation could be an effective method for preserving hLMSCs during transportation, particularly for corneal scar treatment.

7. **Restoration of corneal transparency**: In a mouse model of corneal scarring, treatment with both encapsulated and non-encapsulated hLMSCs resulted in reduced scar area and intensity. Furthermore, the reflectivity of the stroma normalized to baseline levels before debridement,

indicating the potential of hLMSCs to restore corneal transparency and improve visual outcomes.

In short, this thesis work on hLMSCs research provides insights into GMP-optimized protocols, enhanced preservation methods, and the safety and efficacy profiles of hLMSCs, paving the way for further research and potential clinical applications in the future.

Chapter 8

Contributions to Scientific Knowledge

The contributions of the discussed work to science are summarized as follows:

1. **Reproducible methods to isolate and harvest hLMSCs**: The successful isolation and characterization of hLMSCs following cGMP guidelines and regulatory frameworks contribute to the understanding of these cells and their potential applications in corneal regeneration.

2. **Advancement in Cell preservation techniques**: The findings of this thesis work contribute to the field of cell preservation techniques by demonstrating the effectiveness of alginate encapsulation in maintaining the viability and phenotype of hLMSCs during storage and transit. This finding provides a potential solution to the translational bottleneck of reliable storage and transportation of hLMSCs at low cost.

3. **Safety and Efficacy of hLMSCs:** The immunophenotypic analysis confirms the purity and identity of hLMSCs, supporting their safety for potential clinical use. Additionally, the non-immunogenic nature of hLMSCs compared to other treatments like corneal transplantation contributes to their potential for improved outcomes and reduced complications. Restored corneal transparency in murine models provided additional evidences of the healing potential of corneal scars.

Chapter 9

Limitations of the Study

The following are potential study limitations:

1. **Limited expansion of hLMSCs:** This thesis work has designed and employed the hLMSCs isolated, limited to the Passage 3, as cells beyond this passage tend to develop into fibroblasts. The expansion potential of hLMSCs can be improved by finding ways to get around this potential restriction.

2. **Serum-free methods of harvest:** Methods to obtain hLMSCs without employing sera should be developed to make the entire process xeno-free.

3. **Level of inflammatory markers in untreated eye:** Analyzing IgE concentrations might have shed light on the slightly changing concentrations of this marker found in the sera of injured rabbits in safety tests.

Chapter 10

Future Scope

The research reported in this thesis on hLMSCs has paved the way for exciting new directions in the fight against corneal blindness, both in the lab and in the clinic. Based on the findings of this study, few possible future paths and scope that might be explored are outlined hereunder.

1. **Therapeutic applications:**
    - hLMSCs have enormous promise for a variety of therapeutic applications. Further large-scale research may look at their effectiveness in treating corneal problems such corneal ulcers, limbal stem cell deficiency, in addition to corneal scarring.
    - Clinical trials can be designed to evaluate the safety and effectiveness of hLMSC-based therapies compared to current treatment modalities, such as corneal transplantation. These studies will provide valuable insights into the therapeutic potential of hLMSCs and their role in corneal tissue regeneration.

2. **Bioengineering approaches:**
    - Incorporating hLMSCs into bioengineered constructs for corneal tissue engineering is another exciting future avenue. Researchers can explore the development of scaffolds or biomaterials that mimic the native corneal microenvironment to support the growth, differentiation, and integration of hLMSCs onto recipient bed.
    - The bioengineered constructs can be further tested for their biocompatibility, functionality, and long-term stability in preclinical models.

3. **Immunomodulatory properties:**
    - The immunomodulatory properties of hLMSCs hold significant potential for the treatment of autoimmune diseases like Mooren's ulcer and transplantation. Their ability to modulate immune responses and control inflammation can be harnessed for the development of immunotherapeutic approaches. This opens up new possibilities for the management of immune-related corneal and ocular surface disorders.

4. **Clinical translation:**
    - The translation of hLMSC-based therapies from the laboratory to clinical practice requires rigorous regulatory approval and standardized protocols. Further efforts should focus on conducting large-scale, multicenter clinical trials to establish the safety, efficacy, and long-term outcomes of hLMSC-based interventions.
    - Collaboration between researchers, clinicians, and regulatory authorities is crucial to streamline and expedite the translation process and develop guidelines for the clinical use

of hLMSCs, bringing these innovative therapies to patients in need and improve the quality of life for countless individuals worldwide.

The future scope encompasses exploring their therapeutic applications, bioengineering approaches, molecular mechanisms, immunomodulatory properties, and clinical translation. Continued research in these areas will pave the way for innovative treatments and contribute to the development of personalized regenerative therapies for corneal disorders.

References

References

1. *2016DrugsandCosmeticsAct1940Rules1945.pdf*. (n.d.-a). Retrieved June 28, 2023, from https://cdsco.gov.in/opencms/export/sites/CDSCO_WEB/Pdf-documents/acts_rules/2016DrugsandCosmeticsAct1940Rules1945.pdf
2. *2016DrugsandCosmeticsAct1940Rules1945.pdf*. (n.d.-b). Retrieved June 23, 2022, from https://cdsco.gov.in/opencms/export/sites/CDSCO_WEB/Pdf-documents/acts_rules/2016DrugsandCosmeticsAct1940Rules1945.pdf
3. Abdellah, A., Noordin, M. I., & Wan Ismail, W. A. (2015). Importance and globalization status of good manufacturing practice (GMP) requirements for pharmaceutical excipients. *Saudi Pharmaceutical Journal: SPJ: The Official Publication of the Saudi Pharmaceutical Society*, *23*(1), 9–13. https://doi.org/10.1016/j.jsps.2013.06.003
4. Abourehab, M. A. S., Rajendran, R. R., Singh, A., Pramanik, S., Shrivastav, P., Ansari, M. J., Manne, R., Amaral, L. S., & Deepak, A. (2022). Alginate as a Promising Biopolymer in Drug Delivery and Wound Healing: A Review of the State-of-the-Art. *International Journal of Molecular Sciences*, *23*(16), 9035. https://doi.org/10.3390/ijms23169035
5. *Acts & Rules*. (n.d.). Retrieved June 28, 2023, from https://cdsco.gov.in/opencms/opencms/en/Acts-Rules/
6. Ahmad, H. F., & Sambanis, A. (2013). Cryopreservation effects on recombinant myoblasts encapsulated in adhesive alginate hydrogels. *Acta Biomaterialia*, *9*(6), 6814–6822. https://doi.org/10.1016/j.actbio.2013.03.002
7. Akinci, M. A. M., Turner, H., Taveras, M., & Wolosin, J. M. (2009). Differential gene expression in the pig limbal side population: Implications for stem cell cycling, replication, and survival. *Investigative Ophthalmology & Visual Science*, *50*(12), 5630–5638. https://doi.org/10.1167/iovs.09-3791
8. Al Balooshi, N., Jamsheer, A., & Botta, G. A. (2003). Impact of introducing quality control/quality assurance (QC/QA) guidelines in respiratory specimen processing. *Clinical Microbiology and Infection: The Official Publication of the European Society of Clinical Microbiology and Infectious Diseases*, *9*(8), 810–815. https://doi.org/10.1046/j.1469-0691.2003.00658.x
9. Ambati, B. K., Nozaki, M., Singh, N., Takeda, A., Jani, P. D., Suthar, T., Albuquerque, R. J. C., Richter, E., Sakurai, E., Newcomb, M. T., Kleinman, M. E., Caldwell, R. B., Lin, Q., Ogura, Y., Orecchia, A., Samuelson, D. A., Agnew, D. W., St. Leger, J., Green, W. R., … Ambati, J. (2006). Corneal avascularity is due to soluble VEGF receptor-1. *Nature*, *443*(7114), 993–997. https://doi.org/10.1038/nature05249

10. Andrews, P., Baker, D., Benvinisty, N., Miranda, B., Bruce, K., Brüstle, O., Choi, M., Choi, Y.-M., Crook, J., de Sousa, P., Dvorak, P., Freund, C., Firpo, M., Furue, M., Gokhale, P., Ha, H.-Y., Han, E., Haupt, S., Healy, L., … Zhou, Q. (2015). Points to consider in the development of seed stocks of pluripotent stem cells for clinical applications: International Stem Cell Banking Initiative (ISCBI). *Regenerative Medicine*, *10*(2s), 1–44. https://doi.org/10.2217/rme.14.93
11. Badrick, T. (2021). Integrating quality control and external quality assurance. *Clinical Biochemistry*, *95*, 15–27. https://doi.org/10.1016/j.clinbiochem.2021.05.003
12. Barrientez, B., Nicholas, S. E., Whelchel, A., Sharif, R., Hjortdal, J., & Karamichos, D. (2019). Corneal Injury: Clinical and Molecular Aspects. *Experimental Eye Research*, *186*, 107709. https://doi.org/10.1016/j.exer.2019.107709
13. Basu, S., Damala, M., Tavakkoli, F., Mitragotri, N., & Singh, V. (2019a). Human Limbus-derived Mesenchymal/Stromal Stem Cell Therapy for Superficial Corneal Pathologies: Two-Year Outcomes. *Investigative Ophthalmology & Visual Science*, *60*(9), 4146.
14. Basu, S., Damala, M., Tavakkoli, F., Mitragotri, N., & Singh, V. (2019b). Human Limbus-derived Mesenchymal/Stromal Stem Cell Therapy for Superficial Corneal Pathologies: Two-Year Outcomes. *Investigative Ophthalmology & Visual Science*, *60*(9), 4146–4146.
15. Basu, S., Hertsenberg, A. J., Funderburgh, M. L., Burrow, M. K., Mann, M. M., Du, Y., Lathrop, K. L., Syed-Picard, F. N., Adams, S. M., Birk, D. E., & Funderburgh, J. L. (2014a). Human limbal biopsy–derived stromal stem cells prevent corneal scarring. *Science Translational Medicine*, *6*(266), 266ra172. https://doi.org/10.1126/scitranslmed.3009644
16. Basu, S., Hertsenberg, A. J., Funderburgh, M. L., Burrow, M. K., Mann, M. M., Du, Y., Lathrop, K. L., Syed-Picard, F. N., Adams, S. M., Birk, D. E., & Funderburgh, J. L. (2014b). Human limbal biopsy-derived stromal stem cells prevent corneal scarring. *Science Translational Medicine*, *6*(266), 266ra172. https://doi.org/10.1126/scitranslmed.3009644
17. Becker, T. A., Kipke, D. R., & Brandon, T. (2001). Calcium alginate gel: A biocompatible and mechanically stable polymer for endovascular embolization. *Journal of Biomedical Materials Research*, *54*(1), 76–86. https://doi.org/10.1002/1097-4636(200101)54:1<76::aid-jbm9>3.0.co;2-v
18. Bhattacharya, S. (2018). Cryoprotectants and Their Usage in Cryopreservation Process. In *Cryopreservation Biotechnology in Biomedical and Biological Sciences*. IntechOpen. https://doi.org/10.5772/intechopen.80477

19. Bi, D., Yang, X., Yao, L., Hu, Z., Li, H., Xu, X., & Lu, J. (2022). Potential Food and Nutraceutical Applications of Alginate: A Review. *Marine Drugs*, *20*(9), 564. https://doi.org/10.3390/md20090564
20. Blaszkowska, M. K., Bartnik, S. E., Crewe, J. M., Clark, A., & Mackey, D. A. (2022). The epidemiology of eye injuries in Western Australia: A retrospective 10-year study. *Clinical & Experimental Optometry*, 1–7. https://doi.org/10.1080/08164622.2022.2111198
21. Bourne, R. R. A., Flaxman, S. R., Braithwaite, T., Cicinelli, M. V., Das, A., Jonas, J. B., Keeffe, J., Kempen, J. H., Leasher, J., Limburg, H., Naidoo, K., Pesudovs, K., Resnikoff, S., Silvester, A., Stevens, G. A., Tahhan, N., Wong, T. Y., Taylor, H. R., & Vision Loss Expert Group. (2017). Magnitude, temporal trends, and projections of the global prevalence of blindness and distance and near vision impairment: A systematic review and meta-analysis. *The Lancet. Global Health*, *5*(9), e888–e897. https://doi.org/10.1016/S2214-109X(17)30293-0
22. Branch, M. J., Hashmani, K., Dhillon, P., Jones, D. R. E., Dua, H. S., & Hopkinson, A. (2012a). Mesenchymal stem cells in the human corneal limbal stroma. *Investigative Ophthalmology & Visual Science*, *53*(9), 5109–5116. https://doi.org/10.1167/iovs.11-8673
23. Branch, M. J., Hashmani, K., Dhillon, P., Jones, D. R. E., Dua, H. S., & Hopkinson, A. (2012b). Mesenchymal Stem Cells in the Human Corneal Limbal Stroma. *Investigative Ophthalmology & Visual Science*, *53*(9), 5109–5116. https://doi.org/10.1167/iovs.11-8673
24. Bray, L. J., Heazlewood, C. F., Munster, D. J., Hutmacher, D. W., Atkinson, K., & Harkin, D. G. (2014a). Immunosuppressive properties of mesenchymal stromal cell cultures derived from the limbus of human and rabbit corneas. *Cytotherapy*, *16*(1), 64–73. https://doi.org/10.1016/j.jcyt.2013.07.006
25. Bray, L. J., Heazlewood, C. F., Munster, D. J., Hutmacher, D. W., Atkinson, K., & Harkin, D. G. (2014b). Immunosuppressive properties of mesenchymal stromal cell cultures derived from the limbus of human and rabbit corneas. *Cytotherapy*, *16*(1), 64–73. https://doi.org/10.1016/j.jcyt.2013.07.006
26. Brown, G. C. (1999). Vision and quality-of-life. *Transactions of the American Ophthalmological Society*, *97*, 473–511.
27. Buzzonetti, L., Petrocelli, G., & Valente, P. (2012). Amniotic membrane transplantation in corneal melting after anterior lamellar keratoplasty assisted by femtosecond laser in children. *European Journal of Ophthalmology*, *22*(3), 477–480. https://doi.org/10.5301/ejo.5000061

28. Cabrera-Aguas, M., Khoo, P., & Watson, S. L. (2022). Infectious keratitis: A review. *Clinical & Experimental Ophthalmology*, *50*(5), 543. https://doi.org/10.1111/ceo.14113
29. Cao, H., Duan, L., Zhang, Y., Cao, J., & Zhang, K. (2021). Current hydrogel advances in physicochemical and biological response-driven biomedical application diversity. *Signal Transduction and Targeted Therapy*, *6*(1), Article 1. https://doi.org/10.1038/s41392-021-00830-x
30. *CFR - Code of Federal Regulations Title 21*. (n.d.-a). Retrieved August 29, 2022, from https://www.accessdata.fda.gov/scripts/cdrh/cfdocs/cfcfr/cfrsearch.cfm?fr=184.1724
31. *CFR - Code of Federal Regulations Title 21*. (n.d.-b). Retrieved June 28, 2023, from https://www.accessdata.fda.gov/scripts/cdrh/cfdocs/cfcfr/CFRSearch.cfm?CFRPart=211
32. Chang, C.-Y. A., McGhee, J. J., Green, C. R., & Sherwin, T. (2011). Comparison of stem cell properties in cell populations isolated from human central and limbal corneal epithelium. *Cornea*, *30*(10), 1155–1162. https://doi.org/10.1097/ICO.0b013e318213796b
33. Chaurasia, S. S., Lim, R. R., Lakshminarayanan, R., & Mohan, R. R. (2015). Nanomedicine Approaches for Corneal Diseases. *Journal of Functional Biomaterials*, *6*(2), Article 2. https://doi.org/10.3390/jfb6020277
34. Chen, S., Ren, J., & Chen, R. (2019). 5.11—Cryopreservation and Desiccation Preservation of Cells. In M. Moo-Young (Ed.), *Comprehensive Biotechnology (Third Edition)* (pp. 157–166). Pergamon. https://doi.org/10.1016/B978-0-444-64046-8.00451-1
35. Chen, S.-Y., Hayashida, Y., Chen, M.-Y., Xie, H. T., & Tseng, S. C. G. (2011). A New Isolation Method of Human Limbal Progenitor Cells by Maintaining Close Association with Their Niche Cells. *Tissue Engineering. Part C, Methods*, *17*(5), 537–548. https://doi.org/10.1089/ten.tec.2010.0609
36. Chinnadurai, R., Copland, I. B., Garcia, M. A., Petersen, C. T., Lewis, C. N., Waller, E. K., Kirk, A. D., & Galipeau, J. (2016). Cryopreserved Mesenchymal Stromal Cells Are Susceptible to T-Cell Mediated Apoptosis Which Is Partly Rescued by IFNγ Licensing. *Stem Cells (Dayton, Ohio)*, *34*(9), 2429–2442. https://doi.org/10.1002/stem.2415
37. Choong, P.-F., Mok, P.-L., Cheong, S.-K., & Then, K.-Y. (2007). Mesenchymal stromal cell-like characteristics of corneal keratocytes. *Cytotherapy*, *9*(3), 252–258. https://doi.org/10.1080/14653240701218508
38. Commissioner, O. of the. (2020, November 13). *Certificates of Confidentiality*. U.S. Food and Drug Administration; FDA. https://www.fda.gov/regulatory-information/search-fda-guidance-documents/certificates-confidentiality

39. Coppola, A., Tomasello, L., Pitrone, M., Cillino, S., Richiusa, P., Pizzolanti, G., & Giordano, C. (2017). Human limbal fibroblast-like stem cells induce immune-tolerance in autoreactive T lymphocytes from female patients with Hashimoto's thyroiditis. *Stem Cell Research & Therapy*, *8*(1), 154. https://doi.org/10.1186/s13287-017-0611-5
40. Dal-Ré, R., Rid, A., Emanuel, E., & Wendler, D. (2016). The potential exploitation of research participants in high income countries who lack access to health care. *British Journal of Clinical Pharmacology*, *81*(5), 857–864. https://doi.org/10.1111/bcp.12879
41. Damala, M., Pakalapati, N., Singh, V., & Basu, S. (2021). *Safety and toxicity of human limbus-derived stromal/mesenchymal stem cells with and without alginate encapsulation for clinical application* [Preprint]. In Review. https://doi.org/10.21203/rs.3.rs-789579/v1
42. Damala, M., Tavakkoli, F., Koduri, M. A., Gangadharan, A., Rai, A. K., Dash, D., Basu, S., & Singh, V. (2022). Transcriptomic Profiling of Human Limbus-Derived Stromal/Mesenchymal Stem Cells—Novel Mechanistic Insights into the Pathways Involved in Corneal Wound Healing. *International Journal of Molecular Sciences*, *23*(15), Article 15. https://doi.org/10.3390/ijms23158226
43. Dang, D. H., Riaz, K. M., & Karamichos, D. (2022). Treatment of Non-Infectious Corneal Injury: Review of Diagnostic Agents, Therapeutic Medications, and Future Targets. *Drugs*, *82*(2), 145–167. https://doi.org/10.1007/s40265-021-01660-5
44. *Dangerous Goods & Prohibited Items | FedEx India*. (n.d.). FedEx. Retrieved August 29, 2022, from https://www.fedex.com/en-in/shipping/dangerous-goods.html
45. de Boer, F., Dräger, A. M., Pinedo, H. M., Kessler, F. L., Monnee-van Muijen, M., Weijers, G., Westra, G., van der Wall, E., Netelenbos, T., Oberink, J. W., Huijgens, P. C., & Schuurhuis, G. J. (2002). Early apoptosis largely accounts for functional impairment of CD34+ cells in frozen-thawed stem cell grafts. *Journal of Hematotherapy & Stem Cell Research*, *11*(6), 951–963. https://doi.org/10.1089/152581602321080619
46. de Boer, F., Dräger, A. M., Pinedo, H. M., Kessler, F. L., van der Wall, E., Jonkhoff, A. R., van der Lelie, J., Huijgens, P. C., Ossenkoppele, G. J., & Schuurhuis, G. J. (2002). Extensive early apoptosis in frozen-thawed CD34-positive stem cells decreases threshold doses for haematological recovery after autologous peripheral blood progenitor cell transplantation. *Bone Marrow Transplantation*, *29*(3), 249–255. https://doi.org/10.1038/sj.bmt.1703357
47. DelMonte, D. W., & Kim, T. (2011). Anatomy and physiology of the cornea. *Journal of Cataract and Refractive Surgery*, *37*(3), 588–598. https://doi.org/10.1016/j.jcrs.2010.12.037

48. Deshmukh, R., Reddy, J. C., Rapuano, C. J., & Vaddavalli, P. K. (2020). Phototherapeutic keratectomy: Indications, methods and decision making. *Indian Journal of Ophthalmology*, *68*(12), 2856–2866. https://doi.org/10.4103/ijo.IJO_1524_20
49. Di Girolamo, N. (2015). Moving epithelia: Tracking the fate of mammalian limbal epithelial stem cells. *Progress in Retinal and Eye Research*, *48*, 203–225. https://doi.org/10.1016/j.preteyeres.2015.04.002
50. Ding, H., & Wu, F. (2012). Image Guided Biodistribution and Pharmacokinetic Studies of Theranostics. *Theranostics*, *2*(11), 1040–1053. https://doi.org/10.7150/thno.4652
51. *Does GMP apply to Development? - ECA Academy*. (n.d.). Retrieved June 28, 2023, from https://www.gmp-compliance.org/gmp-news/does-gmp-apply-to-development
52. Dominici, M., Le Blanc, K., Mueller, I., Slaper-Cortenbach, I., Marini, F., Krause, D., Deans, R., Keating, A., Prockop, D., & Horwitz, E. (2006). Minimal criteria for defining multipotent mesenchymal stromal cells. The International Society for Cellular Therapy position statement. *Cytotherapy*, *8*(4), 315–317. https://doi.org/10.1080/14653240600855905
53. Dos Santos, A., Lyu, N., Balayan, A., Knight, R., Zhuo, K. S., Sun, Y., Xu, J., Funderburgh, M. L., Funderburgh, J. L., & Deng, S. X. (2022). Generation of Functional Immortalized Human Corneal Stromal Stem Cells. *International Journal of Molecular Sciences*, *23*(21), 13399. https://doi.org/10.3390/ijms232113399
54. Dovgan, B., Miklavčič, D., Knežević, M., Zupan, J., & Barlič, A. (2021). Intracellular delivery of trehalose renders mesenchymal stromal cells viable and immunomodulatory competent after cryopreservation. *Cytotechnology*, *73*(3), 391–411. https://doi.org/10.1007/s10616-021-00465-4
55. Drew, V. J., Tseng, C.-L., Seghatchian, J., & Burnouf, T. (2018). Reflections on Dry Eye Syndrome Treatment: Therapeutic Role of Blood Products. *Frontiers in Medicine*, *5*, 33. https://doi.org/10.3389/fmed.2018.00033
56. *DRUGS CONTROL ADMINISTRATION*. (n.d.). Retrieved June 28, 2023, from https://dca.telangana.gov.in/more.php
57. Du, Y., Funderburgh, M. L., Mann, M. M., SundarRaj, N., & Funderburgh, J. L. (2005). Multipotent stem cells in human corneal stroma. *Stem Cells (Dayton, Ohio)*, *23*(9), 1266–1275. https://doi.org/10.1634/stemcells.2004-0256
58. Duplechain, A., Conrady, C. D., Patel, B. C., & Baker, S. (2023). Uveitis. In *StatPearls [Internet]*. StatPearls Publishing. https://www.ncbi.nlm.nih.gov/books/NBK540993/

59. Dziasko, M. A., Armer, H. E., Levis, H. J., Shortt, A. J., Tuft, S., & Daniels, J. T. (2014). Localisation of epithelial cells capable of holoclone formation in vitro and direct interaction with stromal cells in the native human limbal crypt. *PloS One*, *9*(4), e94283. https://doi.org/10.1371/journal.pone.0094283

60. Dziasko, M. A., Tuft, S. J., & Daniels, J. T. (2015a). Limbal melanocytes support limbal epithelial stem cells in 2D and 3D microenvironments. *Experimental Eye Research*, *138*, 70–79. https://doi.org/10.1016/j.exer.2015.06.026

61. Dziasko, M. A., Tuft, S. J., & Daniels, J. T. (2015b). Limbal melanocytes support limbal epithelial stem cells in 2D and 3D microenvironments. *Experimental Eye Research*, *138*, 70–79. https://doi.org/10.1016/j.exer.2015.06.026

62. Eghrari, A. O., Riazuddin, S. A., & Gottsch, J. D. (2015). Overview of the Cornea: Structure, Function, and Development. *Progress in Molecular Biology and Translational Science*, *134*, 7–23. https://doi.org/10.1016/bs.pmbts.2015.04.001

63. El-Raggal, T. M. (2009). Riboflavin-Ultraviolet A Corneal Cross-linking for Keratoconus. *Middle East African Journal of Ophthalmology*, *16*(4), 256–259. https://doi.org/10.4103/0974-9233.58418

64. *Endotoxin Testing Recommendations for Single-Use Intraocular Ophthalmic Devices—Guidance for Industry and Food and Drug Administration Staff*. (n.d.).

65. Espana, E. M., & Birk, D. E. (2020). Composition, structure and function of the corneal stroma. *Experimental Eye Research*, *198*, 108137. https://doi.org/10.1016/j.exer.2020.108137

66. Espana, E. M., Kawakita, T., Romano, A., Di Pascuale, M., Smiddy, R., Liu, C., & Tseng, S. C. G. (2003). Stromal niche controls the plasticity of limbal and corneal epithelial differentiation in a rabbit model of recombined tissue. *Investigative Ophthalmology & Visual Science*, *44*(12), 5130–5135. https://doi.org/10.1167/iovs.03-0584

67. Fahy, G. M., Wowk, B., Pagotan, R., Chang, A., Phan, J., Thomson, B., & Phan, L. (2009). Physical and biological aspects of renal vitrification. *Organogenesis*, *5*(3), 167–175.

68. Flaxman, S. R., Bourne, R. R. A., Resnikoff, S., Ackland, P., Braithwaite, T., Cicinelli, M. V., Das, A., Jonas, J. B., Keeffe, J., Kempen, J. H., Leasher, J., Limburg, H., Naidoo, K., Pesudovs, K., Silvester, A., Stevens, G. A., Tahhan, N., Wong, T. Y., Taylor, H. R., & Vision Loss Expert Group of the Global Burden of Disease Study. (2017). Global causes of blindness and distance vision impairment 1990-2020: A systematic review and meta-analysis. *The Lancet. Global Health*, *5*(12), e1221–e1234. https://doi.org/10.1016/S2214-109X(17)30393-5

69. Food and Drug Adminsitration, U. (n.d.). *CFR - Code of Federal Regulations Title 21*. Retrieved June 20, 2023, from https://www.accessdata.fda.gov/scripts/cdrh/cfdocs/cfcfr/cfrsearch.cfm?fr=184.1724
70. Freeman, F. E., & Kelly, D. J. (2017). Tuning Alginate Bioink Stiffness and Composition for Controlled Growth Factor Delivery and to Spatially Direct MSC Fate within Bioprinted Tissues. *Scientific Reports*, *7*, 17042. https://doi.org/10.1038/s41598-017-17286-1
71. Fuest, M., Jhanji, V., & Yam, G. H.-F. (2023). Molecular and Cellular Mechanisms of Corneal Scarring and Advances in Therapy. *International Journal of Molecular Sciences*, *24*(9), 7777. https://doi.org/10.3390/ijms24097777
72. Funderburgh, J., Basu, S., Damala, M., Tavakkoli, F., Sangwan, V., & Singh, V. (2018). Limbal Stromal Stem Cell Therapy for Acute and Chronic Superficial Corneal Pathologies: One-Year Outcomes. *Investigative Ophthalmology & Visual Science*, *59*(9), 3455.
73. Funderburgh, J. L., Funderburgh, M. L., & Du, Y. (2016a). Stem Cells in the Limbal Stroma. *The Ocular Surface*, *14*(2), 113–120. https://doi.org/10.1016/j.jtos.2015.12.006
74. Funderburgh, J. L., Funderburgh, M. L., & Du, Y. (2016b). Stem Cells in the Limbal Stroma. *The Ocular Surface*, *14*(2), 113. https://doi.org/10.1016/j.jtos.2015.12.006
75. Funderburgh, M. L., Du, Y., Mann, M. M., SundarRaj, N., & Funderburgh, J. L. (2005). PAX6 expression identifies progenitor cells for corneal keratocytes. *FASEB Journal: Official Publication of the Federation of American Societies for Experimental Biology*, *19*(10), 1371–1373. https://doi.org/10.1096/fj.04-2770fje
76. Gain, P., Jullienne, R., He, Z., Aldossary, M., Acquart, S., Cognasse, F., & Thuret, G. (2016). Global Survey of Corneal Transplantation and Eye Banking. *JAMA Ophthalmology*, *134*(2), 167–173. https://doi.org/10.1001/jamaophthalmol.2015.4776
77. Garfias, Y., Nieves-Hernandez, J., Garcia-Mejia, M., Estrada-Reyes, C., & Jimenez-Martinez, M. C. (2012a). Stem cells isolated from the human stromal limbus possess immunosuppressant properties. *Molecular Vision*, *18*, 2087–2095.
78. Garfias, Y., Nieves-Hernandez, J., Garcia-Mejia, M., Estrada-Reyes, C., & Jimenez-Martinez, M. C. (2012b). Stem cells isolated from the human stromal limbus possess immunosuppressant properties. *Molecular Vision*, *18*, 2087–2095.
79. George, B. (2011). Regulations and guidelines governing stem cell based products: Clinical considerations. *Perspectives in Clinical Research*, *2*(3), 94–99. https://doi.org/10.4103/2229-3485.83228

80. Ghosh, A., Singh, V. K., Singh, V., Basu, S., & Pati, F. (2022). Recent Advancements in Molecular Therapeutics for Corneal Scar Treatment. *Cells*, *11*(20), Article 20. https://doi.org/10.3390/cells11203310
81. Ghoubay, D., Borderie, M., Grieve, K., Martos, R., Bocheux, R., Nguyen, T.-M., Callard, P., Chédotal, A., & Borderie, V. M. (2020). Corneal stromal stem cells restore transparency after N2 injury in mice. *Stem Cells Translational Medicine*, *9*(8), 917–935. https://doi.org/10.1002/sctm.19-0306
82. Giulio, B. D., Orlando, P., Barba, G., Coppola, R., Rosa, M. D., Sada, A., Prisco, P. P. D., & Nazzaro, F. (2005). Use of alginate and cryo-protective sugars to improve the viability of lactic acid bacteria after freezing and freeze-drying. *World Journal of Microbiology and Biotechnology*, *21*(5), 739–746. https://doi.org/10.1007/s11274-004-4735-2
83. Goldberg, M. F., & Bron, A. J. (1982). Limbal palisades of Vogt. *Transactions of the American Ophthalmological Society*, *80*, 155–171.
84. Golubović, S. (1994). [Terrien's marginal corneal degeneration]. *Srpski Arhiv Za Celokupno Lekarstvo*, *122*(3–4), 110–112.
85. Gonzalez, G., Sasamoto, Y., Ksander, B. R., Frank, M. H., & Frank, N. Y. (2018a). Limbal Stem Cells: Identity, Developmental Origin and Therapeutic Potential. *Wiley Interdisciplinary Reviews. Developmental Biology*, *7*(2), 10.1002/wdev.303. https://doi.org/10.1002/wdev.303
86. Gonzalez, G., Sasamoto, Y., Ksander, B. R., Frank, M. H., & Frank, N. Y. (2018b). Limbal Stem Cells: Identity, Developmental Origin and Therapeutic Potential. *Wiley Interdisciplinary Reviews. Developmental Biology*, *7*(2), 10.1002/wdev.303. https://doi.org/10.1002/wdev.303
87. Gonzalez, G., Sasamoto, Y., Ksander, B. R., Frank, M. H., & Frank, N. Y. (2018c). Limbal Stem Cells: Identity, Developmental Origin and Therapeutic Potential. *Wiley Interdisciplinary Reviews. Developmental Biology*, *7*(2), 10.1002/wdev.303. https://doi.org/10.1002/wdev.303
88. Gonzalez, G., Sasamoto, Y., Ksander, B. R., Frank, M. H., & Frank, N. Y. (2018d). Limbal stem cells: Identity, developmental origin, and therapeutic potential. *Wiley Interdisciplinary Reviews. Developmental Biology*, *7*(2). https://doi.org/10.1002/wdev.303
89. González-Gallardo, C., Martínez-Atienza, J., Mataix, B., Muñoz-Ávila, J. I., Daniel Martínez-Rodríguez, J., Medialdea, S., Ruiz-García, A., Lizana-Moreno, A., Arias-Santiago, S., de la Rosa-Fraile, M., Garzon, I., Campos, A., Cuende, N., Alaminos, M., González-Andrades, M., & Mata, R. (2023). Successful restoration of corneal surface

integrity with a tissue-engineered allogeneic implant in severe keratitis patients. *Biomedicine & Pharmacotherapy*, *162*, 114612. https://doi.org/10.1016/j.biopha.2023.114612

90. *Good-Clinical-Practice-Guideline.pdf*. (n.d.). Retrieved June 28, 2023, from https://rgcb.res.in/documents/Good-Clinical-Practice-Guideline.pdf
91. Gouveia, B. G., Rijo, P., Gonçalo, T. S., & Reis, C. P. (2015a). Good manufacturing practices for medicinal products for human use. *Journal of Pharmacy & Bioallied Sciences*, *7*(2), 87–96. https://doi.org/10.4103/0975-7406.154424
92. Gouveia, B. G., Rijo, P., Gonçalo, T. S., & Reis, C. P. (2015b). Good manufacturing practices for medicinal products for human use. *Journal of Pharmacy & Bioallied Sciences*, *7*(2), 87–96. https://doi.org/10.4103/0975-7406.154424
93. Group, B. M. J. P. (1996). The Nuremberg Code (1947). *BMJ*, *313*(7070), 1448. https://doi.org/10.1136/bmj.313.7070.1448
94. *GUIDELINE FOR GOOD CLINICAL PRACTICE*. (n.d.).
95. *Guidelines | Indian Council of Medical Research | Government of India*. (n.d.). Retrieved June 28, 2023, from https://main.icmr.nic.in/content/guidelines-0
96. Gupta, M., Ireland, A. C., & Bordoni, B. (2023). Neuroanatomy, Visual Pathway. In *StatPearls*. StatPearls Publishing. http://www.ncbi.nlm.nih.gov/books/NBK553189/
97. Gupta, U. C. (2013). Informed consent in clinical research: Revisiting few concepts and areas. *Perspectives in Clinical Research*, *4*(1), 26–32. https://doi.org/10.4103/2229-3485.106373
98. Guven, S., & Demirci, U. (2012). Integrating nanoscale technologies with cryogenics: A step towards improved biopreservation. *Nanomedicine (London, England)*, *7*(12), 1787–1789. https://doi.org/10.2217/nnm.12.158
99. Ha, S. Y., Jee, B. C., Suh, C. S., Kim, H. S., Oh, S. K., Kim, S. H., & Moon, S. Y. (2005). Cryopreservation of human embryonic stem cells without the use of a programmable freezer. *Human Reproduction (Oxford, England)*, *20*(7), 1779–1785. https://doi.org/10.1093/humrep/deh854
100. Han, X., Zhang, Y., Zhu, Y., Zhao, Y., Yang, H., Liu, G., Ai, S., Wang, Y., Xie, C., Shi, J., Zhang, T., Huang, G., & He, X. (2022). Quantification of biomechanical properties of human corneal scar using acoustic radiation force optical coherence elastography. *Experimental Biology and Medicine*, *247*(6), 462–469. https://doi.org/10.1177/15353702211061881

101. Harayama, K., Amemiya, T., & Nishimura, H. (1980). Development of the cornea during fetal life: Comparison of corneal and bulbar diameter. *The Anatomical Record*, *198*(3), 531–535. https://doi.org/10.1002/ar.1091980313
102. Hashmani, K., Branch, M. J., Sidney, L. E., Dhillon, P. S., Verma, M., McIntosh, O. D., Hopkinson, A., & Dua, H. S. (2013). Characterization of corneal stromal stem cells with the potential for epithelial transdifferentiation. *Stem Cell Research & Therapy*, *4*(3), 75. https://doi.org/10.1186/scrt226
103. He, X., Park, E. Y. H., Fowler, A., Yarmush, M. L., & Toner, M. (2008). Vitrification by Ultra-fast Cooling at a Low Concentration of Cryoprotectants in a Quartz Microcapillary: A Study Using Murine Embryonic Stem Cells. *Cryobiology*, *56*(3), 223–232. https://doi.org/10.1016/j.cryobiol.2008.03.005
104. Heng, B. C., Kuleshova, L. L., Bested, S. M., Liu, H., & Cao, T. (2005). The cryopreservation of human embryonic stem cells. *Biotechnology and Applied Biochemistry*, *41*(Pt 2), 97–104. https://doi.org/10.1042/BA20040161
105. Heng, B. C., Ye, C. P., Liu, H., Toh, W. S., Rufaihah, A. J., Yang, Z., Bay, B. H., Ge, Z., Ouyang, H. W., Lee, E. H., & Cao, T. (2006). Loss of viability during freeze-thaw of intact and adherent human embryonic stem cells with conventional slow-cooling protocols is predominantly due to apoptosis rather than cellular necrosis. *Journal of Biomedical Science*, *13*(3), 433–445. https://doi.org/10.1007/s11373-005-9051-9
106. Hertsenberg, A. J., & Funderburgh, J. L. (2015). Stem Cells in the Cornea. *Progress in Molecular Biology and Translational Science*, *134*, 25–41. https://doi.org/10.1016/bs.pmbts.2015.04.002
107. Hertsenberg, A. J., Shojaati, G., Funderburgh, M. L., Mann, M. M., Du, Y., & Funderburgh, J. L. (2017a). Corneal stromal stem cells reduce corneal scarring by mediating neutrophil infiltration after wounding. *PloS One*, *12*(3), e0171712. https://doi.org/10.1371/journal.pone.0171712
108. Hertsenberg, A. J., Shojaati, G., Funderburgh, M. L., Mann, M. M., Du, Y., & Funderburgh, J. L. (2017b). Corneal stromal stem cells reduce corneal scarring by mediating neutrophil infiltration after wounding. *PloS One*, *12*(3), e0171712. https://doi.org/10.1371/journal.pone.0171712
109. Higa, K., Kato, N., Yoshida, S., Ogawa, Y., Shimazaki, J., Tsubota, K., & Shimmura, S. (2013). Aquaporin 1-positive stromal niche-like cells directly interact with N-cadherin-positive clusters in the basal limbal epithelium. *Stem Cell Research*, *10*(2), 147–155. https://doi.org/10.1016/j.scr.2012.11.001

110. Hocevar, K. P., Metzger, M., & Flanagin, A. J. (2017). Source Credibility, Expertise, and Trust in Health and Risk Messaging. In K. P. Hocevar, M. Metzger, & A. J. Flanagin, *Oxford Research Encyclopedia of Communication*. Oxford University Press. https://doi.org/10.1093/acrefore/9780190228613.013.287
111. Hori, J. (2008). Mechanisms of immune privilege in the anterior segment of the eye: What we learn from corneal transplantation. *Journal of Ocular Biology, Diseases, and Informatics*, *1*(2–4), 94–100. https://doi.org/10.1007/s12177-008-9010-6
112. Hulley, S. B. (Ed.). (2013). *Designing clinical research* (4th ed). Wolters Kluwer/Lippincott Williams & Wilkins.
113. Hunt, C. J. (2011). Cryopreservation of Human Stem Cells for Clinical Application: A Review. *Transfusion Medicine and Hemotherapy*, *38*(2), 107–123. https://doi.org/10.1159/000326623
114. Hutmacher, F. (2019). Why Is There So Much More Research on Vision Than on Any Other Sensory Modality? *Frontiers in Psychology*, *10*. https://www.frontiersin.org/articles/10.3389/fpsyg.2019.02246
115. Hyun, I. (2010). The bioethics of stem cell research and therapy. *The Journal of Clinical Investigation*, *120*(1), 71–75. https://doi.org/10.1172/JCI40435
116. *ICMR_National_Ethical_Guidelines.pdf*. (n.d.). Retrieved June 28, 2023, from https://ethics.ncdirindia.org/asset/pdf/ICMR_National_Ethical_Guidelines.pdf
117. *India's New Drugs and Clinical Trials Rules: An Industry Perspective*. (n.d.). Retrieved June 28, 2023, from https://www.raps.org/news-and-articles/news-articles/2019/7/indias-new-drugs-and-clinical-trials-rules-an-in
118. Institute of Medicine (US) Committee on Ethical Considerations for Revisions to DHHS Regulations for Protection of Prisoners Involved in Research. (2007). *Ethical Considerations for Research Involving Prisoners* (L. O. Gostin, C. Vanchieri, & A. Pope, Eds.). National Academies Press (US). http://www.ncbi.nlm.nih.gov/books/NBK19882/
119. Ito, A., Yoshioka, K., Masumoto, S., Sato, K., Hatae, Y., Nakai, T., Yamazaki, T., Takahashi, M., Tanoue, S., & Horie, M. (2020). Magnetic heating of nanoparticles as a scalable cryopreservation technology for human induced pluripotent stem cells. *Scientific Reports*, *10*(1), Article 1. https://doi.org/10.1038/s41598-020-70707-6
120. Jabbehdari, S., Yazdanpanah, G., Kanu, L. N., Chen, E., Kang, K., Anwar, K. N., Ghassemi, M., Hematti, P., Rosenblatt, M. I., & Djalilian, A. R. (2020). Therapeutic Effects of Lyophilized Conditioned-Medium Derived from Corneal Mesenchymal

Stromal Cells on Corneal Epithelial Wound Healing. *Current Eye Research*, *45*(12), 1490–1496. https://doi.org/10.1080/02713683.2020.1762227

121. Jeon, S., Rowe, A. M., Carroll, K. L., Harvey, S. A. K., & Hendricks, R. L. (2018). PD-L1/B7-H1 inhibits viral clearance by macrophages in HSV-1-infected corneas. *Journal of Immunology (Baltimore, Md. : 1950)*, *200*(11), 3711–3719. https://doi.org/10.4049/jimmunol.1700417
122. Jester, J. V., Moller-Pedersen, T., Huang, J., Sax, C. M., Kays, W. T., Cavangh, H. D., Petroll, W. M., & Piatigorsky, J. (1999). The cellular basis of corneal transparency: Evidence for "corneal crystallins." *Journal of Cell Science*, *112 (Pt 5)*, 613–622. https://doi.org/10.1242/jcs.112.5.613
123. Jhanji, V., Billig, I., & Yam, G. H.-F. (2021). Cell-Free Biological Approach for Corneal Stromal Wound Healing. *Frontiers in Pharmacology*, *12*. https://www.frontiersin.org/articles/10.3389/fphar.2021.671405
124. Jhanji, V., Santra, M., Riau, A. K., Geary, M. L., Yang, T., Rubin, E., Yusoff, N. Z. B. M., Dhaliwal, D. K., Mehta, J. S., & Yam, G. H.-F. (2022). Combined Therapy Using Human Corneal Stromal Stem Cells and Quiescent Keratocytes to Prevent Corneal Scarring after Injury. *International Journal of Molecular Sciences*, *23*(13), Article 13. https://doi.org/10.3390/ijms23136980
125. Ji, L., de Pablo, J. J., & Palecek, S. P. (2004). Cryopreservation of adherent human embryonic stem cells. *Biotechnology and Bioengineering*, *88*(3), 299–312. https://doi.org/10.1002/bit.20243
126. Joshi, M., & Bhardwaj, P. (2018). Impact of data transparency: Scientific publications. *Perspectives in Clinical Research*, *9*(1), 31–36. https://doi.org/10.4103/picr.PICR_104_17
127. Joyce, N. C., & Zieske, J. D. (1997). Transforming growth factor-beta receptor expression in human cornea. *Investigative Ophthalmology & Visual Science*, *38*(10), 1922–1928.
128. Kamil, S., & Mohan, R. R. (2021a). Corneal stromal wound healing: Major regulators and therapeutic targets. *The Ocular Surface*, *19*, 290–306. https://doi.org/10.1016/j.jtos.2020.10.006
129. Kamil, S., & Mohan, R. R. (2021b). Corneal stromal wound healing: Major regulators and therapeutic targets. *The Ocular Surface*, *19*, 290–306. https://doi.org/10.1016/j.jtos.2020.10.006

130. Kanski, J. K., & Bowling, B. (2016). *Kanski's clinical ophthalmology: A systematic approach | WorldCat.org*. Elsevier. https://www.worldcat.org/title/Kanski's-clinical-ophthalmology-:-a-systematic-approach/oclc/912368712
131. Kapoore, R. V., Huete-Ortega, M., Day, J. G., Okurowska, K., Slocombe, S. P., Stanley, M. S., & Vaidyanathan, S. (2019). Effects of cryopreservation on viability and functional stability of an industrially relevant alga. *Scientific Reports*, *9*(1), Article 1. https://doi.org/10.1038/s41598-019-38588-6
132. Karlsson, J. O., & Toner, M. (1996). Long-term storage of tissues by cryopreservation: Critical issues. *Biomaterials*, *17*(3), 243–256. https://doi.org/10.1016/0142-9612(96)85562-1
133. Kate, A., & Basu, S. (2022). A Review of the Diagnosis and Treatment of Limbal Stem Cell Deficiency. *Frontiers in Medicine*, *9*. https://www.frontiersin.org/articles/10.3389/fmed.2022.836009
134. Katikireddy, K. R., Dana, R., & Jurkunas, U. V. (2014). Differentiation Potential of Limbal Fibroblasts and Bone Marrow Mesenchymal Stem Cells to Corneal Epithelial Cells. *Stem Cells (Dayton, Ohio)*, *32*(3), 717–729. https://doi.org/10.1002/stem.1541
135. Keino, H., Horie, S., & Sugita, S. (2018). Immune Privilege and Eye-Derived T-Regulatory Cells. *Journal of Immunology Research*, *2018*, 1679197. https://doi.org/10.1155/2018/1679197
136. Kerasidou, A. (2017). Trust me, I'm a researcher!: The role of trust in biomedical research. *Medicine, Health Care, and Philosophy*, *20*(1), 43–50. https://doi.org/10.1007/s11019-016-9721-6
137. King, N. M., & Perrin, J. (2014). Ethical issues in stem cell research and therapy. *Stem Cell Research & Therapy*, *5*(4), 85. https://doi.org/10.1186/scrt474
138. Knauer, C., & Pfeiffer, N. (2008). The value of vision. *Graefe's Archive for Clinical and Experimental Ophthalmology = Albrecht Von Graefes Archiv Fur Klinische Und Experimentelle Ophthalmologie*, *246*(4), 477–482. https://doi.org/10.1007/s00417-007-0668-4
139. Kolli, S., Bojic, S., Ghareeb, A. E., Kurzawa-Akanbi, M., Figueiredo, F. C., & Lako, M. (2019). The Role of Nerve Growth Factor in Maintaining Proliferative Capacity, Colony-Forming Efficiency, and the Limbal Stem Cell Phenotype. *Stem Cells (Dayton, Ohio)*, *37*(1), 139–149. https://doi.org/10.1002/stem.2921
140. Kondoh, H., Uchikawa, M., & Kamachi, Y. (2004). Interplay of Pax6 and SOX2 in lens development as a paradigm of genetic switch mechanisms for cell differentiation. *The*

International Journal of Developmental Biology, *48*(8–9), 819–827. https://doi.org/10.1387/ijdb.041868hk

141. Kong, B., & Mi, S. (2016). Electrospun Scaffolds for Corneal Tissue Engineering: A Review. *Materials*, *9*(8), 614. https://doi.org/10.3390/ma9080614
142. Kong, H. J., Smith, M. K., & Mooney, D. J. (2003). Designing alginate hydrogels to maintain viability of immobilized cells. *Biomaterials*, *24*(22), 4023–4029. https://doi.org/10.1016/s0142-9612(03)00295-3
143. Koonrungsesomboon, N., & Karbwang, J. (2016). Ethical considerations in clinical research on herbal medicine for prevention of cardiovascular disease in the ageing. *Phytomedicine: International Journal of Phytotherapy and Phytopharmacology*, *23*(11), 1090–1094. https://doi.org/10.1016/j.phymed.2015.10.017
144. Kowtharapu, B. S., Murín, R., Jünemann, A. G. M., & Stachs, O. (2018). Role of Corneal Stromal Cells on Epithelial Cell Function during Wound Healing. *International Journal of Molecular Sciences*, *19*(2), 464. https://doi.org/10.3390/ijms19020464
145. Kumar, A., Xu, Y., Yang, E., & Du, Y. (2018). Stemness and Regenerative Potential of Corneal Stromal Stem Cells and Their Secretome After Long-Term Storage: Implications for Ocular Regeneration. *Investigative Ophthalmology & Visual Science*, *59*(8), 3728–3738. https://doi.org/10.1167/iovs.18-23824
146. Kumar, A., Yun, H., Funderburgh, M. L., & Du, Y. (2021). Regenerative therapy for the Cornea. *Progress in Retinal and Eye Research*, 101011. https://doi.org/10.1016/j.preteyeres.2021.101011
147. Lahiry, S., Choudhury, S., Sinha, R., & Chatterjee, S. (2019). The National Guidelines for Stem Cell Research (2017): What academicians need to know? *Perspectives in Clinical Research*, *10*(4), 148–154. https://doi.org/10.4103/picr.PICR_23_18
148. Lee, K. C., Bamford, A., Gardiner, F., Agovino, A., ter Horst, B., Bishop, J., Sitch, A., Grover, L., Logan, A., & Moiemen, N. S. (2019). Investigating the intra- and inter-rater reliability of a panel of subjective and objective burn scar measurement tools. *Burns*, *45*(6), 1311–1324. https://doi.org/10.1016/j.burns.2019.02.002
149. Lee, K. Y., & Mooney, D. J. (2012a). Alginate: Properties and biomedical applications. *Progress in Polymer Science*, *37*(1), 106–126. https://doi.org/10.1016/j.progpolymsci.2011.06.003
150. Lee, K. Y., & Mooney, D. J. (2012b). Alginate: Properties and biomedical applications. *Progress in Polymer Science*, *37*(1), 106–126. https://doi.org/10.1016/j.progpolymsci.2011.06.003

151. Li, W., Hayashida, Y., Chen, Y.-T., & Tseng, S. C. (2007). Niche regulation of corneal epithelial stem cells at the limbus. *Cell Research*, *17*(1), Article 1. https://doi.org/10.1038/sj.cr.7310137
152. Liu, G., Zhou, H., Li, Y., Li, G., Cui, L., Liu, W., & Cao, Y. (2008). Evaluation of the viability and osteogenic differentiation of cryopreserved human adipose-derived stem cells. *Cryobiology*, *57*(1), 18–24. https://doi.org/10.1016/j.cryobiol.2008.04.002
153. Liu, X.-N., Mi, S.-L., Chen, Y., & Wang, Y. (2021). Corneal stromal mesenchymal stem cells: Reconstructing a bioactive cornea and repairing the corneal limbus and stromal microenvironment. *International Journal of Ophthalmology*, *14*(3), 448–455. https://doi.org/10.18240/ijo.2021.03.19
154. Ljubimov, A. V., & Saghizadeh, M. (2015a). Progress in corneal wound healing. *Progress in Retinal and Eye Research*, *49*, 17–45. https://doi.org/10.1016/j.preteyeres.2015.07.002
155. Ljubimov, A. V., & Saghizadeh, M. (2015b). Progress in corneal wound healing. *Progress in Retinal and Eye Research*, *49*, 17–45. https://doi.org/10.1016/j.preteyeres.2015.07.002
156. Lo, B., & Parham, L. (2009). Ethical issues in stem cell research. *Endocrine Reviews*, *30*(3), 204–213. https://doi.org/10.1210/er.2008-0031
157. Ma, L., Zhang, B., Deng, S., & Xie, C. (2015). Comparison of the cryoprotective effects of trehalose, alginate, and its oligosaccharides on peeled shrimp (Litopenaeus vannamei) during frozen storage. *Journal of Food Science*, *80*(3), C540-546. https://doi.org/10.1111/1750-3841.12793
158. Mahdavi, S. S., Abdekhodaie, M. J., Mashayekhan, S., Baradaran-Rafii, A., & Djalilian, A. R. (2020). Bioengineering Approaches for Corneal Regenerative Medicine. *Tissue Engineering and Regenerative Medicine*, *17*(5), 567. https://doi.org/10.1007/s13770-020-00262-8
159. Mahler, S., Desille, M., Frémond, B., Chesné, C., Guillouzo, A., Campion, J.-P., & Clément, B. (2003). Hypothermic storage and cryopreservation of hepatocytes: The protective effect of alginate gel against cell damages. *Cell Transplantation*, *12*(6), 579–592. https://doi.org/10.3727/000000003108747181
160. Mann, M. M., Funderburgh, J. L., Du, Y., Funderburgh, M. L., & Zurowski, N. B. (2011). Assessing Potential of Corneal Stromal Stem Cells to Differentiate to Keratocytes. *Investigative Ophthalmology & Visual Science*, *52*(14), 5153.
161. Mannis, M. J., & Holland, E. J. (2021). *Cornea*. Elsevier Health Sciences.
162. Manuchehrabadi, N., Gao, Z., Zhang, J., Ring, H. L., Shao, Q., Liu, F., McDermott, M., Fok, A., Rabin, Y., Brockbank, K. G. M., Garwood, M., Haynes, C. L., & Bischof, J. C.

(2017). Improved tissue cryopreservation using inductive heating of magnetic nanoparticles. *Science Translational Medicine*, *9*(379), eaah4586. https://doi.org/10.1126/scitranslmed.aah4586

163. Mathews, P. M., Lindsley, K., Aldave, A. J., & Akpek, E. K. (2018a). Etiology of Global Corneal Blindness and Current Practices of Corneal Transplantation: A Focused Review. *Cornea*, *37*(9), 1198–1203. https://doi.org/10.1097/ICO.0000000000001666
164. Mathews, P. M., Lindsley, K., Aldave, A. J., & Akpek, E. K. (2018b). Etiology of Global Corneal Blindness and Current Practices of Corneal Transplantation: A Focused Review. *Cornea*, *37*(9), 1198–1203. https://doi.org/10.1097/ICO.0000000000001666
165. Matsushima, D., Heavner, W., & Pevny, L. H. (2011). Combinatorial regulation of optic cup progenitor cell fate by SOX2 and PAX6. *Development (Cambridge, England)*, *138*(3), 443–454. https://doi.org/10.1242/dev.055178
166. Matthaei, M., Hribek, A., Clahsen, T., Bachmann, B., Cursiefen, C., & Jun, A. S. (2019). Fuchs Endothelial Corneal Dystrophy: Clinical, Genetic, Pathophysiologic, and Therapeutic Aspects. *Annual Review of Vision Science*, *5*, 151–175. https://doi.org/10.1146/annurev-vision-091718-014852
167. Matthyssen, S., Van Den Bogerd, B., Dhubhghaill, S. N., Koppen, C., & Zakaria, N. (2018). Corneal regeneration: A review of stromal replacements. *Acta Biomaterialia*, *69*, 31–41. https://doi.org/10.1016/j.actbio.2018.01.023
168. Matthyssen, S., Van den Bogerd, B., Dhubhghaill, S. N., Koppen, C., & Zakaria, N. (2018). Corneal regeneration: A review of stromal replacements. *Acta Biomaterialia*, *69*, 31–41. https://doi.org/10.1016/j.actbio.2018.01.023
169. Maurice, D. M. (1957). The structure and transparency of the cornea. *The Journal of Physiology*, *136*(2), 263–286. https://doi.org/10.1113/jphysiol.1957.sp005758
170. McCally, R. L., Freund, D. E., Zorn, A., Bonney-Ray, J., Grebe, R., de la Cruz, Z., & Green, W. R. (2007). Light Scattering and Ultrastructure of Healed Penetrating Corneal Wounds. *Investigative Ophthalmology & Visual Science*, *48*(1), 157–165. https://doi.org/10.1167/iovs.06-0935
171. McKay, T. B., Karamichos, D., Hutcheon, A. E. K., Guo, X., & Zieske, J. D. (2019). Corneal Epithelial–Stromal Fibroblast Constructs to Study Cell–Cell Communication in Vitro. *Bioengineering*, *6*(4), 110. https://doi.org/10.3390/bioengineering6040110
172. *Medicines: Good manufacturing practices*. (n.d.). Retrieved June 28, 2023, from https://www.who.int/news-room/questions-and-answers/item/medicines-good-manufacturing-processes

173. Meek, K. M., & Boote, C. (2004). The organization of collagen in the corneal stroma. *Experimental Eye Research*, *78*(3), 503–512. https://doi.org/10.1016/j.exer.2003.07.003
174. Menasché, P., Vanneaux, V., Hagège, A., Bel, A., Cholley, B., Cacciapuoti, I., Parouchev, A., Benhamouda, N., Tachdjian, G., Tosca, L., Trouvin, J.-H., Fabreguettes, J.-R., Bellamy, V., Guillemain, R., Suberbielle Boissel, C., Tartour, E., Desnos, M., & Larghero, J. (2015). Human embryonic stem cell-derived cardiac progenitors for severe heart failure treatment: First clinical case report. *European Heart Journal*, *36*(30), 2011–2017. https://doi.org/10.1093/eurheartj/ehv189
175. Mohammadi, A. A., Eskandari, S., Johari, H. G., & Rajabnejad, A. (2017). Using Amniotic Membrane as a Novel Method to Reduce Post-burn Hypertrophic Scar Formation: A Prospective Follow-up Study. *Journal of Cutaneous and Aesthetic Surgery*, *10*(1), 13–17. https://doi.org/10.4103/JCAS.JCAS_109_16
176. Morgan, S. R., Dooley, E. P., Kamma-Lorger, C., Funderburgh, J. L., Funderburgh, M. L., & Meek, K. M. (2016). Early wound healing of laser in situ keratomileusis-like flaps after treatment with human corneal stromal stem cells. *Journal of Cataract and Refractive Surgery*, *42*(2), 302–309. https://doi.org/10.1016/j.jcrs.2015.09.023
177. Mörö, A., Samanta, S., Honkamäki, L., Rangasami, V. K., Puistola, P., Kauppila, M., Narkilahti, S., Miettinen, S., Oommen, O., & Skottman, H. (2022). Hyaluronic acid based next generation bioink for 3D bioprinting of human stem cell derived corneal stromal model with innervation. *Biofabrication*, *15*(1). https://doi.org/10.1088/1758-5090/acab34
178. *National Guidelines for Stem Cell Research, 2017*. (n.d.).
179. Neil, L. (2020). Corneal Stromal Regeneration: Current Status and Future Therapeutic Potential. *Current Eye Research*, *45*(3). https://doi.org/10.1080/02713683.2019.1663874
180. *NewDrugs_CTRules_2019.pdf*. (n.d.-a). Retrieved June 28, 2023, from https://cdsco.gov.in/opencms/export/sites/CDSCO_WEB/Pdf-documents/NewDrugs_CTRules_2019.pdf
181. *NewDrugs_CTRules_2019.pdf*. (n.d.-b). Retrieved June 23, 2022, from https://cdsco.gov.in/opencms/export/sites/CDSCO_WEB/Pdf-documents/NewDrugs_CTRules_2019.pdf
182. Nieto-Miguel, T., Calonge, M., de la Mata, A., López-Paniagua, M., Galindo, S., de la Paz, M. F., & Corrales, R. M. (2011). A comparison of stem cell-related gene expression in the progenitor-rich limbal epithelium and the differentiating central corneal epithelium. *Molecular Vision*, *17*, 2102–2117.

183. Nili, E., Li, F. J., Dawson, R. A., Lau, C., McEwan, B., Barnett, N. L., Weier, S., Walshe, J., Richardson, N. A., & Harkin, D. G. (2019). The Impact of Limbal Mesenchymal Stromal Cells on Healing of Acute Ocular Surface Wounds Is Improved by Pre-cultivation and Implantation in the Presence of Limbal Epithelial Cells. *Cell Transplantation*, *28*(9–10), 1257–1270. https://doi.org/10.1177/0963689719858577

184. Nishimura, A., Carey, J., Erwin, P. J., Tilburt, J. C., Murad, M. H., & McCormick, J. B. (2013). Improving understanding in the research informed consent process: A systematic review of 54 interventions tested in randomized control trials. *BMC Medical Ethics*, *14*, 28. https://doi.org/10.1186/1472-6939-14-28

185. Nita, M., & Grzybowski, A. (2016). The Role of the Reactive Oxygen Species and Oxidative Stress in the Pathomechanism of the Age-Related Ocular Diseases and Other Pathologies of the Anterior and Posterior Eye Segments in Adults. *Oxidative Medicine and Cellular Longevity*, *2016*, 3164734. https://doi.org/10.1155/2016/3164734

186. Nosek, B. A., Alter, G., Banks, G. C., Borsboom, D., Bowman, S. D., Breckler, S. J., Buck, S., Chambers, C. D., Chin, G., Christensen, G., Contestabile, M., Dafoe, A., Eich, E., Freese, J., Glennerster, R., Goroff, D., Green, D. P., Hesse, B., Humphreys, M., … Yarkoni, T. (2015). Promoting an open research culture. *Science (New York, N.Y.)*, *348*(6242), 1422–1425. https://doi.org/10.1126/science.aab2374

187. Office of the Federal Register, N. A. and R. A. (1994, December 12). *59 FR - Citric Acid and Certain Citrate Derivatives; Affirmation of GRAS Status as Direct Human Food Ingredients* [Government]. Govinfo.Gov; Office of the Federal Register, National Archives and Records Administration. https://www.govinfo.gov/app/details/FR-1994-12-12/https%3A%2F%2Fwww.govinfo.gov%2Fapp%2Fdetails%2FFR-1994-12-12%2F94-30496

188. Olson, W. C., Smolkin, M. E., Farris, E. M., Fink, R. J., Czarkowski, A. R., Fink, J. H., Chianese-Bullock, K. A., & Slingluff, C. L. (2011). Shipping blood to a central laboratory in multicenter clinical trials: Effect of ambient temperature on specimen temperature, and effects of temperature on mononuclear cell yield, viability and immunologic function. *Journal of Translational Medicine*, *9*(1), 26. https://doi.org/10.1186/1479-5876-9-26

189. Ong, H. S., Riau, A. K., Yam, G. H.-F., Yusoff, N. Z. B. M., Han, E. J. Y., Goh, T.-W., Lai, R. C., Lim, S. K., & Mehta, J. S. (2023). Mesenchymal Stem Cell Exosomes as Immunomodulatory Therapy for Corneal Scarring. *International Journal of Molecular Sciences*, *24*(8), 7456. https://doi.org/10.3390/ijms24087456

190. O'Sullivan, F., & Clynes, M. (2007). Limbal stem cells, a review of their identification and culture for clinical use. *Cytotechnology*, *53*(1–3), 101–106. https://doi.org/10.1007/s10616-007-9063-6
191. Papas, E. B. (2003). The limbal vasculature. *Contact Lens and Anterior Eye*, *26*(2), 71–76. https://doi.org/10.1016/S1367-0484(02)00054-1
192. Patel, K., & Chotai, N. (2011). Documentation and Records: Harmonized GMP Requirements. *Journal of Young Pharmacists : JYP*, *3*(2), 138–150. https://doi.org/10.4103/0975-1483.80303
193. Pegg, D. E. (2007). Principles of cryopreservation. *Methods in Molecular Biology (Clifton, N.J.)*, *368*, 39–57. https://doi.org/10.1007/978-1-59745-362-2_3
194. Pellegrini, G., Golisano, O., Paterna, P., Lambiase, A., Bonini, S., Rama, P., & De Luca, M. (1999). Location and Clonal Analysis of Stem Cells and Their Differentiated Progeny in the Human Ocular Surface. *The Journal of Cell Biology*, *145*(4), 769–782.
195. Pereira, M. S., Cardoso, L. M. da F., da Silva, T. B., Teixeira, A. J., Mizrahi, S. E., Ferreira, G. S. M., Dantas, F. M. L., Cotta-de-Almeida, V., & Alves, L. A. (2020). A Low-Cost Open Source Device for Cell Microencapsulation. *Materials (Basel, Switzerland)*, *13*(22), 5090. https://doi.org/10.3390/ma13225090
196. Pfister, R. R., Haddox, J. L., & Paterson, C. A. (1982). The Efficacy of Sodium Citrate in the Treatment of Severe Alkali Burns of the Eye Is Influenced by the Route of Administration. *Cornea*, *1*(3), 205–212.
197. Pfister, R. R., Nicolaro, M. L., & Paterson, C. A. (1981). Sodium citrate reduces the incidence of corneal ulcerations and perforations in extreme alkali-burned eyes—Acetylcysteine and ascorbate have no favorable effect. *Investigative Ophthalmology & Visual Science*, *21*(3), 486–490.
198. Pignatti, F., Jonsson, B., Blumenthal, G., & Justice, R. (2015). Assessment of benefits and risks in development of targeted therapies for cancer—The view of regulatory authorities. *Molecular Oncology*, *9*(5), 1034–1041. https://doi.org/10.1016/j.molonc.2014.10.003
199. Pinnamaneni, N., & Funderburgh, J. L. (2012). Concise review: Stem cells in the corneal stroma. *Stem Cells (Dayton, Ohio)*, *30*(6), 1059–1063. https://doi.org/10.1002/stem.1100
200. Popova, O. P., Fedorov, D. N., Khodzhabekian, G. V., Makarov, P. V., Rogovaia, O. S., Vasil'ev, A. V., Ivanov, A. A., & Pal'tsev, M. A. (2006). [Immunomorphological study of time course of repair of corneal deep burn defects after stromal equivalent transplantation]. *Arkhiv Patologii*, *68*(2), 24–28.

201. Pravdyuk, A. I., Petrenko, Y. A., Fuller, B. J., & Petrenko, A. Y. (2013). Cryopreservation of alginate encapsulated mesenchymal stromal cells. *Cryobiology*, *66*(3), 215–222. https://doi.org/10.1016/j.cryobiol.2013.02.002
202. *Publicdisplaydocumentpdf.pdf*. (n.d.). Retrieved June 23, 2022, from https://www.oecd.org/officialdocuments/publicdisplaydocumentpdf/?cote=env/mc/chem(98)17&doclanguage=en
203. Purves, D. (2001). *Neuroscience* (2nd ed.). Sinauer Associates.
204. Remington, L. A. (2012). Chapter 2—Cornea and Sclera. In L. A. Remington (Ed.), *Clinical Anatomy and Physiology of the Visual System (Third Edition)* (pp. 10–39). Butterworth-Heinemann. https://doi.org/10.1016/B978-1-4377-1926-0.10002-5
205. Research, C. for B. E. and. (2020, July 21). *Regulatory Considerations for Human Cells, Tissues, and Cellular and Tissue-Based Products: Minimal Manipulation and Homologous Use*. U.S. Food and Drug Administration; FDA. https://www.fda.gov/regulatory-information/search-fda-guidance-documents/regulatory-considerations-human-cells-tissues-and-cellular-and-tissue-based-products-minimal
206. Richardson, T., Kumta, P. N., & Banerjee, I. (2014). Alginate encapsulation of human embryonic stem cells to enhance directed differentiation to pancreatic islet-like cells. *Tissue Engineering. Part A*, *20*(23–24), 3198–3211. https://doi.org/10.1089/ten.TEA.2013.0659
207. Rodríguez, F. D., & Vecino, E. (2016). Repair of corneal damage with stem cells. *New Frontiers in Ophthalmology*, *1*(1), 6–11. https://doi.org/10.15761/NFO.1000103
208. Sadler, T. W., & Langman. (2012). *Langman's Medical Embryology, 12e | Medical Education | Health Library*. Lippincott Williams & Wilkins. https://lib.ugent.be/catalog/rug01:001694307
209. Sangwan, V. S., Matalia, H. P., Vemuganti, G. K., Fatima, A., Ifthekar, G., Singh, S., Nutheti, R., & Rao, G. N. (2006). Clinical outcome of autologous cultivated limbal epithelium transplantation. *Indian Journal of Ophthalmology*, *54*(1), 29–34. https://doi.org/10.4103/0301-4738.21611
210. Sanmukhani, J., & Tripathi, C. B. (2011). Ethics in Clinical Research: The Indian Perspective. *Indian Journal of Pharmaceutical Sciences*, *73*(2), 125. https://doi.org/10.4103/0250-474X.91564
211. Saxena, P., & Saxena, R. (2014). Clinical Trials: Changing Regulations in India. *Indian Journal of Community Medicine : Official Publication of Indian Association of Preventive & Social Medicine*, *39*(4), 197–202. https://doi.org/10.4103/0970-0218.143018

212. *Schedule Y(ammended version)—CDSCO*. (n.d.-a). 48.
213. *Schedule Y(ammended version)—CDSCO*. (n.d.-b).
214. Schermer, A., Galvin, S., & Sun, T. T. (1986). Differentiation-related expression of a major 64K corneal keratin in vivo and in culture suggests limbal location of corneal epithelial stem cells. *The Journal of Cell Biology*, *103*(1), 49–62. https://doi.org/10.1083/jcb.103.1.49
215. Schlötzer-Schrehardt, U., Dietrich, T., Saito, K., Sorokin, L., Sasaki, T., Paulsson, M., & Kruse, F. E. (2007). Characterization of extracellular matrix components in the limbal epithelial stem cell compartment. *Experimental Eye Research*, *85*(6), 845–860. https://doi.org/10.1016/j.exer.2007.08.020
216. Scott, C. T., & Magnus, D. (2014). Wrongful Termination: Lessons From the Geron Clinical Trial. *Stem Cells Translational Medicine*, *3*(12), 1398–1401. https://doi.org/10.5966/sctm.2014-0147
217. Secker, G. A., & Daniels, J. T. (2008). Limbal epithelial stem cells of the cornea. In *StemBook*. Harvard Stem Cell Institute. http://www.ncbi.nlm.nih.gov/books/NBK27054/
218. Sensebé, L., Gadelorge, M., & Fleury-Cappellesso, S. (2013). Production of mesenchymal stromal/stem cells according to good manufacturing practices: A review. *Stem Cell Research & Therapy*, *4*(3), 66. https://doi.org/10.1186/scrt217
219. Sharma, A., & Coles, W. H. (1989). Kinetics of corneal epithelial maintenance and graft loss. A population balance model. *Investigative Ophthalmology & Visual Science*, *30*(9), 1962–1971.
220. Sharma, A., Kumar, N., Kuppermann, B. D., Bandello, F., & Loewenstein, A. (2020). Ophthalmic biosimilars and biologics—Role of endotoxins. *Eye*, *34*(4), 614–615. https://doi.org/10.1038/s41433-019-0636-3
221. Shimmura-Tomita, M., Wang, M., Taniguchi, H., Akiba, H., Yagita, H., & Hori, J. (2013). Galectin-9-mediated protection from allo-specific T cells as a mechanism of immune privilege of corneal allografts. *PloS One*, *8*(5), e63620. https://doi.org/10.1371/journal.pone.0063620
222. Singh, R., Gupta, N., Vanathi, M., & Tandon, R. (2019). Corneal transplantation in the modern era. *The Indian Journal of Medical Research*, *150*(1), 7–22. https://doi.org/10.4103/ijmr.IJMR_141_19
223. Sridhar, M. S. (2018). Anatomy of cornea and ocular surface. *Indian Journal of Ophthalmology*, *66*(2), 190–194. https://doi.org/10.4103/ijo.IJO_646_17

224. *StemBook*. (2008). Harvard Stem Cell Institute. http://www.ncbi.nlm.nih.gov/books/NBK27044/

225. Stensvaag, V., Furmanek, T., Lønning, K., Terzis, A. J. A., Bjerkvig, R., & Visted, T. (2004). Cryopreservation of alginate-encapsulated recombinant cells for antiangiogenic therapy. *Cell Transplantation*, *13*(1), 35–44. https://doi.org/10.3727/000000004772664879

226. Subbannayya, Y., Pinto, S. M., Mohanty, V., Dagamajalu, S., Prasad, T. S. K., & Murthy, K. R. (2020). What Makes Cornea Immunologically Unique and Privileged? Mechanistic Clues from a High-Resolution Proteomic Landscape of the Human Cornea. *Omics: A Journal of Integrative Biology*, *24*(3), 129–139. https://doi.org/10.1089/omi.2019.0190

227. Sun, J., & Tan, H. (2013a). Alginate-Based Biomaterials for Regenerative Medicine Applications. *Materials*, *6*(4), 1285–1309. https://doi.org/10.3390/ma6041285

228. Sun, J., & Tan, H. (2013b). Alginate-Based Biomaterials for Regenerative Medicine Applications. *Materials*, *6*(4), 1285–1309. https://doi.org/10.3390/ma6041285

229. Sun, T. T., & Green, H. (1977). Cultured epithelial cells of cornea, conjunctiva and skin: Absence of marked intrinsic divergence of their differentiated states. *Nature*, *269*(5628), 489–493. https://doi.org/10.1038/269489a0

230. Swioklo, S., Constantinescu, A., & Connon, C. J. (2016). Alginate-Encapsulation for the Improved Hypothermic Preservation of Human Adipose-Derived Stem Cells. *Stem Cells Translational Medicine*, *5*(3), 339–349. https://doi.org/10.5966/sctm.2015-0131

231. Taylor, A. W. (2016). Ocular Immune Privilege and Transplantation. *Frontiers in Immunology*, *7*, 37. https://doi.org/10.3389/fimmu.2016.00037

232. Thoft, R. A. (1989). The role of the limbus in ocular surface maintenance and repair. *Acta Ophthalmologica. Supplement*, *192*, 91–94. https://doi.org/10.1111/j.1755-3768.1989.tb07099.x

233. Thoft, R. A., & Friend, J. (1983). The X, Y, Z hypothesis of corneal epithelial maintenance. *Investigative Ophthalmology & Visual Science*, *24*(10), 1442–1443.

234. Thoft, R. A., Wiley, L. A., & Sundarraj, N. (1989). The multipotential cells of the limbus. *Eye (London, England)*, *3 (Pt 2)*, 109–113. https://doi.org/10.1038/eye.1989.17

235. Til, D., Amaral, V. L. L., Salvador, R. A., Senn, A., & Paula, T. S. de. (2016). The effects of storing and transporting cryopreserved semen samples on dry ice. *JBRA Assisted Reproduction*, *20*(4), 217–221. https://doi.org/10.5935/1518-0557.20160042

236. Torricelli, A. A. M., Santhanam, A., Wu, J., Singh, V., & Wilson, S. E. (2016). The corneal fibrosis response to epithelial-stromal injury. *Experimental Eye Research*, *142*, 110–118. https://doi.org/10.1016/j.exer.2014.09.012

237. Tran, N. (n.d.). *CONTACT FOR TECHNICAL OR OTHER INFORMATION:* 104.
238. Umemoto, T., Yamato, M., Nishida, K., Yang, J., Tano, Y., & Okano, T. (2006). Limbal epithelial side-population cells have stem cell-like properties, including quiescent state. *Stem Cells (Dayton, Ohio)*, *24*(1), 86–94. https://doi.org/10.1634/stemcells.2005-0064
239. Van Buskirk, E. M. (1989). The anatomy of the limbus. *Eye (London, England)*, *3 (Pt 2)*, 101–108. https://doi.org/10.1038/eye.1989.16
240. Van Buskirk, & Michael, E. (1989). The anatomy of the limbus. *Eye*, *3*(2), Article 2. https://doi.org/10.1038/eye.1989.16
241. Vashist, P., Senjam, S. S., Gupta, V., Gupta, N., Shamanna, B. R., Wadhwani, M., Shukla, P., Manna, S., Yadav, S., & Bharadwaj, A. (2022). Blindness and visual impairment and their causes in India: Results of a nationally representative survey. *PLoS ONE*, *17*(7), e0271736. https://doi.org/10.1371/journal.pone.0271736
242. *Vision impairment and blindness.* (n.d.). Retrieved July 20, 2023, from https://www.who.int/news-room/fact-sheets/detail/blindness-and-visual-impairment
243. Viswanathan, S., Rao, M., Keating, A., & Srivastava, A. (2013). Overcoming Challenges to Initiating Cell Therapy Clinical Trials in Rapidly Developing Countries: India as a Model. *Stem Cells Translational Medicine*, *2*(8), 607–613. https://doi.org/10.5966/sctm.2013-0019
244. W, A., & Al-Sayed, M. (2018). Human subjects in clinical trials: Ethical considerations and concerns. *Journal of Translational Science*, *4*(6). https://doi.org/10.15761/JTS.1000239
245. Wang, J., Shi, X., Xiong, M., Tan, W.-S., & Cai, H. (2022). Trehalose glycopolymers for cryopreservation of tissue-engineered constructs. *Cryobiology*, *104*, 47–55. https://doi.org/10.1016/j.cryobiol.2021.11.004
246. Wang, L.-L., Li, Z.-H., Hu, X.-H., Muyayalo, K. P., Zhang, Y.-H., & Liao, A.-H. (2017). The roles of the PD-1/PD-L1 pathway at immunologically privileged sites. *American Journal of Reproductive Immunology*, *78*(2), e12710. https://doi.org/10.1111/aji.12710
247. Weng, L., Funderburgh, J. L., Khandaker, I., Geary, M. L., Yang, T., Basu, R., Funderburgh, M. L., Du, Y., & Yam, G. H.-F. (2020). The anti-scarring effect of corneal stromal stem cell therapy is mediated by transforming growth factor β3. *Eye and Vision (London, England)*, *7*(1), 52. https://doi.org/10.1186/s40662-020-00217-z
248. West-Mays, J. A., & Dwivedi, D. J. (2006). The keratocyte: Corneal stromal cell with variable repair phenotypes. *The International Journal of Biochemistry & Cell Biology*, *38*(10), 1625–1631. https://doi.org/10.1016/j.biocel.2006.03.010

249. Whaley, D., Damyar, K., Witek, R. P., Mendoza, A., Alexander, M., & Lakey, J. R. (2021). Cryopreservation: An Overview of Principles and Cell-Specific Considerations. *Cell Transplantation*, *30*, 0963689721999617. https://doi.org/10.1177/0963689721999617

250. *Who's who*. (n.d.). Retrieved June 28, 2023, from https://cdsco.gov.in/opencms/opencms/en/About-us/who/

251. Willmann, D., Fu, L., & Melanson, S. W. (2023). Corneal Injury. In *StatPearls*. StatPearls Publishing. http://www.ncbi.nlm.nih.gov/books/NBK459283/

252. Wilson, J. L., Najia, M. A., Saeed, R., & McDevitt, T. C. (2014). Alginate encapsulation parameters influence the differentiation of microencapsulated embryonic stem cell aggregates. *Biotechnology and Bioengineering*, *111*(3), 618–631. https://doi.org/10.1002/bit.25121

253. Wilson, S. (2012). Corneal myofibroblast biology and pathobiology: Generation, persistence, and transparency. *Experimental Eye Research*, *99*(1). https://doi.org/10.1016/j.exer.2012.03.018

254. Wilson, S. E. (2020). Corneal wound healing. *Experimental Eye Research*, *197*, 108089. https://doi.org/10.1016/j.exer.2020.108089

255. *WMA Declaration of Helsinki – Ethical Principles for Medical Research Involving Human Subjects – WMA – The World Medical Association*. (n.d.). Retrieved June 28, 2023, from https://www.wma.net/policies-post/wma-declaration-of-helsinki-ethical-principles-for-medical-research-involving-human-subjects/

256. Wong, T. Y., Lincoln, A., Tielsch, J. M., & Baker, S. P. (1998). The epidemiology of ocular injury in a major US automobile corporation. *Eye (London, England)*, *12 (Pt 5)*, 870–874. https://doi.org/10.1038/eye.1998.220

257. Woods, E. J., & Thirumala, S. (2011). Packaging Considerations for Biopreservation. *Transfusion Medicine and Hemotherapy*, *38*(2), 149–156. https://doi.org/10.1159/000326083

258. Yam, G. H.-F., Yang, T., Geary, M. L., Santra, M., Funderburgh, M., Rubin, E., Du, Y., Sahel, J. A., Jhanji, V., & Funderburgh, J. L. (2023a). Human corneal stromal stem cells express anti-fibrotic microRNA-29a and 381-5p—A robust cell selection tool for stem cell therapy of corneal scarring. *Journal of Advanced Research*, *45*, 141–155. https://doi.org/10.1016/j.jare.2022.05.008

259. Yam, G. H.-F., Yang, T., Geary, M. L., Santra, M., Funderburgh, M., Rubin, E., Du, Y., Sahel, J. A., Jhanji, V., & Funderburgh, J. L. (2023b). Human corneal stromal stem cells express anti-fibrotic microRNA-29a and 381-5p—A robust cell selection tool for stem

cell therapy of corneal scarring. *Journal of Advanced Research*, *45*, 141–155. https://doi.org/10.1016/j.jare.2022.05.008

260. Yu, N.-H., Chun, S. Y., Ha, Y.-S., Kim, H. T., Kim, D. H., Kim, J., Chung, J.-W., Lee, J. N., Song, P. H., Yoo, E. S., Kim, B. S., & Kwon, T. G. (2018). Optimal Stem Cell Transporting Conditions to Maintain Cell Viability and Characteristics. *Tissue Engineering and Regenerative Medicine*, *15*(5), 639–647. https://doi.org/10.1007/s13770-018-0133-y
261. Zadnik, K., Money, S., & Lindsley, K. (2019). Intrastromal corneal ring segments for treating keratoconus. *The Cochrane Database of Systematic Reviews*, *2019*(5), CD011150. https://doi.org/10.1002/14651858.CD011150.pub2
262. Zhang, C., Cao, J., Zhao, S., Luo, H., Yang, Z., Gama, M., Zhang, Q., Su, D., & Wan, Y. (2020). Biocompatibility evaluation of bacterial cellulose as a scaffold material for tissue-engineered corneal stroma. *Cellulose*, *27*(5), 2775–2784. https://doi.org/10.1007/s10570-020-02979-0
263. Zhang, X., Nakahara, Y., Xuan, D., Wu, D., Zhao, F.-K., Li, X.-Y., & Zhang, J.-S. (2012). Study on the optical property and biocompatibility of a tissue engineering cornea. *International Journal of Ophthalmology*, *5*(1), 45–49. https://doi.org/10.3980/j.issn.2222-3959.2012.01.09
264. Zhu, L., Zhang, W., Zhu, J., Chen, C., Mo, K., Guo, H., Wu, S., Huang, H., Li, L., Li, M., Tan, J., Huang, Y., Wang, L., & Ouyang, H. (2022a). Cotransplantation of Limbal Epithelial and Stromal Cells for Ocular Surface Reconstruction. *Ophthalmology Science*, *2*(2), 100148. https://doi.org/10.1016/j.xops.2022.100148
265. Zhu, L., Zhang, W., Zhu, J., Chen, C., Mo, K., Guo, H., Wu, S., Huang, H., Li, L., Li, M., Tan, J., Huang, Y., Wang, L., & Ouyang, H. (2022b). Cotransplantation of Limbal Epithelial and Stromal Cells for Ocular Surface Reconstruction. *Ophthalmology Science*, *2*(2), 100148. https://doi.org/10.1016/j.xops.2022.100148

Annexures

Annexure I

Chemicals/materials/equipment/antibodies used in this thesis work

A. Plasticware

Product	**Make**	**Catalogue Number**
1.5ml micro-centrifuge tube	Eppendorf	0030121589
TC-treated T25 flasks	Eppendorf	0030710126
TC-treated T75 flasks	Eppendorf	0030711122
Petri dishes (60mm)	Eppendorf	0030701119
Petri dishes (35mm)	Eppendorf	0030700112
Pipette (5mL)	Eppendorf	0030127714
Pipette (10mL)	Eppendorf	0030127722
Pipette (25mL)	Eppendorf	0030127730
Dual filter Tips (10 μL)	Eppendorf	022491211
Dual filter Tips (200 μL)	Eppendorf	022491296
Dual filter Tips (1mL)	Eppendorf	0030078578
15 mL Centrifuge Tube	Eppendorf	0030122151
50 mL Centrifuge Tube	Eppendorf	0030122178
0.22μ Syringe Filter	Nalgene	7252520
20mL Syringe	Dispovan	NA
12-well plate	Eppendorf	NA
96-well plate	Eppendorf	NA

B. Glassware

Product	**Make**
Cover glass	BlueStar
Glass slides	BlueStar

C. Surgical Tools

Equipment/Tool	Make	Catalogue Number
Surgical blade	Surgeon	10135
Blade Handle	Asian Surgicals	Bard Parker No.3
Castroviejo Scissors	Asian Surgicals	NA
Tying forceps	Asian Surgicals	JS-4471
Narrow and straight forceps with serrated margin	Asian Surgicals	JS-5400
Corneal Scissors	Asian Surgicals	Js-5421

D. Equipment

S.No.	Equipment	Make	Model/Catalogue Number
1.	Micro Pipettes (0.1-2.5 μL)	Eppendorf	Reference 2/ 4920000016
2.	Micro Pipettes (0.5-10 μL)	Eppendorf	Reference 2/ 4920000024
3.	Micro Pipettes (20-200 μL)	Eppendorf	Reference 2/ 4920000067
4.	Micro Pipettes (100-1000 μL)	Eppendorf	Reference 2/ 4920000083
5.	Pipette Aid	Drummond	Pipet-Aid® Hood-Mate®/ 4000303
6.	Biosafety Cabinet	Telstar	Bio-II-Advance 4
7.	Centrifuge	Eppendorf	Centrifuge 5702R
8.	Biomedical freezer	Panasonic	
9.	Refrigerator	Panasonic	MPR-S163-PE
10.	Inverted Microscope	Zeiss	Primovert
11.	Camera	Zeiss	Axiocam 105
12.	CO_2 Incubator	Eppendorf	CO1711400X/ Galaxy 170S
13.	Bead Bath	Thermo Fisher Scientific	TSGP10
14.	Stereo Microscope	Zeiss	Stemi 305
15.	Cryocooler	ThermoFisher	NA
16.	Cryo-storage system	MVE Biological solutions	MVE Cryosystem 6000

E. Chemicals

Product	**Make**	**Reference**
Paraformaldehyde	Fisher Scientific	30525-89-4
Triton-X 100	ThermoFisher	T8787
BSA	Sigma-Aldrich	A7096
Antibiotic Antimycotic	Gibco	15240062
DPBS	Gibco	14190250
Insulin, recombinant human	Gibco	12585014
Recombinant Human EGF	Thermo Fisher Scientific	PHG0311L
Dulbecco's Modified Eagle Medium / Ham's F12	Lonza	BE04-687F/U1
Serum	Hyclone	SH30084.03
Collagenase IV	Gibco	17104019
DMSO	Sigma-Aldrich	D2650
TrypLE	Thermo Fisher Scientific	A1285901
Trypan Blue	Thermo Fisher Scientific	15250061
Mounting medium with DAPI	Abcam	Ab104139

F. Antibodies

Primary Antibodies

Antibody	Make	Reference	Origin	Clonality
α-SMA	Sigma	A2457	Mouse	Monoclonal
ABCB5	Abcam	Ab140667	Mouse	Monoclonal
ABCG2	Santacruz	Sc18841	Mouse	Monoclonal
CD105	Santacruz	SC376381	Mouse	Monoclonal
CD45	Cell Signaling Technologies	13917s	Rabbit	Monoclonal
CD73	Cell Signaling Technologies	13160s	Rabbit	Polyclonal
CD90	Santacruz	SC-59396	Mouse	Monoclonal
Collagen I	Abcam	Ab138492	Rabbit	Monoclonal
Collagen II	Abcam	Ab34712	Rabbit	Polyclonal
Collagen III	Abcam	Ab7778	Rabbit	Polyclonal
Collagen IV	Abcam	Ab6586	Rabbit	Polyclonal
Collagen V	Abcam	Ab7046	Rabbit	Polyclonal
E-Cadherin	GeneAb	IHC564-100	Mouse	Monoclonal
HLA-DR	Abcam	Ab55152	Mouse	Monoclonal
KERA	LS-Bio	LS-B8216	Rabbit	Polyclonal
N-Cadherin	GeneAb	IHC636-100	Mouse	Monoclonal
P63-α	Cell Signaling Technologies	4892S	Rabbit	Polyclonal
PAX-6	Santacruz	Sc81649	Mouse	Monoclonal
Vimentin	Santacruz	SC6260	Mouse	Monoclonal

Secondary Antibodies

Antibody	Make	Catalogue Number	Origin	Clonality	Dilution ratio
Alexa Fluor 488 anti-rabbit	Invitrogen	A11008	Goat	Polyclonal	1:400
Alexa Fluor 488 anti-mouse	Invitrogen	A11001	Goat	Polyclonal	1:400
Alexa Fluor 594 anti-rabbit	Invitrogen	A11012	Goat	Polyclonal	1:400
Alexa Fluor 594 anti-mouse	Invitrogen	A11005	Goat	Polyclonal	1:400

Annexure II

Study approval by the Institutional Ethics Committee, LV Prasad Eye Institute, Hyderabad.

Hyderabad Eye Research Foundation

World Health Organization
Collaborating Centre for Prevention of Blindness

L V Prasad Eye Institute Ethics Committee
Kallam Anji Reddy Campus, Banjara Hills, Hyderabad
ECR/468/Inst./AP/2013/RR-16

May 22, 2018 **Ethics Ref. No. LEC 05-18-081**

To:

Dr Sayan Basu
Dr Vivek Singh
Principal Investigator
L V Prasad Eye Institute
L V Prasad Marg, Banjara Hills
Hyderabad- 500 034
Telangana

Subject: Ethics Committee Approval Letter

Protocol Entitled: "Optimizing the Processes for Isolation, Preservation, Transportation and Delivery of Human Limbus-derived Stromal/ Mesenchymal Stem Cells for Clinical Use in a cGMP Facility"

Dear Dr Sayan Basu, Dr Vivek Singh:

With reference to your Submission for the approval of above protocol, the Institutional Review Board, L V Prasad Eye Institute, held on May 22, 2018 has reviewed and discussed the below mentioned list of documents submitted by you and approved the same.

Sl No	Documents
1.	Study Protocol
2.	Informed Consent Form

It is understood that the study will be conducted under your direction at L.V. Prasad Eye Institute, Hyderabad

Ethics committee
L.V. Prasad Eye Institute
Kallam Anji Reddy , Campus
Banjara Hills, Hyderabad-500 034
Reg.No. ECR/468/Inst./AP/ 2013/RR-16

LV Prasad Eye Institute, Kallam Anji Reddy Campus, L V Prasad Marg, Banjara Hills, Hyderabad 500034, India
Tel: +91 40 30612345, Fax: +91 40 23548271, Email: info.hyd@lvpei.org, Website: www.lvpei.org

Annexure III

Study approval by the Institutional Committee for Stem Cell Research, LV Prasad Eye Institute, Hyderabad.

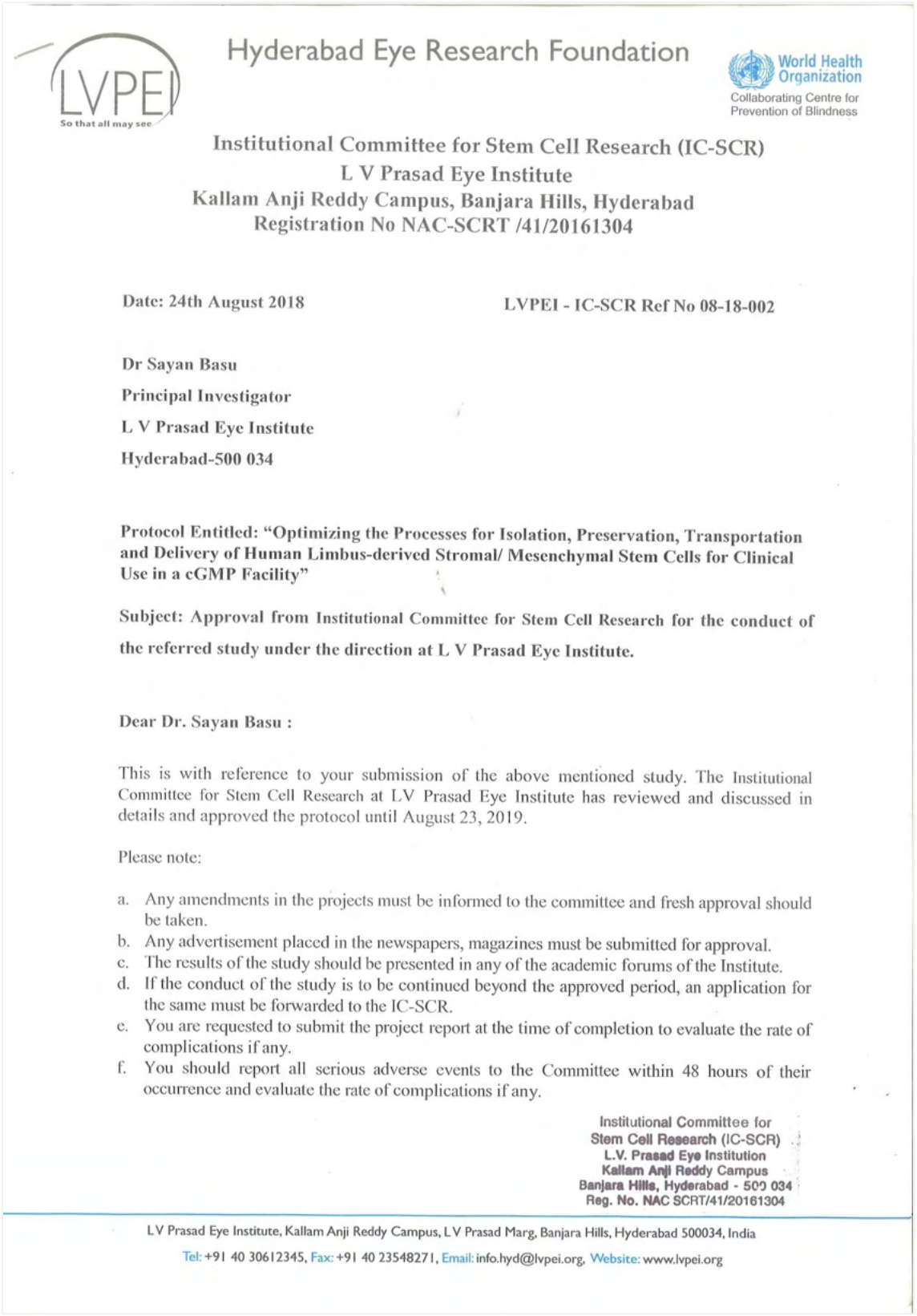

Hyderabad Eye Research Foundation

World Health Organization
Collaborating Centre for Prevention of Blindness

Institutional Committee for Stem Cell Research (IC-SCR)
L V Prasad Eye Institute
Kallam Anji Reddy Campus, Banjara Hills, Hyderabad
Registration No NAC-SCRT /41/20161304

Date: 24th August 2018 **LVPEI - IC-SCR Ref No 08-18-002**

Dr Sayan Basu
Principal Investigator
L V Prasad Eye Institute
Hyderabad-500 034

Protocol Entitled: "Optimizing the Processes for Isolation, Preservation, Transportation and Delivery of Human Limbus-derived Stromal/ Mesenchymal Stem Cells for Clinical Use in a cGMP Facility"

Subject: Approval from Institutional Committee for Stem Cell Research for the conduct of the referred study under the direction at L V Prasad Eye Institute.

Dear Dr. Sayan Basu :

This is with reference to your submission of the above mentioned study. The Institutional Committee for Stem Cell Research at LV Prasad Eye Institute has reviewed and discussed in details and approved the protocol until August 23, 2019.

Please note:

a. Any amendments in the projects must be informed to the committee and fresh approval should be taken.
b. Any advertisement placed in the newspapers, magazines must be submitted for approval.
c. The results of the study should be presented in any of the academic forums of the Institute.
d. If the conduct of the study is to be continued beyond the approved period, an application for the same must be forwarded to the IC-SCR.
e. You are requested to submit the project report at the time of completion to evaluate the rate of complications if any.
f. You should report all serious adverse events to the Committee within 48 hours of their occurrence and evaluate the rate of complications if any.

Institutional Committee for
Stem Cell Research (IC-SCR)
L.V. Prasad Eye Institution
Kallam Anji Reddy Campus
Banjara Hills, Hyderabad - 500 034
Reg. No. NAC SCRT/41/20161304

LV Prasad Eye Institute, Kallam Anji Reddy Campus, L V Prasad Marg, Banjara Hills, Hyderabad 500034, India
Tel: +91 40 30612345, Fax: +91 40 23548271, Email: info.hyd@lvpei.org, Website: www.lvpei.org

Annexure IV

A masked reference copy of the informed consent form, towards donation of eyes.

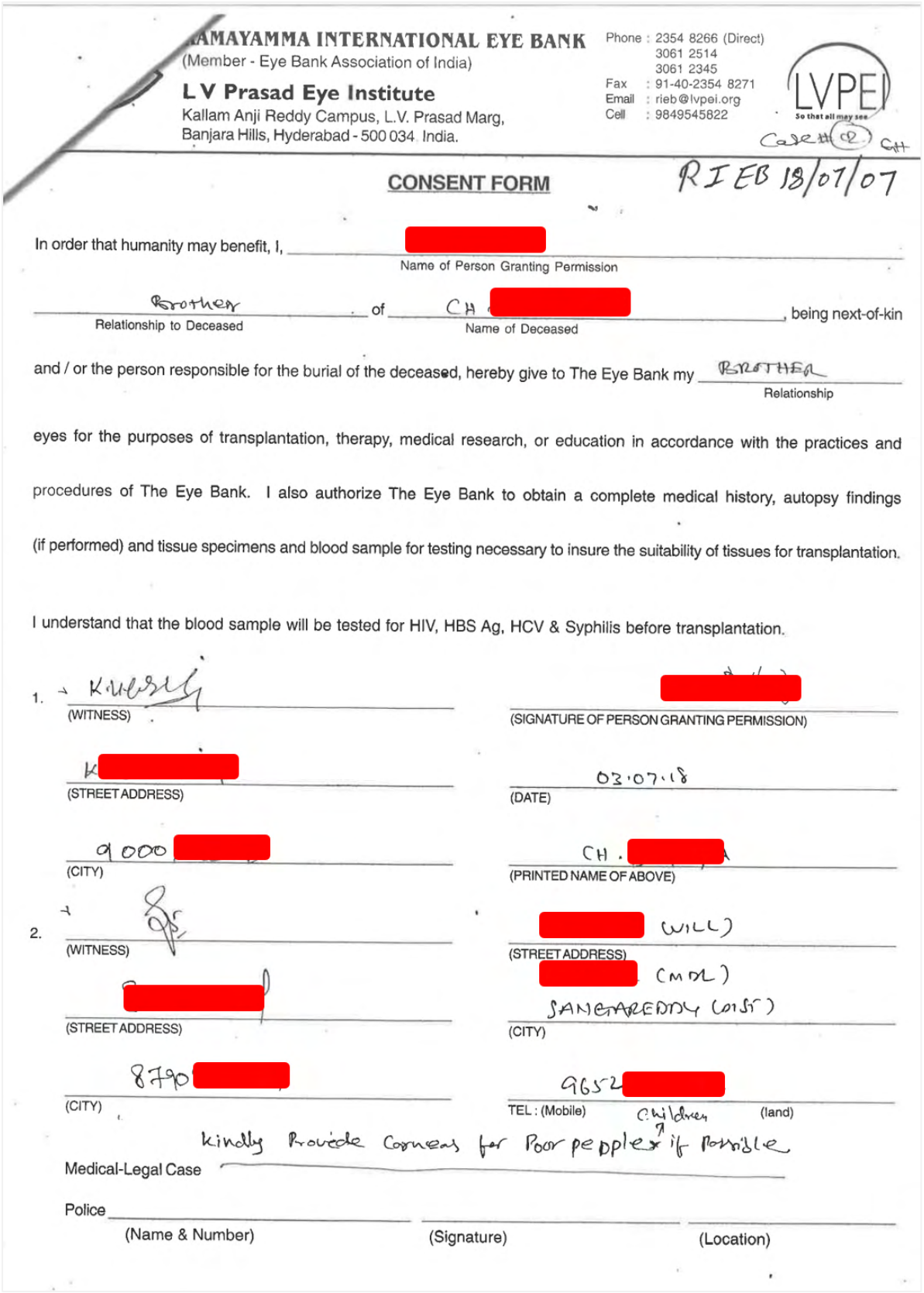

AMAYAMMA INTERNATIONAL EYE BANK
(Member - Eye Bank Association of India)
L V Prasad Eye Institute
Kallam Anji Reddy Campus, L.V. Prasad Marg,
Banjara Hills, Hyderabad - 500 034. India.

Phone : 2354 8266 (Direct)
3061 2514
3061 2345
Fax : 91-40-2354 8271
Email : rieb@lvpei.org
Cell : 9849545822

LVPEI
So that all may see

Case # 02 CH

RIEB 13/07/07

CONSENT FORM

In order that humanity may benefit, I, [redacted]
Name of Person Granting Permission

Brother of CH [redacted], being next-of-kin
Relationship to Deceased — Name of Deceased

and / or the person responsible for the burial of the deceased, hereby give to The Eye Bank my BROTHER
Relationship

eyes for the purposes of transplantation, therapy, medical research, or education in accordance with the practices and procedures of The Eye Bank. I also authorize The Eye Bank to obtain a complete medical history, autopsy findings (if performed) and tissue specimens and blood sample for testing necessary to insure the suitability of tissues for transplantation.

I understand that the blood sample will be tested for HIV, HBS Ag, HCV & Syphilis before transplantation.

1. K[redacted] (WITNESS)
[redacted] (SIGNATURE OF PERSON GRANTING PERMISSION)
K[redacted] (STREET ADDRESS)
03.07.18 (DATE)
9000[redacted] (CITY)
CH.[redacted] (PRINTED NAME OF ABOVE)

2. [redacted] (WITNESS)
[redacted] (WILL) (STREET ADDRESS)
[redacted] (CMDL)
SANGAREDDY (DIST) (CITY)
[redacted] (STREET ADDRESS)
8790[redacted] (CITY)
9652[redacted] TEL : (Mobile) Children (land)

kindly Provide Corneas for Poor people if Possible

Medical-Legal Case

Police _____ _____ _____
(Name & Number) (Signature) (Location)

Annexure V

A reference copy of the tissue evaluation sheet of the donor corneas.

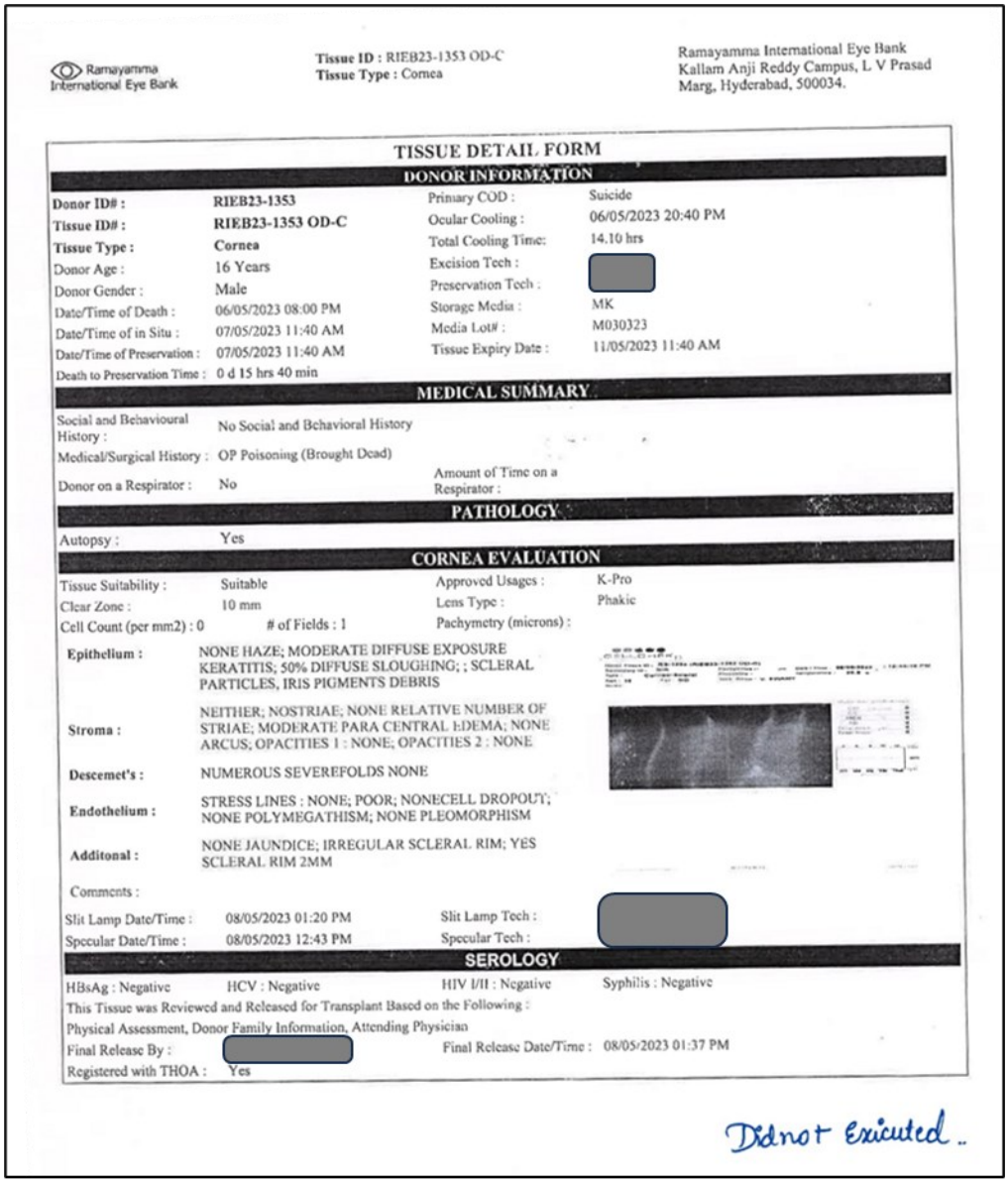

Ramayamma International Eye Bank

Tissue ID : RIEB23-1353 OD-C
Tissue Type : Cornea

Ramayamma International Eye Bank
Kallam Anji Reddy Campus, L V Prasad Marg, Hyderabad, 500034.

TISSUE DETAIL FORM

DONOR INFORMATION

Donor ID# :	**RIEB23-1353**	Primary COD :	Suicide
Tissue ID# :	**RIEB23-1353 OD-C**	Ocular Cooling :	06/05/2023 20:40 PM
Tissue Type :	**Cornea**	Total Cooling Time:	14.10 hrs
Donor Age :	16 Years	Excision Tech :	[redacted]
Donor Gender :	Male	Preservation Tech :	
Date/Time of Death :	06/05/2023 08:00 PM	Storage Media :	MK
Date/Time of in Situ :	07/05/2023 11:40 AM	Media Lot# :	M030323
Date/Time of Preservation :	07/05/2023 11:40 AM	Tissue Expiry Date :	11/05/2023 11:40 AM
Death to Preservation Time :	0 d 15 hrs 40 min		

MEDICAL SUMMARY

Social and Behavioural History :	No Social and Behavioral History
Medical/Surgical History :	OP Poisoning (Brought Dead)
Donor on a Respirator :	No
Amount of Time on a Respirator :	

PATHOLOGY

Autopsy : Yes

CORNEA EVALUATION

Tissue Suitability :	Suitable	Approved Usages :	K-Pro
Clear Zone :	10 mm	Lens Type :	Phakic
Cell Count (per mm2) : 0	# of Fields : 1	Pachymetry (microns) :	

Epithelium : NONE HAZE; MODERATE DIFFUSE EXPOSURE KERATITIS; 50% DIFFUSE SLOUGHING; ; SCLERAL PARTICLES, IRIS PIGMENTS DEBRIS

Stroma : NEITHER; NOSTRIAE; NONE RELATIVE NUMBER OF STRIAE; MODERATE PARA CENTRAL EDEMA; NONE ARCUS; OPACITIES 1 : NONE; OPACITIES 2 : NONE

Descemet's : NUMEROUS SEVEREFOLDS NONE

Endothelium : STRESS LINES : NONE; POOR; NONECELL DROPOUT; NONE POLYMEGATHISM; NONE PLEOMORPHISM

Additonal : NONE JAUNDICE; IRREGULAR SCLERAL RIM; YES SCLERAL RIM 2MM

Comments :

Slit Lamp Date/Time :	08/05/2023 01:20 PM	Slit Lamp Tech :	[redacted]
Specular Date/Time :	08/05/2023 12:43 PM	Specular Tech :	

SEROLOGY

HBsAg : Negative HCV : Negative HIV I/II : Negative Syphilis : Negative

This Tissue was Reviewed and Released for Transplant Based on the Following :

Physical Assessment, Donor Family Information, Attending Physician

Final Release By : [redacted] Final Release Date/Time : 08/05/2023 01:37 PM

Registered with THOA : Yes

Didnot Exicuted..

Annexure VI

Certificate of GLP Compliance, Sipra Labs Limited, Hyderabad.

सत्यमेव जयते

GOVERNMENT OF INDIA

Department of Science and Technology

National Good Laboratory Practice (GLP) Compliance Monitoring Authority (NGCMA)

Certificate of GLP Compliance

Based on the Inspection and the subsequent follow-up actions

Sipra Labs Limited

Industrial Estate, Balanagar
Hyderabad – 500037 (Telangana)

is certified capable of conducting the below-mentioned tests/studies in compliance with Organization for Economic Co-operation & Development (OECD) Principles of GLP:

- **Toxicity Studies**

The specific areas of expertise, types of chemicals and test systems are listed in annexure overleaf.

Validity: October 18, 2017 – October 17, 2020

This certificate is subject to the condition that the test facility complies with the NGCMA's Document No. GLP-101 "Terms & Conditions of NGCMA for obtaining and maintaining GLP certification by a test facility" and OECD Principles of GLP.

Certificate No.: GLP/C-107/2017
Issue Date : 18-10-2017

भारत सरकार ★ Govt. of India
राष्ट्रीय जी एल पी अनुपालन निगरानी प्राधिकरण
National GLP Compliance Monitoring Authority
सत्यमेव जयते
विज्ञान और प्रौद्योगिकी मंत्रालय ★ Dept. of Science and Technology

(Dr. Neeraj Sharma)
Head, NGCMA

Annexure VII

Biological Testing Accredetation Certificate of Sipra Labs Limited, Hyderabad.

National Accreditation Board for Testing and Calibration Laboratories

(A Constituent Board of Quality Council of India)

SCOPE OF ACCREDITATION

Laboratory	**Sipra Labs Limited, 7-2-1813/5/A, Survey No.59/6, Sanathnagar Industrial Area, Hyderabad, Telangana**		
Accreditation Standard	**ISO/IEC 17025: 2005**		
Certificate Number	**TC-5417**	**Page 1 of 14**	
Validity	**31.03.2017 to 30.03.2019**	**Last Amended on 12.06.2017**	

Sl.	Product / Material of Test	Specific Test Performed	Test Method Specification against which tests are performed	Range of Testing / Limits of Detection
		BIOLOGICAL TESTING		
I.	**FOOD AND AGRICULTURAL PRODUCTS**			
1.	**Milk Powder**	Bacterial Count	IS 5402	10 CFU/g to 300 CFU/g
		Coli form count	IS 5401(Part 1)	10 CFU/g to 150 CFU/g
		Staphylococcus aureus	IS 5887(Part 2)	Present or Absent/25g
		Salmonella	IS 5587(Part 3)	Present or Absent/25g
		Shigella	IS 5887(Part 7)	Present or Absent/25g
2.	**Skimmed Milk Powder**	Bacterial Count	IS 5402	10 CFU/g to 300 CFU/g
		coli forms count	IS 5401(Part 1)	10 CFU/g to 150 CFU/g
		Coli form count	IS 5401(Part 1)	≥10 CFU/g
II.	**WATER**			
1.	**Packaged Drinking Water (Other than natural mineral water)**	Escherichia coli	IS15185	Present or Absent/250 mL
		Coliform bacteria	IS15185	Present or Absent /250 mL
		Faecal streptococci	IS15185	Present or Absent /250 mL
		Staphylococcus aureus	IS 5887 (Part 2)	Present or Absent /250 mL
		Sulphite reducing anaerobes	IS 13428 (Annex C)	Present or Absent /50 mL
		Pseudomonas aeruginosa	IS 13428 (Annex D)	Present or Absent /250 mL
		Aerobic microbial count @ 22 °C, 72 hrs	IS 5402	Minimum 1 CFU/mL
		Aerobic microbial count @ 37 °C, 24hrs	IS 5402	Minimum 1 CFU/mL
		Yeast and Mould Count	IS 5403	Present or Absent/250 mL
		Salmonella	IS 15187	Present or Absent /250 mL
		Shigella	IS 5887 (Part 7)	Present or Absent /250 mL
		Vibrio cholera	IS 5887 (Part 5)	Present or Absent /250 mL
		Vibrio parahaemolyticus	IS 5887 (Part 5)	Present or Absent /250 mL

Anuja Anand
Convenor

N. Venkateswaran
Program Director

Annexure VIII

Study approval by the Institutional Animal Ethics Committee of Center for Cellular and Molecular Biology, Hyderabad.

सी सी एम बी CCMB
सीएसआईआर - कोशिकीय एवं आणविक जीव विज्ञान केन्द्र
CSIR-CENTRE FOR CELLULAR AND MOLECULAR BIOLOGY
उप्पल रोड, हैदराबाद तेलंगाणा - 500 007. भारत.
Uppal Road, Hyderabad, Telangana - 500 007. India.

To,
Dr. B. Kiran Kumar Dr.Vivek Singh – LVPEI / Dr.Sayan Basu - LVPEI
Scientist
CCMB

15 th March 2019

Project No: 92/2019

Dear Sir

Institute Animal Ethics Committee (IAEC) has reviewed your research project titled " Optimizing the processes for isolation, preservation, transportation and delivery of human limbus derived stromal / mesenchymal stem cells for clinical use in cGMP facility" (IAEC 92/ 2019) on 15 th March 2019.

The proposal is formally approved for funding and once the project is ready for funding, resubmit the form B for issue of animals.

With regards

Sincerely 15/3/19
Dr. M.J. Mahesh Kumar
Convener, IAEC

MAHESH KUMAR
Principal Scientist & Officer Incharge
Animal House
Centre for Cellular & Molecular Biology
HYDERABAD- 500 007.

फैक्स अंतर्राष्ट्रीय +91-40-27160591, 27160311 दूरभाष +91-40-27160222-41
भारत 040-27160591, 27160311 Telephone
Fax International +91-40-27160591, 27160311 वेब साइट http://www.ccmb.res.in

Annexure IX

Abridged version of the Batch Manufacturing Record proforma of hLMSCs production, is enclosed hereunder. The text explaining the individual steps of the events in this protocol are clipped to shorten the typical 60+ page long document to fewer numbers.

LVPEI	**CENTER FOR OCULAR REGENERATION (CORE)** ***KallamAnji Reddy Campus, L.V Prasad Eye Institute, LV Prasad Marg, Road No.2, Banjara Hills, Hyderabad -500034***				
	BATCH MANUFACTURING RECORD				
Title	LIMBAL TISSUE TO INVESTIGATIONAL MEDICINAL PRODUCT				
Department	Adult Stem Cell		BMR No.	ASCBMR003	
Effective Date		**Revision No.**	00	**Page No.** **New No.**	1 of 59 _____

Batch No.				
Cornea I.D No.				
No.of flasks in generation	**P0 (T25)**	**P1 (T25)**	**P2 (T75)**	**P3 (T75)**

Batch Manufacturing Record Issuance		
Issued By – Issuer has reviewed the Batch Record to ensure that the copy is a complete, accurate copy of the Master Batch Record		
Issued By – Quality Assurance	Signature :	Date:
Issued To – Production has reviewed the Batch Record to ensure that the copy is complete and correct. The concerned department is responsible for the Batch Record following the issuance		
Issued To – Production	Signature:	Date:

	Prepared by	**Verified by**	**Approved by**
Name	**Mukesh Damala**	**Dr Vivek Singh**	**Chethan AJ**
Signature			
Date	dd.mm.18	dd.mm.18	dd.mm.18

	CENTER FOR OCULAR REGENERATION (CORE) ***KallamAnji Reddy Campus, L.V Prasad Eye Institute, LV Prasad Marg, Road No.2, Banjara Hills, Hyderabad -500034***				
	BATCH MANUFACTURING RECORD				
Title	LIMBAL TISSUE TO INVESTIGATIONAL MEDICINAL PRODUCT				
Department	Adult Stem Cell		BMR No.	ASCBMR003	
Effective Date		**Revision No.**	00	**Page No.** **New No.**	2 of 59 _____

Information of no.of flasks per passage/subculture and page number (modified)																			
Batch No.																			
Cornea ID.																			
Passage No.	P0	P1			P2					P3									
Flask No.	**1**	**1**	**2**	**3**	**1**	**2**	**3**	**4**	**5**	**1**	**2**	**3**	**4**	**5**	**6**	**7**	**8**	**9**	**10**
Date of seeding (dd.mm.yy)																			
Source Flask (PN-NN)	NA																		
Media Prep date (dd.mm.yy)																			
No. of cells seeded (million)																			
No. of days in culture																			
Yield (millions)																			
Date of harvest/ subculture (dd.mm.yy)																			
Screening parameters	(Mention the respective new/modified page numbers in below columns)																		
Day 3																			
Day 5																			
Day 7																			
Day 10																			
Day of confluence																			

	CENTER FOR OCULAR REGENERATION (CORE) ***KallamAnji Reddy Campus, L.V Prasad Eye Institute, LV Prasad Marg, Road No.2, Banjara Hills, Hyderabad -500034***				
	BATCH MANUFACTURING RECORD				
Title	LIMBAL TISSUE TO INVESTIGATIONAL MEDICINAL PRODUCT				
Department	Adult Stem Cell		BMR No.	ASCBMR003	
Effective Date		**Revision No.**	00	**Page No.** **New No.**	3 of 59 _____

1. INDEX FOR BATCH MANUFACTURING RECORD

	CENTER FOR OCULAR REGENERATION (CORE) ***KallamAnji Reddy Campus, L.V Prasad Eye Institute, LV Prasad Marg, Road No.2, Banjara Hills, Hyderabad -500034***				
	BATCH MANUFACTURING RECORD				
Title	LIMBAL TISSUE TO INVESTIGATIONAL MEDICINAL PRODUCT				
Department	Adult Stem Cell		BMR No.	ASCBMR003	
Effective Date		**Revision No.**	00	**Page No.** **New No.**	4 of 59 _____

1. INDEX FOR BATCH MANUFACTURING RECORD

	CENTER FOR OCULAR REGENERATION (CORE) ***KallamAnji Reddy Campus, L.V Prasad Eye Institute, LV Prasad Marg, Road No.2, Banjara Hills, Hyderabad -500034***				
	BATCH MANUFACTURING RECORD				
Title	LIMBAL TISSUE TO INVESTIGATIONAL MEDICINAL PRODUCT				
Department	Adult Stem Cell		BMR No.	ASCBMR003	
Effective Date		**Revision No.**	00	**Page No.** **New No.**	5 of 59 _____

2. RAW MATERIAL REQUISITION & DISPENSING RECORD (MEDIA AND REAGENTS)

S. No.	Components	Mfg.	Cat. No.	Batch/ Lot No.	Expiry Date	A.R. No.	Issued By	Checked By
1.	Antibiotic Antimycotic	Gibco	15240062					
2.	DPBS	Gibco	14190250					
3.	Insulin, recombinant human	Gibco	12585014					
4.	Recombinant Human EGF	Thermofisher scientific	PHG0311L					
5.	Dulbecco's Modified Eagle Medium / F12	Lonza	BE04-687F/U1					
6.	Serum	Hyclone	SH30084.03					
7.	Collagenase IV	Gibco	17104019					
8.	DMSO	Sigma	D2650					
9.	TrypLE	Thermofisher scientific	A1285901					
10.	1.5ml micro-centrifuge tube	Eppendorf	0030121589					

	CENTER FOR OCULAR REGENERATION (CORE) ***KallamAnji Reddy Campus, L.V Prasad Eye Institute, LV Prasad Marg, Road No.2, Banjara Hills, Hyderabad -500034***				
	BATCH MANUFACTURING RECORD				
Title	LIMBAL TISSUE TO INVESTIGATIONAL MEDICINAL PRODUCT				
Department	Adult Stem Cell		BMR No.	ASCBMR003	
Effective Date		**Revision No.**	00	**Page No.** **New No.**	6 of 59 _____

3. PLASTIC WARESREQUISITION & DISPENSING RECORD

S. No.	Plastic Ware	Mfg.	Cat. No.	Lot/Batch No.	Expiry Date	Release Note No.	Issued By	Checked By
1.	TC-treated T25 flasks	CytoOne	SLCC76824825					
2.		Eppendorf	0030710126					
3.	TC-treated T75 flasks	CytoOne	SLCC76824875					
4.		Corning	430641U					
5.	Petri dishes(35mm)	CytoOne	SLCC76823340					
6.		Corning	430165					
7.	Petri dishes (60mm)	CytoOne	SLCC76823359					
8.		Corning	430166					
9.	Pipette (5mL)	Eppendorf	0030127714					
10.	Pipette (10mL)	Eppendorf	0030127722					
11.	Pipette (25mL)	Eppendorf	0030127730					
12.	Dual filter Tips (10 µL)	Eppendorf	022491211					
13.	Dual filter Tips(200 µL)	Eppendorf	022491296					
14.	Dual filter Tips(1mL)	Eppendorf	0030078578					
15.	15 mL Centrifuge Tube	(TPP)	91015					
16.	50 mL Centrifuge Tube	(TPP)	91050					
17.	0.22µ Syringe Filter	(TPP)	99722					
18.	Surgical blade #15	Surgeon	10135					
19.	20mL Syringe	Dispovan	NA					

	CENTER FOR OCULAR REGENERATION (CORE) ***KallamAnji Reddy Campus, L.V Prasad Eye Institute, LV Prasad Marg, Road No.2, Banjara Hills, Hyderabad -500034***				
	BATCH MANUFACTURING RECORD				
Title	LIMBAL TISSUE TO INVESTIGATIONAL MEDICINAL PRODUCT				
Department	Adult Stem Cell		BMR No.	ASCBMR003	
Effective Date		**Revision No.**	00	**Page No.** **New No.**	7 of 59 _____

4. LIST OF EQUIPMENT FOR BATCH PROCESSING

S. No.	Item	Company/Model	Location	Equipment/Instrument ID#
1.	Micro Pipettes (0.1-2.5 µL)	Eppendorf/ 4920000016	ASC	N11265F
2.	Micro Pipettes (0.5-10 µL)	Eppendorf/ 4920000024	ASC	L11283F
3.	Micro Pipettes (20-200 µL)	Eppendorf/ 4920000067	ASC	K23326F
4.	Micro Pipettes (100-1000 µL)	Eppendorf/ 4920000083	ASC	L11768F
5.	Pipette Aid	Eppendorf	ASC	093015
6.	Biosafety Cabinet	Telstar/Bio-II-Advance 4	ASC	ACS/BSC-12
7.	Biosafety Cabinet	Telstar/Bio-II-Advance 4	Media Preparation Room	MPR/BSC-26
8.	Centrifuge	Eppendorf/5702R	ASC	ACS/CTF-17
9.	Biomedical freezer	Panasonic	Media Preparation Room	MPR/BMF-27
10.	Refrigerator	Panasonic/MPR-5163-PE,	ASC	ACS/PR-21
11.	Inverted Microscope	Zeiss/Primovert	ASC	ACS/BM-20
12.	CO_2 Incubator	Eppendorf 170S Galaxy	ASC	ACS/COI-15
13.	Water/Bead Bath	Thermo Fisher, TSGP10	ASC	ACS/WB-14
14	Stereo Microscope	Carl Zeiss Microscope/ stemi 305	ASC	ASC/SM-19

5. LIST OF REFERENCE SOP

S. No.	SOP TITLE	SOP NUMBER	VERSION
1.	Entry and Exit and Gowning Procedure for Cleanroom	GN001	02
2.	Procedure for Equipment and Area Monitoring Of Cleanroom	GN002	02
3.	Cleaning and Disinfection of Cleanroom Area	GN004	02
4.	Procedure for Disposal of Biomedical and Cell Culture Waste	GN004	02
5.	Procedure for Fogging in Clean Room Area	GN005	02
6.	Procedure for Numbering and Operation of Dynamic Pass Box	GN006	02
7	Procedure for operation, cleaning and maintenance of Garment cabinet	GN007	02
8.	Procedure for Spillage Management in Production Area	GN008	02
9.	Procedure for Safe Transport and Receipt of Donor Cornea	ASC001	01
10.	Preparation of Media Component Aliquots and Complete Media Preparation	ASC002	01
11.	Digestion, Isolation, Culturing and Monitoring of Cells from Human Corneal Limbal Tissue	ASC003	01
12.	Procedure for Harvesting of Human Limbal Tissue Cells	ASC004	01
13.	Cryopreservation of Limbal cells	ASC005	01
14.	Procedure for Cell Count Using Trypan Blue and Hemocytometer	ASC006	01
15	Procedure for Seeding of Various Passaged Cells	ASC007	01
16.	Procedure for Operation and Cleaning of Biosafety Cabinet	EQ001	01
17	Procedure for Operation and Cleaning of CO_2 Incubator	EQ002	01
18.	Procedure for Operation and Cleaning of Centrifuge	EQ003	01
19.	Procedure for Operation and Cleaning of Water/Bead Bath	EQ004	01
20	Procedure for Operation and Cleaning of Stereo Microscope	EQ005	01
22.	Procedure for Operation and Cleaning of InvertedMicroscope	EQ006	01
23.	Procedure for Operation and Cleaning of Mini Centrifuge	EQ007	01
24.	Procedure for Operation and Cleaning of Pharmaceutical Refrigerator	EQ008	01
25.	Procedure for Operation and Cleaning of Electronic Weighing Balance	EQ010	01
26.	Procedure for Operation and Cleaning of Biomedical Freezer	EQ009	01

	CENTER FOR OCULAR REGENERATION (CORE) ***KallamAnji Reddy Campus, L.V Prasad Eye Institute, LV Prasad Marg, Road No.2, Banjara Hills, Hyderabad -500034***				
	BATCH MANUFACTURING RECORD				
Title	LIMBAL TISSUE TO INVESTIGATIONAL MEDICINAL PRODUCT				
Department	Adult Stem Cell		BMR No.	ASCBMR003	
Effective Date		**Revision No.**	00	**Page No.** **New No.**	__ of 59 _____

6. QUALIFICATION DETAILS OF CORNEA TISSUE							
Date :			**Time :**				
S. No.	**Cornea ID**		**Release Date**	**Received By**		**Expiry Date**	**Checked By**
Cause of Death:							
HBs Ag		**HCV**		**HIV I/II**		**Syphilis**	
POSITIVE		POSITIVE		POSITIVE		POSITIVE	
NEGATIVE		NEGATIVE		NEGATIVE		NEGATIVE	
DONOR AGE		DONOR GENDER	Male			Cell Count per mm^2	
			Female				

	CENTER FOR OCULAR REGENERATION (CORE) ***KallamAnji Reddy Campus, L.V Prasad Eye Institute, LV Prasad Marg, Road No.2, Banjara Hills, Hyderabad -500034***				
	BATCH MANUFACTURING RECORD				
Title	LIMBAL TISSUE TO INVESTIGATIONAL MEDICINAL PRODUCT				
Department	Adult Stem Cell		BMR No.	ASCBMR003	
Effective Date		**Revision No.**	00	**Page No.** **New No.**	__ of 59 _____

7. MEDIUM PREPARATION		
Date :		
Steps	**Preparation Steps**	**Remarks**
7.1	DMEM/F12 Volume of DMEM/F12 added ……mL	
7.2	Serum Volume of Serum added ……mL	
7.3	Insulin Volume of Insulin added ……µL	
7.4	EGF Volume of EGF added ……µL	
7.5	Antibiotic-Antimycotic Volume of Antibiotic-Antimycotic added……µL	
7.6	Total volume of medium prepared ……mL	

Done By: Checked By:

Date: Date:

	CENTER FOR OCULAR REGENERATION (CORE) ***KallamAnji Reddy Campus, L.V Prasad Eye Institute, LV Prasad Marg, Road No.2, Banjara Hills, Hyderabad -500034***				
	BATCH MANUFACTURING RECORD				
Title	LIMBAL TISSUE TO INVESTIGATIONAL MEDICINAL PRODUCT				
Department	Adult Stem Cell		BMR No.	ASCBMR003	
Effective Date		**Revision No.**	00	**Page No.** **New No.**	__ of 59 _____

8. WASHING AND DIGESTION OF CORNEA		
Date :		
Steps	**Processing Steps**	**Remarks**
8.1	**Washing of Cornea:** Wash cornea with 3-5mL of PBS with antibiotic. _____mL of PBS added.	
8.2	Aspirate out the PBS with antibiotic and add 3-5mL fresh 1x PBS to the petridish. _____mL of PBS added.	
. . .	**ALL THE INTERMEDIATE STEPS ARE CLIPPED** **TO CUT SHORT 60 - 80 PAGE DOCUMENT TO < 20 PAGES.**	
. . .		

Done By: Checked By:

Date: Date:

--x--x--x—HEADER CLIPPED --x--x--x—

9. LIMBAL TISSUE CULTURE (P0)
--x--x--x-- CLIPPED --x--x--x--
10. PROCEDURE FOR SUBCULTURE OR PASSAGE (P0 TOP1)
--x--x--x-- CLIPPED --x--x--x--
11. LIMBAL STEM CELL NICHE CULTURE (P1) (Flask No:_____)
--x--x--x-- CLIPPED --x--x--x--
12. PROCEDURE FOR SUBCULTURE OR PASSAGE (P1 TOP2)(Flask No:_____)
--x--x--x-- CLIPPED --x--x--x--
13. LIMBAL STEM CELL NICHE CULTURE (P2) (Flask No:_____)
--x--x--x-- CLIPPED --x--x--x--
14. PROCEDURE FOR SUBCULTURE OR PASSAGE (P2 to P3)(Flask No:_____)
--x--x--x-- CLIPPED --x--x--x--
15. LIMBAL STEM CELL NICHE CULTURE (P3) (Flask No:_____)
--x--x--x-- CLIPPED --x--x--x--
16. HARVESTING OF CELLS(Flask No:_____)
--x--x--x-- CLIPPED --x--x--x--

17. SCREENING PARAMETERS	
Floaters	Significant
	Insignificant
Media Color	Yellow
	Wine Red
	Brick Red
	Pink
Cell Morphology	Cuboidal
	Spindle
	Dendritic
Turbidity	Yes
	No
Confluence	In %
Amount of Media	Sufficient
	Insufficient

18. DAY 3 SCREENING (P0) (Flask No:_____)		
Date :	**--x--x--x-- CLIPPED --x--x--x--**	
Steps	**Processing Steps**	**Remarks**
19. DAY 5 SCREENING (P0) (Flask No:_____)		
Date :	**--x--x--x-- CLIPPED --x--x--x--**	
20. DAY 7 SCREENING (P0) (Flask No:_____)		
Date :	**--x--x--x-- CLIPPED --x--x--x--**	
21. DAY 10 SCREENING (P0) (Flask No:_____)		
Date :	**--x--x--x-- CLIPPED --x--x--x--**	
22. DAY OF CONFLUENCE SCREENING (P0) (Flask No:_____)		
Date :	**--x--x--x-- CLIPPED --x--x--x--**	
23. DAY 3 SCREENING (P1) (Flask No:_____)		
Date :	**--x--x--x-- CLIPPED --x--x--x--**	
24. DAY 5 SCREENING (P1) (Flask No:_____)		
Date :	**--x--x--x-- CLIPPED --x--x--x--**	
25. DAY 7 SCREENING (P1) (Flask No:_____)		
Date :	**--x--x--x-- CLIPPED --x--x--x--**	
26. DAY 10 SCREENING (P1) (Flask No:_____)		
Date :	**--x--x--x-- CLIPPED --x--x--x--**	
27. DAY OF CONFLUENCE SCREENING (P1) (Flask No:_____)		
Date :	**--x--x--x-- CLIPPED --x--x--x--**	
28. DAY 3 SCREENING (P2) (Flask No:_____)		
Date :	**--x--x--x-- CLIPPED --x--x--x--**	
29. DAY 5 SCREENING (P2) (Flask No:_____)		
Date :	**--x--x--x-- CLIPPED --x--x--x--**	
30. DAY 7 SCREENING (P2) (Flask No:_____)		
Date :	**--x--x--x-- CLIPPED --x--x--x--**	
31. DAY 10 SCREENING (P2) (Flask No:_____)		
Date :	**--x--x--x-- CLIPPED --x--x--x--**	
32. DAY OF CONFLUENCE SCREENING (P2) (Flask No:_____)		

Date :	**--x--x--x-- CLIPPED --x--x--x--**
33. DAY 3 SCREENING (P3) (Flask No:_____)	
Date :	**--x--x--x-- CLIPPED --x--x--x--**
34. DAY 5 SCREENING (P3) (Flask No:_____)	
Date :	**--x--x--x-- CLIPPED --x--x--x--**
35. DAY 7 SCREENING (P3) (Flask No:_____)	
Date :	**--x--x--x-- CLIPPED --x--x--x--**
36. DAY 10 SCREENING (P3) (Flask No:_____)	
Date :	**--x--x--x-- CLIPPED --x--x--x--**
37. HARVEST DAY SCREENING(P3) (Flask No:_____)	
Date :	**--x--x--x-- CLIPPED --x--x--x--**

38. FINAL PREPARATION AND TRANSPORT OF CELLS(Flask No:_____)		
Date :		
Steps	**Processing Steps**	**Remarks**
01	Pictures of P3 Cells	
02	Media Collected for Sterility Test	
03	Transfer of Cells to a Sterile vial	
04	Labeling and Sealing the vial with parafilm	
05	Dispatch of cells from the Facility	

Done By: Checked By:

Date: Date:

39. DEVIATIONS				
Date	**Step and Page No.**	**Actual**	**Deviation**	**Reason for Deviation**

40. COMPLIANCE	
DEVIATION REVIEW	
Review Date	

	CENTER FOR OCULAR REGENERATION (CORE) ***KallamAnji Reddy Campus, L.V Prasad Eye Institute, LV Prasad Marg, Road No.2, Banjara Hills, Hyderabad -500034***				
	BATCH MANUFACTURING RECORD				
Title	LIMBAL TISSUE TO INVESTIGATIONAL MEDICINAL PRODUCT				
Department	Adult Stem Cell		BMR No.	ASCBMR003	
Effective Date		**Revision No.**	00	**Page No.** **New No.**	__ of 59 _____

41. REVIEW OF BMR BY SCIENTIST		
S. No.	**Check Point**	**Status**
01.	Manufacturing activities are performed as per SOP	
02.	Details are recorded appropriately /correctly	
03.	Data entries are legible	
04.	No columns are left blank	
05.	Signatures are available	
06.	Errors, if any are corrected appropriately	
07.	Deviations, if any are checked for closure.	
Remarks, if any: **(Scientist- Sign & Date):**		

42. SUBMISSION OF BMR TO QA		
Submitted On		
	Submitted by	**Received by (QA)**
Name		
Signature		
Date		

43. ABBREVIATIONS

Awards and Honours

Fellowships:

1. Senior Research Fellowship, Indian Council of Medical Research, Government of India. 2020 (Ref ID: 2021-7055).
2. Senior Research Fellowship, Council of Scientific & Industrial Research, Government of India. 2020 (Ref ID: 111525/2K19/1) - Not availed.

Travel Awards:

1. ARVO India Chapter Affiliate Travel Grant, to attend and present part of thesis work at the ARVO 2020 Annual Meeting, Baltimore, Maryland, USA

Certifications in GMP and Regulatory training:

1. Elite Certification and Silver Medal, by the National Programme on Technology Enhanced Learning and the Clinical Development Services Agency, India, on *Current regulatory requirements for conducting clinical trials in India for investigational new drugs/new drug*, 2021
2. *Online skill development training program on Good Clinical Laboratory Practic*e certification by the Clinical Development Services Agency, Government of India, 2021
3. Certification of completion, Six-month training on Good Manufacturing Practice and Standard Operating Procedures, Center for Ocular Regeneration, LV Prasad Eye Institute, India, 2021
4. Certification of completion, *cGMP: Introduction to Good Manufacturing Practice* by Biopharma Institute, USA, 2021
5. Certificate of completion, on *GCP: ICH Good Clinical Practice* course by Biopharma Institute, USA, 2021

List of Presentations

International Meetings:

1. **Mukesh Damala**, Naveen Pakalapati, Vivek Singh, Sayan Basu. "In vivo assessment of the toxicity of human limbus-derived stromal/mesenchymal stem cells with or without alginate encapsulation for clinical use," at the 27th Indian Eye Research Group meeting, ARVO-IC India Chapter, LV Prasad Eye Institute, Hyderabad, India, October 2021.

2. Abhishek Sahoo, **Mukesh Damala**, Sayan Basu, Vivek Singh. "Optimizing the xeno-free techniques of human limbus-derived mesenchymal/stromal stem cell expansion using 3D culture methods," at the 27th Indian Eye Research Group meeting, ARVO-IC India Chapter, LV Prasad Eye Institute, Hyderabad, India, October 2021.

3. Mukesh Damala, Steve Swoiklo, Madhuri K. Amulya, Noopur S. Mitragotri, Sayan Basu, Che J. Connon, and Vivek Singh. "Encapsulation of Human Limbus-derived Stromal/Mesenchymal Stem Cells for Storage and Transportation at Room Temperature", at the ARVO Annual Meeting 2019, Vancouver, Canada, May 2019.

4. **Mukesh Damala**, Steve Swoiklo, Madhuri K. Amulya, Noopur S. Mitragotri, Sayan Basu, Che J. Connon, and Vivek Singh. "Encapsulation of human Limbal-Derived Mesenchymal Stromal Stem Cells for Preservation and Transportation at Room Temperature," at the 25th Indian Eye Research Group meeting, ARVO-IC India Chapter, LV Prasad Eye Institute, Hyderabad, India, July 2018.

National Meetings:

5. **Mukesh Damala,** Steve Swoiklo, Madhuri K. Amulya, Noopur S. Mitragotri, Sayan Basu, Che J. Connon, and Vivek Singh. "Encapsulation of human limbus-derived stromal/mesenchymal stem cells for biological preservation and transportation at room temperature for clinical use", at the XLIII All India Cell Biology Conference, IISER Mohali, Mohali, December 2019.

6. Mukesh Damala, Noopur Shriram Mitragotri, Sayan Basu, Vivek Singh. "Characterization and optimization of Human Limbus-derived Stromal/ Mesenchymal Stem cells for clinical application" at 86th Annual Conference of Society of Biological Chemists (SBC), School of Life Sciences, Jawaharlal Nehru University, New Delhi, November 2017.

List of Publications

Research Articles - direct publications of the thesis work:

1. **Damala, M**., et al. Encapsulation of human limbus-derived stromal/mesenchymal stem cells for biological preservation and transportation in extreme Indian conditions for clinical use. Scientific reports, 2023. **IF: 4.122**
2. **Damala M,** et al. Pre-Clinical Evaluation of Efficacy and Safety of Human Limbus-Derived Stromal/Mesenchymal Stem Cells with and without Alginate Encapsulation for Future Clinical Applications, Cells. 2023. DOI:10.3390/cells12060876, **IF:7.666**

Research Articles - extended publications of the thesis work:

1. Chandru A, Agrawal P, Ojha SK, Selvakumar K, Shiva VK, Gharat T, Selvam S, Thomas MB, **Damala M**, et al. Human cadaveric donor cornea-derived extracellular matrix microparticles for minimally invasive healing/regeneration of corneal wounds. Biomolecules. 2021. DOI:10.3390/biom11040532, **IF:6.064**
2. Tavakkoli F, **Damala M,** et al. Transcriptomic profiling of human limbus-derived stromal/mesenchymal stem cells —novel mechanistic insights into the pathways involved in corneal wound healing. Int J Mol Sci. 2022. DOI:10.3390/ijms23158226, **IF:6.028**
3. Sahoo A, **Damala M**, et al. Expansion and characterization of human limbus-derived stromal/mesenchymal stem cells in xeno-free medium for therapeutic applications, Stem Cell Res. Ther. 2023. DOI:10.1186/s13287-023-03299-3, **IF:8.088**

Book Chapters:

1. Sanjay K Ojha, Vijay K Singh, Ashwin K M, **Mukesh Damala**, Shiva K Vaishnavi, Om P Narayan, Vivek Singh. "Aging eye: an insight to common vision problems and associated challenge", – Nova Science Publishers, New York, April 2020**. (ISBN: 978-1-53617-304-8).**
2. Noopur Shriram Mitragotri, **Mukesh Damala**, Vivek Singh, Sayan Basu. "Limbal Stromal Stem Cells in Corneal Wound Healing: Perspective and Current Update", In the book: Alió J., Alió del Barrio J., Arnalich-Montiel F. (eds) Corneal Regeneration. Essentials in Ophthalmology. Springer, Cham, February 2019. **(ISBN: 978-3-030-01303-5).**
3. **Mukesh Damala**, Abhinav Reddy Kethiri, Fatemeh Tavakkoli, Enoch Raju, and Vivek Singh. "The Basics of Stem Cells and Their Role in Vision". In the book: Trends in Life Science Research, Nova Science Publishers, New York, January 2018. **(ISBN: 978-1-53613-241-0).**

Conference proceedings publications:

1. Basu, S., Damala, M., & Singh, V. (2017). Limbal Stromal Stem Cell Therapy for Acute and Chronic Superficial Corneal Pathologies: Early Clinical Outcomes of the Funderburgh Technique. Investigative Ophthalmology & Visual Science, 58(8), 3371–3371.
2. Basu, S., Damala, M., Tavakkoli, F., Mitragotri, N., & Singh, V. (2019). Human Limbus-derived Mesenchymal/Stromal Stem Cell Therapy for Superficial Corneal Pathologies: Two-Year Outcomes. Investigative Ophthalmology & Visual Science, 60(9), 4146–4146.
3. Damala, M., Swioklo, S., Kondapaka, M. A., Mitragotri, N., Basu, S., Connon, C. J., & Singh, V. (2019). Encapsulation of Human Limbus-derived Stromal/Mesenchymal Stem Cells for Storage and Transportation at Room Temperature. Investigative Ophthalmology & Visual Science, 60(9), 4654–4654.
4. Funderburgh, J., Basu, S., Damala, M., Tavakkoli, F., Sangwan, V., & Singh, V. (2018). Limbal Stromal Stem Cell Therapy for Acute and Chronic Superficial Corneal Pathologies: One-Year Outcomes. Investigative Ophthalmology & Visual Science, 59(9), 3455–3455.

Coursework Certificate

Hyderabad Eye Research Foundation

World Health Organization
Collaborating Centre for Prevention of Blindness

LV PRASAD EYE INSTITUTE

Ph D Course Work Grade Sheet

Name of the Candidate	**Mr.Damala Mukesh**
Registration number	**17LAPH16**
Date of Registration	**04-08-2017**
Title of Thesis/ Topic of Research	**Optimizing the processes for Isolation, Preservation, Transportation and Delivery of Human Limbus-derived Stromal/ Mesenchymal Stem Cells for Clinical Use**
Name of the External Supervisor (L V Prasad Eye Institute)	**Dr Vivek Singh**
Name of the Internal Supervisor (University of Hyderabad)	**Dr BinduMadhava Reddy Aramati**

Sl No	Title of Course Work	Credits	Grade
1	Research Methodology/ Laboratory rotation	6	Passed
2	Analytical Technique / Bio Statistics	6	Passed
3	Scientific Writing	3	Passed
4	Clinical Orientation	2	Passed

Head of the Institution **Guide**

Dr. S. SHIVAJI
Director of Research
Hyderabad Eye Research Foundation
Banjara Hills,
Hyderabad-500 034.

LV Prasad Eye Institute, Kallam Anji Reddy Campus, LV Prasad Marg, Banjara Hills, Hyderabad 500034, India
Tel: +91 40 30612345, Fax: +91 40 23548271, Email: info.hyd@lvpei.org, Website: www.lvpei.org

Plagiarism Report

Optimizing the Processes for Isolation, Preservation and Transportation of Human Limbus-derived Stromal/Mesenchymal Stem Cells for Corneal Regeneration

by Damala Mukesh

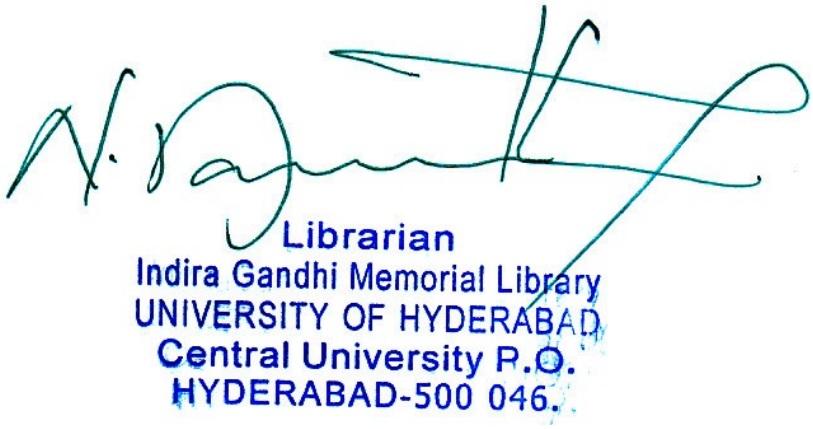

Optimizing the Processes for Isolation, Preservation and Transportation of Human Limbus-derived Stromal/Mesenchymal Stem Cells for Corneal Regeneration

ORIGINALITY REPORT

15%*	13%	13%	2%
SIMILARITY INDEX	INTERNET SOURCES	PUBLICATIONS	STUDENT PAPERS

PRIMARY SOURCES

1	www.researchsquare.com Internet Source	3%
2	www.ncbi.nlm.nih.gov Internet Source	2%
3	www.mdpi.com Internet Source	2%
4	assets.researchsquare.com Internet Source	1%
5	Mukesh Damala, Naveen Pakalapati, Vivek Singh, Sayan Basu. "Safety and toxicity of human limbus-derived stromal/mesenchymal stem cells with and without alginate encapsulation for clinical application", Research Square Platform LLC, 2021 Publication	<1%
6	"Corneal Regeneration", Springer Nature, 2019 Publication	<1%

Dr. A. Bindu Madhava Reddy
Assistant Professor
Dept. of Animal Biology
School of Life Sciences
University of Hyderabad
Hyderabad-500 046.

* Similarity matches of 1-8 are from the part of Student's publications, which are also part of his phd thesis. Thank you (A. Bindu Madhava Reddy (Internal Research Supervisor UOH)

7	livrepository.liverpool.ac.uk Internet Source	<1 %
8	Mukesh Damala, Abhishek Sahoo, Naveen Pakalapati, Vivek Singh, Sayan Basu. "Pre-Clinical Evaluation of Efficacy and Safety of Human Limbus-Derived Stromal/Mesenchymal Stem Cells with and without Alginate Encapsulation for Future Clinical Applications", Cells, 2023 Publication	<1 %
9	Devon Cogswell, Mei Sun, Erin Greenberg, Curtis E. Margo, Edgar M. Espana. "Creation and grading of experimental corneal scars in mice models", The Ocular Surface, 2021 Publication	<1 %
10	www.science.gov Internet Source	<1 %
11	stemjnl.org Internet Source	<1 %
12	"Stem Cells in Regenerative Medicine", Wiley, 2015 Publication	<1 %
13	research.tensorgate.org Internet Source	<1 %
14	www.researchgate.net Internet Source	<1 %

15	Handbook of Global Bioethics, 2014. Publication	<1 %
16	flex.flinders.edu.au Internet Source	<1 %
17	www.consumersinternational.org Internet Source	<1 %
18	ndl.ethernet.edu.et Internet Source	<1 %
19	"Fundamental Neuropathology for Pathologists and Toxicologists", Wiley, 2011 Publication	<1 %
20	Oxidative Stress in Applied Basic Research and Clinical Practice, 2015. Publication	<1 %
21	dokumen.pub Internet Source	<1 %
22	Submitted to Victoria University Student Paper	<1 %
23	Submitted to University of Exeter Student Paper	<1 %
24	Clemence Bonnet, Sheyla Gonzalez, JoAnn S. Roberts, Sarah Robertson, Maxime Ruiz, Jie Zheng, Sophie X. Deng. "Human limbal epithelial stem cell regulation, bioengineering	<1 %

	and function", Progress in Retinal and Eye Research, 2021 Publication	
25	Submitted to Cranfield University Student Paper	<1 %
26	nfburnetthodd.com Internet Source	<1 %
27	patentimages.storage.googleapis.com Internet Source	<1 %
28	www.medrxiv.org Internet Source	<1 %
29	Hongying Yu, M. Habibi, K. Motamedi, D.Toghraie. Semirumi, A. Ghorbani. "Utilizing Stem Cells in Reconstructive Treatments for Sports Injuries: An Innovative Approach", Tissue and Cell, 2023 Publication	<1 %
30	Ajay Kumar, Hongmin Yun, Martha L. Funderburgh, Yiqin Du. "Regenerative therapy for the Cornea", Progress in Retinal and Eye Research, 2022 Publication	<1 %
31	ecommons.aku.edu Internet Source	<1 %
32	stemcellres.biomedcentral.com Internet Source	<1 %

33	Submitted to Granite Hills High School Student Paper	<1 %
34	Philippe Labelle. "The Eye1", Elsevier BV, 2017 Publication	<1 %
35	Rubing Zhao. "Ca2+ influx through both L- and N-type Ca2+ channels increases c-fos expression by electrical stimulation of sympathetic neurons : L- and N-channels stimulate c-fos expression", European Journal of Neuroscience, 02/26/2007 Publication	<1 %
36	journals.plos.org Internet Source	<1 %
37	ndnr.com Internet Source	<1 %
38	Junko Hori, Takefumi Yamaguchi, Hiroshi Keino, Pedram Hamrah, Kazuichi Maruyama. "Immune privilege in corneal transplantation", Progress in Retinal and Eye Research, 2019 Publication	<1 %
39	ashpublications.org Internet Source	<1 %
40	Submitted to Cardiff University Student Paper	<1 %
41	Stem Cell Biology and Regenerative Medicine, 2014.	<1 %

	Publication	
42	Submitted to University of Ulster Student Paper	<1 %
43	"The Textbook of Pharmaceutical Medicine", Wiley, 2009 Publication	<1 %
44	Submitted to University of Lancaster Student Paper	<1 %
45	"Corneal Emergencies", Springer Science and Business Media LLC, 2022 Publication	<1 %
46	Sachin Shukla, Swapna S Shanbhag, Fatemeh Tavakkoli, Shobhit Varma, Vivek Singh, Sayan Basu. "Limbal Epithelial and Mesenchymal Stem Cell Therapy for Corneal Regeneration", Current Eye Research, 2019 Publication	<1 %
47	dspace.library.uvic.ca:8080 Internet Source	<1 %
48	Submitted to Lincoln College, Lincolnshire Student Paper	<1 %
49	Mukesh Damala, Stephen Swioklo, Madhuri A. Koduri, Noopur S. Mitragotri, Sayan Basu, Che J. Connon, Vivek Singh. "Encapsulation of human limbus-derived stromal/mesenchymal stem cells for biological preservation and	<1 %

transportation in extreme Indian conditions for clinical use", Scientific Reports, 2019
Publication

50	Saravana Babu Chidambaram, M. Mohamed Essa, M. Walid Qoronfleh. "Introduction to Toxicological Screening Methods and Good Laboratory Practice", Springer Science and Business Media LLC, 2022 Publication	<1 %
51	Drug Discovery and Evaluation Safety and Pharmacokinetic Assays, 2013. Publication	<1 %
52	Saeed Nazemidashtarjandi, Vishva M. Sharma, Vishwajeet Puri, Amir M. Farnoud, Monica M. Burdick. "Lipid Composition of the Cell Membrane Outer Leaflet Regulates Endocytosis of Nanomaterials through Alterations in Scavenger Receptor Activity", ACS Nano, 2022 Publication	<1 %
53	bmccomplementalternmed.biomedcentral.com Internet Source	<1 %
54	Submitted to National University of Ireland, Galway Student Paper	<1 %
55	mdpi-res.com Internet Source	<1 %

56	Mitsunori Yagame, Daisuke Suzuki, Kazufumi Watanabe, Eiichi Nakao et al. "Significance of Levels of Circulating IgA-Class Immune Complex in Discriminant Analysis of Patients with IgA Nephropathy before Renal Biopsy", Nephron, 2008 Publication	<1 %
57	iclg.com Internet Source	<1 %
58	uknowledge.uky.edu Internet Source	<1 %
59	www.clinicaltrialsregister.eu Internet Source	<1 %
60	Submitted to NIIT University Student Paper	<1 %
61	Submitted to University of Auckland Student Paper	<1 %
62	echa.europa.eu Internet Source	<1 %
63	link.springer.com Internet Source	<1 %
64	www.pubfacts.com Internet Source	<1 %
65	Mohd Tayyab Adil, Jonathan J. Henry. "Understanding cornea epithelial stem cells	<1 %

and stem cell deficiency: Lessons learned using vertebrate model systems", genesis, 2021
Publication

66	Submitted to Southern New Hampshire University - Continuing Education Student Paper	<1%
67	etd.lsu.edu Internet Source	<1%
68	www.dovepress.com Internet Source	<1%
69	Fatemeh Tavakkoli, Mukesh Damala, Madhuri Amulya Koduri, Abhilash Gangadharan et al. "Transcriptomic Profiling of Human Limbus-Derived Stromal/Mesenchymal Stem Cells—Novel Mechanistic Insights into the Pathways Involved in Corneal Wound Healing", International Journal of Molecular Sciences, 2022 Publication	<1%
70	Maria Notara, Yiqin Du, G. Astrid Limb, James L. Funderburgh, Julie T. Daniels. "Chapter 5 Eye", Springer Science and Business Media LLC, 2009 Publication	<1%
71	Submitted to University of Bristol Student Paper	<1%

72	s4fc3bcf49c27ae30.jimcontent.com Internet Source	<1 %
73	Submitted to Fiji National University Student Paper	<1 %
74	Giuseppe F. Pontoriero. "Cell autonomous roles for AP-2α in lens vesicle separation and maintenance of the lens epithelial cell phenotype", Developmental Dynamics, 03/2008 Publication	<1 %
75	Submitted to Sumner College Student Paper	<1 %
76	darts.jaxa.jp Internet Source	<1 %
77	Kagan, M. L., D. W. Sullivan, S. C. Gad, and C. M. Ballou. "Safety Assessment of EPA-Rich Polar Lipid Oil Produced From the Microalgae Nannochloropsis oculata", International Journal of Toxicology, 2014. Publication	<1 %
78	Morris, A.C.. "Studying rod photoreceptor development in zebrafish", Physiology & Behavior, 20051015 Publication	<1 %
79	Pathak, Meeta, O.K. Olstad, Liv Drolsum, Morten C. Moe, Natalia Smorodinova, Sarka	<1 %

Kalasova, Katerina Jirsova, Bjørn Nicolaissen, and Agate Noer. "The effect of culture medium and carrier on explant culture of human limbal epithelium: A comparison of ultrastructure, keratin profile and gene expression", Experimental Eye Research, 2016.
Publication

80	ili.ac.in Internet Source	<1 %
81	nid.pl Internet Source	<1 %
82	orca.cardiff.ac.uk Internet Source	<1 %
83	www.donga-st.com Internet Source	<1 %
84	Helena Rapp-Wright, Fiona Regan, Blánaid White, Leon P. Barron. "A year-long study of the occurrence and risk of over 140 contaminants of emerging concern in wastewater influent, effluent and receiving waters in the Republic of Ireland", Science of The Total Environment, 2022 Publication	<1 %
85	Nidhi B. Agarwal, Manoj Karwa. "Pharmaceutical Regulations in India", Elsevier BV, 2018	<1 %

Publication

86	Rudolf Ott. "Impact of changing immunosuppressive monotherapy from Cyclosporin A to Tacrolimus in long-term, stable liver transplant recipients", Transplant International, 1/2004 Publication	<1 %
87	Submitted to University of New Haven Student Paper	<1 %
88	apvma.gov.au Internet Source	<1 %
89	epdf.pub Internet Source	<1 %
90	patents.google.com Internet Source	<1 %
91	www.ajol.info Internet Source	<1 %
92	Anastassia Kostenko, Stephen Swioklo, Che J Connon. "Alginate in corneal tissue engineering", Biomedical Materials, 2022 Publication	<1 %
93	Chan, Ping, and A Hayes. "Acute Toxicity and Eye Irritancy", Hayes Principles and Methods of Toxicology Sixth Edition, 2014. Publication	<1 %

Methods in Molecular Biology, 2016.

94	Publication	<1 %
95	Submitted to Monash University Student Paper	<1 %
96	www.financialexpress.com Internet Source	<1 %
97	www.frontiersin.org Internet Source	<1 %
98	www.intechopen.com Internet Source	<1 %
99	"Drug Discovery and Development", Springer Science and Business Media LLC, 2021 Publication	<1 %
100	"Veterinary Pharmacovigilance", Wiley, 2009 Publication	<1 %
101	Holly.Y. Chen, Ordan J. Lehmann, Anand Swaroop. "Genetics and therapy for pediatric eye diseases", EBioMedicine, 2021 Publication	<1 %
102	Submitted to Plymouth Devon International College Student Paper	<1 %
103	Submitted to Universidad Miguel Hernandez Servicios Informaticos Student Paper	<1 %

104	justcatsclinic.com Internet Source	<1%
105	www.immunologicalsdirect.com Internet Source	<1%
106	www.paloaltoonline.com Internet Source	<1%
107	Blazka, Mark. "Acute Toxicity and Eye Irritancy", Principles and Methods of Toxicology Fifth Edition, 2007. Publication	<1%
108	Canwei Zhang, Liqun Du, Kunpeng Pang, Xinyi Wu. "Differentiation of human embryonic stem cells into corneal epithelial progenitor cells under defined conditions", PLOS ONE, 2017 Publication	<1%
109	Submitted to City University Student Paper	<1%
110	Submitted to National School of Healthcare Science Student Paper	<1%
111	alclinicalresearch.com Internet Source	<1%
112	ici2016.org Internet Source	<1%

113	ttms.typepad.com Internet Source	<1%
114	www.cambridge.org Internet Source	<1%
115	www.scielo.br Internet Source	<1%

Exclude quotes	On	Exclude matches	< 14 words
Exclude bibliography	On		

Photocopies of Publications

SCIENTIFIC REPORTS
nature research

OPEN

Encapsulation of human limbus-derived stromal/mesenchymal stem cells for biological preservation and transportation in extreme Indian conditions for clinical use

Mukesh Damala[1,2], Stephen Swioklo[3], Madhuri A. Koduri[1], Noopur S. Mitragotri[1], Sayan Basu[1,5], Che J. Connon[4] & Vivek Singh[1,5*]

Human limbus-derived stromal/mesenchymal stem cells (hLMSC) can be one of the alternatives for the treatment of corneal scars. However, reliable methods of storing and transporting hLMSC remains a serious translational bottleneck. This study aimed to address these limitations by encapsulating hLMSC in alginate beads. Encapsulated hLMSC were kept in transit in a temperature-conditioned container at room temperature (RT) or stored at 4 °C for 3–5 days, which is the likely duration for transporting cells from bench-to-bedside. Non-encapsulated cells were used as controls. Post-storage, hLMSC were released from encapsulation, and viability-assessed cells were plated. After 48 and 96-hours in culture the survival, gene-expression and phenotypic characteristics of hLMSC were assessed. During transit, the container maintained an average temperature of 18.6 ± 1.8 °C, while the average ambient temperature was 31.4 ± 1.2 °C ($p = 0.001$). Encapsulated hLMSC under transit at RT were recovered with a higher viability (82.5 ± 0.9% and 76.9 ± 1.9%) after 3 ($p = 0.0008$) and 5-day storage ($p = 0.0104$) respectively as compared to 4 °C (65.2 ± 1.2% and 64.5 ± 0.8% respectively). Cells at RT also showed a trend towards greater survival-rates when cultured (74.3 ± 2.9% and 67.7 ± 9.8%) than cells stored at 4 °C (54.8 ± 9.04% and 52.4 ± 8.1%) after 3 and 5-days storage ($p > 0.2$). Non-encapsulated cells had negligible viability at RT and 4 °C. Encapsulated hLMSC (RT and 4 °C) maintained their characteristic phenotype (ABCG2, Pax6, CD90, p63-α, CD45, CD73, CD105, Vimentin and Collagen III). The findings of this study suggest that alginate encapsulation is an effective method of hLMSC preservation offering high cell viability over prolonged durations in transit at RT, therefore, potentially expanding the scope of cell-based therapy for corneal blindness.

Loss of corneal stromal transparency is a leading cause of blindness and visual impairment impacting millions of individuals globally[1]. The standard treatment for blinding corneal pathologies is corneal transplantation which suffers from several limitations, including global lack of donor tissue, risk of immune rejection, need for long-term follow-up and compliance with life-long medications[2]. Recent progress in regenerative medicine has provided the opportunity of using mesenchymal stem cells (MSC) for treating corneal pathologies. Pre-clinical studies and early clinical trials using MSC from various sources including human limbus-derived stromal/mesenchymal stem cells (hLMSC) have demonstrated a beneficial therapeutic effect in ameliorating corneal opacification[3–5]. However, safe and reliable methods of storage and transportation of cells for prolonged periods and over long distances, still remain an unmet translational roadblock.

[1]Prof. Brien Holden Eye Research Centre, LV Prasad Eye Institute, Hyderabad, Telangana, India. [2]School of Life Sciences, University of Hyderabad, Hyderabad, Telangana, India. [3]Atelerix Ltd., Biomedicine West, International Centre for Life, Newcastle Upon Tyne, UK. [4]Institute of Genetic Medicine, Faculty of Medical Sciences, Newcastle University, Newcastle Upon Tyne, UK. [5]Center for Ocular Regeneration (CORE), LV Prasad Eye Institute, Hyderabad, Telangana, India. *email: viveksingh@lvpei.org

The efficient shipping of cells from production facility to the site of application, while preserving the viability and quality of the cells, is very crucial[6]. Current methods of cryopreservation involve chemicals like dimethyl sulfoxide which itself is harmful to cells. Cryopreserving cells, in addition to being cost ineffective, has the drawbacks of decreased cell-viability[7], impaired post-thaw function and reduced immunomodulatory properties[8]. The logistical complexity of transporting cells in their frozen state, accompanied by potential loss of function when used directly from the thaw, impedes the accessibility of cells for therapy at remote and rural sites. With increased regenerative research and the increased number of clinical trials, efficient transport (3–5 days in the current global scenario) of stem/progenitor cells from one institution to another where there is no GMP facility, is required. Autologous cells are an option but where autologous cells are not available, as in cases of bilateral eye damage/injury, allogeneic cells may be required. Cells, in general are transported using dry ice or liquid nitrogen modes, which is not cost effective, requires expedited shipping and packaging, suitable infrastructure, and specialised training for thawing and administration. In adverse events like a transportation delay, or change in temperature, cells can thaw and become unusable, or undergo stress affecting their viability and characteristic properties of cells[9]. One of the widely practiced alternatives to prevent this loss is encapsulating the cells in a biological matrix. Hypothermic preservation of encapsulated cells where cells are held in a state of suspended animation at temperatures below the normothermic range of 32 °C-37 °C also combats many of the issues associated with methods like cryopreservation[10]. Alginate is a natural polysaccharide exhibiting excellent biocompatibility and a popularly employed polymer for cell encapsulation. Alginate encapsulation has been reported to show more functionally robust spermatozoa[11] and oocytes[12] and to retain the morphological differentiation and adhesion abilities of the Neuroblastoma cells[13]. Recent studies have shown that encapsulating MSCs in alginate hydrogels could be a solution for problems associated with hypothermic storage through extending their preservation shelf life[10,14,15]. However, the reliability of alginate encapsulation has not been previously tested in geographies with high ambient temperatures or after long-distance transportation. This study aimed to test the reliability of alginate encapsulation for storing and transporting hLSMC at room temperature (RT) in temperate climatic conditions.

Methods and Materials

Study protocol and donor corneas. This study protocol was approved by the Institutional Review Board, LV Prasad Eye Institute, Hyderabad, India (LEC 05-18-081). Therapeutically accepted and serologically tested cadaveric donor corneas were obtained from Ramayamma International Eye Bank, LV Prasad Eye Institute, Hyderabad, India (http://www.lvpei.org/services/eyebank). Informed consent for using cadaveric corneas was obtained from the donors' next kin, by the Ramayamma International Eye Bank from where the cadaveric tissues were obtained. Experiments on the human tissue adhered to the declaration of Helsinki. All the experiments in the methodology were performed in triplicates.

Validating the insulated container for maintenance of hypothermic temperature. To have a reliable system that maintains a normalized range of temperatures irrespective of the extreme atmospheric temperatures, an insulated container with cooling packs (Polybox 7, Softbox Systems, India), pre-conditioned to maintain hypothermic temperatures of $\leq$30 °C, was assessed (Supplementary Fig. S1). This assessment was done over a duration of 3–5 days, considering it the likely duration taken to transport cells. The internal temperature of the container and the ambient (atmospheric) temperature was recorded every 4 hours during this period.

Cell culture. The donor corneas were washed with 2% [vol/vol] Antibiotic-Antimycotic (15240062, Thermo Fisher, USA) in Phosphate Buffer Saline (PBS) (14190250, Thermo Fisher, USA) for 2 minutes, followed by another wash with PBS. Iris and endothelial layer were removed for better visibility of the limbus. Complete 360° limbal rims were isolated using a surgical blade in buffered saline and fragmented to minute pieces measuring 1–2 mm long. Tissue fragments were minced for 3–5 minutes using small, curved corneal scissors, in DMEM/F12 media alone (BE04-687F/U1, Lonza, Switzerland). The minced limbal tissue was subjected to collagen digestion by adding 200 IU of reconstituted Collagenase-IV (17104019, Thermo Fisher, USA) in 1 mL of DMEM/F12 media. Tissue digestion was carried out by incubating the limbal tissue for 16 hours at 37 °C with 5% CO_2 in a humidified incubator.

Post 16-hour incubation, the enzymatic digestion was ceased by adding 2 mL of DMEM/F12 fortified with 2% fetal bovine serum (16000036, Thermo Fisher, USA). The enzyme-digested tissue fragments were washed and sedimented twice at 1000 rpm for 3 minutes, at room temperature (RT) in saline. 3 mL of complete media comprising of DMEM/F12 media fortified with 2% FBS, 1% [vol/vol] Antibiotic-Antimycotic, 10 ng/mL epidermal growth factor (PHG0311L, Thermo Fisher, USA) and 5 µg/mL insulin (12585014, Thermo Fisher, USA) was added to the pellet and kept in culture with culture medium being replaced every 2 days. Pure cultures of hLSMCs were obtained by subculturing. Subculturing was done upon 80–90% confluency. Passage 3 cells were used for all experiments post-quantification for viability using 0.4% Trypan Blue (15250061, Thermo Fisher, USA).

Encapsulation of hLSMCs. A cell suspension of hLSMCs harvested from culture was mixed with sodium alginate solution supplied with BeadReady kit commercially available from Atelerix Ltd (UK) at a density of 2.5×10^6 cells/mL. The alginate-cell suspension concoction was slowly dropped into the calcium-chloride based gelation buffer (BeadReady kit) through a 21 1/2 G needle. These droplets of alginate-cell suspension concoction were allowed to stabilize for 8 minutes in the gelation buffer, making the beads polymerize and gelate (Fig. 1). Polymerized beads were washed with complete media and resuspended in 1 mL of fresh complete media.

Storage and transportation of the encapsulated hLSMCs. Vials with alginate-encapsulated cells in the form of polymerized beads were either refrigerated (4 °C; n = 5) or were kept under transit at RT (n = 5). The internal temperature of the container and the ambient (external) temperature was recorded every 4 hours, until 3–5 days (Fig. 1). The encapsulated cells were transported between three towns around Hyderabad, with

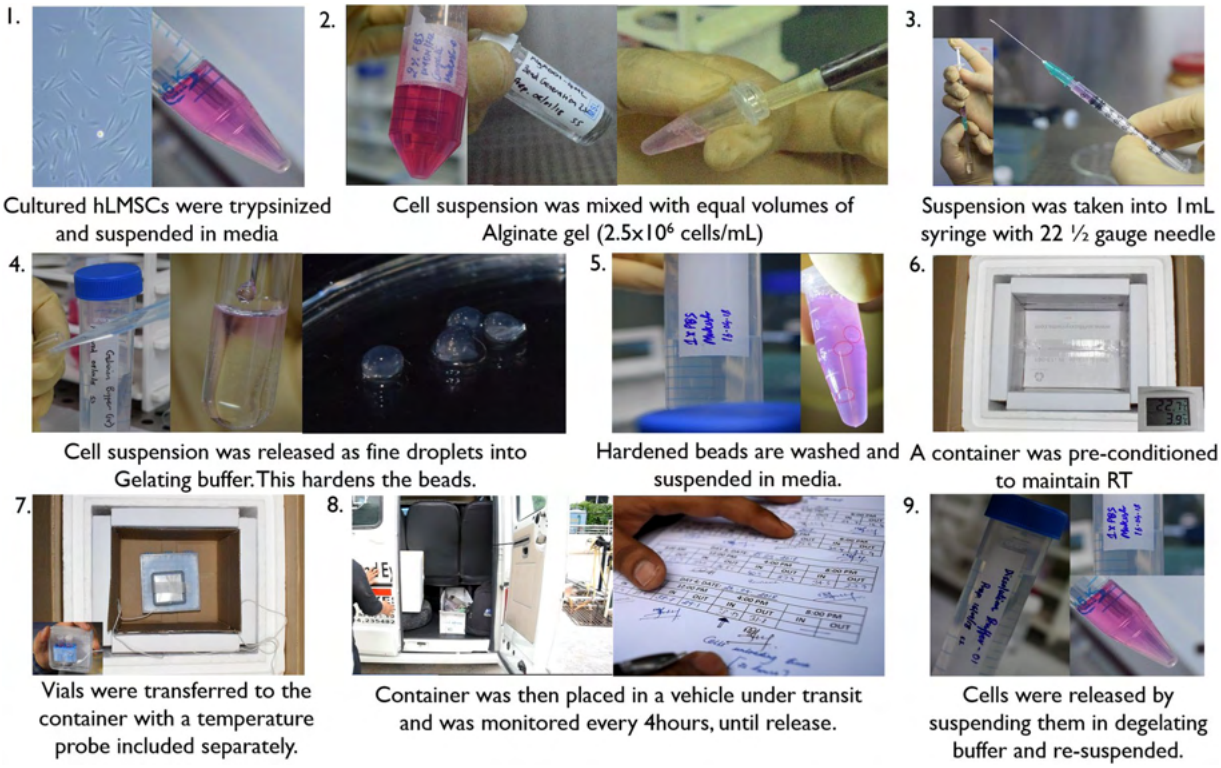

Figure 1. Process of encapsulation and transportation. Schematic diagram of events explaining the encapsulation and transportation of hLMSCs: Alginate-encapsulated hLMSCs, in the form of beads were transported for ~528.67 (±64.2) KMs in real-time conditions for 3–5 days, in a pre-conditioned container.

a transport distance of ~528.67 (±64.2) kms. The vehicle used for the transit was a standard carrier vehicle. The external temperature outside the container was considered as control temperature. An equal number of the non-encapsulated cells were either stored or transported along, as above. All the packaging was done in controlled conditions. This experiment was performed in triplicates.

Release of the hLSMCs from encapsulation. Post transit, alginate beads encapsulating the cells were washed with PBS. They were added to 1.3 mL of dissolution buffer (trisodium citrate based), supplied with BeadReady kit and allowed to dissolve for 5 minutes with gentle agitation releasing the cells from the alginate beads. Cells suspended in the dissolution buffer were sedimented by centrifugation at 1500 rpm for 5 minutes. The sedimented cell pellet was resuspended in complete medium.

Quantifying the viable cells recovered. The number of viable (unstained) cells recovered from each vial that were either stored at 4 °C or transported at RT was quantified using 0.4% Trypan blue solution and counted using a hemocytometer. Post quantification, the cells from the vials of same storage conditions (n = 5, each of RT and 4 °C), were pooled together. Pooled cells, along with non-encapsulated cells (cultured under standard culture conditions) as a control, were plated in equal numbers for further analysis of determining their relative survival, gene expression, and phenotypic biomarkers expression.

Determining the relative rate of survival using MTT assay. Post-release from 3-day and 5-day storage or transit, and their quantification for viability, the cells were plated in triplicates in a 12-well plate, at a density of 20,000 cells/cm^2 and cultured for 48 and 96 hours at 37 °C with 5% CO_2 in a humidified incubator. The relative survival rates of the cells against the control of non-encapsulated (cultured under standard culture conditions) cells were assessed using MTT reagent (M6494, Thermo Fisher, USA). Each well was added with 200 µL of 0.25 mg/mL MTT reagent in culture medium devoid of FBS and incubated for 1 hour at 37 °C in 5% CO_2 chamber. The formazon crystals were solubilized in 200 µL of Dimethyl Sulfoxide (D2650, Sigma Aldrich, USA) for 5 minutes at 37 °C in 5% CO_2 chamber. The concentration was determined by reading the absorbance in duplicates at 570 nm using a spectrophotometer, against a blank.

Assessment of the phenotypic marker expression. Encapsulated cells that were either transported at RT or were under storage at 4 °C for 3–5 days were released and quantified for viability. Cells were cultured on coverslips in 12-well culture plates at a density of 20,000 cells/cm^2 at 37 °C with 5% CO_2 in a humidified incubator for 48 hours. These cells were assessed for the expression of characteristic biomarkers of the hLMSC phenotype. Cultured cells were washed with PBS and fixed using 4% paraformaldehyde in PBS, for 20 minutes, followed by a 10-minute wash in PBS, twice. The cells were permeabilized using 0.03% [vol/vol] Triton-X in PBS, followed by two 5-minute washes in PBS. Cells were incubated for 1 hour with 2.5% BSA in PBS, to block the non-specific

Sl #	Primer	Sequence	Size	T_m (°C)
1	GAPDH	Forward: ACCACAGTCCATGCCATCAC	452 bp	55 °C
		Reverse: TCCACCACCCTGTTGCTGTA		
2	CD90	Forward: CGCTCTCCTGCTAACAGTCTT	142 bp	60 °C
		Reverse: CAGGCTGAACTCGTACTGGA		
3	PAX-6	Forward: ATAACCTGCCTATGCAACCC	208 bp	58 °C
		Reverse: GGAACTTGAACTGGAACTGAC		
4	p63-α	Forward: GAGGTTGGGCTGTTCATCAT	183 bp	57 °C
		Reverse: AGGAGATGAGAAGGGGAGGA		

Table 1. List of primers and their nucleotide sequences used in this study for the gene expression experiments.

protein-protein interactions. All the incubations were carried out at RT in moist conditions. The blocking solution was removed and cells were incubated for 2 hours with primary antibodies in 100 µL of 1% BSA in PBS. The antibody panel was composed of (a) ABCG2 (1:100, 18841, Santa Cruz Biotechnology, USA), Pax6 (1:300, 901301, BioLegend, USA), p63-α (1:100, 4892S, Cell Signalling technology, USA) and Col-III (1:100, ab7778, Abcam, UK), as positive markers of the human limbal stem cell phenotype; HLA-DR (1:100, ab55152, Abcam, UK), and CD45 (1:100, 13197, Cell Signalling Technology, USA) as negative marker for mesenchymal origin, (b) CD73 (1:100, 13160, Cell Signalling Technology, USA), CD105 (1:100, 376381, Santa Cruz Biotechnology, USA), and VIM (1:100, 6260, Santa Cruz Biotechnology, USA) as positive markers of the mesenchymal phenotype. The p63-α antibody used in our study recognizes both ΔNp63-α and TAp63-α components (https://media.cellsignal.com/pdf/4892.pdf). Cells on coverslips were washed twice in PBS for 5 minutes each, after the incubation with primary antibodies. Cells were then incubated for 45 minutes in 100 µL with secondary antibodies (1:400) of 1% BSA in PBS, followed by three 10-minute washes in PBS. This antibody panel was defined abiding by the International Society for Cellular Therapy's guidelines of minimal criteria for defining multipotent mesenchymal stromal cells[16]. The panel of secondary antibodies included anti-mouse Alexa Fluor 488 (A11001, Thermo Fisher, USA) and anti-rabbit Alexa Fluor 488 (A11008, Thermo Fisher, USA). Cells were mounted using Fluorosheild mounting medium with DAPI (ab104139, Abcam, UK) and imaging was done using a fluorescent microscope (Axio Scope A1, Carl Zeiss AG, Germany) with 20x–40x objective. This experiment was repeated thrice. The number of cells positive for a given biomarker is expressed in the form of percentage by analysing the images captured from the central (1 image) and peripheral areas (2 images) of the coverslip. It is represented in the tabular format for better understanding. The lack of expression is denoted by (−) and <25% of cells showing positive expression is denoted by (++), 25–50% is denoted by (+++) and >90% cells being positive is denoted as (++++).

Quantification of the gene expression using real-time PCR. One million cells of each storage category after their release from encapsulation were used for quantifying the gene expression. Freshly lysed *trypsinized* cells from the culture were used as the control. Total RNA was isolated using Trizol (15596018, Thermo Fisher, USA) method and converted to cDNA using the Superscript-III (1808051, Thermo Fisher, USA) at 1 µg/µL of RNA per 20 µL reaction mix. The synthesized cDNA was subjected to real-time PCR, using Maxima SYBR Green kit (K0221, Thermo Fisher, USA) with 200 ng template per 25 µL reaction mix. The reaction was carried out in a detection system (Applied Biosystems, USA). Reactions were run in duplicates. GAPDH was used as a housekeeping gene in these experiments. The gene expression data were normalized to control the variability in expression levels to the geometric mean of the housekeeping gene. The data was analysed using the $2^{-\Delta\Delta CT}$ method. The primer sequences are listed in the Table 1.

Statistical analysis. Statistical analyses were done using the GraphPad software (GraphPad Software, San Diego, CA, http://www.graphpad.com). Comparisons were made using Mann-Whitney U test for non-parametric data. The data is presented as mean values ± SD, obtained from 3–10 independent experiments performed. Values of $p < 0.05$ were considered to be significant. $*p \leq 0.05$, $**p \leq 0.001$. Values of $p > 0.05$ were considered insignificant and were represented with #.

Results

Maintenance of hypothermic temperatures in the pre-conditioned container. The container maintained an average temperature of 18.62 ± 1.82 °C (range: 13.91 °C to 27.52 °C) where the average ambient temperature was 31.43 ± 1.2 °C (range: 28.85 °C to 38.40 °C) over a duration of 3–5 days (Fig. 2). This experiment was repeated (n = 10) and the data was statistically significant ($p < 0.0001$). The container had maintained the hypothermic range of temperatures consistently over a period of varying seasons and weather across the year.

Effect of temperature on viable cell recovery. The temperature in the storage conditions had an insignificant effect on the recovery of viable cells from encapsulation. Encapsulated cells recovered after 3-day transit at RT had an average viable recovery of 82.45 ± 0.87% (n = 3) cells while the cells stored at 4 °C had 65.19 ± 1.19% (n = 3, $p = 0.0008$) viability. After 5-day transit at RT, encapsulated cells had 76.96 ± 1.98% (n = 3) and cells stored at 4 °C had 64.45 ± 0.81% (n = 3, $p = 0.0104$) of viable cell recovery (Fig. 3). The non-encapsulated cells stored at RT did not show more than 1% viability during both 3-day and 5-day transit. Non-encapsulated cells stored at 4 °C showed a mean recovery of 5.33% on 3-day storage and up to 4% after 5-day storage.

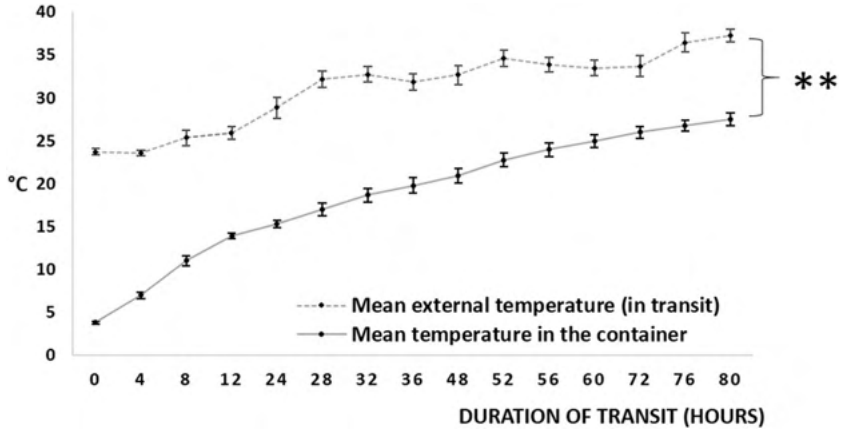

Figure 2. Maintenance of hypothermic temperatures in the pre-conditioned container. Mean external (ambient) and internal temperatures of the conditioned container: A Styrofoam container was conditioned to maintain hypothermic temperatures, by loading with pre-chilled (2–8 °C, 72 hours) gel pads (6 no.s covering all sides of a small box holding vials of cells). This was loaded with alginate beads (without cells) in media, at 13–15 °C of the container's internal temperature, packed, sealed and kept under transit (n = 10). Temperatures were recorded every four hours, up to 80 hours. $^{**}p \leq 0.001$.

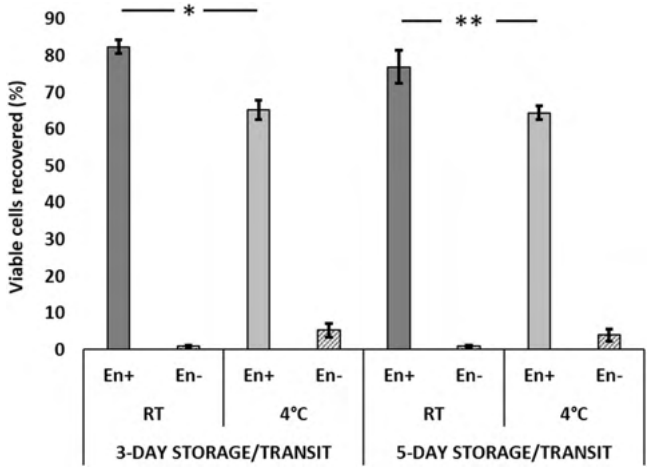

Figure 3. Effect of temperature on viability of encapsulated cells. Mean recovery of the viable encapsulated cells: The storage temperature had an insignificant effect on the viability of encapsulated cells. Encapsulated cells were kept under transit at 4 °C and RT (5 each vials with 0.5×10^6 encapsulated cells/vial) for 3–5 days (n = 3). Cells were released from encapsulation after transit and quantified for viability by dye exclusion method using 0.4% Trypan blue. The average cell viability at given temperature and duration of the storage, was expressed in percentage, with error bars. **En+**: Encapsulated, **En−**: Non-encapsulated. *p = 0.0104, **p = 0.0008.

Relative survival rate of the encapsulated cells. The encapsulated cells kept under transit at RT for 3 days exhibited a relative survival rate of 61.93 ± 1.68% after 48 hours compared to the control group. This increased to 74.34 ± 2.89% in the subsequent 48 hours. Cells that were under transit for 5 days, showed 51.24 ± 1.38% survival after 48 hours that increased to 67.74 ± 9.78% after 96 hours (Fig. 4). On the other hand, the encapsulated cells stored under refrigerated conditions for 3-days, have shown attachment of about 39.67 ± 5.32% after 48 hours and which increased to 54.8 ± 9.04% after 96 hours. Upon 5-day refrigeration, the cell attachment was 43.77 ± 3.53% after 48 hours and 52.35 ± 8.07% after 96 hours.

Phenotypic expression of the biomarkers. Encapsulated cells under transit at RT have shown the similar (default) phenotype with the control group of cells, during both 3-day and 5-day transit. Encapsulated cells under storage at 4 °C showed expression of ABCG2 after 3-day storage but not at 5-day refrigeration (Figs 5 and 6). The expression of the rest of the biomarkers by both RT and 4 °C groups was similar to the control cells, showing the positive expression of $Pax6^+$ and stem cell markers ($p63\text{-}\alpha^+$, $ABCG2^+$) and the biomarkers for mesenchymal origin (VIM^+, $CD105^+$, $CD90^+$, $CD45^-$) and the other surface biomarkers $Col\text{-}III^+$, and $CD73^+$. Although HLA-DR is considered negative marker for the mesenchymal origin, we have found this marker to be positively

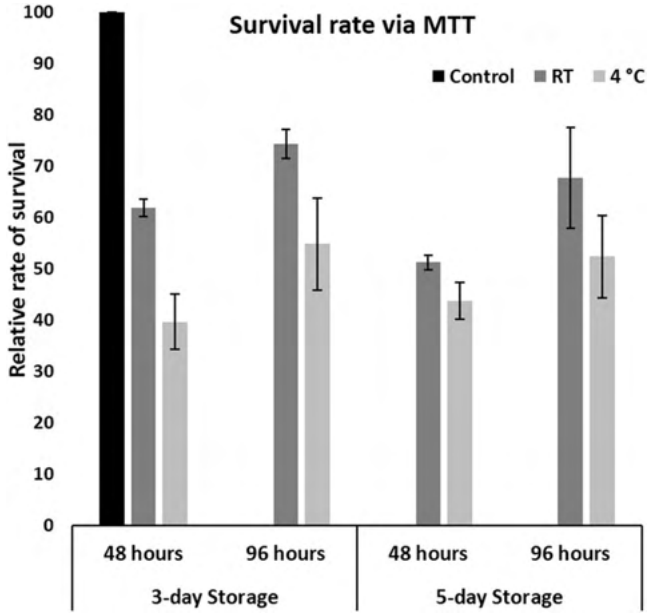

Figure 4. Survival rate of the encapsulated cells. RT-stored encapsulated cells show greater survival than 4 °C-stored encapsulated cells. Alginate encapsulated cells stored/transported at 4 °C and RT for 3–5 days (n = 3), were released and plated in triplicates of equal numbers after quantifying for viability. The regular non-encapsulated cells were plated in same number as controls in all the cases. Cells were cultured for 48 hours and 96 hours and assessed for rate of survival using MTT assay. The average rates of survival were expressed in percentage, by comparing absorbance of given category relative to the standard/control group of cells (capped to 100%).

expressing in all the groups of cells irrespective of encapsulation. The number of cells (categorized to %) with positive expression for a given characteristic biomarker is represented in the tabular format (Table 2).

Quantifying the gene expression (RT-PCR). Although encapsulated cells stored at RT and 4 °C showed higher levels of PAX-6, p63-α, and CD90 expression as compared to the control group, these differences were not statistically significant (Fig. 7, $p > 0.11$).

Discussion

This study aimed to evaluate the efficacy of alginate encapsulation in maintaining the viability and properties of hLMSC while being stored and transported at RT in a real-life ground-transportation scenario. The study found that while non-encapsulated cells had negligible viability at RT and 4 °C, encapsulated hLMSC (RT and 4 °C) maintained high viability, had good survival in culture and retained adequate phenotype expression. The phenotypic assessment of the encapsulated cells in comparison with control groups showing the number of cells positive for a given biomarker is given in Table 2. A similar trend of the percentage of cells expressing a biomarker was observed. We have found positive expression of HLA-DR in all the groups of cells. Many earlier studies have shown similar findings of the positive expression of HLA-DR in the normal cornea towards periphery and the limbus[17–19]. The findings of this study suggest that alginate encapsulation is an effective method of hLMSC preservation and transport at RT for up to 3 to 5 days, which would allow these cells to be shipped to remote locations and therefore, potentially expand the scope of cell-based therapy for corneal blindness.

Corneal stromal stem cells and more recently hLMSC have been studied for their ability to restore corneal transparency[3] through corneal stromal regeneration[20]. The therapeutic potential of these cells for treating various corneal pathologies is currently being explored in clinical trials and the initial reports have shown enhancement in visual parameters and corneal epithelization, neovascularization and clarity[4,21,22]. These cells may eventually evolve into a simpler non-invasive alternative to corneal transplantation, thereby reducing the global demand for donor corneas. Further expansion of this therapeutic advancement is hindered by the bottlenecks of lacking proper preservation and transport methods towards the delivery of these cells without affecting their characteristic properties. The maintenance of appropriate temperature is a crucial and integral factor for optimal shelf life of the cells[23]. Despite the ambient temperature fluctuations between 28.9 to 38.4 °C, not only was the insulated container able to maintain significantly lower temperatures of 13.9 to 27.5 °C, but alginate encapsulation also allowed most cells to survive while in transit. The proportion of the encapsulated cells that were lost in the transit, may be considered to have undergone apoptosis. However, without encapsulation almost all cells perished within the same amount of time. Ability to transport cells at RT circumvents the usage of dry ice, which is currently categorized as restricted item for airborne transport (https://www.fedex.com/in/domestic/services/regulatory-guidelines.html) and of any expensive equipment required to maintain chilled temperature during shipping. This would potentially translate into significantly lower costs for cell storage and transportation.

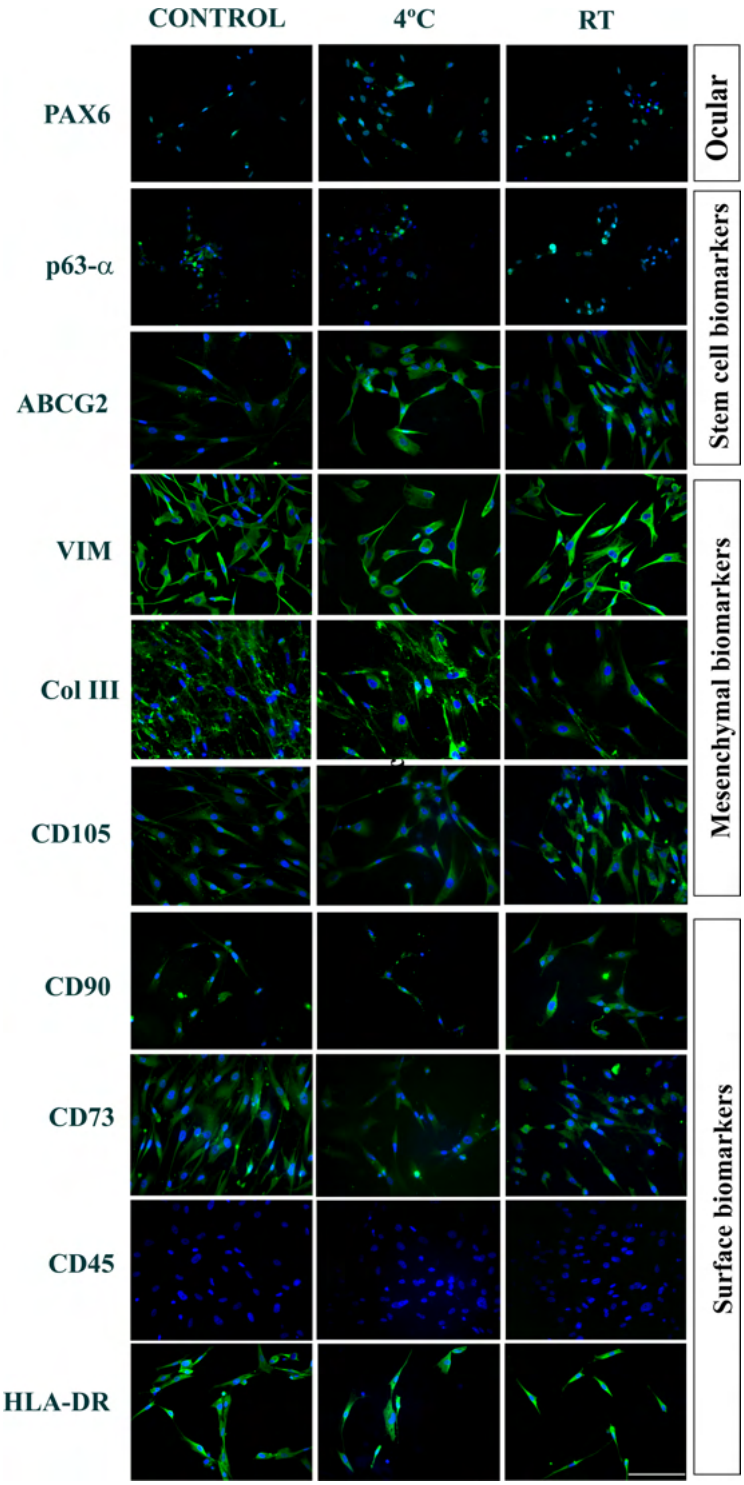

Figure 5. Phenotypic expression of the biomarkers. Immunostaining of the encapsulated hLSMCs under transit for 3 days: Alginate encapsulated hLSMCs of both groups, stored/under transit for 3 days have shown the expression of $Pax6^{+}$, stem-cell biomarkers ($ABCG2^{+}$, p63-α^{+}) and the mesenchymal biomarkers (VIM^{+}, $CD90^{+}$, $CD105^{+}$ and $CD45^{-}$) with respect to the control cells. ***Blue:*** DAPI, nuclear stain. ***Scale:*** 100 µM.

Achieving optimal cell viability and unaffected cell phenotype forms an integral crux of a validated shipping protocol. Similar reports of good viability when stored at room temperatures have been reported earlier with hydrogel encapsulation with[24,25] or without[23] extracellular matrix components. However, there are two distinct novelties of this study: (i) previous studies did not test the efficacy of the preservation methods in retaining the properties of stem cells obtained from primary tissues of human origin, while in actual transit.; (ii) while the

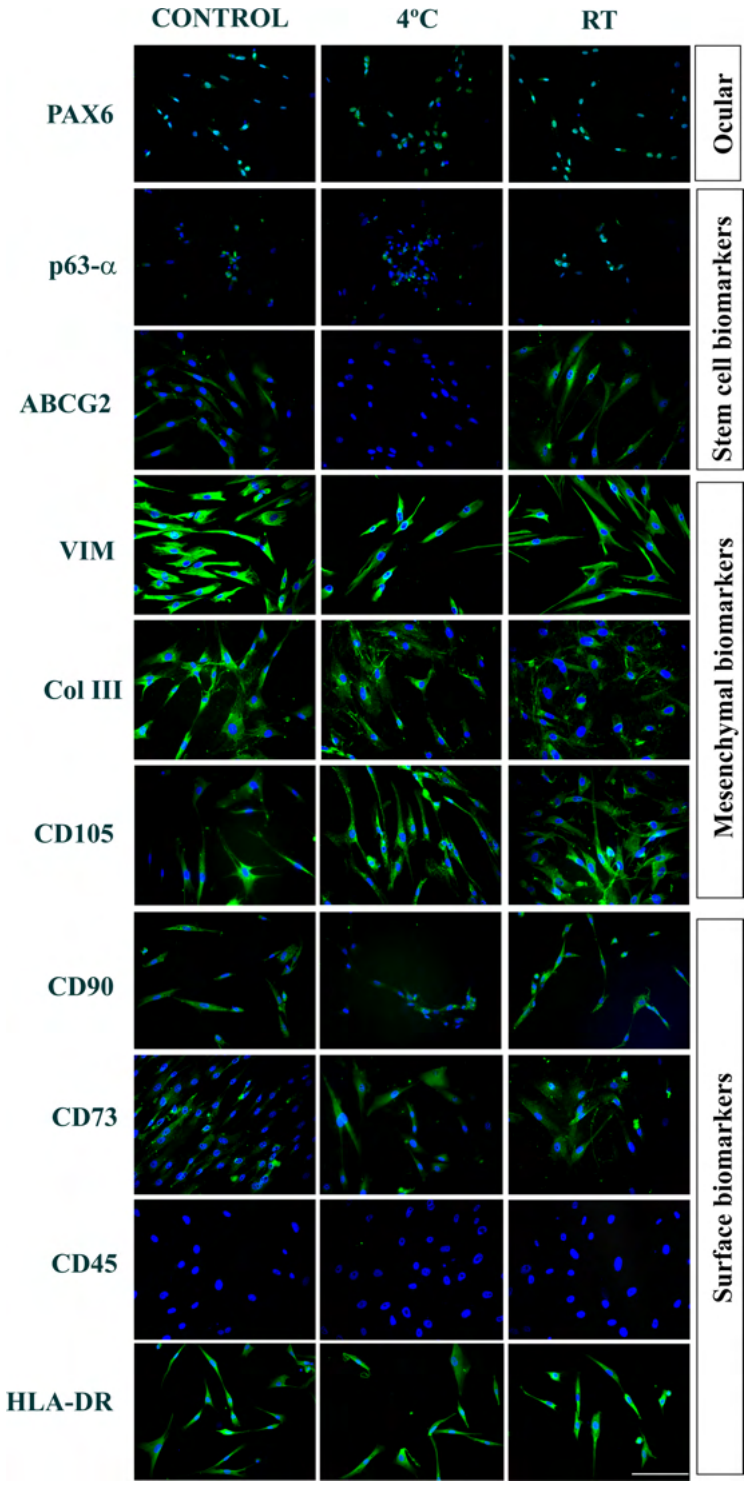

Figure 6. Quantification of the gene expression using real-time PCR. Immunostaining of the encapsulated hLSMCs under transit for 5 days: Alginate encapsulated hLSMCs stored at 4 °C did not show expression of the stem-cell ($ABCG2^{-}$). The RT group cells have showed similar phenotype as the control group ($ABCG2^{+}$, $Pax6^{+}$ p63-α^{+}, VIM^{+}, $CD90^{+}$, $CD105^{+}$, $CD45^{-}$, $HLADR^{+}$, Col-III^{+}, and $CD73^{+}$). ***Blue:*** DAPI, nuclear stain. ***Scale:*** 100 μM.

experimental temperature ranges tested previously were 22–25 °C[16] or 11–23 °C[10] in controlled laboratory set-ups, in this study the external ambient temperature ranged from 28.9 to 38.4 °C in real-life conditions. These results imply that it may be possible to send the alginate encapsulated cells to remote locations for their application using ground transportation, which would significantly lower the shipping costs involved. The remote and rural areas,

Type	Biomarker	In transit for 3 days			In transit for 5 days		
		Control	4 °C	RT	Control	4 °C	RT
Ocular	Pax6	++	++	++	++	++	++
Stem Cell	p63-α	+	+	+	+	+	+
	ABCG2	+++	+++	+++	+++	–	+++
Mesenchymal	VIM	++++	++++	++++	++++	++++	++++
	Col III	++++	++++	++++	++++	++++	++++
	CD105	++++	++++	++++	++++	++++	++++
Surface	CD90	++++	++++	++++	++++	++++	++++
	CD73	++++	++++	++++	++++	++++	++++
	CD45	–	–	–	–	–	–
	HLA-DR	++++	++++	++++	++++	++++	++++

Table 2. Tabular format denoting the number of cells showing positive expression of the phenotypic biomarkers. (−): No expression; (+): <25% cells are positive, (++): 25–50%, (+++): 50–90%, (++++): >90% cells are positive.

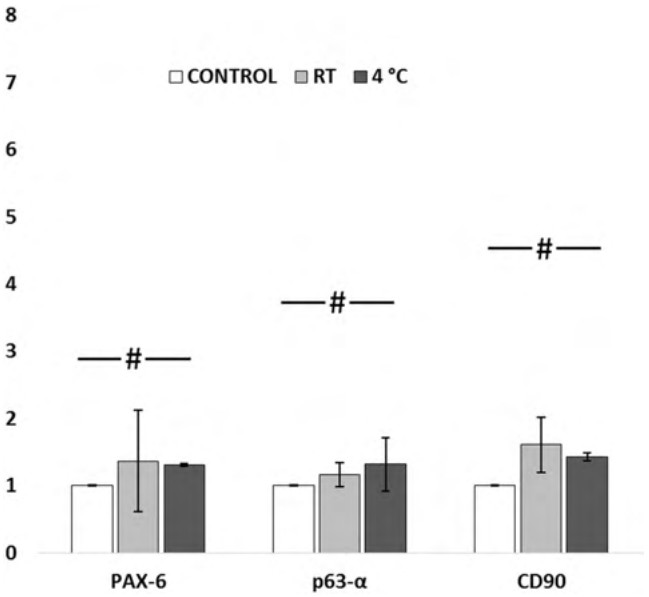

Figure 7. Quantification of gene expression of encapsulated cells, under transit for 3 days: Cells stored at 4 °C have shown 0.6-fold increased expression of ABCG2, PAX-6 and p63-α; ~2-fold increased expression of CD90 when compared to control. Insignificant fold change of expression was found between the control and RT groups for all the three markers. $^{\#}p > 0.11$.

by having equipped with one centrifuge and a pipette, shall be able to release the encapsulated cells, without the necessity of having a cell culture facility. Additionally, all the reagents and procedures employed in the process of cell encapsulation are FDA approved. This would ease the regulatory constraints on the clinical translation and expansion of the technique[26]. However, this study is limited by lacking serum free culture methods and the study of therapeutic properties of the encapsulated cells, which are underway in the further phase of this study.

In conclusion, this study aimed to test the reliability of alginate encapsulation for storing and transporting hLSMC at RT in temperate climatic conditions and the findings of this study suggest that alginate encapsulation is an effective method of hLMSC preservation offering high cell viability over prolonged durations in real-life transit conditions. The simplicity of the encapsulation process combined with the cost-effectiveness of ground-transportation makes alginate encapsulation an attractive option for furthering the scope and scale of cell-based therapy for corneal blindness particularly in the developing world.

Received: 1 March 2019; Accepted: 22 October 2019;
Published online: 18 November 2019

References

1. Whitcher, J. P., Srinivasan, M. & Upadhyay, M. P. Corneal blindness: a global perspective. *Bull. World Health Organ.* **79**, 214–221 (2001).
2. Williams, K. A. *et al*. How effective is penetrating corneal transplantation? Factors influencing long-term outcome in multivariate analysis. *Transplantation*. **81**(No. 6), 896–901 (2006).
3. Basu, S. *et al*. Human limbal biopsy–derived stromal stem cells prevent corneal scarring. *Sci transl med.* **6**(266), 266ra172–266ra172 (2014).
4. Basu, S., Damala, M. & Singh, V. Limbal stromal stem cell therapy for acute and chronic superficial corneal pathologies: early clinical outcomes of the Funderburgh technique. *Invest. Ophthalmol. & Vis. Sci.* **58**(8), 3371–3371 (2017).
5. Calonge, M. *et al*. A proof-of-concept clinical trial using mesenchymal stem cells for the treatment of corneal epithelial stem cell deficiency. *Transl Res.* **11**, 003, https://doi.org/10.1016/j.trsl.2018.11.003 (2018).
6. Whiteside, T. L. *et al*. Shipping of therapeutic somatic cell products. *Cytotherapy.* **13**(No. 2), 201–213 (2011).
7. Karlsson, J. O. & Toner, M. Long-term storage of tissues by cryopreservation: critical issues. *Biomaterials*. **17**(3), 243–256 (1996).
8. Chinnadurai, R. *et al*. Cryopreserved mesenchymal stromal cells are susceptible to T-cell mediated apoptosis which is partly rescued by IFNγ licensing. *Stem Cells.* **34**(9), 2429–2442 (2016).
9. Lioznov, M. *et al*. Transportation and cryopreservation may impair haematopoietic stem cell function and engraftment of allogeneic PBSCs, but not BM. *Bone marrow transplantation* **42**(2), 121 (2008).
10. Swioklo, S. & Connon, C. J. Keeping cells in their place: the future of stem cell encapsulation. *Expert. Opin. Biol. Ther.* **16**(10), 1181–3 (2016).
11. Faustini, M. *et al*. Boar sperm encapsulation reduces *in vitro* polyspermy. *Reproduction in Domestic Animals* **45**(2), 359–362 (2010).
12. Sakurai, T., Kimura, M. & Sato, M. Temporary developmental arrest after storage of fertilized mouse oocytes at 4 C: effects on embryonic development, maternal mRNA processing and cell cycle. *Molecular human reproduction* **11**(5), 325–333 (2005).
13. Tamponnet, C. *et al*. Storage and growth of neuroblastoma cells immobilized in calcium-alginate beads. *Applied microbiology and biotechnology* **33**(4), 442–447 (1990).
14. Swioklo, S., Constantinescu, A. & Connon, C. J. Alginate-encapsulation for the improved hypothermic preservation of human adipose-derived stem cells. *Stem Cells Transl. Med.* **5**(3), 339–49 (2016).
15. Swioklo, S., Ding, P., Pacek, A. W. & Connon, C. J. Process parameters for the high-scale production of alginate-encapsulated stem cells for storage and distribution throughout the cell therapy supply chain. *Process Biochem.* **59**(B), 289–96 (2017).
16. Dominici, M. *et al*. Minimal criteria for defining multipotent mesenchymal stromal cells. The International Society for Cellular Therapy position statement. *Cytotherapy.* **8**(No. 4), 315–317 (2006).
17. Treseler, P. A., Sanfilippo, F. & Foulks, G. N. The expression of HLA antigens by cells in the human cornea. *Am J Ophthalmol.* **98**(6), 763–772 (1984).
18. Hamrah, P., Zhang, Q., Liu, Y. & Dana, M. R. Novel characterization of MHC class II–negative population of resident corneal Langerhans cell–type dendritic cells. *Invest. Ophthalmol. & Vis. Sci.* **43**(3), 639–646 (2002).
19. Hamrah, P., Huq, S. O., Liu, Y., Zhang, Q. & Dana, M. R. Corneal immunity is mediated by heterogeneous population of antigen-presenting cells. *J Leukoc Biol.* **74**(2), 172–178 (2003).
20. Hassell, J. R. & Birk, D. E. The molecular basis of corneal transparency. *Exp. Eye Res.* **91**(3), 326–335 (2010).
21. Damala, M., Kethiri, A. R., Tavakkoli, F., Raju, E. & Singh. V. The basics of stem cells and their role in vision in *Trends in Life Science Research* (ed. Sinha P. R., and Umesh P. S.). 97–124 (Nova Science, 2018).
22. Funderburgh, J. *et al*. Limbal stromal stem cell therapy for acute and chronic superficial corneal pathologies: one-year outcomes. *Invest. Ophthalmol. & Vis. Sci.* **59**(9), 3455–3455 (2018).
23. Olson, W. C. *et al*. Shipping blood to a central laboratory in multicenter clinical trials: effect of ambient temperature on specimen temperature, and effects of temperature on mononuclear cell yield, viability and immunologic function. *J. Transl. Med.* **9**(No. 1), 26 (2011).
24. Wang, J. *et al*. Transporting cells in semi-solid gel condition and at ambient temperature. *PLoS One.* **10**(No. 6), e0128229 (2015).
25. Nicodemus, G. D. & Bryant, S. J. Cell encapsulation in biodegradable hydrogels for tissue engineering applications. *Tissue. Eng. Part B Rev.* **14**(2), 149–165 (2008).
26. Wright, B. *et al*. Enhanced viability of corneal epithelial cells for efficient transport/storage using a structurally modified calcium alginate hydrogel. *Regenerative medicine* **7.3**, 295–307 (2012).

Acknowledgements

This work was supported by Science and Engineering Research Board, Department of Science and Technology, Government of India (EMR/2017/005086). Support in part was provided by Champalimaud Translational Centre for Eye Research, Hyderabad Eye Research Foundation, Hyderabad, India. Part of this study is accepted for submission at ARVO Annual Meeting, 2019.

Author contributions

Conception and design: Vivek Singh, Che J. Connon, Sayan Basu, Steve Swioklo, Mukesh Damala. Analysis and interpretation: Mukesh Damala, Vivek Singh, Steve Swioklo, and Che J. Connon. Data collection: Mukesh Damala, Steve Swioklo, Madhuri A. Kondapaka, Noopur S. Mitragotri. Supervision and direction: Vivek Singh, Che J. Connon and Sayan Basu.

Competing interests

S.S. and C.J.C. have a proprietary and commercial relationship with Atelerix Ltd, UK that supplied the alginate within the BeadReady kit used.

Additional information

Supplementary information is available for this paper at https://doi.org/10.1038/s41598-019-53315-x.

Correspondence and requests for materials should be addressed to V.S.

Reprints and permissions information is available at www.nature.com/reprints.

Publisher's note Springer Nature remains neutral with regard to jurisdictional claims in published maps and institutional affiliations.

cells

IMPACT FACTOR 7.666

Indexed in: PubMed

Article

Pre-Clinical Evaluation of Efficacy and Safety of Human Limbus-Derived Stromal/Mesenchymal Stem Cells with and without Alginate Encapsulation for Future Clinical Applications

Mukesh Damala, Abhishek Sahoo, Naveen Pakalapati, Vivek Singh and Sayan Basu

Special Issue

Stem Cell Biotechnology in Ocular Regenerative Medicine and Drug Discovery

Edited by

Prof. Dr. Heli Skottman and Prof. Dr. Sayan Basu

MDPI

https://doi.org/10.3390/cells12060876

cells

MDPI

Article

Pre-Clinical Evaluation of Efficacy and Safety of Human Limbus-Derived Stromal/Mesenchymal Stem Cells with and without Alginate Encapsulation for Future Clinical Applications

Mukesh Damala [1,2], Abhishek Sahoo [1], Naveen Pakalapati [1], Vivek Singh [1,*] and Sayan Basu [1,*]

[1] Centre for Ocular Regeneration (CORE), Prof Brien Holden Eye Research Centre, LV Prasad Eye Institute, Hyderabad 500034, India
[2] School of Life Sciences, University of Hyderabad, Hyderabad 500046, India
* Correspondence: viveksingh@lvpei.org (V.S.); sayanbasu@lvpei.org (S.B.); Tel.: +91-40-6810-2286 (V.S.); +91-40-6810-2555 (S.B.)

Abstract: Corneal opacification or scarring is one of the leading causes of blindness worldwide. Human limbus-derived stromal/mesenchymal stem cells (hLMSCs) have the potential of clearing corneal scarring. In the current preclinical studies, we aimed to determine their ability to heal the scarred corneas, in a murine model of corneal scar, and examined their ocular and systemic toxicity after topical administration to rabbit eyes. The hLMSCs were derived from human donor corneas and were cultivated in a clean room facility in compliance with the current good manufacturing practices (cGMP). Before the administration, the hLMSCs were analyzed for their characteristic properties including immunostaining, and were further subjected to sterility and stability analysis. The corneas (right eye) of C57BL/6 mice (n = 56) were stripped of their central epithelium and superficial anterior stroma using a rotary burr (Alger Brush® II). Few mice were left untreated (n = 8), while few (n = 24) were treated immediately with hLMSCs after debridement (prophylaxis group). The rest (n = 24, scar group) were allowed to develop corneal scarring for 2 weeks and then treated with hLMSCs. In both groups, the treatment modalities included encapsulated (En+) and non-encapsulated (En−) hLMSCs and sham (vehicle) treatment. The follow-up (4 weeks) after the treatment or debridement included clinical photography, fluorescein staining, and optical coherence tomography at regular intervals. All the images and scans were analyzed using ImageJ software to assess the changes in corneal haze, scar area, and the reflectivity ratio of the epithelium to the stroma. The scar area and the scar intensity were found to be decreased in the groups that received hLMSCs. The reflectivity of the stroma was found to be normalized to the baseline levels before the debridement in the eyes that were treated with hLMSCs, relative to the untreated. In the safety study, the central corneas of the left eye of 18 New Zealand rabbits were scraped with a needle and then treated with En+ hLMSCs, En− hLMSCs, and the sham (n = 6 each). Rabbits were then followed up for 4 weeks, during which blood and tear samples were collected at regular intervals. These rabbits were then assessed for changes in the quantities of inflammatory markers (TNF-α, IL-6, and IgE) in the sera and tears, changes in the ocular surface observations such as intraocular pressure (IOP), and the hematological and clinical chemistry parameters. Four weeks later, the rabbits were euthanized and examined histopathologically. No significant changes in conjunctival congestion, corneal clarity, or IOP were noticed during the ophthalmic examination. The level of inflammatory molecules (TNF-α and IL-6 TNF-α) and the hematological parameters were similar in all groups without any significant changes. Histological examination of the internal organs and ocular tissues did not reveal any abnormalities. The results of these studies summarize that the En+ and En− hLMSCs are not harmful to the recipient and potentially restore the transparency of debrided or scarred corneas, indicating that hLMSCs can be assessed for clinical use in humans.

Keywords: cornea; limbus; limbal stromal stem cells; stromal cell; immune response; toxicity; safety; cell encapsulation; efficacy; alginate; transport at room temperature

Citation: Damala, M.; Sahoo, A.; Pakalapati, N.; Singh, V.; Basu, S. Pre-Clinical Evaluation of Efficacy and Safety of Human Limbus-Derived Stromal/Mesenchymal Stem Cells with and without Alginate Encapsulation for Future Clinical Applications. *Cells* **2023**, *12*, 876. https://doi.org/10.3390/cells12060876

Academic Editors: W. Matthew Petroll and Dimitrios Karamichos

Received: 18 January 2023
Revised: 1 March 2023
Accepted: 9 March 2023
Published: 11 March 2023

1. Introduction

The cornea, also called the window of the eye, is a transparent structure in front of the eye. Light passes through it onto the retina, for the perception of light. Anatomically speaking, the ultrastructure of the cornea comprises three main layers: epithelium, followed by stroma, and followed by endothelium. The transparency of the cornea is due to the highly organized collagen fibrils in its stroma [1,2]. Corneal opacity or haze occurs when a person is exposed to infection, inflammation, or trauma [3,4]. Corneal scarring, a resultant of irregular fibrillogenesis following a wound, is one of the major causes affecting corneal transparency. Scarring involves the formation of atypical proteoglycans and the differentiation of the native keratocytes to the myofibroblastic phenotype [5–8].

The unavailability of standard treatments to clear corneal scarring makes corneal transplantation a pre-eminent mode of care for patients suffering from partial impairment of vision to complete blindness. The requirement for longer follow-up and the chances of graft rejection and the low rate of graft survival are the major limitations of corneal transplantation. Additionally, the unmet balance between the supply and the demand for donor corneas necessitates the need for alternative approaches to curb corneal scarring. Cell-based therapy is one of the emerging alternatives that could prevent and heal corneal scarring without the need for whole corneal transplantation [9–11].

Many groups across the globe have shown the potential of hLMSCs in preventing corneal haze [4,12–16]. Reports from the investigations by Basu et al. (2014) [4] and Du et al. (2009) [17] indicated that hLMSCs did not cause any immune reaction in the murine models of corneal scars. These cells are safe because it has been demonstrated that they can regulate the immune system [18] and that they do not produce any xenogeneic reactions in mouse models [4,18]. Various clinical studies are currently evaluating the safety and potency of hLMSCs and other mesenchymal stem cells [19–24]. By decreasing the need for donor corneas, the hLMSCs may reduce the need for corneal transplants. In addition, it has been demonstrated that hLMSCs preserved their viability and phenotype by being encapsulated in sodium alginate for 3–5 days while being transported or stored at various temperatures [25]. Without involving the patient in hundreds or thousands of kilometers of travel, this straightforward method, which does not require a costly cold chain, could expand access to hLMSC-based therapy, especially in rural and underdeveloped countries. However, before these novel techniques can be used in clinical settings, the toxicity and efficacy profiles of these cells, with or without encapsulation, must first be determined.

The objective of this study was to evaluate the cGMP-manufactured therapeutic-class hLMSCs for (a) harmlessness as well as detrimental effects following topical treatment in an animal model of corneal wound healing according to Indian regulatory guidelines, and (b) their effectiveness in preventing the formation of corneal scar and the regeneration of the corneal surface following treatment of the corneal scar with En−/En+ hLMSCs. Additionally, the information from the findings includes the vitality and stability of cGMP-grade hLMSCs throughout culturing and passages as well as the several quality checks that must be completed before these cells may be used in a clinical study.

2. Materials and Methods

2.1. Study Design and Ethical Approvals

2.1.1. Approvals

The research ethics committee (Approval reference number 05-18-081) and the panel of the Institutional Committee for Stem Cell Research (Approval reference number ICSCR 08-18-002) at the LV Prasad Eye Institute, Hyderabad, approved the study methodology (Figure 1). The experimental protocols (safety study) on the animals were approved by the Animal Ethics Committee of Sipra Labs (Project reference number 110-19), Hyderabad, and adhered to the guidelines of Schedule–Y (26), Drugs and Cosmetics Rules act, 2019, Government of India (27).

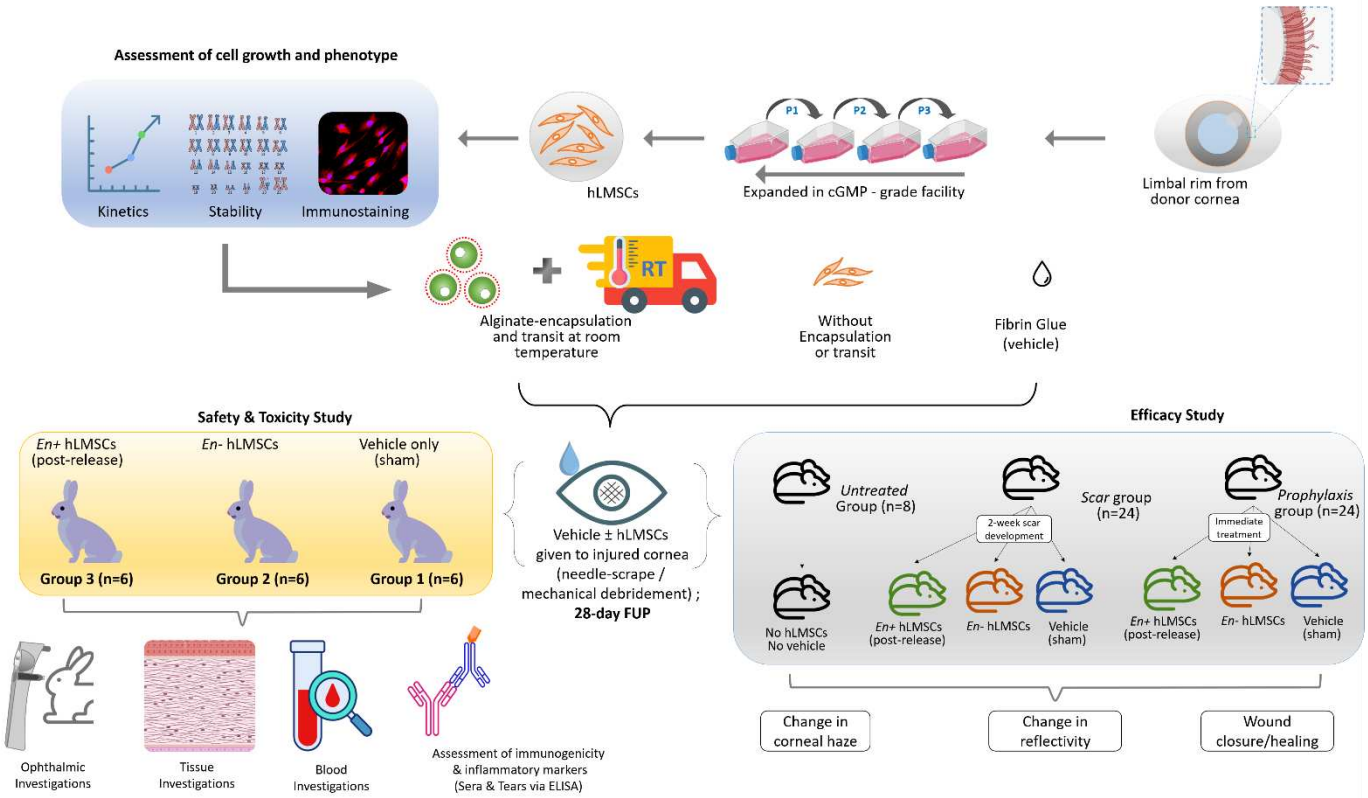

Figure 1. Graphical abstract of the experimental plan for assessing the safety and efficacy of human limbus−derived stromal/mesenchymal stem cells.

The protocols used in the efficacy and safety studies were created in a way that complies with the ARVO Statement for the Use of Animals in Ophthalmic and Vision Research [26] issued by the Association for Research in Vision and Ophthalmology. All investigations conformed to generally accepted procedures, minimized or avoided the potential for animal suffering, and maintained their general health.

The International Council for Harmonization of Technical Requirements for Pharmaceuticals for Human Use (ICH) M3 (R2) [27] and the OECD (Organization for Economic Cooperation and Development) standards [28] of Good Laboratory Practice, 1997 were also followed in the conduct of this investigation.

2.1.2. Donor Corneas

Therapeutic-grade donor corneas (n = 28) to harvest hLMSCs were obtained from Ramayamma International Eye Bank (RIEB), Hyderabad, India. The guidelines of the Declaration of Helsinki for the usage of human tissues were followed.

2.1.3. Characterization of hLMSCs Expanded in GMP-Compliant Clean Room

All the batches of hLMSCs that were isolated and expanded using the optimized protocols underwent a series of tests and analyses (at both in-process and end-product stages) to ensure stability, sterility, and similitude of the characteristic properties. The tests included: qualitative and quantitative assessment of the phenotype through immunofluorescence and FACS (fluorescence-assisted cell sorting), karyotyping, quantification of the viability of hLMSCs in the cell pellet, microbial and mycoplasma analysis, determination of endotoxin content, and growth kinetics. The batches of hLMSCs that qualified for all of the tested parameters were used for the pre-clinical assessment in animal models.

2.1.4. Assessment of the Efficacy of hLMSCs in a Murine Model of Corneal Scar

C57BL/6 mice (n = 56) of 6–8 weeks of age, weighing 20 to 25 g, were used for this study. A normal diet was provided. All mice were acclimatized to the cages at least a week before the beginning of the experimental procedures. The allocation was conducted through simple randomization. The mice were allocated to three study groups viz (a) the scar group (n = 24), (b) prophylaxis group (n = 24), and (c) untreated group (n = 8). The central epithelium and anterior stroma were debrided in the right eye of the mice. After debridement, the mice were treated either prophylactically (prophylaxis group) or therapeutically after allowing them to develop corneal scars for two weeks (scar group). Based on the method of treatment, these groups were divided into three subgroups, each based on the method of treatment: (i) sham (n = 8, vehicle only); (ii) En− hLMSCs (n = 8, cells that were neither encapsulated nor transported); and (iii) En+ hLMSCs (n = 8, cells released from transit after encapsulation). The untreated group was not provided with any treatment.

A clinical assessment of both eyes was undertaken before and after the debridement and treatment of the corneas. Clinical photographs of the ocular surface and optical coherence tomography (OCT) scans of the corneal ultrastructure were taken to detect the changes in the reflectivity and thickness of the corneal layers. Additionally, fluorescein staining of the ocular surface was performed to track the wound closure and reepithelization of the corneas debrided. The assessment was conducted at the stages of the pre-wound, wound, pre-op (on days 1, 7, and 14 during the development of the scar), and post-op stages (days 7, 14, 21, and 28).

2.1.5. Determination of Safety and Toxicity of hLMSCs in Rabbits with Corneal Wounds

Three to four-month-old rabbits of the New Zealand White strain (n = 18) were used in this part of the study. The rabbits were allocated to the study groups through the stratified randomization method. Three groups of six rabbits each with three male and three female members received the following treatment: sham-treated group (G1) or control group; the G2 (En− hLMSCs) group received unencapsulated hLMSCs, while the G3 (En+ hLMSCs) group received encapsulated hLMSCs that were transported at room temperature.

The rabbits were anesthetized on the day of the experiment by injecting a formulation of ketamine (35 µg/g body weight) and xylazine (10 µg/g body weight). After that, 1–2 drops of topical anesthesia were applied to the eye (0.5 percent proparacaine). Next, a sterile needle was used to carefully scrape the corneal surfaces, as soon as they had been cleaned with a cotton swab soaked in 0.5 percent povidone-iodine. Then, the eyes of the G2 and G3 groups received 5×10^5 En− hLMSCs and 50×10^5 En+ hLMSCs, respectively, mixed with 100 uL of the fibrin glue formulation that is available for purchase (TISSEEL LYO, Baxter International Inc., Deerfield, IL, USA). The control group was treated with the vehicle alone (sham treatment) (i.e., fibrin glue) at the same time. To prevent the test item from being lost after the analytes were given, the eyes were closed for about 3 to 5 s. Finally, a sterile dressing pad was used to apply the treated eyes until the rabbits recovered from anesthesia. At each time point, additional ophthalmic examinations and blood analysis as well as the collection of serum and tear fluid were carried out. After the animals had been sacrificed, the pathological assessments were carried out on day 29.

2.2. Isolation and Expansion of hLMSCs

As previously reported [25], the limbal rim from the donor corneas served as the source of the hLMSCs. Briefly, limbal rims were dissected, cut to small fragments of 1–2 mm, and gently minced after the donor cornea was washed with the penicillin-streptomycin-gentamycin composition (15240062, Thermo Fisher Scientific, Waltham, MA, USA) diluted in PBS (14190250, Thermo Fisher Scientific, Waltham, MA, USA). Using the enzyme collagenase-IV (17104019, Thermo Fisher Scientific, Waltham, MA, USA), the minced limbal fragments were digested. After the digested tissue was washed, it was cultured in DMEM/F12 medium (BE04-687F/U1, Lonza, Basel, Switzerland) supplemented with 2%

fetal bovine serum (SH30084.03, Cytiva Life Sciences, Marlborough, MA, USA). After reaching 80–90% confluence, the primary cultures (P0) were divided and subcultured for three generations or passages. At passage 3 (P3), a pure hLMSC culture was obtained, and post-viability checks were performed with 0.4% Trypan Blue (15250061, Thermo Fisher Scientific, Massachusetts, MA, USA).

A commercially available BeadReady^{TM} Kit [25] from Atelerix Ltd., Newcastle upon Tyne, TWR, UK was used to encapsulate hLMSCs with sodium-alginate. Using a sterile needle, the 2.5 $\times$ 10^6 formulation of the alginate-cell suspension was released into a gelating buffer, where it polymerized into bead-like structures. For three to five days, these hLMSC-containing beads were in transit in a pre-standardized Styrofoam container that could maintain room temperature. These were suspended in the culture medium during the transit. The cells were then sedimented and released from the beads using a buffer containing trisodium citrate. For further analysis, the sedimented cell pellet was resuspended in a new complete medium. Before they were topically applied to the ocular surface, the pellet was washed with PBS/saline and the cell suspension was centrifuged at 1000 rpm for three minutes.

2.3. Analyzing the Distinctive Phenotype of hLMSCs

2.3.1. Immunostaining

Until confluence, cells were cultured in 12-well culture plates with coverslips with a diameter of 18 mm at a density of 2 $\times$ 10^4 cells per cm^2 at 37 °C and 5% CO_2. As described previously [25], hLMSCs were examined for the expression of typical markers of the MSC phenotype. The antibody panel featured markers for the human limbal stem cell trait such as Pax6, ABCG2, p63-α, and Col-III as well as markers for the MSC phenotype such as CD45, a negative indicator for mesenchymal cells, CD73, VIM, CD105, and CD90.

The minimum requirements for multipotent mesenchymal stromal cells as defined by the International Society for Cellular Therapy [29] were used to select this antibody panel. Alexa Fluor 594 (anti-mouse and anti-rabbit) from Thermo Fisher Scientific, Massachusetts, MA, USA, were included in the secondary antibody panel. A mounting medium (Fluoroshield, ab104139, Abcam, Cambridge, Cambs, UK) containing DAPI was used to mount the cells, and a Carl Zeiss Axio Scope A1 fluorescent microscope with a 20× or 40× objective was used for imaging. Biologic triplets were used in this experiment.

The number of viable cells was counted in a Neubauer chamber using the dye-exclusion method, which makes use of 0.4% Trypan Blue solution, and was used to measure the cell viability in both experimental groups. The minimum acceptance criterion was 70%, and the viability was expressed as percentage + SD.

2.3.2. FACS

Fluorescence-assisted cell sorting (FACS) was used to quantitatively evaluate a portion of the populations of En−/En+ hLMSCs prior to administration to the murine corneas. After trypsinization from the cultures, viability checks were performed on both En− and En+ hLMSCs, and 10 uL of each primary antibody (diluted as per manufacturer's instructions) was added to 50,000 En− hLMSCs in PBS after recovery from encapsulation, transport, and viability checks. The cells were then kept at 2–8 °C for 45–60 min in the dark. CD45, CD90, ABCG2, P63-α, and HLA-DR were the antibodies on the panel. As a control, no primary antibody was added to the cell suspension, so an "unstained" set of cells was used. After being incubated with the primary antibody, the cell suspensions were added to 200 mL of sheath fluid, and the CytoFLEX analyzer (Beckman Coulter, Indianapolis, IN, USA) was used for cytometric analysis.

2.4. Assessment of hLMSC Stability

2.4.1. Evaluation of the Viability of Pelletized hLMSCs

The post-harvest cells from cultures and post-release cell suspensions after encapsulation (En−/En+ hLMSCs cell suspensions, respectively) were centrifuged at 1000 rpm

for three minutes to eliminate the supernatant before being applied to the corneal surface. Since the process of transplanting the cell to the patient's eyes usually takes some time, as does the journey from the GMP laboratory to the operation room, these pelleted cells were preserved at temperatures from 2 to 4 °C. To find the best window of time to transplant the cells onto the corneal surface, it is advised to evaluate their stability as a pellet. This was found by measuring the viability of these cells in pellet from the first hour to the end of 24 h from trypsinization. The cell suspension was evenly divided among six separate vials (0.5×10^6 cells per vial/time point) and was preserved at temperatures from 2 to 4 °C following the initial viability evaluation. Using the dye-exclusion method, the amount (%) of viable cells at 30-min, 1-h, 3-h, 6-h, 12-h, and 24-h time points was measured and plotted.

2.4.2. Karyotyping

A licensed third-party laboratory used karyotyping to look for chromatic defects and abnormalities in the hLMSCs. Colcemide was used to stop the spindle formation in hLMSC cultures that were three to four days old (with and without encapsulation). The chromosomes were then released from the cells by giving them a hypnotic treatment. After that, the G-banding method was used to prepare the slides, and a bright-field microscope was used to look at them. Cytovision® software was used to carry out the analysis.

2.4.3. Growth Kinetics

From the hour of seeding the cells to the completion of day 6 of expansion in the cell culture flask, the number of viable cells was measured using the MTT assay as well as the dye-exclusion methods. The doubling time and growth curve of the hLMSCs were obtained by plotting the data on a graph.

2.5. Assessment of the Sterility of hLMSCs

2.5.1. Mycoplasma Assessment

Following the manufacturer's directions when using the kit (LT07-318, MycoAlert™, Lonza, Basel, Switzerland), the existence or absence of mycoplasma contamination was tested in the hLMSCs culture. A Luminometer (E5321, Promega, Wisconsin, WI, USA) was used to read the emitted light signal and check for mycoplasma in the cells' spent media at the end of each passage and passage 3.

2.5.2. Endotoxin Levels

A gel clot-based technique (N283-125, Lonza, Basel, Switzerland) was used to measure the amount of bacterial endotoxins (BET) existing in the hLMSC-suspension in conformity with the manufacturer's protocol. The FDA's rules [30] state that endotoxins cannot be present in amounts of more than 0.2 EU/mL.

2.6. Generation of the Murine Model of Corneal Scar

In normal saline, a mixture of xylazine and ketamine was used to anesthetize the mice. The mice were given 100 mg of xylazine (ilium Xylazil-100, Troy Laboratories Australia Pty. Ltd., NSW, Glendenning, Australia) and 10 mg of ketamine (Aneket®, Neon Laboratories Limited, Mumbai, India) per kilogram of body weight. Intraperitoneal administration of general anesthesia was conducted. Tearsplus (Allergan, Bangalore, India) lubricating eye drops were given to both eyes to keep them from drying out during the experiments. A surgical spear (EYETEC, Gujarat, India) was used to remove any objects or particles from the eyes, and the eyes were lubricated once more. After that, 0.5% proparacaine (Paracain, Sunways India Pvt Ltd., Mumbai, India) was applied topically to anesthetize both eyes.

Algerbrush® II (Accutome Inc., Pennsylvania, PA, USA) with a 0.5 mm burr was used to gently rotate the right eye's central cornea in a circular motion for 15–20 s. This removed the epithelium and a portion of the anterior stroma in the central cornea. The damage only affected the central cornea, not the limbus, sclera, or any other ocular surface area. The mice were either treated immediately or allowed to grow the scar for two weeks. After

being gently scraped with a #15 surgical blade to remove the damaged tissue, the scarred or debrided corneas were treated with 5×10^4 En−/En+ hLMSCs mixed in 2 µL of fibrin glue. Within one minute of application, this fibrin glue hardened into a gel-like clot. In each group, the contralateral eye (left) served as the normal control.

2.7. Assessment of Safety and Toxicity of hLMSCs

2.7.1. Rabbit Body Weights and Death Rates

Every rabbit was checked for morbidity and demise twice daily. Additionally, on the first day of treatment and then every week after, the specific body weights (kg) were measured.

2.7.2. Ophthalmic Investigations

The cornea, conjunctiva, iris, and aqueous humor were all examined using slit lamps (PSLAIA-11, Appasamy Associates, Chennai, TN, India). For corneal and conjunctival ophthalmic examinations, fluorescein ophthalmic strips were utilized. The ophthalmic observations were rated utilizing a numerical scoring procedure outlined in the OECD chemical testing guidelines, Test 405 "Scoring of the Lesions on Ocular surface" [28] and in accordance with Schedule Y [31] Before dosing, slit lamp and IOP readings were taken as well as at 3, 6, 12, and 24 h on day 1, and on days 7, 14, 21, and 28 after dosing. Supplementary Table S1 outlines the scoring guidelines.

2.7.3. Inflammatory Marker Quantification

At the end of 1, 6, 12, and 24 h on the day of treatment as well as on the days 7, 14, 21, and 28, blood samples ranging from 3 to 4 mL were taken from each animal using standard vacutainers. The blood samples were used to separate the sera, which was stored at –80 °C. Tear strips were used to collect samples of tear fluid at 1, 3, 6, 12, and 24 h as well as on days 7, 14, 21, and 28. For the purpose of determining the expression of the IL-6, TNF-α, and IgE markers, the collected samples were stored at –80 °C.

Schirmer Strip Tear Fluid Extraction

Applying the methodology that Posa et al. had previously published [32], Schirmer's strip (Tear Strip, Care Group, Vadodara, GJ, India) was used to extract the tears. Using forceps, the frozen strips were inserted into a sterile 0.5 mL microcentrifuge tube. A fresh 22 1/2 gauze needle was used to puncture these microcentrifuge tubes containing 0.5 mL. A 1.5 mL microcentrifuge tube was used to store the entire arrangement. Next, 10–50 mL of 1× PBS was added to the strip, based on the strip length in millimeters. The strip was then incubated for 30 min at 2–4 °C. Afterward, the apparatus was centrifuged at 4 °C for 5 min at 13,000 rpm. Each microliter of the collected tear fluid was evaluated to determine the level of protein, with the remaining volume being subsequently frozen at −80 °C for further study.

BCA Protein Quantitation

In accordance with the manufacturer's instructions, the bicinchoninic acid (BCA) assay (786-570, G-Biosciences, Geno Technology Inc., St. Louis, MO, USA) was used to measure the amount of protein in the tear samples collected. The standard graph obtained was compared to the concentration of the unknown samples. Using a SpectraMax M3 spectrophotometer (Molecular Devices, San Jose, CA, USA), the absorbance was measured at 562 nm for the standards, which ranged from 2000 pg to 0 µg/mL.

Quantification of Markers through Immunoassay

Using sandwich ELISA, the levels of inflammatory markers in rabbits were measured. KinesisDx, Krishgen Biosystems, USA, supplied commercially available antibody-coated kits for the quantification (IgE, K09-0071; IL-6, Ref: KLX0065), TNF-α, and KLX0003. Briefly, 10 µL of each biotinylated antibody was added to each well after 40 µL of each

sample (sera/tear) was added. There were no biotinylated antibodies in the standards. The streptavidin-HRP conjugate solution was then added to all wells and stored in an incubator at 37 °C for one hour in the dark. The wells were then thoroughly tapped onto absorbent paper and washed four times with washing buffer by utilizing an automatic washer (Erba Lisa Wash II, Erba Mannheim, Brentford, LDN, UK). After that, 50 µL of substrate A, 50 µL of substrate B, were added to the wells and incubated for 10 min. The SpectraMax M3 spectrophotometer was used to read the formed color at 450 nm following the addition of 50 uL of stop solution per well to halt the reaction.

2.7.4. Blood Investigations

Using a hematology cell quantifier (SYSMEX-XP 100, Kobe, OC, Japan), the hematological parameters were determined. The Leishman stain was used to stain the hematology sample to make blood smears. Utilizing standard microscopy, for these smears, the differential leukocyte count was performed. Clinical chemistry analysis was performed on the sera that were extracted from the blood specimens. A fully automated Random Access Biochemical Analyzer was used to perform the clinical chemistry test (EM-360, Erba Mannheim, Brentford, LDN, UK).

2.7.5. Tissue Evaluations

External Examinations and Necropsies

After the study duration, every single rabbit was sacrificed and underwent a thorough necropsy. The gross findings that might point to abnormalities were noted. During an in situ examination, the individual organs were investigated for histomorphological anomalies.

Organs Weights and Histopathology

The organs were collected and weighed after the gross pathology examination was finished. The ratios of organ weight to body weight were calculated. For histopathological examination, 10% buffered formalin preserved the organs.

2.8. Statistical Analysis

Mean + SD was used to represent all of the data. Using GraphPad software, the findings were all put through statistical analysis with a significance level (of 0.05). The Student's *t*-test (safety study—organ and body weights, clinical and hematological parameters) and non-parametric one-way ANOVA (Kruskal–Wallis) tests (safety study—IOP, inflammatory marker assessment; efficacy study—changes scar intensity, scar area, and E:S ratios) were used to analyze the data.

3. Results

3.1. Characteristic Analysis of hLMSCs

3.1.1. Phenotypic Assessment of hLMSCs

Col-III, p63-α, Pax6, and ABCG2 were both expressed positively by the cells. As expected, mesenchymal biomarkers such as CD73, VIM, CD73, CD105, and CD90 were expressed positively, but CD45 was not. Overall, the phenotypic expression of the hLMSCs of the biomarkers was found to be unaltered (Figure 2A).

3.1.2. Evaluation of the Viability and Stability of hLMSCs

Karyotyping revealed no numerical or chromatic aberrations in either of the En− or En+ hLMSC cell populations (Figure 2B). At the end of six hours, 88.33 ± 2.37% of the pelleted hLMSCs were still alive, while at the end of 24 h, 78.21 ± 1.47% of the cells were still alive (Figure 2C). The doubling time of hLMSCs was less than 61 h, according to the growth kinetics studies. In both of the En−/En+ hLMSCs that were administered to the study's test animals, there was no evidence of Mycoplasma species contamination. The En− hLMSCs and En+ hLMSCs cell suspensions had levels of bacterial endotoxins that were within the acceptable range (<0.12 EU/mL).

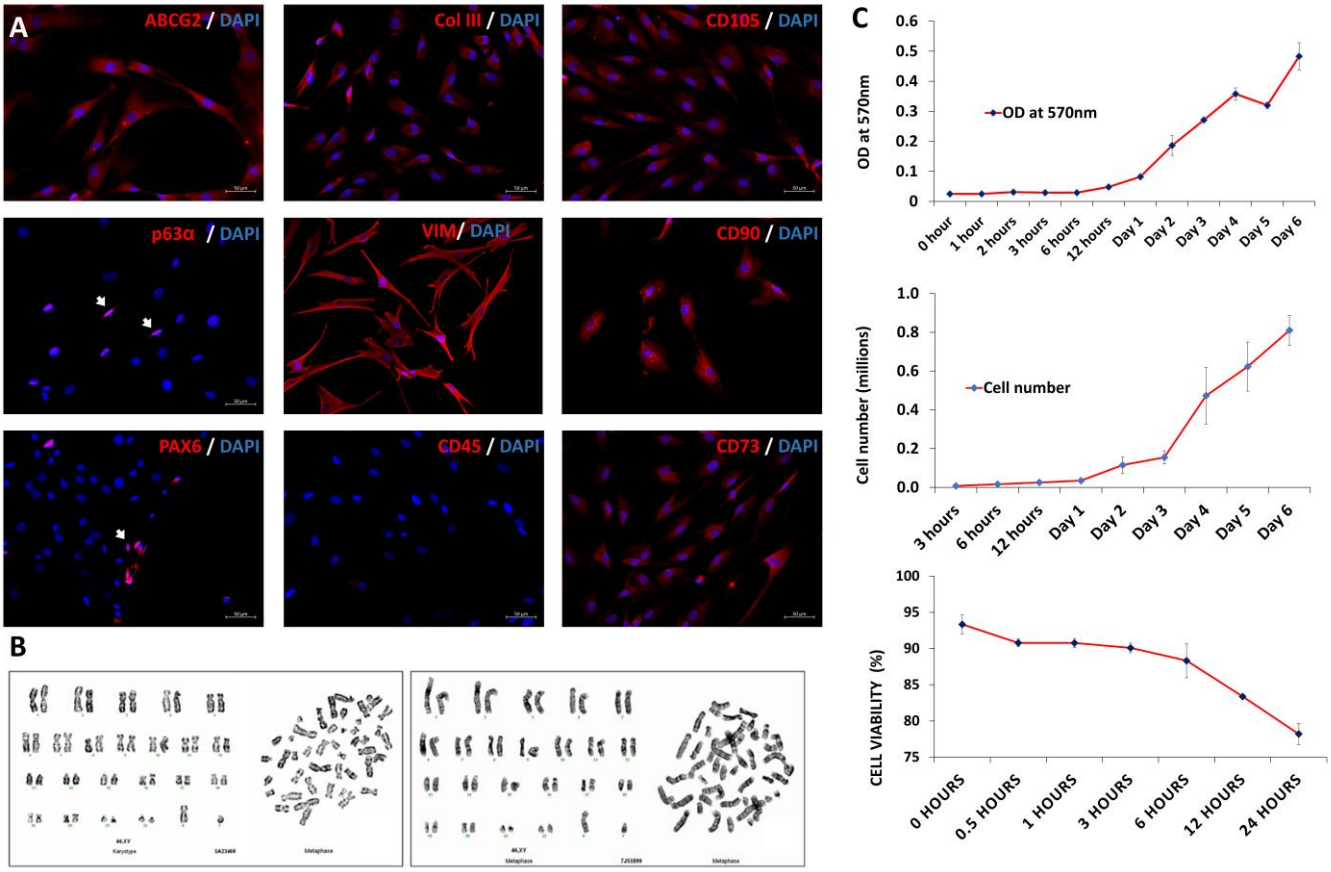

Figure 2. hLMSC phenotyping and stability. (**A**) Immunostaining assessment of the hLMSC phenotype before administering them to rabbit corneas. The panel shows stem-cell biomarkers (p63+, Pax6+, ABCG2+) and mesenchymal biomarkers (VIM+, CD45−, CD73+, CD90+, and CD105+) stained red against DAPI, nuclear stain (blue). 40×; 50 µM. (**B**) Karyotyping of hLMSCs before and after encapsulation and transport (n = 3). Both groups showed no numerical or significant reforms. (**C**) Top graph shows the hLMSC growth in culture. Third-passage cells were seeded in equal numbers into well plates and assessed via the MTT assay for 7 days (n = 3). The 570 nm absorbance was plotted against culture duration. The dye-exclusion graph of the hLMSC culture growth (middle). The bottom graph shows the viable cell percentage in pellet at various time points when stored at 2–8 °C. The hLMSCs were stable with 90.09 ± 0.06 percent viability at 3 h and 88.33 ± 2.37 percent viability at 6 h (n = 3), the timeframe for corneal transplantation.

3.2. Comparison of the Effectiveness of the hLMSCs with and without the Incorporation of Alginate

Debridement of the corneal epithelium and stroma successfully led to the formation of scarring or haze (Figure 3). The reepithelization of the cornea was observed to happen more or less in the first two weeks in all groups. Groups that received hLMSCs in both the scar and prophylaxis groups were found with similar levels of tissue regeneration and the restoration of the transparency in terms of the scar intensity (Figures 4 and 5A,B,D,E).

3.2.1. Change in Corneal Haze

In both the prophylaxis and scar groups, the intensity of the corneal scar or haze in the eyes that received En−/En+ hLMSCs decreased toward the conclusion of the investigation in comparison to the pre-treatment ($p < 0.0001$, n = 6). In mice that received En− and En+ hLMSCs, the intensity of corneal haze decreased from 164 ± 12 GSU and 164 ± 11 GSU on day 14 of scar formation to 121 ± 6 GSU and 124 ± 11 GSU at the end of day 28 (Figure 5A–C).

In a similar vein, the prophylaxis group's haze decreased to 138 ± 19 and 136 ± 11 GSU on day 28 after treatment, as opposed to 151 ± 14 and 173 ± 13 GSU on day 1 of the wounding and transplantation of En+ hLMSCs, respectively (Figure 5B). In contrast, there was no significant change in the corneal scar intensity in the eyes that received the sham treatment or no treatment (Figure 5A,C) compared to the baseline prior to transplantation.

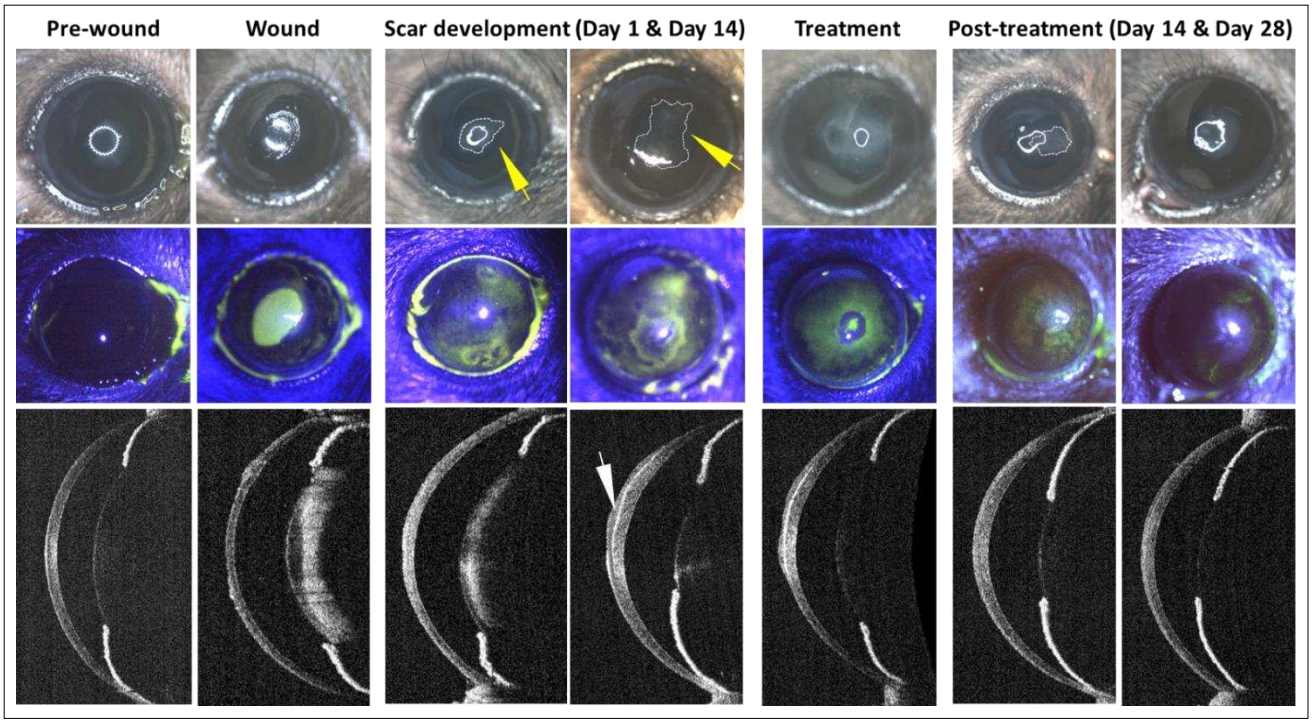

Figure 3. Generation of the corneal scar, treatment, and clinical follow-up. Collage of the representative (scar group) clinical photographs (top row) of the normal corneal surface (pre-wound) before debriding the central cornea (wound), and the respective fluorescein staining images confirming the compromised epithelial integrity (middle row). The debrided corneas developed clouding or haze (marked with a dotted line, indicated with a yellow arrow) on day 1 after the debridement and by the end of two weeks, the debrided area developed a scar. The respective OCT scan on the lower panel shows the scarring in the anterior stroma (indicated by a white arrow) and altered corneal thickness. The scarred tissue was scraped away and treated with hLMSCs (treatment) in fibrin glue. The OCT scan on day 28 post-treatment shows stabilized corneal transparency relative to the scarred sections.

3.2.2. Reduction in the Scar Area

The scarred corneal surface area gradually decreased in all treatment arms (Figure 5D,E) after En− and En+ hLMSC treatment, over the course of the two-week scar development period. From day 7 of scar development to day 28 of treatment, the mice that received the sham treatment maintained corneal scarring of the same size (Figure 5D,E).

By the end of the study, the eyes that received En−/En+ hLMSCs immediately after debridement had a level of scarred corneal surface that was consistent, with a slight decrease in the area that was statistically insignificant ($p = 0.0875$). On the other hand, similar to the scar ($p < 0.001$, Figure 5D) and untreated ($p < 0.0001$, Figure 5F) groups, the eyes that received the sham treatment prophylactically displayed an increase in the scarred area that remained unchanged throughout the follow-up.

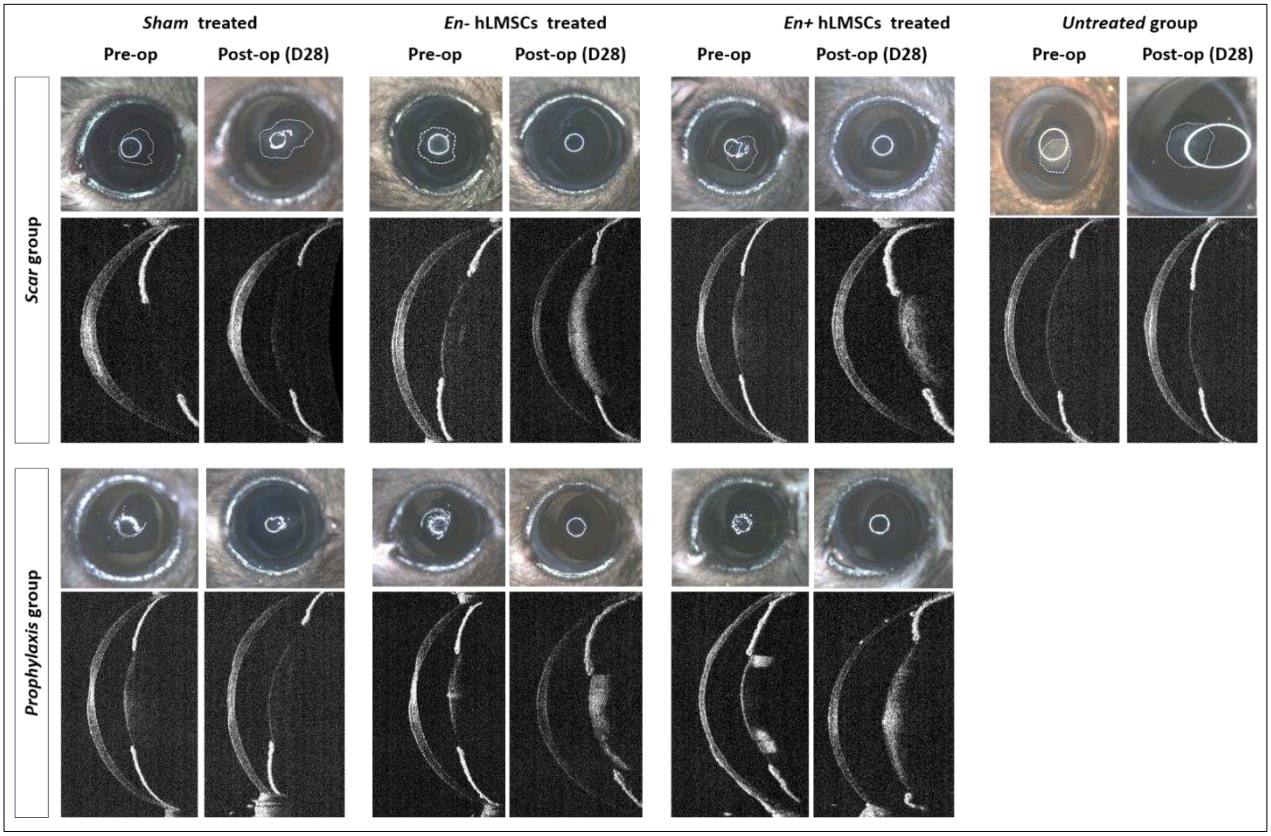

Figure 4. Outcomes of the treatment with hLMSCs: Collage of representative microphotographs and scans showing the scarring of debrided corneas before and after treatment with hLMSCs. Eyes of the untreated and sham treated arms show the unhealed corneas post debridement/treatment. Eyes treated with En−/En+ hLMSCs showed relatively clear corneas with less haze and scarring.

3.2.3. Epithelium to Stroma Reflectivity

Before any wound was made, the average E:S reflectivity ratio of the three groups ranged from 0.87 ± 0.03 to 0.96 ± 0.01.

While the eyes that received En−/En+ hLMSCs were able to normalize to the baseline E:S ratio in all of the treated arms (Figure 5G,H), this ratio was found to gradually de-crease in the untreated (0.96 ± 0.01 to 0.65 ± 0.02) or sham-treated arms (scar: 0.93 ± 0.04 to 0.68 ± 01 and prophylaxis: 0.96 ± 0.01 to 0.76 ± 0.1) in all of the groups, indicating the elevated stromal reflectivity (Figure 5I).

3.3. Determination of the Safety and Toxicity of hLMSCs

3.3.1. Clinical Symptoms, Body Weights, and Death Rate

All of the animals in the sham and test (En+/En− hLMSC) groups showed no clinical signs. In both the sham and test groups, there was no mortality. When compared to the control group, a normal weight increase was determined to have occurred in all of the test groups (Supplementary Figure S1).

3.3.2. Ophthalmic Observations and IOP

It was found that all of the ophthalmic findings were normal. However, at the three-hour time point, the left conjunctivas of all three groups showed Grade 1 ocular inflammation. At the 6 h time point, the same happened to one of the six sham group animals and to all animals in the En− hLMSC group. From the 12th hour onward, there were no symptoms of ocular irritation observed. In all three groups, the contralateral (normal) eyes did not exhibit any ocular lesions and remained normal at all time points throughout the study (Figure 6 and Supplementary Table S2).

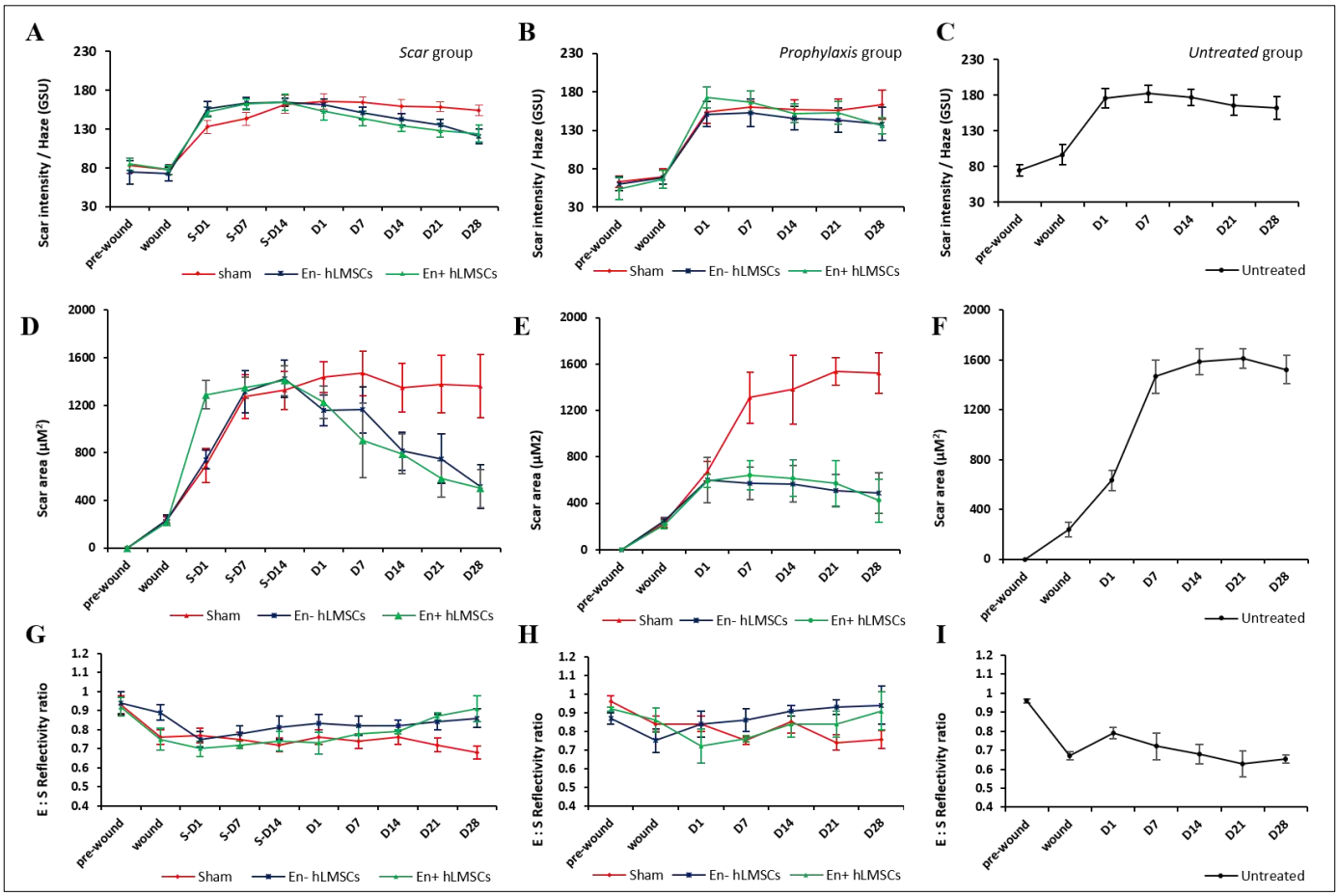

Figure 5. Changes in the corneal scar intensity, area, and reflectivity. (**A**–**C**) Graph plots showing the relative decrease in the corneal haze or the scar intensity of the murine eyes treated with encapsulated and non-encapsulated hLMSCs, and both. Corneas treated with vehicle alone (sham) or left untreated remained without any significant change up to the endpoint of the study. (**D**–**F**) Graph plots showing the reduction in the size of the corneal scars. Mice treated with hLMSCs after scar development (**D**) showed a significant decrease ($p < 0.0001$, n = 8) in the scar area, relative to pre-treatment (S-D1 to S-D14), whereas the mice that received hLMSCs prophylactically did not show any significant ($p = 0.08$, n = 8) increase in the scar area. (**G**–**I**) The reflectivity of the corneal surface normalized to the baseline readings in the eyes that received hLMSCs in both the scar (**G**) and prophylaxis (**H**) groups. The reflectivity of the stroma increased in eyes that received the sham (**G,H**) or no treatment (**I**).

In all three groups, the intraocular pressure was found to be comparable within the normal range. The IOP of the treated eyes in either the test group or the control group was not significantly dissimilar from the sham or control group. In all groups, the IOP of the opposite eye (normal) also did not change significantly, with the exception of a single time point, day 28 (Figure 6 and Supplementary Table S3).

3.3.3. Evaluation of Immunogenicity and Inflammatory Markers

The rabbit sera showed that the inflammatory markers TNF-α and IL-6 declined. In both test groups (En+/En− hLMSCs), the mean concentrations of these analytes were found to decrease in a manner that was comparable to that of the control group (G1) (Figure 7E,F). The outliers were a few occurrences in the very early stages (level of TNF-α in tears at hours 1 and 3 after treatment), and it was discovered that the TNF-α and IL-6 levels, two inflammatory chemicals, were pointedly low and also seen to decline throughout the study (Figures 6C and 7B). At five of the eight time points, the serum IgE levels in the En+ hLMSC group were higher than those of the other two groups (Figure 7D). In contrast,

except for the first and third hours of treatment for the En−hLMSC group, IgE levels in the tear samples were shown to decrease (Figure 7A). In general, all three groups maintained comparable levels of IgE in the tears.

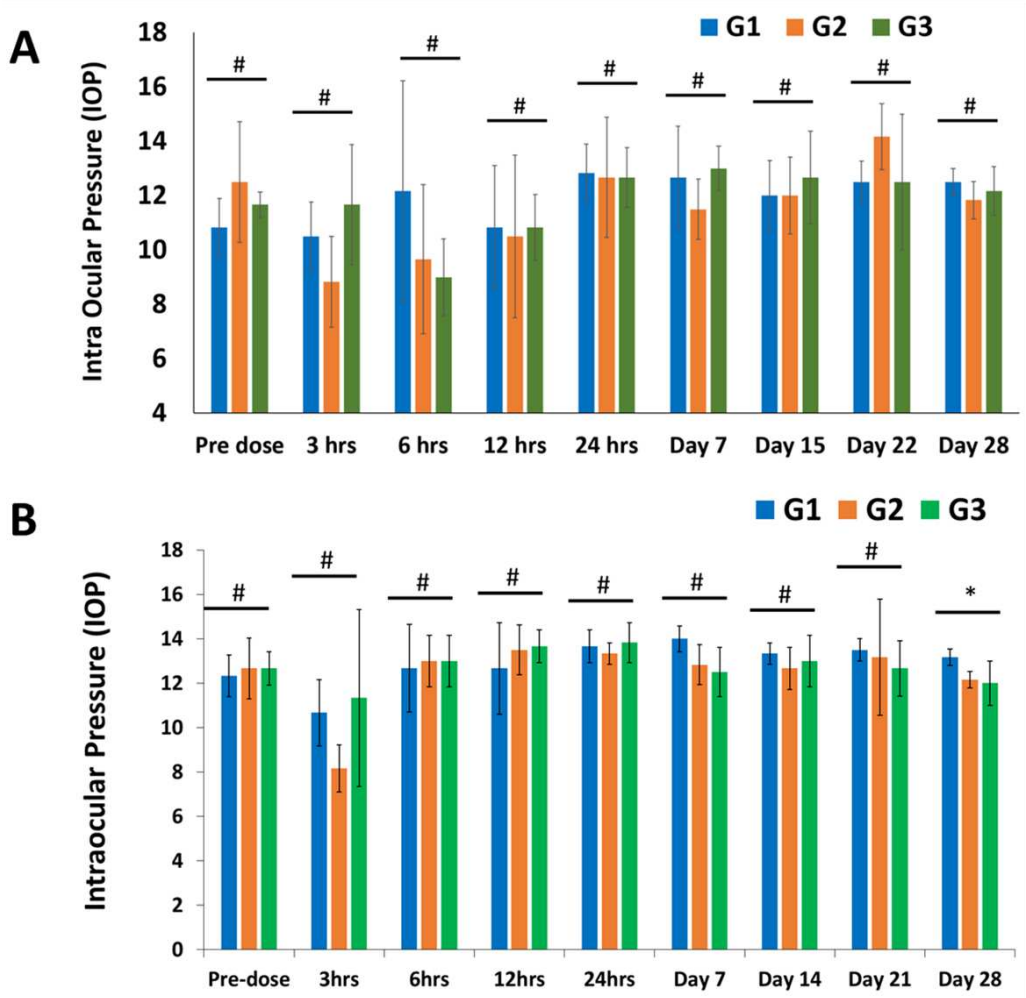

Figure 6. Changes in the intraocular pressure of the rabbits at different study time points. (**A**) Intraocular pressure (IOP) was monitored before and after treatment and is depicted as a bar graph. Comparing the experimental groups (G2 and G3) to the control group, no statistically significant differences were found in IOP levels (G1). n = 6; * $p < 0.05$, # $p > 0.05$. (**B**) Intraocular pressure (IOP) variations in healthy eyes, represented as a bar graph. Except for one time point, there were no statistically significant differences between the IOP levels of the experimental groups (G2 and G3) and the control group (G1) (Day 28). n = 6; * $p < 0.05$, # $p > 0.05$. G1—Sham treated group; G2—Treated with En− hLMSCs; G3—Treated with En+ hLMSCs.

3.3.4. Hematology

The sham and test item transplanted groups (En+/En− hLMSCs) had similar hematological values (Supplementary Table S5). The bone marrow showed no hematopoietic system changes. In the sham/control group, no test group showed erythropoiesis, granulopoiesis, or lymphopoiesis. Supplementary Table S5 shows that none of the G1, G2, or G3 animals had hypocellularity, hypercellularity, or hypochromatism.

One G1 and G2 rabbit produced granulopoietic cells. These modifications were absent in G3 (En+ hLMSCs) granulopoietic cells. The cells did not impact granulopoietic activity in comparison to the sham group. Some animals in the control and hLMSC transplanted groups showed changes in granulopoietic activity, indicating that their immune systems spontaneously changed.

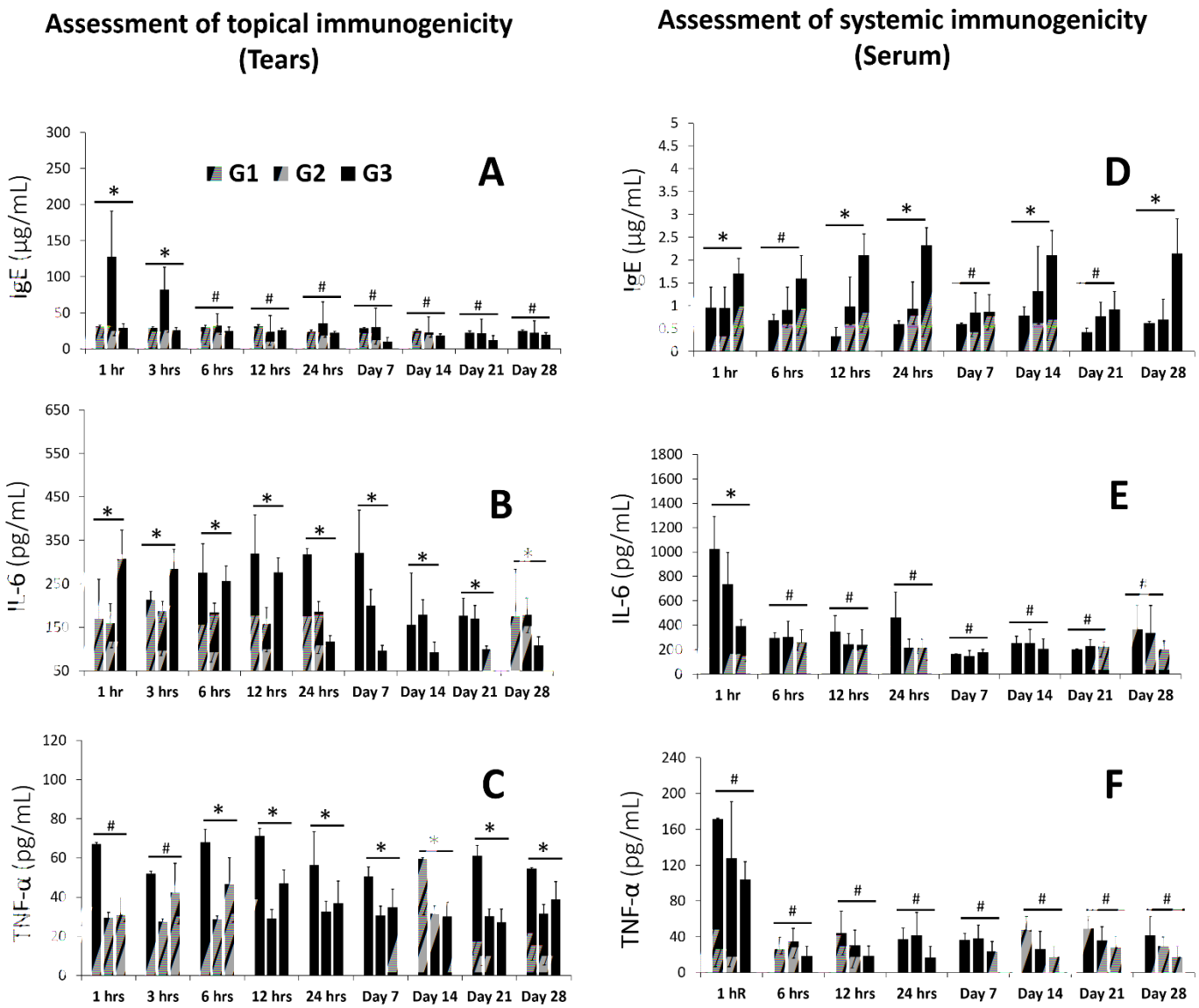

Figure 7. Serum and tear levels of IgE, IL-6, and TNF-α after treatment with En+/En− hLMSCs in rabbits. (**A**–**C**) Bar charts displaying the ELISA-determined concentrations of the cytokines IgE, IL-6, and TNF-α in rabbit serum. (**D**–**F**) Quantitative analysis of rabbit tear samples for the cytokines interleukin (IL)-6, tumor necrosis factor α, and interleukin (IL)-1 presented as bar graphs. Both the experimental and control groups showed a downward trend in cytokine levels, suggesting that there was no localized toxicity in the eyes of the recipients. * $p \leq 0.05$; # $p > 0.05$. G1—Sham treated group; G2—Treated with En− hLMSCs; G3—Treated with En+ hLMSCs.

Bone marrow smears taken from all of the animals in groups G1, G2, and G3 indicated that there was no toxicity or dose-dependent change in the synthesis of precursor cells for myeloid, erythroid, or lymphoid cells. This was the case in comparison to the "sham" or "control" group, which was given zero doses of the cells.

3.3.5. Clinical Chemistry

Except for the following observations, all of the clinical chemistry values were found to be normal. When compared to the sham group, the levels of phosphorus in the G3 group were higher (7.35 ± 1.11 mg/dL) (5.83 ± 0.39 mg/dL). Total proteins decreased by 5.63 ± 0.38 g/dL, globulin decreased by 3.27 ± 0.21 g/dL, and sodium decreased by 153.26 ±5.01 mmol/L in the G2 group. When compared to the animals in the sham

group, the level of sodium in the G3 group animals was lower (152.47 ± 1.86 mmol/L) (Supplementary Table S6). The internal organs of the animals were unaffected by the observed changes.

3.3.6. Organ Weights, Gross Observations, and Necropsy

In all animal groups, both external and internal examinations of the organs revealed no abnormalities (Supplementary Tables S7 and S8). In each of the G2 and G3 groups, the organ weights were found to be normal. When compared to the animals in the control group, the test item administered animals underwent no significant changes.

3.3.7. Histopathology

Compared to the control group, the majority of organs did not show any abnormal findings or changes (Supplementary Table S8).

Two rabbits from each group—the G1, G2, and G3 groups—had sinusoidal hemorrhages in their livers [2 of 6]. One animal from the G1 group showed necroses and infiltration of inflammatory cells, but the livers of the other groups were unaffected. Five G1 and five G2 animals had alveolar thickening or inflammation.

One animal of the G2 group and the G3 group both had kidneys with tubular degeneration. All groups—G1 group [3 animals], G2 group [1 animal], and G3 group—were found to have foci of tubular or interstitial inflammation. Two G1 and one G2 animals had cerebral hemisphere necrosis, and G3 did not show brain alterations. One G1 male, one G2 male, and one G3 female developed submucosal lymphoid tissue hyperplasia in their ilium mucosa.

However, when compared to the G1 group, the ileum, lung, liver, kidney, eye, and kidneys showed no dose-related adverse effects. Since these organ lesions emerged in both the vehicle control group and the test item group, it is possible that they developed on their own. Additionally, there were no consistent or significant lesions in these organs between the vehicle control animals and animals given the test item. In conclusion, none of the systemic organs underwent significant reactive or toxic changes (Supplementary Tables S7 and S8).

4. Discussion

In recent years, numerous potential treatments for corneal opacification and scarring other than corneal transplantation have emerged. Biomimetic hydrogels, cell-based methods, and molecular methods are examples of these. Different hydrogels—with or without cells—have been demonstrated in several studies to be an effective option for stromal replacement using donor tissue. [33–36]. Exosomes [37], anti-TGF- [6,7,38], anti-PDGF [7,39,40], and HGF [41,42] have all been shown to play a role in either preventing or reversing corneal scars. During wound healing, researchers have found that corneal scars can be repaired in two ways: by reversing the conversion of myofibroblasts to fibroblasts or by inhibiting TGF-/SMAD signaling [4,43–46]. In the past few years, hLMSCs have demonstrated promising latent for non-scarring wound healing from various pathologies [4]. When these cells are encased in alginate, it has also been demonstrated that they maintain their characteristic properties and have a longer shelf life when subjected to a variety of temperature conditions [25]. Without the need for costly cold-chain systems, alginate encapsulation can make it easier for these cells to travel over long distances. As stromal scarring or opacification-related corneal blindness prevalence is highest in developing nations, more affordable and simpler transportation will make patients in remote areas more accessible to cell-based treatments at lower costs. The aim of this study was to determine the toxicity of hLMSCs after they were applied topically to rabbit corneas and their potential in healing and preventing corneal scars in a murine model.

According to previously reported studies [25], the limbus-isolated LMSC donor corneas were cultivated in a CGMP-grade cell culture suite. After topical treatment on rabbit and mouse eyes with corneal lesions and scars, the efficacy and toxicity of LMSCs encapsulated in alginate and transited for three days and those not encapsulated were

assessed. The vehicle served as a sham for the control group, which received no cells. After the treatment, clinical imaging and optical coherence tomography were used to examine the eyes of mice for a period of four weeks. Through ophthalmic, hematological, and tissue examinations of the rabbits, comprehensive evaluations of the toxicity to the system as well as the eyes were carried out. Throughout the course of the study, there was no mortality in the animals.

In groups that received therapeutic (scar group) or prophylactic (prophylaxis group) treatment for the murine eyes, the scarring was cleared or prevented. When compared to the sham-treated or untreated groups, these arms showed a decrease in corneal haze, or scar area and intensity.

At the conclusion of the safety study, all rabbits were sacrificed, and all major organs including the eyes were taken and examined histologically in detail. The intraocular pressure of the treated rabbits did not significantly change during the ophthalmic examinations (Figure 7 and Supplementary Table S2), which also revealed normal observations of IOP (Supplementary Tables S2 and S3 and Figure 7). In all three groups, the hematological examination parameters were comparable (Supplementary Table S5). Histopathological examination revealed no abnormalities in the corneal tissues (Figure 8). Against the sham group, neither the tears nor the sera of the experimental groups displayed any significant signs of an inflammatory response (TNF-α and IL-6) (Figure 7A–F). This study offers additional proof for the safety of hLMSCs, suggesting that human clinical trials may evaluate these cells for clinical applications.

Regenerative medicine's recent advancements have made it possible to treat a wide range of diseases and disorders. One of the main therapies being tested in clinical trials around the world for their efficacy in treating heart, ear, bone, and eye diseases is mesenchymal stem cell therapy [47,48]. However, guaranteeing the patient's safety is the most crucial element and the top concern of any clinical investigation or pharmaceutical development process. In order to determine the toxicity or safety profile of the drug or cell product, preclinical testing and compliance with various regulatory requirements are required. MSCs derived from bone marrow have been shown to be safe and effective for corneal repair in a recent study by Putra et al. [49]. The aforementioned study was carried out in advance of the Phase I clinical trial. However, the safety of GMP-manufactured human limbus-derived MSCs for upcoming clinical trials is poorly documented in the literature. The Drug Controller General of India, part of the Central Drugs Standards Control Organization (CDSCO), regulates India's pharmaceuticals as the FDA does in the U.S. According to The Government of India's Drugs and Cosmetics Rules, 2018 (Schedule Y) [31,50], these bodies require the safety evaluation of each drug and surgical procedure [31,50]. In this study, hLMSCs were evaluated in accordance with the above laws and the Good Laboratory Practice (GLP) guidelines by the OECD. It has been demonstrated that encapsulating corneal epithelium and hLMSCs in sodium alginate [25,51] may increase the cells' shelf life, enabling room-temperature transport while maintaining their distinctive phenotype and vitality. With the potential to considerably reduce associated expenses, this technique significantly improves the costs of this new advanced cell-based therapy. Because it eliminates the time-consuming and costly cold-chain transport and has the potential to considerably reduce associated expenses, this technique significantly improves the finances of this new advanced cell-based therapy.

In the scar group that were treated after the scar developed, the cross-sections of murine corneas in the OCT scans revealed a significant reduction in the area affected by scarring (Figure 5D). In the group that received the En−/En+ hLMSCs prophylactically, there was also a decrease in the scar area (Figure 5E), but it was not statistically significant. However, all of the groups that received hLMSCs had significantly less corneal haze (Figure 5A,B). In terms of the scar area and intensity of the treated corneas, the groups that received sham or no treatment had comparable outcomes (Figure 5C,F). This clearly demonstrates that the hLMSCs assist in the repair of corneal wounds or scars.

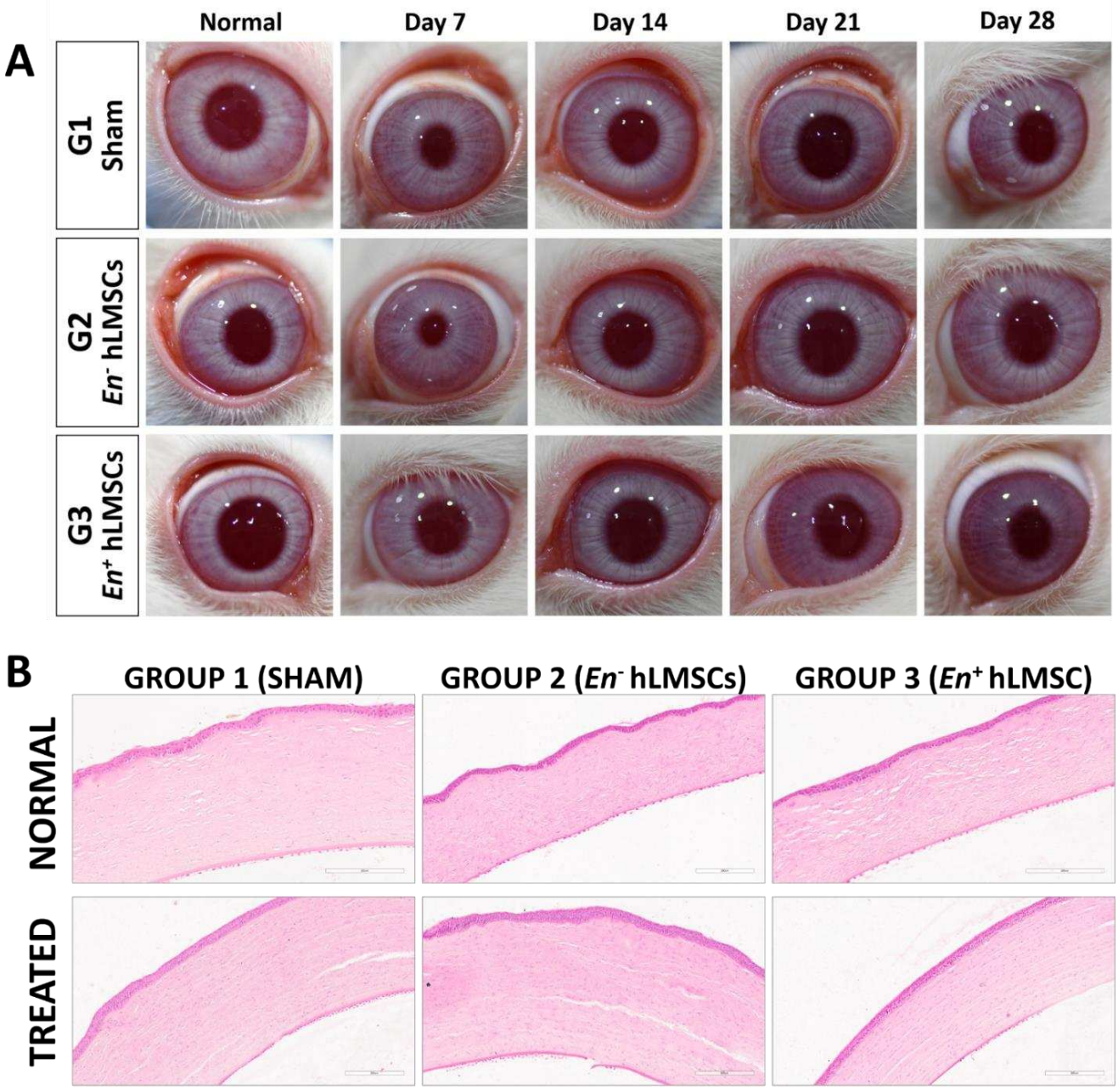

Figure 8. Rabbit eyes and corneal histopathology after En+/En− hLMSC treatment. (**A**) Clinical photographs of normal and injured rabbit eyes taken over a 28-day period showed no evidence of inflammation or irritation in the injured eyes. The Nikon D7200 and Nikon AF-S VR Micro-NIKKOR 105 mm f/2.8 G IF-ED lens were used to take the images. (**B**) Histopathological sections of normal and treated corneas represented by a panel of representative photomicrographs. Magnification: 40×; Scale: 200 µM. Group 1 received no treatment (sham group); Group 2 received En−hLMSCs; and Group 3 received En+ hLMSCs.

In addition, during the same time period following treatment, the scar area had diminished to numbers that were comparable (ranging from 412 to 488 microns in the prophylaxis group and 501 to 512 microns in the scar groups). This degree of similarity in the scar area demonstrates that the hLMSCs are able to restore the damaged corneal surface without causing any scarring and heal corneal scars (scar group, treated two weeks after scar development). Additionally, it demonstrates that the alginate encapsulation has no effect on the efficacy of hLMSCs (Figure 5A,B,D,E).

In the arms of both the scar and prophylaxis groups that received hLMSCs, the corneal surface transparency returned to its pre-debridement readings (Figure 5G,H). The transparency of the cornea was impacted by the increased reflectivity of the stromal surface in the eyes of the untreated group (Figure 5I). The untreated groups' corneal reflectivity increased by 32.3%, while the scar and prophylaxis groups' reflectivity increased by 26.7 percent and 20.8 percent, respectively, in the sham-treated arms.

According to the rather small amounts of cytokine molecules IL-6 and TNF-α in the tears, the evaluation of inflammatory cytokines demonstrated that these cells did not cause eye toxicity (Figure 7B,C). Similar findings were made regarding the systemic toxicity of these cells from the levels of the analytes TNF-α (Figure 7F) and IL-6 (Figure 7E) in the rabbits' blood serum. At specific time points, animals that were given cells released from transit had significantly higher levels of IgE molecules than the control/sham group and the group treated with non-encapsulated cells, indicating any potential allergens. However, neither the amounts of IgE in the tears of the hLMSC-treated animals nor the varying levels of IgE were accompanied by a clear trend (Figure 7D). The TNF-α and IL-6 expression in the tear samples were significantly lower in both experimental arms (Supplementary Table S4 and Figure 7B,C). In addition, no ocular lesions were observed after 12 h post-treatment until the study's conclusion, and eye examination proved to have insignificant variations in IOP levels (Figure 6 and Supplementary Table S3). According to the results of the histopathological examinations (Figure 8 and Supplementary Tables S7 and S8), the variations that were observed in the clinical chemistry parameters (Supplementary Table S6) and hematological indicators (Supplementary Table S5) did not affect the systemic organs. In addition, the data in Figure 5B demonstrate the stability of the cells, sterility, and no chromosomal abnormalities support the safety of the cells for human testing.

The fact that this study was conducted at a GLP-certified animal facility with a NABL accreditation (National Accreditation Board for Testing and Calibration Laboratories) facility is a strength. Veterinarians, biochemists, and pathologists were all hidden from the intervention under investigation. Compared to the previous study [25], this one did not include the hLMSCs transiting for more than three days after alginate encapsulation, which may be a limitation. However, this time frame was chosen in light of the fact that the cells would be able to reach any faraway part of the country within three days of being distributed. It is possible that by evaluating tears from an untreated or healthy eye, ocular toxicity may have been better assessed. These LSMCs were solely applied to the corneal surface in this study, which is also the planned route of administration for the clinical trials. However, introducing these hLMSCs to the subconjunctival area might provide the possibility of investigating not just the various delivery mechanisms, but also their safety. This will be investigated in the future.

5. Conclusions

The purpose of our study was to establish the efficacy and toxicity of hLMSCs in wounded rabbits and murine corneas, and whether they were encapsulated in alginate or not. Our study suggests that the hLMSCs are safe because they do not harm the recipient and do not cause any inflammatory response. hLMSCs are able to repair traumatized tissues and effectively restore corneal surface transparency. This ensures that these cells can be used on humans to test their efficacy in treating corneal wound healing. In the end, this will make them more affordable and available to people in the most remote places, eliminating the need for long-distance travel.

Supplementary Materials: The following supporting information can be downloaded at: https://www.mdpi.com/article/10.3390/cells12060876/s1, Figure S1: The rabbit's relative body weight growth (%) after hLMSC therapy; Table S1: Ophthalmic lesion grading; Table S2: Summary of ocular lesions in ophthalmic observations; Table S3: Serial evaluation of IOP after treatment with *En+/En-* hLMSCs; Table S4: Serum and tear immunological and inflammatory markers after En+/En- hLMSCs treatment; Table S5: Hematological observations made on rabbits following treatment with hLMSCs; Table S6: Rabbit clinical chemistry after En-/En+ hLMSC treatment; Table S7: Summary of histopathological observations of rabbit organs post-treatment with hLMSCs; Table S8: Organ weight summaries after hLMSC treatment in rabbits.

Author Contributions: Conceptualization, M.D., V.S. and S.B.; Methodology, M.D., N.P., A.S., V.S. and S.B.; Validation, M.D., V.S. and S.B.; Formal analysis, M.D., V.S. and S.B.; Investigation, M.D., N.P. and A.S; Resources, V.S. and S.B.; Data curation, S.B. and V.S.; Writing—original draft preparation, M.D.; Writing—review and editing, M.D., A.S., V.S. and S.B.; Visualization, M.D., V.S. and S.B.; Supervision, V.S. and S.B.; Project administration, V.S. and S.B.; Funding acquisition, V.S. and S.B. All authors have read and agreed to the published version of the manuscript.

Funding: This research was funded by the Science and Engineering Research Board, Government of India, grant number EMR/2017/005086. This work was supported in part by the Hyderabad Eye Research Foundation, Hyderabad, India. MD thankfully acknowledges the Senior Research Fellowship grant, File No. 2020-7055/CMB-BMS, from the Indian Council of Medical Research, Government of India.

Institutional Review Board Statement: The study was conducted in accordance with the Declaration of Helsinki, and approved by the Institutional Ethics Committee of LV Prasad Eye Institute (LEC 05-18-081, approved on 22 May 2018) and the Institutional Committee for Stem Cell Research (IC-SCR-Ref No:08-18-002, approved on 24 August 2018). The animal study protocol for the safety study was approved by the Committee for the Purpose of Control and Supervision of Experiments on Animals (CPCSEA) of SIPRA Labs Limited, Hyderabad (SLL/PCT/IAEC/110-19, approved on 22 January 2020). The animal study protocol for efficacy study was approved by the Institutional Animal Ethics Committee (IAEC) of the Center for Cellular and Molecular Biology, Hyderabad (IAEC 92/2019, approved on 15 March 2019).

Informed Consent Statement: Informed consent was obtained from the next-of-kin of all the donors. The consent forms are available at the Ramayamma International Eye Bank, Hyderabad.

Data Availability Statement: Data are available on request due to institutional policies.

Acknowledgments: We thank the Ramayamma International Eye Bank, LV Prasad Eye Institute for providing the cadaveric corneas.

Conflicts of Interest: The authors declare no conflict of interest. The funders had no role in the design of the study; in the collection, analyses, or interpretation of data; in the writing of the manuscript, or in the decision to publish the results.

References

1. Maurice, D.M. The Structure and Transparency of the Cornea. *J. Physiol.* **1957**, *136*, 263–286. [CrossRef] [PubMed]
2. Meek, K.M.; Boote, C. The Organization of Collagen in the Corneal Stroma. *Exp. Eye Res.* **2004**, *78*, 503–512. [CrossRef] [PubMed]
3. Funderburgh, J.L.; Mann, M.M.; Funderburgh, M.L. Keratocyte Phenotype Mediates Proteoglycan Structure: A Role for Fibroblasts in Corneal Fibrosis. *J. Biol. Chem.* **2003**, *278*, 45629–45637. [CrossRef] [PubMed]
4. Basu, S.; Hertsenberg, A.J.; Funderburgh, M.L.; Burrow, M.K.; Mann, M.M.; Du, Y.; Lathrop, K.L.; Syed-Picard, F.N.; Adams, S.M.; Birk, D.E.; et al. Human Limbal Biopsy-Derived Stromal Stem Cells Prevent Corneal Scarring. *Sci. Transl. Med.* **2014**, *6*, 266ra172. [CrossRef] [PubMed]
5. Jester, J.V.; Rodrigues, M.M.; Herman, I.M. Characterization of Avascular Corneal Wound Healing Fibroblasts. New Insights into the Myofibroblast. *Am. J. Pathol.* **1987**, *127*, 140–148.
6. Torricelli, A.A.M.; Santhanam, A.; Wu, J.; Singh, V.; Wilson, S.E. The Corneal Fibrosis Response to Epithelial-Stromal Injury. *Exp. Eye Res.* **2016**, *142*, 110–118. [CrossRef]
7. Singh, V.; Santhiago, M.R.; Barbosa, F.L.; Agrawal, V.; Singh, N.; Ambati, B.K.; Wilson, S.E. Effect of TGFβ and PDGF-B Blockade on Corneal Myofibroblast Development in Mice. *Exp. Eye Res.* **2011**, *93*, 810–817. [CrossRef]
8. Wilson, S.E. TGF Beta -1, -2 and -3 in the Modulation of Fibrosis in the Cornea and Other Organs. *Exp. Eye Res.* **2021**, *207*, 108594. [CrossRef]

9. Thompson, R.W.; Price, M.O.; Bowers, P.J.; Price, F.W. Long-Term Graft Survival after Penetrating Keratoplasty. *Ophthalmology* **2003**, *110*, 1396–1402. [CrossRef]
10. Coster, D.J.; Williams, K.A. The Impact of Corneal Allograft Rejection on the Long-Term Outcome of Corneal Transplantation. *Am. J. Ophthalmol.* **2005**, *140*, 1112–1122. [CrossRef]
11. Williams, K.A.; Lowe, M.; Bartlett, C.; Kelly, T.-L.; Coster, D.J. All Contributors Risk Factors for Human Corneal Graft Failure within the Australian Corneal Graft Registry. *Transplantation* **2008**, *86*, 1720–1724. [CrossRef]
12. Mittal, S.K.; Omoto, M.; Amouzegar, A.; Sahu, A.; Rezazadeh, A.; Katikireddy, K.R.; Shah, D.I.; Sahu, S.K.; Chauhan, S.K. Restoration of Corneal Transparency by Mesenchymal Stem Cells. *Stem Cell Rep.* **2016**, *7*, 583–590. [CrossRef] [PubMed]
13. Du, Y.; Funderburgh, M.L.; Mann, M.M.; SundarRaj, N.; Funderburgh, J.L. Multipotent Stem Cells in Human Corneal Stroma. *Stem Cells* **2005**, *23*, 1266–1275. [CrossRef] [PubMed]
14. Kureshi, A.K.; Dziasko, M.; Funderburgh, J.L.; Daniels, J.T. Human Corneal Stromal Stem Cells Support Limbal Epithelial Cells Cultured on RAFT Tissue Equivalents. *Sci. Rep.* **2015**, *5*, 16186. [CrossRef]
15. Funderburgh, J.L.; Funderburgh, M.L.; Du, Y. Stem Cells in the Limbal Stroma. *Ocul. Surf.* **2016**, *14*, 113–120. [CrossRef]
16. Dos Santos, A.; Balayan, A.; Funderburgh, M.L.; Ngo, J.; Funderburgh, J.L.; Deng, S.X. Differentiation Capacity of Human Mesenchymal Stem Cells into Keratocyte Lineage. *Investig. Ophthalmol. Vis. Sci.* **2019**, *60*, 3013–3023. [CrossRef]
17. Du, Y.; Carlson, E.C.; Funderburgh, M.L.; Birk, D.E.; Pearlman, E.; Guo, N.; Kao, W.W.-Y.; Funderburgh, J.L. Stem Cell Therapy Restores Transparency to Defective Murine Corneas. *Stem Cells* **2009**, *27*, 1635–1642. [CrossRef]
18. Coppola, A.; Tomasello, L.; Pitrone, M.; Cillino, S.; Richiusa, P.; Pizzolanti, G.; Giordano, C. Human Limbal Fibroblast-like Stem Cells Induce Immune-Tolerance in Autoreactive T Lymphocytes from Female Patients with Hashimoto's Thyroiditis. *Stem Cell Res. Ther.* **2017**, *8*, 154. [CrossRef]
19. Mitragotri, N.; Damala, M.; Singh, V.; Basu, S. Limbal Stromal Stem Cells in Corneal Wound Healing: Current Perspectives and Future Applications. In *Corneal Regeneration: Therapy and Surgery*; Alió, J.L., Alió del Barrio, J.L., Arnalich-Montiel, F., Eds.; Essentials in Ophthalmology; Springer International Publishing: Cham, Switzerland, 2019; pp. 387–402; ISBN 978-3-030-01304-2.
20. Del Barrio, J.L.A.; El Zarif, M.; de Miguel, M.P.; Azaar, A.; Makdissy, N.; Harb, W.; El Achkar, I.; Arnalich-Montiel, F.; Alió, J.L. Cellular Therapy With Human Autologous Adipose-Derived Adult Stem Cells for Advanced Keratoconus. *Cornea* **2017**, *36*, 952–960. [CrossRef]
21. Basu, S.; Damala, M.; Singh, V. Limbal Stromal Stem Cell Therapy for Acute and Chronic Superficial Corneal Pathologies: Early Clinical Outcomes of The Funderburgh Technique. *Investig. Ophthalmol. Vis. Sci.* **2017**, *58*, 3371.
22. Funderburgh, J.; Basu, S.; Damala, M.; Tavakkoli, F.; Sangwan, V.; Singh, V. Limbal Stromal Stem Cell Therapy for Acute and Chronic Superficial Corneal Pathologies: One-Year Outcomes. *Investig. Ophthalmol. Vis. Sci.* **2018**, *59*, 3455.
23. Singh, V.; Agarwal, H.; Kethiri, A.R.; Damala, M.; Basu, S.; Sangwan, V.S. Immunological Characterization of Chemical Burn-Induced Ocular Surface Pannus in Humans, Rabbits and Mice after Limbal Stem Cell Deficiency. *Investig. Ophthalmol. Vis. Sci.* **2017**, *58*, 1423.
24. Nurković, J.S.; Vojinović, R.; Dolićanin, Z. Corneal Stem Cells as a Source of Regenerative Cell-Based Therapy. *Stem Cells Int.* **2020**, *2020*, 8813447. [CrossRef]
25. Damala, M.; Swioklo, S.; Koduri, M.A.; Mitragotri, N.S.; Basu, S.; Connon, C.J.; Singh, V. Encapsulation of Human Limbus-Derived Stromal/Mesenchymal Stem Cells for Biological Preservation and Transportation in Extreme Indian Conditions for Clinical Use. *Sci. Rep.* **2019**, *9*, 16950. [CrossRef] [PubMed]
26. The Association for Research in Vision and Ophthalmology-Statement for the Use of Animals in Ophthalmic and Vision Research. Available online: https://www.arvo.org/About/policies/statement-for-the-use-of-animals-in-ophthalmic-and-vision-research/#three (accessed on 3 September 2022).
27. Ich-m-3-R2-Non-Clinical-Safety-Studies-Conduct-Human-Clinical-Trials-Marketing-Authorization_en.Pdf. Available online: https://www.ema.europa.eu/en/documents/scientific-guideline/ich-m-3-r2-non-clinical-safety-studies-conduct-human-clinical-trials-marketing-authorization_en.pdf (accessed on 7 November 2022).
28. OECD. *Test No. 405: Acute Eye Irritation/Corrosion*; Organisation for Economic Co-Operation and Development: Paris, France, 2021.
29. Dominici, M.; Le Blanc, K.; Mueller, I.; Slaper-Cortenbach, I.; Marini, F.; Krause, D.; Deans, R.; Keating, A.; Prockop, D.; Horwitz, E. Minimal Criteria for Defining Multipotent Mesenchymal Stromal Cells. The International Society for Cellular Therapy Position Statement. *Cytotherapy* **2006**, *8*, 315–317. [CrossRef] [PubMed]
30. Endotoxin Testing Recommendations for Single-Use Intraocular Ophthalmic Devices—Guidance for Industry and Food and Drug Administration Staff. 9. Available online: https://www.fda.gov/media/88615/download (accessed on 7 November 2022).
31. Schedule Y(Ammended Version)—CDSCO. 48. Available online: https://rgcb.res.in/documents/Schedule-Y.pdf (accessed on 7 November 2022).
32. Posa, A.; Bräuer, L.; Schicht, M.; Garreis, F.; Beileke, S.; Paulsen, F. Schirmer Strip vs. Capillary Tube Method: Non-Invasive Methods of Obtaining Proteins from Tear Fluid. *Ann. Anat.-Anat. Anz. Ann.* **2013**, *195*, 137–142. [CrossRef]
33. McTiernan, C.D.; Simpson, F.C.; Haagdorens, M.; Samarawickrama, C.; Hunter, D.; Buznyk, O.; Fagerholm, P.; Ljunggren, M.K.; Lewis, P.; Pintelon, I.; et al. LiQD Cornea: Pro-Regeneration Collagen Mimetics as Patches and Alternatives to Corneal Transplantation. *Sci. Adv.* **2020**, *6*, eaba2187. [CrossRef]
34. Fernández-Pérez, J.; Madden, P.W.; Ahearne, M. Engineering a Corneal Stromal Equivalent Using a Novel Multilayered Fabrication Assembly Technique. *Tissue Eng. Part A* **2020**, *26*, 1030–1041. [CrossRef]

35. Wang, F.; Shi, W.; Li, H.; Wang, H.; Sun, D.; Zhao, L.; Yang, L.; Liu, T.; Zhou, Q.; Xie, L. Decellularized Porcine Cornea-Derived Hydrogels for the Regeneration of Epithelium and Stroma in Focal Corneal Defects. *Ocul. Surf.* **2020**, *18*, 748–760. [CrossRef]
36. Chameettachal, S.; Prasad, D.; Parekh, Y.; Basu, S.; Singh, V.; Bokara, K.K.; Pati, F. Prevention of Corneal Myofibroblastic Differentiation In Vitro Using a Biomimetic ECM Hydrogel for Corneal Tissue Regeneration. *ACS Appl. Bio Mater.* **2021**, *4*, 533–544. [CrossRef]
37. WO2019169380A1-Stem Cell-Derived Exosomes for the Treatment of Corneal Scarring—Google Patents. Available online: https://patents.google.com/patent/WO2019169380A1/en (accessed on 11 July 2022).
38. Saika, S.; Yamanaka, O.; Okada, Y.; Tanaka, S.-I.; Miyamoto, T.; Sumioka, T.; Kitano, A.; Shirai, K.; Ikeda, K. TGF Beta in Fibroproliferative Diseases in the Eye. *Front. Biosci.-Sch.* **2009**, *1*, 376–390. [CrossRef] [PubMed]
39. Kamiyama, K.; Iguchi, I.; Wang, X.; Imanishi, J. Effects of PDGF on the Migration of Rabbit Corneal Fibroblasts and Epithelial Cells. *Cornea* **1998**, *17*, 315–325. [CrossRef]
40. Kim, W.J.; Mohan, R.R.; Mohan, R.R.; Wilson, S.E. Effect of PDGF, IL-1alpha, and BMP2/4 on Corneal Fibroblast Chemotaxis: Expression of the Platelet-Derived Growth Factor System in the Cornea. *Investig. Ophthalmol. Vis. Sci.* **1999**, *40*, 1364–1372.
41. Miyagi, H.; Thomasy, S.M.; Russell, P.; Murphy, C.J. The Role of Hepatocyte Growth Factor in Corneal Wound Healing. *Exp. Eye Res.* **2018**, *166*, 49–55. [CrossRef]
42. de Oliveira, R.C.; Murillo, S.; Saikia, P.; Wilson, S.E. The Efficacy of Topical HGF on Corneal Fibrosis and Epithelial Healing after Scar-Producing PRK Injury in Rabbits. *Transl. Vis. Sci. Technol.* **2020**, *9*, 29. [CrossRef]
43. Maltseva, O.; Folger, P.; Zekaria, D.; Petridou, S.; Masur, S.K. Fibroblast Growth Factor Reversal of the Corneal Myofibroblast Phenotype. *Investig. Ophthalmol. Vis. Sci.* **2001**, *42*, 2490–2495.
44. Ljubimov, A.V.; Saghizadeh, M. Progress in Corneal Wound Healing. *Prog. Retin. Eye Res.* **2015**, *49*, 17–45. [CrossRef] [PubMed]
45. Medeiros, C.S.; Marino, G.K.; Santhiago, M.R.; Wilson, S.E. The Corneal Basement Membranes and Stromal Fibrosis. *Investig. Ophthalmol. Vis. Sci.* **2018**, *59*, 4044–4053. [CrossRef]
46. Wilson, S.E. Corneal Wound Healing. *Exp. Eye Res.* **2020**, *197*, 108089. [CrossRef]
47. Mathew, B.; Ravindran, S.; Liu, X.; Torres, L.; Chennakesavalu, M.; Huang, C.-C.; Feng, L.; Zelka, R.; Lopez, J.; Sharma, M.; et al. Mesenchymal Stem Cell-Derived Extracellular Vesicles and Retinal Ischemia-Reperfusion. *Biomaterials* **2019**, *197*, 146–160. [CrossRef]
48. Bagno, L.; Hatzistergos, K.E.; Balkan, W.; Hare, J.M. Mesenchymal Stem Cell-Based Therapy for Cardiovascular Disease: Progress and Challenges. *Mol. Ther.* **2018**, *26*, 1610–1623. [CrossRef] [PubMed]
49. Putra, I.; Shen, X.; Anwar, K.N.; Rabiee, B.; Samaeekia, R.; Almazyad, E.; Giri, P.; Jabbehdari, S.; Hayat, M.R.; Elhusseiny, A.M.; et al. Preclinical Evaluation of the Safety and Efficacy of Cryopreserved Bone Marrow Mesenchymal Stromal Cells for Corneal Repair. *Transl. Vis. Sci. Technol.* **2021**, *10*, 3. [CrossRef] [PubMed]
50. NewDrugs_CTRules_2019.Pdf. Available online: https://cdsco.gov.in/opencms/export/sites/CDSCO_WEB/Pdf-documents/NewDrugs_CTRules_2019.pdf (accessed on 7 November 2022).
51. Wright, B.; Cave, R.A.; Cook, J.P.; Khutoryanskiy, V.V.; Mi, S.; Chen, B.; Leyland, M.; Connon, C.J. Enhanced Viability of Corneal Epithelial Cells for Efficient Transport/Storage Using a Structurally Modified Calcium Alginate Hydrogel. *Regen. Med.* **2012**, *7*, 295–307. [CrossRef] [PubMed]

International Journal of
Molecular Sciences

IMPACT FACTOR 6.208

Indexed in: PubMed

Article

Transcriptomic Profiling of Human Limbus-Derived Stromal/Mesenchymal Stem Cells—Novel Mechanistic Insights into the Pathways Involved in Corneal Wound Healing

Fatemeh Tavakkoli, Mukesh Damala, Madhuri Amulya Koduri, Abhilash Gangadharan, Amit K. Rai, Debasis Dash, Sayan Basu and Vivek Singh

Special Issue
Molecular and Cellular Mechanisms of Corneal Fibrosis/Scarring and Advances in Therapy

Edited by
Dr. Gary Hin-Fai Yam, Prof. Dr. Vishal Jhanji and Dr. Matthias Fuest

MDPI

https://doi.org/10.3390/ijms23158226

International Journal of
Molecular Sciences

MDPI

Article

Transcriptomic Profiling of Human Limbus-Derived Stromal/Mesenchymal Stem Cells—Novel Mechanistic Insights into the Pathways Involved in Corneal Wound Healing

Fatemeh Tavakkoli [1,2,†], Mukesh Damala [1,3,†], Madhuri Amulya Koduri [1,4], Abhilash Gangadharan [5], Amit K. Rai [2], Debasis Dash [5], Sayan Basu [1,6] and Vivek Singh [1,6,*]

1 Prof. Brien Holden Eye Research Center, LV Prasad Eye Institute, Hyderabad 500034, India; fatemehtavakkoli88@gmail.com (F.T.); mukeshdamala@lvpei.org (M.D.); madhurikamulya333@gmail.com (M.A.K.); sayanbasu@lvpei.org (S.B.)
2 Center for Genetic Disorders, Banaras Hindu University, Varanasi 221005, India; akrai10@gmail.com
3 School of Life Sciences, University of Hyderabad, Hyderabad 500046, India
4 Manipal Academy of Higher Education, Manipal 576104, India
5 CSIR-Institute of Genomics and Integrative Biology, Mathura Road Campus, New Delhi 110025, India; gangutalk@gmail.com (A.G.); ddash@igib.in (D.D.)
6 Center for Ocular Regeneration (CORE), Prof. Brien Holden Eye Research Center, LV Prasad Eye Institute, Hyderabad 500034, India
* Correspondence: viveksingh@lvpei.org; Tel.: +91-40-6810-2286
† These authors contributed equally to this work.

Citation: Tavakkoli, F.; Damala, M.; Koduri, M.A.; Gangadharan, A.; Rai, A.K.; Dash, D.; Basu, S.; Singh, V. Transcriptomic Profiling of Human Limbus-Derived Stromal/Mesenchymal Stem Cells—Novel Mechanistic Insights into the Pathways Involved in Corneal Wound Healing. *Int. J. Mol. Sci.* **2022**, *23*, 8226. https://doi.org/10.3390/ijms23158226

Academic Editors: Vishal Jhanji, Gary Hin-Fai Yam and Matthias Fuest

Received: 21 June 2022
Accepted: 16 July 2022
Published: 26 July 2022

Abstract: Limbus-derived stromal/mesenchymal stem cells (LMSCs) are vital for corneal homeostasis and wound healing. However, despite multiple pre-clinical and clinical studies reporting the potency of LMSCs in avoiding inflammation and scarring during corneal wound healing, the molecular basis for the ability of LMSCs remains unknown. This study aimed to uncover the factors and pathways involved in LMSC-mediated corneal wound healing by employing RNA-Sequencing (RNA-Seq) in human LMSCs for the first time. We characterized the cultured LMSCs at the stages of initiation (LMSC−P0) and pure population (LMSC−P3) and subjected them to RNA-Seq to identify the differentially expressed genes (DEGs) in comparison to native limbus and cornea, and scleral tissues. Of the 28,000 genes detected, 7800 DEGs were subjected to pathway-specific enrichment Gene Ontology (GO) analysis. These DEGs were involved in Wnt, TGF-β signaling pathways, and 16 other biological processes, including apoptosis, cell motility, tissue remodeling, and stem cell maintenance, etc. Two hundred fifty-four genes were related to wound healing pathways. *COL5A1* (11.81 ± 0.48) and *TIMP1* (20.44 ± 0.94) genes were exclusively up-regulated in LMSC−P3. Our findings provide new insights involved in LMSC-mediated corneal wound healing.

Keywords: cornea; limbus; mesenchymal stem cells; wound healing; stromal cells; RNA sequencing; transcriptome; ocular surface; tissue remodeling; regeneration

1. Introduction

The cornea is the transparent and highly specialized tissue located in the anterior portion of the eye. In addition to its function as a protective barrier, the cornea is largely responsible for the transmission of light onto the retina, accounting for two-thirds of the eye's refractive power [1–3]. Anatomically, the cornea is made of three major layers: epithelium, stroma, and endothelium. The epithelium is a 4–6 layered outermost structure made of non-keratinized stratified squamous cells. Stroma is the middle layer comprising ~90% of the corneal thickness and contributing to most of the structural framework. It is made of an extensive network of collagen fibrils with interstitially embedded cells called keratocytes, and proteoglycans such as lumican, keratocan, and decorin. The stroma is followed by endothelium, the innermost layer. Endothelium is majorly responsible for the

maintenance of stromal dehydration via pumping out excess water/fluids, which in turn prevents corneal edema and resultant opacity. Any damage to one or more of these layers due to extrinsic or intrinsic factors affects the cornea's transparency [4], a crucial factor for optimal vision [5]. Between the transparent cornea and opaque sclera is the transitional zone, limbus. This acts as a storehouse of the stem cells required for corneal homeostasis and regeneration [6–8].

Corneal epithelium, the outermost surface, is subjected to microscopic wear and tear, which requires constant renewal of the lost cells or damaged tissue. The maintenance of the corneal epithelium and stroma relies on the populations of limbal epithelial stem cells (LESCs) and limbal stromal stem cells. Located at the base of limbal crypts [9,10], the LESCs interact with the underlying cells of the limbal stroma [11] through the interruptions in the basement membrane. Limbal stroma is a highly vascularized tissue [12] that has a mixed population of fibroblast-like cells, melanocytes, myofibroblasts, and nerve cells, as well as transmigrating immune cells such as dendritic cells, lymphocytes, mast cells, and macrophages. Derived from the neural crest [13], these limbus-derived stromal cells are multipotent [14–17] mesenchymal stem cells that conform to the ICST (International Society for Cellular Therapy) criteria [18], demonstrating their trilineage differentiation potential [19,20]. Multiple studies have shown that these LMSCs can also trans-differentiate to keratocyte lineage [14,20–23] and epithelium [24,25]. They support and regulate the plasticity and niche of the LESCs towards the restoration of the impaired limbal niche and corneal wound healing [12,26–31]. The migration of both LESCs and LMSCs to the site of injury and the subsequent combined repair mechanisms are responsible for the maintenance of the stem cell functions and restoration of corneal transparency, a pre-requisite for optimal vision [22,32–39].

In case of injuries involving the stroma, the native keratocytes transdifferentiate into fibroblasts and then myofibroblast cells, facilitating the migration and healing of the damage in the corneal stroma. However, this wound healing mechanism is undesirable, as it leads to fibrosis causing corneal haze and scar formation. This obscures the visual pathway leading to partial or complete visual impairment [40–42].

The most common surgical means of treating an injured, melted, or the perforated cornea is partially or completely replacing it [43]. The currently available modes of treating these pathologies are often challenged by risks such as graft failure or rejections, inflammatory responses, long-term follow–up, and the inadequate supply of donor corneas [5]. Besides, the current procedures do not offer longevity and unaffected or optimal visual acuity post-transplantation [44–48].

Limbal stromal stem cells were earlier reported for their safety and efficacy [8,9] in preventing corneal scars and the regeneration of corneal stroma. However, the underlying molecular mechanisms behind the stem cell-based for cornel regeneration are not well studied.

In the current study, we have attempted to uncover the regulatory pathways in-volved in LMSC-mediated corneal wound healing. We examined the human LMSCs in comparison to the native tissues of the limbus and cornea using the RNA-Seq. Scleral tissue was used as a control. The detected DEGs were subjected to pathways through the Gene Ontology studies to obtain insights into various biological/signaling pathways. The differences in the frequency distribution of fold-change values of pathway-specific genes were compared to that of all the other genes in the transcriptome. The exclusively up-regulated genes in the corneal wound healing process were checked for their known and probable interactions with other genes through STRING analysis and validated through qRT-PCR. Our data provides molecular/mechanistic insights into corneal wound healing mediated by LMSCs.

2. Results

2.1. Expansion of Limbal Stem Cells in Culture

Both limbal epithelial (round cells which grow as a layer) and limbal stromal (spindle-shaped and individual) cell populations were obtained from the explants in the initial

(Figure 1A) and late stages (Figure 1B,C) of the primary culture (>80% confluence, days 8–10). Further subcultures were observed to show the elevated number of stromal cells and the gradual decrease in the epithelial cells from passages P1 (Figure 1D) to passages P2 (Figure 1E). A pure population of the limbal stromal cells without any presence of the epithelial cells was derived in passage P3. This population of stromal cells also featured the presence of few myofibroblasts in their undifferentiated state, (Figure 1F; orange arrow), dendritic cells (Figure 1F; black arrow), and few quiescent fibroblastic cells (Figure 1F; white arrow), similar to the native corneal stroma.

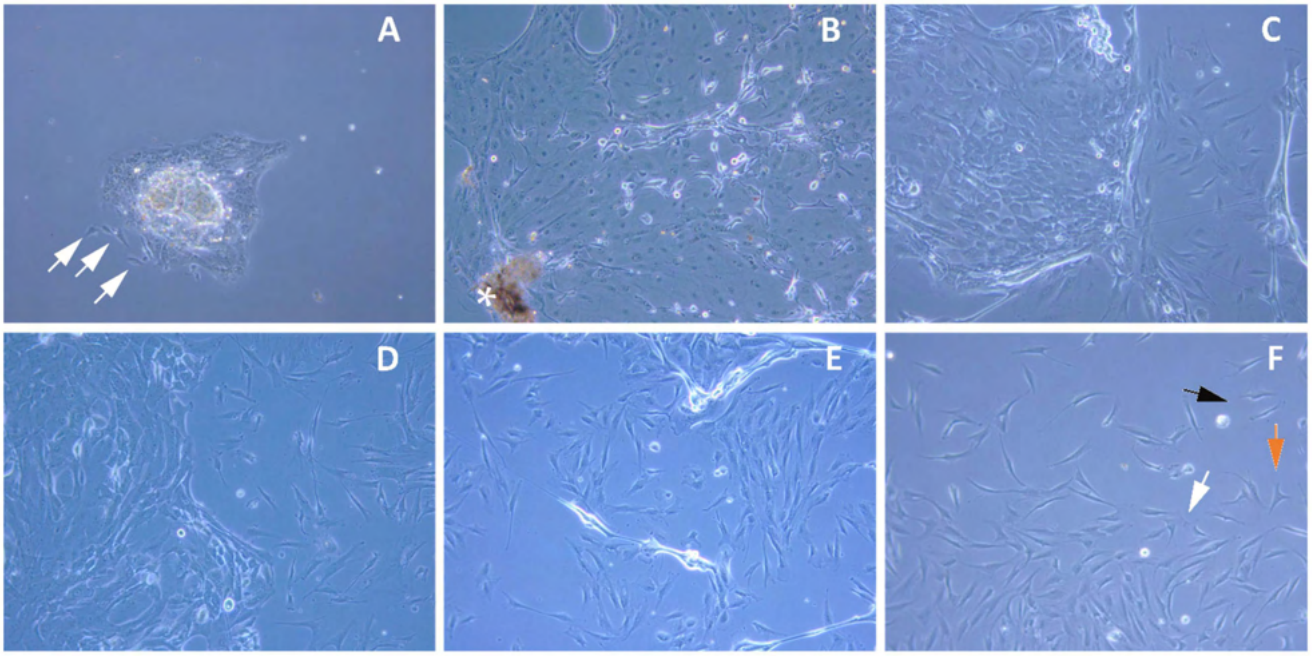

Figure 1. Expansion of the limbal stem cells in culture. Representative images of the limbal stem cells in the primary culture: initiation (**A**) and at confluence (**B**,**C**), passage P1 (**D**), passage P2 (**E**) and passage P3 (**F**). Epithelial cells (round morphology) and stromal/progenitor cells (spindle morphology, indicated with white arrows) derived from the limbal explant (**A**). Gradual increase in limbal stromal cells population and simultaneous fading of limbal epithelial cells (**C**–**E**). Pure population of the limbal stromal cells obtained in passage P3 including dendritic cells ((**F**); black), undifferentiated myofibroblastic cells ((**F**); orange), and quiescent fibroblastic cells ((**F**); white); * Limbal Explant.

2.2. Cell Type Biomarker Changes during Culture Passages

2.2.1. Stem Cell and Ocular Biomarkers

The immunostaining analysis has revealed a similar pattern of the expression (positive) of the stem cell (ABCG2, p63-α) and ocular biomarkers (PAX6) at both LMSC−P0 and LMSC−P3 stages of the culture. However, ABCB5 was found to be expressed in a low number of cells in P0 relative to P3. Additionally, the number of cells positive for p63-α were high in P0 relative to P3 (Figure 2). ABCB5 plays a vital role in the differentiation of limbal stem cells and is essential for corneal repair [34].

However, the RT-PCR data have revealed significant up-regulation of *ABCG2* in LMSC−P3 with respect to that of LMSC−P0 and native limbus (Figure 2). *ABCB5* was found to be significantly down-regulated in both LMSC−P0 and LMSC−P3 and *PAX6* was found to be significantly up-regulated relative to limbal tissue. *P63α* was found to be down-regulated by 3-fold in LMSC−P3 relative to native limbal tissue. On the contrary, the level of *P63α* was found to be up-regulated 3-fold in LMSC−P0 relative to the control.

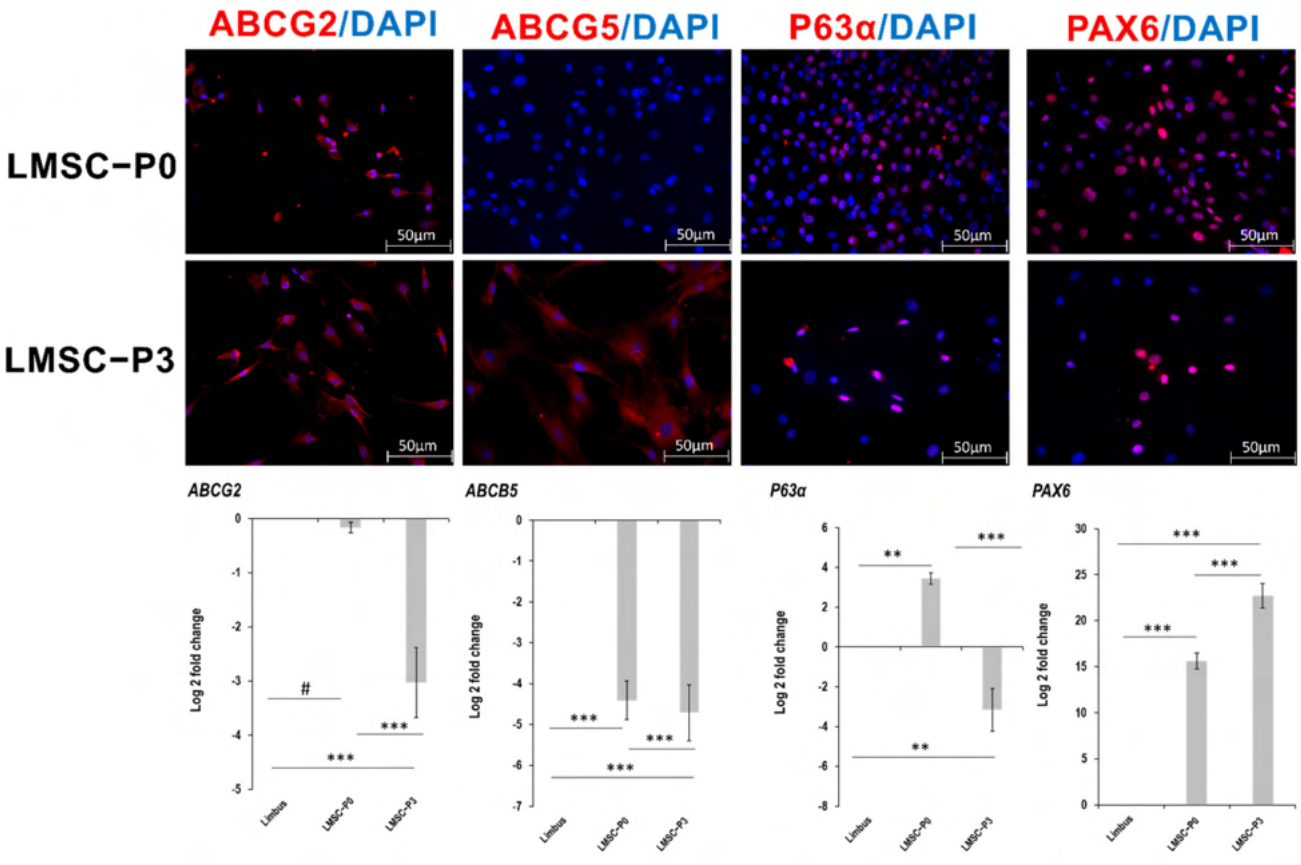

Figure 2. Expression of the stem cell and ocular biomarkers in limbal stem cells. Panel of the representative images of the limbal stem cells showing positive expression of ABCG2, ABCB5, P63-α, and PAX6 (red) in both epithelial (LMSC−P0) and stromal cell (LMSC−P3) populations, counterstained with DAPI (blue). Scale: 50 μm. Level of expression (lower panel) of *ABCG2*, *ABCB5*, *P63α*, and *PAX6* genes quantified using qRT-PCR in limbal epithelial (LMSC−P0) and stromal (LMSC−P3) cells, relative to native limbal tissue (n = 5). *P63α* was found to be down-regulated in LMSC−P3 where all the other stem cell genes *ABCG2*, *ABCB5* and *PAX6* were found to follow same pattern of expression in both early and late passages of the culture. The results were plotted as mean log 2-fold change ± SD. The statistical analysis was performed using Kruskal–Wallis one-way ANOVA test. # $p > 0.05$, ** $p < 0.01$, *** $p < 0.001$.

2.2.2. Mesenchymal Stem Cell Markers

The limbal stem cells at LMSC−P0 were found to be positive in relatively low numbers for the mesenchymal stem cell (MSC) biomarkers CD90, CD105, and VIM (Vimentin). However, most of the cells at LMSC−P3 were found to be positive for the above markers (Figure 3). The qRT-PCR analysis revealed a down-regulated expression of markers *CD90*, *VIM* (1-fold), and *CD105* (6-fold) in LMSC−P0 relative to the control, limbal tissue. On the contrary, the levels were found to be up-regulated in LMSC−P3 by 2-fold of *CD105*, 3-fold of *VIM*, and ~20-fold of CD*90* relative to the control (Figure 3).

The transmembrane proteins NCAD (N-cadherin) and ECAD (E-cadherin) were observed to express positively in LMSC−P0 through the immunostaining analysis. However, Ecad was found to be negative in LMSC−P3, and Ncad showed positive expression. The qRT-PCR analysis showed that *NCAD* was found to be up-regulated in both LMSC−P0 (8-fold) and LMSC−P3 (26-fold) compared to the native limbus. *ECAD* was found to be down-regulated in LMSC−P3 (3-fold), while it was found to have an increased expression in LMSC−P0 (3-fold) relative to the control (Figure 3).

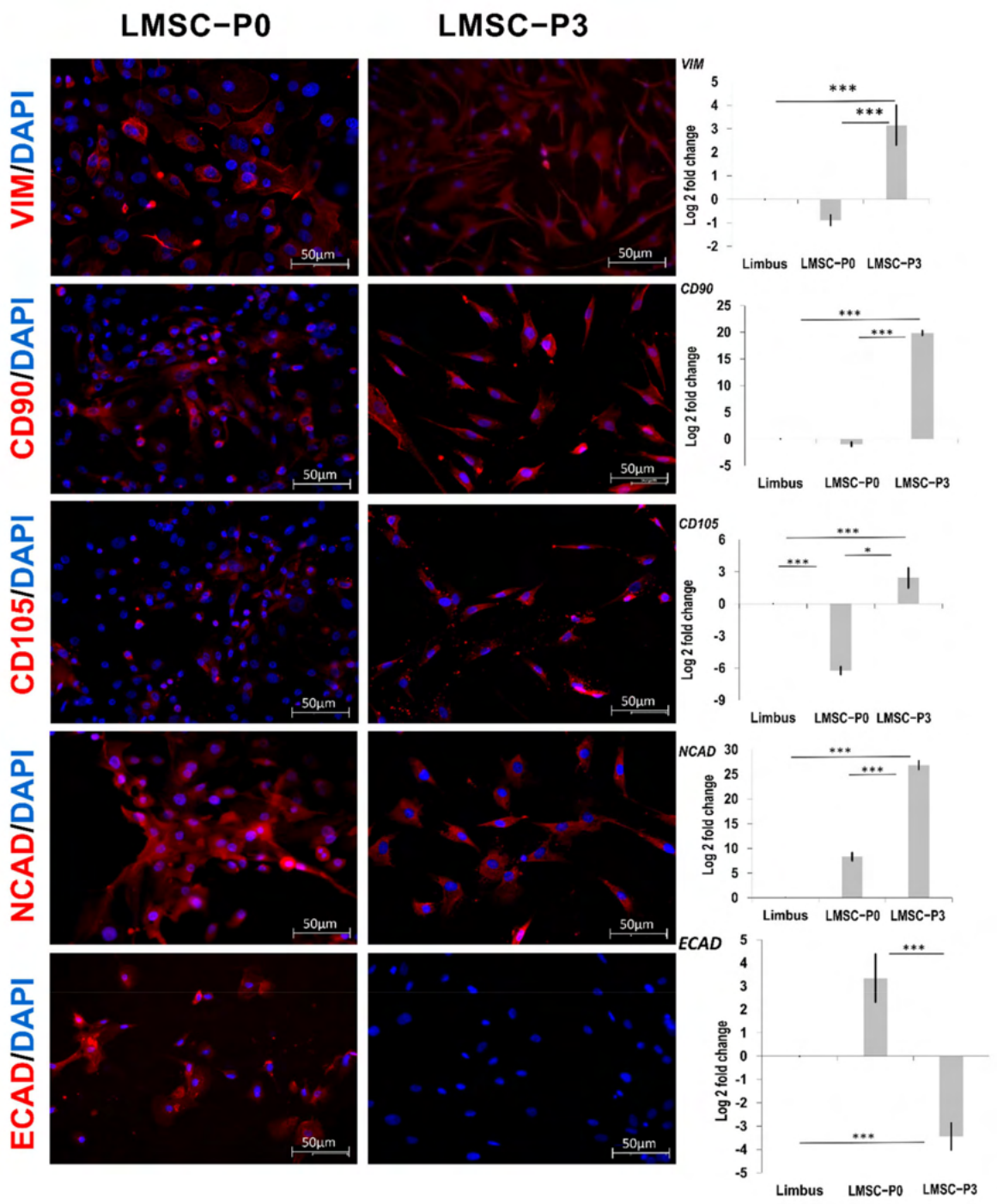

Figure 3. Limbal stem cells showing mesenchymal stem cell biomarkers. Panel of the representative images of the limbal stem cells showing positive expression of Vim (Vimentin), CD90, and CD105 in both LMSC−P0 (n = 3) and LMSC−P3 (n = 3) populations, counterstained with DAPI (blue). Ncad (N-cadherin) were positive (red) in LMSC−P3 cells and Ecad (E-cadherin) did not show any expression in LMSC−P3. Level of expression of *VIM*, *CD90*, *CD105*, *NCAD*, *ECAD* genes quantified using qRT-PCR in LMSC−P0 and LMSC−P3 relative to native limbal tissue (n = 5). Except *ECAD* remaining genes were found to be up-regulated in LMSC−P3 with fold-change ranging between 2 to 20, which were down-regulated in LMSC−P0. Scale: 50 µm. The results were plotted as mean log 2-fold change ± SD. The statistical analysis was performed using Kruskal–Wallis one-way ANOVA test. * $p < 0.05$, *** $p < 0.001$.

2.3. Genome Wide Transcriptomics Analysis Using RNA-Seq

2.3.1. Transcriptome Overview Using Principal Components Analysis Plot

To visualize the overall similarities or differences between gene expression patterns in different cell types, the counts were analyzed through Principal Component analysis (PCA). The counts data was subjected to Box-Cox transformation to stabilize the skewness in the data before PCA analysis. This analysis has showed the overall differences in the expression patterns of the samples in terms of the distances between them, which indicates the similarity between their expression profiles. It was found that sclera and cornea clustered together and are quite distant from the other samples. This indicates that the differences in their gene expression is not as heterogeneous (Figure 4A) as compared to the rest of the analytes (Limbus, LMSC−P0, LMSC−P3 and ESC (embryonic stem cell)).

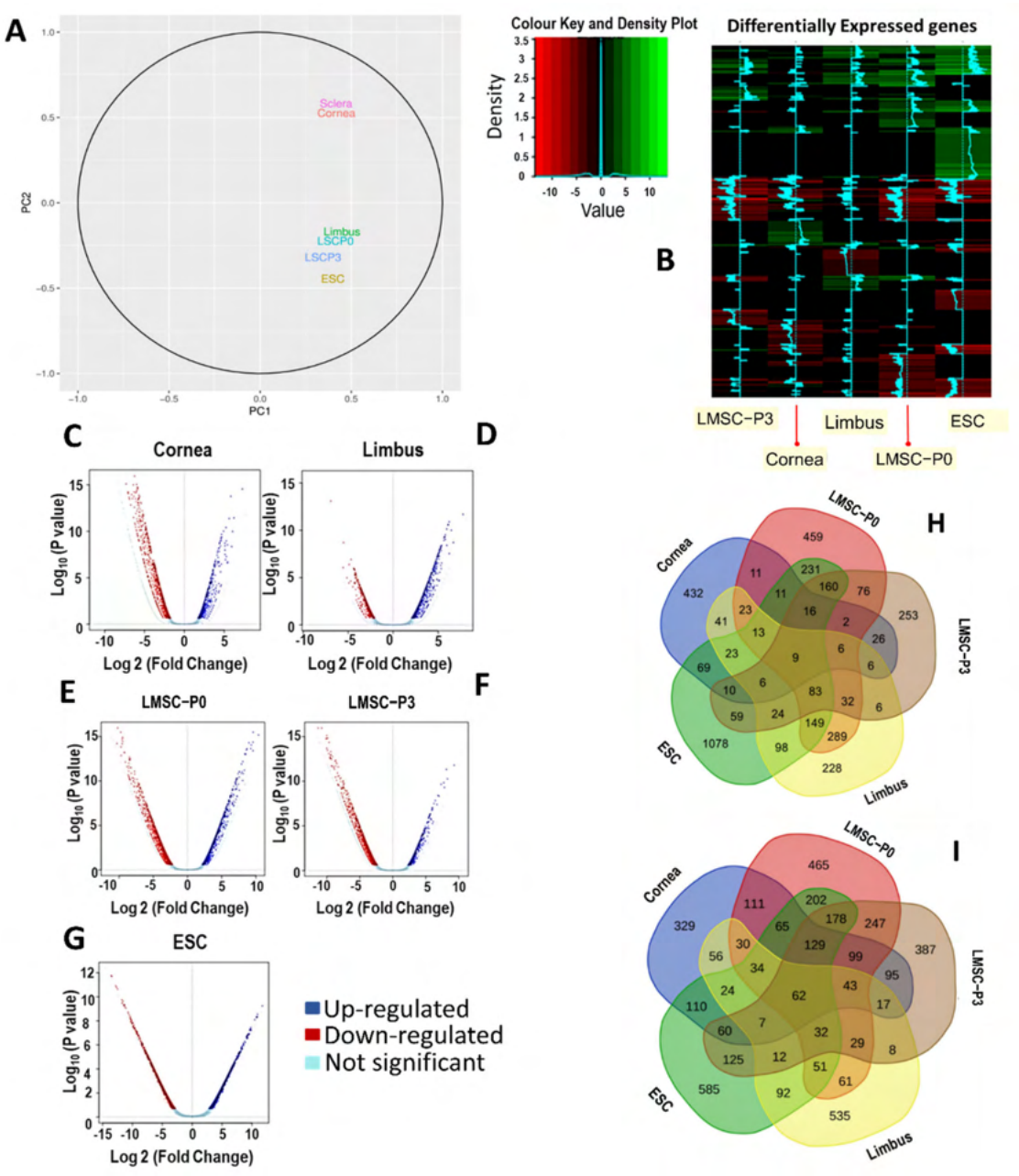

Figure 4. Similarities and asymmetry in the gene expression. (**A**) The count data from all the samples were transformed using Box-Cox transform to compensate for skewness before PCA analysis. The

closer proximity of the samples indicates similarity of the expression profiles of those samples. Sclera and cornea were found to show high similarity in whole transcriptome of expression and were clustered together. Similarly, LMSC−P0 and native limbal tissue were in close proximity, indicating similar transcriptomic signature. LMSC−P3 and ESC were found to be further away from one another, indicating an altered or different expression profile relative to the rest of the analytes. (**B**) The heat map representing the DEGs in all 5 samples relative to the control (scleral tissue). The rows indicate the genes and columns indicate the samples (cells or tissues). The color intensity represents the level of changes in expression. All significantly up-regulated genes are indicated in green and all significantly down-regulated genes are indicated in red. $p < 0.05$ was considered to be a statistically significant change in the gene expression. (**C**–**G**) Volcano plots of each cell/tissue samples showing the distribution of genes up-regulated (blue) and down-regulated (red). Majority of the genes in corneal tissue were down-regulated while majority of genes in limbus were up-regulated. The primary culture of limbal stromal cells (LMSC−P0) had nearly equal distribution of the genes that were up-regulated and down-regulated. (**H**,**I**) Tissue-specific differential expression of the genes: Venn diagrams showing the number of genes that are common and exclusively up-regulated (**H**) or exclusively down-regulated (**I**) in cornea, limbus, LMSC−P0, LMSC−P3, and ESC with respect to the scleral tissue (control).

The limbus tissue and LMSC−P0 were observed to form an isolated cluster away from LMSC−P3 and ESC. The altered transcriptomic signature of LMSC−P3 may possibly be the result of repeated passaging and de-epithelialization. However, it was not very distinct from ESC, indicating possible shared/similar gene expression patterns such as pluripotent nature and dedifferentiation.

2.3.2. Visualizing the Asymmetry in Gene Expression of Various Tissues

Around 28,000 genes were detected via RNA-Seq in all the analytes. Among them, 7800 genes were differentially expressed (either up-regulated or down-regulated) against scleral tissue as a control (Figure 4B). In limbal tissue, a total of 1036 genes were up-regulated and 1093 genes down-regulated. LMSC−P0 had 1570 genes up-regulated and 1838 genes down-regulated, wherein LMSC−P3 774 and 1530 genes were up-regulated and down-regulated, respectively.

The asymmetry in gene expression by cornea, limbus, LMSC−P0, LMSC−P3, and ESC was visualized by plotting their transcriptome through volcanic plots. Volcanic plots provide a visual representation of the DEGs, showing their statistical significance (p values) versus the magnitude of change (fold-change). These scattered plots have shown that the transcriptome of corneal tissue had a major proportion of the down-regulated genes (Figure 4C). On the other hand, limbal tissue had a distinct asymmetry, with a major proportion of the genes significantly up-regulated (Figure 4D). LMSC−P0 showed a near symmetry in the plot (Figure 4E), while LMSC−P3 has a smaller proportion of up-regulated genes (Figure 4F). The ESC had shown a large number of down-regulated genes (Figure 4G).

2.4. Tissue-Specific Differential Expression and Pathway Enrichment Analysis

The differential expression of the genes that were either specific to a particular type of cell or tissue was analyzed using 5-way Venn diagrams (Figure 4H,I). The information on the number of genes commonly expressed in one or more cells/tissues was obtained. In addition, the number of genes that were either exclusively up-regulated or exclusively down-regulated in one particular type of cell/tissue was also obtained. The number of genes exclusively up-regulated in LMSC−P0 and LMSC−P3 was 459 and 223, respectively, while the exclusively down-regulated ones were 465 and 387, respectively (Figure 4H,I).

Pathway-specific Gene Ontology (GO) enrichment analysis using the Enrichr tool provided insights into various cellular processes and pathways such as apoptosis, cell motility etc., where one or two particular cells/tissues were playing a major role. This was evident from the statistically significant gene expression with respect to the control (sclera). The relative median change indicated the up-regulation or down-regulation of such genes with respect to the basal expression levels of the whole transcriptome (Figure 5A). Few

of the prominent or majorly observed cellular processes were plotted against the relative expressions of DEGs specific to each of these processes.

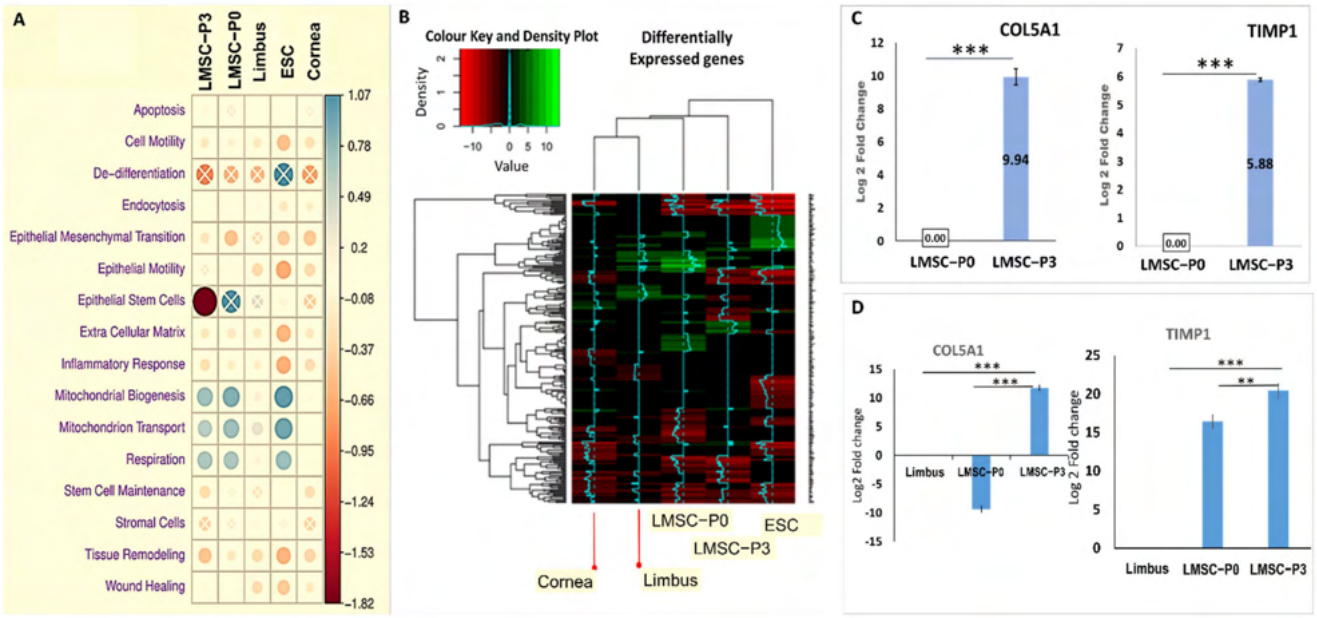

Figure 5. Interpretations from Gene Ontology enrichment analysis. (**A**) Gene ontology pathway-specific analysis: Each row represents the genes belonging to a particular pathway/biological process in the GO database. The dot color/size represents the difference in median expression between genes of a particular pathway and rest of genes in whole transcriptome. A positive value indicates up-regulation (blue) and a negative value indicates down-regulation (red). The difference was tested using Mann–Whitney–Wilcoxon test and statistically insignificant ones were denoted with crosses. Inflammatory response is down-regulated more strongly in P3 versus P0, which may reflect why the use of P3 stage cells does not cause fibrosis in corneal stromal transplants. The stronger down-regulation in ESC may reflect on the immune privilege of embryonic stem cells. The cell motility pathways are active in P3, cornea, and ESC. This is easily explained for the stromal stem cells in P3 and the ESC in terms of their proliferation and migration activity before differentiation, but for cornea may be representative of continuous cell migration required to replace lost corneal tissue. (**B**) The heatmap of 254 genes belonging to wound healing pathway. The rows indicate the genes and columns indicate the samples (cells or tissues). The color intensity represents the level of changes in expression. All significantly up-regulated genes are indicated in green and all significantly down-regulated genes are indicated in red. $p < 0.05$ was considered to be statistically significant change in the gene expression. (**C**,**D**) Genes of wound healing pathway exclusively expressed in LMSC−P3: The levels of COL5A1 and TIMP1 in LMSC−P0 and LMSC−P3 assessed through RNA-Seq (**C**) and qRT-PCR (**D**). The LMSC−P3 has ~10-fold ($n = 3$. $p < 0.001$) high expression of COL5A1, which was down-regulated in LMSC−P0, evident from both techniques. The levels of TIMP1 were ~6-fold high ($n = 3$, $p < 0.001$) and 4-fold higher ($n = 5$, $p < 0.01$) in LMSC−P3, when assessed through RNA-Seq and qRT-PCR respectively. ** $p < 0.01$, *** $p < 0.001$. The results were plotted as mean log 2-fold change ± SD. The statistical analysis was performed using Kruskal–Wallis one-way ANOVA test for qRT-PCR and two-tailed T test for RNA-Seq analysis.

2.4.1. Interpretations from Gene Ontology Enrichment Analysis

A total of 6634 unique genes belonging to 16 relevant biological processes were found to be expressed by the corneal and limbal tissues and cells LMSC−P3, LMSC−P0 and ESC. The relative comparison of DEGs specific to various cell processes expressed by the cells of interest in this study—LMSC−P3 and LMSC−P0 cells—has provided interesting results.

2.4.2. GO Pathway Level Gene Expression Changes with Respect to Whole Transcriptome

The LMSC−P0 was found to have relatively high numbers of genes of the cellular processes apoptosis (*BAX*, *BCL2*, etc.,), mitochondrial biogenesis (*SIRT3*, *CASP8*, etc.,) and its transport (*ATP5F1A*, *BCL2*, etc.,) and respiration (*BID*, *COX10*, etc.,) relative to that of LMSC−P3, and were significantly up-regulated (Figure 5A). Genes of wound healing (*COL5A1*, *TIMP1*, *ANXA1* etc.,), tissue remodeling (*HIF1α*, *NOX2*, *NOTCH4* etc.,), stem cell maintenance (*FOXO1*, *SOX2*, *TP63* etc.,), and cell motility (*MAPK*, *MMP1*, etc.,) were found to be more expressed in high numbers in LMSC−P3 than that of LMSC−P0; however, they were down-regulated with respect to the control (sclera). Genes of epithelial phenotype were found to be strongly down-regulated in LMSC−P3. Genes of the epithelial-to-mesenchymal transition (*SNAI1*, *TWIST1*) were down-regulated in both LMSC−P0 and LMSC−P3. Inflammatory response (*C3*, *CXCL8*, etc.) and tissue remodeling genes (*MMP14*, *MMP2*, *IL15*, etc.) were down-regulated more strongly in LMSC−P3 relative to LMSC−P0. In addition to these processes, the GO analysis revealed the DEGs of various signaling pathways such as Wnt, TGF-β and stem cell pathways (Supplementary Figure S3 and Supplementary Table S6).

2.4.3. Genes of Multiple Cell Signaling Pathways

Genes Involved in Wound Healing Pathway

Around 254 genes belonging to the wound healing pathway were found to be differentially expressed (GO consortium accession number 0042060). The heat map showing the relative expression of these DEGs (Figure 5B) has shown that more significantly up-regulated genes were expressed by LMSC−P0 cells (relative to sclera), followed by limbal tissue and LMSC−P3. Among these DEGs, 21 genes (*CASP3*, *EPB41L4B*, *AJUBA*, *NFE2*, *EGFR*, *IL24*, *ANXA2*, *HMGCR*, *PRKCQ*, *DSP*, *F3*, *IL1A*, *KLK6*, *UBASH3B*, *RHOC*, *TFPI2*, *ADAM15*, *METAP1*, *RAC2*, *DGKA*, *DCBLD2*) were found be exclusively up-regulated or expressed by LMSC−P0 alone. On the other hand, LMSC−P3 has shown exclusive up-regulation of *TIMP1* and *COL5A1* genes (Figure 5C). These two genes were validated through qRT-PCR with native limbus tissue as control, which revealed that in LMSC−P0, the level of *TIMP1* (16.44 ± 0.87) is up-regulated and *COL5A1* (−9.32 ± 0.53) is down-regulated. In LMSCP3, both the genes were up-regulated: *COL5A1* (11.81 ± 0.48) and *TIMP1* (20.44 ± 0.94) (Figure 5D).

Other Signaling Pathways

The AmiGO gene ontology analysis of the total DEGs has revealed that 211 genes playing a role in the Wnt signaling pathway were differentially expressed by cornea, limbus, ESC, LMSC−P3, and LMSC−P0. The relative expression levels of these genes from the RNA-Seq by each cell/tissue were plotted in Supplementary Figure S3B, tabulated in Supplementary Table S6. A total of 85genes belonging to the TGF-β signaling pathway were found to be differentially expressed by one or more cells/tissues. Among them, *COL3A1* was found to be exclusively up-regulated in LMSC−P3 alone.

Of the 23 genes available in the GO database which belong to stem cell pathway, 13 DEGs (Supplementary Table S6) were found to be expressed by the cells or tissues analyzed in this study (GO consortium accession CL 00000034). The plot of their relative expression levels has shown (Supplementary Figure S3A) that the majority of genes were found to be significantly down-regulated in LMSC−P0.

2.5. Quantification of Genes Interacting among the Exclusively Up-Regulated Genes in LMSC−P3

String database revealed 17 more genes were interacting with exclusively up-regulated genes, i.e., *COL5A1* and *TIMP1* (Figure 5D). The STRING network was formed with a PPI enrichment *p*-value of $<1.0 \times 10^{-16}$ (Figure 6B). The highly co-expressive genes were *COL1A1* and *COL3A1* with the RNA co-expression score of 0.944 (Figure 6C). Biological process involved among these 17 genes were mentioned earlier (Table 1).

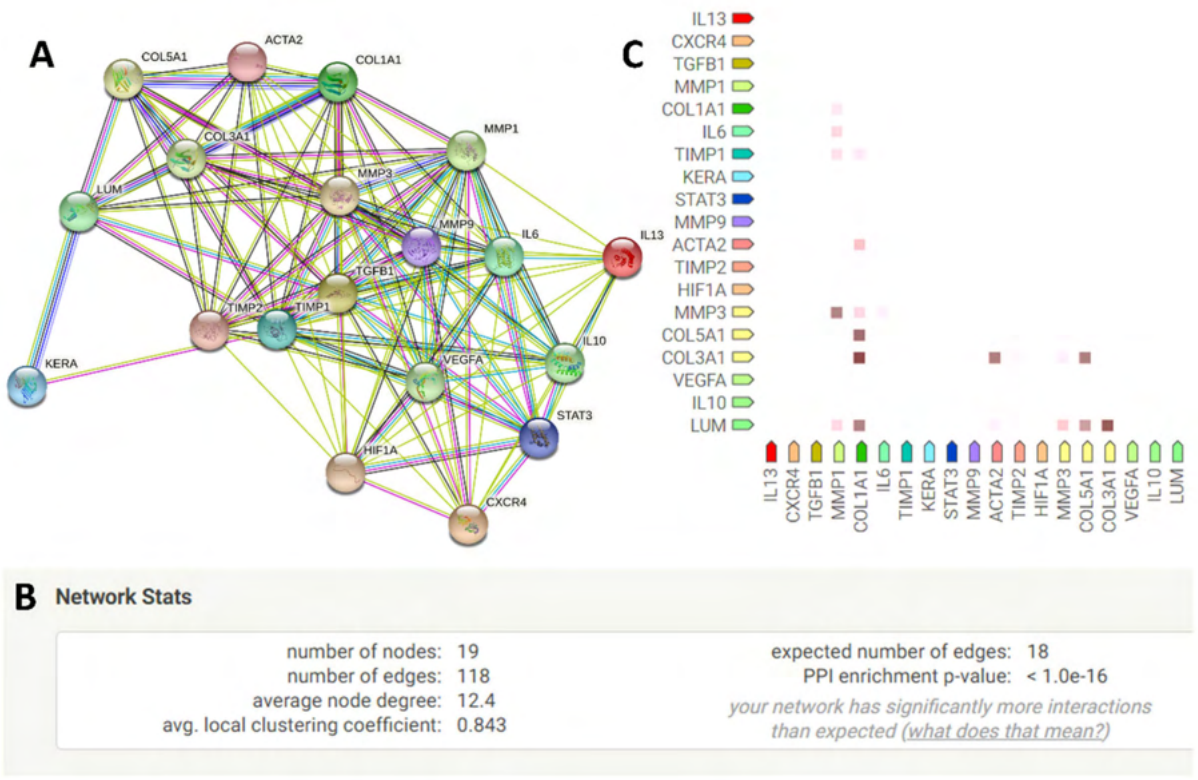

Figure 6. The network generated from the gene interactions involved between COL5A1 and TIMP1 (**A**). The network stats of the network in (**A**) showing the significance value of $<1.0 \times 10^{-16}$ (**B**). The RNA co-expression analysis from STRING software shows for the above network shows the COL3A1 and COL1A1 are highly co-expressing in the homeostatic conditions (**C**).

Table 1. The above table shows the genes playing roles in specific biological processes from the network generated between COL5A1 and TIMP1 gene interactions, which has a significant role in corneal wound healing.

Gene Ontology ID	Biological Process	Genes Involved	False Discovery Ratio
GO:0032964	Collagen biosynthetic process	COL5A1, COL1A1	0.0028
GO:1905048	Regulation of metallopeptidase activity	TIMP1, TIMP2, STAT3	0.00013
GO:0070102	Interleukin-6-mediated signaling pathway	IL-6, STAT3,	0.0061
GO:0030199	Collagen fibril organization	COL5A1, COL1A1, COL3A1, LUM	3.5×10^{-5}
GO:0035633	Maintenance of blood-brain barrier	VEGF, IL-6	0.0171
GO:0048661	Positive regulation of smooth muscle cell proliferation	MMP9, IL-6, IL-13, IL-10	0.00021
GO:0042060	Wound healing	COL5A1, COL1A1, COL3A1, TIMP1, HIF1A, VEGFA, IL-6, TGFB-1	3.4×10^{-6}
GO:0060485	Mesenchyme development	ACTA2/SMA, TGFB1, HIF1A	0.0299

Seventeen genes (*CXCR4*, *HIF1A*, *LUM*, *MMP1*, *MMP3*, *MMP9*, *ACTA2*, *VEGF*, *WNT7A*, *HLADR*, *IL10*, *IL13*, *IL6*, *KERA*, *STAT3*, *TGFB1*, *TIMP2*) were hypothesized through string analysis based on their interactions with exclusively up-regulated genes *TIMP1* and *COL5A1* (Figure 6A). These 17 genes were validated through RT-qPCR. When compared with the native limbal tissue, in LMSC−P0, nine genes were up-regulated, i.e., *CXCR4*

(9.23 ± 3.31), *HIF1A* (7.84 ± 0.47), *LUM* (4.06 ± 1.35), *MMP1* (12.83 ± 1.49), *MMP3* (1.88 ± 1.01), *MMP9* (1.88 ± 1.01), *ACTA2/αSMA* (14.58 ± 2.86), *VEGF* (9.65 ± 1.30), and *WNT7A* (6.90 ± 1.30), and 8 genes were down-regulated, i.e., *HLADR* (−2.01 ± 0.11), *IL10* (−7.95 ± 1.09), *IL13* (−1.43 ± 0.97), *IL6* (−2.25 ± 0.46), *KERA* (−1.36 ± 1.42), *STAT3* (−0.72 ± 0.63), *TGFB1* (−2.90 ± 1.29), and *TIMP2* (−5.36 ± 1.37) (Figure 7).

In the pure population of LMSCs, i.e., LMSC−P3, five genes were down-regulated: *IL13* (−3.97 ± 1.06), *MMP3* (−0.96 ± 0.52), *STAT3* (−1.23 ± 0.87), *TGFB1* (−1.04 ± 0.26), and *TIMP2* (−1.70 ± 0.32). Meanwhile, 12 genes were up-regulated: *CXCR4* (4.53 ± 0.36), *HIF1A* (22.51 ± 1.12), *HLADR* (11.22 ± 0.41), *IL10* (4.78 ± 0.43), *IL6* (7.65 ± 1.49), *KERA* (16.45 ± 0.54), *LUM* (8.60 ± 0.92), *MMP1* (13.40 ± 1.13), *MMP9* (3.34 ± 0.38), *ACTA2/αSMA* (30.76 ± 1.70), *VEGF* (26.74 ± 0.76), and *WNT7A* (13.69 ± 1.68) (Figure 7). Among these, 17 genes—*CXCR4*, *HIF1A*, *LUM*, *MMP1*, *MMP9*, *ACTA2/αSMA*, and *VEGF*—were commonly up-regulated, and *IL13*, *TIMP2*, and *TGFB1* were commonly down-regulated in both LMSC−P0 and P3.

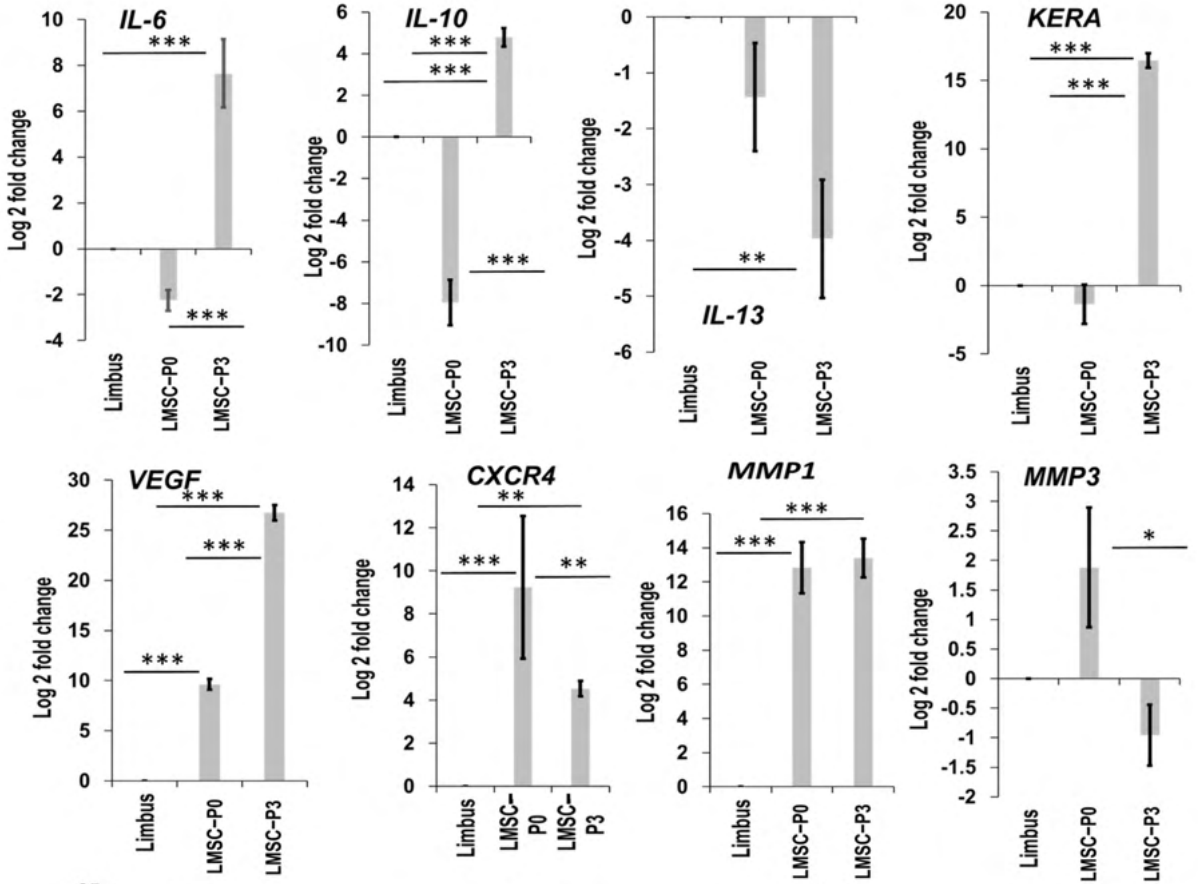

Figure 7. *Cont.*

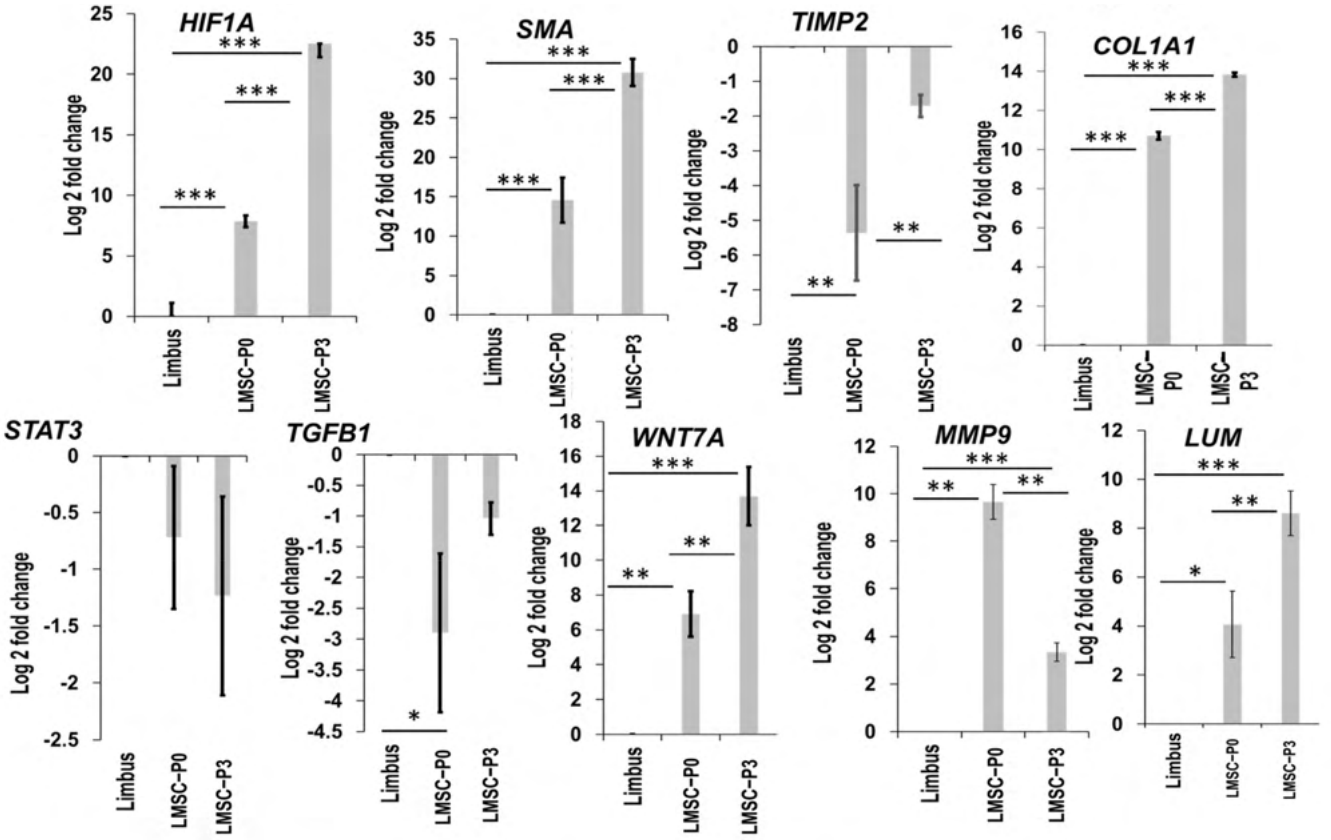

Figure 7. Validating the levels of DEGs. Level of expression of the differentially expressed genes validated through qRT-PCR. The levels of DEGs in limbal epithelial (LMSC−P0) and stromal (LMSC−P3) cells was quantified relative to native limbal tissue (n = 5). The results were plotted as mean log 2-fold change ± SD. The statistical analysis was performed using Kruskal–Wallis one-way ANOVA test. * $p < 0.05$, ** $p < 0.01$, *** $p < 0.001$.

3. Discussion

Various groups across the globe have attempted to understand the basic biology and the mechanisms involved in the healing or repair of the corneal wounds resulting from trauma [49–51] or the regeneration of the corneal epithelium and stroma lost due to the regular wear and tear [30,52]. The epithelial homeostasis is achieved primarily through the LESCs residing in the limbal crypts [53], in which the systematic synthesis and the degradation of the collagens in the stromal extracellular matrix (ECM) released by the native keratocytes helps in the maintenance of the corneal stromal integrity and homeostasis [54]. The interactions between the epithelial and stromal cells affect the repair of the cornea after an injury. Earlier studies have shown that the communication or the interaction between the LESCs and the stromal cells through their cytokines and other secretory molecules is essential for maintaining the corneal integrity [28,37,53] and thereby its transparency. IL-1 and its isoforms (IL-1α and IL-1β), produced by the epithelial cells during corneal injury, promote the production of TNF-α, KGF, and HGF [55,56]. Together with TNF-α, IL-1 also modulates the production of growth factors (PDGF and family) that modulate the chemotaxis and proliferation of corneal fibroblasts [57]. They also enhance the levels of cytokines such as G-CSF, neutrophil-activating peptide, IL-3 precursor, IL-4, IL-6, IL-7, IL-8, IL-9, and IL-17 [58]. These cytokines trigger the entry of inflammatory cells to the site of injury [59,60]. HGF and KGF released by the stromal fibroblasts, along with bFGF, IGF, and EGF, modulate the interactions between epithelial and stromal cells, regulating the migration and differentiation of damaged epithelial cells [61–65]. IL-6, a multifunctional cytokine, modulates the repair of the cornea in many ways. It enhances the epithelial wound closure, and low levels of IL-6 delays the healing [66–68]. Additionally, it

reduces the levels of IL-1 and TNF-α, lowering inflammation [69]. A study by Samaeekia et al. [37] has shown that the exosomes isolated from the corneal and peripheral limbal MSCs enhance the migration and proliferation of corneal epithelial cells in vitro. The co-culture of corneal epithelial cells and corneal stromal cells has been shown to reduce the levels of pro-inflammatory cytokines and enhance the number of viable epithelial cells following an injury [70].

However, in the cases of corneal injuries (limited to the layers of epithelium and its surface, as well as the stroma), the healing process that follows involves one or more factors such as the native cells, growth factors, genes, cytokines, and antigen-presenting cells and even lipids [71–75]. The healing/repair process could involve just one of the above factors or a cascade of multiple events and reactions based on the site/location and the severity of the wound. Additionally, not all of them can be favorable towards the transparency of cornea. Mechanisms such as corneal fibrosis result in opaque/scarred cornea obscuring the visual pathway. The LMSCs were proven to be one of the promising intervention which could prevent and repair the corneal wound without needing a whole corneal replacement [22,38]. These cells are capable of differentiating into the native keratocyte phenotype [22,23]. Recent studies by Orozco Morales et al. [70], Hertsenberg et al. [76], Weng et al. [77] Chameettachal et al. [78] and Chandru et al. [79] have shown the potential of these cells in healing the cornea both in vitro and in vivo in animal models. However, the underlying mechanisms of how these cells achieve the scarless wound healing is not clearly studied. The current study aimed in uncovering the pathways and genes or other factors involved in the corneal wound repair by the LMSCs.

The LMSCs were isolated from cadaveric donor corneo-limbal rims and cultivated in a GMP-certified clean-room facility. Cells at the primary cultures (P0) where both mesenchymal/stromal stem cells of limbus and LESCs were obtained and cell population at the third passage where a pure population of the limbal mesenchymal/stromal cells were obtained (Figure 1), were subjected to RNA sequencing and immunostaining analysis. The outcomes of these two methods were further validated through the qRT-PCR. The mix population of the cells at primary culture were termed LMSC−P0 and the latter was termed LMSC−P3. The digestion of limbal tissue with collagenase alone and maintenance of low serum levels may possibly have led to the propagation of limbal mesenchymal/stromal cells only. The complete removal of serum may lead to the generation of fibroblastic cells with reduced keratocyte phenotype [80]. Conversely, a low quantity of serum (2%) [22] after digestion with collagenase alone [81] would allow stromal cells to proliferate with gradual loss of epithelial islands in the culture. Cells in both populations were found to express the stem cell ocular biomarkers positively (Figure 2). However, the number of cells positive for collagens and mesenchymal biomarkers was more in LMSC−P3 (Figure 3). The collagens of corneal stromal ECM also followed a similar trend, with more expression in LMSC−P3 (Figure 4).

The principle component analysis plot revealed an altered transcriptomic signature of the LMSC−P3 from the rest of the clusters. Of the 28,000 genes detected, nearly 7800 were found to DEGs from all the samples, with LMSC−P0 having more number of DEGs. The asymmetry of the up-regulated or down-regulated genes visualized through volcanic plots revealed a near symmetry in LMSC−P0 (Figure 5). The gene ontology enrichment revealed 6344 unique genes with functions in more than 16 biological processes (Figure 6 and Supplementary Table S4). Genes belonging to signaling pathways such as Wnt (211 DEGs), TGF-β (85 DEGs), stem cell (23 DEGs), and wound healing pathways (254 DEGs) were also obtained (Supplementary Figure S1, and Supplementary Tables S5 and S6). Many studies have proven the anti-inflammatory and immunomodulatory properties of the LMSCs [70,76,77,82]. The findings of the current study also support the anti-inflammatory nature of these cells. The overall genes of the inflammatory response (734) were down-regulated in LMSC−P3 relative to LMSC−P0 (Figure 5A). The pro-fibrotic gene IL-13 (Figure 7), and inflammatory genes C3 and CXCL8 which may lead to corneal neovascular-

ization, etc., were down-regulated in LMSC−P3. Additionally, the anti-inflammatory gene 1L-10 (Figure 7) was up-regulated in LMSC−P3 relative to LMSC−P0.

COL5A1 is a prominent and vital regulator of fibrillogenesis [83], the levels of which were reported to be high during the healing of scars [84,85]. During wound healing, the fibroblasts recruited to the site of injury produce collagens type I and V for extracellular matrix regeneration and restoration of the corneal thickness. In our study, the levels of COL5A1 were found to be higher in LMSC−P3 when compared to LMSC−P0 and native cornea. A similar finding was reported by Ruggiero et al. [86], who have shown that the amount of type V collagen produced by corneal fibroblasts in vitro is higher than that of the native cornea. Moreover, studies by McLaughlin et al. [87] and DeNigris et al. [88] have reported that the altered fibroblasts affect the level of collagen V in vitro. This also justifies and explains the levels of COL5A1 being proportionate to the number of fibroblasts in cells/tissues analyzed, i.e., LMSC−P3, followed by LMSC−P0, cornea, and limbus (Supplementary Table S5 and Figure S5C). The number of fibroblasts was also relatively high in LMSC−P3 compared to LMSC−P0 (Figure 1A–C,F). These findings were similar to the study by Z.H. Guo et al. [89], who provided insights into the molecular mechanisms of differentiation and stemness maintenance by limbal stem cell niche in mice. The collagen genes of corneal stroma are responsible for collagen synthesis, which is predominantly regulated by COL5A1 [90]. The exclusive up-regulation of the COL5A1 by the LMSC−P3 cells evidently shows their ability and makes them an ideal source for repair and regeneration of corneal tissue through collagen fibrillogenesis (Figure 5C,D).

The other gene exclusively up-regulated in LMSC−P3 was TIMP-1, an inhibitor of the matrix metalloproteinases (MMPs), the genes responsible for cleaving collagens. The tissue inhibitor of metalloproteinases (TIMPs), inhibit these MMP genes, highly regulating the corneal ECM. The binding of TIMPs to the MMPs prevents the degradation of the ECM. TIMP-1 inhibits all active MMPs, except membrane type matrixins (MT1-MMP), whereas TIMP-2 inhibits MMP-2, in particular [91,92]. These two groups of genes, i.e., the MMP family and the TIMP family, also a play vital role in the development of cornea [93]. In this study, we have found that TIMP-1, MMP-1, and MMP-9 were found to be up-regulated and that TIMP-2 and MMP-3 were down-regulated in LMSC−P3. A similar trend was observed in the LMSC−P0, except for the levels of MMP-3. Although MMP-9 in LMSC−P3 was up-regulated, the levels of TIMP-1 were much higher in terms of fold-change. Unlike the earlier studies [94,95], the positive correlation between the levels of TGF-β and TIMP1 was also not observed in our study (Figures 5C,D and 7), which did not involve disease condition or the altering of their concentration in culture. Assessing all these genes in a disease condition may provide a better understanding of their respective roles in corneal regeneration.

The exclusively elevated genes on LMSC−P3 interact through various genes and biological processes. The network functional enrichment analysis performed to understand their interactions has revealed a set of interleukins, matrixins, chemokine receptors, and growth factors. Most of these were up-regulated in LMSC−P3 relative to LMSC−P0 (Figure 7). Corneal ECM genes such as Keratocan, Lumican, and SMA were expressed significantly higher in LMSC−P3 relative to LMSC−P0 and native limbus. Lumican and keratocan belong to the SLRP (small leucine-rich proteoglycan) family, which is critical for corneal clarity. They are responsible for the fibrillar organization of the collagens in the ECM of the corneal stroma [96,97]. Both these proteoglycans play a crucial role in corneal wound healing and regulate inflammation by localizing the macrophages to the site of injury and recruiting neutrophils [97]. The levels of lumican and keratocan were reported to decrease during the scarring of cornea [98]. Unlike the studies [99,100] that reported low expression of keratocan by keratocytes in vitro, we observed relatively high levels of keratocan in LMSC−P3. However, when compared to LMSC−P0, where there is no chance of differentiating the expression of keratocyte markers by a diverse set of cell populations and the relatively less number of stromal cells, the high number of stromal cells in LMSC−P3 could attribute to the high levels of keratocan and lumican. The

down-regulation of TGF-β could also be attributed to the keratocan levels, as shown by Kawakita et al. [101], with decreasing levels of TGF-β maintaining the levels of keratocan. This indicates the strong keratocyte-like nature of the cells in LMSC−P3 with respect to LMSC−P0. The increased expression of SMA in LMSC−P3 relative to LMSC−P0 could be attributed to the relatively high number of myofibroblastic cells in LMSC−P3 than in LMSC−P0.

We have also found that the expression of VEGFA, a proangiogenic factor, was also significantly high in LMSC−P3. The continuous maintenance of corneal avascularity is important for optimal visual acuity. Angiogenesis is one of the many vital processes in wound healing for the successful repair of damaged tissue. The balance between the proangiogenic and anti-angiogenic factors is mandatory for maintaining corneal avascularity [102]. To assess the levels of angiogeneic factors that regulate the formation of vasculature on corneal surface, certain genes were quantified through qRT-PCR. VEGFA is one of the proangiogenic factors which, besides FGF-2 [102], plays a role in multiple processes such as immune-modulation, epithelialization, collagen deposition, and cell migration [103]. It decreases the duration of wound healing [104]. Although MSCs were reported to potentially lower angiogenesis [105], the surprisingly high expression of the VEGFA in LMSC−P3 (Figure 7) is questionable due to the fact that elevated vasculature over the surface of cornea can potentially affect the visual acuity [106,107]. However, the elevated levels of VEGFA (growth factor-induced or transfected or topically applied) in the wound bed were reported to enhance the wound repair of dermis/skin [108–111], but not many studies on corneal surface were reported. These elevated levels of VEGFA also contradict decreased expression of MMP9, the factors reported to feedback regulation mechanism [112]. However, other proangiogenic factors such as PDGF and its family (PDGFB, PDGFC, PDGFD, PDGFRA, and PDGFRB) are either unexpressed or down-regulated in LMSC−P3 (Supplementary Table S5). Although native corneal epithelial tissue is reported to have detectable levels of VEGFA and sflt-1 [113,114], not much information is available regarding the levels of VEGFA in native limbal tissue. However, the levels of VEGF expression occurs differently in different cells in vitro. The limbal epithelial cells were earlier reported [115] to be anti-angiogenic in nature and the limbal fibroblasts proangiogenic in nature. The corresponding high and low levels of the limbal fibroblasts in LMSC−P3 and LMSC−P0, respectively, could possibly explain the increased levels of VEGFA. However, a contradicting observation was reported much later in a study by Eslani et al. [116], who have shown that the LMSCs are anti-angiogenic. Low levels of VEGFA and high levels of the anti-angiogeneic factors SFLT-1 and PDGF were observed in the secretome of LMSCs. In the current study, determining the levels of SFLT-1, MMP-2, MMP-14, and CTGF genes in the cell populations/tissues tested could have provided a better answer to this conundrum. Further studies to explore/evaluate the levels of VEGF in a corneal wound model treated with LMSCs and monitoring of the progress of healing may be required.

4. Materials and Methods

4.1. Ethics Approval and Tissue Collection

Human donor corneas (donor age ranged between 18–60 years) were collected from the Ramayamma International Eye Bank (RIEB), LV Prasad Eye Institute, Hyderabad. Overall, 21 therapeutic-grade donor corneas, unutilized for surgical purposes, were used in this study (n = 21). The corneas were collected with informed consent and in compliance with the guidelines of the Declaration of Helsinki. Ethical approval was obtained from the Institutional Ethics Committee (Reference number LEC 05-18-081) and the Institutional Committee for Stem Cell Research, of LV Prasad Eye Institute, Hyderabad, India (IC-SCR-Ref No: 08-18-002).

4.2. Establishment of Limbal Stem Cell Culture

The tissue processing was done using a stereomicroscope (SZX10, Olympus, Japan) to set up the limbal stromal stem cell culture, as described previously [117], and for total RNA

extraction. Briefly, cadaveric corneas were washed with 1X PBS (14190250, Thermo Fisher Scientific, Waltham, MA, USA) fortified with 2× antibiotics (15240062, Thermo Fisher Scientific, Waltham, MA, USA) and were stripped of endothelium and iris. Full thickness limbus was excised in 1× PBS and then fragmented to small pieces in plain DMEM/F12 media (BE04-687F/U1, Lonza, Basel, Switzerland). These tissue fragments were minced for 1–2 min. The dissected limbal tissue is then enzymatically digested by Collagenase type IV (17104019, Thermo Fisher Scientific, Waltham, MA, USA) enzyme (200 IU per one donor rim), added to 1 mL of plain DMEM/F12 media and then incubated for 16 h. The digested tissue is sedimented twice at 1000 rpm/3 min in PBS. The pellet is then suspended in complete media, i.e., DMEM/F12 fortified with 2% Fetal Bovine Serum (SH30084.03, Cytiva Life Sciences, Shrewsbury, MA, USA) and supplemented with human recombinant Epidermal Growth Factor (PHG0311L, Thermo Fisher Scientific, Waltham, MA, USA) and human recombinant Insulin (12585014, Thermo Fisher Scientific, Waltham, MA, USA). This suspension was plated and cultured for 3 generations. Cells upon confluence, at the stages of primary culture (LMSC−P0) and passage 1 (LMSC−P1) and passage 3 (LMSC−P3), were used for analysis.

4.3. Immunofluorescence Assay

Cells were grown on the surface of glass coverslips in complete media until confluence. The cells were then fixed with 4% Formaldehyde (30525-89-4- 500G, Fisher Scientific, Bangalore, India) for 10 min and washed twice with 1× PBS before permeabilization with 0.3% Triton-X (T8787-100ML, Sigma-Aldrich, St. Louis, MO, USA) for 20 min and washed thrice. Later, the cells were blocked with 2.5% Bovine Serum Albumin (BSA) (A7096-50G, Sigma-Aldrich, St. Louis, MO, USA) in PBS for one hour at room temperature and incubated overnight at 4 °C with primary antibody (Supplementary Table S1) diluted in 1% BSA. This was followed by a wash with PBS thrice for 10 min and incubation with secondary antibody (Supplementary Table S1) (diluted in 1% BSA) for 45 min, which was further washed thrice and mounted onto a glass slide using Fluoroshield Mounting Medium with DAPI (ab104139, Abcam, San Francisco, CA, USA) for nuclei counterstaining. Staining of negative controls was done by omitting the primary antibody. Images were documented using an inverted fluorescence microscope (Axio Scope A1, Carl Zeiss AG, Oberkochen, Germany). The biomarker panel of the MSC phenotype was chosen in accordance with the minimal criteria set for multipotent mesenchymal stem cells [18].

4.4. RNA Isolation

Total RNA was isolated from tissues (sclera, limbus, and cornea) and limbal stem cells (LMSC−P0 and LMSC−P3) and embryonic stem cell line (ESC) using TRIzol™ reagent (15596018, Thermo Fisher Scientific, Waltham, MA, USA). The spent medium was removed from the 80% confluent cell culture. Cells were then washed with 1× PBS (prepared with DEPC-treated distilled water for RNA isolation) (AM9920, Thermo Fisher Scientific, Waltham, MA, USA), and an appropriate volume of TRIzol™ reagent was added to the cells. The cell lysate was mixed several times through a pipette and transferred to a sterile 1.5 mL micro-centrifuge tube. To the lysate, 0.5 mL of Chloroform (96764, Sisco Research Laboratories, Mumbai, India) was added per every 1mL of TRIzol™ reagent and incubated at room temperature for 15 min. This was followed by centrifugation at 12,000 rpm for 15 min at 4 °C. The aqueous phase was collected in a fresh tube and 1 mL of Isopropanol (Q13825, Thermo Fisher Scientific, Waltham, MA, USA) was added (in equal volumes with TRIzol™ reagent) and incubated at room temperature for 3 min followed by centrifugation at 12,000 rpm for 3 min at 4 °C. RNA pellet was washed with 75% Ethanol (24102, Sigma-Aldrich, St. Louis, MO, USA), air dried, and dissolved in 25 µL of nuclease-free water (AM7020) (volume dependent on size of RNA pellet). RNA was quantified by measuring the absorbance using a spectrophotometer along with the purity evaluation by the ratio of A260/280 (NanoVue™ Plus, 28956058, GE Healthcare Bio-Sciences AB, Chicago, IL, USA). Further confirmation was done through gel electrophoresis, using 1%

agarose gel (50004, Lonza, Basel, Switzerland) stained with Ethidium Bromide (93079, Sisco Research Laboratories Private Limited, Mumbai, India). The RNA was treated with DNase I (AM2222, Thermo Fisher Scientific, Waltham, MA, USA) according to manufacturers' protocol. Briefly, a 30 µL reaction volume containing 30 µg of total cellular RNA, 1× reaction buffer, 6U of DNase I (RNase free), and nuclease-free water. The reaction mix was incubated at 37 °C for 30 min. After incubation, 70 µL DEPC water was added to the reaction mix and the RNA was purified by adding 100 µL TRIzol™ reagent. The RNA was quantified by measuring the absorbance using a spectrophotometer, as previously described, and 1µg each of the RNA from the analytes was used for the RNA-Seq study.

4.5. Next Generation RNA Sequencing (RNA-Seq) and Library Preparation

One microgram each of the total RNA from limbus, cornea, sclera, LMSC−P0, LMSC−P3, and embryonic stem cells (ESC) were subjected to RNA sequencing via Illumina platform using the reagents provided in the Illumina® TruSeq® Stranded Total RNA Sample Preparation Ribo-Zero™ kit (RS-122-2201, Illumina, San Diego, CA, USA). The first step involves the removal of ribosomal RNA using Ribo-Zero™ rRNA removal beads provided in the kit. The Ribo-Zero™ rRNA reagent depletes samples of cytoplasmic ribosomal RNA. Following purification, the RNA was fragmented into small pieces by heat digestion using divalent cations (magnesium or zinc) under elevated temperature. The cleaved RNA fragments were copied into first strand cDNA using reverse transcriptase and random primers. This is followed by second strand cDNA synthesis using DNA polymerase I and RNase H. These cDNA fragments then have the addition of a single 'A' base and subsequent ligation of the adapter. The products have been purified and enriched with PCR to create the final cDNA library. This sample preparation protocol provides the advantages of (i) strand information on RNA transcript and (ii) library capture of both coding RNA and multiple forms of non-coding RNA. The processed cDNA library of all 6 samples was used for paired end sequencing run (50 × 2 cycles) on the Illumina HiSeq 2500 platform (SY–401–2501, Illumina, San Diego, CA, USA).

4.5.1. Pre-Processing of the RNA-Seq Data for Data Analysis

The Fastq file was obtained from sequencer after trimming the adapter sequences using bcl2fastq program. Fastq data was used for alignment with the hg19 version of the human genome using the TopHat program with options provided as transcript annotation file. The alignment data has been used for guided transcript assembly using the Cufflinks program. After that, we merged transcripts across samples using the Cuffmerge program to make a reference transcript assembly. This merged transcript assembly has been used as a reference to compare for differential gene expression between a pair of samples with the use of Cuffdiff program. The resultant Cuffdiff output file has provided the normalized expression of genes/transcript in the form of counts, and the fold differences converted into log2 values. The details of the reference links of all the software/programs/bioinformatics tools used in analysis of the RNA-Seq data were provided in the Supplementary Table S3.

4.5.2. Differential Expression Analysis

The counts obtained for each sample were analyzed by using the EBSeq tool (Supplementary Table S3) for differential expression by considering scleral tissue as the control. A list of DEGs was obtained for the tissues with pairwise comparison to sclera, and multiple testing corrections were applied at a False Discovery Rate (FDR) of 0.05 percent. The heatmaps were generated using R software.

4.5.3. Delineating Cell-Specific Gene Expression Patterns and Testing for Pathway Enrichment

To delineate the DEGs in different tissues and cells according to their cellular specific expression, 5-way Venn diagrams were used to find the genes which were exclusively up-regulated and down-regulated. Two types of the gene expression patterns were analyzed.

The cell type-specific gene expression to find genes that were exclusively differentially regulated in only one type of the cell/tissue and which may therefore serve as transcriptomic markers to identify the unique cell type. Pairwise overlapping genes that are differentially regulated only in two cell types may indicate a shared functionality between the two cell types. To obtain pathway-level insights into the significance of the exclusively differentially regulated genes, we have conducted pathway enrichment analysis through the Gene Ontology studies using Enrichr tool. This analysis indicates statistically significant groups of genes that are belong to various biological/signaling pathways.

4.5.4. Gene Ontology Pathway-Specific Gene Expression Changes

Using the ontology keywords derived from the pathway enrichments obtained in the Enrichr analysis, the lists of genes specific to the pathway-keywords were obtained from the gene ontology database using the AmiGO tool. These gene lists were used to examine the differences in the frequency distribution of fold-change values of pathway-specific genes as compared to that of all the other genes in the transcriptome. These differences in the distributions were tested for statistical significance using the nonparametric Mann–Whitney–Wilcoxon U test. The median difference between the distributions was used to detect the direction of the shift in expression value. The values of median shift of the pathways across different samples were plotted against the crossed out the values which were not statistically significant ($p \leq 0.05$).

4.6. Reverse Transcriptase PCR

One microgram each of the RNA was reverse transcribed to cDNA using the Superscript™ III First-Strand Synthesis System (18080051, Thermo Fisher Scientific, Waltham, MA, USA) according to the manufacturer's instructions.

4.7. qRT-PCR

Quantitative PCR was performed using 200 ng of cDNA in a final volume of 25 µL reaction mix (K0221, Maxima SYBR Green/ROX qPCR Master Mix (2X), Thermo Fisher Scientific, Waltham, MA, USA) and a 0.2 µM primer concentration. The reaction was carried out using Step One (Applied Biosystems, Life technologies) hardware and software. The reactions were run in triplicates. The gene expression data were normalized to control the variability in expression levels to the geometric mean of the housekeeping gene. The expression level of target genes was represented as a relative expression by using $2^{-\Delta\Delta Ct}$ formula and the graphs were plotted using their Log2 fold-change values. The primer sequences are listed in the Supplementary Table S2.

4.8. Statistical Analysis

All the experiments were repeated at least thrice with biological triplicates. Statistical analysis was performed using the Graphpad Prism 6 software. The tests employed were Student's two-tailed *t*-tests, Kruskal–Wallis test, and a nonparametric one-way ANOVA test with p values ≤ 0.05 to assess the statistical significance. The results are presented as the mean ± standard deviation.

5. Conclusions

In the current study, we report the genes, biological processes, and pathways involved in the limbal stromal/mesenchymal stem cell-mediated corneal wound healing by employing RNA-Sequencing in human LMSCs (LMSC−Passage-0 and LMSC−Passage-3), for the first time. Differential expression of the genes (7800) belonging to the following pathways, namely, apoptosis, cell motility, dedifferentiation, inflammatory response, stem cell maintenance, tissue remodeling, and wound healing pathways, etc., were found. The interactions between the DEGs exclusively up-regulated by the LMSC−P3 in the wound healing pathway (COL5A1, COL1A1 and TIMP1) have revealed the processes involved in tissue remodeling and repair (collagen fibril reorganization, collagen biosynthesis, regula-

tion of the metallopeptidase activity etc.) and the cytokines and other key genes regulating these processes. However, this study is limited by the small sample size, and further comprehensive studies needed to explore and understand all the DEGs and their biological relevance in corneal wound healing. On the whole, the findings of this study provide a brief glimpse into the molecular basis of tissue repair, and the remodeling of the cornea by human LMSCs and the therapeutic potential of this.

Supplementary Materials: The following supporting information can be downloaded at: https://www.mdpi.com/article/10.3390/ijms23158226/s1.

Author Contributions: Conceptualization, F.T., M.D., A.K.R., S.B. and V.S.; methodology, F.T., M.D., A.G., D.D., A.K.R. and V.S.; validation, F.T., M.D., M.A.K., A.G. and D.D.; formal analysis, F.T., M.D., M.A.K. and V.S.; investigation, F.T., M.D., M.A.K. and V.S.; resources, F.T., M.D. and V.S.; data curation, S.B. and V.S.; writing—original draft preparation, F.T. and M.D.; writing—review and editing, F.T., M.D., M.A.K., S.B. and V.S.; visualization, F.T. and M.D.; supervision, A.K.R., S.B. and V.S.; project administration, A.K.R. and V.S.; funding acquisition, A.K.R., S.B. and V.S. All authors have read and agreed to the published version of the manuscript.

Funding: This research was funded by the SCIENCE AND ENGINEERING RESEARCH BOARD, Government of India, grant number EMR/2017/005086 and CRG/2018/003514 (EMR and CORE research grant to Dr Vivek Singh and Dr Sayan Basu). This work was partly supported by the Hyderabad Eye Research Foundation, Hyderabad, India. MD thankfully acknowledges the Senior Research Fellowship grant, File No. 2020-7055/CMB-BMS, from the INDIAN COUNCIL OF MEDICAL RESEARCH, Government of India.

Institutional Review Board Statement: The study was conducted in accordance with the Declaration of Helsinki, and approved by the Institutional Ethics Committee (LEC 05-18-081, approved on 22 May 2018) and Institutional Committee for Stem Cell Research (IC-SCR-Ref No:08-18-002, approved on 24 August 2018) of LV PRASAD EYE INSTITUTE.

Informed Consent Statement: Informed consent was obtained from the next-of-kin of all the donors. The consent forms are available with the Ramayamma International Eye Bank, Hyderabad.

Data Availability Statement: Data available upon request from the corresponding author, due to the Institutional policies.

Acknowledgments: We thank Indumati Mariappan for generously providing the embryonic stem cell line and the Ramayamma International Eye Bank, LV Prasad Eye Institute for providing cadaveric corneas. We would also like to thank NGS facility, Centre for Genetic Disorders, Banaras Hindu University for performing the RNA Sequencing.

Conflicts of Interest: The authors have no proprietary or commercial interest in any materials discussed in this article. The funders had no role in the design of the study; in the collection, analyses, or interpretation of data; in the writing of the manuscript, or in the decision to publish the results.

References

1. Meek, K.M.; Knupp, C. Corneal structure and transparency. *Prog. Retin. Eye Res.* **2015**, *49*, 1–16. [CrossRef] [PubMed]
2. DelMonte, D.W.; Kim, T. Anatomy and physiology of the cornea. *J. Cataract Refract. Surg.* **2011**, *37*, 588–598. [CrossRef]
3. Eghrari, A.O.; Riazuddin, S.A.; Gottsch, J.D. Overview of the Cornea: Structure, Function, and Development. *Prog. Mol. Biol. Transl. Sci.* **2015**, *134*, 7–23. [CrossRef] [PubMed]
4. Kumar, A.; Yun, H.; Funderburgh, M.L.; Du, Y. Regenerative therapy for the Cornea. *Prog. Retin. Eye Res.* **2021**, *87*, 101011. [CrossRef] [PubMed]
5. Barrientez, B.; Nicholas, S.E.; Whelchel, A.; Sharif, R.; Hjortdal, J.; Karamichos, D. Corneal injury: Clinical and molecular aspects. *Exp. Eye Res.* **2019**, *186*, 107709. [CrossRef] [PubMed]
6. Van Buskirk, E.M. The anatomy of the limbus. *Eye* **1989**, *3*, 101–108. [CrossRef] [PubMed]
7. Mitragotri, N.; Damala, M.; Singh, V.; Basu, S. Limbal Stromal Stem Cells in Corneal Wound Healing: Current Perspectives and Future Applications. In *Corneal Regeneration*; Alió, J.L., Alió del Barrio, J.L., Arnalich-Montiel, F., Eds.; Essentials in Ophthalmology; Springer International Publishing: Cham, Switzerland, 2019; pp. 387–402; ISBN 978-3-030-01303-5.
8. Seyed-Safi, A.G.; Daniels, J.T. The limbus: Structure and function. *Exp. Eye Res.* **2020**, *197*, 108074. [CrossRef]
9. Dua, H.S.; Shanmuganathan, V.A.; Powell-Richards, A.O.; Tighe, P.J.; Joseph, A. Limbal epithelial crypts: A novel anatomical structure and a putative limbal stem cell niche. *Br. J. Ophthalmol.* **2005**, *89*, 529–532. [CrossRef]

10. Dziasko, M.A.; Armer, H.E.; Levis, H.J.; Shortt, A.J.; Tuft, S.; Daniels, J.T. Localisation of epithelial cells capable of holoclone formation in vitro and direct interaction with stromal cells in the native human limbal crypt. *PLoS ONE* **2014**, *9*, e94283. [CrossRef]
11. Higa, K.; Shimmura, S.; Miyashita, H.; Shimazaki, J.; Tsubota, K. Melanocytes in the corneal limbus interact with K19-positive basal epithelial cells. *Exp. Eye Res.* **2005**, *81*, 218–223. [CrossRef] [PubMed]
12. Huang, M.; Wang, B.; Wan, P.; Liang, X.; Wang, X.; Liu, Y.; Zhou, Q.; Wang, Z. Roles of limbal microvascular net and limbal stroma in regulating maintenance of limbal epithelial stem cells. *Cell Tissue Res.* **2015**, *359*, 547–563. [CrossRef] [PubMed]
13. Gage, P.J.; Rhoades, W.; Prucka, S.K.; Hjalt, T. Fate maps of neural crest and mesoderm in the mammalian eye. *Investig. Ophthalmol. Vis. Sci.* **2005**, *46*, 4200–4208. [CrossRef] [PubMed]
14. Du, Y.; Funderburgh, M.L.; Mann, M.M.; SundarRaj, N.; Funderburgh, J.L. Multipotent stem cells in human corneal stroma. *Stem Cells Dayt. Ohio* **2005**, *23*, 1266–1275. [CrossRef] [PubMed]
15. Polisetty, N.; Fatima, A.; Madhira, S.L.; Sangwan, V.S.; Vemuganti, G.K. Mesenchymal cells from limbal stroma of human eye. *Mol. Vis.* **2008**, *14*, 431–442. [PubMed]
16. Li, G.-G.; Zhu, Y.-T.; Xie, H.-T.; Chen, S.-Y.; Tseng, S.C.G. Mesenchymal stem cells derived from human limbal niche cells. *Investig. Ophthalmol. Vis. Sci.* **2012**, *53*, 5686–5697. [CrossRef]
17. Funderburgh, J.L.; Funderburgh, M.L.; Du, Y. Stem Cells in the Limbal Stroma. *Ocul. Surf.* **2016**, *14*, 113–120. [CrossRef]
18. Dominici, M.; Le Blanc, K.; Mueller, I.; Slaper-Cortenbach, I.; Marini, F.; Krause, D.; Deans, R.; Keating, A.; Prockop, D.; Horwitz, E. Minimal criteria for defining multipotent mesenchymal stromal cells. The International Society for Cellular Therapy position statement. *Cytotherapy* **2006**, *8*, 315–317. [CrossRef]
19. Pinnamaneni, N.; Funderburgh, J.L. Concise review: Stem cells in the corneal stroma. *Stem Cells Dayt. Ohio* **2012**, *30*, 1059–1063. [CrossRef]
20. Sidney, L.E.; Hopkinson, A. Corneal keratocyte transition to mesenchymal stem cell phenotype and reversal using serum-free medium supplemented with fibroblast growth factor-2, transforming growth factor-β3 and retinoic acid. *J. Tissue Eng. Regen. Med.* **2018**, *12*, e203–e215. [CrossRef]
21. Park, S.H.; Kim, K.W.; Chun, Y.S.; Kim, J.C. Human mesenchymal stem cells differentiate into keratocyte-like cells in keratocyte-conditioned medium. *Exp. Eye Res.* **2012**, *101*, 16–26. [CrossRef]
22. Basu, S.; Hertsenberg, A.J.; Funderburgh, M.L.; Burrow, M.K.; Mann, M.M.; Du, Y.; Lathrop, K.L.; Syed-Picard, F.N.; Adams, S.M.; Birk, D.E.; et al. Human limbal biopsy-derived stromal stem cells prevent corneal scarring. *Sci. Transl. Med.* **2014**, *6*, 266ra172. [CrossRef] [PubMed]
23. Dos Santos, A.; Balayan, A.; Funderburgh, M.L.; Ngo, J.; Funderburgh, J.L.; Deng, S.X. Differentiation Capacity of Human Mesenchymal Stem Cells into Keratocyte Lineage. *Investig. Ophthalmol. Vis. Sci.* **2019**, *60*, 3013–3023. [CrossRef] [PubMed]
24. Hashmani, K.; Branch, M.J.; Sidney, L.E.; Dhillon, P.S.; Verma, M.; McIntosh, O.D.; Hopkinson, A.; Dua, H.S. Characterization of corneal stromal stem cells with the potential for epithelial transdifferentiation. *Stem Cell Res. Ther.* **2013**, *4*, 75. [CrossRef]
25. Katikireddy, K.R.; Dana, R.; Jurkunas, U.V. Differentiation potential of limbal fibroblasts and bone marrow mesenchymal stem cells to corneal epithelial cells. *Stem Cells Dayt. Ohio* **2014**, *32*, 717–729. [CrossRef]
26. Espana, E.M.; Kawakita, T.; Romano, A.; Di Pascuale, M.; Smiddy, R.; Liu, C.; Tseng, S.C.G. Stromal niche controls the plasticity of limbal and corneal epithelial differentiation in a rabbit model of recombined tissue. *Investig. Ophthalmol. Vis. Sci.* **2003**, *44*, 5130–5135. [CrossRef] [PubMed]
27. Dziasko, M.A.; Tuft, S.J.; Daniels, J.T. Limbal melanocytes support limbal epithelial stem cells in 2D and 3D microenvironments. *Exp. Eye Res.* **2015**, *138*, 70–79. [CrossRef]
28. Kureshi, A.K.; Dziasko, M.; Funderburgh, J.L.; Daniels, J.T. Human corneal stromal stem cells support limbal epithelial cells cultured on RAFT tissue equivalents. *Sci. Rep.* **2015**, *5*, 16186. [CrossRef] [PubMed]
29. Polisetti, N.; Zenkel, M.; Menzel-Severing, J.; Kruse, F.E.; Schlötzer-Schrehardt, U. Cell Adhesion Molecules and Stem Cell-Niche-Interactions in the Limbal Stem Cell Niche. *Stem Cells Dayt. Ohio* **2016**, *34*, 203–219. [CrossRef]
30. Yazdanpanah, G.; Jabbehdari, S.; Djalilian, A.R. Limbal and corneal epithelial homeostasis. *Curr. Opin. Ophthalmol.* **2017**, *28*, 348–354. [CrossRef]
31. Polisetti, N.; Gießl, A.; Zenkel, M.; Heger, L.; Dudziak, D.; Naschberger, E.; Stich, L.; Steinkasserer, A.; Kruse, F.E.; Schlötzer-Schrehardt, U. Melanocytes as emerging key players in niche regulation of limbal epithelial stem cells. *Ocul. Surf.* **2021**, *22*, 172–189. [CrossRef]
32. Zhao, J.; Mo, V.; Nagasaki, T. Distribution of label-retaining cells in the limbal epithelium of a mouse eye. *J. Histochem. Cytochem.* **2009**, *57*, 177–185. [CrossRef] [PubMed]
33. Ljubimov, A.V.; Saghizadeh, M. Progress in corneal wound healing. *Prog. Retin. Eye Res.* **2015**, *49*, 17–45. [CrossRef] [PubMed]
34. Ksander, B.R.; Kolovou, P.E.; Wilson, B.J.; Saab, K.R.; Guo, Q.; Ma, J.; McGuire, S.P.; Gregory, M.S.; Vincent, W.J.B.; Perez, V.L.; et al. ABCB5 is a limbal stem cell gene required for corneal development and repair. *Nature* **2014**, *511*, 353–357. [CrossRef]
35. Amitai-Lange, A.; Altshuler, A.; Bubley, J.; Dbayat, N.; Tiosano, B.; Shalom-Feuerstein, R. Lineage tracing of stem and progenitor cells of the murine corneal epithelium. *Stem Cells Dayt. Ohio* **2015**, *33*, 230–239. [CrossRef] [PubMed]
36. Reinshagen, H.; Auw-Haedrich, C.; Sorg, R.V.; Boehringer, D.; Eberwein, P.; Schwartzkopff, J.; Sundmacher, R.; Reinhard, T. Corneal surface reconstruction using adult mesenchymal stem cells in experimental limbal stem cell deficiency in rabbits. *Acta Ophthalmol.* **2011**, *89*, 741–748. [CrossRef] [PubMed]

37. Samaeekia, R.; Rabiee, B.; Putra, I.; Shen, X.; Park, Y.J.; Hematti, P.; Eslani, M.; Djalilian, A.R. Effect of Human Corneal Mesenchymal Stromal Cell-derived Exosomes on Corneal Epithelial Wound Healing. *Investig. Ophthalmol. Vis. Sci.* **2018**, *59*, 5194–5200. [CrossRef]
38. Basu, S.; Damala, M.; Tavakkoli, F.; Mitragotri, N.; Singh, V. Human Limbus-derived Mesenchymal/Stromal Stem Cell Therapy for Superficial Corneal Pathologies: Two-Year Outcomes. *Investig. Ophthalmol. Vis. Sci.* **2019**, *60*, 4146.
39. Liu, X.-N.; Mi, S.-L.; Chen, Y.; Wang, Y. Corneal stromal mesenchymal stem cells: Reconstructing a bioactive cornea and repairing the corneal limbus and stromal microenvironment. *Int. J. Ophthalmol.* **2021**, *14*, 448–455. [CrossRef]
40. Netto, M.V.; Mohan, R.R.; Sinha, S.; Sharma, A.; Dupps, W.; Wilson, S.E. Stromal haze, myofibroblasts, and surface irregularity after PRK. *Exp. Eye Res.* **2006**, *82*, 788–797. [CrossRef]
41. Torricelli, A.A.M.; Santhanam, A.; Wu, J.; Singh, V.; Wilson, S.E. The corneal fibrosis response to epithelial-stromal injury. *Exp. Eye Res.* **2016**, *142*, 110–118. [CrossRef]
42. Medeiros, C.S.; Marino, G.K.; Santhiago, M.R.; Wilson, S.E. The Corneal Basement Membranes and Stromal Fibrosis. *Investig. Ophthalmol. Vis. Sci.* **2018**, *59*, 4044–4053. [CrossRef] [PubMed]
43. Barbosa, A.P.; Alves, M.; Furtado, J.M.F.; Adriano, L.; Nominato, L.F.; Dias, L.C.; Fantucci, M.Z.; de Andrade Batista Murashima, A.; Rocha, E.M. Corneal blindness in Plato's cave: The acting forces to prevent and revert corneal opacity. Part I: Epidemiology and new physiopathological concepts. *Arq. Bras. Oftalmol.* **2020**, *83*, 437–446. [CrossRef] [PubMed]
44. Niederkorn, J.Y.; Larkin, D.F.P. Immune privilege of corneal allografts. *Ocul. Immunol. Inflamm.* **2010**, *18*, 162–171. [CrossRef] [PubMed]
45. Borderie, V.M.; Boëlle, P.-Y.; Touzeau, O.; Allouch, C.; Boutboul, S.; Laroche, L. Predicted long-term outcome of corneal transplantation. *Ophthalmology* **2009**, *116*, 2354–2360. [CrossRef] [PubMed]
46. Klebe, S.; Coster, D.J.; Williams, K.A. Rejection and acceptance of corneal allografts. *Curr. Opin. Organ Transplant.* **2009**, *14*, 4–9. [CrossRef]
47. Pantanelli, S.M.; Sabesan, R.; Ching, S.S.T.; Yoon, G.; Hindman, H.B. Visual performance with wave aberration correction after penetrating, deep anterior lamellar, or endothelial keratoplasty. *Investig. Ophthalmol. Vis. Sci.* **2012**, *53*, 4797–4804. [CrossRef]
48. Nielsen, E.; Hjortdal, J. Visual acuity and contrast sensitivity after posterior lamellar keratoplasty. *Acta Ophthalmol.* **2012**, *90*, 756–760. [CrossRef]
49. Dupps, W.J.; Wilson, S.E. Biomechanics and Wound Healing in the Cornea. *Exp. Eye Res.* **2006**, *83*, 709–720. [CrossRef]
50. Chawla, S.; Ghosh, S. Establishment of in vitro model of corneal scar pathophysiology. *J. Cell. Physiol.* **2018**, *233*, 3817–3830. [CrossRef]
51. Cogswell, D.; Sun, M.; Greenberg, E.; Margo, C.E.; Espana, E.M. Creation and grading of experimental corneal scars in mice models. *Ocul. Surf.* **2021**, *19*, 53–62. [CrossRef]
52. Sherwin, T.; McGhee, C.N.J. Corneal epithelial homeostasis. *Ophthalmology* **2010**, *117*, 190–191; author reply 191–192. [CrossRef] [PubMed]
53. Altshuler, A.; Amitai-Lange, A.; Tarazi, N.; Dey, S.; Strinkovsky, L.; Hadad-Porat, S.; Bhattacharya, S.; Nasser, W.; Imeri, J.; Ben-David, G.; et al. Discrete limbal epithelial stem cell populations mediate corneal homeostasis and wound healing. *Cell Stem Cell* **2021**, *28*, 1248–1261.e8. [CrossRef] [PubMed]
54. Keratocyte Biology—PubMed. Available online: https://pubmed.ncbi.nlm.nih.gov/32442558/ (accessed on 18 June 2022).
55. Weng, J.; Mohan, R.R.; Li, Q.; Wilson, S.E. IL-1 upregulates keratinocyte growth factor and hepatocyte growth factor mRNA and protein production by cultured stromal fibroblast cells: Interleukin-1 beta expression in the cornea. *Cornea* **1997**, *16*, 465–471. [CrossRef] [PubMed]
56. Ylä-Outinen, H.; Aaltonen, V.; Björkstrand, A.S.; Hirvonen, O.; Lakkakorpi, J.; Vähä-Kreula, M.; Laato, M.; Peltonen, J. Upregulation of tumor suppressor protein neurofibromin in normal human wound healing and in vitro evidence for platelet derived growth factor (PDGF) and transforming growth factor-beta1 (TGF-beta1) elicited increase in neurofibromin mRNA steady-state levels in dermal fibroblasts. *J. Investig. Dermatol.* **1998**, *110*, 232–237. [CrossRef]
57. Kim, W.J.; Mohan, R.R.; Mohan, R.R.; Wilson, S.E. Effect of PDGF, IL-1alpha, and BMP2/4 on corneal fibroblast chemotaxis: Expression of the platelet-derived growth factor system in the cornea. *Investig. Ophthalmol. Vis. Sci.* **1999**, *40*, 1364–1372.
58. Hong, J.W.; Liu, J.J.; Lee, J.S.; Mohan, R.R.; Mohan, R.R.; Woods, D.J.; He, Y.G.; Wilson, S.E. Proinflammatory chemokine induction in keratocytes and inflammatory cell infiltration into the cornea. *Investig. Ophthalmol. Vis. Sci.* **2001**, *42*, 2795–2803.
59. O'Brien, T.P.; Li, Q.; Ashraf, M.F.; Matteson, D.M.; Stark, W.J.; Chan, C.C. Inflammatory response in the early stages of wound healing after excimer laser keratectomy. *Arch. Ophthalmol.* **1998**, *116*, 1470–1474. [CrossRef]
60. Wright, B.; Hopkinson, A.; Leyland, M.; Connon, C.J. The secretome of alginate-encapsulated limbal epithelial stem cells modulates corneal epithelial cell proliferation. *PLoS ONE* **2013**, *8*, e70860. [CrossRef]
61. Hassell, J.R.; Kane, B.P.; Alexandrou, B.; Musselmann, K. IGF-II Is Present in the Cornea Stroma and Activates Keratocytes to Proliferate in vitro. *Investig. Ophthalmol. Vis. Sci.* **2008**, *49*, 4814.
62. Nagano, T.; Nakamura, M.; Nakata, K.; Yamaguchi, T.; Takase, K.; Okahara, A.; Ikuse, T.; Nishida, T. Effects of Substance P and IGF-1 in Corneal Epithelial Barrier Function and Wound Healing in a Rat Model of Neurotrophic Keratopathy. *Investig. Ophthalmol. Vis. Sci.* **2003**, *44*, 3810–3815. [CrossRef]

63. Wilson, S.E.; He, Y.G.; Weng, J.; Zieske, J.D.; Jester, J.V.; Schultz, G.S. Effect of epidermal growth factor, hepatocyte growth factor, and keratinocyte growth factor, on proliferation, motility and differentiation of human corneal epithelial cells. *Exp. Eye Res.* **1994**, *59*, 665–678. [CrossRef]
64. Li, D.Q.; Tseng, S.C. Differential regulation of keratinocyte growth factor and hepatocyte growth factor/scatter factor by different cytokines in human corneal and limbal fibroblasts. *J. Cell. Physiol.* **1997**, *172*, 361–372. [CrossRef]
65. David, T.; Rieck, P.; Renard, G.; Hartmann, C.; Courtois, Y.; Pouliquen, Y. Corneal wound healing modulation using basic fibroblast growth factor after excimer laser photorefractive keratectomy. *Cornea* **1995**, *14*, 227–234. [CrossRef] [PubMed]
66. Hafezi, F.; Gatzioufas, Z.; Angunawela, R.; Ittner, L.M. Absence of IL-6 prevents corneal wound healing after deep excimer laser ablation in vivo. *Eye* **2018**, *32*, 156–157. [CrossRef] [PubMed]
67. Cole, N.; Bao, S.; Willcox, M.; Husband, A.J. Expression of Interleukin-6 in the Cornea in Response to Infection with Different Strains of Pseudomonas aeruginosa. *Infect. Immun.* **1999**, *67*, 2497–2502. [CrossRef] [PubMed]
68. Nishida, T.; Nakamura, M.; Mishima, H.; Otori, T.; Hikida, M. Interleukin 6 Facilitates Corneal Epithelial Wound Closure In Vivo. *Arch. Ophthalmol.* **1992**, *110*, 1292–1294. [CrossRef] [PubMed]
69. Akira, S.; Hirano, T.; Taga, T.; Kishimoto, T. Biology of multifunctional cytokines: IL 6 and related molecules (IL 1 and TNF). *FASEB J.* **1990**, *4*, 2860–2867. [CrossRef]
70. Orozco Morales, M.L.; Marsit, N.M.; McIntosh, O.D.; Hopkinson, A.; Sidney, L.E. Anti-inflammatory potential of human corneal stroma-derived stem cells determined by a novel in vitro corneal epithelial injury model. *World J. Stem Cells* **2019**, *11*, 84–99. [CrossRef]
71. Wilson, S.E. Corneal wound healing. *Exp. Eye Res.* **2020**, *197*, 108089. [CrossRef] [PubMed]
72. De Oliveira, R.C.; Wilson, S.E. Fibrocytes, Wound Healing, and Corneal Fibrosis. *Investig. Ophthalmol. Vis. Sci.* **2020**, *61*, 28. [CrossRef]
73. McKay, T.B.; Hutcheon, A.E.K.; Zieske, J.D. Biology of corneal fibrosis: Soluble mediators, integrins, and extracellular vesicles. *Eye* **2020**, *34*, 271–278. [CrossRef] [PubMed]
74. Kamil, S.; Mohan, R.R. Corneal stromal wound healing: Major regulators and therapeutic targets. *Ocul. Surf.* **2021**, *19*, 290–306. [CrossRef] [PubMed]
75. Bazan, H.E.P. Cellular and molecular events in corneal wound healing: Significance of lipid signalling. *Exp. Eye Res.* **2005**, *80*, 453–463. [CrossRef] [PubMed]
76. Hertsenberg, A.J.; Shojaati, G.; Funderburgh, M.L.; Mann, M.M.; Du, Y.; Funderburgh, J.L. Corneal stromal stem cells reduce corneal scarring by mediating neutrophil infiltration after wounding. *PLoS ONE* **2017**, *12*, e0171712. [CrossRef] [PubMed]
77. Weng, L.; Funderburgh, J.L.; Khandaker, I.; Geary, M.L.; Yang, T.; Basu, R.; Funderburgh, M.L.; Du, Y.; Yam, G.H.-F. The anti-scarring effect of corneal stromal stem cell therapy is mediated by transforming growth factor β3. *Eye Vis.* **2020**, *7*, 52. [CrossRef]
78. Chameettachal, S.; Prasad, D.; Parekh, Y.; Basu, S.; Singh, V.; Bokara, K.K.; Pati, F. Prevention of Corneal Myofibroblastic Differentiation In Vitro Using a Biomimetic ECM Hydrogel for Corneal Tissue Regeneration. *ACS Appl. Bio Mater.* **2021**, *4*, 533–544. [CrossRef]
79. Chandru, A.; Agrawal, P.; Ojha, S.K.; Selvakumar, K.; Shiva, V.K.; Gharat, T.; Selvam, S.; Thomas, M.B.; Damala, M.; Prasad, D.; et al. Human Cadaveric Donor Cornea Derived Extra Cellular Matrix Microparticles for Minimally Invasive Healing/Regeneration of Corneal Wounds. *Biomolecules* **2021**, *11*, 532. [CrossRef]
80. Du, Y.; SundarRaj, N.; Funderburgh, M.L.; Harvey, S.A.; Birk, D.E.; Funderburgh, J.L. Secretion and Organization of a Cornea-like Tissue In Vitro by Stem Cells from Human Corneal Stroma. *Investig. Ophthalmol. Vis. Sci.* **2007**, *48*, 5038–5045. [CrossRef]
81. Chen, S.-Y.; Hayashida, Y.; Chen, M.-Y.; Xie, H.T.; Tseng, S.C.G. A New Isolation Method of Human Limbal Progenitor Cells by Maintaining Close Association with Their Niche Cells. *Tissue Eng. Part C Methods* **2011**, *17*, 537. [CrossRef]
82. Yam, G.H.-F.; Yang, T.; Geary, M.L.; Santra, M.; Funderburgh, M.; Rubin, E.; Du, Y.; Sahel, J.A.; Jhanji, V.; Funderburgh, J.L. Human corneal stromal stem cells express anti-fibrotic microRNA-29a and 381-5p—A robust cell selection tool for stem cell therapy of corneal scarring. *J. Adv. Res.* 2022, *in press*. [CrossRef]
83. Birk, D.E.; Fitch, J.M.; Linsenmayer, T.F. Organization of collagen types I and V in the embryonic chicken cornea. *Investig. Ophthalmol. Vis. Sci.* **1986**, *27*, 1470–1477.
84. Yokota, T.; McCourt, J.; Ma, F.; Ren, S.; Li, S.; Kim, T.-H.; Kurmangaliyev, Y.Z.; Nasiri, R.; Ahadian, S.; Nguyen, T.; et al. Type V Collagen in Scar Tissue Regulates the Size of Scar after Heart Injury. *Cell* **2020**, *182*, 545–562.e23. [CrossRef] [PubMed]
85. Niyibizi, C.; Kavalkovich, K.; Yamaji, T.; Woo, S.L. Type V collagen is increased during rabbit medial collateral ligament healing. *Knee Surg. Sports Traumatol. Arthrosc.* **2000**, *8*, 281–285. [CrossRef] [PubMed]
86. Ruggiero, F.; Burillon, C.; Garrone, R. Human corneal fibrillogenesis. Collagen V structural analysis and fibrillar assembly by stromal fibroblasts in culture. *Investig. Ophthalmol. Vis. Sci.* **1996**, *37*, 1749–1760.
87. McLaughlin, J.S.; Linsenmayer, T.F.; Birk, D.E. Type V collagen synthesis and deposition by chicken embryo corneal fibroblasts in vitro. *J. Cell Sci.* **1989**, *94*, 371–379. [CrossRef]
88. DeNigris, J.; Yao, Q.; Birk, E.K.; Birk, D.E. Altered dermal fibroblast behavior in a collagen V haploinsufficient murine model of classic Ehlers-Danlos syndrome. *Connect. Tissue Res.* **2016**, *57*, 1–9. [CrossRef]
89. Guo, Z.H.; Jia, Y.Y.S.; Zeng, Y.M.; Li, Z.F.; Lin, J.S. Transcriptome analysis identifies the differentially expressed genes related to the stemness of limbal stem cells in mice. *Gene* **2021**, *775*, 145447. [CrossRef]

90. Call, M.; Elzarka, M.; Kunesh, M.; Hura, N.; Birk, D.E.; Kao, W.W. Therapeutic efficacy of mesenchymal stem cells for the treatment of congenital and acquired corneal opacity. *Mol. Vis.* **2019**, *25*, 415–426.
91. Pietruszewska, W.; Bojanowska-Poźniak, K.; Kobos, J. Matrix metalloproteinases MMP1, MMP2, MMP9 and their tissue inhibitors TIMP1, TIMP2, TIMP3 in head and neck cancer: An immunohistochemical study. *Otolaryngol. Pol. Pol. Otolaryngol.* **2016**, *70*, 32–43. [CrossRef]
92. Visse, R.; Nagase, H. Matrix Metalloproteinases and Tissue Inhibitors of Metalloproteinases. *Circ. Res.* **2003**, *92*, 827–839. [CrossRef]
93. Huh, M.-I.; Lee, Y.-M.; Seo, S.-K.; Kang, B.-S.; Chang, Y.; Lee, Y.-S.; Fini, M.E.; Kang, S.-S.; Jung, J.-C. Roles of MMP/TIMP in regulating matrix swelling and cell migration during chick corneal development. *J. Cell. Biochem.* **2007**, *101*, 1222–1237. [CrossRef] [PubMed]
94. Kwak, H.-J.; Park, M.-J.; Cho, H.; Park, C.-M.; Moon, S.-I.; Lee, H.-C.; Park, I.-C.; Kim, M.-S.; Rhee, C.H.; Hong, S.-I. Transforming growth factor-beta1 induces tissue inhibitor of metalloproteinase-1 expression via activation of extracellular signal-regulated kinase and Sp1 in human fibrosarcoma cells. *Mol. Cancer Res.* **2006**, *4*, 209–220. [CrossRef] [PubMed]
95. Leivonen, S.-K.; Lazaridis, K.; Decock, J.; Chantry, A.; Edwards, D.R.; Kähäri, V.-M. TGF-β-Elicited Induction of Tissue Inhibitor of Metalloproteinases (TIMP)-3 Expression in Fibroblasts Involves Complex Interplay between Smad3, p38α, and ERK1/2. *PLoS ONE* **2013**, *8*, e57474. [CrossRef] [PubMed]
96. Amjadi, S.; Mai, K.; McCluskey, P.; Wakefield, D. The Role of Lumican in Ocular Disease. *ISRN Ophthalmol.* **2013**, *2013*, 632302. [CrossRef] [PubMed]
97. Carlson, E.C.; Lin, M.; Liu, C.-Y.; Kao, W.W.-Y.; Perez, V.L.; Pearlman, E. Keratocan and Lumican Regulate Neutrophil Infiltration and Corneal Clarity in Lipopolysaccharide-induced Keratitis by Direct Interaction with CXCL1*. *J. Biol. Chem.* **2007**, *282*, 35502–35509. [CrossRef] [PubMed]
98. Funderburgh, J.L. The Corneal Stroma. In *Encyclopedia of the Eye*; Dartt, D.A., Ed.; Academic Press: Oxford, UK, 2010; pp. 515–521. ISBN 978-0-12-374203-2.
99. Espana, E.M.; He, H.; Kawakita, T.; Di Pascuale, M.A.; Raju, V.K.; Liu, C.-Y.; Tseng, S.C.G. Human Keratocytes Cultured on Amniotic Membrane Stroma Preserve Morphology and Express Keratocan. *Investig. Ophthalmol. Vis. Sci.* **2003**, *44*, 5136–5141. [CrossRef] [PubMed]
100. Uchida, S.; Yokoo, S.; Yanagi, Y.; Usui, T.; Yokota, C.; Mimura, T.; Araie, M.; Yamagami, S.; Amano, S. Sphere Formation and Expression of Neural Proteins by Human Corneal Stromal Cells In Vitro. *Investig. Ophthalmol. Vis. Sci.* **2005**, *46*, 1620–1625. [CrossRef] [PubMed]
101. Kawakita, T.; Espana, E.M.; He, H.; Hornia, A.; Yeh, L.-K.; Ouang, J.; Liu, C.-Y.; Tseng, S.C.G. Keratocan expression of murine keratocytes is maintained on amniotic membrane by downregulating tgf-β signaling. *J. Biol. Chem.* **2005**, *280*, 27085–27092. [CrossRef]
102. Pouw, A.E.; Greiner, M.A.; Coussa, R.G.; Jiao, C.; Han, I.C.; Skeie, J.M.; Fingert, J.H.; Mullins, R.F.; Sohn, E.H. Cell-Matrix Interactions in the Eye: From Cornea to Choroid. *Cells* **2021**, *10*, 687. [CrossRef] [PubMed]
103. Brem, H.; Kodra, A.; Golinko, M.S.; Entero, H.; Stojadinovic, O.; Wang, V.M.; Sheahan, C.M.; Weinberg, A.D.; Woo, S.L.C.; Ehrlich, H.P.; et al. Mechanism of sustained release of vascular endothelial growth factor in accelerating experimental diabetic healing. *J. Investig. Dermatol.* **2009**, *129*, 2275–2287. [CrossRef]
104. Losi, P.; Briganti, E.; Errico, C.; Lisella, A.; Sanguinetti, E.; Chiellini, F.; Soldani, G. Fibrin-based scaffold incorporating VEGF- and bFGF-loaded nanoparticles stimulates wound healing in diabetic mice. *Acta Biomater.* **2013**, *9*, 7814–7821. [CrossRef]
105. Yao, L.; Li, Z.; Su, W.; Li, Y.; Lin, M.; Zhang, W.; Liu, Y.; Wan, Q.; Liang, D. Role of mesenchymal stem cells on cornea wound healing induced by acute alkali burn. *PLoS ONE* **2012**, *7*, e30842. [CrossRef] [PubMed]
106. Han, K.-Y.; Chang, J.-H.; Lee, H.; Azar, D.T. Proangiogenic Interactions of Vascular Endothelial MMP14 With VEGF Receptor 1 in VEGFA-Mediated Corneal Angiogenesis. *Investig. Ophthalmol. Vis. Sci.* **2016**, *57*, 3313–3322. [CrossRef] [PubMed]
107. Stepp, M.A.; Menko, A.S. Immune responses to injury and their links to eye disease. *Transl. Res. J. Lab. Clin. Med.* **2021**, *236*, 52–71. [CrossRef]
108. Frank, S.; Hübner, G.; Breier, G.; Longaker, M.T.; Greenhalgh, D.G.; Werner, S. Regulation of vascular endothelial growth factor expression in cultured keratinocytes. Implications for normal and impaired wound healing. *J. Biol. Chem.* **1995**, *270*, 12607–12613. [CrossRef] [PubMed]
109. Matsumoto, R.; Omura, T.; Yoshiyama, M.; Hayashi, T.; Inamoto, S.; Koh, K.-R.; Ohta, K.; Izumi, Y.; Nakamura, Y.; Akioka, K.; et al. Vascular endothelial growth factor-expressing mesenchymal stem cell transplantation for the treatment of acute myocardial infarction. *Arterioscler. Thromb. Vasc. Biol.* **2005**, *25*, 1168–1173. [CrossRef] [PubMed]
110. Fu, Q.; Li, C.; Yu, L. Gambogic acid inhibits spinal cord injury and inflammation through suppressing the p38 and Akt signaling pathways. *Mol. Med. Rep.* **2018**, *17*, 2026–2032. [CrossRef]
111. Michaels, J.; Dobryansky, M.; Galiano, R.D.; Bhatt, K.A.; Ashinoff, R.; Ceradini, D.J.; Gurtner, G.C. Topical vascular endothelial growth factor reverses delayed wound healing secondary to angiogenesis inhibitor administration. *Wound Repair Regen.* **2005**, *13*, 506–512. [CrossRef]
112. Hollborn, M.; Stathopoulos, C.; Steffen, A.; Wiedemann, P.; Kohen, L.; Bringmann, A. Positive feedback regulation between MMP-9 and VEGF in human RPE cells. *Investig. Ophthalmol. Vis. Sci.* **2007**, *48*, 4360–4367. [CrossRef]

113. Van Setten, G.B. Vascular endothelial growth factor (VEGF) in normal human corneal epithelium: Detection and physiological importance. *Acta Ophthalmol. Scand.* **1997**, *75*, 649–652. [CrossRef]
114. Ambati, B.K.; Nozaki, M.; Singh, N.; Takeda, A.; Jani, P.D.; Suthar, T.; Albuquerque, R.J.C.; Richter, E.; Sakurai, E.; Newcomb, M.T.; et al. Corneal avascularity is due to soluble VEGF receptor-1. *Nature* **2006**, *443*, 993–997. [CrossRef] [PubMed]
115. Ma, D.H.-K.; Tsai, R.J.-F.; Chu, W.-K.; Kao, C.-H.; Chen, J.-K. Inhibition of Vascular Endothelial Cell Morphogenesis in Cultures by Limbal Epithelial Cells. *Investig. Ophthalmol. Vis. Sci.* **1999**, *40*, 1822–1828.
116. Eslani, M.; Putra, I.; Shen, X.; Hamouie, J.; Afsharkhamseh, N.; Besharat, S.; Rosenblatt, M.I.; Dana, R.; Hematti, P.; Djalilian, A.R. Corneal Mesenchymal Stromal Cells Are Directly Antiangiogenic via PEDF and sFLT-1. *Investig. Ophthalmol. Vis. Sci.* **2017**, *58*, 5507–5517. [CrossRef] [PubMed]
117. Damala, M.; Swioklo, S.; Koduri, M.A.; Mitragotri, N.S.; Basu, S.; Connon, C.J.; Singh, V. Encapsulation of human limbus-derived stromal/mesenchymal stem cells for biological preservation and transportation in extreme Indian conditions for clinical use. *Sci. Rep.* **2019**, *9*, 16950. [CrossRef]

Stem Cell Research & Therapy

RESEARCH

Open Access

Expansion and characterization of human limbus-derived stromal/mesenchymal stem cells in xeno-free medium for therapeutic applications

Abhishek Sahoo[1], Mukesh Damala[1,2], Jilu Jaffet[1,3], Deeksha Prasad[1,3], Sayan Basu[1*] and Vivek Singh[1*]

Abstract

Background Mesenchymal stem cells (MSCs) have been proven to prevent and clear corneal scarring and limbal stem cell deficiency. However, using animal-derived serum in a culture medium raises the ethical and regulatory bar. This study aims to expand and characterize human limbus-derived stromal/mesenchymal stem cells (hLMSCs) for the first time in vitro in the xeno-free medium.

Methods Limbal tissue was obtained from therapeutic grade corneoscleral rims and subjected to explant culture till tertiary passage in media with and without serum (STEM MACS XF; SM), to obtain pure hLMSCs. Population doubling time, cell proliferation, expression of phenotypic markers, tri-lineage differentiation, colony-forming potential and gene expression analysis were carried out to assess the retention of phenotypic and genotypic characteristics of hLMSCs.

Results The serum-free medium supported the growth of hLMSCs, retaining similar morphology but a significantly lower doubling time of 23 h ($*p < 0.01$) compared to the control medium. FACS analysis demonstrated ≥ 90% hLMSCs were positive for *CD90*$^+$, *CD73*$^+$, *CD105*$^+$, and ≤ 6% were positive for *CD45*$^-$, *CD34*$^-$ *and HLA-DR*$^-$. Immunofluorescence analysis confirmed similar expression of *Pax6*$^+$, *COL IV*$^+$, *ABCG2*$^+$, *ABCB5*$^+$, *VIM*$^+$, *CD90*$^+$, *CD105*$^+$, *CD73*$^+$, *HLA-DR*$^-$ *and CD45*$^-$, *αSMA*$^-$ in both the media. Tri-lineage differentiation potential and gene expression of hLMSCs were retained similarly to that of the control medium.

Conclusion The findings of this study demonstrate successful isolation, characterization and culture optimization of hLMSCs for the first time in vitro in a serum-free environment. This will help in the future pre-clinical and clinical applications of MSCs in translational research.

Key findings

- This study successfully optimizes the growth and expansion of hLMSCs in a serum-free environment using commercially available SM medium, retaining their spindle-shaped morphology till higher generations (P8).

*Correspondence:
Sayan Basu
sayanbasu@lvpei.org
Vivek Singh
viveksingh@lvpei.org
Full list of author information is available at the end of the article

- hLMSCs cultured in SM maintained significantly lower population doubling time, tri-lineage differentiation potential and significantly higher colony-forming ability than the control medium. Immunofluorescence and FACS analysis showed expression of MSC markers and absence of expression of myo-fibroblastic marker (αSMA), and haematopoietic markers (CD45, CD34 and HLA-DR).
- The qPCR data suggested similar expression of MSC phenotypic markers, wound healing markers and inflammatory markers identical to that of the control medium.

Keywords hLMSCs, Xeno-free media, Corneal scarring, Regenerative medicine, Therapeutic applications

Background

MSCs originate from mesoderm during embryo development, possess fibroblastic and spindle shape morphology, adhere to the plastic surface, and positively express phenotypic cell surface markers CD105 (endoglin-recognized by SH2), CD90 (Thy-1), CD73 (ecto 5′ nucleotidase -recognized by SH3 and SH4), CD106, CD166, COL-I, COL-III and is negative for hematopoietic markers CD34 (primitive hematopoietic progenitors and endothelial cell marker), CD45 (pan-leukocyte marker), CD19, HLA-DR, CD14 & 11b (monocytes and macrophages) and α-SMA [1, 2]. Another specific criterion of MSC is to differentiate into Adipocytes (Oil Red O staining), Osteocytes (Alizarin Red staining for Ca^{2+} deposits) and Chondrocytes (Alcian Blue staining for collagen type II and GAGs) upon induction. In vitro culture and expansion of these cells are of utmost necessity for cell-based therapies. Isolation and culture of MSC date back to the 1970s, when Friedenstein et al. [3] first described them, and since then, various methods and protocols have been devised to cultivate these cells. The field of regenerative medicine has paved the way for MSCs to become an emerging player owing to its translational applications [4]. Cell-based therapies have become immensely popular in regenerative medicine to repair or regenerate a tissue through stem cell transplantation [5]. Currently, 352 clinical trials have been completed, and 339 are ongoing using MSCs as cellular therapy; (https://clinicaltrials.gov/ct2/home); 26/11/2022.

MSCs have been isolated from various tissues in the body like bone marrow (BM), umbilical cord (UC), adipose tissue (AD), dental pulp, corneal and limbal stroma [6, 7]. The cornea is a transparent and avascular connective tissue on the anterior eye, forming a barrier between the eye and the outside world [8]. It is divided into five layers depending on function and anatomy. The outermost layer is corneal epithelium followed by compactly arranged stroma consisting predominantly of type I and V collagen fibrils, separated by Bowman's membrane. Inner to stroma lies Descemet's membrane preceding a monolayer of cuboidal cells known as corneal endothelium. To perceive vision, the cornea refracts two-thirds of the total light onto the retina [7]. As evident from the literature, corneal stroma houses a specific cell population satisfying the MSC criterion known as corneal stromal stem cells (CSSC) that eventually differentiate into stromal keratocytes [7–11]. These stromal keratocytes differentiate into fibroblastic scar tissue upon corneal injury, thus opacifying the transparent cornea and leading to vision deterioration [12–19]. The most common and accepted treatment owing to this visual impairment is corneal transplantation (keratoplasty); however, the availability of suitable donor corneas falls behind the demand. Furthermore, post-operative complications and immune rejection of corneal allografts add to the disadvantages [20, 21]. To cater to the above needs, various therapeutic alternatives to keratoplasty, like stem cell therapy, 3D printed corneas, and bio-mimetic hydrogels, are currently being explored [11, 22].

Mesenchymal stem cells (MSCs) have become promising candidates for various biologically engineered therapeutic applications. The presence of multipotent mesenchymal stem cells in corneal stroma has paved the way for cellular therapy against disorders like limbal stem cell deficiency (LSCD). The efficacy of MSCs as a therapeutic agent in restoring corneal transparency has been confirmed in previous studies. Moreover, MSCs being immunosuppressant, post-operative complications like immune rejection and inflammation can be ruled out [23–25]. The corneoscleral junction of the human eye, known as limbus, houses mesenchymal stromal cells in finger-like projections called palisades of Vogt. These cells can be cultured from limbal biopsy, expanded using an appropriate growth medium and used for treating LSCD, corneal burns, scars and various ocular surface injuries [19]. MSCs isolated from human umbilical cord have been shown to restore corneal transparency in Lumican knockout mice, thus confirming that stem cells from different organs aid in corneal regeneration [26]. In humans, MSCs from other tissues also have been reported to cure corneal scarring and restore transparency [27–30].

As the evolvement of science is marching forward, the procedure to develop an optimal culturing condition is also being looked for alternative ways to cultivate MSCs [31, 32]. For half a century, FBS has been acting as a supplement to the basal media in most of the studies and even in clinical trials [33–45]. FBS is an ill-defined pool of macro- and micro-molecules required for the growth and sustainability of cells. Being of xenogeneic origin and with lot-to-lot variance, FBS is prone to cause zoonotic diseases like anthrax, Q fever, and Creutzfeldt–Jakob Disease (CJD). Bovine Spongiform Encephalopathies and their relation to the new variant of CJD can also be caused due to the presence of harmful pathogens like unknown viruses, bacteria, prions and endotoxins in FBS [46]. Cells cultured in FBS are prone to be contaminated with mycoplasma which is unnoticeable and can easily pass through 0.22μ filters [47, 48]. Furthermore, slaughtering a bovine foetus for serum extraction is inhumane and questions the ethical issues in many countries [49]. Large-scale production of serum is uneconomical, pointing to the high cost of feeding, maintenance and infrastructure for bovine rearing [50].

To tackle these limitations, the regulatory authorities have emphasized looking for a serum-free medium to delineate a standardized paradigm that can preserve the therapeutic potential of MSCs [5]. Serum-free or xeno-free medium formulations are chemically defined mediums that need strict optimization and characterization based on specific cell types [51]. Recently various industry groups like RoosterBio, Inc., MD, USA (RoosterNourish-MSC XF); Miltenyi Biotec, Germany (STEM MACS XF); Merck, USA (PLTMax Human Platelet Lysate); R&D Systems, USA (StemXVivo Serum free Human Mesenchymal Stem Cell Expansion media) and many more are focusing on optimizing FBS free culture medium [52]. Several research groups are looking into preparing in-house xeno-free medium for the growth and expansion of MSCs [39, 53–58].

This study aims to optimize and characterize SM to expand hLMSCs to higher passages and check their suitability for therapeutic use. This chemically defined xeno-free medium is formulated by Miltenyi Biotec and manufactured in compliance with cGMP regulations. This is a patented proprietary chemically defined medium, (cat no.- 130-104-182) so disclosure of individual components is limited to the manufacturer only. The details about SM can be accessed from; (https://www.miltenyibiotec.com/US-en/products/stemmacs-msc-expansion-media-kit-xf-human.html#gref). SM had previously been reported to support the growth and expansion of adult mesenchymal stem cells, [4] which prompted us to test it in human limbal stromal cells.

Materials and methods

Isolation and culture of hLMSCs

The complete limbal rim was dissected from the therapeutic grade and biologically tested cadaveric corneas obtained from Ramayamma International Eye Bank (RIEB) (http://www.lvpei.org/services/eyebank) with proper documentation. This study was approved by the Institutional Review Board (IRB) of the LV Prasad Eye Institute (Ethics Ref. No. LEC-05-18-081) and Institutional Committee for Stem Cell Research (IC-SCR Ref No 08-18-002) and followed the tenets of the declaration of Helsinki. Briefly, the corneoscleral rim was first washed with 2× [vol/vol] Antibiotic–Antimycotic solution (15240062, Thermo Fisher, USA) in sterile filtered Phosphate Buffer Saline (PBS) (D5652-10L, Sigma-Aldrich). Iris and tissue debris, if any, were cleaned with the help of a scalpel blade (15 no.) in 1X PBS. Carefully, a 360° limbal rim of about 1–2 mm diameter was dissected from the corneoscleral rim and cut into small fragments of 1–2 mm length. The fragmented tissue was minced with the help of curved scissors in 1 mL of sterile-filtered DMEM/F12 medium (D0547-10X1L, Sigma-Aldrich). The minced tissue was subjected to collagenase digestion by adding 200 IU of reconstituted collagenase IV (17104019, Thermo Fisher, USA) in HBSS buffer (14025092, Thermo Fisher, USA) and incubated for 16 h at 37 °C and 5% CO_2.

Post-digestion, 1 mL of DMEM/F12 complete medium fortified with 2% of foetal bovine serum (SH30396.03, Cytiva Life Sciences), 1% [vol/vol] Antibiotic–Antimycotic, 10 ng/mL epidermal growth factor (PHG0311L, Thermo Fisher, USA) and 5 μg/mL insulin (12585014, Thermo Fisher, USA), was added. The solution was spun down at 1000 rpm for 3 min at 25 °C. The pellet was then washed twice with 1X PBS. 2 mL of complete medium was added to the final pellet, mixed well and kept for growth in a T25 flask at 37 °C and 5% CO_2 with media changed every 3rd day. This served as a control for this study.

For culturing the cells in SM (130-104-182, Miltenyi Biotec), post-enzymatic digestion, 1 mL of SM medium was added and centrifuged at 1000 rpm for 3 min, following two PBS washes. 2 mL of SM medium was added to the pellet and was kept in culture maintained at 37 °C, and 5% CO_2 with media changed every 3rd day.

As this is a primary culture, we obtain a mixed population of limbal epithelial and stromal cells in the first two passages. Pure population of MSCs are obtained at third passage of the culture. Hence, this pure

population of MSCs (henceforth referred to as P3 hLMSCs) were used for all the characterization experiments post-viability quantification using 0.4% Trypan Blue (15250061, Thermo Fisher, USA).

Population doubling time (PDT) and cumulative population doublings (CPD)

To look into the growth kinetics, hLMSCs cultured in both media were used. Briefly, 1×10^4 cells were seeded in triplicates in a 48-well plate and harvested upon 80–90% confluency, and the growth duration was noted. The total viable cell number was recorded, and Population Doubling Time (PDT) was calculated from P3 to P8 using the formula below from https://www.doublingtime.com/compute.php.

$$\text{Doubling Time} = \frac{\text{Duration} * \log(2)}{\text{Log(Final Concentration)} - \log(\text{Initial Concentration})}$$

Cumulative Population Doublings (CPD) were calculated using the formula (Initial PDT + 3.322*(log (Cell no. at confluency) − log (seeding cell no.)).

Relative viability assay using MTT

5000 cells/cm^2 of hLMSCs were seeded in a 48-well plate in triplicates separately in SM and serum-based medium and cultured for 24, 48, 72, 96 and 120 h at 37 °C and 5% CO_2 in a humidified incubator. Post 24 h of seeding (termed as T_0), spent media was removed, and 200 µL of 2 mg/mL of MTT (M6494, Thermo Fisher, USA) dissolved in DMEM/F12 devoid of growth supplements and FBS was added preceding a PBS wash and incubated for 3 h at 37 °C and 5% CO_2. Post-incubation, 200 µL DMSO (D2650, Sigma-Aldrich, USA) was added following 10 min incubation to solubilize the formazan crystals. 100 µL of supernatant was transferred to a transparent bottom 96-well plate, and absorbance was taken in triplicates at 570 nm in a UV–Vis spectrophotometer against DMSO as blank. The same steps were repeated for T_{24}, T_{48}, T_{72}, T_{96}, and T_{120} h.

Immunophenotypic markers expression by immunofluorescence and flow cytometry

To assess the expressivity of MSC phenotypic markers, hLMSCs grown in both the medium were subjected to immunofluorescence (IF) and FACS analysis. In brief, for IF, cells were seeded on coverslips placed in 12-well plates at a density of 5000 cells/cm^2. Upon 60–70% confluency, the cells were washed with 1× PBS, fixed in 4% paraformaldehyde for 20 min, followed by two PBS washes for 5 min each. The fixed cells were permeabilized using 0.5% triton-X for 5 min, following three PBS washes of 5 min each. Thereafter, hLMSCs were incubated for 45 min at room temperature in 2.5% BSA in PBS (blocking buffer) to restrict non-specific interactions. Post-blocking, the cells were incubated with primary antibody dissolved in 1% BSA solution and kept at 4 °C overnight. The antibody panel consisted of CD105 (1:200, ab156756, Abcam, UK), CD90 (1:200, ab181469, Abcam, UK), ABCG2 (1:200, ab229193, Abcam, UK), ABCB5 (1:200, ab140667, Abcam, UK), COLIV (1:200, ab6586, Abcam, UK), CD73 (1:100, 13160S, Cell Signalling Technology, USA), p63-α (1:100, ab124762, Abcam, UK), and Vimentin (1:100, sc-6260, Santa Cruz Biotechnology, USA) as positive markers of the mesenchymal phenotype, Pax6 (1:200, ab195045, Abcam, UK) as positive markers of the human limbal stem cell phenotype; HLA-DR (1:100, ab92511, Abcam, UK), and CD45 (1:100, ab154885, Abcam, UK), αSMA (1:100, MA5-11547, Invitrogen, USA), as negative markers for mesenchymal stem cells origin according to the guidelines of ISCT. To nullify the presence of epithelial phenotype in P3 hLMSCs, IF was carried out using epithelial markers, CK3/2P (1:100, sc-80000, Santa Cruz Biotechnology, USA), CK14 (1:100, sc-53253, Santa Cruz Biotechnology, USA) and CK15 (1:100, sc-47697, Santa Cruz Biotechnology, USA); (Additional file 1: figure S1).

Post-incubation, cells were washed twice for 5 min each with PBS, and 1:400 dilution of secondary antibodies in 1% BSA was added, followed by incubation at R.T. Secondary antibodies included anti-mouse Alexa Flour 488 (A11001, Thermo Fisher, USA) and anti-rabbit Alexa Flour 488 (A11008, Thermo Fisher, USA). After 45 min of incubation, cells were washed thrice with PBS to remove the background stain and mounted using a Mounting Medium with DAPI - Aqueous, Fluoroshield (ab104139, Abcam, USA). Fluorescent images of mounted cells were captured with Zeiss LSM 880(Carl Zeiss AG, Germany).

FACS analysis of hLMSCs cultured in SM and control medium was carried out to quantify the expression of phenotypic markers. P3 hLMSCs were trypsinized upon 70–80% confluency, and around 1×10^5 cells were added to 1.5 mL vials. The cell suspension was spun down at 400 g for 5 min following two PBS washes. Conjugated antibodies were dissolved in 2% FBS in PBS (blocking buffer) in 1:100 dilution following incubation for 20 min in the dark at room temperature. The phenotypic markers analysed were CD105$^+$ (B76299), CD90$^+$ (B36121), CD73$^+$ (B68176), CD45$^-$ (A07783), CD34$^-$ (IMI870), HLA-DR$^-$ (B36291), all from Beckman Coulter (Brea, CA, USA). Post-incubation, cells were washed twice in

1X PBS, and the pellet was resuspended in 200 µL of PBS. The stained cells were analysed using CytoFLEX flow cytometer (Beckman Coulter, CA, USA), and the data analysis was carried out using CytExpert software (Beckman Coulter, CA, USA).

Tri-lineage differentiation

The potential of both the medium to support tri-lineage differentiation was evaluated using MesenCult™ Adipogenic (05412), Osteogenic (05465), and Chondrogenic (05455) differentiation kit (Stem Cell Technologies, USA). Briefly, 5000 cells/cm^2 of hLMSCs were seeded in triplicates in 24 well plate. Upon 60–70% confluency, the cells were induced to differentiate for 21 days. The media was changed every 3rd day, and the plate was periodically observed for differentiation. Post 21 days, the cells were fixed with 4% paraformaldehyde for 10 min following two PBS washes. Staining was carried out using alizarin red for osteogenic differentiation, Alcian blue for chondrogenic differentiation, and oil red O for adipogenic differentiation for 10 min, 1 h and 20 min, respectively. Three washes with Milli-Q water were given to drain out excessive stains, and differentiated cells were imaged in PBS under a bright field microscope.

To quantify the extent of differentiation in SM and control media, stain from individual wells was eluted using various dye elution techniques [59–61] and the intensity was measured using a UV–Vis spectrophotometer (SpectraMax M3, Molecular Devices, California, USA).

Colony forming unit (CFU) assay

hLMSCs (1000 cells) were seeded in 70 mm tissue culture Petri dishes in SM and control medium for 14 days at 37 °C and 5% CO_2, replenishing media every 3–4 days. Post day 14, the colonies were fixed with ice-cold methanol for 10 min at 4°C following incubation with 0.5% crystal violet for 10 min. The dish was washed 2–3 times with tap water and Milli-Q water to remove the excess stain. The no. of visible colonies with a size more than 2 mm was counted manually. A histogram was plotted between means of the total no. of colonies observed in both media.

In vitro wound-healing assay

hLMSCs were cultured in serum-based and SM medium in a six-well plate till 80%-90% confluency. The monolayer of cells was scratched using a sterile 200 µL pipette, following a PBS wash to remove the floating cells. Images were taken immediately after scratching and after 12, 24, 36 and 48 h, respectively, to look for the cell migration for wound healing. The decrease in the wounded area was measured using ImageJ software [62], to determine the healing potency.

Table 1 List of primers used in this study for gene expression analysis

Sl. no	Genes	Primer sequence		Size (bp)
1	LUMICAN	Fwd	GCACAATCGGCTGAAAGAGG	228
		Rev	TCAGCCAGTTCGTTGTGAGA	
2	IL10	Fwd	GCTGGAGGACTTTAAGGGTTACCT	109
		Rev	CTTGATGTCTGGGTCTTGGTTCT	
3	IL 6	Fwd	GCGATGGAGTCAGAGGAAACT	218
		Rev	AGTGACTCAGCACTTTGGCA	
4	COL1A1	Fwd	GTCACCCACCGACCAAGAAACC	121
		Rev	AAGTCCAGGCTGTCCAGGGATG	
5	COL5A1	Fwd	TTCAAGCGTGGGAAACTGCT	115
		Rev	GGTAGGTGACGTTCTGGTGG	
6	TGFβ1	Fwd	TACCTGAACCCGTGTTGCTCTC	122
		Rev	GTTGCTGAGGTATCGCCAGGAA	
7	COL3A1	Fwd	TGAAAGGACACAGAGGCTTCG	532
		Rev	GCACCATTCTTACCAGGCTC	
8	P63α	Fwd	ACCTGGAAAACAATGCCCAGA	369
		Rev	GAGGTGGGGTCATCACCTTG	
9	VIM	Fwd	GGACCAGCTAACCAACGACA	178
		Rev	AAGGTCAAGACGTGCCAGAG	
10	CD105	Fwd	CGGTGGTCAATATCCTGTCGAG	109
		Rev	AGGAAGTGTGGGCTGAGGTAGA	
11	CD90	Fwd	AGCATCGCTCTCCTGCTAAC	230
		Rev	CTGGTGAAGTTGGTTCGGGA	
12	CD73	Fwd	GGCTGCTGTATTGCCCTTTG	175
		Rev	TACTCTGTCTCCAGGTTTTCGG	
13	RUNX2	Fwd	CCACTGAACCAAAAAGAAATCCC	129
		Rev	GAAAACAACACATAGCCAAACGC	
14	CD45	Fwd	CTTCAGTGGTCCCATTGTGGTG	107
		Rev	CCACTTTGTTCTCGGCTTCCAG	
15	KERA	Fwd	GACACAGGACTCAACGGTGT	205
		Rev	GTAGGAAAACTGGGTGGGCA	
16	ALDH3A1	Fwd	CAGTTACCGGGAGAGGCTGT	345
		Rev	GTGGCTCCGAGTGGATGTAG	
17	SEMA3A	Fwd	AGACTCACTTGTACGCCTGTG	242
		Rev	CCCAAGAGTTCGGAAGATAGCAA	
18	DCN	Fwd	ATGAAGGCCACTATCATCCTCC	135
		Rev	GTCGCGGTCATCAGGAACTT	
19	COL4A1	Fwd	TGTTGACGGCTTACCTGGAGAC	120
		Rev	GGTAGACCAACTCCAGGCTCTC	
20	PAX6	Fwd	ATAACCTGCCTATGCAACCC	208
		Rev	GGAACTTGAACTGGAACTGAC	
21	IL1β	Fwd	CCTGTCCTGCGTGTTGAAAGA	149
		Rev	GGGAACTGGGCAGACTCAAA	
22	TNFα	Fwd	CCCCAGGGACCTCTCTCTAATC	94
		Rev	GGTTTGCTACAACATGGGCTACA	

Gene expression analysis using real-time PCR

Total RNA was isolated after resuspending in RNAiso Plus (9108/9109, TAKARA). RNA isolation was done

using the traditional phenol–chloroform method following quantification using Nanodrop. cDNA was synthesized using SuperScript™ III First-Strand Synthesis System (18080051, Thermo Scientific™) by taking an equal RNA concentration in all the samples. Maxima SYBR Green/ROX qPCR Master Mix- 2X (F416L, Thermo Scientific™) kit was used for gene expression analysis on QuantStudio™ 3 Real-Time PCR System (A28567, Applied Biosystems™) using gene-specific primers as listed in Table 1. GAPDH was taken as the reference gene. RNA from human cadaveric limbal tissue was used as the control for this assay. The relative fold change of various genes was calculated using the $2^{-(\Delta\Delta ct)}$ method. The graph was plotted on a logarithmic scale, taking relative fold change on the *Y* axis and genes on the *X* axis.

Statistical analysis

All the mean, standard deviation and standard error of mean were calculated in Microsoft Excel, and the graphs were plotted using the GraphPad Prism application (GraphPad Software, SanDiego, USA). Statistical significance was analysed using the student's *t* test for non-parametric data. $p < 0.05$ were considered significant and represented by *, whereas $p > 0.05$ meant non-significant and is represented as "ns".

Results

Isolation and culture of hLMSCs

Serum-free (SM) and control media supported the attachment and growth of cells from limbal explants ($n = 3$). At P0, a mixed population of limbal epithelial and stromal cells were seen (Fig. 1a). The epithelial cells were cuboidal/polygonal in shape, and stromal cells showed spindle morphology. The microscopic images revealed that subsequent passages resulted in a decrease in epithelial cell population and an increase in the number of elongated, spindle-shaped stromal cells. A pure population of hLMSCs (P3 cells) were obtained at the end of 3rd passage; hence, these cells were used for further characterization.

PDT, CPD and relative viability rate using MTT

At each passage, viable cell count in SM outnumbered cells in the control medium. The total viable cell count at various passages in both the media is represented in Table 2. The population doubling time (25 ± 2 h.) was retained until further passages in SM, whereas it increased to 66 h. in the control medium. The graph was plotted taking PDT on the Y-axis and subsequent passages on the X-axis (Fig. 1b).

As Cumulative Population Doublings (CPD) and PDT are inversely proportional to each other, CPD was seen to be increasing significantly in case of SM in comparison with the control medium due to significantly lower PDT of SM (Fig. 1c). Owing to a significant difference in PDT between two media, the relative viable rate was evaluated in both media. To assess the relative viability rate of hLMSCs, an MTT assay was carried out. As evident from the graph (Fig. 1e), cells in serum-free medium (SM) showed significantly higher viability than in the control medium. The data were normalized to that of the control medium, which was taken as 100%. ($^*p < 0.01$, for graphs 1 b–e).

Phenotypic expression of markers using immunofluorescence and flow cytometry

The immunophenotype marker expression of hLMSCs cultured in serum-free (SM) and serum-based media (control medium) was evaluated using immunofluorescence (IF) staining and flow cytometry. hLMSCs stained their characteristics phenotype ocular surface marker ($Pax6^+$, COL IV^+), stem cell biomarkers ($P63\alpha^+$, $ABCG2^+$, $ABCB5^+$) and the mesenchymal biomarkers (VIM^+, $CD90^+$, $CD105^+$, $CD73^+$, HLA-DR^-, αSM A^- and $CD45^-$) adapting to serum-free conditions (Fig. 2a).

FACS analysis showed no significant difference in the expression of phenotypic markers of hLMSCs grown in both media. The expression was $\leq 6\%$ of negative MSC markers (CD45, CD34 and HLA-DR) and $\geq 97\%$ expression of positive markers (CD105, CD73, CD90). (Fig. 2b, c).

(See figure on next page.)

Fig. 1 **a** Micrographs of hLMSCs cultured in SM and Control medium, respectively. Cells grown in SM retained spindle-shaped morphology till passage P8, but cells grown in the control medium showed elongated fibroblastic morphology from P4. At P3, hLMSCs had spindle morphology in both the media. Magnification: × 10, Scale: 200 μM; **b** relative Population Doubling Time (PDT) of hLMSCs. hLMSCs cultured in SM displayed lower PDT than in the control medium. PDT was maintained till passage 8 in SM, which increased relatively in the control medium after passage 4. The data are represented as mean ± SD; **c** cumulative population doublings of hLMSCs in control and SM. SM showed comparatively more population doublings than the control medium; **d** bar graph representing total no. of viable cells at subsequent passages in control and SM medium; **e** percentage viability of hLMSCs cultured in SM and control medium was measured by MTT assay. SM cultures displayed cell viability similar to the control medium till 96 h and increased after that. The X and Y axes represent the time point and percentage cell viability, respectively. The percentage viability of cells in the control medium is taken as 100%. Data are expressed as mean ± SD in triplicates; $n = 3$; $p < 0.01$

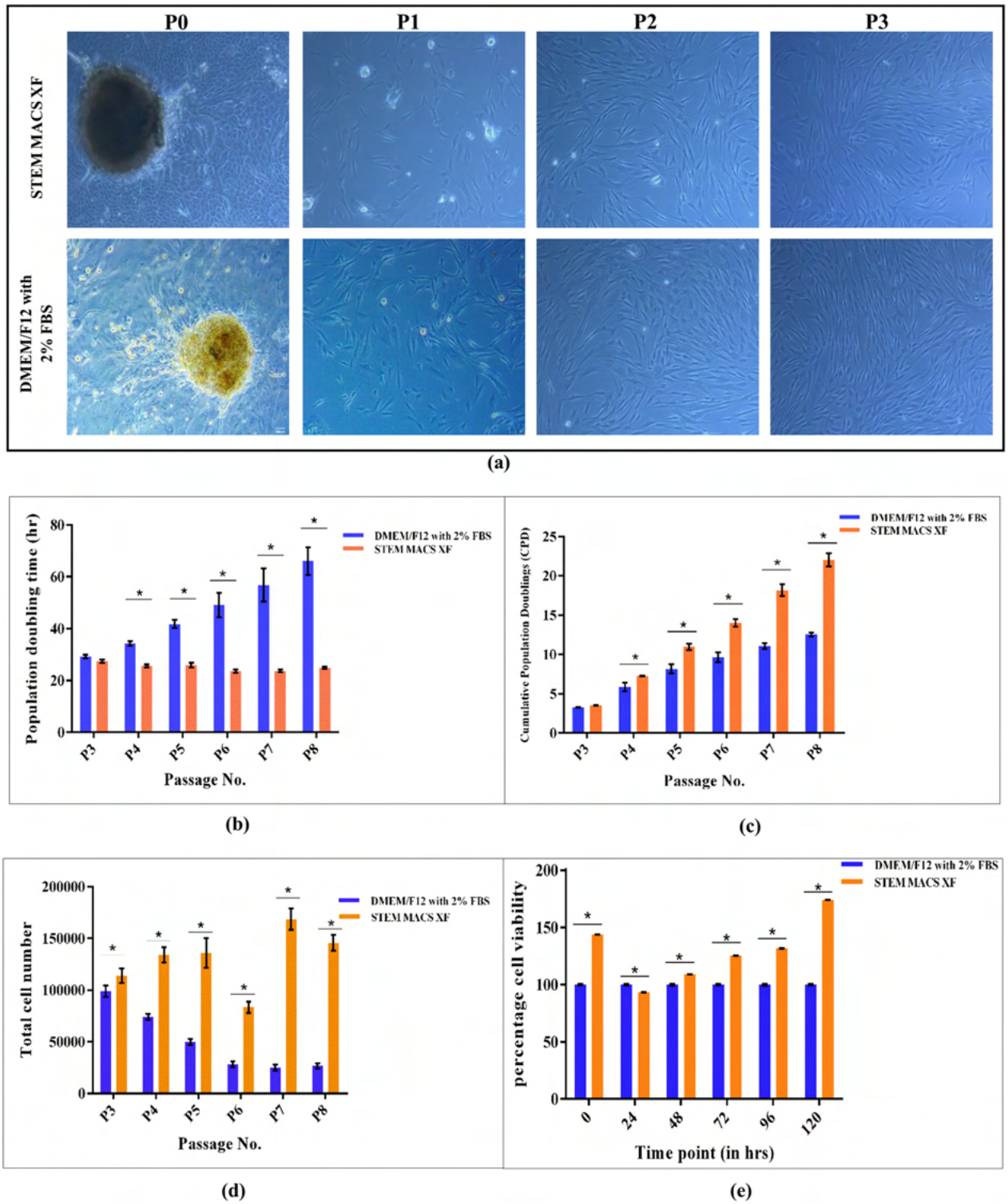

Fig. 1 (See legend on previous page.)

Table 2 The viable count of hLMSCs cultured in SM and in control medium at different passages

Passage No	Cell count in control medium	Cell count in SM
P3	$0.98 \times 10^5 \pm 0.054$	$1.1 \times 10^5 \pm 0.068$
P4	$0.62 \times 10^5 \pm 0.028$	$1.34 \times 10^5 \pm 0.074$
P5	$0.49 \times 10^5 \pm 0.028$	$1.36 \times 10^5 \pm 0.143$
P6	$0.27 \times 10^5 \pm 0.027$	$0.83 \times 10^5 \pm 0.054$
P7	$0.27 \times 10^5 \pm 0.031$	$1.6 \times 10^5 \pm 0.10$
P8	$0.27 \times 10^5 \pm 0.026$	$1.2 \times 10^5 \pm 0.076$

Tri-lineage differentiation

To assess the effect of serum-free medium on the tri-lineage differentiation potential of hLMSCs, in vitro differentiation was carried out. Osteogenic differentiation was marked as deep red colour calcium deposits after staining with Alizarin Red. Approximately 80–90% of the total area was stained red in both media showing efficient differentiation. Red fat droplets identified adipogenic differentiation after staining with Oil Red O. Cells grown in SM had clustered droplets, whereas control cells showed individual fat vacuoles. Glycosaminoglycan (GAG) deposits stained with Alcian Blue marked the chondrogenic differentiation.

In SM, the cells were seen to aggregate and form a pellet-like structure when viewed under a microscope, whereas in control medium, scattered deposits of GAGs were seen. The undifferentiated hLMSCs grown in control medium and SM served as control (Fig. 3a).

The graph in Fig. 3b clearly depicts a non-significant ($p > 0.05$) difference between the extent of differentiation in both media.

Colony forming unit (CFU) assay

MSCs produce holoclones and grow in colonies when seeded at lower densities. The colonies in SM were higher and more compactly arranged, whereas, in control, they were less and scattered (Fig. 4a, b). SM had significantly more colonies than the control medium, with mean values of 93 ± 9.17 and 60.6 ± 16.01 in SM and control medium, respectively (Fig. 4c) ($p = 0.038$).

In vitro wound-healing assay

hLMSCs cultured in both media displayed migration towards the wounded area without significant difference. The injured area was filled at 96 h post-wounding as shown in Fig. 5a. The average wounded area in the case of SM was found to be $886{,}387.5 \pm 51{,}124.53$, $556{,}339 \pm 35{,}011.69$, $375{,}298.5 \pm 20{,}965.01$, $53{,}199 \pm 1149.756$ and 0 at T_0, T_{24}, T_{48}, T_{72} and T_{96}, respectively. Similarly, in the case of the control medium, the average wounded area was $932{,}640 \pm 61{,}407.98$, $606{,}297 \pm 31{,}133.91$, $466{,}128.5 \pm 20{,}034.46$, $52{,}400.5 \pm 6537.202$ and 0 at T_0, T_{24}, T_{48}, T_{72} and T_{96}, respectively. The above data are represented on a bar graph ($p > 0.05$).

Quantitative gene expression (qRT-PCR)

The expression patterns of specific genes were analysed to assess the impact of xeno-free medium on various stem cell markers, wound healing and inflammatory markers. The fold change was calculated using the $2^{-(\Delta\Delta ct)}$ formula. All the markers showed approximately similar fold change in both the media without any significant difference except IL1β ($p = 0.0007$). The MSC markers were upregulated compared to the control except for Vimentin and PAX6 (ns). (Fig. 6a). The inflammatory markers' expression was downregulated except IL6 compared to the native limbus (Fig. 6b). Wound healing markers like Lumican and Semaphorin were upregulated(non-significant) in both the medium, whereas Decorin and ALDH3A1 were downregulated (Fig. 6c).

Discussion

MSCs have been used as therapeutic agents in various systemic disorders, as evident from reported clinical trials. Human corneal/limbal stroma has finger-like projections known as palisades of Vogt that house MSCs [23, 24], which promote corneal wound healing [19]. Various scientific groups have discovered diverse applications of these cells in the case of corneal scarring and haze [63] but all of them using FBS as the growth supplement to the basal media [7, 9, 10, 18]. FBS contains zoonotic antigens, which might result in cross-contamination, immune rejection and chances of bovine disease occurrence in the human population, thus compromising

(See figure on next page.)

Fig. 2 **a** Immunofluorescence analysis showed approximately similar biomarker expression of hLMSCs in SM for ocular surface marker ($Pax6^+$), stem-cell biomarkers ($ABCG2^+$, $P63\alpha^+$, $ABCB5^+$) and the mesenchymal biomarkers (VIM^+, $CD90^+$, $CD105^+$, $CD\ 34^-$, $HLA\text{-}DR^-$ and $CD45^-$) with respect to the cells in control medium; **b** the expression of MSC markers in hLMSCs grown in both the media was quantified using flow cytometry. More than 97% of cells were positive for CD105, CD90, and CD73, whereas less than 1% showed expression for negative markers CD45 and HLA-DR and approx. 6% of total cells were positive for CD34; **c** graphical representation of flow cytometry data. Blue: DAPI; Scale: 50 μM; Magnification: × 20 (all other micrographs) and 20 μM (CD73 of DMEM/F12 with 2% FBS; × 40 magnification)

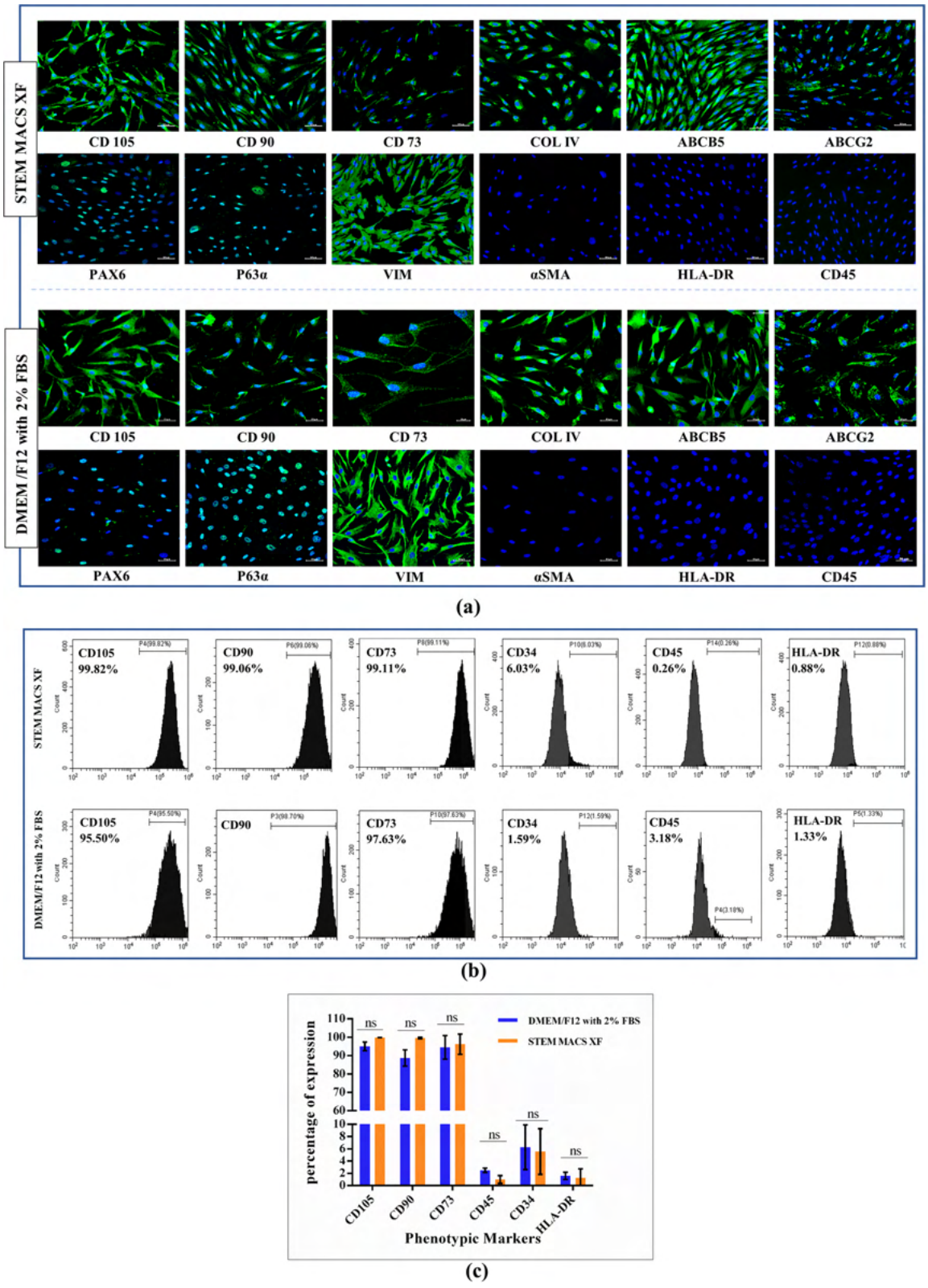

Fig. 2 (See legend on previous page.)

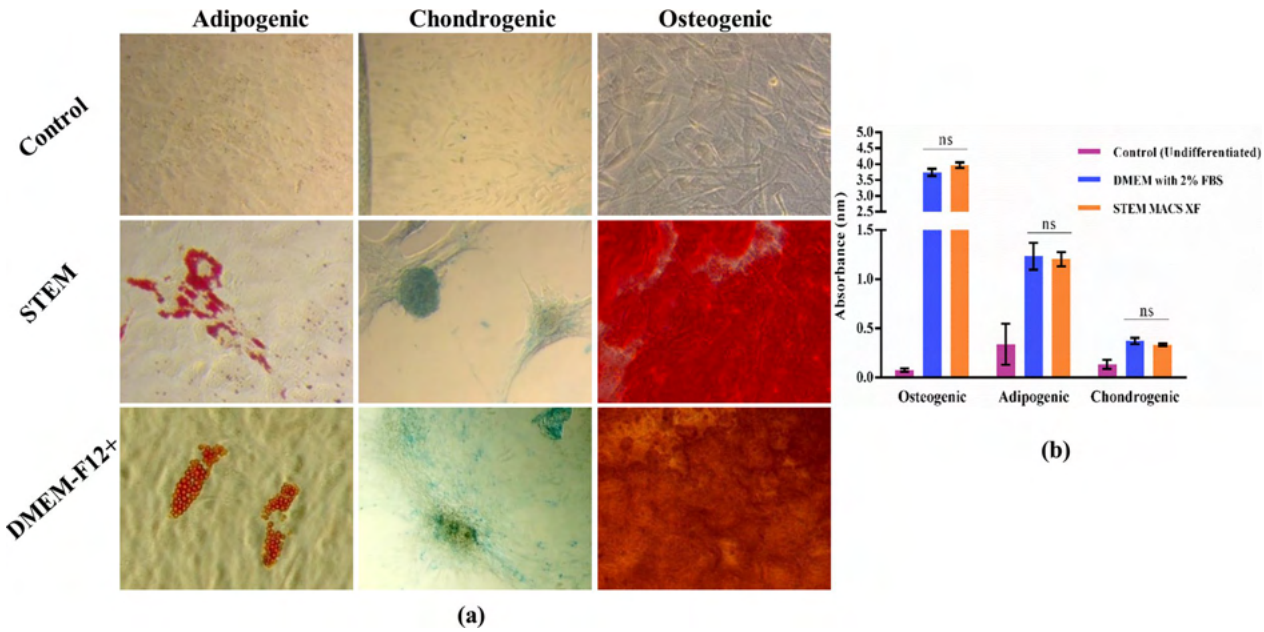

Fig. 3 **a** Tri-lineage differentiation potential of hLMSCs cultured in SM and control medium. Control represents undifferentiated cells. Adipogenic differentiation was identified by the formation of oil droplets stained by Oil Red O stain. Chondrogenic differentiation had glycosaminoglycans stained by an acidic stain, Alcian Blue. Osteogenic differentiation was identified as a large number of calcium deposits stained by Alizarin Red stain. hLMSCs cultured in both the medium showed a significant amount of tri-lineage differentiation; **b** graph of quantification of tri-lineage differentiation of hLMSCs into osteocytes, adipocytes and chondrocytes. The respective stains were eluted, and the intensity of colour was measured using a spectrophotometer. Both the media supported tri-lineage differentiation to an approximately equal extent. Control represents undifferentiated cells. Data are represented as mean ± SD ($n = 3$)

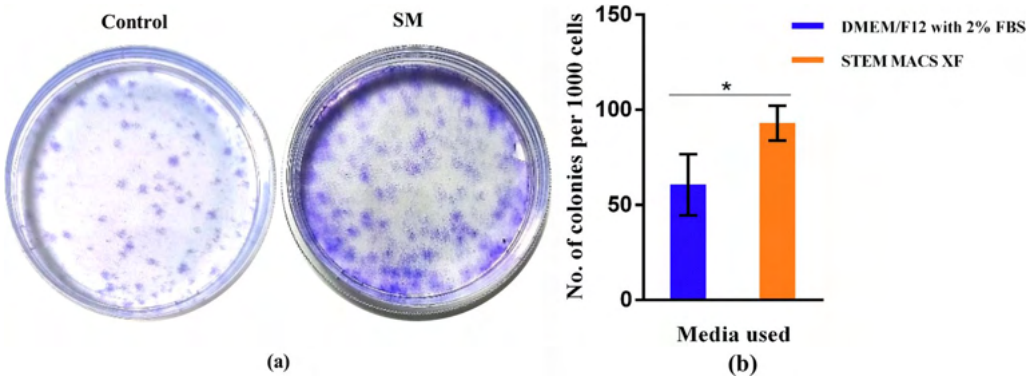

Fig. 4 **a** Representative photograph of colony forming unit of hLMSCs: SM showed a higher number of colonies than the control medium. **b** Bar graph showing the comparison of number of colonies per 1000 cells in both the media

regulatory guidelines for transplantation. To date, MSCs have been used in various clinical trials worldwide, but they are cultured in FBS fortified medium. Hence, establishing a xeno-free method of culturing these cells has an immediate translational approach.

Some studies have cultured MSCs in low serum-containing medium [64, 65], but the idea of the complete elimination of serum would be better for therapeutic use, which led several research groups to formulate in-house xeno-free medium for MSC expansion using defined chemical compounds as supplements [66–69]. However, the safety of these in-house media haven't been ensured, and some studies have markedly shown a difference in the growth rate of MSCs isolated from different tissues of the same organism [51, 53, 70] or from the same tissues of various organisms [71, 72]. To avoid

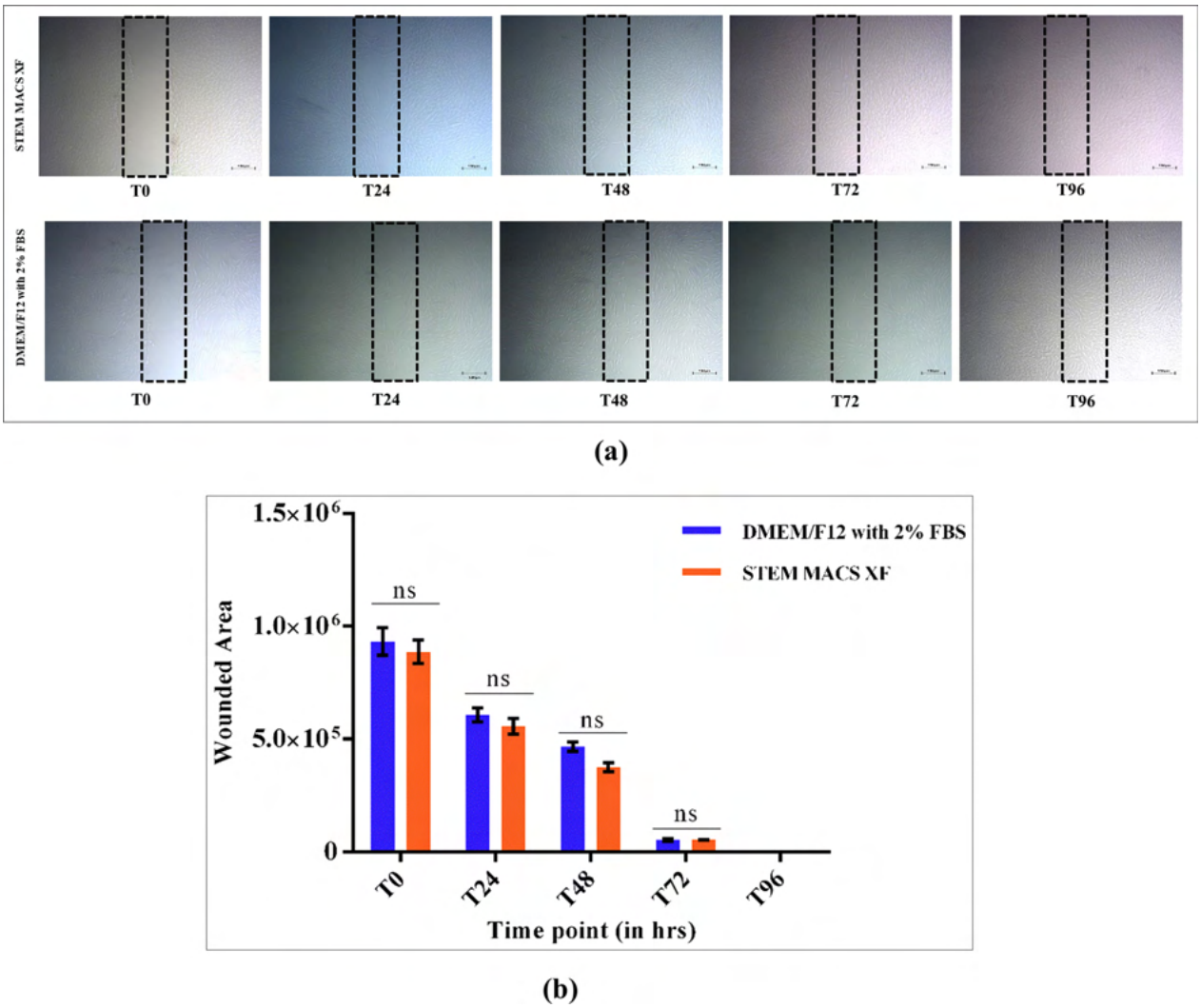

Fig. 5 **a** Representative photograph of the wounded area of hLMSCs cultured in SM and control. **b** Bar graph showing the relative decrease in the wounded area at different time points in both media. Scale: 500 μM

these complications, proprietary commercially available serum-free medium like RoosterBio, Inc., MD, USA (RoosterNourish-MSC XF); Miltenyi Biotec, Germany (STEM MACS XF); Merck, USA (PLTMax Human Platelet Lysate); R&D Systems, USA (StemXVivo Serum free Human Mesenchymal Stem Cell Expansion media) for MSC growth and expansion are promising alternatives. These media contain all chemically defined supplements devoid of any zoonotic components for healthy growth of MSCs [52, 73, 74]. A study by Ghoubay et al. followed different culture conditions along with 3T3 feeder cells. They have mainly characterized the epithelial and stromal stem cells. However, our study has shown isolation of hLMSCs by looking into all the MSC-specific markers using FACS, IF and qRT PCR following the ISCT guidelines using GMP grade media. Our findings also show comparatively less culture duration of MSCs reducing the population doubling time, thereby reducing the time consumed [75].

In a similar study, Aussel C group have demonstrated the successful expansion of MSCs in serum and xeno-free medium satisfying all the required parameters similar to the results obtained in our study. There are a number of serum and xeno-free media available in the market, so different groups test MSC from different origins and using different media [76].

Another group led by Gerby S have used a single serum-free medium which has supported the growth of bone marrow mesenchymal stem cells as evident from

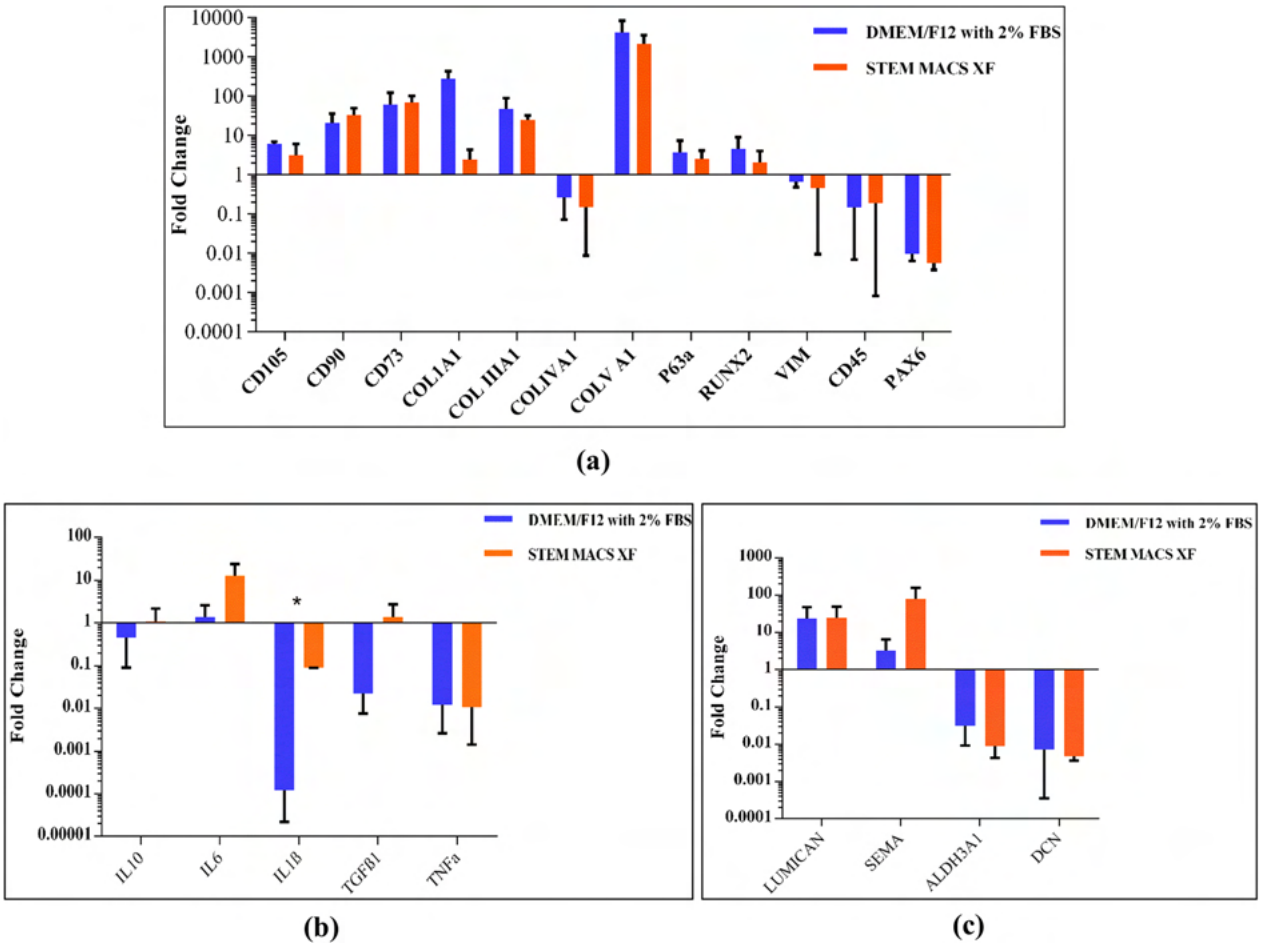

Fig. 6 Bar graph showing log fold change of various MSC-specific genes (**a**), genes involved in inflammatory pathways (**b**), and wound healing markers (**c**). No statistically significant difference between fold change demonstrates that hLMSCs retain their genotypic and phenotyping characteristics adapting to the serum-free environment. The data are represented as mean ± SD; $n = 3$; $^{*}p < 0.5$

different experiments except CFU. It would be inappropriate to say the cells are not stem cells by just using one medium to characterize. In our opinion, the Gerby S group can try other medium to characterize the cells. Other independent research groups have shown successful expansion and characterization of BM-MSCs using different other xeno-free medium [77].

As per earlier studies, optimal seeding density is required for efficient growth of MSCs, minimizing patchy growths [78]. According to a study by Abrahamsen et al., MSCs perhaps expand optimally when seeded at lower densities due to the property of contact inhibition regulated by the Wnt pathway [79]. In this study, the hLMSCs were seeded at 5000 cells/cm^2 for all the functional assays. Maintaining a consistent PDT is vital for the translational use of MSCs. Several previous studies have claimed an equivalent doubling time of MSCs in a serum-free environment to that of serum-based medium [56, 80, 81]. The doubling time of hLMSCs in SM was maintained at 25 ± 5 h even at higher passages, while it rose significantly higher in the control medium (Fig. 1b). The cell viability percentage was also significantly higher in SM (Fig. 1e), representing better division in comparison with the control medium.

Immunofluorescence analysis of phenotypic markers revealed expression of MSC-specific surface markers (CD105$^+$, CD90$^+$, ABCG2$^+$, ABCB5$^+$, COLIV$^+$, CD73$^+$, and VIM$^+$), negligible expression of haematopoietic markers (CD45$^-$, CD34$^-$, HLA-DR$^-$) and fibroblastic marker (αSMA$^-$) satisfying MSC criterion [2]. Earlier studies that employed serum-fortified medium to culture MSCs have reported positive expression of HLA-DR, possibly due to the presence of FGF in serum [82–84]. The depletion or complete absence of serum in culture media used in this study might have aided in minimizing

HLA-DR expression in large-scale production, enhancing the therapeutic value of MSCs. In our study, the HLA-DR expression was found to be 0.88% in SM and 1.33% in the control medium (with 2% FBS) (Fig. 2b).

Differentiation of hLMSCs into all three lineages was supported by SM without any significant difference compared to the control medium (Fig. 3). Even though there was no difference in the extent of chondrogenic differentiation between the two media, the pellets were microscopically different in size (Fig. 3 middle panel). In case of SM, the pellet was more prominent, whereas the GAG deposits were scattered throughout the plate in the control medium. Further, the colony-forming ability was significantly higher in SM compared to the control medium (Fig. 4; $p=0.038$). In vitro wound healing assay, a property well exhibited by MSCs, was also retained in the serum-free formulation. In fact, SM demonstrated better healing potential of hLMSCs than the control medium, due to comparatively lower population doubling time (Fig. 5a).

The gene expression pattern was observed to be similar in both media, as evident from the calculated fold change in qRT PCR (Fig. 6). Various stem cell markers were overexpressed in both media as compared to the native limbus, except Collagen IV, Vimentin and PAX6. As collagen IV is mainly present in Descemet's membrane, the expression is supposed to be higher in native tissue [85, 86]. Similarly, concerning PAX6, which is omnipresent in both corneal and limbal epithelia relative to the stroma, its decreased expression in hLMSCs is self-explanatory [87].

The culture of corneal/limbal stromal cells in the serum-free medium has been reported in previous studies, but those media weren't adequately characterized. Some studies used human platelet lysate, which again has lot-to-lot variation [88]. In this study, we demonstrated the growth and expansion of hLMSCs in vitro in serum-free conditions using a commercially available xeno-free medium, SM. SM was chosen as it has been successfully used in the expansion of BM-MSC [4] and was readily available. As SM hasn't been used in the culture of limbal stromal cells, we tried to explore its potential for hLMSCs. This medium is manufactured in a GMP-compliant facility, which is an added advantage for therapeutic use.

Undoubtedly, we acknowledge certain limitations of this study, like characterization and optimization of only P3 hLMSCs and usage of only one serum-free medium. However, this study successfully addresses the aim of expanding P3 hLMSCs in a serum-free environment.

Optimization of hLMSCs in SM at higher passages and to study the safety and toxicity of these cells in animal models needs to be further explored.

Conclusion

The findings of this study suggest that the phenotypic and functional property of hLMSCs is retained in serum-free environment. Further, their ability for wound closure and multi-lineage differentiation also remains unaltered. This indicates that the serum-free medium not only supports but also enhances its characteristic features, in addition to overcoming regulatory and ethical constraints.

Abbreviations

hLMSCs	Human limbus-derived stromal/mesenchymal stem cells
MSC	Mesenchymal stem cells
LSCD	Limbal stem cell deficiency
SM	STEM MACS XF
FBS	Foetal bovine serum
PDT	Population doubling time
BM	Bone marrow
UC	Umbilical cord
AD	Adipose tissue
CSSC	Corneal stromal stem cells
RIEB	Ramayamma International Eye Bank
PBS	Phosphate-buffered saline
IF	Immunofluorescence
BSA	Bovine serum albumin
CPD	Cumulative population doublings
GAG	Glycosaminoglycans
EGF	Epidermal growth factor
DMEM	Dulbecco's modified eagle medium
CD	Cluster of differentiation
T	Time
P3	Passage 3

Supplementary Information

The online version contains supplementary material available at https://doi.org/10.1186/s13287-023-03299-3.

Additional file 1. Immunofluorescence analysis of epithelial markers in Human Corneal Epithelial (HCE) cell line and hLMSCs.

Acknowledgements

The current work was supported by Science and Engineering Research Board, Department of Science and Technology, Government of India (EMR/2017/005086); Science and Engineering Research Board, Department of Science and Technology, Government of India (CRG/2018/003514); Sree Ramakrishna Paramahamsa Research Grant for Translational Biomedical Research 2022", funded by "Sree Padmavathi Venkateswara Foundation (SreePVF), Vijayawada, Andhra Pradesh (Sree PVF/G/TS/21/1). The authors thank Udaya Chandrika Kamepalli, senior technician of FACS and Imaging facility, for her support in confocal imaging and flow cytometry; and Hyderabad Eye Research Foundation, Hyderabad, India, for the infrastructural support.

Author contributions

AS designed and performed the experiments, collected and analysed the data and prepared and reviewed the manuscript. JJ performed the experiments, collected the data and proofread the manuscript. MD analysed the data, reviewed, and proofread the manuscript. DP performed the experiments and collected and analysed the data. SB provided a conceptual design and reviewed the manuscript. VS provided conceptual guidance for the study; supervised the experiments, and data analysis; reviewed and approved the manuscript. All authors read and approved the final manuscript.

Funding
Not applicable.

Availability of data and materials
All the data are available with the corresponding author upon request.

Declarations

Ethics approval and consent to participate
This work was carried out under the project entitled "Optimizing the Processes for Isolation, Preservation, Transportation and Delivery of human limbus-derived stromal/mesenchymal stem cells for Clinical Use in a cGMP Facility". This study was approved by the Institutional Review Board (IRB) of the LV Prasad Eye Institute Ethics Committee (Ethics Ref. No. LEC-05-18-081), dated 22nd May 2018 and Institutional Committee for Stem Cell Research (LVPEI- IC-SCR Ref No 08-18-002), dated 24th August 2018. The informed consent for use of cadaveric corneas was obtained from Ramayamma International Eye Bank housed in L V Prasad Eye Institute.

Consent for publication
Not applicable.

Competing interests
The authors declare that they have no competing interests.

Author details
[1]Centre for Ocular Regeneration, Prof. Brien Holden Eye Research Centre, L V Prasad Eye Institute, Hyderabad, Telangana, India. [2]Department of Animal Biology, School of Life Sciences, University of Hyderabad, Hyderabad, Telangana, India. [3]Manipal Academy of Higher Education, Manipal, Karnataka, India.

Received: 7 December 2022 Accepted: 24 March 2023
Published online: 15 April 2023

References

1. Horwitz EM, Andreef M, Frassoni F. Mesenchymal stromal cells. Curr Opin Hematol. 2006;13:419.
2. Dominici M, le Blanc K, Mueller I, Slaper-Cortenbach I, Marini FC, Krause DS, et al. Minimal criteria for defining multipotent mesenchymal stromal cells. The International Society for Cellular Therapy position statement. Cytotherapy. 2006;8:315–7.
3. Friedenstein AJ, Chailakhjan RK, Lalykina KS. The development of fibroblast colonies in monolayer cultures of guinea-pig bone marrow and spleen cells. Cell Prolif. 1970;3:393–403.
4. Bhat S, Viswanathan P, Chandanala S, Prasanna SJ, Seetharam RN. Expansion and characterization of bone marrow derived human mesenchymal stromal cells in serum-free conditions. Sci Rep. 2021;11:1–18.
5. Cimino M, Gonçalves RM, Barrias CC, Martins MCL. Xeno-free strategies for safe human mesenchymal stem/stromal cell expansion: supplements and coatings. Stem Cells Int. 2017;2017:6597815.
6. Singh V, Shukla S, Ramachandran C, Mishra DK, Katikireddy KR, Lal I, et al. Science and art of cell-based ocular surface regeneration. Int Rev Cell Mol Biol. 2015;319:45–106.
7. Shojaati G, Khandaker I, Funderburgh ML, Mann MM, Basu R, Stolz DB, et al. Mesenchymal stem cells reduce corneal fibrosis and inflammation via extracellular vesicle-mediated delivery of miRNA. Stem Cells Transl Med. 2019;8:1192–201.
8. Pinnamaneni N, Funderburgh JL. Concise review: stem cells in the corneal stroma. Stem Cells. 2012;30:1059–63.
9. Du Y, SundarRaj N, Funderburgh ML, Harvey SA, Birk DE, Funderburgh JL. Secretion and organization of a cornea-like tissue in vitro by stem cells from human corneal stroma. Invest Ophthalmol Vis Sci. 2007;48:5038–45.
10. Du Y, Funderburgh ML, Mann MM, SundarRaj N, Funderburgh JL. Multipotent stem cells in human corneal stroma. Stem Cells. 2005;23:1266–75.
11. Wu J, Du Y, Mann MM, Yang E, Funderburgh JL, Wagner WR. Bioengineering organized, multilamellar human corneal stromal tissue by growth factor supplementation on highly aligned synthetic substrates. Tissue Eng Part A. 2013;19:2063.
12. Singh V, Barbosa FL, Torricelli AAM, Santhiago MR, Wilson SE. Transforming growth factor β and platelet-derived growth factor modulation of myofibroblast development from corneal fibroblasts in vitro. Exp Eye Res. 2014;120:152–60.
13. Singh V, Jaini R, Torricelli AAM, Santhiago MR, Singh N, Ambati BK, et al. TGFβ and PDGF-B signaling blockade inhibits myofibroblast development from both bone marrow-derived and keratocyte-derived precursor cells in vivo. Exp Eye Res. 2014;121:35–40.
14. Singh V, Agrawal V, Santhiago MR, Wilson SE. Stromal fibroblast–bone marrow-derived cell interactions: implications for myofibroblast development in the cornea. Exp Eye Res. 2012;98:1–8.
15. Patel SV, McLaren JW, Hodge DO, Baratz KH. Scattered light and visual function in a randomized trial of deep lamellar endothelial keratoplasty and penetrating keratoplasty. Am J Ophthalmol. 2008;145:97–105.
16. Koh S, Maeda N, Nakagawa T, Nishida K. Quality of vision in eyes after selective lamellar keratoplasty. Cornea. 2012;31(Suppl 1):S45–9.
17. Jester JV, Barry-Lane PA, Cavanagh HD, Petroll WM. Induction of alpha-smooth muscle actin expression and myofibroblast transformation in cultured corneal keratocytes. Cornea. 1996;15:505–16.
18. Funderburgh JL, Mann MM, Funderburgh ML. Keratocyte phenotype mediates proteoglycan structure: a role for fibroblasts in corneal fibrosis. J Biol Chem. 2003;278:45629.
19. Basu S, Hertsenberg AJ, Funderburgh ML, Burrow MK, Mann MM, Du Y, et al. Human limbal biopsy–derived stromal stem cells prevent corneal scarring. Sci Transl Med. 2014;6:266ra172.
20. Coster DJ, Williams KA. The impact of corneal allograft rejection on the long-term outcome of corneal transplantation. Am J Ophthalmol. 2005;140:1112–22.
21. Dandona L, Naduvilath TJ, Janarthanan M, Ragu K, Rao GN. Survival analysis and visual outcome in a large series of corneal transplants in India. Br J Ophthalmol. 1997;81:726.
22. Tan DTH, Dart JKG, Holland EJ, Kinoshita S. Corneal transplantation. Lancet. 2012;379:1749–61.
23. Polisetty N, Fatima A, Madhira SL, Sangwan VS, Vemuganti GK. Mesenchymal cells from limbal stroma of human eye. Mol Vis. 2008;14:431.
24. Branch MJ, Hashmani K, Dhillon P, Jones DRE, Dua HS, Hopkinson A. Mesenchymal stem cells in the human corneal limbal stroma. Invest Ophthalmol Vis Sci. 2012;53:5109–16.
25. Bray LJ, Heazlewood CF, Munster DJ, Hutmacher DW, Atkinson K, Harkin DG. Immunosuppressive properties of mesenchymal stromal cell cultures derived from the limbus of human and rabbit corneas. Cytotherapy. 2014;16:64–73.
26. Liu H, Zhang J, Liu CY, Wang IJ, Sieber M, Chang J, et al. Cell therapy of congenital corneal diseases with umbilical mesenchymal stem cells: lumican null mice. PLoS ONE. 2010;5:e10707.
27. Mörö A, Samanta S, Honkamäki L, Rangasami VK, Puistola P, Kauppila M, et al. Hyaluronic acid based next generation bioink for 3D bioprinting of human stem cell derived corneal stromal model with innervation. Biofabrication. 2022;15:015020.
28. Alió del Barrio JL, de la Mata A, de Miguel MP, Arnalich-Montiel F, Nieto-Miguel T, el Zarif M, et al. Corneal regeneration using adipose-derived mesenchymal stem cells. Cells. 2022;11:2549–2549.
29. Saccu G, Menchise V, Gai C, Bertolin M, Ferrari S, Giordano C, et al. Bone marrow mesenchymal stromal/stem cell-derived extracellular vesicles promote corneal wound repair by regulating inflammation and angiogenesis. Cells. 2022;11:3892.
30. Galindo S, de la Mata A, López-Paniagua M, Herreras JM, Pérez I, Calonge M, et al. Subconjunctival injection of mesenchymal stem cells for corneal failure due to limbal stem cell deficiency: state of the art. Stem Cell Res Ther. 2021;12:1–12.
31. Lavrentieva A, Hoffmann A, Lee-Thedieck C. Limited potential or unfavorable manipulations? Strategies toward efficient mesenchymal stem/stromal cell applications. Front Cell Dev Biol. 2020;8:316.
32. Spees JL, Lee RH, Gregory CA. Mechanisms of mesenchymal stem/stromal cell function. Stem Cell Res Ther. 2016;7:1–13.
33. Wagner M, Yoshihara M, Douagi I, Damdimopoulos A, Panula S, Petropoulos S, et al. Single-cell analysis of human ovarian cortex identifies distinct cell populations but no oogonial stem cells. Nat Commun. 2020;11:1147.

34. Gstraunthaler G, Lindl T, van der Valk J. A plea to reduce or replace fetal bovine serum in cell culture media. Cytotechnology. 2013;65:791–3.
35. Karnieli O, Friedner OM, Allickson JG, Zhang N, Jung S, Fiorentini D, et al. A consensus introduction to serum replacements and serum-free media for cellular therapies. Cytotherapy. 2017;19:155–69.
36. Lindroos B, Boucher S, Chase L, Kuokkanen H, Huhtala H, Haataja R, et al. Serum-free, xeno-free culture media maintain the proliferation rate and multipotentiality of adipose stem cells in vitro. Cytotherapy. 2009;11:958–72.
37. Bieback K. Platelet lysate as replacement for fetal bovine serum in mesenchymal stromal cell cultures. Transfus Med Hemother. 2013;40:326.
38. Jonsdottir-Buch SM, Lieder R, Sigurjonsson OE. Platelet lysates produced from expired platelet concentrates support growth and osteogenic differentiation of mesenchymal stem cells. PLoS ONE. 2013;8:68984.
39. Hemeda H, Giebel B, Wagner W. Evaluation of human platelet lysate versus fetal bovine serum for culture of mesenchymal stromal cells. Cytotherapy. 2014;16:170–80.
40. Burnouf T, Strunk D, Koh MBC, Schallmoser K. Human platelet lysate: replacing fetal bovine serum as a gold standard for human cell propagation? Biomaterials. 2016;76:371–87.
41. Monsanto MM, White KS, Kim T, Wang BJ, Fisher K, Ilves K, et al. Concurrent isolation of 3 distinct cardiac stem cell populations from a single human heart biopsy. Circ Res. 2017;121:113–24.
42. Motedayyen H, Esmaeil N, Tajik N, Khadem F, Ghotloo S, Khani B, et al. Method and key points for isolation of human amniotic epithelial cells with high yield, viability and purity. BMC Res Notes. 2017;10:1–8.
43. Lee MS, Wang J, Yuan H, Jiao H, Tsai TL, Squire MW, et al. Endothelin-1 differentially directs lineage specification of adipose- and bone marrow-derived mesenchymal stem cells. FASEB J. 2019;33:996–1007.
44. Cherian DS, Bhuvan T, Meagher L, Heng TSP. Biological considerations in scaling up therapeutic cell manufacturing. Front Pharmacol. 2020;11:654.
45. Wagner M, Yoshihara M, Douagi I, Damdimopoulos A, Panula S, Petropoulos S, et al. Single-cell analysis of human ovarian cortex identifies distinct cell populations but no oogonial stem cells. Nat Commun. 2020;11:1–15.
46. de Sousa PA, Galea G, Turner M. The road to providing human embryo stem cells for therapeutic use: the UK experience. Reproduction. 2006;132:681–9.
47. Nikfarjam L, Farzaneh P. Prevention and detection of mycoplasma contamination in cell culture. Cell J (Yakhteh). 2012;13:203.
48. Rottem S, Barile MF. Beware of mycoplasmas. Trends Biotechnol. 1993;11:143–51.
49. Bjare U. Serum-free cell culture. Pharmacol Ther. 1992;53:355–74.
50. Brindley DA, Davie NL, Culme-Seymour EJ, Mason C, Smith DW, Rowley JA. Peak serum: implications of serum supply for cell therapy manufacturing. Regen Med. 2012;7:7–13.
51. Tan KY, Teo KL, Lim JFY, Chen AKL, Reuveny S, Oh SKW. Serum-free media formulations are cell line-specific and require optimization for microcarrier culture. Cytotherapy. 2015;17:1152–65.
52. Bhat S, Viswanathan P, Chandanala S, Prasanna SJ, Seetharam RN. Expansion and characterization of bone marrow derived human mesenchymal stromal cells in serum-free conditions. Sci Rep. 2021;11:1–18.
53. Al-Saqi SH, Saliem M, Asikainen S, Quezada HC, Ekblad Å, Hovatta O, et al. Defined serum-free media for in vitro expansion of adipose-derived mesenchymal stem cells. Cytotherapy. 2014;16:915–26.
54. Chase LG, Yang S, Zachar V, Yang Z, Lakshmipathy U, Bradford J, et al. Development and characterization of a clinically compliant xeno-free culture medium in good manufacturing practice for human multipotent mesenchymal stem cells. Stem Cells Transl Med. 2012;1:750–8.
55. Mimura S, Kimura N, Hirata M, Tateyama D, Hayashida M, Umezawa A, et al. Growth factor-defined culture medium for human mesenchymal stem cells. Int J Dev Biol. 2011;55:181–7.
56. Jung S, Sen A, Rosenberg L, Behie LA. Human mesenchymal stem cell culture: rapid and efficient isolation and expansion in a defined serum-free medium. J Tissue Eng Regen Med. 2012;6:391–403.
57. Fekete N, Gadelorge M, Frst D, Maurer C, Dausend J, Fleury-Cappellesso S, et al. Platelet lysate from whole blood-derived pooled platelet concentrates and apheresis-derived platelet concentrates for the isolation and expansion of human bone marrow mesenchymal stromal cells: production process, content and identification of active components. Cytotherapy. 2012;14:540–54.
58. Schallmoser K, Strunk D. Preparation of pooled human platelet lysate (pHPL) as an efficient supplement for animal serum-free human stem cell cultures. J Vis Exp. 2009;32:1523.
59. Prosser A, Scotchford C, Roberts G, Grant D, Sottile V. Integrated multi-assay culture model for stem cell chondrogenic differentiation. Int J Mol Sci. 2019;20:951.
60. Kraus NA, Ehebauer F, Zapp B, Rudolphi B, Kraus BJ, Kraus D. Quantitative assessment of adipocyte differentiation in cell culture. Adipocyte. 2016;5:351.
61. Gregory CA, Gunn WG, Peister A, Prockop DJ. An Alizarin red-based assay of mineralization by adherent cells in culture: comparison with cetylpyridinium chloride extraction. Anal Biochem. 2004;329:77–84.
62. Movahedan A, Majdi M, Afsharkhamseh N, Sagha HM, Saadat NS, Shalileh K, et al. Notch inhibition during corneal epithelial wound healing promotes migration. Invest Ophthalmol Vis Sci. 2012;53:7476.
63. Kacham S, Bhure TS, Eswaramoorthy SD, Naik G, Rath SN, Parcha SR, et al. Human umbilical cord-derived mesenchymal stem cells promote corneal epithelial repair in vitro. Cells. 2021;10:1254.
64. Montzka K, Führmann T, Wöltje M, Brook GA. Expansion of human bone marrow-derived mesenchymal stromal cells: serum-reduced medium is better than conventional medium. Cytotherapy. 2010;12:587–92.
65. Wappler J, Rath B, Läufer T, Heidenreich A, Montzka K. Eliminating the need of serum testing using low serum culture conditions for human bone marrow-derived mesenchymal stromal cell expansion. Biomed Eng Online. 2013;12:1–10.
66. Liu CH, Wu ML, Hwang SM. Optimization of serum free medium for cord blood mesenchymal stem cells. Biochem Eng J. 2007;33:1–9.
67. Gharibi B, Hughes FJ. Effects of medium supplements on proliferation, differentiation potential, and in vitro expansion of mesenchymal stem cells. Stem Cells Transl Med. 2012;1:771–82.
68. Rajala K, Lindroos B, Hussein SM, Lappalainen RS, Pekkanen-Mattila M, Inzunza J, et al. A defined and xeno-free culture method enabling the establishment of clinical-grade human embryonic, induced pluripotent and adipose stem cells. PLoS ONE. 2010;5:e10246.
69. Lennon DP, Haynesworth SE, Young RG, Dennis JE, Caplan AI. A chemically defined medium supports in vitro proliferation and maintains the osteochondral potential of rat marrow-derived mesenchymal stem cells. Exp Cell Res. 1995;219:211–22.
70. Lopes VS, Ngo A, Ni H-T. A xeno-free, serum-free expansion medium for ex-vivo expansion and maintenance of major human tissue-derived mesenchymal stromal cells. Transl Biomed. 2018;9:2172.
71. Devireddy LR, Myers M, Screven R, Liu Z, Boxer L. A serum-free medium formulation efficiently supports isolation and propagation of canine adipose-derived mesenchymal stem/stromal cells. PLoS ONE. 2019;14:e0210250.
72. Schubert S, Brehm W, Hillmann A, Burk J. Serum-free human MSC medium supports consistency in human but not in equine adipose-derived multipotent mesenchymal stromal cell culture. Cytometry A. 2018;93:60–72.
73. Takao S, Nakashima T, Masuda T, Namba M, Sakamoto S, Yamaguchi K, et al. Human bone marrow-derived mesenchymal stromal cells cultured in serum-free media demonstrate enhanced antifibrotic abilities via prolonged survival and robust regulatory T cell induction in murine bleomycin-induced pulmonary fibrosis. Stem Cell Res Ther. 2021;12:1–16.
74. Hoang VT, Trinh QM, Phuong DTM, Bui HTH, Hang LM, Ngan NTH, et al. Standardized xeno- and serum-free culture platform enables large-scale expansion of high-quality mesenchymal stem/stromal cells from perinatal and adult tissue sources. Cytotherapy. 2021;23:88–99.
75. Ghoubay-Benallaoua D, de Sousa C, Martos R, Latour G, Schanne-Klein MC, Dupin E, et al. Easy xeno-free and feeder-free method for isolating and growing limbal stromal and epithelial stem cells of the human cornea. PLoS ONE. 2017;12:e0188398.
76. Aussel C, Busson E, Vantomme H, Peltzer J, Martinaud C. Quality assessment of a serum and xenofree medium for the expansion of human GMP-grade mesenchymal stromal cells. PeerJ. 2022;10:e13391.
77. Gerby S, Attebi E, Vlaski M, Ivanovic Z. A new clinical-scale serum-free xeno-free medium efficient in ex vivo amplification of mesenchymal stromal cells does not support mesenchymal stem cells. Transfusion (Paris). 2017;57:433–9.

78. Colter DC, Class R, DiGirolamo CM, Prockop DJ. Rapid expansion of recycling stem cells in cultures of plastic-adherent cells from human bone marrow. Proc Natl Acad Sci USA. 2000;97:3213–8.
79. Abrahamsen JF, Bakken AM, Bruserud Ø. Cryopreserving human peripheral blood progenitor cells with 5-percent rather than 10-percent DMSO results in less apoptosis and necrosis in CD34+ cells. Transfusion (Paris). 2002;42:1573–80.
80. Lindroos B, Boucher S, Chase L, Kuokkanen H, Huhtala H, Haataja R, et al. Serum-free, xeno-free culture media maintain the proliferation rate and multipotentiality of adipose stem cells in vitro. Cytotherapy. 2009;11:958–72.
81. Bobis-Wozowicz S, Kmiotek K, Kania K, Karnas E, Labedz-Maslowska A, Sekula M, et al. Diverse impact of xeno-free conditions on biological and regenerative properties of hUC-MSCs and their extracellular vesicles. J Mol Med (Berl). 2017;95:205–20.
82. Bocelli-Tyndall C, Zajac P, di Maggio N, Trella E, Benvenuto F, Iezzi G, et al. Fibroblast growth factor 2 and platelet-derived growth factor, but not platelet lysate, induce proliferation-dependent, functional class II major histocompatibility complex antigen in human mesenchymal stem cells. Arthritis Rheum. 2010;62:3815–25.
83. Sotiropoulou PA, Perez SA, Salagianni M, Baxevanis CN, Papamichail M. Characterization of the optimal culture conditions for clinical scale production of human mesenchymal stem cells. Stem Cells. 2006;24:462–71.
84. Damala M, Swioklo S, Koduri MA, Mitragotri NS, Basu S, Connon CJ, et al. Encapsulation of human limbus-derived stromal/mesenchymal stem cells for biological preservation and transportation in extreme Indian conditions for clinical use. Sci Rep. 2019;9:1–11.
85. Kabosova A, Azar DT, Bannikov GA, Campbell KP, Durbeej M, Ghohestani RF, et al. Compositional differences between infant and adult human corneal basement membranes. Invest Ophthalmol Vis Sci. 2007;48:4989–99.
86. Eghrari AO, Riazuddin SA, Gottsch JD. Overview of the cornea: structure, function, and development. Prog Mol Biol Transl Sci. 2015;134:7–23.
87. Tavakkoli F, Damala M, Koduri MA, Gangadharan A, Rai AK, Dash D, et al. Transcriptomic profiling of human limbus-derived stromal/mesenchymal stem cells—novel mechanistic insights into the pathways involved in corneal wound healing. Int J Mol Sci. 2022;23:8226.
88. Gupta P, Hall GN, Geris L, Luyten FP, Papantoniou I. Human platelet lysate improves bone forming potential of human progenitor cells expanded in microcarrier-based dynamic culture. Stem Cells Transl Med. 2019;8:810–21.

Publisher's Note

biomolecules

IMPACT FACTOR 6.064

Indexed in: PubMed

Article

Human Cadaveric Donor Cornea Derived Extra Cellular Matrix Microparticles for Minimally Invasive Healing/Regeneration of Corneal Wounds

Arun Chandru, Parinita Agrawal, Sanjay Kumar Ojha, Kamalnath Selvakumar, Vaishnavi K. Shiva, Tanmay Gharat, Shivaram Selvam, Midhun Ben Thomas, Mukesh Damala, Deeksha Prasad et al.

Special Issue
Ocular Diseases and Therapeutics

Edited by
Prof. Dr. Hemant Khanna

MDPI

https://doi.org/10.3390/biom11040532

biomolecules

MDPI

Article

Human Cadaveric Donor Cornea Derived Extra Cellular Matrix Microparticles for Minimally Invasive Healing/Regeneration of Corneal Wounds

Arun Chandru [1,*], Parinita Agrawal [1,†], Sanjay Kumar Ojha [1,†], Kamalnath Selvakumar [1], Vaishnavi K. Shiva [1], Tanmay Gharat [1], Shivaram Selvam [1], Midhun Ben Thomas [1], Mukesh Damala [2], Deeksha Prasad [2], Sayan Basu [2,3], Tuhin Bhowmick [1,*], Virender Singh Sangwan [2,3] and Vivek Singh [2,3,*]

1 Pandorum Technologies Private Limited, Bangalore, Karnataka 560100, India; parinita.agrawal@pandorumtechnologies.in (P.A.); sanjay.ojha@pandorumtechnologies.in (S.K.O.); kamalnath.s@pandorumtechnologies.in (K.S.); vaishnavioptom@gmail.com (V.K.S.); tanmay.gharat@pandorumtechnologies.in (T.G.); selvam.shivaram@pandorumtechnologies.in (S.S.); ben.thomas@pandorumtechnologies.in (M.B.T.)

2 Brien Holden Eye Research Center, LV Prasad Eye Institute, Hyderabad, Telangana 500034, India; mukeshdamala@lvpei.org (M.D.); deekshaprasad317@gmail.com (D.P.); sayanbasu@lvpei.org (S.B.); virender.sangwan@sceh.net (V.S.S.)

3 Center for Ocular Regeneration (CORE), LV Prasad Eye Institute, Hyderabad, Telangana 500034, India

* Correspondence: arun@pandorumtechnologies.in (A.C.); tuhin@pandorumtechnologies.in (T.B.); viveksingh@lvpei.org (V.S.); Tel.: +91-40-6810-2286 (V.S.)

† These authors contributed equally to this work.

check for updates

Citation: Chandru, A.; Agrawal, P.; Ojha, S.K.; Selvakumar, K.; Shiva, V.K.; Gharat, T.; Selvam, S.; Thomas, M.B.; Damala, M.; Prasad, D.; et al. Human Cadaveric Donor Cornea Derived Extra Cellular Matrix Microparticles for Minimally Invasive Healing/Regeneration of Corneal Wounds. *Biomolecules* **2021**, *11*, 532. https://doi.org/10.3390/biom11040532

Academic Editor: Hemant Khanna

Received: 2 March 2021
Accepted: 25 March 2021
Published: 2 April 2021

Abstract: Biological materials derived from extracellular matrix (ECM) proteins have garnered interest as their composition is very similar to that of native tissue. Herein, we report the use of human cornea derived decellularized ECM (dECM) microparticles dispersed in human fibrin sealant as an accessible therapeutic alternative for corneal anterior stromal reconstruction. dECM microparticles had good particle size distribution (≤10 µm) and retained the majority of corneal ECM components found in native tissue. Fibrin–dECM hydrogels exhibited compressive modulus of 70.83 ± 9.17 kPa matching that of native tissue, maximum burst pressure of 34.3 ± 3.7 kPa, and demonstrated a short crosslinking time of ~17 min. The fibrin–dECM hydrogels were found to be biodegradable, cytocompatible, non-mutagenic, non-sensitive, non-irritant, and supported the growth and maintained the phenotype of encapsulated human corneal stem cells (hCSCs) in vitro. In a rabbit model of anterior lamellar keratectomy, fibrin–dECM bio-adhesives promoted corneal re-epithelialization within 14 days, induced stromal tissue repair, and displayed integration with corneal tissues in vivo. Overall, our results suggest that the incorporation of cornea tissue-derived ECM microparticles in fibrin hydrogels is non-toxic, safe, and shows tremendous promise as a minimally invasive therapeutic approach for the treatment of superficial corneal epithelial wounds and anterior stromal injuries.

Keywords: decellularization; human cornea; extracellular matrix; fibrin hydrogels; in vivo imaging

1. Introduction

Cornea is the transparent window of the eye and the most significant refractive element responsible for the creation of vision. However, at times, vision is compromised due to various factors including dystrophic, degenerative, infectious (bacterial and fungal infections), and secondary damage, such as scarring, chemical burns, and allergies, all of which if left untreated ultimately lead to irreversible loss of vision [1]. Among the various types of visual impairments, corneal blindness is the fourth leading cause of blindness globally [2]. On an average, 1.5–2 million new cases are estimated to occur worldwide each year [3]. In severe corneal injuries, the epithelium along with the stroma could be

significantly compromised, threatening the structural integrity of the ocular surface. In such conditions, the most common treatment involves the replacement of a part or whole of the cornea with human donor tissue [1]. However, studies have shown that less than 5% of the patient population has access to corneal transplantation due to severe shortage of donor tissues and high cost of corneal transplantation [4]. Moreover, more than half of donated corneas do not meet the standards for transplantation due to low endothelial cell count, transmissible diseases, short shelf life, etc. Hence, other standard care options for treatment of corneal scars and perforation typically include application of tissue bioadhesives, use of artificial corneas, and biomaterial-mediated stem cell therapy [5–8].

Ocular tissue adhesives based on natural (fibrin, hyaluronic acid, collagen, and gelatin) or synthetic (cyanoacrylate- and PEG-based (ReSure and OcuSeal®) polymers have been extensively used as suture substitutes for closure of corneal incisions/perforation and conjunctival wounds [5]. For serious ocular complications, replacement of the diseased cornea with a synthetic "artificial" cornea has been actively investigated as an alternate option to a conventional corneal tissue graft [3,6,9]. In this regard, cell-free biomaterial implants composed of recombinant human collagen type III (RHCIII) or fabricated from poly(2-hydroxyethyl methacrylate) (AlphaCor®) have been evaluated on patients with severe corneal pathologies [3,6]. For instance, long-term assessment of patients with RHCIII implants demonstrated that the biosynthetic implants presented no serious adverse reactions, including pain or discomfort, excessive redness, and swelling of adjacent corneal tissues [3]. However, problems related to cytotoxicity from residual contaminants were one of the notable drawbacks of this approach [9]. Besides, cell-free systems are inherently limited by their capacity to homogenously recruit and integrate keratocytes from nearby stromal tissue which could severely impair biointegration and impede corneal stromal repair and regeneration in vivo. Hence, there is a demand for safer, efficacious, and cost-effective alternatives that would allow for successful treatment of corneal diseases in a minimally invasive manner.

Recently, the incorporation of extracellular matrix (ECM) components obtained from decellularized native tissues has gained importance as they offer tissue-specific biological cues that could stimulate host-cell migration, mediate stem cell differentiation, and offer pro-regenerative microenvironment conducive for tissue regeneration [10,11]. In this regard, decellularized freeze milled cornea powder has been reported for use in corneal repair and regeneration [12,13]. For instance, decellularized bovine and porcine corneas have been shown to be biocompatible and demonstrated the ability to maintain optical clarity, mechanical, and structural integrity favorable for transplantation procedures in vivo [14,15]. In addition, acellular porcine cornea matrix implanted in inter-lamellar stromal pockets in a rabbit model demonstrated excellent biocompatibility with optical transparency comparable to that of normal corneas eight weeks post-implantation [16]. In the present study, decellularized cornea ECM microparticles (dECM microparticles), derived from cadaveric human corneas that were unfit for transplantation, were dispersed in fibrin glue and their potential for facilitating cornea stromal wound healing was evaluated. To this end, dECM microparticles incorporated in fibrin hydrogels were characterized for their physical and mechanical properties in vitro. Additionally, fibrin–dECM hydrogel biocompatibility and its influence on human corneal stem cells (hCSCs) phenotype were demonstrated via fluorescence imaging in vitro. Lastly, dECM-dispersed fibrin hydrogels, with and without hCSCs, were evaluated in a rabbit model of anterior lamellar keratectomy [17] to demonstrate corneal re-epithelialization, stromal tissue repair, and integration with native tissue in vivo.

2. Materials and Methods

Study Design, Location, Duration, and Approvals: It was prospective study and conducted at LV Prasad Eye Institute, Pandorum Technologies Pvt. Ltd., Bangalore and Vimta Laboratories, in Hyderabad. The work was approved by the ethics committees (IRB and IC-SCRT, LV Prasad Eye Institute) of the respective institutes and animals were handled

in accordance with the Association for Research in Vision and Ophthalmology (ARVO) statement for the animal use in Ophthalmic and Vision Research as well as in accordance with the tenets of declaration from Helsinki. The animal study was conducted after IRB approval from the ethics committee at LV Prasad Eye Institute and animal ethics committee of Vimta Labs Limited (Ethics Ref: LEC-12-19-372) (LVPEI-IC-SCR REF No 02-19-001).

2.1. Decellularization of Human Cadaveric Donor Corneas

The decellularization procedures were performed under mild chemical conditions with NaCl solution modifying previously published protocols [18,19] (Figure 1A). Briefly, human cadaveric corneas, unfit for clinical transplantation but suitable for research, were collected from Ramayamma International Eye Bank (LVPEI, Hyderabad, India) and processed in a cGMP facility. Corneas stripped of the epithelium and endothelium were cut using trephine (9.25 mm) and the resultant cornea buttons were washed with phosphate buffered saline (PBS) solution. They were later washed with betadine solution (1.5%, purified water) for 30 s, incubated in sodium chloride solution (NaCl, 1.5 M), and placed on a rocker at room temperature (RT) for 48 h with NaCl solution changed once every 24 h. The decellularized corneas were then incubated in PBS containing Pen-Strep (P/S, 100 U/mL Penicillin, 100 µg/mL streptomycin, and Lonza) for 24 h, following which they were treated in PBS containing DNase in an orbital shaker (200 RPM) for another 24 h at 37 °C. Finally, the corneas were incubated in PBS containing 2× P/S for 24 h at RT and were tested by immunostaining to make sure no cellular debris or foreign DNA was present in the tissue before further processing.

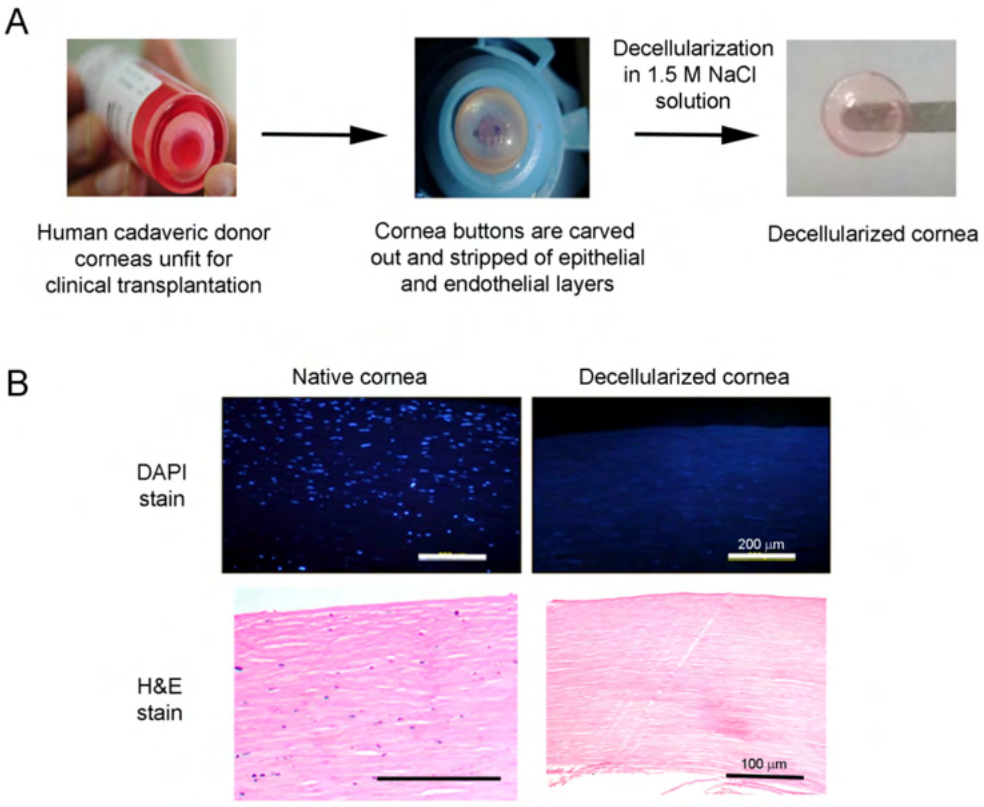

Figure 1. *Cont.*

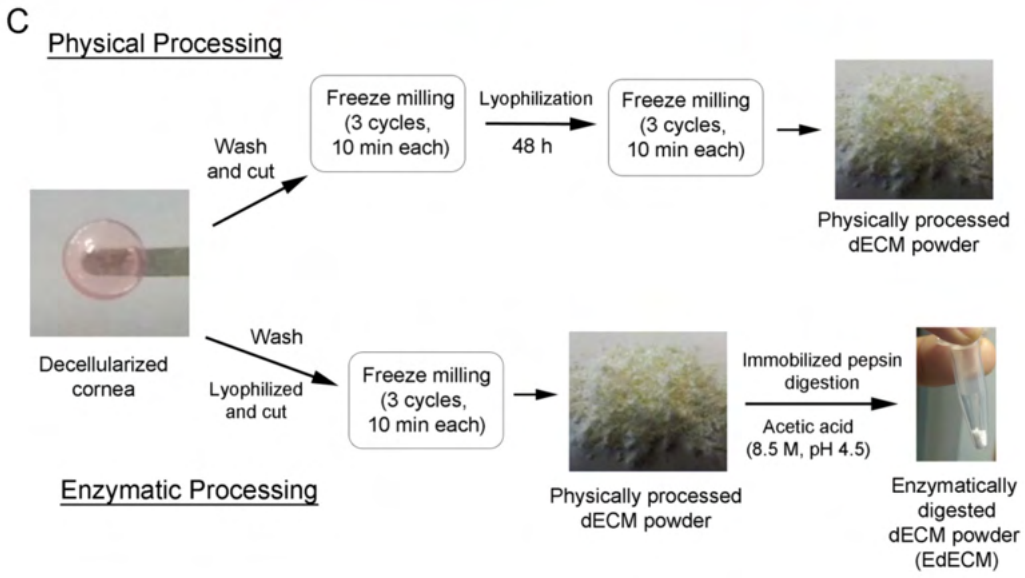

Figure 1. Schematic representation depicting the preparation of physically milled and enzymatically digested human cadaveric cornea derived decellularized ECM microparticles. (**A**) Decellularization process of cadaveric human donor corneas unfit for clinical transplantation; (**B**) nuclei (DAPI) and H&E stain demonstrating the absence of genetic material; and (**C**) preparation of physically processed and pepsin enzyme digested dECM microparticles from decellularized human corneas.

2.2. Processing of Decellularized Tissues

The decellularized corneas were washed three times with deionized water for 30 min at RT to remove salts and antibiotics. After washing, the wet corneas were cut into small pieces (<20 mm^3) and transferred to the micro vial set of the freeze-miller. Of note, we have evidence to show that water present in the cornea pieces form icicles upon freezing which might act as a grinding agent during the milling process to yield fine microparticles (Figure S1). The cornea pieces were then allowed to pre-cool in liquid nitrogen for 5 min, following which they were freeze-milled in liquid nitrogen for 10 min (SPEX SamplePrep, USA, #6775-230). This cycle was repeated two more times to yield a finely milled cornea decellularized extracellular matrix (dECM) paste. The dECM paste was frozen at −80 °C and lyophilized in a freeze dryer (Labcogene, Scanvac CoolSafe Pro #110-4) 48 h. After lyophilization, the dECM was freeze milled again (3 cycles, 10 min each) to yield a finely milled powder that was weighed and stored at −80 °C until further use.

For enzymatic digestion, decellularized corneas were washed three times with deionized water, lyophilized for 48 h, and chopped into small pieces (<20 mm^3). The cornea pieces were then freeze milled to yield dECM powder which was subjected to enzymatic digestion using pepsin immobilized on agarose beads (Protein A Agarose beads, #20333, Thermo-Scientific). Briefly, dECM (10 mg) was UV-sterilized (20 min) and dispersed in sterile acetic acid solution (0.22 micron-filtered, 8.5 M, pH 4.5). The concentration of the enzyme slurry used was ~0.025 mL slurry/mg of dECM. The digestion was carried out at 37 °C in 8.5 M acetic acid (Merck) at pH 4.5 for 72 h. Post-digestion, the beads were separated from the enzyme digested dECM (EdECM) suspension via centrifugation at ~200× *g* for 5 min. The final EdECM was dialyzed, and the resultant suspension was lyophilized to yield a fine, dry powder. Both physically processed and EdECM microparticles were used for various characterizations, as detailed in Table 1.

Table 1. List of formulations used for the various characterization studies.

dECM Microparticle Characterization	
SEM	**Physically processed dECM and EdECM**
Thermogravimetric analysis (TGA)	Physically processed dECM
Dynamic Light Scattering (DLS)	Physically processed dECM and EdECM
Fourier Transform Infrared (FTIR)	Physically processed dECM and EdECM
Sandwich ELISA assay	EdECM
Mass Spectrometry	EdECM
Hydrogel Characterization	
Compressive modulus	EdECM
Crosslinking kinetics	EdECM
Ex-vivo burst pressure	EdECM
In vitro Cell Culture Studies with hCSCS	
MTT assay on hydrogel extracts	Physically processed dECM
Bacterial reverse mutation test on hydrogel extracts	Physically processed dECM
Cell encapsulation in hydrogels	EdECM
Live/Dead assay	EdECM
Biomarker expression	EdECM
Biodegradation Study in vitro	EdECM
In Vivo Studies	
Skin sensitization test in Guinea pigs	Physically processed dECM
Acute ocular irritation test in rabbits	Physically processed dECM
Treatment of corneal stromal injury in rabbit model	Physically processed dECM

2.3. dECM Microparticle Characterization

2.3.1. Scanning Electron Microscopy (SEM) with Energy Dispersive X-Ray Analysis (EDAX)

Physically processed and enzymatically digested corneal dECM microparticle (EdECM) size and morphology were recorded using a field-emission scanning electron microscopy (Zeiss Ultra-55, Oberkochen, Germany) operating at a voltage of 5 kV (Figure 2). Briefly, lyophilized physically processed or EdECM microparticles were sputter-coated with gold/palladium to achieve a 10-nm coating and visualized under low vacuum conditions. Elemental analysis by energy dispersive X-ray spectroscopy was also performed to determine molecular constituents of EdECM samples (Zeiss Ultra-55, Oberkochen, Germany).

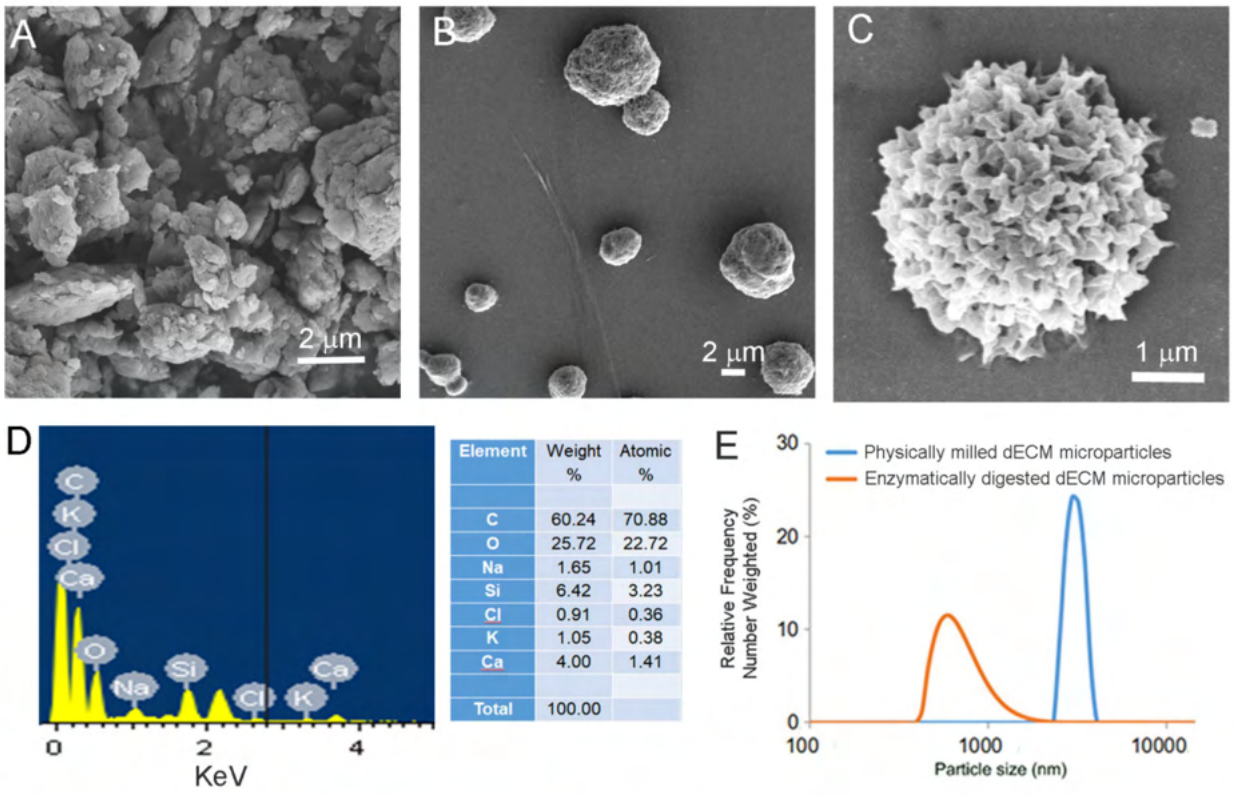

Figure 2. Physical characterization of dECM microparticles: (**A**) representative SEM image of physically processed dECM microparticles; (**B**) SEM image of enzymatically digested dECM microparticles; (**C**) SEM images of a EdECM microparticle showing petaloid-like architecture; (**D**) elemental analysis of EdECM microparticles demonstrating that its primarily composed of carbon and oxygen moieties confirming its ECM origin; and (**E**) hydrodynamic sizes of dECM microparticles via DLS measurements.

2.3.2. Thermogravimetric Analysis (TGA)

TGA analysis was performed on thermogravimetric analyzer (TGA Q500 V20.13, TA Instruments) at a heating rate of 10 °C/min from RT to 350 °C under nitrogen atmosphere.

2.3.3. Dynamic Light Scattering (DLS)

For DLS measurements, dECM microparticles were dispersed in PBS (1 mg/mL), and the average hydrodynamic particle size and polydispersity index (PDI) were measured using a particle size analyzer (Litesizer 500, AntonPaar) at RT.

2.3.4. Fourier Transform Infrared (FTIR)

The Fourier transform infrared (FTIR) spectrum of lyophilized dECM powder in the region of 400–4000 cm^{-1} was obtained using a FTIR spectrometer (Spectrum Two, Perkin Elmer) at RT.

2.3.5. Sandwich ELISA Assay

Analysis of carryover pepsin from the immobilized pepsin digestion was verified using porcine pepsin quantitative sandwich ELISA kit (MyBioSource, San Diego, CA, USA) as per the manual provided by the manufacturer.

2.3.6. Mass Spectrometry

Briefly, dECM microparticles were processed with 4% SDS lysis buffer and heated at 90 °C for 5 min. The treated sample was then sonicated for 3 cycles at 40% amplitude including intermittent resting for 1 min on ice between cycles. The samples were then

sonicated at 12,000 rpm for 15 min at 4 °C and the supernatant was transferred to a fresh tube. After protein estimation, the samples (200 µg) were further processed with dithiothreitol (Merck), iodoacetamide (Merck), and chilled acetone (Merck). The resultant sample was centrifuged and the pellet was dissolved in urea (6 M). The dissolved sample was further subjected to trypsin digestion and LysC solution (Lys C protease in 50 mM triethyl ammonium bicarbonate buffer, Merck) treatment. The resultant peptide digest was acidified with 1% formic acid and cleaned using Sep-Pak C18 columns. The eluent was dried using a vacuum concentrator and analyzed in a mass spectrometer (LTQ Orbitrap Velos, Thermo Scientific).

2.4. Hydrogel Preparation

To prepare the working pre-gel fibrin solution, thrombin was reconstituted in calcium chloride solution (1 mL) to obtain a 500 IU/mL solution, and aprotinin solution (1 mL) was added to fibrinogen powder to yield 90 mg/mL solution (Tisseel Lyo, Deerfield, Baxter). The fibrinogen solution was kept under stirring at 37 °C to obtain clear liquid. For preparation of dECM based fibrin hydrogels, dECM microparticles were first dispersed in reconstituted thrombin solution and this solution was mixed with an equal volume of reconstituted fibrinogen solution. The mixture was allowed to gel at 37 °C for 20 min to obtain the liquid cornea hydrogel (Schematic representation in Figure 3A). The final dECM concentration in the resultant fibrin gel was 30 mg/mL (3% w/v). Hydrogels with dECM concentrations higher than 30 mg/mL were not considered as it was difficult to mix this dECM/thrombin mixture with highly viscous fibrinogen solution which severely affected the homogenous distribution of the microparticles in the fibrin glue. Fibrin hydrogels prepared in the absence of dECM microparticles was used as control gels.

2.5. Hydrogel Characterization

2.5.1. Compressive Modulus

Cylindrical hydrogel discs were prepared using molds (6 mm diameter and 1 mm height) and were subjected to a crosshead speed of 1 mm/min and compressed to a maximum strain of 50% using BiSS mechanical tester (OmniTest 5kN with Vector Pro NT). The values for compressive strain (mm) and load (N) were recorded and the compressive moduli were calculated from the slope of the linear region between 0.1–0.2 mm/mm strain on the stress (kPa) versus strain (mm/mm) curves using BiSS software.

2.5.2. Crosslinking Kinetics

The crosslinking kinetics of fibrin and fibrin–EdECM hydrogels was determined using a rheometer (Anton Paar Rheometer, MCR105). Briefly, pre-gel solution, comprising of 125 µL fibrinogen and 125 µL thrombin, was placed in between the parallel plate geometry (25 mm diameter) with 0.2 mm gap. The change in rheological behavior (storage modulus) of the hydrogels was then measured at constant a frequency of 1 Hz when subjected to an oscillatory load of 0.2% strain.

2.5.3. Ex-Vivo Burst Pressure

The sealing ability of fibrin-based hydrogels was evaluated on rejected human donor corneas. Briefly, a full thickness corneal wound was created by punching a hole (2 mm diameter) using a commercially available leather hole punch (Armor Heavy Rotary Leather hole punch, Visking). The cornea was then mounted on a Barron artificial anterior chamber (Katena, Denville, NJ, USA) and 15–20 µL of fibrin glue was applied to seal the hole. After gelation, air was gradually pumped into the system (2 mL/min) using a syringe pump (New Era Pump System Inc., Farmingdale, NY, USA, #NE-1600) and the pressure at which the hydrogel ruptured or delaminated from the cornea was recorded (PASCO wireless pressure sensor, #PS-3203) as the maximum burst pressure.

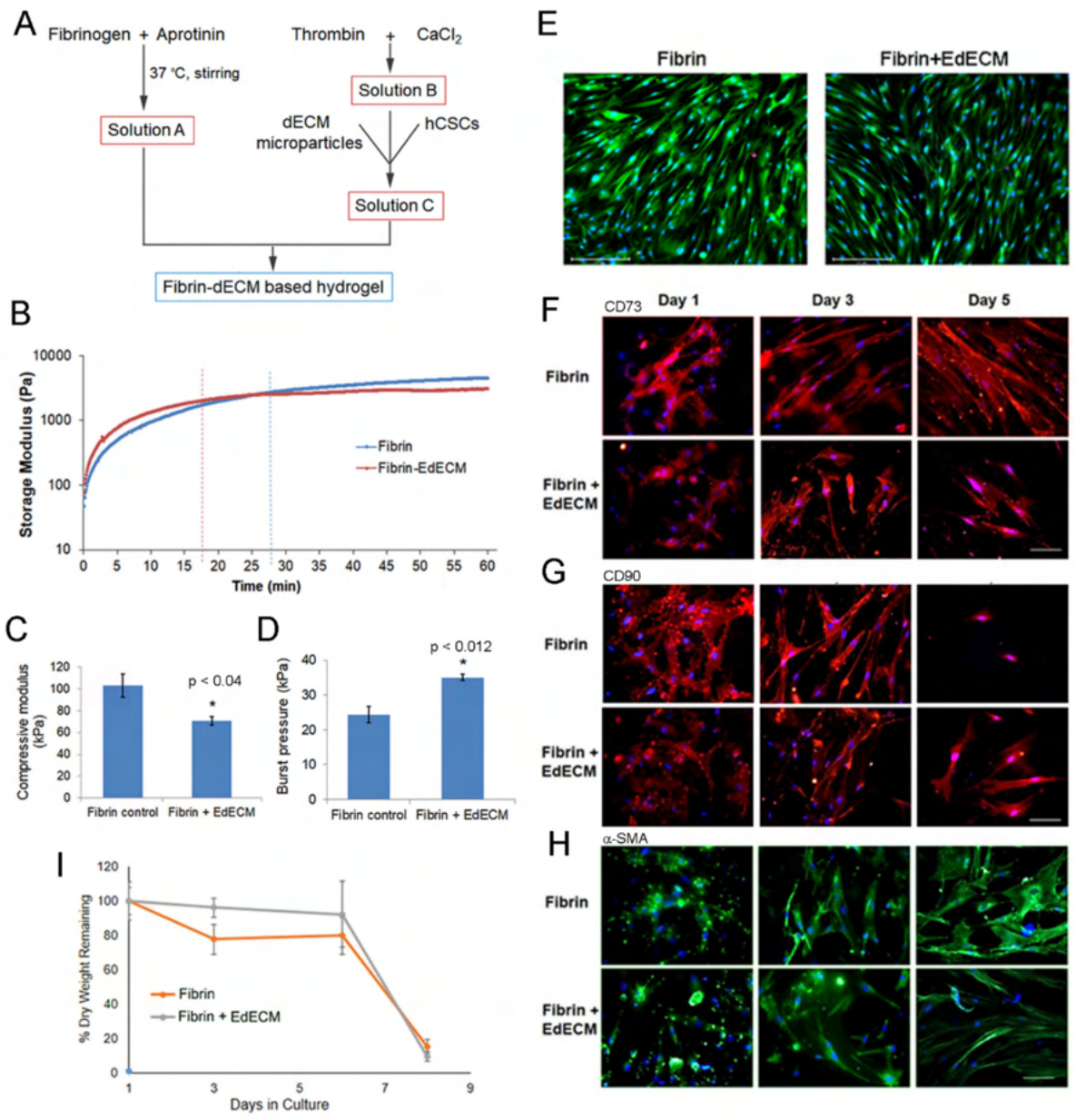

Figure 3. Characterization of fibrin–EdECM based hydrogels: (**A**) schematic for the preparation of fibrin–dECM based hydrogels; (**B**) crosslinking kinetics of fibrin and fibrin–EdECM hydrogels; (**C**) compressive modulus of fibrin and fibrin–EdECM hydrogels; (**D**) maximum burst pressure of fibrin and fibrin–EdECM hydrogels; (**E**) cell viability of hCSCs encapsulated in fibrin and fibrin–EdECM hydrogel on Day 5 via live/dead stain, where reen denotes live cells and red denotes dead cells and nuclei are labeled blue; (**F**,**G**) CD73 and CD90 biomarker expression of hCSCs encapsulated in fibrin and fibrin–EdECM hydrogels; (**H**) expression of α-SMA in hCSCs encapsulated in fibrin and fibrin–EdECM hydrogels; and (**I**) biodegradation of hCSC encapsulated fibrin and fibrin–EdECM hydrogels in vitro. Data are represented as mean ± SE with n≥3 samples/group. * $p \leq 0.05$ denotes significant differences observed between fibrin and fibrin–EdECM hydrogels.

2.5.4. MTT Assay on Hydrogel Extracts

MTT cell proliferation assay is a simple method for determination of viability of cells and was performed as per the International Standards (ISO) 10993-5 with six replicate samples. Briefly, fibrin and fibrin–dECM hydrogels were incubated in complete cell culture medium (0.2 g/mL Minimal Essential Medium (MEM) supplemented with 10% fetal bovine serum (FBS) and P/S) for a period of 24 h. Later, the hydrogel extracts and degradation products were diluted with MEM to yield test concentrations of 25%, 50%, and 75%

and evaluated on L929 fibroblast cultures. For cell culture, L929 cells were seeded at 1×10^4 cells/well in a 96-well plate in 100 µL of culture medium and incubated at 37 °C. After 24 h, media containing hydrogel extracts were added to complete cell culture medium at the concentrations mentioned above. After 24 h incubation, MTT solution (HiMedia, India; 50 µL, 1 mg/mL) was added to each well and the plate was incubated for 2 h at 37 °C. The resulting formazan was then solubilized and quantified spectrophotometrically at 570 nm using an automated microplate reader (Perkin Elmer, EnSpire®, Waltham, MA, USA).

2.5.5. Bacterial Reverse Mutation Test on Hydrogel Extracts

To study the genotoxicity of hydrogel extracts in vitro, a bacterial reverse mutation assay was performed using *S. typhimurium* and *E. coli* tester strains as per ISO 10993-3. For preparation of hydrogel extracts, fibrin and fibrin–dECM hydrogels (0.2 g/mL) were incubated under agitation in polar (0.9% *w*/*v* NaCl) and non-polar (sesame oil, MP Biomedicals) solvents at 50 °C for 70 h. Then, the mutagenicity of polar and non-polar hydrogel extracts was assessed based on the results of precipitation test and initial cytotoxicity test. For the mutation assay, plate incorporation and pre-incubation methods were carried out with 100% extract solution/plate, as the maximum limit of concentration under study groups along with solvent controls and positive controls, as mentioned in Table S2. In the plate incorporation method, the tester strains along with induced rat liver S9 homogenate in PBS (used as the metabolic activation system) were mixed directly with 2 mL soft agar containing histidine-biotin for *S. typhimurium* and tryptophan for *E. coli* and poured on to minimal glucose agar plates (HiMedia). In the pre-incubation method, the strains along with S9 homogenate in PBS were incubated in a shaker at 100 RPM at 37 °C for 30 min prior to mixing with agar. Later, 100 µL of hydrogel extract were plated with each of the following tester strains: *S. typhimurium* TA98, TA100, TA1535, TA1537 and *E. coli* WP2 uvrA (pKM101) (Molecular Toxicology Inc., Boone, NC, USA), with and without metabolic activation, and the plates were incubated at 37 °C for 65 h. The condition of the bacterial background lawn was evaluated for evidence of hydrogel extract cytotoxicity using a code system and revertant colonies for a given strain exposed to different dilutions were counted manually.

2.6. In Vitro Cell Culture Studies with hCSCS

2.6.1. Human Corneal Stem Cell Harvest and Expansion

Human corneal stem cells (hCSCs) were isolated and expanded as per our previously published protocol [20]. Briefly, hCSCs were isolated from collagenase digested limbal stromal tissue of human corneal rims from which central tissue had been removed. The isolated cells were cultured in Advanced DMEM/F12 medium containing 2% fetal bovine serum, epidermal growth factor (10 ng/mL), platelet-derived growth factor (PDGF-BB, 10 ng/mL), and gentamicin (50 ng/mL). Once confluent, hCSCs were passaged by trypsinizing with TrypLE and re-seeded at a density of ~10^4 cells/cm^2. The cells were cultured for up to three passages and used at passage four for subsequent experiments. On average, one cornea rim provided ~8–10 million hCSCs at passage 3 and around 3–5 corneas were used for in vitro cell culture studies.

2.6.2. Cell Encapsulation in Hydrogels

Briefly, EdECM microparticles were UV sterilized inside a biosafety cabinet for 30 min and were suspended in reconstituted thrombin solution containing hCSCs. Next, the cell/EdECM suspension in thrombin was pipetted onto the culture surface and mixed with an equal volume of reconstituted fibrinogen solution. The mixture was allowed to gel at 37 °C for 20 min after which culture medium was added to the gel. The cell encapsulated hydrogels were then incubated at 37 °C in a 5% CO_2 incubator. The final EdECM concentration in fibrin glue gel was 30 mg/mL (3% *w*/*v*) with a final cell density of ~1.5–2.0 million cells/mL of the hydrogel.

2.6.3. Live/Dead Assay

Briefly, thin hydrogels encapsulating hCSCs (2×10^6 cells/mL) were prepared by placing a drop of hydrogel formulation (12 µL) at the center of a sterile coverslip. Then, another coverslip was placed immediately on top of the drop to yield a hydrogel sandwiched between the coverslips. The sandwiched hydrogel was then placed in culture media for a few minutes and then the top coverslip was gently released and pushed aside using a pair of sharp pointed forceps without damaging the underlying hydrogel. The hydrogels were cultured for a period of 5 days, following which they were incubated in calcein acetoxymethyl (calcein-AM, 0.2 µg/mL) and ethidium homodimer (2.5 µg/mL) (Invitrogen, Paisley, UK) for 15 min in supplemented DMEM at 37 °C to stain for live cells and dead cells. Live cells were visualized as green and dead cells as red under a fluorescence microscope (EVOS FL Auto2, Thermo Fisher Scientific, Waltham, MA, USA).

2.6.4. Biomarker Expression

Briefly, fibrin derived hydrogels with encapsulated hCSCs (12 µL) were prepared between cover slips to yield thin samples. The thin hydrogel samples were recovered at different time points and washed with PBS. After washing, the hydrogel samples were fixed with 3.7% formalin solution in PBS (Sigma-Aldrich, India) for 10 min at RT and washed with PBS again. Immunohistochemistry (fluorescence) was performed to visualize the expression of scarless-wound healing related markers. Primary anti-CD73, anti-CD90 and anti-alpha smooth muscle actin (α-SMA) antibody were procured from Abcam. Goat anti-mouse and anti-rat antibodies (conjugated with Alexa Fluor 594 and Alexa Fluor 488; Thermo Fisher Scientific) were used as secondary antibodies. Briefly, after washing, the hydrogel samples were blocked in BSA (5% in PBS, 1 h) and were incubated with primary antibodies at 4 °C overnight (1:100 dilution in 1% BSA). The samples were then washed (PBS, 3 times, 5 min each) and incubated with an appropriate secondary antibody (1:200 dilution in 1% BSA) at room temperature for 1 h. The sections were then washed (PBS, 3 times, 10 min each), semi dried, and mounted with Vectashield antifade mounting medium containing DAPI (#H1200, Vector Labs, Burlingame, CA, USA). The sections were imaged under a fluorescence imaging system (Evos FL Auto 2).

2.6.5. Biodegradation Study In Vitro

To assess in vitro biodegradation, hydrogels loaded with hCSCs (12 µL, 2×10^6 cells/mL) were cultured for a maximum period of 9 days. At various time points, hydrogel samples were collected, lyophilized, weighed, and the mass remaining was calculated using the formula below:

$$\%\ mass\ remaining = \frac{(Mo - Mt)\ *\ 100}{Mo} \quad (1)$$

where *Mo* is the initial dry mass of the hydrogel and *Mt* is the dry mass of the hydrogel at various time points.

2.7. In Vivo Studies

Skin sensitization test in Guinea pigs and acute ocular irritation test in rabbits were performed in an AAALAC accredited facility in accordance with the recommendation of the Committee for the Purpose of Control and Supervision of Experiments on Animals (CPCSEA) guidelines for laboratory animal facility published in the Gazette of India, 2018, in accordance with the protocol approved by Institutional Animal Ethics Committee (IAEC) (Protocol Nos. BIO-IAEC-3579 and BIO-IAEC-3385) and in accordance with the International Standard ISO 10993 Second Edition: 2006-07-15, "Biological Evaluation of Medical Devices—Part 2: Animal Welfare Requirements" (Reference Number: ISO 10993-2:2006(E)).

The corneal stromal injury in rabbit model was conducted after IRB approval from the ethics committee at LV Prasad Eye Institute and animal ethics committee of Vimta Labs Limited in accordance with the tenets of declaration from Helsinki (Ethics Ref: LEC-12-19-371).

2.7.1. Skin Sensitization Test in Guinea Pigs

For the study, animals were divided into the following four groups with at least 5 animals per group: polar solvent control extract, polar hydrogel extract, non-polar solvent control extract, and non-polar hydrogel extract, prepared using the method described in Section 2.5.5. The polar and non-polar extracts were then injected intradermally during induction phase (Day 1) and applied topically during boosting (Day 8) and challenge (Day 22) phases. For intradermal injections, animals received 0.1 mL of injection at the shoulder region, and, for topical application, filter papers soaked with polar or non-polar extracts were placed as a patch at the test site for 24 h. Animals were then observed for at least 24 h to see whether the extracts produced any skin reactions. In addition, all animals were observed once daily for clinical signs of toxicity and twice daily for mortality. Body weight was recorded prior to initiation of the treatment (Day 1) and at termination of study.

2.7.2. Acute Ocular Irritation Test in Rabbits

The ocular irritation potential of fibrin and fibrin–dECM hydrogel extracts was evaluated via acute ocular irritation test in three New Zealand White rabbits. Hydrogel extracts were prepared using the method described in Section 2.5.5. The study was performed in two phases, initial test with one animal and confirmatory test with two animals. For both tests, a volume of 0.1 mL of undiluted extracts was instilled into the lower conjunctival sac of the eye and eyes were examined for ocular reactions at 1, 24, 48 and 72 h after instillation. At each interval, the cornea, iris, and conjunctivae were examined and scored according to a numerical scoring system. All three animals were observed once daily for clinical signs of toxicity and twice daily for mortality throughout the study period. Body weight was recorded on the day of instillation (Day 1 prior to instillation) and at termination (Day 4) of the experiment.

2.7.3. Treatment of Corneal Stromal Injury in Rabbit Model

Nine 8–10-week-old New Zealand White rabbits weighing 2–3 kg each were chosen for the corneal wound healing study and acclimatized for at least 1 week. Wound model was created as per our previously published literature [17]. Briefly, rabbits were anesthetized using ketamine and xylazine, after which they were shifted to a surgical table and draped for surgery. The wound creation was performed on the left eye at the central zone of the cornea with the help of a skin-marking pen and trephine (Joja Surgicals Private Limited, Kolkata, West Bengal, India). Then, a guarded knife (400 µm) and crescent blade (Joja Surgicals) were used to make the corneal wound (3 mm dia, 150–200 µm depth), after which an Alger brush was used to clear the remnant corneal pieces. Animals were divided into the following four groups. These were untreated control (2 rabbits), fibrin (2 rabbits), fibrin + EdECM (30 mg/mL) (3 rabbits), and fibrin + EdECM + hCSCs (5×10^6 cells/mL) (2 rabbits). Animals received one dose of ~4–8 µL of the formulation based on wound dimensions and clinician's discretion. Lastly, a soft bandage contact lens (Purecon Lenses Private Limited, New Delhi, India) was placed and tarsorrhaphy was performed to ensure that the hydrogels were properly secured in the eye. Animals that underwent surgery but received no treatment were used as untreated controls and the healthy contralateral eyes of all rabbits were used as normal experimental controls. The schematic diagram of the procedure is shown in Figure 4A. All animals were treated with corticosteroids and antibiotics for a week post wound creation.

Rabbit corneas were imaged using standard protocols pre-surgery and at 1, 2, 4 and 8 weeks postoperatively (±1 day). To monitor epithelialization, a digital SLR camera (Nikon D3300) and a handheld slit lamp (PSLAIA-11, Appasamy Associate, Chennai) with blue filter were used to photograph and capture fluorescein-stained images of the cornea. Anterior segment optical coherence tomography (ASOCT) imaging was performed using Ivue (Optovue, USA) to visualize cross sections of the cornea to discern scar depth, corneal thickness, and corneal edema. Scheimpflug imaging was performed using Galilei

G4 (Zeimer, Switzerland) in both horizontal and vertical meridians to analyze corneal topography and densitometry.

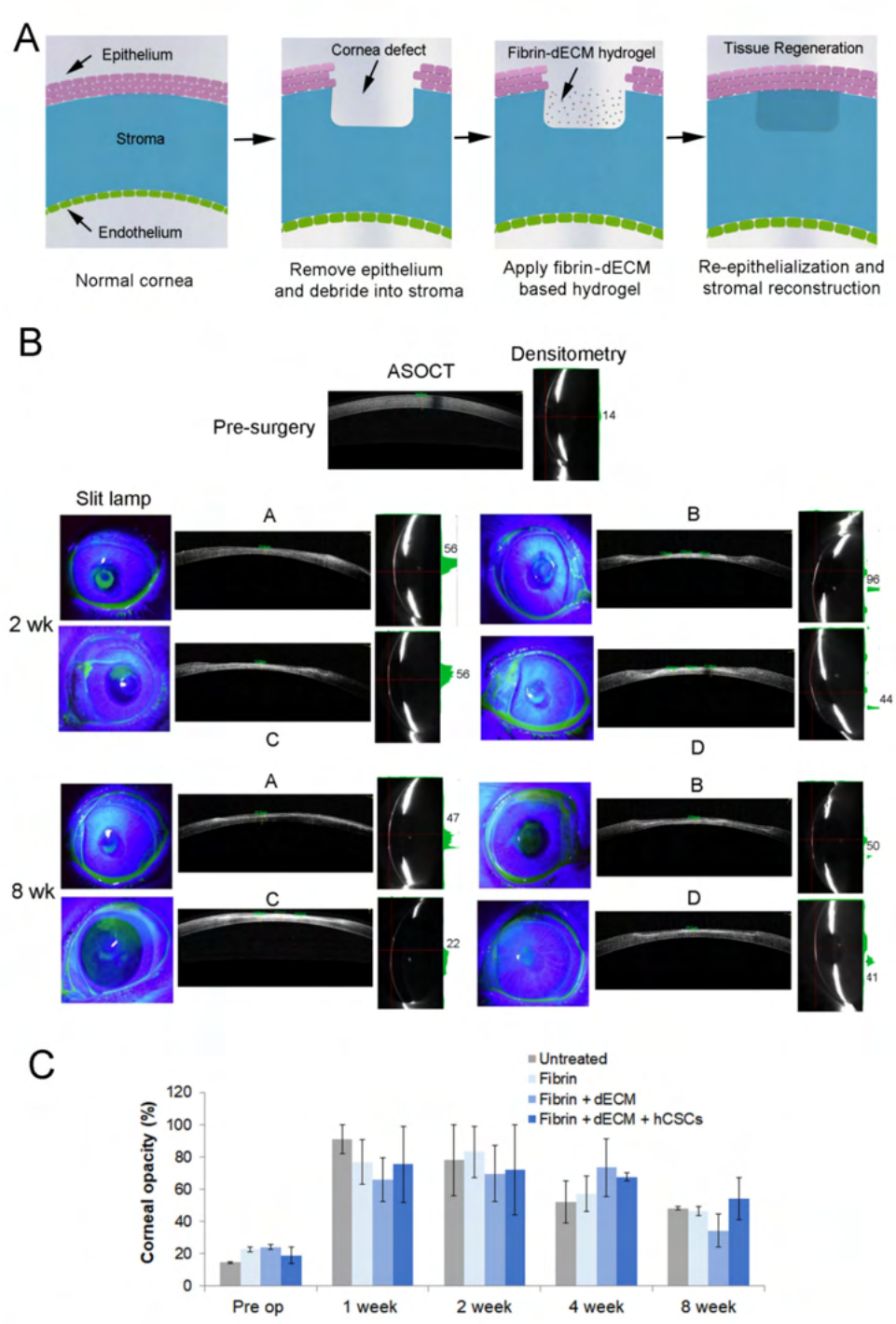

Figure 4. Rabbit cornea imaging in vivo. (**A**) Schematic depicting the creation of corneal defect and application of fibrin–dECM based hydrogels for ocular tissue reconstruction. (**B**) Representative images of rabbit corneas obtained using slit lamp with fluorescein staining, ASOCT and densitometry two and eight weeks post-application of fibrin based hydrogels. Corneas are represented as: (A) untreated; (B) fibrin controls; (C) fibrin + dECM microparticles; and (D) fibrin + dECM + hCSCs. Prior to surgery, corneas of all animals exhibited nominal corneal thickness with good optical clarity. (**C**) Bar graph depicts the decrease in corneal haze, an indicator of corneal wound healing, determined via densitometric evaluations during the eight-week time period.

2.8. Histopathology

After euthanasia at 8 weeks, rabbit corneas were punched out using 14 mm trephine and preserved in formalin. They were later cut into two halves, dehydrated, embedded in paraffin wax, and sectioned at a thickness of 4 µm. The cornea sections were then deparaffinized at 70 °C for 2 min and dipped in xylene solution immediately. After a series (100%, 90%, and 80%) of xylene wash, the sections were air dried and were subjected to an alcohol gradient wash (100%, 90%, and 80%) for 5 min each. Later, the slides were rehydrated in water for 10 min and stored in PBS. The deparaffinized sections were then stained with hematoxylin and eosin (H&E) and periodic acid-Schiff (PAS) staining respectively, as per standard protocols [21]. After completion of the staining protocols, the sections were mounted with DPX mounting media for imaging.

2.9. Immunofluorescence Staining

Heat induced antigen retrieval was performed on deparaffinized sections placed in sodium citrate buffer (pH 6.0). The sections were then washed (PBS, 3 times, 5 min each) and incubated in a permeabilizing agent (0.3% triton-X100, 30 min). After washing, the sections were blocked in BSA (2.5% in PBS, 1 h) and incubated with primary antibodies, cytokeratin 3 (CK3, 1:200) (SC-80000, Santa Cruz Biotechnology, USA) at 4 °C overnight, and alpha smooth muscle actin (α-SMA, 1:600) (A2547, Sigma-Aldrich, USA) at room temperature for 2 h. The sections were then washed (PBS, 3 times, 5 min each) and incubated with an appropriate secondary antibody (1:500 dilution in 1% BSA) (A11005, Invitrogen, USA) at room temperature for 1 h. The sections were then washed (PBS, 3 times, 10 min each), semi dried, and mounted with Fluoroshield medium containing DAPI (ab104139, Abcam, UK). The stained sections were then imaged under a fluorescent microscope (Axio Scope A1, Carl Zeiss AG, Germany) with 20–40× objective.

2.10. Statistical Analysis

Data are represented as mean ± standard error (SE) with n ≥ 3 samples/group. A two-tailed, unpaired Student's *t*-test or Multiple *t*-test was performed as applicable to detect differences between two groups with p values ≤ 0.05 considered statistically significant.

3. Results and Discussion

Globally, millions of people suffer from corneal blindness and the most common treatment option for these patients is a corneal transplantation. However, due to acute shortages of donor corneas, only one in 70 patients benefits from it [4]. Furthermore, as approximately one-third of corneal transplantations end up in graft rejection or revision surgery in the long term [22], there is a clinical need for exploring other therapeutic avenues for patients with corneal pathologies. Although options such as the use of artificial corneas for restoring corneal clarity are employed in some cases [3,6,9], these prefabricated implants fundamentally require the need of a certified surgeon with surgical skills and advanced instrumentation for corneal surgery. In this study, we developed a minimally invasive methodology combining a biocompatible tissue adhesive, fibrin glue, and decellularized corneal ECM microparticles for treatment of superficial corneal epithelial defects and anterior stromal disorders. We hypothesized that the decellularized biological components, which possess structural and biochemical similarities to that of native microenvironment, should aid in homeostasis and regeneration of neo-tissues in vivo [10,11,23]. To this end, discarded human cadaveric donor corneas that screened negative for infectious diseases and viruses were decellularized, milled, and enzymatically digested to yield microparticles for ocular surface reconstruction.

3.1. Decellularization of Cadaveric Human Corneas

Decellularization of cadaveric donor corneas was performed under mild chemical conditions with hypertonic NaCl solution as this methodology yielded corneal tissues with minimal loss in transparency and stromal disruption [18,19] (Figure 1A). Of note, NaCl-

based decellularization is biocompatible, compared to techniques that involve ionic/non-ionic detergents, as it relies only on osmotic shock to trigger cell rupture and cell death without significantly altering the structural integrity of native cornea tissue [18]. The resultant acellular corneal scaffolds obtained after NaCl treatment were characterized and evaluated to ensure the completeness of the decellularization protocol. The decellularization efficiency of the human corneal tissues was confirmed via H&E and DAPI staining (Figure 1B). Cross-sections of stained decellularized tissues demonstrated the absence of remnant cells and DNA. These results show that the employed NaCl-based decellularization protocol efficiently removed all cell debris and associated genetic material while preserving the structural, biochemical, and biomechanical cues of the corneal ECM structure.

3.2. Characterization of Cornea Derived dECM Microparticles

After decellularization, the cornea buttons were incised and milled in a freeze miller to yield particles (Figure 1C) that ranged 7–10 μm. More notably, the physically processed dECM microparticles were found to be non-homogenous and had the tendency to form large agglomerates over time (Figure 2A). As high moisture content in samples promote agglomeration and is often correlated to poor stability under long-term storage conditions [24], we determined the moisture content in the freeze-milled samples using thermogravimetric analysis (Figure S2). TGA data demonstrate that the freeze-milled dECM microparticles possessed ~7.7% moisture content at 100 °C which increased to 9.5% at 200 °C (Figure S2). To circumvent the issue of microparticle agglomeration and yield particles of smaller size with homogenous particle distribution for easy dispersion in fibrin glue, we explored the possibility of enzymatically digesting the dECM powder with porcine pepsin immobilized on agarose beads (Figure 1C).

SEM data show that the resultant enzymatically-digested corneal dECM microparticles averaged <4 μm in size, which was a two-fold decrease in particle size compared to physically-milled dECM powder (Figure 2B). Furthermore, EdECM particles were mostly found to be spherical in shape with characteristic petaloid-like architectures (Figure 2C). This observation was unique and is considered advantageous as these ultrastructures could increase the availability of cell binding RGD epitopes and facilitate cell–ECM interactions at the macroscopic level [25]. In addition, elemental analysis of EdECM microparticles confirmed its ECM origin (not inorganic or salt particles) as it was primarily composed of carbon and oxygen moieties (Figure 2D). The size of EdECM microparticles dispersed in aqueous solution was evaluated using dynamic light scattering. DLS measurements demonstrated a homogenous particle distribution with polydispersity indices <0.3 and particle sizes <1 μm (Figure 2E).

To demonstrate that enzymatic digestion did not modify or alter the ECM protein structure, lyophilized dECM microparticles were analyzed using FTIR spectroscopy. The results demonstrate that FTIR spectra of both physically processed and EdECM microparticles exhibited characteristic amide peaks [26], commonly seen in biological proteins, with no significant differences observed between them (Figure S3). The C=O stretching vibration in the amide group of the dECM protein was seen at 1630 cm^{-1}, while the out-of-phase and in-phase combination of N-H bending and C-N stretching vibration were observed at 1542 and 1403 cm^{-1}, respectively [26].

Xenogenic components have the tendency to elicit strong immune responses compared to allogenic materials in vivo [27]. To rule out the possibility of porcine pepsin in EdECM microparticles, a sandwich ELISA assay was performed on lyophilized EdECM microparticles (Figure S4). Our ELISA results demonstrate an insignificant amount of porcine pepsin (0.0001%) present in the dECM powder digested with immobilized pepsin under mild acidic conditions. Next, to demonstrate that most corneal dECM components were retained after immobilized pepsin treatment, mass spectrometric analysis was performed on the EdECM powder (Table S1). MS results show that majority of corneal ECM components, including collagen I, collagen V, and cornea-specific proteoglycans, such as

keratocan, decorin, lumican, and biglycan, as reported previously [28], were preserved in the pepsin-digested dECM powder. More importantly, MS analysis established the absence of run-away porcine pepsin in the final EdECM digest. Cumulatively, these observations indicate that enzymatic digestion of dECM microparticles is an alternative, safe and effective technique for obtaining homogenous particle size distribution. In addition, this methodology efficiently preserves the molecular constituents of native tissue which can help support a constructive, site-appropriate, remodeling response when implanted in vivo [29].

3.3. Characterization of Fibrin and Fibrin–dECM Hydrogels

Human fibrin sealant or glue (TISSEEL®) was employed as a vehicle for the delivery of dECM microparticles for scarless wound healing of cornea. The fibrin derived hydrogels were prepared with minor modifications to the manufacturer's protocol, as depicted in Figure 3A. The physical and mechanical properties of the prepared fibrin-based hydrogels were evaluated using several techniques in vitro. The crosslinking kinetics of the prepared fibrin derived hydrogels was evaluated using a parallel plate rheometer. Our results show that the storage modulus of fibrin glue plateaued at 28 min, whereas fibrin–EdECM hydrogels attained saturation within 17 min (Figure 3B). This observation suggests that the time required for complete crosslinking of fibrin–EdECM hydrogels is significantly shorter compared to fibrin hydrogels, which should in turn reduce the postoperative recovery time of a patient in a clinical setting.

We next evaluated the compressive modulus of fibrin hydrogels using a mechanical testing instrument. The results demonstrate that fibrin hydrogels displayed significantly higher compressive strength (102.97 $\pm$ 23.95 kPa) compared to fibrin–EdECM hydrogels (70.83 $\pm$ 9.17 kPa) (Figure 3C). Although studies have shown that incorporation of micro-/nanoparticles improve the mechanical properties of fabricated hydrogels [30,31], surprisingly, the inclusion of EdECM microparticles in fibrin glue did not improve the compressive modulus of fibrin–EdECM hydrogels. Nevertheless, as the compressive modulus values of both hydrogel groups fall within the range of 25–100 kPa, reported to be the Young's modulus of human cornea tissue [32,33], the engineered fibrin–EdECM hydrogels are favorably poised to support cell adhesion and promote stromal tissue regeneration in vivo.

Application of fibrin glue has been shown to be effective for treatment of corneal perforations [34]. Hence, to evaluate the sealing ability of fibrin–EdECM hydrogels, burst pressure assessment was performed on perforated cadaveric human corneas ex vivo. Maximum burst pressure values for fibrin controls were observed at 21.7 $\pm$ 4.3 kPa, whereas fibrin–EdECM hydrogels sustained significantly higher burst pressures of 34.3 $\pm$ 3.7 kPa (Figure 3D). These data indicate that fibrin–dECM hydrogels possess sufficient adhesive strength to sustain pressures in the order of magnitude higher than the nominal intraocular pressure (IOP) of the human eye (~2 kPa) [35].

Furthermore, MTT assay on L929 cells incubated in fibrin and fibrin–dECM hydrogel extracts demonstrated negligible cytotoxicity with percentage cell viability ranging 82–97% compared to media control at all four tested concentrations (25%, 50%, 75%, and 100%) (Figure S5). These results show that the prepared fibrin-based hydrogels and their degradation products were non-cytotoxic to L929 cells in vitro. In addition, results from genotoxicity assay demonstrate that the mean number of revertant colonies at the concentration of polar and non-polar extracts of fibrin derived hydrogels was comparable to those of solvent controls, in both the presence and absence of metabolic activation. These data suggest that the fibrin derived hydrogel extracts were "non-mutagenic" to *S. typhimurium* and *E. coli* strains at the concentration of 100% extract solution as assessed via bacterial reverse mutation test (Table S2).

3.4. In Vitro hCSC Culture Studies

To demonstrate the cytocompatibility of EdECM microparticles, hCSCs were encapsulated and cultured in fibrin–EdECM hydrogels for a period of five days in vitro. The results from the live–dead assay demonstrate that the EdECM microparticles displayed very good cytocompatibility, comparable to fibrin-only controls, with cell viability exceeding >95% by the end of Day 5 (Figure 3E). Next, to study the influence of biological-derived EdECM microparticles on the phenotype of hCSCs encapsulated in fibrin hydrogels, cells were stained for specific mesenchymal stem cell (MSC) markers, CD73 and CD90. Of note, CD73 and CD90 are common stem cell markers that are routinely employed for the identification of MSCs arising from various tissue types in the body [36]. The results from immunofluorescence studies show that hCSCs cultured in fibrin–EdECM hydrogels exhibited significantly higher expression of CD73 and lower of CD90 compared to fibrin controls at the end of the five-day culture period (Figure 3F,G and Figure S6). In addition, the fibrocytic marker α-SMA, a standard marker used for labeling activated fibrocytes/myofibroblasts that play a major role in tissue fibrosis [37], was significantly downregulated in cells cultured in the presence of EdECM microparticles compared to fibrin controls (Figure 3H and Figure S6) at all three time points. This data clearly indicate that EdECM microparticles inhibit the differentiation of hCSCs to a myofibroblast lineage which plays a major role in fibrotic ECM deposition that leads to corneal opacity [38]. Overall, these data demonstrate that dECM microparticles support and maintain hCSC phenotypic characteristics that are beneficial for tissue repair and regeneration in vivo.

Biodegradation studies on cell-laden fibrin-based hydrogels showed that both hydrogel groups lost only 20% of their mass by the end of Day 6 (Figure 3I). However, both groups significantly lost >80% mass by the end of Day 8. Moreover, no significant differences in percentage mass loss were observed between the two groups at any time point during the eight-day study period. These data correlate well with other studies that show that fibrin gels possess weak physical properties and hence are associated with a fast degradation rate [5,39].

3.5. Animal Studies

For in vivo studies, physically processed dECM microparticles were employed in the hydrogel preparation process as enzymatic digestion of physically milled dECM powder generated very low yield of EdECM microparticles. Skin sensitization studies with the polar and non-polar fibrin-based hydrogel extracts demonstrated that no treatment related skin reactions were observed at sites after intradermal injection. However, skin reactions such as erythema (of varying degree) and very slight edema (barely perceptible) were observed at all other injection sites in all animal groups. In topical induction and challenge phases, no treatment-related skin reactions such as erythema and edema were observed in any of the animals of all groups tested. Cumulatively, our results indicate that extracts of fibrin and fibrin–dECM hydrogels were found to be "non-sensitive" to the skin of Guinea pigs under the employed experimental conditions (Table S3).

Ocular irritation studies demonstrated that no treatment related ocular lesions were observed for up to 72 h in initial and confirmatory test animals after single ocular instillation of polar hydrogel extracts (Table S4). In addition, no treatment related clinical signs of toxicity, mortality, and gross pathological changes were observed in any of the animals in both initial and confirmatory test groups, post-instillation. Taken together, based on the observed results under the experimental conditions followed as per ISO 10993 guidelines, it can be concluded that the fibrin derived hydrogel extracts were found to be a "non-irritant" to the eyes of New Zealand white rabbits.

We next assessed the use of fibrin-based hydrogels in a rabbit model of corneal stromal injury. Animals that received hydrogel formulations did not exhibit adverse reactions but displayed moderate ocular irritation and some mucus release for the initial 2–3 days post-surgery. However, there was no sign of edema, opacity or neo vascularization in the cornea and no significant differences in IOP were observed between the experimental and

normal eyes of rabbits in all four groups. Clinical photographs demonstrated that a clear demarcation of the wound site was visible in all animals at the end of Day 7 (data not shown). Cobalt blue slit lamp photographs with fluorescein staining demonstrated that all four groups re-epithelialized by Day 14 post-surgery, implying successful migration of corneal epithelial cells over the fibrin-based hydrogels (Figure 4B). However, corneal healing and scar formation were also observed, but their magnitude varied across all four groups. For instance, slit lamp images of untreated corneas revealed severe scar formation that was visible until Day 14 but gradually decreased over the next few weeks. On the other hand, corneas treated with the various treatment formulations demonstrated a gradual decrease in corneal haze that was no longer visible after four weeks.

ASOCT is an established platform for evaluating corneal thickness and has been used to identify and evaluate changes occurring along the corneal surface non-invasively. ASOCT imaging demonstrated that all animals exhibited nominal corneal thickness with no pathological conditions prior to surgery. After surgery, ASOCT images showed a reduced corneal thickness with an epithelial defect measuring 150–200 μm depth. Interestingly, one week post-surgery, corneas that received fibrin hydrogels with dECM microparticles retained the bioadhesive more prominently compared to fibrin-only controls, suggesting that dECM microparticles played an important role in stabilizing the hydrogels in vivo (data not shown). In addition, ASOCT imaging also indicated scar formation, visible as a hyper-reflective layer due to incident light scatter from the underlying stromal layer, with varying degrees along with signs of re-epithelialization in all four groups across all time points during the eight-week study period.

Corneal densitometry has been employed clinically to quantify corneal haze and to determine the extent of scarring in the cornea. Prior to surgery, animals demonstrated nominal densitometric values (~20%), which was suggestive of good optical clarity and absence of deformities in the cornea. However, post-surgery, densitometric scans indicated high light scattering, similar to ASOCT imaging, which is indicative of scar development in the injured eye of the rabbit. Corneal opacity was close to 70% across all groups during the first two weeks post-surgery, following which the values gradually decreased, suggesting wound stabilization and healing at the injured site (Figure 4C). By the end of eight weeks, densitometric values dropped to ~45%, suggesting gradual recovery of vision in the injured eye of the rabbits. It was observed that animals that received fibrin with dECM microparticles exhibited the lowest corneal opacity values at the eight-week time point, suggesting that the presence of dECM might have minimized corneal stromal scarring compared to the other groups. Corneas that received fibrin hydrogels with dECM microparticles and hCSCs displayed slightly higher densitometric values compared to other three groups.

Histopathological evaluation demonstrated that corneas from all four groups showed evidence of re-epithelialization and stromal reconstruction (Figure 5). More importantly, histological sections revealed strong adhesion of the fibrin-based hydrogels at the defect site after application. It was observed that corneas that received fibrin + dECM microparticles showed the presence of voids due to the absence of microparticles in the fibrin hydrogel. It is not clear whether the microparticles degraded overtime in vivo or were lost during histological sample processing and preparation. In contrast, corneas that received fibrin hydrogel with microparticles and hCSCs displayed a compacted epithelium at the injured site. However, epithelial hyperplasia due to the injury was visible across all four groups. PAS staining exhibited no sign of goblet cells, which suggests that there was no infiltration in cornea. Immunofluorescence imaging demonstrated a positive stain for the epithelial marker CK3. This result is noteworthy as cytokeratins, CK3 and CK12, are widely known to be expressed in differentiated human corneal epithelial cells [40].

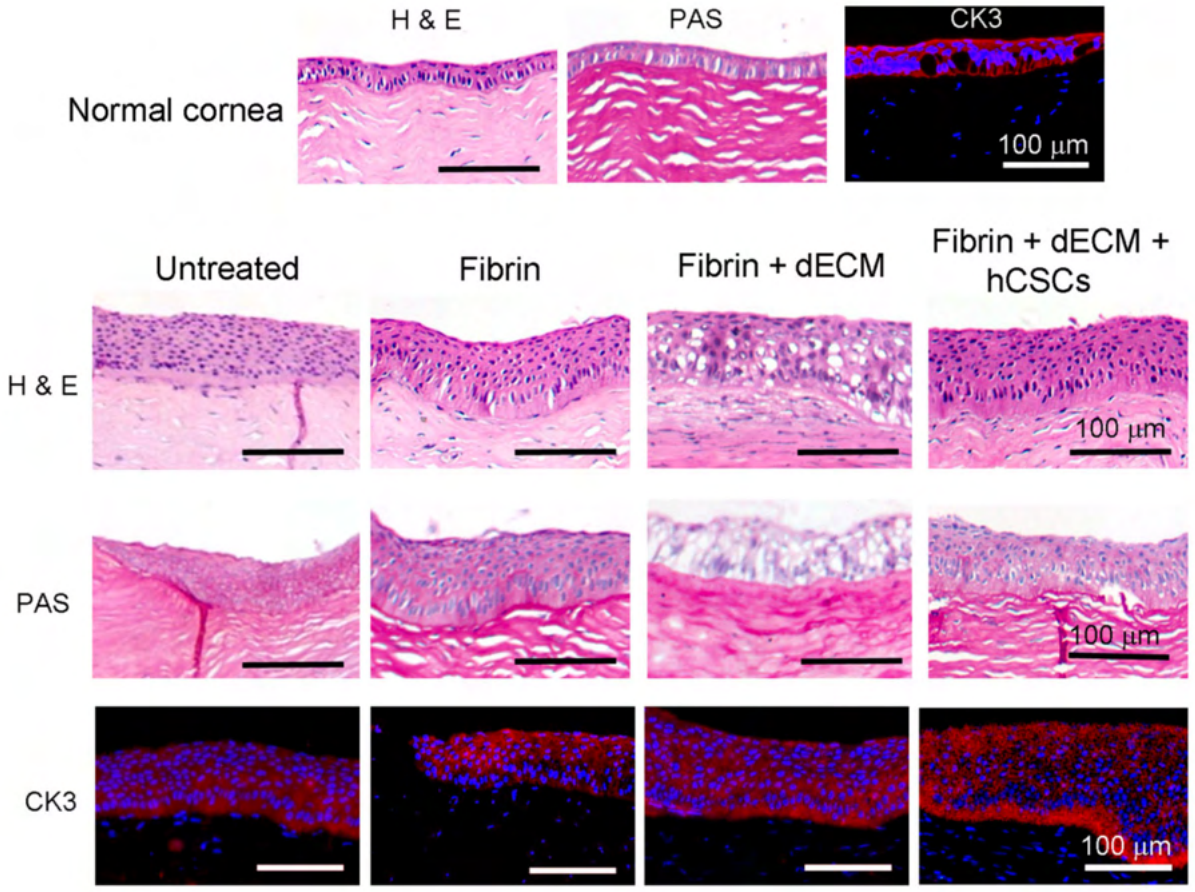

Figure 5. Histopathology and immunofluorescence imaging of paraffin-embedded rabbit cornea sections. H&E imaging revealed strong adhesion of the fibrin-based adhesives to the cornea and demonstrated evidence of re-epithelialization and stromal reconstruction with signs of epithelial hyperplasia. PAS staining denoted the absence of goblet cell infiltration in the cornea. Immunofluorescence staining demonstrated a positive stain for cytokeratin 3, observed across all groups, confirming corneal re-epithelialization by the end of eight weeks.

Overall, our preclinical pilot study demonstrates that human cornea-derived ECM microparticles have an excellent safety profile and suggests that they can be potentially used for the treatment of surface epithelial defects and anterior stromal injuries in a minimally invasive manner. As the animal study performed was based on a pilot study design with very few animals, the efficacy of the various treatment formulations via standard statistical methods of analysis could not be established. In our previous study using Bovine DCM hydrogel, we showed its advantage over existing materials including easy availability, affordability, and simple formulation procedures, which make it a promising biomaterial to prevent scar development in an injured cornea [41]. Moreover, based on the data in hand, we are in the process of refining the stromal wound model as our results indicate that epithelial/stromal defects in rabbits heal rapidly as untreated corneas exhibited accelerated wound healing and speedy recovery without any therapeutic intervention. In view of this, studies have been focused on developing delayed wound healing models that mimic persistent corneal epithelial defects observed in several chronic ocular pathologies [21,42,43]. To overcome the above limitation and for plausible assessment of treatment outcomes, we are in the process of establishing and validating an alkali-induced stromal wound model for subsequent preclinical investigations.

4. Conclusions

In this study, we report the use of dECM microparticles derived via physical and enzymatic processing of cadaveric human corneas as an accessible therapeutic option for

the reconstruction of corneal surface post-injury. dECM microparticles averaged <10 µm in size and were readily dispersible in the precursor solution of thrombin. Hydrogels derived from fibrin–EdECM formulations were moderately transparent and exhibited physical and mechanical properties that matched the microenvironment of native cornea tissue. More specifically, fibrin–EdECM hydrogels exhibited good compressive modulus and sustained pressures 17-fold higher than the nominal IOP of the human eye. Furthermore, fibrin–dECM hydrogels demonstrated excellent biocompatibility, non-mutagenicity, and, in addition, was found to be non-sensitive and non-irritable to the ocular surface as assessed via in vivo studies following ISO 10993 guidelines. Moreover, the prepared hydrogels supported the growth and maintained the phenotype of encapsulated hCSCs in vitro. Most importantly, fibrin–dECM hydrogels demonstrated safety and promoted corneal re-epithelialization and stromal regeneration in a rabbit model of anterior lamellar keratectomy in vivo. However, the limitation of our study is the small animal number in each group, and this needs to be further explored in a large preclinical study using both mice and rabbit scar models. Viewed comprehensively, our results indicate that dECM microparticles hold great promise for inducing constructive corneal remodeling for reparation of epithelial surface defects and anterior stromal wounds. Evidently, this methodology should reduce the dependence on donor corneas for full corneal transplant (keratoplasty) and circumvent issues associated with current corneal transplantation procedures, making it a viable, minimally invasive approach that will lead to faster recovery, improved visual acuity, minimized photosensitivity to light, reduced pain, and better the quality of life of patients.

Supplementary Materials: The following are available online at https://www.mdpi.com/article/10.3390/biom11040532/s1, Figure S1: Average size of freeze milled corneal dECM microparticles obtained from lyophilized corneas and wet corneas as measured through scanning electron microscopy, Figure S2: TGA analysis on physically milled dECM microparticles; Figure S3: FTIR spectroscopy on physically milled and enzymatically digested dECM microparticles; Figure S4: quantification of Pepsin using Sandwich ELISA; Table S1: components of pepsin digested cornea dECM via mass spectrometry analysis; Figure S5: MTT assay; Figure S6: Quantification of immunofluorescence signals from CD73, CD90 and α-SMA from hCSC encapsulated fibrin and fibrin+EdECM hydrogel samples using ImageJ; Table S2: bacterial reverse mutation test study report; Table S3: skin sensitization test study report; Table S4: acute ocular irritation test study report.

Author Contributions: A.C., T.B., V.S.S., V.S. and S.B., were involved in the experimental design of the study. P.A., K.S., T.G., S.S., M.D. and D.P., were involved in the production, characterization and in vitro studies related to dECM microparticles. Animal studies were performed by S.K.O., V.K.S., V.S. and S.B., T.G., S.S., P.A., M.B.T., S.K.O. and M.D. were involved in manuscript writing and preparation. All authors have read and agreed to the published version of the manuscript.

Funding: This study was funded by the Hyderabad Eye Research Foundation, Hyderabad, Telangana, 500034, India and Pandorum Technologies Pvt. Ltd., Bengaluru, Karnataka, 560100, India. The authors would like to acknowledge Science and Engineering Research Board, Government of India, for the grant to SB and supporting the Junior Research Fellowship to MD (EMR/2017/005086).

Institutional Review Board Statement: The study was conducted according to the guidelines of the Declaration of Helsinki, and approved by the Institutional Ethics Committee of LV Prasad Eye Institute, Hyderabad, India (LEC 12-9-372, 6 December 2019).

Informed Consent Statement: Informed consent is not applicable for this study as it does not involve any human subjects. However, towards the usage of corneas utilized in this study, informed consent was obtained from the donor's families, by the Ramayamma International Eye Bank, LV Prasad Eye Institute, Hyderabad, India, who provided human corneal tissue.

Data Availability Statement: The data presented in this study are available on request from the corresponding author. The data are not publicly available due to intellectual property restrictions and institutional policies.

Acknowledgments: The authors would like to gratefully acknowledge the Ramayamma International Eye Bank (RIEB), LV Prasad Eye Institute, Hyderabad India for providing human donor corneal tissue (not otherwise suitable for clinical transplantation) for the experiments.

Conflicts of Interest: The authors declare no competing financial interest. The authors have two patents on the hydro-gel described in the study (WO2019211873 and WO2019211874).

References

1. Tan, D.T.; Dart, J.K.; Holland, E.J.; Kinoshita, S. Corneal transplantation. *Lancet* **2012**, *379*, 1749–1761. [CrossRef]
2. Stevens, G.A.; White, R.A.; Flaxman, S.R.; Price, H.; Jonas, J.B.; Keeffe, J.; Leasher, J.; Naidoo, K.; Pesudovs, K.; Resnikoff, S.; et al. Global prevalence of vision impairment and blindness: Magnitude and temporal trends, 1990–2010. *Ophthalmology* **2013**, *120*, 2377–2384. [CrossRef] [PubMed]
3. Islam, M.M.; Buznyk, O.; Reddy, J.C.; Pasyechnikova, N.; Alarcon, E.I.; Hayes, S.; Lewis, P.; Fagerholm, P.; He, C.; Iakymenko, S.; et al. Biomaterials-enabled cornea regeneration in patients at high risk for rejection of donor tissue transplantation. *NPJ Regen. Med.* **2018**, *3*, 1–10. [CrossRef] [PubMed]
4. Gain, P.; Jullienne, R.; He, Z.; Aldossary, M.; Acquart, S.; Cognasse, F.; Thuret, G. Global Survey of Corneal Transplantation and Eye Banking. *JAMA Ophthalmol.* **2016**, *134*, 167–173. [CrossRef]
5. Trujillo-de Santiago, G.; Sharifi, R.; Yue, K.; Sani, E.S.; Kashaf, S.S.; Alvarez, M.M.; Leijten, J.; Khademhosseini, A.; Dana, R.; Annabi, N. Ocular adhesives: Design, chemistry, crosslinking mechanisms, and applications. *Biomaterials* **2019**, *197*, 345–367. [CrossRef]
6. Jirásková, N.; Rozsival, P.; Burova, M.; Kalfertova, M. AlphaCor artificial cornea: Clinical outcome. *Eye* **2011**, *25*, 1138–1146. [CrossRef]
7. Basu, S.; Hertsenberg, A.J.; Funderburgh, M.L.; Burrow, M.K.; Mann, M.M.; Du, Y.; Lathrop, K.L.; Syed-Picard, F.N.; Adams, S.M.; Birk, D.E.; et al. Human limbal biopsy-derived stromal stem cells prevent corneal scarring. *Sci. Transl. Med.* **2014**, *6*, 266ra172. [CrossRef]
8. Singh, V.; Shukla, S.; Ramachandran, C.; Mishra, D.K.; Katikireddy, K.R.; Lal, I.; Chauhan, S.K.; Sangwan, V.S. Science and Art of Cell-Based Ocular Surface Regeneration. *Int. Rev. Cell Mol. Biol.* **2015**, *319*, 45–106. [CrossRef]
9. Fagerholm, P.; Lagali, N.S.; Ong, J.A.; Merrett, K.; Jackson, W.B.; Polarek, J.W.; Suuronen, E.J.; Liu, Y.; Brunette, I.; Griffith, M. Stable corneal regeneration four years after implantation of a cell-free recombinant human collagen scaffold. *Biomaterials* **2014**, *35*, 2420–2427. [CrossRef]
10. Badylak, S.; Kokini, K.; Tullius, B.; Simmons-Byrd, A.; Morff, R. Morphologic Study of Small Intestinal Submucosa as a Body Wall Repair Device. *J. Surg. Res.* **2002**, *103*, 190–202. [CrossRef]
11. Gilbert, T.W.; Wognum, S.; Joyce, E.M.; Freytes, D.O.; Sacks, M.S.; Badylak, S.F. Collagen fiber alignment and biaxial mechanical behavior of porcine urinary bladder derived extracellular matrix. *Biomaterials* **2008**, *29*, 4775–4782. [CrossRef]
12. Yin, H.; Lu, Q.; Wang, X.; Majumdar, S.; Jun, A.S.; Stark, W.J.; Grant, M.P.; Elisseeff, J.H. Tissue-derived microparticles reduce inflammation and fibrosis in cornea wounds. *Acta Biomater.* **2019**, *85*, 192–202. [CrossRef]
13. Kim, H.; Park, M.-N.; Kim, J.; Jang, J.; Kim, H.-K.; Cho, D.-W. Characterization of cornea-specific bioink: High transparency, improved in vivo safety. *J. Tissue Eng.* **2019**, *10*, 2041731418823382. [CrossRef]
14. Du, L.; Wu, X.; Pang, K.; Yang, Y. Histological evaluation and biomechanical characterisation of an acellular porcine cornea scaffold. *Br. J. Ophthalmol.* **2010**, *95*, 410–414. [CrossRef]
15. Márquez, S.P.; Martínez, V.S.; Ambrose, W.M.; Wang, J.; Gantxegui, N.G.; Schein, O.; Elisseeff, J. Decellularization of bovine corneas for tissue engineering applications. *Acta Biomater.* **2009**, *5*, 1839–1847. [CrossRef]
16. Du, L.; Wu, X. Development and Characterization of a Full-Thickness Acellular Porcine Cornea Matrix for Tissue Engineering. *Artif. Organs* **2011**, *35*, 691–705. [CrossRef]
17. Joshi, V.P.; Ojha, S.K.; Singh, V.; Basu, S. A reliable animal model of corneal stromal opacity: Development and validation using in vivo imaging. *Ocul. Surf.* **2020**, *18*, 681–688. [CrossRef]
18. Wilson, S.L.; Sidney, L.E.; Dunphy, S.E.; Dua, H.S.; Hopkinson, A. Corneal Decellularization: A Method of Recycling Unsuitable Donor Tissue for Clinical Translation? *Curr. Eye Res.* **2015**, *41*, 769–782. [CrossRef]
19. Gonzalez-Andrades, M.; Cardona, J.D.L.C.; Ionescu, A.M.; Campos, A.; Perez, M.D.M.; Alaminos, M. Generation of Bioengineered Corneas with Decellularized Xenografts and Human Keratocytes. *Investig. Opthalmol. Vis. Sci.* **2011**, *52*, 215–222. [CrossRef]
20. Damala, M.; Swioklo, S.; Koduri, M.A.; Mitragotri, N.S.; Basu, S.; Connon, C.J.; Singh, V. Encapsulation of human limbus-derived stromal/mesenchymal stem cells for biological preservation and transportation in extreme Indian conditions for clinical use. *Sci. Rep.* **2019**, *9*, 16950. [CrossRef]
21. Kethiri, A.R.; Raju, E.; Bokara, K.K.; Mishra, D.K.; Basu, S.; Rao, C.M.; Sangwan, V.S.; Singh, V. Inflammation, vascularization and goblet cell differences in LSCD: Validating animal models of corneal alkali burns. *Exp. Eye Res.* **2019**, *185*, 107665. [CrossRef]
22. Coster, D.J.; Jessup, C.F.; Williams, K.A. Mechanisms of corneal allograft rejection and regional immunosuppression. *Eye* **2009**, *23*, 1894–1897. [CrossRef]
23. Nie, X.; Wang, D.-A. Decellularized orthopaedic tissue-engineered grafts: Biomaterial scaffolds synthesised by therapeutic cells. *Biomater. Sci.* **2018**, *6*, 2798–2811. [CrossRef]

24. Breen, E.D.; Curley, J.G.; Overcashier, D.E.; Hsu, C.C.; Shire, S.J. Effect of Moisture on the Stability of a Lyophilized Humanized Monoclonal Antibody Formulation. *Pharm. Res.* **2001**, *18*, 1345–1353. [CrossRef]
25. Nakamura, K.; Iwazawa, R.; Yoshioka, Y. Introduction to a new cell transplantation platform via recombinant peptide petaloid pieces and its application to islet transplantation with mesenchymal stem cells. *Transpl. Int.* **2016**, *29*, 1039–1050. [CrossRef]
26. Barth, A. Infrared spectroscopy of proteins. *Biochim. Biophys. Acta (BBA)—Bioenerg.* **2007**, *1767*, 1073–1101. [CrossRef]
27. Rieder, E.; Steinacher-Nigisch, A.; Weigel, G. Human immune-cell response towards diverse xenogeneic and allogeneic decellularized biomaterials. *Int. J. Surg.* **2016**, *36*, 347–351. [CrossRef]
28. Dyrlund, T.F.; Poulsen, E.T.; Scavenius, C.; Nikolajsen, C.L.; Thøgersen, I.B.; Vorum, H.; Enghild, J.J. Human Cornea Proteome: Identification and Quantitation of the Proteins of the Three Main Layers Including Epithelium, Stroma, and Endothelium. *J. Proteome Res.* **2012**, *11*, 4231–4239. [CrossRef]
29. Pouliot, R.A.; Young, B.M.; Link, P.A.; Park, H.E.; Kahn, A.R.; Shankar, K.; Schneck, M.B.; Weiss, D.J.; Heise, R.L. Porcine Lung-Derived Extracellular Matrix Hydrogel Properties Are Dependent on Pepsin Digestion Time. *Tissue Eng. Part C Methods* **2020**, *26*, 332–346. [CrossRef]
30. Fu, J. Strong and tough hydrogels crosslinked by multi-functional polymer colloids. *J. Polym. Sci. Part B Polym. Phys.* **2018**, *56*, 1336–1350. [CrossRef]
31. Huang, C.; Li, Y.; Duan, L.; Wang, L.; Ren, X.; Gao, G. Enhancing the self-recovery and mechanical property of hydrogels by macromolecular microspheres with thermal and redox initiation systems. *RSC Adv.* **2017**, *7*, 16015–16021. [CrossRef]
32. Ramirez-Garcia, M.A.; Sloan, S.R.; Nidenberg, B.; Khalifa, Y.M.; Buckley, M.R. Depth-Dependent Out-of-Plane Young's Modulus of the Human Cornea. *Curr. Eye Res.* **2017**, *43*, 595–604. [CrossRef] [PubMed]
33. Sjøntoft, E.; Edmund, C. In vivo determination of young's modulus for the human cornea. *Bull. Math. Biol.* **1987**, *49*, 217–232. [CrossRef] [PubMed]
34. Duchesne, B.; Tahi, H.; Galand, A. Use of Human Fibrin Glue and Amniotic Membrane Transplant in Corneal Perforation. *Cornea* **2001**, *20*, 230–232. [CrossRef]
35. Wang, Y.X.; Xu, L.; Bin Wei, W.; Jonas, J.B. Intraocular pressure and its normal range adjusted for ocular and systemic parameters. The Beijing Eye Study 2011. *PLoS ONE* **2018**, *13*, e0196926. [CrossRef]
36. Lv, F.-J.; Tuan, R.S.; Cheung, K.M.; Leung, V.Y. Concise Review: The Surface Markers and Identity of Human Mesenchymal Stem Cells. *Stem Cells* **2014**, *32*, 1408–1419. [CrossRef]
37. De Oliveira, R.C.; Wilson, S.E. Fibrocytes, Wound Healing, and Corneal Fibrosis. *Investig. Ophthalmol. Vis. Sci.* **2020**, *61*, 28. [CrossRef]
38. Wilson, S.E. Corneal myofibroblast biology and pathobiology: Generation, persistence, and transparency. *Exp. Eye Res.* **2012**, *99*, 78–88. [CrossRef]
39. Li, Y.; Meng, H.; Liu, Y.; Lee, B.P. Fibrin Gel as an Injectable Biodegradable Scaffold and Cell Carrier for Tissue Engineering. *Sci. World J.* **2015**, *2015*, 685690. [CrossRef]
40. Sun, T.-T.; Tseng, S.C.G.; Huang, A.J.-W.; Cooper, D.; Schermer, A.; Lynch, M.H.; Weiss, R.; Eichner, R. Monoclonal Antibody Studies of Mammalian Epithelial Keratins: A Review. *Ann. N. Y. Acad. Sci.* **1985**, *455*, 307–329. [CrossRef]
41. Chameettachal, S.; Prasad, D.; Parekh, Y.; Basu, S.; Singh, V.; Bokara, K.K.; Pati, F. Prevention of Corneal Myofi-broblastic Differentiation in vitro Using a Biomimetic ECM Hydrogel for Corneal Tissue Regeneration. *ACS Appl. BioMater.* **2021**, *4*, 533–544. [CrossRef]
42. Gum, G.; Wirostko, B.; Rafii, M.; Pritt, S.; Gutierrez, D. Corneal Wound Healing Model in New Zealand White Rabbits for Evaluating Persistent Corneal Epithelial Defects. *Investig. Opthalmol. Vis. Sci.* **2013**, *54*, 3903.
43. Chang, S.-W.; Chou, S.-F.; Chuang, J.-L. Mechanical corneal epithelium scraping and ethanol treatment up-regulate cytokine gene expression differently in rabbit cornea. *J. Refract. Surg.* **2008**, *24*, 150–159. [CrossRef]

OPEN ACCESS
ARVO Annual Meeting Abstract | June 2017

Limbal Stromal Stem Cell Therapy for Acute and Chronic Superficial Corneal Pathologies: Early Clinical Outcomes of The Funderburgh Technique

Sayan Basu; Mukesh Damala; Vivek Singh

— Author Affiliations & Notes

Sayan Basu
Tej Kohli Cornea Institute, L V Prasad Eye Institute, Hyderabad, Telangana, India

Mukesh Damala
Tej Kohli Cornea Institute, L V Prasad Eye Institute, Hyderabad, Telangana, India

Vivek Singh
Tej Kohli Cornea Institute, L V Prasad Eye Institute, Hyderabad, Telangana, India

Footnotes

Commercial Relationships **Sayan Basu**, None; **Mukesh Damala**, None; **Vivek Singh**, None

Support None

Investigative Ophthalmology & Visual Science June 2017, Vol.58, 3371. doi:

Abstract

Purpose : Conventional therapies for potentially blinding corneal disorders like burns, ulcers and scars have several limitations. We aimed to clinically validate the findings of previous animal studies, which had indicated that application of limbal stromal stem cells (LSSC) to the wounded corneal surface promoted corneal stromal regeneration, prevented fibrosis and restored corneal transparency.

Methods : In this pilot-clinical trial, one-clock hour wide limbal biopsies were obtained from donor eyes. The LSSC were isolated ex-vivo using a previously standardized xeno-free cultivation technique. The Funderbugh technique of LSSC delivery involved: (i) debridement of the corneal epithelium using a dry sponge; (ii) mixing 0.5 million LSSC in 0.05ml of the fibrinogen component of commercially available fibrin sealant and layering it over the bared corneal stroma; (iii) adding 0.05ml of the thrombin component and allowing the two components to gel; and (iv) placing a bandage contact lens on the eye. Patients in the study group were prescribed prophylactic topical antibiotics without any corticosteroids. Patients in the control group received the standard medical therapy, including topical corticosteroids, along with debridement and fibrin glue but without the cells.

Results : The study group included 5 eyes each with acute corneal burns and sterile non-healing ulcers, which received allogeneic LSSC; and 5 eyes with chronic post-infectious scars, which received autologous LSSC. The control group was matched both in terms of numbers and baseline characteristics. At 4 weeks, when compared to controls, the eyes receiving LSSC, irrespective of the source, showed: (i) greater improvement in best-corrected visual acuity (P=0.003); (ii) faster corneal epithelization (p=0.002); (iii) better corneal clarity, evaluated both clinically (P=0.012) and on scheimpflug imaging (P<0.0001); and lesser corneal vascularization (p<0.0001). None of the 15 eyes receiving LSSC required a second surgical intervention as compared to 6 of 15 (40%) eyes in the control group (p=0.017).

Conclusions : The Funderburgh technique of delivering autologous and allogeneic LSSC was effective in enhancing vision, promoting corneal epithelization, improving corneal clarity, reducing corneal scarring and thus obviating the need for corneal transplantation in eyes with corneal burns, ulcers and scars.

This is an abstract that was submitted for the 2017 ARVO Annual Meeting, held in Baltimore, MD, May 7-11, 2017.

OPEN ACCESS
ARVO Annual Meeting Abstract | July 2018

Limbal Stromal Stem Cell Therapy for Acute and Chronic Superficial Corneal Pathologies: One-Year Outcomes

James Funderburgh; Sayan Basu; Mukesh Damala; Fateme Tavakkoli; Virender Sangwan; Vivek Singh

Author Affiliations & Notes

James Funderburgh
Ophthalmology, Univ of Pittsburgh School of Medicine, Pittsburgh, Pennsylvania, United States

Sayan Basu
Tej Kohli Cornea Institute, L V Prasad Eye Institute, Hyderabad, Telangana, India

Mukesh Damala
Tej Kohli Cornea Institute, L V Prasad Eye Institute, Hyderabad, Telangana, India

Fateme Tavakkoli
Tej Kohli Cornea Institute, L V Prasad Eye Institute, Hyderabad, Telangana, India

Virender Sangwan
Tej Kohli Cornea Institute, L V Prasad Eye Institute, Hyderabad, Telangana, India

Vivek Singh
Tej Kohli Cornea Institute, L V Prasad Eye Institute, Hyderabad, Telangana, India

Footnotes

Commercial Relationships **James Funderburgh**, None; **Sayan Basu**, None; **Mukesh Damala**, None; **Fateme Tavakkoli**, None; **Virender Sangwan**, None; **Vivek Singh**, None

Support Stein Innovator Award, Research to Prevent Blindness Inc. (JLF)

Investigative Ophthalmology & Visual Science July 2018, Vol.59, 3455. doi:

Abstract

Purpose : Conventional corneal transplantation is prone to failure in severe blinding pathologies like burns, ulcers and scars. Alternative strategies are being pursued globally to find better solutions. This study evaluated the long-term safety and efficacy of one such approach, using a novel minimally invasive technique to deliver allogeneic limbal stromal stem cells (LSSC) to restore corneal clarity and improve vision.

Methods : In this pilot-clinical trial, one-clock hour wide limbal biopsies were obtained from human cadaveric corneo-scleral rims. The LSSC were isolated using a previously standardized xeno-free ex-vivo cultivation technique. The technique of LSSC delivery involved: (i) debridement of the corneal epithelium using a dry sponge; (ii) mixing 0.5 million LSSC in 0.05ml of the fibrinogen component of commercially available fibrin sealant and layering it over the bared corneal stroma; (iii) adding 0.05ml of the thrombin component and allowing the two components to gel; and (iv) placing a bandage contact lens on the eye. Patients in the study group were prescribed prophylactic topical antibiotics without any corticosteroids. Patients in the control group received fibrin sealant without cells, along with standard therapy, including topical corticosteroids, as indicated. Both cases and controls were followed up for 1-year post-operatively.

Results : The study group included 5 eyes each with acute corneal burns, sterile non-healing ulcers and chronic post-keratitis scars. The control group was matched both in terms of numbers and baseline characteristics. At 6-weeks, 3-months, 6-months and 1 year, when compared to controls, the eyes receiving LSSC had: (i) greater UCVA ($P<0.03$); (ii) greater BCVA ($P<0.01$); (iii) better corneal clarity, evaluated both clinically ($P<0.001$) and on scheimpflug imaging ($P<0.007$); and lesser corneal vascularization ($P<0.0001$), irrespective of the original indication. Only 1 (6.7%) of the 15 eyes receiving LSSC required a second surgical intervention as compared to 7 of 15 (46.7%) eyes in the control group ($P=0.013$).

Conclusions : This minimally-invasive technique of delivering allogeneic LSSC was effective in enhancing vision, improving corneal clarity, reducing corneal opacification and vascularization, thus obviating the need for corneal transplantation in eyes with corneal burns, ulcers and scars.

This is an abstract that was submitted for the 2018 ARVO Annual Meeting, held in Honolulu, Hawaii, April 29 - May 3, 2018.

OPEN ACCESS
ARVO Annual Meeting Abstract | July 2019

Human Limbus-derived Mesenchymal/Stromal Stem Cell Therapy for Superficial Corneal Pathologies: Two-Year Outcomes

Sayan Basu; Mukesh Damala; Fateme Tavakkoli; Noopur Mitragotri; Vivek Singh

— Author Affiliations & Notes

Sayan Basu
Center for Ocular Regeneration (CORE), L V Prasad Eye Institute, Hyderabad, India
Cornea and Anterior Segment Services, L V Prasad Eye Institute, Hyderabad, ANDHRA PRADESH, India

Mukesh Damala
Center for Ocular Regeneration (CORE), L V Prasad Eye Institute, Hyderabad, India

Fateme Tavakkoli
Center for Ocular Regeneration (CORE), L V Prasad Eye Institute, Hyderabad, India

Noopur Mitragotri
Center for Ocular Regeneration (CORE), L V Prasad Eye Institute, Hyderabad, India

Vivek Singh
Center for Ocular Regeneration (CORE), L V Prasad Eye Institute, Hyderabad, India

Footnotes

Commercial Relationships **Sayan Basu**, None; **Mukesh Damala**, None; **Fateme Tavakkoli**, None; **Noopur Mitragotri**, None; **Vivek Singh**, None

Support none

Investigative Ophthalmology & Visual Science July 2019, Vol.60, 4146. doi:

Abstract

Purpose : Corneal transplantation is prone to failure in severe inflammatory pathologies like burns, ulcers and scars. Alternative strategies are being pursued globally to find better solutions. This study evaluated the long-term safety and efficacy of using a novel minimally invasive technique of delivering allogeneic human limbus-derived mesenchymal/stromal stem cells (hLMSC) to treat potentially blinding superficial corneal diseases.

Methods : In this registered and approved pilot-clinical trial, limbal biopsies were obtained from human cadaveric corneo-scleral rims, sourced from an accredited eye bank. The hLMSC were isolated using a previously standardized xeno-free ex-vivo cultivation technique. The technique of hLMSC delivery involved: (i) debridement of the corneal epithelium using a dry sponge; (ii) mixing 0.5 million hLMSC in 0.05ml of the sealer protein component of commercially available fibrin sealant and layering it over the bared corneal stroma; (iii) adding 0.05ml of the thrombin component and allowing the two components of the fibrin sealant to gel together; and (iv) placing a bandage contact lens on the eye. The study group recieved prophylactic topical antibiotics without any corticosteroids. The control group received fibrin sealant without cells, along with standard therapy, including topical corticosteroids, as indicated. Both groups were followed up for 2-years post-operatively.

Results : The study group included 5 eyes each with acute corneal burns, sterile non-healing ulcers and chronic post-keratitis scars. The control group was matched both in terms of numbers, indications and baseline characteristics. At 2 years, when compared to controls, the eyes receiving hLMSC had: (i) greater best corrected visual acuity (P=0.006); (iii) better corneal clarity, evaluated both clinically (P=0.001) and on scheimpflug imaging (P=0.005); and lesser corneal vascularization (P<0.0001), irrespective of the original indication. Only 2 (13.3%) of the 15 eyes receiving hLMSC required a second surgical intervention as compared to 9 of 15 (60%) eyes in the control group (P=0.005).

Conclusions : This minimally-invasive technique of delivering allogeneic hLMSC was effective in enhancing vision, improving corneal clarity and reducing corneal opacification and vascularization, thus obviating the need for corneal transplantation in eyes with corneal burns, ulcers and scars.

This abstract was presented at the 2019 ARVO Annual Meeting, held in Vancouver, Canada, April 28 - May 2, 2019.

OPEN ACCESS
ARVO Annual Meeting Abstract | July 2019

Encapsulation of Human Limbus-derived Stromal/Mesenchymal Stem Cells for Storage and Transportation at Room Temperature

Mukesh Damala; Stephen Swioklo; Madhuri Amulya Kondapaka; Noopur Mitragotri; Sayan Basu; Che John Connon; Vivek Singh

— Author Affiliations & Notes

Mukesh Damala
Brien Holden Eye Research Center, LV Prasad Eye Institute, Hyderabad, Telangana, India
Department of Animal Biology, School of Life Sciences, University of Hyderabad, Hyderabad, Telangana, India

Stephen Swioklo
Institute of Genetic Medicine, Newcastle University, Newcastle Upon Tyne, England, United Kingdom
Atelerix Ltd, Newcastle Upon Tyne, England, United Kingdom

Madhuri Amulya Kondapaka
Brien Holden Eye Research Center, LV Prasad Eye Institute, Hyderabad, Telangana, India
Manipal Academy of Higher Education, Manipal, India

Noopur Mitragotri
Brien Holden Eye Research Center, LV Prasad Eye Institute, Hyderabad, Telangana, India

Sayan Basu
Brien Holden Eye Research Center, LV Prasad Eye Institute, Hyderabad, Telangana, India
Center for Ocular Regeneration, LV Prasad Eye Institute, Hyderabad, Telangana, India

Che John Connon
Institute of Genetic Medicine, Newcastle University, Newcastle Upon Tyne, England, United Kingdom
Atelerix Ltd, Newcastle Upon Tyne, England, United Kingdom

Vivek Singh
Brien Holden Eye Research Center, LV Prasad Eye Institute, Hyderabad, Telangana, India
Center for Ocular Regeneration, LV Prasad Eye Institute, Hyderabad, Telangana, India

Footnotes

Commercial Relationships **Mukesh Damala**, None; **Stephen Swioklo**, None; **Madhuri Kondapaka**, None; **Noopur Mitragotri**, None; **Sayan Basu**, None; **Che Connon**, None; **Vivek Singh**, None

Support None

Investigative Ophthalmology & Visual Science July 2019, Vol.60, 4654. doi:

Abstract

Purpose : Cell-based therapy for corneal scarring using human limbus-derived mesenchymal/stromal stem cells (hLMSCs) is a promising alternative to conventional corneal transplantation. However, reliable methods of storing and transporting these cells for prolonged periods of time and over long distances remains challenging. This study aimed to test a novel method of storing and transporting hLSMCs at room temperature by encapsulating them.

Methods : The cell suspension of hLMSCs was mixed in equal volumes with sodium alginate solution, at a final density of $2.5x10^6$/mL. Encapsulated hLSMCs with complete media were kept in transit at room temperature (RT) or 4°C for 3-5 days, considering it to be the likely maximum duration of transporting cells from bench-to-bedside. Cells without encapsulation were also transported at RT as controls. A specialized container pre-conditioned to maintain temperatures of ≤30°C was used for transportation. Post-storage, hLMSCs were released from encapsulation, their viability was assessed, and they were placed in culture. After 48 and 96-hours in culture, hLSMCs were quantified for their proliferation, gene-expression and phenotypic assessment.

Results : Overall 5 vials were transported in 3 batches of 3-5 days duration. The container under transit maintained an average temperature of 18.6±1.8°C, where the average atmospheric temperature was 31.4±1.2°C. Encapsulated hLSMCs under transit at RT were recovered with a high viability of 82.5±0.9% after a 3-day storage and 76.9±1.9% over a 5-day storage as compared to 4°C that showed 65.2±1.2% and 64.5±0.8% respectively (p=0.01). Cells under transit at RT had better proliferation rates of 74.3±2.9% and 67.7±9.8% than cells stored at 4°C (54.8±9.04% and 52.4±8.1%) after 3 and 5 days of storage, respectively (p<0.001). Non-encapsulated cells at RT had no viability after 3-5 days. Cells after transit maintained their characteristic phenotype, showing the expression of $CD105^+$, $CD45^-$, $CD73^+$, VIM^+, COL-III^+, HLA-DR^-(mesenchymal) and P63-α^+, $ABCG2^+$, PAX-6^+ (stem cell) markers.

Conclusions : Alginate encapsulation is a promising method of cell storage and transportation, offering high cell viability over prolonged durations, in transit and at room temperatures. This provides the opportunity of expanding the scope of cell-based therapy for corneal blindness to remote centers without cell-cultivation cGMP facilities.

This abstract was presented at the 2019 ARVO Annual Meeting, held in Vancouver, Canada, April 28 - May 2, 2019.

OPEN ACCESS
ARVO Annual Meeting Abstract | July 2019

A Novel Extracellular Matrix-Mimetic Hydrogel for Corneal Regeneration

Vivek Singh; Mukesh Damala; Tanmay Gharat; Shivaram Selvam; Sanjay Kumar Ojha; Tuhin Bhowmick; Arun Chandru; Virender Singh Sangwan; Sayan Basu

— Author Affiliations & Notes

Vivek Singh
SSR-Stem cell biology laboratory, Prof. Brien Holden Eye Research Center, L V Prasad Eye Institute, Hyderabad, Telangana, India
Center for Ocular Regeneration (CORE), L V Prasad Eye Institute, Hyderabad, India

Mukesh Damala
SSR-Stem cell biology laboratory, Prof. Brien Holden Eye Research Center, L V Prasad Eye Institute, Hyderabad, Telangana, India
University of Hyderabad, Hyderabad, Telangana, India

Tanmay Gharat
Pandorum Technologies Private Limited, Bangalore, Karnataka, India

Shivaram Selvam
Pandorum Technologies Private Limited, Bangalore, Karnataka, India

Sanjay Kumar Ojha
Pandorum Technologies Private Limited, Bangalore, Karnataka, India

Tuhin Bhowmick
Pandorum Technologies Private Limited, Bangalore, Karnataka, India

Arun Chandru
Pandorum Technologies Private Limited, Bangalore, Karnataka, India

Virender Singh Sangwan
SSR-Stem cell biology laboratory, Prof. Brien Holden Eye Research Center, L V Prasad Eye Institute, Hyderabad, Telangana, India
Center for Ocular Regeneration (CORE), L V Prasad Eye Institute, Hyderabad, India

Sayan Basu
Cornea and Anterior Segment Services, L V Prasad Eye Institute, Hyderabad, Telangana, India
Center for Ocular Regeneration (CORE), L V Prasad Eye Institute, Hyderabad, India

Footnotes

Commercial Relationships **Vivek Singh**, None; **Mukesh Damala**, None; **Tanmay Gharat**, None; **Shivaram Selvam**, None; **Sanjay Ojha**, None; **Tuhin Bhowmick**, None; **Arun Chandru**, None; **Virender Sangwan**, None; **Sayan Basu**, None

Support None

Investigative Ophthalmology & Visual Science July 2019, Vol.60, 4687. doi:

Abstract

Purpose : Corneal stromal scarring is a serious cause of visual impairment and blindness worldwide. Human limbus-derived mesenchymal/stromal stem cells (hLMSCs) have been found to be effective in amelioration of superficial corneal scars. This study aimed to develop a novel extracellular matrix (ECM)-mimetic hydrogel formulation that can incorporate hLMSCs for use in deeper wounds to promote scar-less corneal healing.

Methods : Human cadaveric corneas were obtained from the eye-bank. The corneas were decellularized and the ECM was extracted as powder using freeze-miller and enzymatic digestion. After the ECM-powder was assessed for sterility and level of endotoxins, the ECM-mimetic hydrogel was developed by entrapping enzymatically-digested ECM-derived proteins and glycosaminoglycans within a semi-interpenetrating hydrogel network. The final product was analyzed by using scanning-electron microscopy (SEM) and dynamic light scattering for its physical and transmittance properties. The hLMSCs were then encapsulated and cultured inside this 3D hydrogel for 72-hours to test their viability and proliferation. Immunohistochemistry for hLMSCs markers (ABCG2, PAX-6, Vimentin, Collagen-III, CD73, CD90) and fibroblast marker α-SMA was performed to assess the phenotypic properties of encapsulated hLMSCs.

Results : The SEM analysis of ECM-powder showed intact collagen fibril structure. The ECM-derived proteins' particle size averaged 2 (±0.5) µm on dynamic light scattering analysis. The encapsulated hLMSCs in the ECM-mimetic 3D hydrogel showed similar cell viability (92±3%) as compared to 2D hLMSCs culture ($p=0.12$). The hLMSCs were able to maintain phenotypic expression of ABCG2, PAX-6, Vimentin, Collagen-III, CD73 and CD90 biomarkers, in the presence of ECM-derived proteins within the hydrogel matrix. However, in 2D culture without ECM-derived components, the hLMSCs showed significantly higher expression of α-SMA ($p<0.0001$).

Conclusions : The findings of this study suggest that the novel ECM-mimetic hydrogel possesses the ability to maintain viability and phenotype of encapsulated hLMSCs. This opens the possibility of using hLMSCs encapsulated in the ECM-mimetic hydrogel for application in deeper corneal wounds, which needs to be tested in pre-clinical studies.

This abstract was presented at the 2019 ARVO Annual Meeting, held in Vancouver, Canada, April 28 - May 2, 2019.